Science and Technology Facilities Council

Technical Report
STFC-TR-2026-013

Next-Generation XFEL Science and Technology Case

J Marangos, et.al.

July 2026

©2026 UK Research and Innovation



This work is licensed under a Creative Commons Attribution 4.0 International License.

Enquiries concerning this report should be addressed to:

RAL Library
STFC Rutherford Appleton Laboratory
Harwell Oxford
Didcot
OX11 0QX

Tel: +44(0)1235 445577
email: library@stfc.ac.uk

Science and Technology Facilities Council reports are available online at:
https://epubs.stfc.ac.uk

Accessibility: a Microsoft Word version of this document (for use with assistive technology) may be available on request.

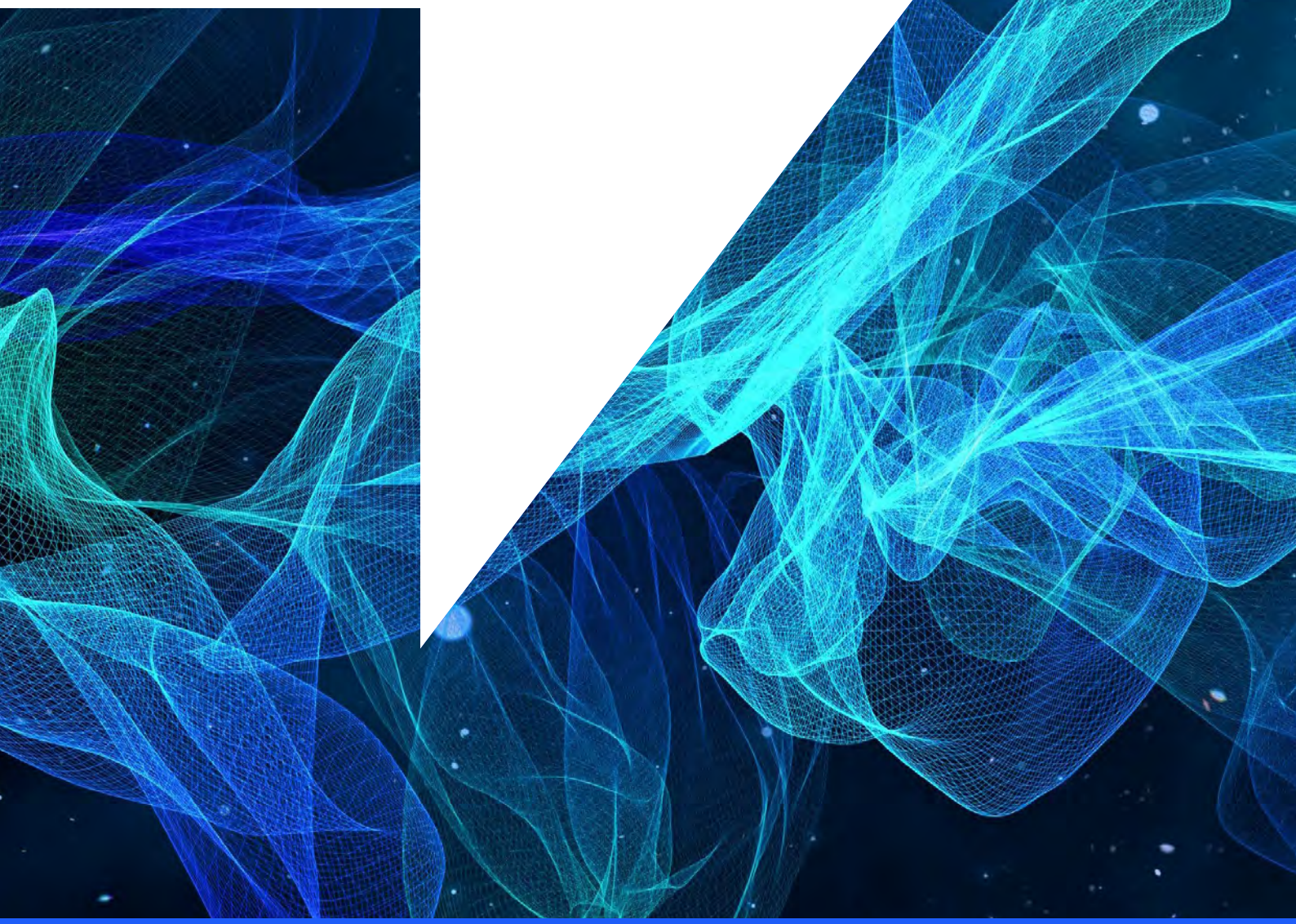
DOI: 10.5286/stfctr.2026013

ISSN 2753-5797

Neither the Council nor the Laboratory accept any responsibility for loss or damage arising from the use of information contained in any of their reports or in any communication about their tests or investigations.

Science and Technology Facilities Council

Next-Generation XFEL Science and Technology Case



xfel.ac.uk

The production team for the Next-Generation XFEL Science and Technology Case was as follows:

Lead Author: Jon Marangos (Imperial College)

STFC Sponsor: John Collier

Production: Paul Aden, Tracey Burge, Jon Marangos

Editors: Tracey Burge, Jon Marangos, Marcus Newton, Allen Orville, Sven Schroeder, Sam Vinko, Julia Weinstein and Amelle Zair

Project Leadership: Jon Marangos, Paul Aden, Deepa Angal-Kalinin, Jim Clarke, John Collier, David Dunning and Edward Snedden

Copyright © 2026 UK Research and Innovation

Technical Report - STFC-TR-2026-013 - DOI: 10.5286/stfctr.2026013

Authors from the Science Team: Shakil Awan, Aliaksandr Baidak, Marco Borghesi, Mark Brouard, Andrew Burnett, Andrew Comley, Mark Dean, Sarnjeet Dhesi, Sofia Diaz Moreno, David Dye, Daniel Eakins, Mike Fitzpatrick, Tian Geng, Jason Greenwood, Andrew Higginbotham, Rebecca Ingle, Adam Kirrander, Adrian Mancuso, Jon Marangos, Emma McBride, Malcolm McMahon, Russell Minns, Marcus Newton, Allen Orville, Thomas Penfold, Paolo Radaelli, Anna Regoutz, Ian Robinson, David Rugg, Sven Schroeder, Elaine Seddon, Claire Vallance, Jasper van Thor, Sam Vinko, Simon Wall, Justin Wark, Julia Weinstein, Amelle Zair and Xiaodong Zhang

Contributing authors: Paul Aden, Massimo Altarelli, Frederico Alves Lima, Deepa Angal-Kalinin, Graham Appleby, Moataz Attallah, David Ayuso, Camila Bacellar, Artem Bakulin, Sneha Banerjee, Stuart Bartlett, James Baxter, Andrew Beale, Richard Bean, Colin Berry, Uwe Bergmann, Jens Biegert, Matthew Bird, Thomas Blackburn, Simon Bland, Rebecca Boll, Stefano Bonetti, Stewart Boogert, Archie Bott, Alice Bowen, Steven Boyes, Christian Bressler, Bill Brockelsby, Andrew Brown, Colin Brown, Philip Bucksbaum, Carlo Callegari, Richard Catlow, Giulio Cerullo, Roy Chantrell, Henry Chapman FRS, Adrien Chauvet, Vadim Cherezov, Majed Chergui, Jenny Clark, Jim Clarke, Aina Cohen, Simon Coles, John Collier, Andrew Cook, John Costello, Matthew Cotton, Tom Cowan, James Cryan, Basile Curchod, Frederick Currell, Richard Curry, Serena de Beer, Georgi Dakovski, Katerina Dörner, Paul Donaldson, Peter Dowding, Leora Dresselhaus-Marais, Brendan Dromey, Mike Dunne, David Dunning, John Dyke, Radoslav Enchev, Gwyndaf Evans, Olena Fedchenko, Robert Feidenhansl, Michael Först, Andrea Folli, Leszek Frasinski, Kelly Gaffney, Luigi Genovese, Simon Gerber, Gianluca Gregori, Mark Gilbert, Darren Graham, Ross Gray, James Green, Alice Green, Dave Grills, Markus Gühr, Ahmad Fahim Habib, Dave Hall, Samar Hasnain, Lauren Hatcher, Thomas Heinzl, Michael Hennig, Bernhard Hidding, Matthias Hoffmann, Simon Hooker, Robert House, Nils Huse, Olof Johansson, Philip Johnson, Steve Johnson, Gabriel Karras, David Keen, Philip King, Ben King, Přemysl Kolorenč, Soonam Kwon, Cristina Lazzeroni FRS, Peter Lee, David Leys, Ken Long, Jason Lynam, Stuart Mangles, Agostino Marinelli, Mattias Marklund, Mikael Martinez, Claudio Masciovecchio, Karim Massri, Steve Matthews, Martin McCoustra, David McGonegle, Paul McKenna, Brian McNeil, Stewart McWilliams, Christopher Milne, Keith Moffat, Henrike Müller-Werkmeister, Shaul Mukamel, Ben Murdin, James Naismith FRS, Eriko Nango, Colin Nave, Keith Nelson, Richard Neutze, Abbas Ourmazd, Robin Owen, Raj Pandya, Jason Parsons, Mitesh Patel, Foivos Perakis, Louis Piper, Colin Pulham, Patrick Rabe, Patrick Rauer, Dave Riley, Alex Robinson, Steven Robinson, John Rodenburg, Nina Rohringer, Kai Rossnagel, Marco Ruberti, Daniela Rupp, Christopher Russo, Danny Sahtoe, Alvaro Sanchez-Gonzalez, Charlotte Sanders, Subir Sarkar, Andreas Schaefer, Markus Scheck, Paul Scherkl, Christopher Schofield, Ralf Schützhold, Robbie Scott, Elizabeth Shotton, Alistair Siebert, Graham Smith, Peter Smowton, Edward Snedden, Edward Snell, Emma Springate, Claudiu Stan, Jergus Strucka, David Stuart FRS, Cristian Svetina, David Thompsett, Geoff Thornton, Kiyoshi Ueda, Patrick Vagovic, Joachim von Zanthier, Dave Walsh, Martin Walsh, Ryan Wang, Mark Warren, Dan Watts, Peter Weber, Philippe Wernet, Peter Williams, Thomas Wolf, Junko Yano, Mark Yeung, Briony Yorke and Linda Young

Acknowledgements: Thomas Feurer, Peter Knight FRS, Thomas Lane, Matt Lunt, Randy Read FRS and Ilme Schlichting

Foreword



It is my pleasure to introduce these reports examining the Conceptual Design, an Options Analysis, and The Scientific and Technology Case for a transformative Next-Generation XFEL (X-ray Free Electron Laser). The work undertaken to compile these reports is part of the contribution that the expert teams in STFC's research infrastructure, both nationally and through international partnerships, makes as a crucial component of UKRI's mission to advance knowledge, improve lives, and drive economic growth.

The UK is already a partner and shareholder in the European XFEL, with UK researchers currently being one of the largest XFEL users worldwide, so it is natural that we should rigorously evaluate the case for a Next-Generation XFEL. This process follows the 2016 strategic FEL review and the 2020 UK XFEL Science Case. The reports assess various options available, ranging from a new facility in the UK to expansion of an existing international facility to more reactive options.

Since the world's first XFEL began operation in 2009 at Stanford, these machines have rapidly proven to be a transformative new tool for science. Through time-resolved X-ray methods, spectroscopy, imaging and scattering, they offer a unique window into the structural and electronic dynamics of matter at the nanoscale, providing profound new insights into challenging questions from stellar interiors to protein dynamics and chemical reactions.

Recent advances in XFELs, in areas such as attosecond science, AI integration, dynamic structural biology, imaging techniques, chemical dynamics in batteries and catalysis, carry direct relevance to UK industrial priorities, from more efficient energy storage to the precision materials science underpinning defence and advanced manufacturing. These reports address how, over the coming decades, the technological and scientific opportunities enabled by XFELs will develop and what impact there might be from access to a Next-Generation XFEL.

I wish to express my gratitude to the project's International Advisory Committee, chaired by Massimo Altarelli, for their expert oversight and invaluable advice throughout the project, and for all the help of the international XFEL community. We are indebted to the UK XFEL Leadership Team, comprising John Collier (Project Sponsor), Paul Aden (Project Manager), Deepa Angal-Kalinin, Jim Clarke, David Dunning (Technical Lead), Jon Marangos (Science Lead) and Edward Snedden, along with experts from across the STFC, for steering the work on the Conceptual Design over a period of three years. The Science and Technology Case was authored by a science team of 40 experts, who refined the opportunities and technical requirements through exchanges with over 500 community members at events including Town Halls in Belfast, Glasgow, Plymouth, Manchester, Sheffield, London, Harwell and Cardiff. The Conceptual Design translated these requirements into a concept machine that is deliverable across a series of options for implementation at existing XFELs or as a new standalone facility.

Together, these documents deliver the evidence the UK needs to make clear, strategic decisions on the future of these innovative light sources.

Professor Michele Dougherty CBE FRS FRAS
Executive Chair, Science and Technology Facilities Council

Contents

Foreword - Professor Michele Dougherty, Executive Chair, STFC

1. Next-generation XFEL Science and Technology Case — Executive Summary

2. Introduction
2.1 Overview of the impact of XFELs on science
2.2 Recent high impact science with XFELs
2.3 Time and space resolved measurement with an XFEL
2.4 Survey of existing facilities and capabilities
2.5 Outlook for a next-generation XFEL
2.6 Overview of the Science and Technology Case
2.7 References for Chapter 2

3. Science Opportunities in Physics and X-ray Photonics
3.1 Frontiers in ultrafast chemical physics
3.2 New concepts in scattering
3.3 Attosecond science and non-linear X-ray spectroscopy
3.4 Capturing conformational dynamics and rare thermodynamic states
3.5 Non-linear X-ray physics and physics beyond the Standard Model with XFELs
3.6 High brightness relativistic electron beam science
3.7 References for Chapter 3

4. Science Opportunities for Matter in Extreme Conditions
4.1 Shocked materials and matter at extremes
4.2 Quantum plasmas: warm and hot dense matter
4.3 X-ray interactions with laser accelerated electrons
4.4 Coupling an XFEL to a laser-driven spherical compression facility
4.5 References for Chapter 4

5. Science Opportunities in Condensed Matter, Quantum and Nanomaterials
5.1 Magnetic materials and control of ultrafast magnetisation
5.2 Structural dynamics and light induced phases in quantum materials
5.3 Imaging dynamics in nanomaterials
5.4 Electronic dynamics in quantum materials
5.5 Time resolved pair distribution functions
5.6 Concluding remarks
5.7 References for Chapter 5

6. Science Opportunities in the Chemical Sciences and Energy

6.1 Fundamentals of reaction dynamics: Coupling between nuclear, electronic and spin degrees of freedom
6.2 Exploring complex energy landscapes through chemical activation
6.3 Pulse radiolysis and radiation damage mechanisms
6.4 Understanding catalysis
6.5 Chemistry and the environment: Aerosols, atmospheric, space chemistry, combustion, corrosion
6.6 Conclusions and vision: XFEL and chemical sciences
6.7 References for Chapter 6

7. Science Opportunities in the Life Sciences

7.1 Serial femtosecond crystallography enabled by XFELs and adopted by synchrotrons - a new era in structural biology
7.2 Dynamic structural biology: Photosensitive systems
7.3 Dynamic structural biology: Molecular movies of enzyme catalysis
7.4 Controlling and measuring nuclear and electronic coherence within biological systems
7.5 Capturing biological function in single molecules
7.6 Conclusion and summary
7.7 References for Chapter 7

8. Opportunities for Technology and Applications

8.1 Properties of shocked materials for engineering and defence
8.2 Multiphase-multicomponent formulated products
8.3 Dynamic processes in additive manufacturing, laser machining and photolithography
8.4 Applied and industrial catalysis
8.5 Industrial inspirations from deeper insights into biology: Pharma to clean energy
8.6 Energy materials and devices: Solar cells and batteries
8.7 References for Chapter 8

9. Next-generation XFEL Capabilities and Unique High Impact Opportunities

9.1 Next-generation XFEL capabilities
9.2 Facility general requirements to match scientific needs
9.3 Facility end-stations and their capabilities
9.4 High impact Flagship Science and Technology Programmes
9.5 References for Chapter 9

10. Alignment to National Priorities and International Engagement for a Next-generation XFEL
10.1 Addressing national strategic priorities in technology
10.2 Defence technology
10.3 Industrial engagement
10.4 Synergies with other national facilities and capability: Synergistic technology transfer among XFELs, neutrons, synchrotrons, and electron microscopy/diffraction
10.5 International engagement and partnerships
10.6 References for Chapter 9

Appendices

Appendix 1: Complementarity of Techniques
A1.1 Cryo-Electron Microscopy (cryo-EM), Tomography (cryo-ET), and Diffraction (cryo-ED)
A1.2 Next-generation synchrotron light sources
A1.3 Ultrafast electron diffraction
A1.4 Life Sciences Hub and roadmap
A1.5 References for Appendix 1

Appendix 2: Complementary Technologies
A2.1 Complementary pulsed X-ray technologies
A2.2 Plasma and laser wakefield acceleration
A2.3 High harmonic sources
A2.4 Energy Recovery Linac upgrade
A2.5 References for Appendix 2

Appendix 3: Community Engagement
A3.1 Townhall Events and Workshops
A3.2 Community engagement summary
A3.3 Other external engagements of UK XFEL team
A3.4 Science Team
A3.5 Contributors to the 2026 Science and Technology Case
A3.6 Engagements and surveys from the 2020 edition of the Science Case

Glossary

Units

> Whilst the aim of realising the next generation of XFELs is a truly international endeavour, towards which our many international collaborators are striving, UK access to such a facility is vital, and will help to underpin future national economic growth and industrial competitiveness.



1. Next-generation XFEL Science and Technology Case – Executive Summary

This report makes the science and technology case for UK access to a next-generation X-ray free electron laser facility. The new opportunities arising from access are very deep and wide ranging, with impact across all areas of science and technology. These opportunities include boosting the development of technologies for the green transition, fusion energy, advanced materials and advanced manufacturing, defence and biotechnology. At the same time, a next-generation XFEL facility will drive frontier science in extreme states of matter, ultrafast dynamical processes in molecules and condensed phase, and dynamical processes in biochemistry.

In this Science and Technology Case we address how access to a next-generation X-ray free electron laser (XFEL) facility would support national economic and industrial competitiveness, forming a vital part of a UK science infrastructure landscape that ensures a vibrant, high technology environment, and helping to build and retain cutting-edge skills in the UK workforce. This Science and Technology Case is making *the case for access* to a next-generation XFEL regardless of how that access is made available, such as by building a unique new facility in the UK supported by international partnerships or investing in upgrading the existing facilities at the European XFEL or SLAC. This Case builds on the 2020 UK XFEL Science Case and significantly updates it, by inclusion of the many breakthrough advances in science and technology made with XFELs since it was published. Moreover, by focusing on the benefits to research and innovation of UK access to a next-generation XFEL, it supports the broader mission of the project and should be considered in conjunction with the Conceptual Design and Options Analysis reports.

The last five years have been a hugely exciting period in the development of XFELs and in their science and technology impact. This period has seen the first advances driven by XFELs in the emerging area of attosecond science, the advent of powerful new non-linear X-ray techniques, breakthroughs in tracking chemical dynamics including applications to batteries and catalysis, and advances in understanding the behaviour of matter at extreme conditions. Further it has led to advances in dynamic imaging of bulk materials and in uncovering the mechanisms behind vital biological processes, such as vision and photosynthesis. **Section 2.2** contains recent examples of high impact science and technology achieved with XFELs to illustrate the power of these facilities.

Ultrafast X-rays from free electron lasers allow us to image the workings of matter at all relevant scales of both space and time. In common with neutron, synchrotron X-ray sources and electron microscopy, XFELs can establish the static structure of matter at the atomic scale. XFELs, however, are unique in that they can also allow us to follow the innumerable types of structural and electronic dynamics that are essential to understanding the workings of matter at the quantum scale, i.e. at their natural timescales of attoseconds to nanoseconds. They are therefore transformative in enabling the understanding and control of matter at the quantum *spatial and temporal* scales. Examples of big scientific questions that an advanced next-generation XFEL will be able to answer include:

- How do materials behave at the high pressures of planetary cores?
- How do enzyme-catalysed reactions occur in a living cell?
- How can we control states in quantum materials (e.g. superconductivity) with light?
- How do molecular machines efficiently cross energy barriers to drive biological processes?
- How do X-rays propagate in the interior of stars?
- How do liquids, like water, change and fluctuate at the nanoscopic scale?
- How are small inert molecules, especially CO_2 and N_2, activated in key catalytic processes?
- How can we optimally exploit quantum mechanics in solar and information technologies?

As well as underpinning a vast array of science, the capability and understanding delivered by a next-generation XFEL will also be critical in the advancement of emerging technologies with great potential importance to UK industry and sovereign capability, including:

- Developing fast, energy efficient, compact data storage
- Optimising novel quantum sensors and quantum elements for information processing
- Advancing light harvesting, carbon capture and utilisation of solar biofuel production, and energy storage technologies
- Imaging compression of fusion targets and radiation damage of materials of relevance to fusion energy technology
- Discovering advanced drugs, antibiotics and antivirals
- Advancing catalysis and facilitating sustainable chemistry using Earth-abundant elements
- Designing advanced materials for use in defence, industry and nuclear energy.

The new science and technology enabled by a next-generation XFEL will boost delivery of the **UK government's (2025) Industrial Strategy** including advances in the **IS-8 growth-driving sectors**. This would be through directly addressing key technology challenges for **Advanced Manufacturing**, **Clean Energy Industries**, **Digital and Technologies**, **Life Sciences** and **Defence**. Next-generation XFELs will be among the world's largest sources of high-value scientific **data**, with a highly synergistic relationship with **AI and machine learning** that is critical to harness for the UK. Just as the highly successful AlphaFold protein structure prediction tool relied on ~200,000 experimentally-determined protein structures, equivalent AI tools for predicting dynamics and mechanisms will require far larger datasets, which will be enabled by next-generation XFELs. Large numbers of highly trained scientists and engineers, whose skills will be honed working with the facility, will ultimately join the workforce thereby boosting all sectors including the **Creative Industries**, **Financial Services** and **Professional and Business Services**.

In addressing the Industrial Strategy, a next-generation XFEL will also address key topics integral to the UK's science and technology environment:

- **Advancing the frontiers of knowledge** through the ability to probe quantum processes in matter and understand the couplings and interactions that underpin, for example, chemistry, materials science and the life sciences, as well as through the potential to study matter at the extreme conditions found in the universe
- **Advancing technology** through the boost provided by space- and time-resolved understanding, leading to the development of new energy, data, quantum, nuclear and materials technologies
- **Furthering healthcare** by profound advances in the understanding of biochemical and biomolecular functions, facilitating better guidance in developing drugs and therapies
- **Underpinning net zero goals** by the space- and time-resolved data that is essential to developing sustainable approaches to catalysis, optimised combustion and carbon capture, and understanding the action of pollutants and particulates in the environment.

Together these capabilities will combine to boost **economic strengths** as well as provide vital sovereign capabilities for the defence and wellbeing of the nation. Moreover, the research enabled is critical to the missions of multiple **UKRI** research councils: **EPSRC** through impact in physics, chemistry, materials, advanced manufacturing, green energy, quantum technology, AI/Exascale computing and nuclear fission; **STFC** through impact in accelerator technology, astrophysics, dark matter searches and tests of the standard model and potential for new muon and kaon science facilities through access to the primary electron beam; **NERC** through enabling new research impacting atmospheric chemistry, geophysics, geochemistry and palaeontology; **BBSRC** through advancing biochemistry, structural biology and potentially brain imaging; **MRC** through impact upon tissue imaging, drug discovery and drug interactions at the molecular level; and **AHRC** through opening up new imaging capabilities for cultural heritage and archaeology. Other agencies will also be direct beneficiaries, including **UKAEA** through the ability to image the processes in nuclear fusion energy including compression of material and radiation damage mechanisms, and potentially **AWE/MOD** through advances in defence technology and matter at extreme conditions.

This Science and Technology Case explores these far-reaching science and technology opportunities and outlines the **key next-generation capabilities** required for their delivery. **Figure 1.1** shows the conceptual design for a next-generation XFEL that would deliver these capabilities and ensure a high throughput facility that will be world-leading and able to tackle some of the most challenging research problems for industry, defence and medicine.

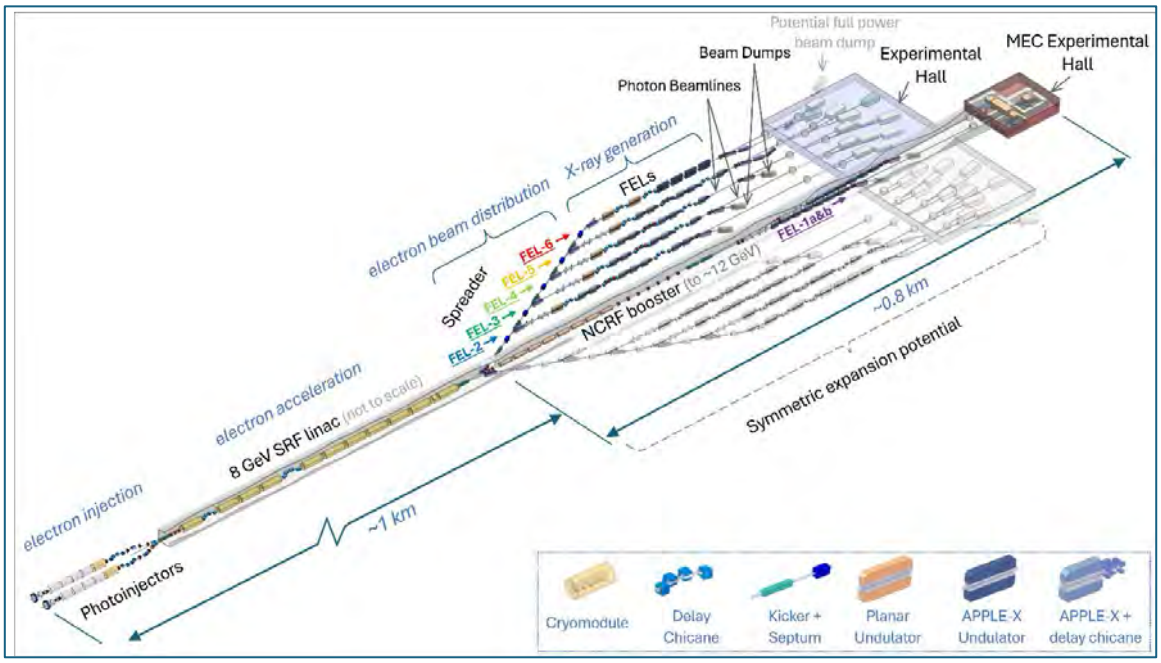


Figure 1.1: An outline of the conceptual design for a next-generation XFEL that would provide a unique combination of capabilities, able to deliver the opportunities discussed in this Case

In recognition of the growing importance of XFELs to current and future science and technology, leading industrial nations across the globe have established their own XFEL capability, with systems now in operation or under construction in the USA, Germany, Italy, Switzerland, Japan, Korea and China. XFELs are recognised as indispensable to the development of new technologies where the quantum scale structural dynamics of matter must be understood and exploited. A primary driver for the Linac Coherent Light Source (LCLS) II in the USA was its fundamental contribution to the Department of Energy's mission, most critically in Basic Energy Sciences. Similarly, the other international XFELs are seen as making essential contributions to science and to future economic and national strength.

With the Diamond-II upgrade now being prepared, the UK will maintain a strong presence in that technology and its application to increase understanding of the static structure of matter. What the UK must now secure is the next generation of light source technology and the capability to perform the most advanced time-resolved science for which we will need extensive access to the very best next-generation XFEL facilities. **The UK has the opportunity to play a leading role in next-generation XFELs** and thus reinforce its place as a leading scientific and industrial power. Failure to do so could see strategic competitors grasping these opportunities ahead of us and reaping the benefits by outpacing our technology and science.

A survey of research groups in the UK in 2019 indicated that over 500 UK scientists had had active involvement in XFEL science in the previous decade. This number has grown rapidly over the last few years, with UK researchers now amongst the major users at the European XFEL and LCLS (see use survey figures in Chapter 10). A huge advantage can be gained through a next-generation XFEL facility that massively boosts access opportunities and is optimised with the most advanced features matched to future needs, ensuring widened access to the new capabilities of direct benefit to the UK economy. The conceptual design (**Figure 1.1**) would enable parallel operation of more than 10 scientific end-stations and rapid switching between experiments, increasing the amount of research access more than ten-fold compared to existing facilities and revolutionising direct commercial access.

Ease of accessibility for individual users, and for new user communities, is a critically important issue if a facility is to deliver the fullest range of the potential science and technology. In part, this can be addressed by designing appropriate technical configurations of instruments, end stations and data systems into a facility from the outset. For example, in scientific areas that are currently at an advanced level of technical maturity, such as serial nano-crystallography, it will be possible to conduct experiments solely via user-supplied samples, without on-site users, thereby significantly boosting throughput and lowering the threshold to access. Improved training and support for new users will also lower barriers to access, by developing, and widely propagating, the required expertise needed to use a facility effectively: we recommend that work on this should continue, building on the actions already undertaken by the Life and Physical Sciences Hubs at Harwell that currently support UK access. Related actions, such as establishing dedicated Centres for Doctoral Training across a variety of science areas, should be undertaken with urgency. These measures are important to ensure readiness for a next-generation XFEL facility, but equally will allow UK science to continue to compete successfully for access to the existing international XFELs.

The transformative capabilities brought about by a next-generation XFEL are in real-time imaging and measurement at the quantum scale, which will underpin many future technological and scientific advances and developments in human health (**Figure 1.2**). No single technology will, however, solve all scientific problems. The solution to the challenges we face now, and to those we will face in the future, will inevitably require a combination of technologies. An XFEL should be seen as an essential component of a wide-suite of capabilities that includes, for example, lasers, spectroscopy, mass spectrometry, cryo-EM, synchrotron X-rays, ultrafast electron diffraction and neutrons. These synergies are further discussed in this Case and its appendices.

The UK currently benefits from membership of the European XFEL in Hamburg. We must continue as a full member of this organisation, as this facility will remain one of the world's premier XFELs. A next-generation XFEL would deliver new capability beyond that at any existing facility and would remain complementary to the European XFEL or may even be incorporated within that facility. **Secured access to the best XFEL facilities for UK researchers** is vital for ensuring, in the longer term, **technologically** and **industrially critical capabilities**. It signals the UK commitment to research and innovation.

In this Case we discuss **the science and technology that will be enabled by access to a next-generation XFEL** and **specify the new capabilities** such a facility must have to maximise the research and innovation impact.

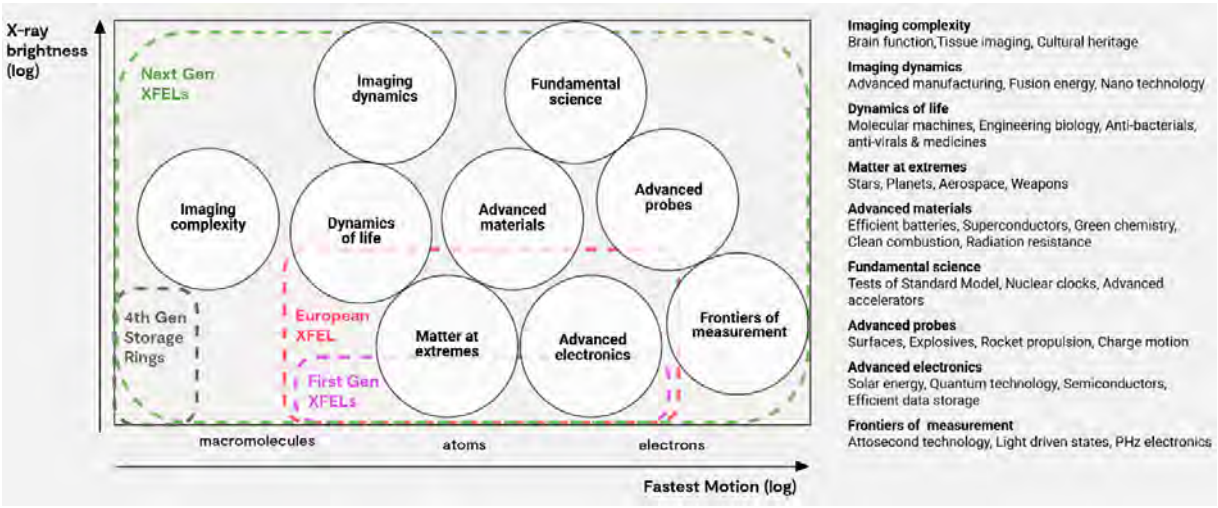


Figure 1.2: The high X-ray average brightness coupled to extreme time resolution of a next-generation XFEL enable new classes of measurement that will drive discovery in science and technology

2. Introduction

X-ray pulses emitted by X-ray free electron lasers (XFELs) are a billion times brighter and more than ten-thousand times shorter than pulses from any other X-ray sources. This makes time-resolved X-ray measurements possible, to access the quantum scales of space and time in matter. The impact of this new capability on science and technology through the 21st century promises to be as large as the applications of lasers and synchrotrons were in the 20th century.

This chapter begins with an introduction to the light source that underlies this Science and Technology Case, starting with a primer on XFEL sources, followed by a broad-brush preview of the scientific opportunities. The dominant science driver for XFELs is access to the dynamical processes in matter on the quantum length and time scales that are relevant to chemistry, biology, materials and quantum technology. XFELs are strongly positioned to support the materials, manufacturing, biomedical and data technologies vital to advancing the UK's Modern Industrial Strategy 2025.

In the 17 years since they became available, XFELs have made a very substantial scientific impact. Unlike some large-scale research infrastructures (e.g. particle colliders) that are primarily designed to address research in a single discipline, XFELs have impact across a wide swathe of science and technology. Consequently, it is not easy to provide an answer to the simple single question, “What will be the major scientific outcome of a next-generation XFEL?” Instead, we need to look across this breadth of research and frame the query more as, “What are the multiple major research outcomes that a next-generation XFEL will deliver across science and technology?” In this chapter, we look at a selection of recent high-profile papers that illustrate the breadth and depth of the scientific outcomes made possible by XFELs. These examples are explained as simply as possible, to enable them to be understood by people without specialist technical knowledge of the respective fields. For each example we try to map out why the result of the research was significant and where it may lead in the future. Greater detail of the science and technology opportunities created is given in the rest of this case.

Later in this chapter, we introduce the powerful time-resolved methods – X-ray spectroscopy, imaging and scattering – that are enabled by an XFEL. This is intended as a primer for the non-specialist: more complete accounts are included in **Chapters 3 to 8**. By way of establishing an international context for this project, we present a brief survey of existing XFELs that are already being extensively used by UK researchers, and the capabilities on offer. It is against this array of facilities that we can best understand the overwhelming case for a next-generation facility that can go far beyond what any of these can currently achieve, and for securing access to that facility for UK researchers.

Finally within this chapter, we discuss the array of new capabilities that should be provided by an ambitious next-generation XFEL, and which would lead to ground-breaking scientific and technological opportunities. As a new facility, a next-generation XFEL would be superbly positioned to implement recent and emerging advances in X-ray modes, expanding the scientific reach made possible and delivering still more transformative science and technology.

2.1 Overview of the impact of XFELs on science

XFELs have led to transformative developments in light source science over the last decade and a half. Numerous scientific applications have already been achieved, and original methods and approaches are being developed in many areas where future impact will be made. The discoveries enabled by XFELs continue to expand and new ideas are being explored, but, after only 17 years, the impact is already well demonstrated.

The mechanism of X-ray free electron laser radiation has its origins in the formation of self-modulation of a relativistic electron beam as it radiates in an undulator (**Figure 2.1**). In an XFEL, high quality relativistic (3 – 15 GeV) electron bunches of low emittance are required, necessitating the use of large-scale, high-performance linear electron accelerators. On entering the alternating polarity magnetic field structure of the undulator, the electrons begin to radiate and, critically, there is a back reaction of the radiation upon the electrons in the bunch. Passage through a sufficient length of undulators leads to a regular structuring of the electron density in the bunch, the consequence of which is coherent, high brightness X-ray radiation. This process, termed Self-Amplified Spontaneous Emission[1,2] (SASE), is the dominant principle of operation of free electron lasers in the X-ray region.

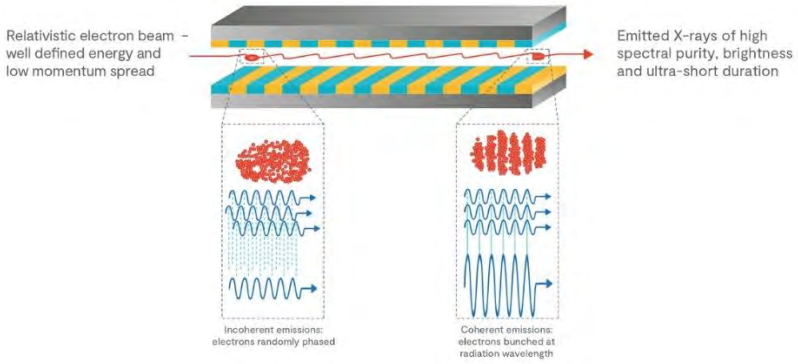


Figure 2.1: Principle of operation of a SASE X-ray free electron laser
Reprinted by permission from Springer Nature: B.W.J. McNeil and N.R. Thompson Nat. Phot. 4, 814-821 (2010). https://doi.org/10.1038/nphoton.2010.239 Copyright (2010)

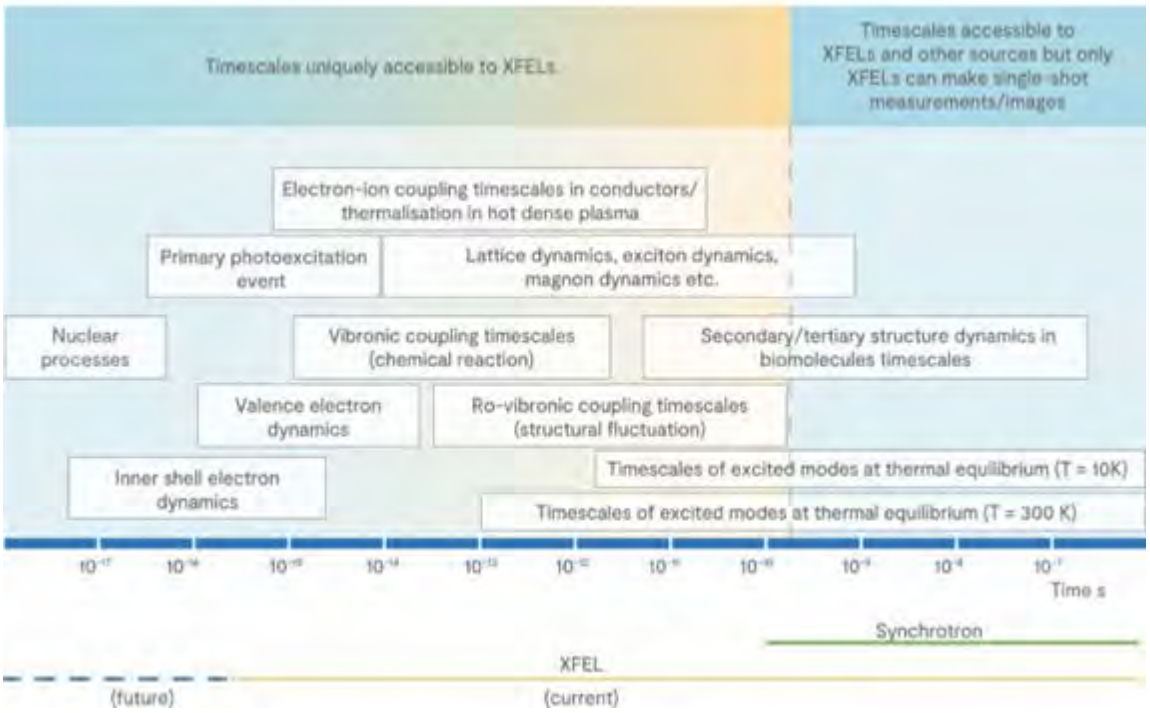
Lasing in the vacuum ultra-violet range via this method was achieved at the Deutsches Elektronen-Synchrotron (DESY) in Hamburg, and this machine began operating as the FLASH user facility from 2005, with more recent extension into the soft X-ray (SXR) range.[3] The Linac Coherent Light Source (LCLS) at the SLAC National Accelerator Laboratory in California first lased in the X-ray range in April 2009,[4] heralding a new dawn in X-ray science. Since then, there have been numerous demonstrations of important new science (as discussed later in this Science and Technology Case) and a number of new X-ray facilities have begun operation around the world. Other concepts are now being explored to extend the capabilities of X-ray lasers, including the first demonstration of oscillator-based lasing, as originally envisioned by John Madey[5] (the inventor of the FEL concept). Laser preconditioning of the electron bunch (seeding) before it enters the undulator has proved effective at greatly improving the coherence properties and stability of the output, with this approach successfully demonstrated in the soft X-ray range at the FERMI facility[6] in Italy. Lasing on a very short, single SASE spike, leading to near transform limited operation, was developed through manipulation of the phase space of the incoming electron bunch, with the first demonstration of attosecond time domain isolated pulses[7] at LCLS in 2018. New facilities are increasing repetition rates up to ~1 MHz using superconducting acceleration technology, compared to ~100 Hz in the first-generation machines.

With the capabilities of these light sources developing so rapidly, we are heading into the next generation of XFELs, with far greater control of the X-ray pulses and application to a still wider range of scientific challenges. Next-generation XFELs will be some of the biggest sources of high-value data in the world, and they will have a highly synergistic relationship with AI. It is these opportunities that this XFEL project is evaluating, to enable UK researchers to access these advanced capabilities.

The properties of light from free electron lasers are dramatically different from those of storage rings and conventional lasers. Storage ring synchrotron radiation has enormous spectral coverage and can deliver a high photon fluence (photons per second) up to hard X-rays (10s of keV), which has allowed these sources to be the dominant tool for crystallography, X-ray spectroscopy and many other areas of X-ray science for the last four decades. These sources do, however, have low peak brightness, especially if a narrow spectral bandwidth or a short pulse is selected. With advanced pulse slicing, they can provide sub-picosecond temporal resolution, but only with a tiny flux, which severely limits the utility for measuring rapid changes. Conventional lasers have advanced hugely in recent years and can produce extremely short pulses (~5 fs) at very high brightness, but these capabilities are limited to a restricted spectral range (0.5 – 5 eV). With high harmonic generation (HHG) the accessible range can be extended, but the low inherent conversion efficiency (< 10^{-6} in the extreme ultraviolet (XUV) and < 10^{-8} in the SXR) is a severe restriction to fully exploiting incisive X-ray techniques, like X-ray spectroscopy at atomic edges, and atomic position resolution by X-ray diffraction.

XFELs are having a revolutionary impact on the science we do with light, potentially as far-reaching in impact as that created by the laser and synchrotron radiation in earlier decades. XFELs deliver coherent radiation across an exceptional spectral range (< 10 eV to > 20 keV), with narrow bandwidth (~0.1% of photon energy) and very energetic (millijoule/10^{12} photons per pulse) short pulses (~1 fs duration), and therefore with exceptional brightness. A FEL undulator produces this very bright pulse at the fundamental frequency, but also bright pulses at three- and five-times that frequency (the harmonics), with the photon number dropping by a factor of around 100 at each harmonic step. This is a vastly wider spectral range than that covered by conventional lasers, and the pulses are typically a hundred thousand times shorter and millions of times brighter than those that a storage ring can provide. Next-generation XFELs will also deliver an average photon fluence 1000 higher than 4th generation synchrotrons.

Box 2.1: XFELs provide unique access to the structure and dynamics of matter at the quantum scale: nanometre spatial and ultrafast temporal scales



Ultrafast X-rays from free electron lasers allow us to image the workings of matter at all relevant scales of both space and time. XFELs, in common with neutron, synchrotron X-ray sources and electron microscopy, can establish the static structure of matter at the atomic scale. XFELs, however, are unique in that they also allow us to follow, at their natural attosecond – nanosecond timescales, the myriad structural dynamics that are essential to understanding the workings of matter at the quantum scale. They are transformative in enabling the understanding and control of matter at the quantum spatial and temporal scales.

The main science driver for X-ray FELs is the need to uncover the structural dynamics of matter at the quantum scale (see **Box 2.1**). XFELs provide access to the atomic (ångstrom) spatial and few-to-sub-femtosecond temporal scales of matter. This is achieved by way of time-resolved X-ray scattering and X-ray spectroscopy (**Section 2.3**), which together enable determination of the instantaneous geometric structure and electronic-state characteristics. Incisive time-resolved probing allows measurement of dynamical processes and the coupling between different components of a quantum system, including that between electronic excitations, and vibrational and rotational dynamics in molecules and macromolecules, as well as collective modes, such as phonons, excitons, polaritons and magnons, in condensed-phase systems. The practical importance of understanding these couplings and quantum dynamics is clear; for example, much sustainable technology is energised by the absorption of light from the Sun, and efficient and cost-effective devices and processes require a quantum-level understanding of the chain of events that follow the initial electronic photoexcitation.

In the years since their first operation, numerous XFEL applications have been demonstrated. It is impossible to detail all of this work, but a representative sample is covered within this Science and Technology Case. **Section 2.2** features a few recent examples of significant results that serve to illustrate the impact of XFELs across multiple scientific disciplines: these topics are discussed further in **Chapters 3 to 8.** Although these achievements are already impressive, it should be kept in mind the short time in which XFEL light sources have been available. Much development has taken place and much more must be anticipated as the newer and upgraded facilities start to operate.

There remains enormous, as yet untapped, scientific and technological potential for these light sources. A next-generation XFEL with increased control over the X-ray output, a large data acquisition rate, multiplex operation of multiple experiments simultaneously and the most innovative accompanying capabilities at the interaction point (e.g. lasers, THz, electron and ion beams) will be transformative in tapping this full potential. An advanced next-generation XFEL will be able to answer key questions in physical science around, for example, the behaviour of materials at extreme pressures, the propagation of X-rays in stellar interiors, the control of superconductivity in quantum materials, the nanoscopic fluctuations in liquids and solute-solvent interaction, and the behaviour of matter and energy at the atomic spatial and length scale. In the life sciences, it will address questions such as how molecular machines efficiently cross energy barriers to drive biological processes and how enzyme-catalysed reactions occur in living cells. Knowledge gained will help to drive progress in many areas, including advanced manufacturing, inertial confinement fusion, solar technologies, batteries, drug development and catalysis.

In the sections that follow, these topics and many others are considered in greater detail and emerging opportunities across a wide range of science are highlighted and discussed.

2.2 Recent high impact science with XFELs

We have reviewed recent high impact science and technology achieved with XFELs, and summarise selected examples that show the power of these facilities. XFELs have delivered substantial scientific advances and discoveries across many fields of science – from physics to chemistry, laboratory geophysics and astrophysics to the life sciences – and towards industrial application. While these examples only cover a tiny portion of the advances already being made by XFELs in science and technology, they do provide a useful primer for those curious to find out more.

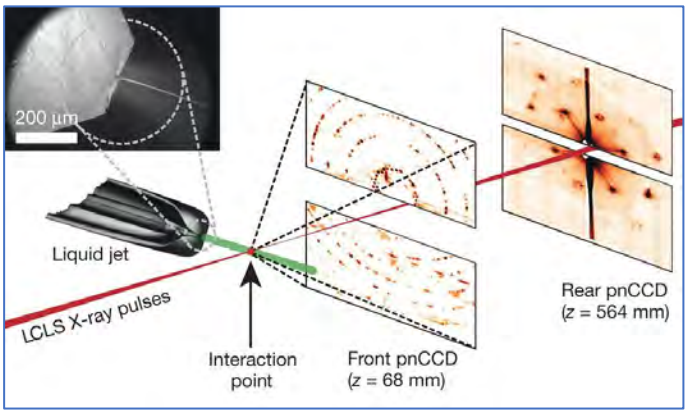
The opportunities afforded by XFELs in time-resolved studies have already advanced research in the **chemical and physical sciences**. Recent liquid and gas phase chemistry studies have improved our understanding of chemical dynamics of relevance to catalysis,[8,9] where X-ray emission spectroscopy has proved a decisive method in resolving research questions. Combining X-ray diffraction and X-ray emission from molecules of interest in biochemistry is also proving very promising, with work by Kern *et al.*[10] leading to new insights on the photosystem II complex photocycle. Much opportunity has also been enabled in physics, where pump-probe methods have allowed the interrogation and study of dynamics in states only transiently accessible, such as high pressure shocks, hot dense matter, matter dressed by lasers and matter in extreme electric and magnetic fields. Noted examples for matter at extreme conditions include probing shock compression of materials[11] and probing laser generated dense matter.[12] Optical and terahertz (THz) field dressing of quantum materials probed by XFEL pulses is leading to the understanding of hidden phases of significance to high T_c superconductivity and other functional properties.[13,14] Further opportunities in time-resolved X-ray emission spectroscopy (XES) and X-ray photoelectron spectroscopy (XPS) for chemical dynamics, and resonant inelastic X-ray scattering (RIXS) for materials science, will be enabled by the far higher sensitivity offered by the high repetition rate XFELs that are now becoming operational.

In the **life sciences**, an important early scientific breakthrough with FLASH, the XUV FEL at DESY, Hamburg, was the coherent diffractive single shot imaging of biological and non-biological structures led by Hajdu and Chapman.[15] These same ideas have since been implemented at LCLS, and promising results are emerging on imaging non-periodic, non-reproducible structures and nanocrystals utilising the single shot coherent diffraction imaging (CDI) methodology. In the future, there is potential for such a technique to provide nanoscopic imaging of biological assemblies and molecular machines within the necessary time resolution and operating conditions (i.e. living cell temperatures). It has, however, been in the sphere of serial femtosecond nano-crystallography (SFX) that XFELs have had the largest impact, so far, in the life sciences. SFX is opening up the study of otherwise inaccessible proteins, such as membrane proteins that frequently cannot be made to form macroscopic crystals, and is also allowing structures to be studied free of radiation damage and potential cryo-artefacts. Selected examples include investigations of light harvesting in photosystem II,[16] and studies of the protein that is a critical agent in sleeping sickness[17] and of the machinery of neuronal molecular transport.[18] Moreover, XFELs bring the unique possibility of studying the structural dynamics of light-activated proteins, something that has not been possible before. Pande *et al.*[19] resolved the structural dynamics occurring in the photo-excited cis/trans isomerisation induced in the photo-active yellow protein. One ground-breaking study has also shown the possibility of using the snap-shot imaging capability of an XFEL to study rare, but functionally critical, conformational changes in a virus.[20]

The following sub-sections attempt to capture a flavour of the broad but profound impact that XFELs are having on scientific research. We present selected examples of publications across a range of research disciplines including key papers on advances in methods, applications, physics and X-ray photonics, matter at extreme conditions, condensed matter, chemical sciences and the life sciences. The criteria for selection was not rigorous, and was based largely on the preferences of our Science Team; doubtless an entirely different set of 21 papers could have been presented that are just as significant, which further illustrates the wealth of research advances now being driven by XFELs.

2.2.1 Advances in methods

"Femtosecond X-ray protein nanocrystallography" published in Nature, February 2011,[21] used extremely short X-ray laser pulses from LCLS, each lasting less than 100 femtoseconds (100 x 10^{-15} s), to take rapid diffraction "snapshots" of millions of tiny protein crystals in a flowing stream, before the intense X-rays could damage them. They demonstrated this by studying Photosystem I, a complex membrane protein involved in photosynthesis, using nanocrystals far too small for traditional X-ray methods . By combining over three million individual diffraction patterns, they reconstructed a detailed three-dimensional structure without growing large crystals. This "*diffraction before destruction*" technique works because the X-ray pulse records data before any damage occurs, effectively outrunning the damage problem that has limited protein imaging in the past. Their breakthrough opened a new way called Serial Femtosecond Crystallography (SFX) to study important, fragile proteins, like those found in cell membranes, at high resolution under realistic, hydrated conditions.



Reprinted with permission from Springer Nature from H.N. Chapman et al. Nature 470, 73 (2011). DOI: 10.1038/nature09750

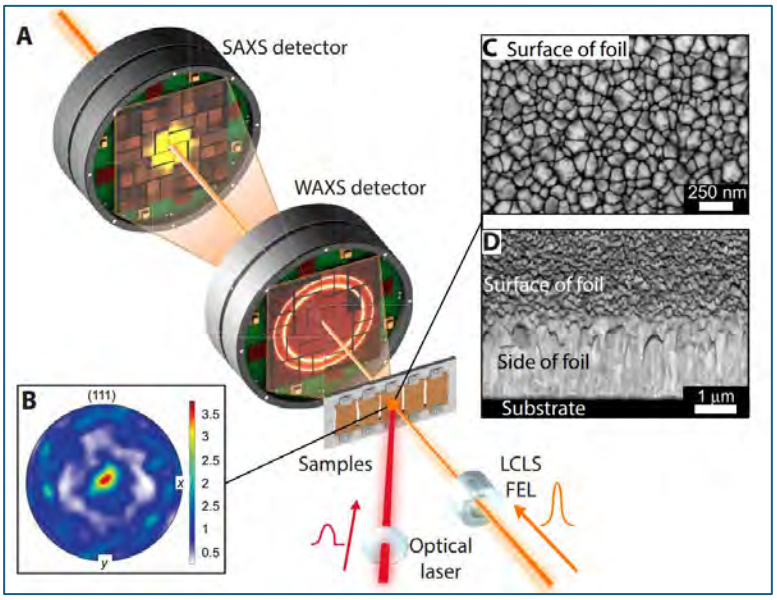
"Tunable isolated attosecond X-ray pulses with gigawatt peak power from a free-electron laser" published in Nature Photonics, January 2020,[7] was the first demonstration of XFEL-generated pulses lasting less than 400 attoseconds (400 x 10^{-18} s) with gigawatt-scale peak power in the soft X-ray range. These pulses are "tunable," meaning that their colour (photon energy) can be adjusted to match specific atomic resonances in matter. They used a method called ESASE (Enhanced Self-Amplified Spontaneous Emission) to compress an electron bunch into a brief spike, which then emitted the intense single X-ray burst. The team confirmed that these pulses lasted only a few hundred attoseconds and had enough energy – tens to hundreds of gigawatts – to potentially do advanced experiments like non-linear X-ray spectroscopy or single-shot imaging of individual particles. This breakthrough has opened the door to watching electrons move on their natural timescale and studying matter with unprecedented speed and clarity (see below) .

In **"Attosecond pulse shaping using a seeded free-electron laser" published in Nature, February 2020**,[22] researchers at the FERMI FEL demonstrated the generation of reproducible attosecond X-ray pulse trains using a seeded FEL. This approach allows precise manipulation of both the amplitude and phase of the attosecond pulse train. By employing a novel technique for temporal reconstruction, the team achieved high-energy (microjoule-level) attosecond waveforms with consistent characteristics. This innovation paves the way for detailed studies of ultrafast electron dynamics in atoms and small molecules, enabling time-resolved experiments that were previously unattainable. The successful shaping of attosecond pulses using a seeded FEL marks a significant milestone in the field. Taken along with the work at LCLS (above), these methods are opening new avenues for exploring the fundamental processes of matter on their natural timescales, and go beyond the achievements recognised in the Nobel Prize in Physics 2023 for the development of attosecond physics and technology.

2.2.2 Advances towards industrial applications

"Femtosecond quantification of void evolution during rapid material failure" published in Science Advances, December 2020,[23] reports the use of X-ray scattering from the LCLS XFEL to capture how

tiny voids (empty spaces) form and grow inside materials as they break under extreme stress. This process happens on a picosecond timescale, so the team used femtosecond imaging to observe it in real time. Understanding this rapid failure will help researchers to predict when and how materials will break, especially in high-speed impacts like car crashes or explosions. These insights could lead to stronger, safer materials for use in aerospace, defence, and construction. Ultimately, this research may help design materials that resist breaking under sudden, intense forces.



Reprinted from J. Coakley et al., Sci. Adv. 6: eabb4434 (2020) under the terms of a Creative Commons Attribution License 4.0 (CC BY). DOI: 10.1126/sciadv.abb4434

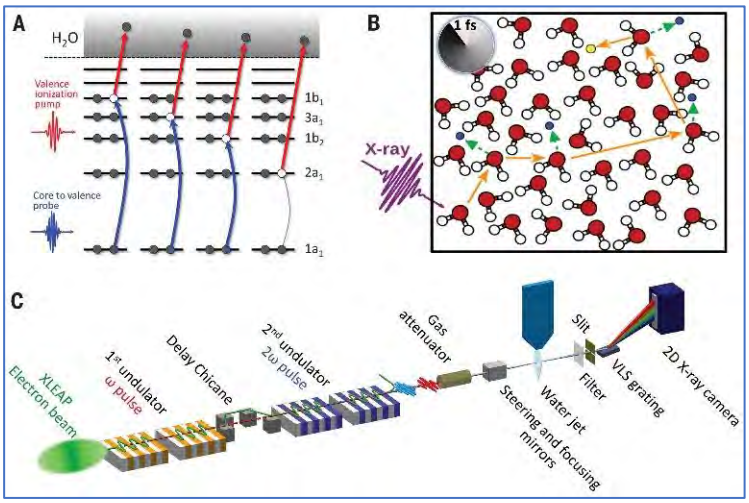
"Direct observation of charge separation in an organic light harvesting system by femtosecond time-resolved XPS" published in Nature Communications, February 2021,[24] used femtosecond time-resolved X-ray photoelectron spectroscopy (XPS) at the FLASH soft X-ray FEL in Hamburg to watch how electric charges separate in an organic material that captures light. This charge separation is a key step in turning sunlight into electricity, essential in photovoltaic devices (solar panels). By directly observing this process for the first time with X-rays, scientists gained deeper insight into how energy moves through these materials. This knowledge could help improve the efficiency of organic solar cells, which are lightweight, flexible and potentially cheaper than traditional ones. Ultimately, the findings could lead to better renewable energy technologies for everyday use.

"Real-time imaging of acoustic waves in bulk materials with X-ray microscopy" published in PNAS, September 2023,[25] used advanced X-ray microscopy to watch sound waves (phonons) travel through solid materials in real time. These waves move very fast and are usually hard to see, but the researchers captured them with high precision using powerful X-rays from LCLS. Understanding how sound waves move through materials can reveal hidden damage or weaknesses deep inside. This technique could be used to improve structures, for example, earthquake-resistant buildings, safer airplanes or stronger electronic devices. In the future, it may advance geoscience and help engineers design materials that are more durable and reliable under stress.

2.2.3 Advances in physics and X-ray photonics

"Attosecond-pump attosecond-probe X-ray spectroscopy of liquid water" published in Science, February 2024,[26] used the attosecond X-ray method at LCLS to probe the very fastest dynamics of ionised water. The X-rays with a pulse duration of ~300 attoseconds act like a super-fast camera to watch how electrons in liquid water react. In this measurement, they sent two of these X-ray bursts through water, one to kick out an electron and the second, almost immediately after, to check what happened next. Because the second burst arrives so quickly (within a few hundred attoseconds), the atoms themselves do not have time to move, effectively freezing the motion of the water molecule. They discovered that a previously unexplained feature in a specific X-ray spectral signal, seen in earlier longer timescale measurements, was caused by water molecules moving on femtosecond timescales

that were eliminated in the current attosecond measurement. This powerful snapshot settled that longstanding puzzle and demonstrated how attosecond X-ray spectroscopy can reveal how electrons behave in liquids.



Reprinted with permission from AAAS from S. Li et al. Science 383, Issue 6687 1118-1122 (2024) DOI: 10.1126/science.adn6059

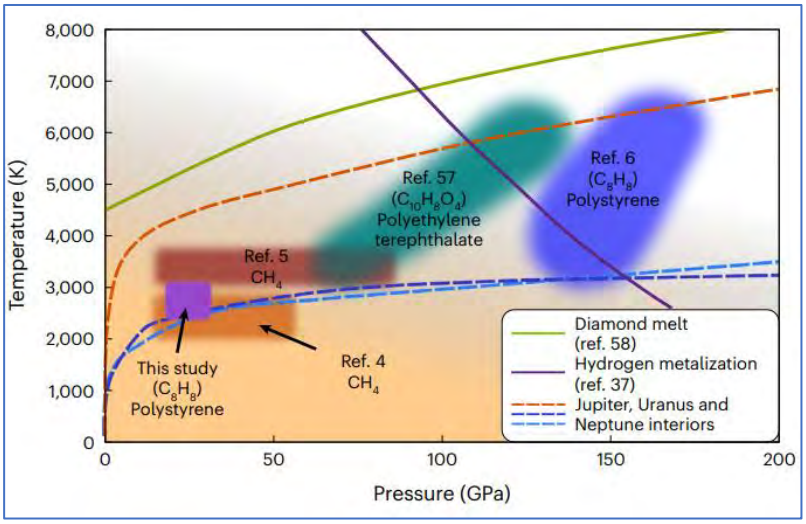
"Resonant X-ray excitation of the nuclear clock isomer 45Sc" published in Nature, September 2023,[27] used narrow bandwidth capabilities at the European XFEL to excite a special state within the nucleus of the element scandium. This was a breakthrough step towards building a "nuclear clock" that could outperform today's best atomic clocks by a huge margin. They fired 12.4 keV X-rays from the XFEL at scandium metal, which caused a tiny fraction of the nuclei to jump into an excited isomeric state that lasted about half a second. By detecting the specific radiation released as the excited nuclei returned to their ground state, the team confirmed the excitation and identified the exact energy of the nuclear transition with two orders of magnitude greater precision than before. Oscillations based on nuclear transitions are much less disturbed by outside forces than the electronic oscillations used in conventional atomic clocks. With this experimental success, researchers are now one step closer to developing a new generation of clocks that could keep time so accurately they might only drift by a second every 300 billion years, and so could ultimately advance fundamental tests of physics and global positioning technology.

"Attosecond coherent electron motion in Auger-Meitner decay" published in Science, January 2022,[28] used X-ray pulses of a few hundred attoseconds to study a rapid electronic process called Auger–Meitner decay, which occurs when matter is excited by energetic photons. The attosecond X-ray pulse knocks out a deeply bound electron, creating an unstable "core hole" state in a molecule. The molecule then loses energy by ejecting another electron (the Auger–Meitner electron), and the researchers used a second, circularly polarised infrared laser as an "attoclock" to time precisely when that ejection happened. They discovered extra, oscillating "quantum beats" in the time profile of the emitted electrons, showing that the electrons were not just decaying randomly, but were moving together in a coherent, wave-like way before escaping. This is the first time scientists have watched the detailed, ultrafast choreography of electrons in the core excited states of matter in real time, opening up new possibilities for understanding fast electron behaviour inside matter.

2.2.4 Advances in matter at extreme conditions

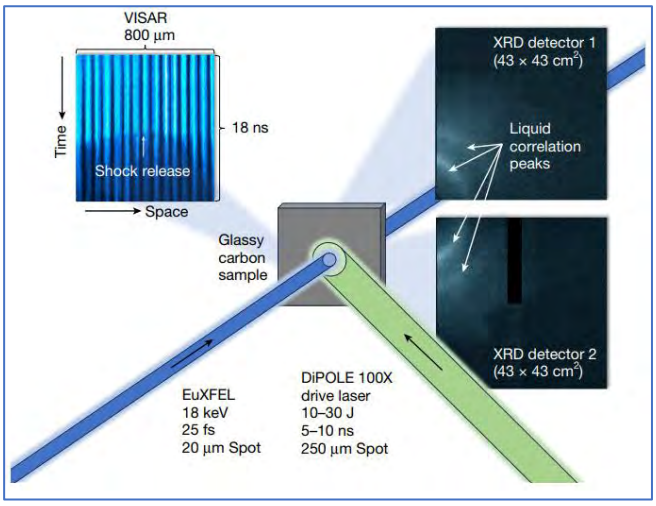
In **"Diamond precipitation dynamics from hydrocarbons at icy planet interior conditions" published in Nature Astronomy, January 2024**,[29] a thin film of polystyrene was squeezed between diamond anvils and exposed to ultra-fast X-ray pulses from the European XFEL, duplicating the pressures (190,000 – 270,000 times atmospheric pressure) and temperatures (>2,500°C) that exist a few thousand kilometres inside Neptune and Uranus. Within 30 – 40 microseconds they directly observed carbon atoms separating from hydrogen and crystallising into diamond. This leads to the phenomena of "diamond rain" thought to occur in giant planets. The study showed that it can begin sooner and at much lower pressures than earlier nanosecond shock-wave experiments had suggested. This work

resolved a decade-long experimental discrepancy and reset the boundary conditions for carbon-hydrogen demixing in planetary interiors. Because newly forged diamonds are heavier than the surrounding ice, they would sink, releasing gravitational energy and stirring conductive fluid layers; the team argues that this extra heat and convection help explain the unusual magnetic fields of Neptune and Uranus, and suggests that the same process could operate in the abundant class of exoplanets dubbed "mini-Neptunes," where it would begin at even shallower depths than previously assumed. The refined pressure-temperature map for diamond formation will now feed directly into interior-structure, heat-flow and dynamo simulations, improving our understanding of how icy giant planets and their extrasolar cousins evolve over time.



Reprinted with permission from Springer Nature from M. Frost et al. Nature Astronomy 8, 174-181 (2024) DOI: 10.1038/s41550-023-02147-x

"The structure of liquid carbon elucidated by in situ X-ray diffraction" published in Nature, May 2025,[30] achieved the first direct experimental measurement of liquid carbon's atomic structure under extreme conditions. Utilising the DiPOLE100 high-energy laser, supplied by the Central Laser Facility, in conjunction with the European XFEL's ultrafast X-ray pulses, the team transiently liquefied carbon at pressures exceeding one million atmospheres and temperatures around 7,000 K. This enabled the capture of time-resolved diffraction patterns, revealing a complex liquid structure characterised by transient bonding of carbon atoms to an average number of four neighbours – akin to the tetrahedral arrangement in diamond. The study precisely delineated how carbon melts under such extreme conditions, resolving longstanding discrepancies in theoretical predictions. This advance holds significant implications for understanding carbon-rich planetary interiors, the development of carbon-based materials and inertial confinement fusion technologies. The successful integration of high-powered laser compression with ultrafast X-ray diffraction not only overcomes previous experimental limitations, but also establishes a versatile methodology for probing the structures of other light-element liquids under extreme conditions.



Reprinted from D. Kraus et al. Nature 642, 351-355 (2025) under the terms of a Creative Commons Attribution License 4.0 (CC BY). DOI: 10.1038/s41586-025-09035-6

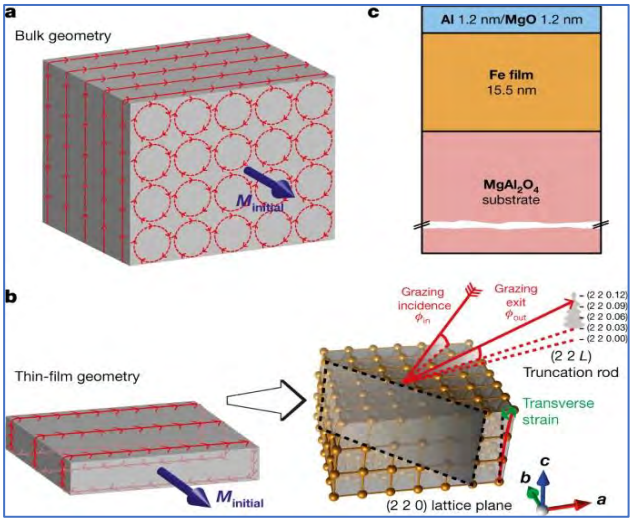
"Superheating gold beyond the predicted entropy catastrophe threshold" published in Nature, July 2025,[31] reports a new method developed to measure temperatures in warm dense matter using inelastic X-ray scattering at the LCLS. This warm dense matter regime is notoriously difficult to probe, as standard diagnostic techniques often fail or require complex modelling. The strength of this approach lies in its directness – it measures the ion velocity distribution from the inelastic scattering signal, without relying on detailed solid-state or plasma models for interpretation. The team applied the technique to gold samples rapidly heated with a 50 fs optical laser and found that the material remained crystalline even at temperatures up to 19,000 K – about 14-times the melt temperature of gold. This far exceeds the theoretical limit for superheating predicted in the 1980s based on thermodynamics considerations. The method provides a robust new diagnostic tool for probing temperature in systems such as inertial fusion targets, where warm dense matter conditions emerge and accurate temperature measurements remain a critical challenge.

2.2.5 Advances in condensed matter, quantum and nanotechnology

"Nonlinear lattice dynamics as a basis for enhanced superconductivity in $YBa_2Cu_3O_{6.5}$" published in Nature, December 2014,[14] used ultrafast laser pulses to strongly excite specific vibrations in the crystal structure of a material called $YBa_2Cu_3O_{6.5}$. This non-linear lattice excitation caused atoms to shift in a way that improved how electrons move through the material. To observe these rapid changes, the team used the technique of femtosecond X-ray diffraction, which allowed them to capture snapshots of the atomic structure in motion. Their results showed that the vibrations altered the distances between layers of atoms and changed the shape of certain bonds, creating conditions that favour superconductivity – even at temperatures much higher than usual. This discovery is significant because it shows that light can be used to control and enhance superconductivity in real time. It opens up new possibilities for designing materials that could one day lead to more efficient power grids, faster electronics and powerful magnets for medical, technological and scientific use.

"**Ultrafast disordering of vanadium dimers in photoexcited VO_2" published in Science, November 2018**,[32] studied vanadium dioxide (VO_2), which is a special material that can switch from an insulator to a metal (i.e. from a poor to a good electrical conductor) when heated or exposed to light. In this study, scientists used ultrafast laser pulses to trigger this switch and then observed what happened using the powerful technique of femtosecond X-ray diffraction. This method allowed them to take ultrafast snapshots of the atoms in VO_2. They discovered that the key to the transition is the rapid breaking apart – or "disordering" – of pairs of vanadium atoms, called dimers, which normally keep the material in its insulating state. This finding is important because it shows that the change to a metallic state can happen extremely fast and does not require the entire structure to rearrange first. The research will help scientists better understand how to control materials like VO_2 with light, which could lead to faster electronics, smart windows and energy-efficient devices that respond instantly to changes in their environment.

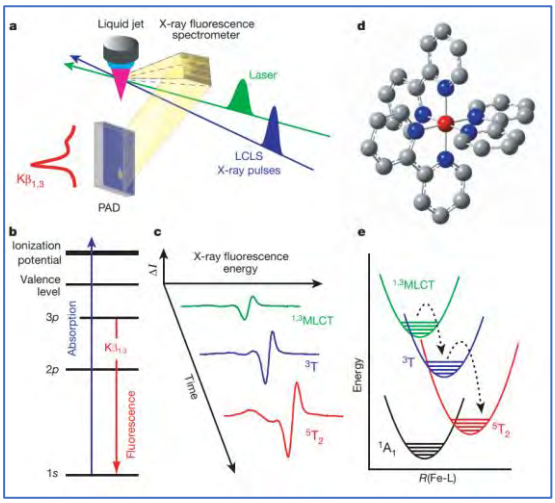
In **"The ultrafast Einstein-de Haas effect" published in Nature, January 2019**,[33] scientists explored how fast the Einstein-de Haas effect can happen by using ultrafast laser pulses to demagnetise a thin piece of iron. The Einstein-de Haas effect shows that when the direction of magnetisation in a material changes, it also causes the material to physically rotate – proving that magnetism is linked to angular momentum. In this study, they then used femtosecond time-resolved X-ray diffraction to watch how the atoms in the material responded in real time. The researchers discovered that within just 200 femtoseconds most of the angular momentum lost from the electrons' spins was transferred to the atoms in the crystal lattice. This transfer launched a tiny mechanical wave through the material. The study is significant because it shows that the lattice – the structure of atoms – plays a key role in ultrafast magnetic changes. Understanding this process could help scientists develop faster magnetic storage devices and improve our control over materials using light.



Reprinted with permission from Springer Nature from C. Dornes et al. Nature 565, 209-212 (2019) DOI: 10.1038/s41586-018-0822-7

2.2.6 Advances in chemical sciences

"Tracking excited-state charge and spin dynamics in iron coordination complexes" published in Nature, May 2014,[9] is a landmark study that employed femtosecond X-ray emission spectroscopy to directly track, in real time, the excited-state charge and spin dynamics of an archetypal metal complex, Fe(II) polypyridyl. By launching a charge transfer excitation between the metal and surrounding parts of the molecule (ligands), and monitoring the highly spin-sensitive X-ray emission, the authors revealed that spin state change proceeds not as a simple two-state jump but involves a critical intermediate triplet state. This clear identification of a transient intermediate species – bridging the initial and the ultimate high-spin state – resolves longstanding debates about the mechanistic pathway. The work not only showcases a powerful new spectroscopic tool with sub-100 femtosecond time resolution, but also provides unprecedented molecular-level insight into the ultrafast interplay of charge, spin, and structure in light-activated 3d transition-metal complexes critical in emerging quantum technologies.



Reprinted with permission from Springer Nature from W. Zhang et al. Nature 509, 345 (2014) DOI: 10.1038/nature13252

"Observation of the fastest chemical processes in the radiolysis of water", published in Science, January 2020,[34] was a groundbreaking study using femtosecond soft X-ray pulses to directly observe, in real time, the earliest steps of water radiolysis following strong-field ionisation. For the first time, researchers tracked water fragments following ionisation, witnessing the ultrafast proton-transfer event leading to OH formation, and following the emergent hydrated electron within tens of femtoseconds. This illuminated the sub-100 femtosecond chemical fragmentation and the subsequent solvent reorganization dynamics when water is ionised. These insights not only advance our molecular-level understanding of radiation-water interactions, but also showcase the power of ultrafast X-ray methods to capture the fastest chemical processes essential to chemistry, biology and radiation science.

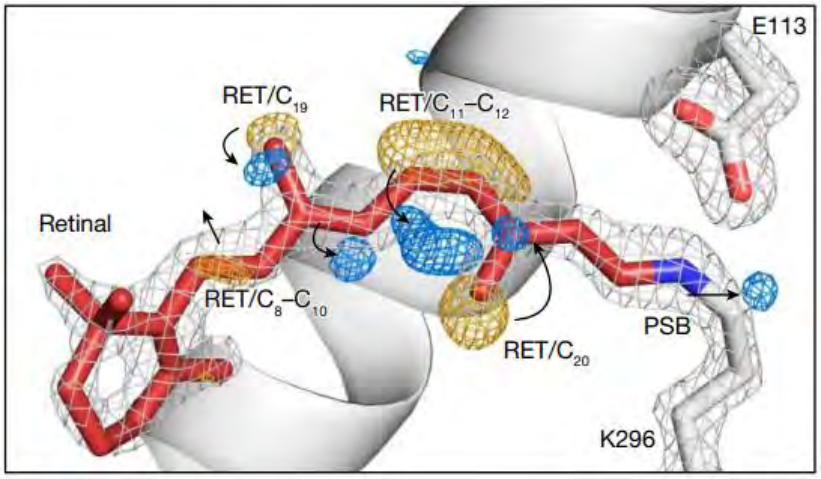
"Tracking C–H activation with orbital resolution", published in Science, June 2023,[35] harnessed ultrafast, metal-specific and electronic state sensitive X-ray absorption spectroscopy to directly observe, with femtosecond-to-nanosecond time resolution, the intricate electronic orbital resolved charge-transfer events driving C–H bond activation in a catalytic complex (rhodium cyclopentadienyl-carbonyl) reacting with octane. C–H bond activation in a metal complex is a critical step in many industrially relevant catalytic processes. This work deciphers how orbital-specific electron exchange governs reactivity in C–H bond activation. This capability to dissect charge-transfer interactions with orbital resolution opens a formidable avenue for rational catalyst design in C–H activation and beyond.

2.2.7 Advances in life sciences

"Identification of Phosphorylation Codes for Arrestin Recruitment by G Protein-Coupled Receptors", published in Cell, July 2017,[36] was carried out at LCLS using serial femtosecond crystallography (SFX). G protein-coupled receptors (GPCRs) are proteins on cell surfaces that help cells respond to signals like hormones or light. When these receptors are activated, they can be turned off or reshaped by a protein called arrestin. This study shows that specific patterns of chemical tags, called phosphorylation codes, on the receptors control how arrestin attaches. By figuring out these codes, scientists can better understand how cells fine-tune their responses to signals. This knowledge could help in designing more precise medicines that target these important cell pathways.

In the landmark study **"Ultrafast structural changes direct the first molecular events of vision", published in Nature, March 2023**,[37] researchers used ultrafast time-resolved serial femtosecond crystallography at LCLS to capture, within just one picosecond after photon absorption, how human vision occurs. It showed how the 11-cis retinal in rhodopsin protein isomerises to a twisted all-*trans* form, breaking away from roughly half of its binding-pocket contacts. The excess energy stored in this distorted chromophore is rapidly channelled into an anisotropic "breathing" motion of the protein toward the extracellular space, specifically involving side chains in regions known to participate in G protein-coupled receptor activation. By revealing these sub-picosecond structural ripples, the work elucidates how a single photon triggers a cascade of conformational changes that prime rhodopsin for

G-protein signalling—offering unprecedented, atomic-level insight into the very first molecular events of vision.



Reprinted from T. Grul et al. Nature 615, 939–944 (2023) under the terms of a Creative Commons Attribution License 4.0 (CC BY). DOI: 10.1038/s41586-023-05863-6

"Structural evidence for intermediates during O_2 formation in photosystem II", published in Nature, May 2023,[38] employs SFX to address a key cycle in biology – photosynthesis, which is responsible for nearly all oxygen (O_2) generation on Earth. Photosystem II is a very large protein complex in plants and photosynthetic microbes in the oceans, that helps turn water into oxygen during photosynthesis. Scientists have long wondered exactly how photons from the Sun drive O_2 formation during this process. This paper and other recent XFEL-related work[39] provide experimental data showing the steps the protein goes through as it sequentially absorbs energy from the Sun (four photons in total) to eventually "split" two water molecules and transfers the four electrons and four protons to other biological processes. In the end, however, the enzyme brings the two oxygen atoms together to make one dioxygen molecule and thereby resets itself for another round of reaction. These snapshots capture several photon-driven, sequential and short-lived "intermediates" – temporary states that the molecules pass through during the catalytic cycle. Understanding these steps also helps explain how nature uses energy from the Sun to separate charge (preferential electron flow) that is already inspiring new ways to produce clean energy, such as improved photovoltaic panels.

2.3 Time and space-resolved measurement with an XFEL

The combination of time-resolved X-ray scattering, X-ray spectroscopy and X-ray dynamic imaging that can be performed at XFELs is proving transformative. These methods enable measurements, resolved in space and time, of the electronic and structural dynamics at the fundamental quantum scales for solids, liquids, nano-assemblies and molecules relevant to physics, chemistry, and material and life sciences.

2.3.1 X-ray structural and electronic probes

The short wavelengths of X-ray photons, and the short de Broglie wavelengths of electrons and neutrons of appropriate energy, permit diffraction imaging of the structure of matter at the atomic spatial scale. In contrast to the case for neutrons and electrons, with X-rays it is also possible to interrogate the electronic states of matter through various types of spectroscopy, and this has proved key to elucidating the electronic and geometric structure of materials, molecules and biomolecules. The frontier challenge is also to measure the dynamics of these electronic and structural properties, which at the nanoscopic/quantum scale are typically very fast (attosecond – nanosecond) (see **Box 2.1**). Such time-resolved measurements require very short duration X-ray probes to enable this structural information to be sampled at a sufficiently high temporal resolution. X-ray pulses from XFELs are routinely generated with 10 femtosecond or shorter duration, with sub-femtosecond modes now available, which match to this task. In this Section, we briefly overview the classes of time-resolved X-ray probing techniques that are available, and then discuss the types of measurements that are currently being made (see **Box 2.2**).

2.3.2 Time-resolved X-ray scattering

X-rays may interact with matter via either elastic or inelastic scattering (the latter is discussed with X-ray spectroscopy in **Section 2.3.3**). The elastic scattering signal is dominated by Thomson scattering from the large number of electrons localised to the atomic sites. If the scattering is from a periodic structure (see **Figure 2.2)**, such as a crystal lattice, constructive interference between the scattered X-ray waves leads to strong peaks at certain angles (Bragg peaks),[40] which give the reciprocal space information from which the lattice structure can be readily retrieved. Through serial exposures, high brightness X-rays, such as those available from an XFEL, enable the lattice structure of nanocrystals to be retrieved with atomic resolution. This has proven of significant value, as many proteins can only be crystallized to form nanoscopic, rather than macroscopic, crystals.[21]

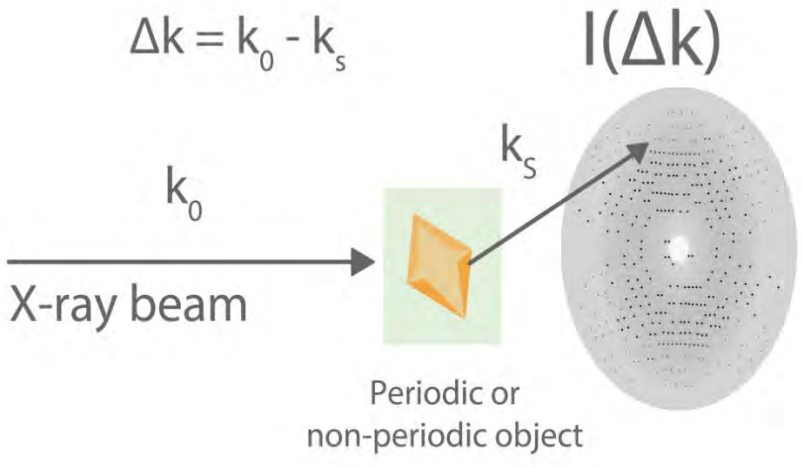


Figure 2.2: X-ray scattering, from either a crystal or a non-periodic object, leads to a distinct diffraction pattern from which the structure can be reconstructed. Through the high temporal resolution now available at XFELs, structural dynamics can be followed in full detail.

Even in a non-periodic structure, the X-ray scattering signal for spatially coherent X-rays can give a complex diffraction pattern from which the structure can be retrieved, using powerful algorithms that numerically solve the phase problem by applying various physical constraints in an iterative retrieval procedure.[41,42] This coherent diffraction imaging (CDI) procedure is well suited to the high brightness coherent X-rays from XFELs, and the concept of "diffract-before-destroy" for imaging non-periodic structures has been used to gain nanometre resolution in a variety of biological[43] and non-biological[44] nanoscale structures. Although not yet reaching atomic resolution, advances towards 0.5 nm resolution are being made as the technique develops. The possibilities for static nanoscale imaging of single particles by CDI are being actively pursued at all of the XFELs currently in operation and progress is regularly being reported (see **Sections 3.4** and **7.5**).

The X-ray pulses from XFELs have a very short duration, as well as a very high brightness; consequently, if they are applied time-synchronised with another interaction that can initiate structural change, then time-resolved X-ray diffraction becomes possible. Such a scenario is termed a 'pump-probe measurement,' with temporal information gained by repeating the measurement over the appropriate range of pump-probe delays. A significant number of recent experiments illustrating this possibility have been carried out at the LCLS, Swiss FEL, European XFEL, PAL XFEL and SACLA (SPring-8 Angstrom Compact free-electron LAser in Japan) XFELs. The X-ray brightness is high enough even to capture structural changes in an ensemble of gas phase small molecules,[45] and pump-probe measurements of laser activated molecular dynamics have revealed photochemical structural changes that occur over a few hundreds of femtoseconds. Structural changes of much larger photoactive protein molecules, in a nanocrystalline form, have also been captured in a number of cases.[19] Optical and THz fields can be used to induce non-equilibrium phases in strongly correlated quantum condensed phase materials with new emergent properties, and these too have been captured by time-resolved X-ray diffraction.[16] Recently, progress has been made on short electron pulse generation for ultrafast electron diffraction (UED),[46,47,48] although accessing the sub-10 femtosecond temporal range remains challenging and UED returns no information on the electronic quantum states. The synergy of XFEL and UED techniques is discussed in **Appendix 1.3**.

For time-resolved studies, unless picosecond resolution is sufficient, technical effort must be applied to establish the relative timing of X-ray and optical pulses. In the LCLS (the first X-ray FEL), there was an intrinsic temporal jitter of up to several hundred femtoseconds; in the newer facilities, this has been reduced through improved temporal synchronization technology and the development of a number of so called "time-tools",[49,50] at LCLS and elsewhere, that can sort the pulse timing to a fidelity of better than 10 femtoseconds. Future machines with lower intrinsic jitter and higher resolution time-tools are under development;[51,52] these are anticipated for widespread use that will improve the achievable resolution eventually to better than 1 fs. This timing technology is also vital for the time-resolved X-ray spectroscopy techniques discussed in **Section 2.3.3** below.

2.3.3 Time-resolved X-ray spectroscopy

Inelastic X-ray interactions can be enormously powerful, and their measurement via various channels forms the basis of several well-established X-ray spectroscopy techniques (see **Figure 2.3**): X-ray photoelectron spectroscopy (XPS); Auger electron spectroscopy; X-ray absorption spectroscopy (XAS); X-ray emission spectroscopies (XES) and resonant inelastic X-ray scattering (RIXS). With XFEL pulses, these X-ray spectroscopy tools can be made time-resolved, with temporal resolution in the femtosecond and even the sub-femtosecond range.

Photoelectron emission results when an X-ray photon is absorbed by the target and a bound electron is excited to the continuum from valence to inner shell states. If X-rays of well-defined energy are used, the energy analysis of the photoelectrons emitted from the valence and inner shells gives direct information on the binding energies of these states. Angularly-resolved measurements of the photoelectrons can give additional detailed information on state symmetries. This technique has been widely exploited to investigate the chemical state of materials and, in this form, is often termed

Electron Spectroscopy for Chemical Analysis (ESCA), following the pioneering developments by Siegbahn[53] that led to his Nobel Prize in Physics in 1981.

Ionisation of an inner shell electron can lead to an unstable electronic hole, which can undergo decay through electron-electron correlation with the emission of further Auger-Meitner electrons.[54] Auger-Meitner electrons carry information on the energy levels of the involved ionic forms. It has been shown to be possible to track mechanisms of radiation damage in biomolecules[55] using time-resolved X-ray Auger-Meitner and absorption spectroscopy probing of optically excited molecules at an XFEL. Streaking in a laser field of atomic photoelectrons and Auger-Meitner electrons has been used to resolve temporal delays in emissions from different states, with as little as a few tens of attosecond difference,[56] and these methods are being developed at XFELs.

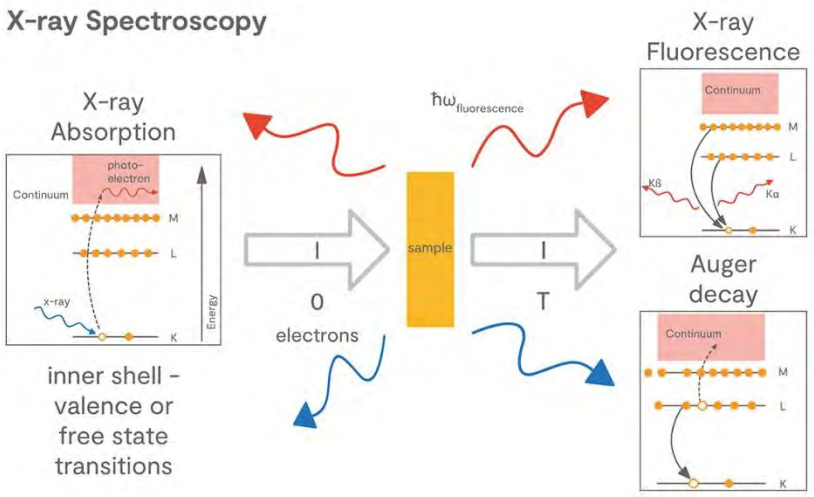


Figure 2.3: X-ray spectroscopy is sensitive to the electronic states, their energies, populations, symmetries and interactions. Utilising the specificity afforded by atomic X-ray absorption edges, time-resolved X-ray spectroscopy can give access to the local evolution of states in space and time

Resonant ionisation close to an absorption edge of a particular atom, corresponding to a transition from an inner shell state to an unoccupied valence or low-lying continuum state, is a powerful way to learn about the electronic structure in the vicinity of that atom. The cross-section for photo-absorption at different X-ray energies can be determined from absorption or electron yield measurements in a condensed phase or gaseous system, and can reveal the details of the unoccupied and partially occupied valence and low continuum states near the ionisation threshold. This method of X-ray absorption near edge structure (XANES) is widely used to establish critical local electronic structure information.[57] Further into the continuum, the absorption modulations are termed extended X-ray absorption fine structure (EXAFS) and have been used for many years to establish local bond lengths around a specific atomic site.[58] Time-resolved X-ray absorption and emission (XAS and XES) using XFELs are now proven techniques for photochemistry studies.[8-10]

X-ray photon emission measurement methods are now being used in time-resolved mode using XFELs. For example, with RIXS, a core excited intermediate state relaxes to one or other of the neutral valence states by emission of a photon, and the energy and direction (momentum transfer) of the emitted photons are measured using an angularly resolving X-ray spectrometer. In the language of non-linear optics, this process is termed spontaneous Raman scattering. The energy levels of the occupied and partially occupied states can be registered from this signal, as well as the existence of the low energy collective excitation modes and their momenta. This provides a powerful way to probe low energy (eV to meV) excitation modes in a condensed phase material. Time-resolved RIXS studies have proved valuable in elucidating the nature of excitations in photoexcited correlated materials.[59]

RIXS and other photon in/photon out methods using spontaneous emission are two-photon in nature, although scale only linearly with X-ray field intensity. The spontaneous emission is, however, into

unoccupied field modes and is therefore not controlled by the applied X-ray fields. High brightness X-ray sources provide new opportunities for controlled non-linear X-ray processes. One example is stimulated X-ray Raman, demonstrated experimentally by Rohringer *et al*.[60,61]

High brightness, high repetition rate XFELs open the possibility of non-linear X-ray spectroscopy with entirely new capabilities. An early proposal in this direction is the possibility of impulsive X-ray electronic Raman creating and probing atomically localised valence electronic excitation, and so tracking ultrafast electronic coupling through a molecule even on attosecond timescales.[62] This is just becoming possible through recent advances with attosecond pulses and is discussed further in **Section 3.3**. Another new concept is for non-linear X-ray diffraction involving a two-photon (optical and X-ray) scattering into an X-ray mode that can be heterodyne detected against an applied X-ray field in the same mode. This method is predicted to have the potential to image the charge density evolution of excited electronic states.[63]

2.3.4 X-ray dynamic imaging

Harnessing the capability of X-rays to penetrate through macroscopic and mesoscopic objects has been one of the driving applications of X-rays in technology and medicine for over a century. XFELs unleash new opportunities in this area by providing exceptional brightness (both instantaneous and time averaged) and unprecedented temporal resolution. This enables a full array of X-ray microscopy and wide angle tomographic imaging methods, offering nanometre-scale imaging of multi-millimetre scale objects. Dynamic imaging with picosecond resolution is being actively developed and will be very important for characterising key technological processes in advanced manufacturing, mechanical engineering and fusion technology. There has been recent progress in this direction, extending techniques from synchrotrons to the higher temporal resolution and pulse energy available from XFELs[64 65].

Moreover, the next generation of XFELs will have 100 to 1000 times greater average spectral flux than even the brightest 4th generation synchrotron in operation today. This will enable high resolution static tomographic imaging of much larger volumes of material than is currently possible, and will enable imaging and spectroscopically (chemically) sensitive methods like X-ray fluorescence imaging to be applied with greater fields of view and sensitivity. This will have an impact on, for example, the imaging of biological tissues (e.g. in whole mammalian brain imaging), fossils[66] (e.g. to uncover previously unseen structural detail) and cultural heritage objects[67 68] (e.g. fragile ancient papyri and manuscripts).

2.3.5 Classes of measurements with XFELs

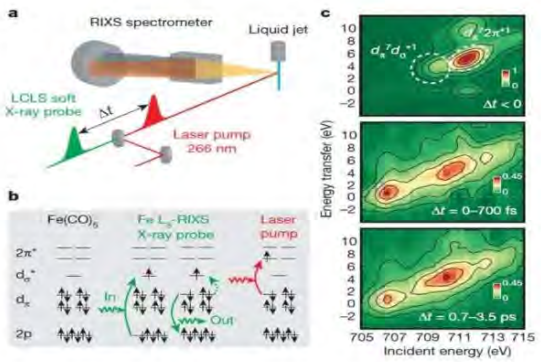
To date, the majority of studies conducted at XFELs have fitted into the categories of measurements of **structural dynamics**, **properties of transient state** and **nano-crystallography**. These use a combination of X-ray scattering and spectroscopy. As repetition rates increase, and the X-ray properties become more controlled, it is likely that classes of measurement based around coherent diffraction imaging, X-ray microscopy and imaging spectroscopy will become more important, along with studying fluctuations with X-ray correlation spectroscopy, time-resolved pair distribution functions and **mapping out conformational trajectories**. The current state-of-the-art is illustrated in **Box 2.2**.

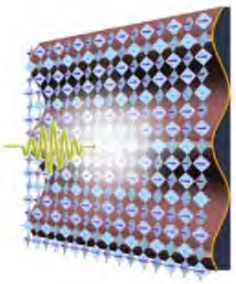
Looking ahead, we anticipate that a next-generation XFEL, with its suite of leading capabilities, will provide transformative opportunities including: higher temporal resolution, access to matter in a wider range of extreme states, greater data rates to capture the full range of fluctuations and rare events, and time-resolved structural information on scarce samples. In this way, it will be able to expand the scope of scientific investigation of the electronic and structural dynamics of matter, thereby profoundly increasing our understanding of the nanoscopic world that underpins so much of science and technology.

Box 2.2: Current forms of measurement being made at XFELs

Access to structural dynamics: Dynamical phenomena can be probed after laser excitation on a timescale down to femtoseconds, thus covering electronic dynamics, lattice dynamics and chemical bonds breaking/forming.

*Figure reproduced from P. Wernet et al., "Orbital-specific mapping of the ligand exchange dynamics of $Fe(CO)_5$ in solution" Nature **520**, 78 (2015), Springer Nature. DOI: 10.1038/nature14296*



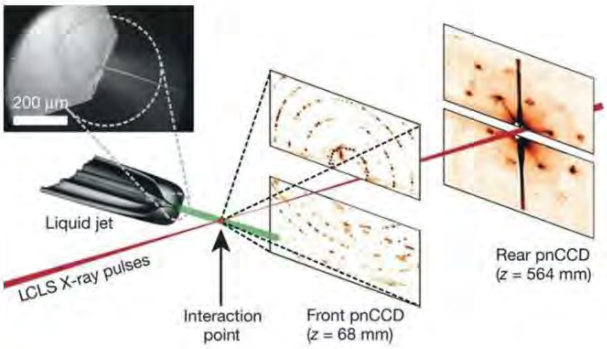


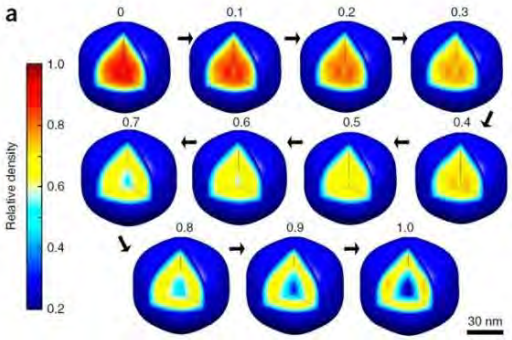
Access to transient states: Matter can be probed under only transiently attainable conditions of extreme pressure, high E and B fields, laser dressing and high energy density.

Courtesy of A. Cavalleri

New modes of crystallography and nanoscopic imaging: For seeing the nanoscopic arrangements relevant to nanotechnology and life-sciences free from radiation damage and adverse effects of sample preparation.

*Reprinted by permission from Springer Nature: H.N. Chapman et al. Nature **470**, 73 (2011). DOI: 10.1038/nature09750*





Capturing rare events: In physical, chemical and biological systems, critical processes can proceed through brief rare events (e.g. barrier crossings) arising from intrinsic fluctuations.

*Reprinted by permission from Springer Nature: A. Hosseinizadeh et al. Nature Methods **14**, 877 (2017). DOI: 10.1038/nmeth.4395*

2.4 Survey of existing facilities and capabilities

For the next decade, the UK will remain reliant on the international XFEL facilities in Germany, the USA, Japan, Switzerland, Italy, South Korea and China. To develop a future next-generation XFEL facility with unique capability, it is essential to plan this in the context of these existing facilities and other planned facilities in the pipeline. Here we briefly review the capabilities of the existing facilities and others due to start operating during the decade.

Now, and in the coming decades, the key frontier for a broad range of important scientific and technological disciplines will develop into the quantum realm, i.e. in a domain requiring measurement and understanding on ultra-small length scales, simultaneously with associated ultrafast time scales. Accessing this domain – which is crucial for new knowledge, discovery and technological progress – is possible with an XFEL that provides insight into structural and electronic dynamics at the quantum scale.

Recognising this, there are currently five XFELs and three soft X-ray machines operating in the world, with several others under construction, notably in Asia. These few machines are already having significant global scientific impact, with a high proportion of their scientific output published in high impact journals. It is a signpost to the future, in much the same way that, decades ago, early synchrotrons, lasers, electron microscopes, etc. signalled new multi-disciplinary tools that we take for granted today.

Table 2.1: Summary of existing XFELs (March 2026)

Facility (Year of First Operation)	Max Photon Energy (keV)	Beam Energy (GeV)	Pulses/s	Bunch Charge (nC)	Facility Length (km)	RF Technology
FLASH, Hamburg (2005)	0.3	1.2	27000	1	0.32	SC
LCLS-I, Stanford (2009)	11	13.6	120	0.25	1.7	NC
SACLA, Harima (2011)	15	8.5	60	0.2	0.8	NC
FERMI, Trieste (2011)	0.3	1.5	50	0.5	0.5	NC
European XFEL, Hamburg (2017)	25	17.5	27000	1	3.4	SC
SwissFEL, Viligen (2017)	12	5.8	100	0.2	0.7	NC
PAL XFEL, Pohang (2017)	12	10	60	0.2	1	NC
LCLS-II, Stanford (since 2023)	5	4	10^5	0.1	4	SC
	25	15	120	0.125	4	NC
HE UPGRADE (~2027)	12	8	10^6	0.1	4	SC
SHINE, Shanghai (~2026 1st FEL)	25	8	10^6	0.1	3.1	SC

Table 2.1 lists the main parameters of short-wavelength FEL facilities in order of their year for coming online, and includes two facilities that are under construction and will be online in the next five years. The colour coding relates to the RF technology – superconducting (SC, blue) or normal conducting (NC, pink). The first facility to offer short-wavelength FEL light to users was the pioneering FLASH in 2005, recently upgraded to FLASH-II by including gap tunable undulators. FLASH was originally constructed as an SC linac test facility and the technological advances it produced were critical to the design and success of the European XFEL. The first hard X-ray facility was LCLS-I, which started operations in 2009, and has since been joined by facilities in Japan, Germany, Switzerland and South Korea.

SC technology permits a higher pulse repetition rate than NC. The European XFEL (in common with FLASH) operates in a pulsed mode, where the RF cavities are switched on and off 10 times per second. This limits the total number of FEL pulses per second and is not favourable for some uses. LCLS-II, online from 2023, operates in a continuous wave (CW) mode, generating evenly spaced pulses at up to 1 MHz and photon energies up to 5 keV. LCLS-I continues to deliver higher photon energies, the beam being accelerated up to 15 GeV using the existing NC linac sections, so the FEL output is limited

to 120 Hz. The high-energy (HE) upgrade to LCLS-II (upgrade started in January 2026 and is expected to be operational later in 2027) will add extra SC linac sections to allow 1 MHz operation at 8 GeV, with expected photon energy 12 keV or higher. Finally, the SHINE facility is under construction in a tunnel underneath Shanghai and is expected to begin operating later this year. SHINE will also be driven by an 8 GeV SC accelerator and will produce 1 MHz FEL pulses at energies up to 25 keV.

It should be noted that the accelerating gradients available from SC cavities are significantly less than those available from NC cavities – this is the reason that the length of linac used at the European XFEL is twice as long as that used at LCLS-I, although the two facilities have similar beam energies. Another trend revealed by **Table 2.1** is that the required beam energy to produce hard X-ray photons has reduced over time. This is due to advances in undulator technology, such as narrow-gap in-vacuum devices or superconducting devices, which mean that shorter periods with stronger on-axis fields are now available.

All the operational machines listed have large international user communities, built up in the time since they first began operating. UK users have been very actively involved in science at FLASH, LCLS, SACLA, PAL-XFEL, Swiss FEL, the European XFEL and FERMI (shown in **Figure 2.4**). The UK XFEL user community is currently smaller than the synchrotron user community but has grown substantially over the last decade. Critically, the UK user community is now one of the biggest users of the major international facilities, behind only those of Germany and the USA that both host their own facilities. The growth of the UK user community has been helped by initiatives such as the Life Sciences and Physical Sciences Hubs at Diamond and the CLF, respectively, and by the promotion of XFEL science through activities like the UK XFEL project. It is vital for the strength of UK science across a wide range of areas that we do everything possible to support and further grow this community, to remain competitive in key areas of frontier science and advanced technology, regardless of whether or not the UK builds a next-generation XFEL.



Figure 2.4: Aerial views of operating XFELs: LCLS, USA (top left) started operating in 2009; SACLA, Japan (top right) operating since 2012; European XFEL, Germany (centre) operating since 2017; Swiss FEL, Switzerland (bottom left) operating since 2017; PAL XFEL, South Korea (bottom right) operating since 2017

2.5 Outlook for a next-generation XFEL

In the 17 years since the first XFEL, remarkable progress has been made in adding new capabilities to this technology. Furthermore, the progress to date represents only the very early stages in XFEL development – a host of further capabilities are being developed that could be incorporated into a next-generation XFEL. Building a new XFEL or undertaking a major upgrade at an existing facility offers the opportunity to integrate the most exciting emerging features in an optimal way, to provide a combination of capabilities that will establish a facility of scientifically transformative potential. This blue-sky thinking has enabled a set of key next-generation capabilities to be defined that will shape the future possibilities for science and technology.

The time is ripe to consider a new XFEL that builds upon what has been learnt from the first generation of machines. The first light from a free electron laser in the X-ray range was observed just 17 years ago (March 2009). The intervening years have not only seen the construction of some half dozen machines around the world, but also enormous advances in the ability to simulate and implement new X-ray modes that are constantly advancing the scientific reach made possible by XFELs. These capabilities offer for example: two-colour, two-pulse X-rays; variable polarisation states; high spectral purity X-rays; higher brightness X-rays; and sub-femtosecond X-ray pulses. Many of these new capabilities go beyond SASE by manipulating the electron bunch (e.g. using pre-modulation of density or controlled emittance spoiling) prior to it entering the undulator. Modes such as XFELO (X-ray FEL Oscillator)[1] and RAFEL (Regenerative Amplifier Free-Electron Laser), which use oscillator and regenerative amplifier concepts from laser technology, are even more radical and promise to provide unprecedented spectral brightness. Although all of these modes are underpinned by access to an excellent electron beam driver, they are ultimately controlled by the operating modes of the undulator and so, by using a versatile undulator design, all can potentially be made available at a single facility if properly configured.

Existing facilities are often constrained by site and machine design factors, making it hard to offer all of these newer options or the combinations needed to optimise scientific impact. A next-generation XFEL starting from a clean slate could, therefore, leapfrog the existing facilities and would be superbly positioned to implement all of these advances, and to add to them other emerging capabilities. Balanced against this is the cost effectiveness of starting from a suitable existing facility that will reduce overall cost and delivery time.

In this section we define the next-generation XFEL capabilities that we consider will drive science forward. The integration of these into a **self-consistent conceptual design is discussed fully in the Conceptual Design Report**.

[1] The XFELO concept saw a first successful test at European XFEL in 2025.

2.5.1 Next-generation XFEL capabilities

Since publication of the previous Science Case in 2020, we have continued to monitor XFEL advancements and to consider all of the potential developments that might be delivered in the foreseeable future that would advance their science impact. This exercise has resulted in a full definition of the **capabilities needed for a next-generation XFEL facility**:

- **Near transform-limited operation across the X-ray range**
- **High efficiency facility, with a step-change in the simultaneous operation of multiple end stations in parallel**
- **Evenly spaced, high repetition rate pulses to match samples, lasers, and detectors**
- **New AI approaches for operation, data analysis and interpretation of vast data volumes generated**
- **Improved synchronisation/timing data with external lasers to <1 fs by harnessing state-of-the-art synchronization strategies and implementing the most advanced timing tools**
- **Widely separated, multiple colour X-rays to at least one end station by combining the outputs from two FELs**
- **Full array of synchronised sources including optical lasers + nonlinear optical conversion across the EM spectrum from XUV – THz, charge particle beams, high energy and high power lasers**
- **Sustainable facility meeting Net Zero targets**

These capabilities formed the starting point for development of this Science and Technology Case, and of the Conceptual Design. They are further developed and matched to the driving research fields in **Section 9.1**.

2.5.2 High repetition rate laser seeding

One area with exceptionally high potential for a next-generation XFEL is extending the range of seeding [6] (introduced in **Section 2.1**) to much higher repetition rates and to higher photon energy. Seeding greatly improves the coherence properties and stability of the output. The FERMI facility in Italy has demonstrated seeding up to approximately 400 eV at a repetition rate of 50 Hz. In a recent demonstration,[69] two external lasers were used to precisely tailor the longitudinal phase space in the electron bunch before it entered the undulator. An advanced XFEL could operate with a thousand-times as many seeded pulses per second by utilising superconducting linear acceleration with high repetition rate (~100 kHz) lasers – both areas of UK expertise. In combination with high repetition rate sample delivery and detectors, the massively enhanced data acquisition rate would greatly speed up existing experimental techniques. In addition, this would also open up entirely new classes of experiment due to the excellent X-ray coherence and stability, for example in: X-ray emission spectroscopy[10] of dilute samples; X-ray angularly resolved photoelectron spectroscopy using the high repetition-rate to gain sufficient signal in the low space-charge limit; and transient grating measurements[70] of transport rates at sub-nanometre scales in materials. Furthermore, using the latest non-linear optical laser technology to generate the appropriate seeding would extend the range over which seeding operates to reach higher photon energies (> 1 keV), thereby extending the benefits to new areas of science by spanning an important range of critical absorption edges in carbon, nitrogen, oxygen and metals.

2.5.3 High spectral purity X-rays

Laser seeding is anticipated to be less effective above 1 keV, but alternative technologies are being developed to improve coherence and stability at the higher photon energies. A useful figure of merit related to coherence is the relative spectral bandwidth, with smaller values indicating a higher degree of spectral purity. While existing XFELs typically operate with bandwidth between 1×10^{-3} for the default SASE mode and 2×10^{-4} for self-seeding (already introduced), new techniques are expected to far surpass this performance. Double self-seeding,[71] employing two monochromatisation stages within

the FEL, has the potential to achieve bandwidths < 10^{-4}. High-Brightness SASE (HB-SASE),[72,73] a scheme developed by UK FEL physicists, could achieve a bandwidth of ~2×10^{-5}, and was demonstrated in the soft X-ray range at the SwissFEL. Its use of magnetic delay chicanes rather than optics could prove more flexible to different energies and higher repetition rates.

A method that may promise the highest spectral purity in the future is the XFELO[74] (X-ray FEL Oscillator), which uses a low gain FEL enclosed in an optical cavity comprising diamond crystal Bragg mirrors with a geometry allowing a tunability of a few percent. Bandwidths of ~1×10^{-7} are anticipated, with modest pulse energies but exceptional shot-to-shot stability. The first demonstration of an XFELO was achieved recently at the European XFEL[75], and experiments to address the challenging cavity alignment tolerances are underway at LCLS-II. Such a scheme is, however, only possible on an accelerator with a repetition rate of around 1 MHz or higher, as optical cavity lengths become unfeasibly large below this rate. A facility with a high repetition beam at lower energy only (e.g. 2 GeV) could employ an oscillator FEL at soft X-ray/EUV wavelength, to provide good stability and spectral purity and potentially provide seed pulses for an XFEL. Another future possibility is to seed directly at hard X-ray wavelengths, and a potential seed source is under development at Arizona State University.[76] With this source, a compact low energy accelerator transforms a transverse electron diffraction pattern into coherent longitudinal electron bunching, into which a laser pulse is counter-propagated to produce a pulse of coherent hard X-rays with sufficient power to act as a seed for a longer XFEL amplifier. Experiments are still underway and the results will be important to further planning.

2.5.4 Higher pulse energy

Pulses of high spectral purity, produced via any of the methods above, can be further amplified very efficiently by extending the FEL undulator beyond the normal saturation point, whilst tapering down the field strength to keep the FEL pulse in resonance with the decreasing electron bunch energy.[77] It is expected that increases in pulse energy of one to two orders of magnitude can be achieved using this tapering technique, with a simultaneous damping of the shot-to-shot fluctuations to a few percent. For example, by using low charge, highly compressed electron bunches in combination with self-seeding/HB-SASE and post-saturation tapering, it is anticipated that few-femtosecond, nearly transform-limited pulses, with greater than millijoule pulse energies and few-percent shot-to-shot stability, could be produced.

2.5.5 Attosecond pulses

The recent demonstration of ~400 attosecond duration pulses at the LCLS facility (2018)[7] is a particularly significant development, and is a feature that would be a major focus of a next-generation XFEL facility. The LCLS study reports one- and two-colour attosecond pulse generation over the photon energy range 500 eV – 1 keV, but related methods have now been demonstrated through to the hard X-ray range. The study of dynamics on ultrafast timescales is one of the defining features of XFELs and is made possible by the ultrashort duration of the XFEL pulses. Moreover, the large coherent bandwidth (5 – 8 eV in the pulses generated so far) is a key resource for future multi-dimensional, non-linear X-ray spectroscopies. A significant number of experiments have now been carried out at LCLS using the attosecond X-rays (see **Section 3.3**), e.g. measuring relative photo-electron emission delays for ionisation from different states of a molecule, and demonstrating impulsive electronic X-ray Raman excitation. Attosecond modes are now available for user operation at both soft and hard X-rays at LCLS, LCLS-II and the European XFEL. All XFEL facilities are making progress towards refining attosecond modes and offering these to users .

2.5.6 High average power

As well as high pulse energy, high average power from the X-rays and from the electron beam would open up unprecedented opportunities. The development of the relativistic high brightness linac required to drive the X-ray laser (**see Section 3.6**) will offer the chance to develop a high repetition rate electron acceleration test facility. A further opportunity that emerged in our consultation was the

potential for developing a novel kaon science experiment using the electron beam after X-ray lasing in an undulator (see **Section 3.6.4**).

To date, the potential of XFELs in direct industrial processing – for example for photolithography at soft X-ray wavelengths to achieve deep sub-nanometre feature resolutions – is a little explored area. Interest in this from companies in the semiconductor chip sector was registered in our information gathering exercise for the 2020 edition of the Science Case, but it is clear that an exceptionally high repetition rate (multi-MHz) will be required, even for a test facility to prove the concepts. Adding a return loop or an energy recovery configured accelerator section at the front end (perhaps up to 1 GeV) could be used for such a purpose, before the bunches to be accelerated to a higher energy pass through a conventional linac section (see **Appendix 2**). This is seen as an important upgrade option for a next-generation XFEL. It would create opportunities for direct science access to a GeV range electron beam at a high repetition rate. An additional potential benefit of this is the construction of an ultra-high average brightness gamma source based upon inverse Compton scattering (discussed in **Appendix 2**).

2.5.7 Combining X-rays with other sources

Beyond the potential for advanced X-ray modes outlined above, an enormous extension to science reach can be accomplished by combining other advanced capability at the X-ray interaction point. Ultrafast lasers, used with the X-rays in pump-probe configuration, are a mainstay of time-resolved XFEL research. Hitherto the laser photon energy ranges on offer at XFELs, and their pulse duration, have typically been rather limited due to practicalities and budgetary issues. In a machine designed to optimise these capabilities from scratch, the full range of pulse compressed laser/non-linear optical sources – spanning from < 100 nm to 10 µm – can be used for science (see **Section 9.2**), with a repetition rate commensurate with experimental demands. By developing synchronised electron gun technology (in the 1 – 10 MeV energy range) at a number of end-stations, new opportunities in THz and electron-initiated biology, chemistry and physics, will become possible (see **Section 9.2**). A state-of-the-art, high repetition-rate, high power laser – essential for science in the area of X-ray non-linear interactions (see **Chapter 3**) and matter at extreme conditions research (see **Chapter 4**) – will also be able to launch synchronised energetic electrons or ions/protons into the sample at the interaction point, permitting a wide range of new experiments for material science, defence and astrophysical applications.

2.5.8 Further considerations

Only a sample of the possibilities for unique capability in a next-generation XFEL are covered above. It is also expected that advanced undulators[78] (e.g. superconducting) and ultra-low emittance electron sources will **extend photon energy reach** for a given electron beam energy, as well as facilitating higher energy per pulse. Harmonic lasing[79] will offer intense X-rays at higher photon energies, too. In addition to combining X-rays with other advanced capabilities, **the two-colour (or multi-colour) FEL capability[80,81] could be greatly enhanced** in a facility designed for this purpose, with broader ranges of temporal and spectral separation. Advances are anticipated in the control of pulse structures beyond that already described, to include **control of polarisation, orbital angular momentum and carrier-envelope phase**. It is expected that **facility capacity can be increased**, e.g. following the approach of using fast-kickers demonstrated at the European XFEL, and advanced controls incorporating machine learning will enable more **rapid optimisation and restoration of setups**.

2.6 Overview of Science and Technology Case

This Science and Technology Case contains an analysis of the scientific and technological opportunities that can be addressed by a next-generation XFEL. These opportunities exist across a broad range of disciplines – physics and X-ray photonics, matter at extreme conditions, quantum and nanomaterials, chemical sciences and energy, and the life sciences – with applications to industry, medicine and defence. These opportunities are discussed in their respective chapters (**3 to 8**). In **Chapter 9**, we examine the technical capabilities required to capture these opportunities, and discuss how the integration with other capabilities in the UK landscape will be vital. Within that chapter we also present a set of **Flagship Scientific Programmes** that would be enabled by a next-generation XFEL to illustrate high potential for new science and technology. In **Chapter 10**, we look at the strategic alignment of the Science and Technology Case for a next-generation XFEL with the UK's industrial strategy, with defence and with various industrial sectors, and consider the potential for international engagement. A set of Appendices is included that present: the broader developing methodological landscape (**Appendix 1**); assessments of synergies with other technologies and potential upgrade paths (**Appendix 2**); and a survey of the community engagement exercises undertaken (**Appendix 3**).

2.7 References for Chapter 2

1 A.M. Kondratenko and E.L.Saldin, "Generation of coherent radiation by a relativistic electron beam in an ondulator," *Part. Accel.* **10**, 207-216 (1980)

2 R. Bonifacio, C. Pellegrini and L.M. Narducci, "Collective instabilities and high-gain regime in a free electron laser", *Opt.Comm.* **50**, 373 (1984) DOI: 10.1016/0030-4018(84)90105-6

3 W. Ackermann, G. Asova, V. Ayvazyan *et al.* "Operation of a Free Electron Laser in the Wavelength Range from the Extreme Ultraviolet to the Water Window," *Nat. Photonics* **1**, 336-342 (2007) DOI: 10.1038/nphoton.2007.76

4 P. Emma, R. Akre, J. Artur *et al.* "First lasing and operation of an ångstrom-wavelength free electron laser," *Nat. Photonics* **4**, 64 (2010) DOI: 10.1038/NPHOTON.2010.176

5 J. Madey, "Stimulated emission of bremsstrahlung in a periodic magnetic field," *J.Applied Physics* **42**, 1906 (1971) DOI: 10.1063/1.1660466

6 E. Allaria, R. Appio, L. Badano *et al.* "Highly coherent and stable pulses from the FERMI seeded free-electron laser in the extreme ultraviolet," *Nat. Photonics* **6**, 699 (2012) DOI: 10.1038/nphoton.2012.233

7 J. Duris, S. Li, T. Driver *et al.* "Tunable isolated attosecond X-ray pulses with gigawatt peak power from a free-electron laser," *Nat. Photonics* **14**, 30 (2020) DOI: 10.1038/s41566-019-0549-5

8 Ph. Wernet, K. Kunnus, I. Josefsson *et al.* "Orbital-specific mapping of the ligand exchange dynamics of $Fe(CO)_5$ in solution" *Nature* **520**, 78 (2015) DOI: 10.1038/nature14296

9 W. Zhang, R. Alonso-Mori, U. Bergmann *et al.* "Tracking excited-state charge and spin dynamics in iron coordination complexes" *Nature* **509**, 345 (2014) DOI: 10.1038/nature13252

10 J. Kern, R. Chatterjee, I.D. Young *et al.* "Structures of the intermediates of Kok's photosynthetic water oxidation clock," *Nature* **563**, 421-425 (2018) DOI: 10.1038/s41586-018-0681-2

11 M.G. Gorman, R. Briggs, E.E. McBride *et al.* "Direct observation of melting in shock compressed bismuth with fs X-ray diffraction *PRL* **115**, 095701 (2015) DOI: 10.1103/PhysRevLett.115.095701

12 L.B. Fletcher, H.J. Lee, T. Döppner *et al.* "Ultra-bright X-ray laser scattering for dynamic warm dense matter physics" *Nature Photon* **9**, 274-279 (2015) DOI: 10.1038/nphoton.2015.41

13 M. Först, R.I Tobey, H. Bromberger *et al.* "Melting of charge stripes in vibrationally driven $La_{1.875}Ba_{0.125}CuO_4$: Assessing the Respective Roles of Electronic and Lattice Order in Frustrated Superconductors," *Phys. Rev. Lett.* **112**, 157002 (2014) DOI: 10.1103/PhysRevLett.112.157002

14 R. Mankowsky, A. Subedi, M. Först *et al.* "Nonlinear lattice dynamics as a basis for enhanced superconductivity in $YBa_2Cu_3O_{6.5}$," *Nature* **516**, 71-73 (2014) DOI: 10.1038/nature13875

15 A. Barty, S. Boutet, M. Bogan *et al.* "Ultrafast single-shot diffraction imaging of nanoscale dynamics," *Nature Photon* **2**, 415–419 (2008). DOI: 10.1038/nphoton.2008.128

16 C. Kupitz, S. Basu, I. Grotjohann *et al.* "Serial time resolved crystallography of photosystem II using a femtosecond X-ray laser," *Nature* **513**, 261-265 (2014) DOI: 10.1038/nature13453

17 L. Redecke, K. Nass, D.P. DePonte *et al.* "Natively inhibited Trypanosoma brucei cathepsin B structure determined by using an X-ray laser" *Science* **339**, 227 (2013) DOI: 10.1126/science.1229663

18 Q. Zhou, Y. Lai, T. Bacaj *et al.* "Architecture of the synaptotagmin-SNARE machinery for neuronal exocytosis" *Nature* **525**, 62-67 (2015) DOI: 10.1038/nature14975

19 K.Pande, C.M. Hutchison, G. Groenhof *et al.* "Femtosecond structural dynamics drives the trans/cis isomerization in photoactive yellow protein" *Science* **352**, 725-729 (2016) DOI: 10.1126/science.aad5081

20 A. Hosseinizadeh, G. Mashayekhi, J. Copperman *et al.* "Conformational landscape of a virus by single-particle X-ray scattering" *Nat Methods* **14**, 877-881 (2017) DOI: 10.1038/nmeth.4395

21 H.N. Chapman *et al.* "Femtosecond X-ray protein nanocrystallography" *Nature* **470**, 73–77 (2011) DOI: 10.1038/nature09750

22 P.K. Maroju *et al*. "Attosecond pulse shaping using a seeded free-electron laser" *Nature* **578**, 386–391 (2020) DOI: 10.1038/s41586-020-2005-6

23 J. Coakley *et al*. "Femtosecond quantification of void evolution during rapid material failure," *Sci. Adv*. **6**: eabb4434 (2020) DOI: 10.1126/sciadv.abb4434

24 F. Roth *et al*. "Direct observation of charge separation in an organic light harvesting system by femtosecond time-resolved XPS" *Nat. Comms*, **12**:1196 (2021) DOI: 10.1038/s41467-021-21454-3

25 T.S. Holdstadt *et al.* "Real-time imaging of acoustic waves in bulk materials with X-ray microscopy " *PNAS* **120**, 39, e2307049120 (2023) DOI: 10.1073/pnas.2307049120

26 S. Li *et al.* "Attosecond-pump attosecond-probe X-ray spectroscopy of liquid water" *Science* **383**, Issue 6687 1118-1122 (2024) DOI: 10.1126/science.adn6059

27 Y. Shvyd'ko *et al*. "Resonant X-ray excitation of the nuclear clock isomer 45Sc" *Nature,* **622**, 471 (2023) DOI: 10.1038/s41586-023-06491-w

28 S. Li *et al.* "Attosecond coherent electron motion in Auger-Meitner decay " *Science* **375**, Issue 6578, 285-290 (2022) DOI: 10.1126/science.abj2096

[29] M. Frost *et al*. "Diamond precipitation dynamics from hydrocarbons at icy planet interior conditions," *Nature Astronomy* **8**, 174-181 (2024) DOI: 10.1038/s41550-023-02147-x

[30] D. Kraus *et al*. "The structure of liquid carbon elucidated by in situ X-ray diffraction," *Nature* **642**, 351-355 (2025) DOI: 10.1038/s41586-025-09035-6

[31] T.G. White, T.D. Griffin, D. Haden *et al.* "Superheating gold beyond the predicted entropy catastrophe threshold," *Nature* **643**, 950–954 (2025) DOI: 10.1038/s41586-025-09253-y

[32] S. Wall *et al.* "Ultrafast disordering of vanadium dimers in photoexcited VO_2" *Science* **362**, 572-576 (2018) DOI: 10.1126/science.aau3873

[33] C. Dornes, Y. Acremann, M. Savoini *et al*. "The ultrafast Einstein-de Haas effect," *Nature* **565**, 209-212 (2019) DOI: 10.1038/s41586-018-0822-7

[34] Z-H. Loh *et al.* "Observation of the fastest chemical processes in the radiolysis of water," *Science,* **367**, Issue 6474, 179-182 (2020) DOI: 10.1126/science.aaz474

[35] R.M. Jay *et al.* "Tracking C–H activation with orbital resolution," *Science,* **380**, Issue 6648, 955-960 (2023) DOI: 10.1126/science.adf8042

[36] X. Edward Zhou *et al.* "Identification of Phosphorylation Codes for Arrestin Recruitment by G Protein-Coupled Receptors," *Cell* **170**, 457–469, (2017) DOI: 10.1016/j.cell.2017.07.002

[37] T. Gruhl *et a*l. "Ultrafast structural changes direct the first molecular events of vision," *Nature* **615**, 939-944 (2023) DOI:10.1038/s41586-023-05863-6

[38] A. Bhowmick *et al.* "Structural evidence for intermediates during O_2 formation in photosystem II" *Nature* **617**, 629-636 (2023) DOI: 10.1038/s41586-023-06038-z

[39] H. Li et al. Oxygen-evolving photosystem II structures during S1–S2–S3 transitions. Nature 626, 670-677, doi:10.1038/s41586-023-06987-5 (2024)

[40] W.H. Bragg and W.L. Bragg, "The reflexion of X-rays by crystals," *Proc. R. Soc. Lond. A*. **88**, 428-38 (1913) DOI: 10.1098/rspa.1913.0040

[41] D. Sayre, "Some implications of a theorem due to Shannon," *Acta. Cryst*. **5**, 843-843 (1952) DOI: 10.1107/S0365110X52002276

[42] J. Miao, P. Charalambous, J. Kirz *et al.* "Extending the methodology of X-ray crystallography to allow imaging of micrometre-sized non-crystalline specimens," *Nature* **400**, 342-344 (1999) DOI: 10.1038/22498

[43] M.M. Siebert, T. Ekeberg, F. Maia *et al.* "Single mimivirus particles intercepted and imaged with an X-ray laser," *Nature* **470**, 78-81 (2011) DOI: 10.1038/nature09748

[44] J.N. Clark, L. Beitra, G. Xiong *et al.* "Ultrafast three-dimensional imaging of lattice dynamics in individual gold nanocrystals," *Science* **341**, 6141 (2013) DOI: 10.1126/science.1236034

[45] J.M. Glownia, A. Natan, J.P. Cryan *et al.* "Self-referenced coherent diffraction X-ray movie of Angstrom and femtosecond-scale atomic motion," *Phys. Rev. Lett*. **117**, 153003 (2016) DOI: 10.1103/PhysRevLett.117.153003

[46] T. Ishikawa, S.A. Hayes, S. Keskin *et al.* "Direct observation of collective modes coupled to molecular orbital-driven charge transfer," *Science* **350**, 1501-1505 (2015) DOI: 10.1126/science.aab3480

[47] M.Z. Mo, Z. Chen, R.K. Li *et al*. "Heterogeneous to homogeneous melting transition visualized with ultrafast electron diffraction," *Science* **360**, 1451-1455 (2018) DOI: 10.1126/science.aar2058

[48] J. Yang, X. Zhu, J.A. Thomas *et al.* "Imaging CF_3I conical intersection and photodissociation dynamics with ultrafast electron dynamics," *Science* **361**, 64-67 (2018) DOI: 10.1126/science.aat0049

[49] M. Harmand, R. Coffee, M. Bionta *et al.* "Achieving few-femtosecond time-sorting at hard X-ray free-electron lasers". *Nature Photon* **7**, 215-218 (2013) DOI: 10.1038/nphoton.2013.11

[50] M.R. Bionta, N. Hartmann, M. Weaver *et al.* "Spectral encoding method for measuring the relative arrival time between X-ray/optical pulses," Rev. Sci. Instrum. **85**(8):083116 (2014) DOI: 10.1063/1.4893657

[51] N. Hartmann, G. Hartmann, R. Heider *et al.* "Attosecond time-energy structure of X-ray free-electron laser pulses," *Nature Photon* **12**, 215–220 (2018) DOI: 10.1038/s41566-018-0107-6

[52] Y. Ding, C. Behrens, P. Emma *et al.* "Femtosecond X-ray pulse temporal characterization in free-electron lasers using a transverse deflector," Phys. Rev. ST Accel. Beams **14**, 120701 (2011) DOI: 10.1103/PhysRevSTAB.14.120701

[53] A. Fahlman, C. Nordling, K. Siegbahn *et al.* "ESCA: atomic, molecular and solid state structure studied by means of electron spectroscopy," Uppsala: Almqvist and Wiksell (1967)

[54] L. Meitner, "Über die Entstehung der β-Strahl-Spektren radioaktiver Substanzen," *Z. Physik* **9**, 131-144 (1922) DOI: 10.1007/BF01326962

[55] T.J.A. Wolf, R.H. Myhre, J.P. Cryan *et al.* "Probing ultrafast ππ* /nπ* internal conversion in organic chromophores via K-edge resonant absorption," *Nat. Commun*. **8**, 29 (2017) DOI: 10.1038/s41467-017-00069-7

[56] M. Drescher, M. Hentschel, R. Kienberger *et al.* "Time-resolved atomic inner-shell spectroscopy," *Nature* **419**, 803–807 (2002) DOI: 10.1038/nature01143

[57] J. Stöhr, "NEXAFS Spectroscopy," *Springer Series in Surface Sciences* **25** (1992) DOI: 10.1007/978-3-662-02853-7

[58] J.J. Rehr and R.C. Albers, "Theoretical approaches to X-ray absorption fine structure," *Rev. Mod. Phys*. **72** 621-654 (2000) DOI: 10.1103/RevModPhys.72.621

[59] M.M. Dean, Y. Cao, X. Liu *et al.* "Ultrafast energy- and momentum-resolved dynamics of magnetic correlations in the photo-doped Mott insulator

Sr_2IrO_4," *Nature Mater* **15**, 601-605 (2016) DOI: 10.1038/nmat4641

[60] C. Weninger, M. Purvis, D. Ryan *et al.* "Stimulated electronic X-ray Raman scattering," *Phys. Rev. Lett.* **111**, 233902 (2013) DOI: 10.1103/PhysRevLett.111.233902

[61] T. Kroll, C. Weninger, R. Alonsi-Mori *et al.* "Stimulated X-ray emission spectroscopy in transition metal complexes," *Phys. Rev. Lett.* **120**, 133203 (2018) DOI: 10.1103/PhysRevLett.120.133203

[62] J.D. Biggs, Y. Zhang, D. Healion, S. Mukamel, "Watching energy transfer in metalloporphyrin heterodimers using stimulated X-ray Raman spectroscopy," *Proc Natl Acad Sci USA* **110**(39):15597-15601 (2013) DOI: 10.1073/pnas.1308604110

[63] J.R. Rouxel, M. Kowalewski, K. Bennett, S. Mukamel, "X-ray sum frequency diffraction for direct imaging of ultrafast electron dynamics," *Phys. Rev. Lett*. **120**, 243902 (2018) DOI: 10.1103/PhysRevLett.120.243902

[64] P. Vagovic *et al.* "Megahertz X-ray microscopy at X-ray free electron lasers and synchrotron sources," *Optica* **6**, 1106 (2019) DOI: 10.1364/OPTICA6.001106

[65] J.C.P. Koliyadu *et al.* "Development of MHz phase contrast imaging at the European XFEL," *Journal of Synchrotron Radiation* **32**, 17 (2025) DOI: 10.1107/S160057724009860X

[66] U. Bergmann *et al.* "Chemical mapping of ancient artifacts and fossils," *Synchrotron Light Sources and Free Electron Lasers* (ed E.J. Jaeschke *et al.),* p2393 (2020) DOI: 10.1007978-3-030-23201-6-6_77

[67] M. Amati *et al.* "Looking at ancient objects under a different light: cultural heritage at Elettra," *Radiation Effects and Defects in Solids*, **177**, 1271 (2022) DOI: 10.1080/10420150.2022.2136080

[68] E. Elia and D. Baratto, "Recent developments in X-ray imaging applied to cultural heritage," 14th International Conference on non-destructive investigations and microanalysis for the diagnostics and conservation of cultural and environmental heritage - 2023 - Brescia (Italy) (art 2023)

[69] P. Rebernik Ribič, A. Abrami, L. Badano *et al.* "Coherent soft X-ray pulses from an echo-enabled harmonic generation free-electron laser," *Nat. Photonics* **13**, 555-561 (2019) DOI: 10.1038/s41566-019-0427-1

[70] F. Bencivenga, R. Mincigrucci, F.Capotondi *et al.* "Nanoscale transient gratings excited and probed by extreme ultraviolet femtosecond pulses," *Science Advances* **5**, eaaw5805 (2019) DOI: 10.1126/sciadv.aaw5805

[71] S. Liu, W. Decking, V. Kocharyan *et al.* "Preparing for high-repetition rate hard X-ray self seeding at the European X-ray Free Electron Laser: Challenges and opportunities," *Phys. Rev. Accel. Beams* **22**, 060704 (2019) DOI: 10.1103/PhysRevAccelBeams.22.060704

[72] N.R. Thompson *et al.* "Improved Temporal Coherence in SASE FELs," *Proc. IPAC2010* **TUPE050** 2257-2259 (2010)

[73] B.W.J. McNeil, N.R. Thompson, D.J. Dunning, "Transform-Limited X-ray Pulse Generation from a High-Brightness Self-Amplified Spontaneous-Emission Free-Electron Laser," *Phys. Rev. Lett*. **110**, 134802 (2013) DOI: 10.1103/PhysRevLett.110.134802

[74] K.-J. Kim, Y. Shvyd'ko, S. Reiche, "A proposal for an X-ray free-electron laser oscillator with an energy-recovery linac," *Phys. Rev. Lett*. **100** 244802 (2008) DOI: 10.1103/PhysRevLett.100.244802

[75] Rauer, P., Bahns, I., Friedrich, B. *et al.* Lasing of a cavity-based X-ray source. *Nature* **650**, 93–96 (2026). DOI: 10.1038/s41586-025-10025-x

[76] W.S. Graves *et al.* "ASU Compact XFEL," *Proc. of FEL2017* DOI: 10.18429/JACoW-FEL2017-TUB03

[77] W. M. Fawley *et al.* "Tapered undulators for SASE FELs," *Nucl. Instrum. Meth.A* **483**, 537-541 (2002) DOI: 10.1016/S0168-9002(02)00377-7

[78] F. Nguyen *et al.* "Technologies for the Compact Light undulator," *XLS-Report-2019-004* (2019)

[79] E.A. Schneidmiller *et al.* "First operation of a harmonic lasing self-seeded free electron laser," *Phys. Rev. Accel. Beams* **20**, 020705 (2017) DOI: 10.1103/PhysRevAccelBeams.20.020705

[80] A. Marinelli, D. Ratner, A. Lutman *et al.* "High-intensity double-pulse X-ray free-electron laser," *Nat Commun* **6**, 6369 (2015) DOI: 10.1038/ncomms7369

[81] A. Lutman, T. Maxwell. J. MacArthur *et al.* "Fresh-slice multicolour X-ray free-electron lasers," *Nature Photon* **10**, 745-750 (2015) DOI: 10.1038/nphoton.2016.201

3. Science Opportunities in Physics and X-ray Photonics

High intensity, ultrashort pulses of X-rays create new possibilities in physics and new potential in X-ray photonics that will find future application across the sciences. Here we consider new basic physics enabled by XFELs, and the exciting science opportunities provided by new X-ray based measurement methods. Further we identify new scientific opportunities enabled by the access to the high-quality relativistic electron beam in addition to the generation of X-rays.

Physics, and the exploration of new physical principles and methods, has been a major driver in the development of new light sources and their applications in science. From X-ray diffraction to the broad range of X-ray spectroscopy, the initial steps required the elucidation of physical principles, refinement of the measurement and analysis methods, and development of new instrumentation, in which physics played a primary and driving role. Given the unique new X-ray properties on offer from next-generation XFELs, for instance ultrashort pulses, large coherent bandwidth and ultra-high brightness, it is imperative that the new X-ray photonics and the physics of their interaction with matter is fully explored, not only because of the basic physics interest in its own right, but also in order to spur the development of new measurement methods and applications for future science. Moreover, these unique X-ray characteristics provide opportunities for fundamental physics experiments and tests. This section explores a range of these opportunities, with an emphasis on looking forwards to exciting new discoveries and frontiers.

The new capabilities are poised to answer some basic questions in the physical sciences, many of which have the potential to find wide application in other disciplines including:

- What role does electronic quantum coherence play in the photo-excitation of matter?
- How do electron-nuclear couplings proceed and what role do conical intersections play in chemical reactions?
- What are the dynamical mechanisms for radiation damage in materials and biomolecules?
- Can we map the conformational pathways of macromolecules traversing their energy landscape as they perform their function?
- Can we use X-rays to detect dark matter and for other fundamental tests?

First, in **Section 3.1**, we examine the basic interaction of intense X-rays with matter, and the opportunities this affords in chemical physics and solving basic questions of energy and charge transfer following photoexcitation, which can be applied to understanding the dynamics of radiation damage of biomolecules, probing and controlling chirality, and developing new probes for ultrafast quantum coherent phenomena. Next, in **Section 3.2**, we review new opportunities in X-ray scattering that go beyond the conventional approaches of elastic non-resonant scattering and employ new concepts, by exploiting higher order photon correlation functions, quantum imaging concepts, inelastic scattering and signatures of electronic coherence in scattering. In **Section 3.3**, we look at the new opportunities unlocked by the attosecond domain X-ray pulses that are now available, which includes the ultrafast probing of electronic coherence in new pump-probe X-ray spectroscopies. There is also the potential to exploit the large coherent bandwidth to develop new classes of non-linear X-ray spectroscopy that are able to fully follow the propagation in space and time of electronic excitations in matter, and their decoherence pathways. In **Section 3.4**, we consider the options opened by using high repetition-rate coherent diffraction imaging and related methods, along with AI algorithms, to track the trajectory of molecular conformational change through the complex energy landscapes typical of biological and liquid systems. In **Section 3.5**, we turn to tests of fundamental X-ray interaction physics, looking at non-linear QED physics and the potential for tests of the Standard Model using X-rays of extreme brightness in a facility offering a high repetition rate in order to capture rare events. Finally, in **Section 3.6**, we consider the added opportunity of directly using the high-quality relativistic electron beam that drives the XFEL to investigate new approaches in future accelerator and light source physics, and to drive a new generation of kaon science experiments.

3.1 Frontiers in ultrafast chemical physics

Ultrafast X-ray probing provides unprecedented insight into how energy and charge is transferred within and between molecules in processes such as photoexcitation or X-ray ionisation. Taking inspiration from non-linear optical spectroscopy techniques, and implementing them in the X-ray regime, will enable dynamic probing of electronic properties and their coupling to molecular structure. These techniques will prove key in finding answers to questions such as how DNA responds to ionising radiation and how to control photophysical processes at the quantum level.

3.1.1 Introduction

Interactions between light and molecules were essential to the development of the conditions that made possible life on Earth. Irradiation of interstellar media created the molecular building blocks of life, while absorption and conversion of solar energy continue to sustain the processes that allow complex life to thrive. Light interactions are also critical for studying molecules during chemical reactions and biological processes, illuminating the structure and dynamics of reactants, catalysts and products as they evolve in time.

Conversion of light energy into molecular potential energy is initiated by the displacement of electrons in the molecule by an electromagnetic field. Coupling of electronic states results in charge displacement, which occurs on extremely fast (attosecond) timescales. Understanding and/or controlling how this charge is subsequently transferred and coupled to the molecular structure is key to determining how this energy is used to break or form bonds.

Photochemical processes are found in natural systems, such as those that govern vision,[1] vitamin D production,[2] photosynthesis,[3] UV photo-protection of DNA bases,[4] and the magnetic "vision" of migrating birds.[5] The charge transfer at the heart of these processes is equally relevant in determining the function of catalysts and batteries, and combustion and corrosion/degradation processes, enabling them to be optimised for particular applications. Questions remain about how electromagnetic energy is converted into chemical or electrical energy via coupling of electronic excitation into the molecular framework, with the experimental and theoretical tools available today unable to provide comprehensive answers.

Chemistry has predominantly relied upon an adiabatic description of chemical processes, where any atomic motion results in an almost instantaneous rearrangement of the electrons that "glue" the atoms together via bonds. In most situations, this assumption – known as the Born-Oppenheimer (BO) approximation – is reasonable, as the electrons are lighter and therefore move faster than the atoms. Following absorption of a photon, however, the potential energy surface of the excited electronic state has points or seams, called conical intersections, which cross with other electronic states. Near these intersections, as the separation of the electronic states becomes smaller, electron wavepacket motion slows down to the point where it becomes similar in magnitude to the motion of the atoms, and the BO approximation breaks down.

Theoretical simulations of molecules at conical intersections are particularly challenging to model, as the electronic and atomic motion cannot be de-coupled. With current models and computing power, this complex behaviour cannot be described accurately, even for relatively simple molecules, without significant approximation. Likewise, experimental methods currently lack the tools and observables that can broadly probe the motion of the system through a conical intersection.

3.1.2 New X-ray spectroscopy techniques

A range of ultrafast X-ray spectroscopy techniques has been developed at XFELs to exploit site-selective absorption by inner shell electrons in molecules. For example, X-ray near edge absorption spectroscopy, X-ray fluorescence spectroscopy, resonant inelastic X-ray scattering, and X-ray angle resolved photoelectron spectroscopy have been used as sensitive probes of chemical states and

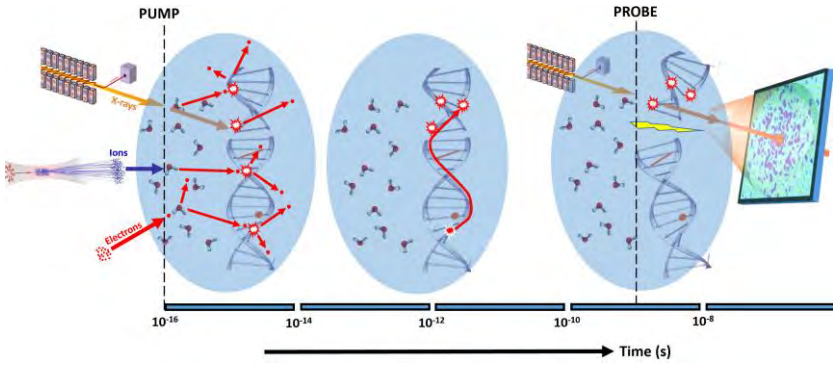
electronic structure. The advent of beamlines producing circularly polarised X-rays[6] has also enabled the chiral and magnetic properties of molecules and materials to be probed.

The high brightness and ultrafast pulse capability of free electron lasers revolutionises X-ray spectroscopy by bringing it into the non-linear regime, facilitating the study of dynamical chemical processes with unprecedented temporal and spatial resolution. Non-linear spectroscopy, based on various absorption, fluorescence, wave mixing and Raman schemes, has already been exploited in the optical domain to reveal details of the inter- and intra-molecular processes that govern transient chemical dynamics. This has shown how motion at the atomic level influences complex molecules and their biological function, but by translating these techniques into the X-ray regime with an XFEL, researchers can delve down to the level of the electrons that underpin all molecular behaviour. As a result, the critical electronic-nuclear couplings can be probed with atomic specificity, unravelling the behaviour at conical intersections and determining how charge and energy flows across and between molecules,[7,8] with sub-Ångström resolution.

A range of X-ray spectroscopy techniques, coupled with optical techniques and X-ray diffraction imaging, can be combined in multi-pulse schemes to stimulate, observe and even control chemical dynamics. These schemes provide a powerful toolbox to answer some fundamental questions, such as how DNA reacts to ionising radiation[9] so that the mechanisms for cancer induction are understood and new ways of enhancing radiotherapy outcomes can be developed. For example, research has shown that high dose rate radiotherapy, which can be simulated in FEL experiments, is less toxic to healthy cells than to cancer cells.[10]

Box 3.1 illustrates how a next generation XFEL could be used to study the effects of radiation on isolated or solvated DNA in extraordinary detail. Different pulsed radiation sources (electrons, ions, X-rays) would initiate an interaction. The ionisation process and initial charge migration proceeds on an attosecond timescale but, after as little as a few femtoseconds, the electron displacement couples to the molecular structure: this determines the ultimate destination of the charge, weakening or breaking bonds and transferring energy within the molecule or to its surroundings, on timescales from femtoseconds to microseconds. The electronic and nuclear coupling could be tracked over these timescales using the new non-linear spectroscopies and ultrafast diffraction available with XFEL pulses, in combination with synchronised optical lasers.

Box 3.1: Studying the effects of radiation on isolated or solvated DNA



Ionisation of DNA and its surroundings is initiated by a short burst of radiation (electrons, ions or X-rays). Charge is transferred on attosecond to picosecond timescales, ultimately causing bond cleavage and damage to the DNA. These steps can be probed at different times by XFEL pulses with linear and non-linear X-ray spectroscopies or ultrafast diffraction imaging.

(Left) Image courtesy of Lawrence Livermore National Laboratory; (Right) Diffraction image and undulator illustration by Horst Frank, reproduced under terms of the Creative Commons Attribution License 3.0 BY

The development of new X-ray spectroscopies could be transformative for our understanding of one of the most fundamental processes in photo-chemistry – the coupling of different electronic states at conical intersections that act as 'gateways' through which excited molecules can undergo rapid, non-radiative de-excitation. For example, these transitions lead to the UV stability of DNA bases, which is essential for the development of life. Despite absorbing strongly in the ultraviolet, these molecules are able to dissipate excited electronic energy into vibrational energy (and eventually into the surrounding environment) via conical intersections. Normally the Born-Oppenheimer approximation is used to theoretically model the dynamics of excited molecular states, as the timescale for electronic motion is much faster than that of the nuclei. In the vicinity of degeneracies between two potential energy surfaces, however, these timescales are similar and de-coupling of the electron and nuclear motion is not possible.

Obtaining direct evidence of the behaviour at a conical intersection is just as challenging for experiments. Existing pump-probe techniques are incapable of tracking the structural dynamics at conical intersections with sufficient temporal resolution (typically 10 fs or less). Few-femtosecond pulses are available at optical frequencies, but the uncertainty principle means such pulses are unable to spectrally resolve passage through the conical intersection. Instead, the presence and action of conical intersections is indirectly inferred from measured decay rates. Similarly, techniques like ultrafast electron diffraction and time-resolved X-ray diffraction have so far lacked the necessary temporal resolution to follow de-excitation through conical intersections.

The capability of XFELs to produce ultrashort pulses at X-ray frequencies provides access to tools with sufficient temporal and spatial resolution to track molecular dynamics at conical intersections. This tracking could be achieved through a number of complementary approaches (see below) based on both spectroscopy and scattering (see **Sections 3.2** and **3.4**).

Attosecond Transient Absorption Spectroscopy (ATAS)

In transient absorption spectroscopy, the bandwidth of ultrashort pulses is exploited to give spectroscopic as well as temporal resolution of a dynamic process. The use of X-ray pulses enables changes to be tracked through core transitions that are sensitive to the electronic and structural dynamics in the molecule. Using soft X-ray pulses from high harmonic generation, it was demonstrated that following ionisation of ethylene into an excited state of the cation, relaxation to the ground state through a conical intersection took only 7 fs.[11] The speed of this transition indicates that electronic coherence might be maintained and potentially controlled during these transitions. Attosecond XFEL pulses offer much higher fluxes, temporal resolution and site-specific absorption so that investigations of conical intersections in much larger molecules will become possible. ATAS has already been used to resolve a long-standing question about the structural motifs of liquid water, which was only possible due to the attosecond capability at LCLS for both the pump and probe pulses.[12] These opportunities are discussed further in **Section 3.3**.

Time-Resolved X-ray Photo-Electron and Auger Electron Spectroscopy (TR-XPES and TR-XAES)

If the X-ray absorption leads to a transition to the continuum, the energies of the photoelectrons provide an alternative probe of the molecular dynamics. Compared to absorption spectroscopy, this approach has a higher detection efficiency and is particularly sensitive to the electronic dynamics. This could provide a way of probing core electronic dynamics for the first time. For example, an attosecond XFEL pulse could excite a core electron wavepacket and the second harmonic be used to ionise a core electron with the energy of the photoelectron modulated by the charge oscillations.[13] Auger-Meitner decay of the core hole left behind could provide additional insight. As this process is particularly sensitive to bond lengths in the vicinity of the core hole and the local electronic structure, it has the potential to track non-BO behaviour at conical intersections. The combination of time-resolved XPES and XAES is a powerful tool through which charge flow and molecular configuration can be observed, such as showing how light harvesting complexes can efficiently inject charge into semiconductor nanostructures.[14]

X-ray Stimulated Raman Scattering (XSRS)

Raman spectroscopy is extensively used in the optical regime via spontaneous or stimulated scattering. In the X-ray regime, stimulated Raman scattering of core transitions localised around specific atoms has the potential to both generate and probe electronic wavepackets in molecules.[15] This is challenging to realise experimentally as it is a non-linear process requiring a range of wavelengths. The intensity, bandwidth and wavelength tunability of attosecond XFEL pulses provide the opportunity for impulsive stimulated X-ray Raman scattering (ISXRS) studies of the dynamics of conical intersections and charge flow in molecules. Numerous promising multi-dimensional IXSRS-based schemes have been proposed theoretically but have yet to be fully implemented experimentally.[16,17,18,] This is discussed further in **Section 3.3.4**.

3.1.3 Chiral X-ray probes

One of the most intriguing scientific questions is why the molecular building blocks of life on Earth, such as amino acids and sugars, exist predominantly with 'one handedness.' This reflection asymmetry in molecules was termed *chirality* by Kelvin, and the mirror images are known as *enantiomers*. As a consequence of this chirality, the action of most biological processes depends critically on the handedness of receptors, enzymes and drugs. Currently, the only way of identifying enantiomers is through interaction with another chiral object of known handedness. While circularly polarised light has long been exploited to help reveal structural asymmetries in molecules, the very small differences in the interaction of circularly polarised light with the opposite enantiomers limits the ability of light to identify and control molecular chirality. These chiroptical effects are weak because, from a molecule's perspective, the electric field's spiral rotation is much longer than the dimensions of the molecule itself, i.e. it is not present in the dipole approximation. Chiral differentiation relies on magnetic dipole and electric quadrupole interactions, which are orders of magnitude weaker, such that differences in the excitation rates of left- and right-handed enantiomers (circular dichroism) is typically <0.1%.

Chiral interactions can, however, be amplified in the X-ray regime and be used to interrogate different parts of molecules. When this is combined with the time resolution and complex polarisation offered by next-generation XFEL facilities, chirality will be able to be probed and even controlled across the spatial and temporal landscapes of molecules.

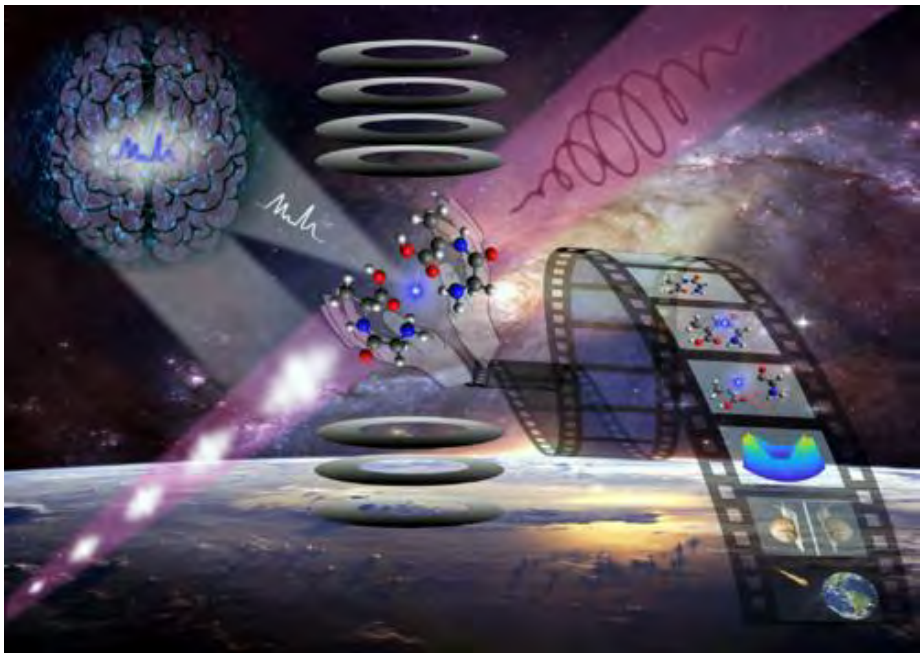


Figure 3.1: An artist's impression of how optical and XFEL pulses can be combined to reveal and control chiral molecular dynamics, through optimisation of the pulse shape and polarisation

Figure reproduced Ilchen et al.[37] under the terms of the Creative Commons Attribution 4.0 International

X-ray Circular Dichroism (XCD)

Time-resolved studies using circular dichroism at optical wavelengths are challenging but can give a unique insight into the chemical reaction dynamics of chiral molecules.[19] As the contribution of multipole interaction scales as a/λ for each higher order, where a is the molecular length scale, XCD is much stronger than in the optical domain. The power of XCD to probe the spatial extent of chiral centres has already been realised for static molecular structures.[20] XFELs could be used in pump-probe experiments to observe how chirality evolves within molecules on ultrafast timescales. For example, **Figure 3.2** demonstrates a proposed experiment in which transient chirality induced in an achiral molecule by a circularly polarised UV pulse could be probed by X-ray circular dichroism.[21] Time-resolved, magnetically-induced circular dichroism with X-rays has also been proposed as a way of interrogating electronic coherences found in excited molecules passing through conical intersections.

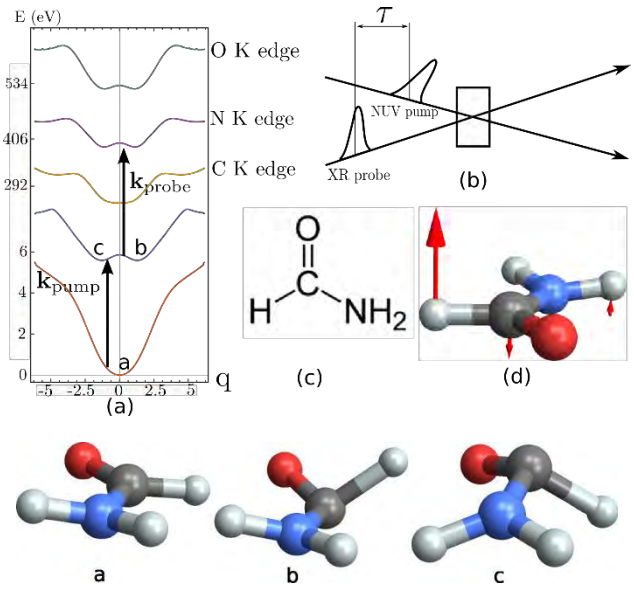


Figure 3.2: Potential for inducing, probing and controlling chirality [21]

Chiral induction and ultrafast reversal in the planar molecule formamide: The formamide molecule is excited into a state which oscillates between two opposite chiral configurations. This transient chirality could be probed by circular dichroism in X-ray absorption or photoionisation. Such a flagship experiment offers a first step on the road to exploiting light to control the creation and/or separation of specific enantiomers.

*Figure reproduced from J.R. Rouxel et al. Structural Dynamics **4**, 044006 (2017) under the terms of a Creative Commons Attribution (CC BY) license. DOI: 10.1063/1.4974260*

Photoelectron Circular Dichroism (PECD)

Rather than relying on differential absorption rates in molecules, analysis of the angular distribution of photoelectrons provides even greater asymmetries, typically 1-20%.[22,23,24] This photoelectron circular dichroism (PECD) originates from the interaction of the outgoing electron with the chiral potential of the molecule, with the electron being preferentially scattered parallel or anti-parallel to the light direction. As this is manifested in the dipole approximation, it is prevalent whether a valence or inner shell is being ionised,[25] and is present in the single photon, multiphoton and tunnelling ionisation regimes.[26] As PECD is also very sensitive to the molecular potential and orientation, it has been shown to be a sensitive observable of chiral dynamics.[27,28] In a recent experiment, 10fs electronic dynamics were captured in enantiomers of methyl lactate.[29]

There is now the opportunity to conduct time-resolved X-ray PECD experiments through the installation of helical undulators at XFELs. In a two-colour X-ray pump – X-ray probe experiment on trifluoromethyloxirane at LCLS, ionisation of a 1s electron from one of the fluorine atoms initiated fast Coulomb explosion of the molecule, which was probed by measuring the PECD from 1s ionisation in another fluorine atom, allowing the dissociation process to be tracked.[30] In another experiment at FERMI, localised, time-resolved PECD within a chiral enantiomer was achieved for the first time.[31] By exploiting the chemical shift in the K edge of the carbon atoms in fenchone between the ground state

and a 3s Rydberg state populated with a UV pump pulse, the core level chiral signal originating from the carbon atoms near the carbonyl group was identified. With the help of theoretical calculations, site specific contributions to the overall PECD, and how they dynamically evolve as the 3s state decays, were determined. This provided the first demonstration of how XFELs can be used to determine localised, dynamic contributions to the circular dichroism in chiral molecules.

These pioneering experiments show how chiral dynamics can be studied in isolated molecules, but there will also be future opportunities to measure X-ray PECD for liquid and solvated targets. This has already been demonstrated for core C(1s) photoionisation at synchrotrons in liquid jets of fenchone[32] and an aqueous solution of the amino acid alanine.[33] The latter experiment allowed the local PECD contributions of each of alanine's carbon atoms to be determined and showed that these were sensitive to changes in the molecular structure induced by protonation or de-protonation through control of the pH of the solution. Translation of these techniques to XFEL facilities would enable *in situ* studies of site-specific dynamics within biomolecules.[34]

A phenomenon related to PECD is photoexcitation circular dichroism, where a superposition of excited states creates chiral electron wavepackets,[35] which can be induced even in an achiral system. The chirality of this transient state could be probed with an XFEL pulse by direct ionisation at energies well above the threshold, so that its chirality is projected onto the photoelectron continuum.[36] Alternatively, nearby inner-shell orbitals could be ionised, with the low energy photoelectrons probing the chiral distribution as they emerge from the molecule. This latter technique could also use site-selective K-shell ionisation to image the chiral electron cloud in a tomographic way.

XFEL beams with exotic spin and orbital angular momentum configurations

Control of the polarisation state of XFEL pulses is crucial for studies of chiral systems as well as other forms of matter. All current XFELs have, or will be developing, beamlines with helical undulators for polarisation control.[37] Schemes are also underway to allow for fast switching between opposite polarisation states without the need for mechanical movement of the magnets within undulators. For example, at FERMI the delay between orthogonal polarisation states in cross-polarised undulators is controlled by a magnetic chicane phase shifter, so that the full range of polarisation states can be accessed within a few seconds.[38] This scheme can also be used for polarisation shaping within the combined pulse in similar way to that achieved in the optical domain.[39]

More exotic X-ray polarisation states can be accessed by overlapping orthogonal linearly polarised first and second harmonic pulses so that the electric field maps out a 'C' or '8' shape in space, depending on the phase between the two colours.[40] In these configurations there are sub-cycle variations in the rotation of the electric field vector, which have been shown to imprint chiral tensorial footprints onto photoelectron angular distributions in the optical regime (**Figure 3.3**).[41] Implementing this polarisation scheme at XFEL wavelengths offers the possibility of measuring the chiral-dependent phase transitions in the interference between 1ω and 2ω photoionisation pathways. Resonantly enhanced two photon ionisation with the fundamental could be referenced to direct photoionisation by the second harmonic in the photo-angular distribution. [41]

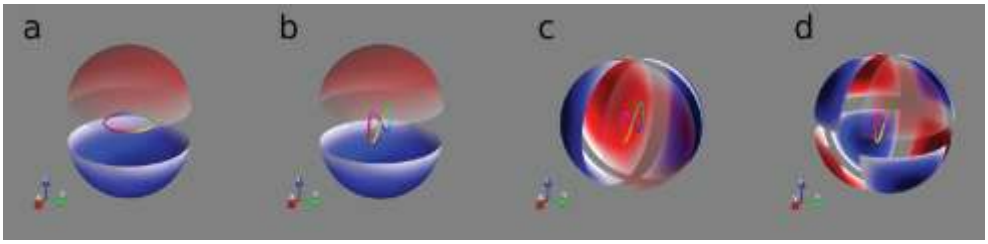


Figure 3.3: Chiral (a, c and d) and achiral (b) detection setups relative to electric fields with circular polarisation (a) and '8' polarisation (b,c,d), demonstrating detection of tensor observables for photoelectron emission from a chiral molecule.

Figure reproduced from Ordonez and Smirnova under the terms of the Creative Commons Attribution 3.0 [41]

A further ambition is to combine multiple colours in a non-collinear arrangement to create a locally chiral field which maps out a 3D Lissajous figure, enabling strong, direct coupling of the electric field to the chiral properties of the molecules via electric dipole interactions.[42] Combining optical and XFEL pulses of this nature will offer an unprecedented way of sensitively probing global and local changes in the symmetry of molecules on sub-optical cycle timescales.

The polarisation of an XFEL pulse can also be configured to vary across the wavefront[43] or, by controlling the azimuthal phase, create vortex beams that carry orbital angular momentum (OAM). OAM pulses have already been produced at FERMI, either naturally from second harmonics generated in the undulator or by introducing a spiral zone plate into the beam.[44] Combining both the spin and orbital angular momentum of the pulse provides a unique way of probing and manipulating matter.

Helical dichroism – the differential in the light absorption between the left- and right-handed OAM of light – is weak for linear interactions at optical wavelengths due to the mismatch between the length scale of the wavefront rotation and the size of the target. Stronger coupling has been found for non-linear absorption.[45] At FERMI, XUV pulses have been used to create a continuum electron wavepacket from the ionisation of helium atoms, which was dressed by a strong IR vortex laser field. The photoelectron angular distribution showed a dependence on the topological charge of the field showing that the OAM was coherently imprinted onto this emerging electron wave.[46]

Direct interactions of vortex XFEL pulses with molecules will offer stronger helical dichroism as, in principle, they can be focused down to spot sizes of a few nanometres,[47] with the potential to deliver more than one quanta of angular momentum to site-specific parts of molecules.[48] As well as producing another degree of freedom that could be used to develop new chiro-optical spectroscopy and analysis, vortex beams also be a powerful tool, particularly for triggering light driven molecular switches and motors or switching enantiomeric configurations.

XFEL beamlines with complete control of the spin and orbital angular momentum of the emitted light, which can be combined at different angles and with different colours or polarisation states, will offer remarkable control of chiro-optical interactions. The site-specificity of core orbital absorption will provide opportunities for probing chiral properties in different parts of molecules, and even to induce or modify this chirality. For example, the possibility of identifying the loss of chiral specificity within single proteins, which is believed to contribute to age-related illnesses such as cataracts and Alzheimer's disease, would be groundbreaking.[49] Ultimately, these pulses will be remarkable tools, capable of interrogating the strength, and even the phase, of chiral interactions across molecular frameworks with attosecond temporal resolution.

3.1.4 Molecules in intense X-ray fields

The high brightness of XFEL pulses presents opportunities to perform diffraction imaging of single molecules. At intensities of up to 10^{20} W cm^{-2}, however, is it possible to obtain scattering data from an unperturbed molecule before it is inevitably destroyed by the pulse? Conversely, could complementary structural information be derived from the resulting fragmentation dynamics? To answer these questions requires a fundamental understanding of how complex molecules couple to intense X-ray fields.

It would be expected that molecules attain high ionisation states before they explode through Coulomb repulsion of the multiply-charged fragments, as with intense optical laser pulses; however, for X-rays, sequential single photon ionisation of inner shell electrons is prevalent. If a heavy atom is present in the molecules, the X-ray field efficiently ionises its inner shell electrons. Within a few femtoseconds, Auger processes ionise outer electrons while re-filling the inner shell holes. This results in sequential photoionisation-Auger events, generating an even higher charge state of the atom.[50] This charge has been found to quickly distribute around the molecule, via processes such as inter-atomic Coulombic decay (ICD), such that further absorption and ionisation of X-ray photons take place. These mechanisms produce a charge state of the molecule that is higher than could be obtained for the atom by itself.[51]

This dramatic and ultrafast shift in electrons within the molecule means that it suffers radiation damage, since the initial electron distribution is altered substantially. Additionally, on timescales as short as 10 fs, Coulomb repulsion is already pushing the atoms from their equilibrium positions. This has consequences for XFEL diffraction imaging of single molecules, and these effects need to be considered to enable correct interpretation of single-molecule scattering patterns. These processes have been observed in atoms and simple molecules,[52,53] but much more complex molecules need to be studied in order to see how electronic coupling behaves over greater spatial extents. Encouragingly, recent studies have demonstrated that transient ion resonances may significantly enhance the spatial resolution in diffraction with sub-femtosecond temporal precision at the nanoscale[54].

Fragmentation patterns of complex molecules can themselves yield important structural information and can reveal details of how biological structures are damaged by ionising radiation. Coulomb explosion imaging (CEI) has been established using intense optical pulses, with the momentum vectors of the fragment ions used to recreate the molecular structure.[55] It has already been applied to obtain the absolute configuration of simple chiral molecules[56] and some exemplar organic ring and chain molecules.[57] This opens up the possibility of using CEI to map out transiently chiral structures, or observe ring opening dynamics.

Even higher charge states can be reached by XFEL pulses through efficient inner shell ionisation of a heavy atom in the molecule. This enables the CEI reconstruction of the molecular structure to be achieved with higher resolution. Molecular models are also being developed to include the initial vibrational motion of the atoms and the subsequent nuclear dynamics,[58] giving multi-pulse schemes the potential to generate high resolution, ultrafast molecular movies of atomic motion in the molecule. The ability to observe fast proton migration within molecules is particularly important, as this migration drives many chemical processes, but cannot be seen with X-ray diffraction techniques that rely on scattering from electrons.

The potential of XFEL CEI to image single, isolated molecules with 11 atoms has been demonstrated at the European XFEL using 10 fs, 2 keV pulses at intensities greater than 10^{18} Wcm^{-2}.[59] The combination of high intensity and short pulses means that charging of the whole molecule proceeds within a few femtoseconds, from which the momenta vectors of individual atoms were produced with unprecedented resolution. Although only partial coincidences were obtained (it is impossible to detect all atoms in coincidence), it was demonstrated that coincidence of only three ions was sufficient to determine the overall structure, including the positions of all the hydrogens. This shows that imaging of even larger molecules is feasible and time-resolved dynamics of photochemical processes can be tracked with exceptional structural detail.

Challenges remain to be overcome if XFEL CEI is to fully reach its enormous potential, such as the continued development of multi-hit detector technology[60] and correlation mapping,[61, 62] to enable the complex fragmentation patterns generated from large molecules to be mapped out. Visualisation schemes will need to be developed so that the multi-dimensional momentum space can be meaningfully interpreted. There is also still the question of whether high quality data can be obtained without the need for a substituted heavy atom (such as iodine) to act as an X-ray absorber for efficient ionisation. These advances must also go hand-in-hand with development of accurate theoretical models needed to simulate the ultrafast electron redistribution in the molecule and resulting nuclear dynamics. While the current state-of-the-art uses a fully quantum description of the atomic orbital binding energies, photoionisation cross-sections, and Auger and fluorescence decay rates, the electron and nuclear motion is simulated with classical molecular dynamics.

3.1.5 Future vision

The development of a next-generation XFEL with high repetition rates, high pulse energies, multi-pulse sequences consisting of individually configurable wavelengths and polarisation states, and attosecond pulse durations will revolutionise how molecular systems are studied and understood. Huge steps forward in detector technology, capable of handling MHz repetition rates and manifold coincident hits

(100s per pulse), will herald the dawn of multi-dimensional non-linear X-ray spectroscopy and fragmentation imaging. When placed alongside innovative X-ray diffraction techniques, this will provide sub-ångstrom and sub-femtosecond resolution of all molecular components – electrons, protons and ions. Using the comprehensive data provided by these complementary techniques, artificial intelligence advances will be exploited to re-create accurate, multi-faceted movies of the structure and dynamics of complex molecular systems, such as real-time atomic resolution of enzymatic action (see **Section 7.3**).

In addition, site-selective X-ray absorption within complex molecules, combined with spatial and temporal control of the pulse's electric field, will be a powerful probe of localised quantum properties within the molecule. In this way the properties of chromophores, reaction nodes and chiral centres critical to molecular functionality will be revealed, by mapping out the electronic and nuclear motion on the multi-dimensional landscape that is found near conical intersections. These will provide insight, for instance, into how photosynthetic systems efficiently convert light into charge separation and how the chirality of life can be compromised, thus leading to age-related diseases.

Ultimately, this knowledge will enable the design of functionalised molecules, which can emit light of different colours and polarisation depending on the environment and nature of the stimulus, transform the efficiency of solar harvesting devices, or change their pharmacological action inside patients following absorption of infrared light or X-rays.

3.2 New concepts in scattering

The arrangement of atoms in matter and their motion are fundamental to understanding the function of material systems. XFELs enable us to determine dynamic changes in structure, providing insight that will allow us to engineer molecular machines and devise new catalytic processes. By combining ultrafast X-ray scattering with novel ideas from quantum optics and scattering physics, we will be able to explore new physics, circumvent the phase problem that currently restricts imaging of matter, study samples that are too disordered or fragile for today's technologies, and image important but elusive phenomena such as electron dynamics and coherent transport.

3.2.1 Introduction

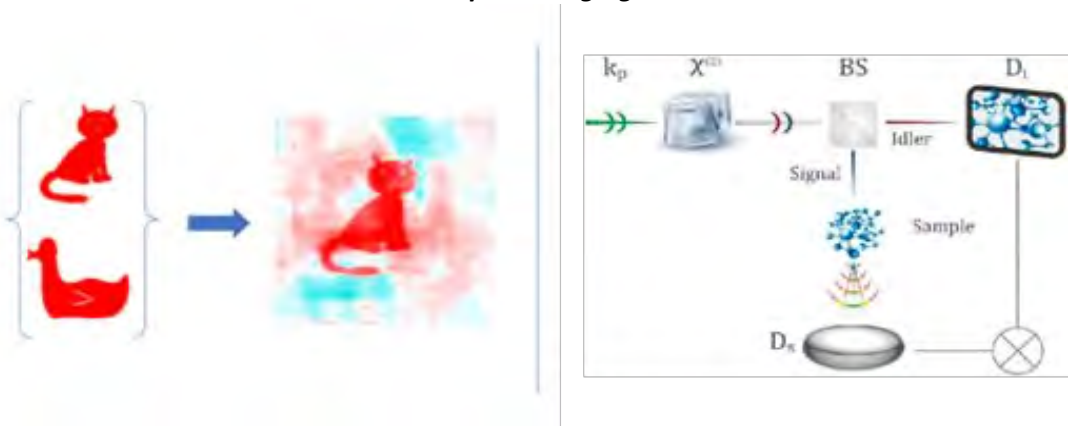
X-ray scattering has shaped our understanding of the structure of matter. The iconic renderings of the arrangement of atoms in the DNA double-helix,[63] in proteins,[64] and in crystalline matter[65] constitute early breakthroughs that were awarded Nobel Prizes. The number of known structures is growing exponentially[66] (see also **Chapter 7**), reflecting the importance of structure-function relationships in many branches of modern science and high-tech industries. This success notwithstanding, great opportunities remain to be explored.

The large photon-flux and coherence of XFELs, combined with cutting-edge ideas from, for example, quantum optics, may enable forms of single-particle imaging[67] that circumvent the requirement of crystalline targets and allow molecules to be observed in their natural state, avoiding distortion due to the crystalline environment. In many systems, the structure constantly fluctuates between many distinct thermodynamic states, with the rarest, and thus most difficult to observe, states playing important roles in the function of molecular machines such as enzymes. XFELs aided by powerful AI algorithms may allow us to image the whole range of thermodynamic states (see also **Section 3.4**). Furthermore, greater information might be extracted for delicate, fragile or disordered materials that are challenging or impossible to study with the technologies available today. Perhaps most revolutionary are concepts that may overcome the *phase problem*, arguably the defining challenge for all forms of X-ray imaging (see **Box 3.2**).

The short pulse duration at XFELs can have even greater impact. The absence of dynamics from the current structure-function dogma reflects the limitations of traditional imaging methods, which provide static and time-averaged images. With the ability to measure the transformation of one structure into another, XFELs may revolutionise the development of future nanoscale technologies and bring greater understanding to all aspects of structural science. For instance, by measuring time-resolved sequences of molecular structures on a femtosecond timescale, the motion of atoms in a molecule following the interaction with light can be revealed, with great impact on our understanding of energy and charge transport and chemical reactivity, which could be exploited in areas such as photonics, catalysis and molecular electronics.

These new opportunities come alongside new and exciting physics. Imaging techniques, such as ghost imaging, exploit ideas from quantum optics and involve the detection of photons that never interact with the sample, with the quantum version of ghost imaging going one step further by using entangled photons. Likewise, ultrafast measurements with hard X-rays may transgress current distinctions between structural dynamics and spectroscopy, and provide insights into the fundamental nature of the combined motions of electrons and nuclei that cannot be achieved by other means. Finally, theoretical predictions indicate that, for sufficient time-resolution and coherence, new quantum interference phenomena in scattering will appear, carrying unique information about ultrafast electron dynamics and transient coherences in material systems.

Box 3.2: Real-space imaging with XFELs



Current imaging techniques measure the amplitudes but not the phases of the light. This so-called phase problem imposes significant limitations on imaging, as illustrated on the left. If we combine the phases for the cat with the amplitudes for the duck, the resulting image looks more like a cat than a duck (http://www.ysbl.york.ac.uk/~cowtan/fourier/fourier.html). Ideas from quantum optics, e.g. ghost imaging or incoherent diffraction, may overcome this problem. On the right, a proposed quantum diffraction setup is shown that would be capable of measuring phase. [80]

*Figure (right) reproduced from S. Asban et al. PNAS **116** 11673-11678. Copyright (2019) National Academy of Sciences*

3.2.2 New imaging techniques

Correlated X-ray scattering, or fluctuation X-ray scattering, detects momentum-transfer correlations between two or more photons scattered by the same molecule, making it possible to determine structure in the absence of short- or long-range order. The concept, advanced in the late 1970s,[68,69] remained largely undeveloped until the emergence of XFELs, which finally provided sufficient photon fluence and pulse durations shorter than rotational diffusion times. At LCLS in 2017, it was demonstrated that angular correlations can determine nanoscale structural features of viruses.[70] With currently existing XFELs, the signal to noise ratio is still insufficient to determine the atomic structure of particles as complex as proteins, but the technology may attain this goal with further improvements in photon fluence. Apart from studies in native environments, the method could also become instrumental in single-particle imaging, where it could overcome the issue of unknown sample orientations.[71]

Ghost imaging originates in quantum optics[72] and exploits the observation of photon correlations. These protocols have been extended to classical light based on statistical correlations,[73,74] making them relevant to non-seeded XFEL sources. The immediate advantage of ghost imaging is that the radiation dose absorbed by a fragile sample can be lowered dramatically.[75] The approach also offers distinct improvements in resolution, signal to noise and, under specific circumstances, greater efficiency in data collection.[76] At optical wavelengths, it has been demonstrated that ghost imaging can provide special performance when parametric down-conversion is phase-matched to give non-degenerate signal and idler wavelengths.[77] This allows an object to be illuminated at one wavelength and the spatial information recorded at another, perhaps where the imaging detector is more sensitive or less noisy. Ghost tomography schemes have been proposed that aim at atomic resolution of complex targets,[78] and analogous ideas have been put forward that exploit the random time-structure of SASE pulses to achieve pump-probe resolution of dynamics without actual time-delay scans.[79] An interesting opportunity at future high-flux XFELs is quantum ghost imaging via parametric down-conversion of X-ray photons, allowing one photon of an entangled pair to be diffracted off a sample and detected in coincidence with its twin.[80] By scanning the photon that did not interact with the target, the phase information imprinted in the state of the field can be detected, which could yield real-space images that avoid the phase problem altogether (see **Box 3.2**). Recently a demonstration was made of X-ray coincidence imaging using spontaneous parametric down-conversion (SPDC) of synchrotron radiation

to generate correlated X-ray photon pairs[81]. With the far higher photon flux from an XFEL the yield of SPDC will be orders of magnitude greater. Other proposals to circumvent the phase problem at XFELs include measuring energy-resolved scattering from a target driven by an external periodic field, resulting in time-dependent changes in the electron density.[82]

Another exciting technique, which originates in ideas originally put forward by Hanbury Brown and Twiss, is incoherent diffractive imaging[83,84,85] that exploits higher-order correlations between fluorescence emission from different atoms to retrieve structural information. This approach may provide striking advantages, such as element specificity, and opportunities for phasing in a manner analogous to anomalous dispersion when performed in conjunction with coherent diffraction. Since the cross-section for incoherent fluorescence emission is higher than that for elastic scattering, incoherent diffraction can produce stronger signals than standard coherent diffraction and detect higher momentum transfer, thanks to the uniform angular distribution of fluorescence emission. The cumulative result is a potential for rapid structure determination that requires a significantly smaller number of observations to fill the full 3D Fourier space than conventional methods,[50] and sub-Abbe resolution may be achieved if higher than second order correlations are exploited.[86] The concept has recently been demonstrated at the FLASH XFEL using a patterned mask,[84] as shown in **Figure 3.4.** Similarly to the other techniques discussed in this section, incoherent diffractive imaging requires the extreme brilliance and high pulse repetition rate of new XFEL sources. It also requires pulse durations shorter than the radiative lifetime of fluorescence (e.g. 2.6 fs for the K_α fluorescence in Fe atoms). A striking prospective application could be ultra-high resolution of yet unresolved structural changes in metal clusters in Photosystem II, which are essential for how water is oxidised during photosynthesis.

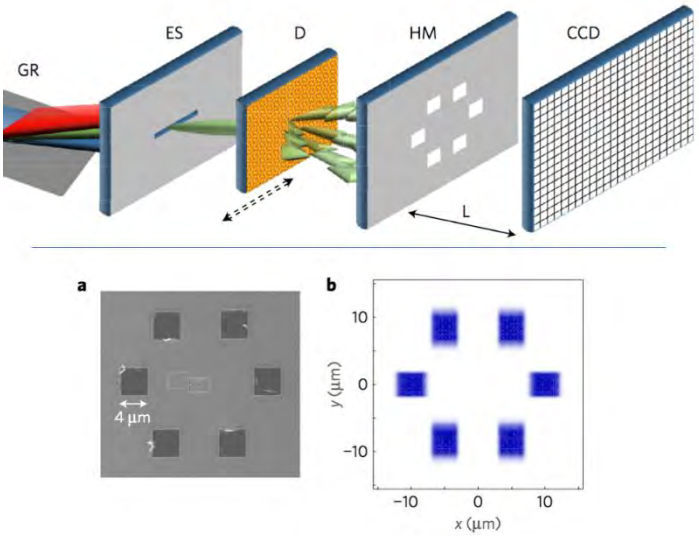


Figure 3.4: The first demonstration of incoherent diffraction using a microscale patterned mask at the FLASH XFEL.[85] (Top) Experimental setup with grating (GR), exit slit (ES), diffusor (D), hole mask (HM), and a CCD detector. a) Hole mask, b) reconstructed image.

*Figure reproduced from R. Schneider et al. "Quantum imaging with incoherently scattered light from a free-electron laser" Nat. Phys. **14**, 126-129 (2018), Springer Nature. DOI: 10.1038/nphys4301*

3.2.3 Structural dynamics and beyond

Ultrafast X-ray scattering at XFELs is opening the door to observations of structural dynamics at the fundamental timescale of nuclear motion, on the order of femtoseconds (10^{-15} s). This information is not directly available from ultrafast spectroscopy and brings unique insights into the atomic motions that underpin transformations in matter. With sufficient spatial and temporal resolution, it is possible to observe the fundamental steps in bond-breaking, bond-making, and atomic re-arrangements, for instance following photoexcitation. Experiments at LCLS have demonstrated structure determination in excited molecules undergoing coherent vibrations,[87] as shown in **Figure 3.5** (*right*), observed the dynamics associated with rapid electrocyclic ring-opening reactions,[88] charge transfer,[89] and the stability of the biologically important disulphide bond.[90] Such measurements will transgress simplistic

notions of structural dynamics, as analysis of the ultrafast X-ray scattering data can reveal normal modes and associated frequencies, thus combining sub-ångström resolution of atomic displacements with resolution of e.g. harmonic spectroscopic modes.[91,92] As the resolution increases further, it will become possible to track the time-evolution of the quantum wavepacket for excited systems, identify excited electronic states, and directly observe intrinsically quantum phenomena such as dispersion, coherence, and interference.[93, 94,95]

Importantly, the scattered X-ray photons carry an imprint of the actual electron density of the material system. A recent experiment shown in **Figure 3.5** (*left*) demonstrates that short-lived electronic states can be observed using ultrafast X-ray scattering at XFELs.[96] Taking into account expected improvements in signal-to-noise at a next-generation XFEL with a higher repetition rate, it is reasonable to expect that it will be possible to simultaneously track both the structural dynamics and the changes in electronic structure that drive the nuclear motion. Such aspects were already part of the analysis in previous experiments[87,97], and were demonstrated beautifully in a recent study of excited state dynamics in ammonia.[88] The ability to characterise nuclear and electronic motions in a single experiment will boost our ability to diagnose and improve molecular devices such as fluorescent probes, photocatalyst and photovoltaics. On a more fundamental level, accurate measurements made possible by the large X-ray photon flux may reveal intrinsic correlation effects in electronic structure, leading to advances in electronic structure theory and the computational modelling of materials.[98] Recent experiments at SACLA also demonstrated how sequential X-ray pulses enable non-resonant hard X-ray scattering experiments initiated by hard X-rays, with the X-ray pump giving access to processes inaccessible to pumping by optical light.[99]

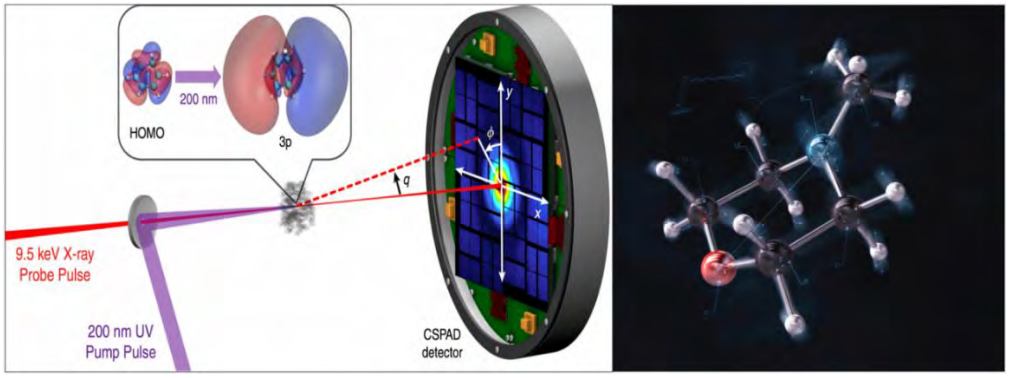


Figure 3.5: (Left) Schematic of the first experiment to directly observe an excited electronic state in a molecule using ultrafast X-ray scattering. (Right) A recent experiment has been able to accurately measure bond distances in an excited molecule undergoing harmonic vibration.[96]

Figure reproduced from H. Yong et al. "Observation of the molecular response to light upon photoexcitation" Nat. Comms. ***11****, 2157 (2020), Springer Nature. DOI: 10.1038/s41467-020-15680-4*

3.2.4 Physics of scattering with coherent X-rays

The coherence in the incident X-ray radiation, combined with the ultrashort time-duration of the pulses, is expected to lead to new observable phenomena due to interferences between different inelastic transitions. Such interferences in X-ray scattering, sometimes referred to as coherent mixed scattering,[100] have been theoretically predicted to carry the signatures of ultrafast electron dynamics,[101] transient nuclear coherences and transitions between different electronic states due to nonadiabatic coupling[102] or at conical intersections.[103] **Figure 3.6** shows how transient nuclear coherences may manifest in scattering.

The coherent mixed scattering will appear alongside elastic and inelastic scattering, and stems from an interference of scattering amplitudes from different electronic states populated in an excited molecule,[100,104] as shown in **Figure 3.6** and **Figure 3.7**. The effect requires coherence between populated electronic states, meaning that their nuclear wavefunctions must overlap. Such coherences emerge transiently during photochemical reactions, when electronic states are coupled and transitions between them occur. Coherent mixed scattering, possibly combined with X-ray spectroscopy,[105] should

thus provide distinct fingerprints of internal conversion and intersystem crossing during photochemical and photophysical processes.[106] It could furthermore be used to measure the role of coherence in energy transport[107] and charge migration.[108]

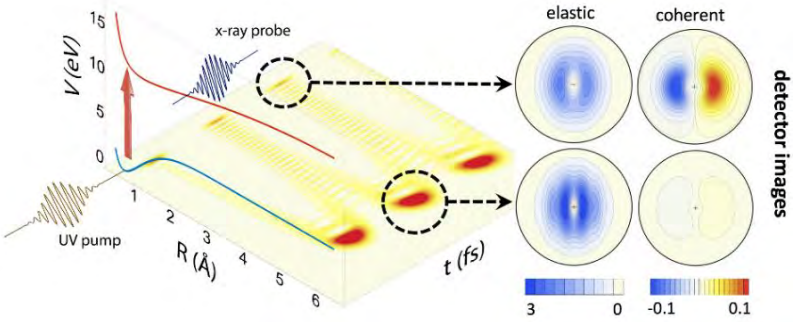


Figure 3.6: Coherent mixed scattering appears as a consequence of coherent electron dynamics and may help characterise complex dynamic processes in matter. On the left-hand side, an optically pumped wavepacket is shown, with the X-ray scattering detector images showing elastic and coherent mixed scattering shown on the right[100]

*Figure reproduced from M. Simmermacher et al. "Electronic Coherence in Ultrafast X-Ray Scattering from Molecular Wave Packets" Phys. Rev. Lett **122**, 073003 (2019), American Physical Society. DOI: 10.1103/PhysRevLett.122.073003*

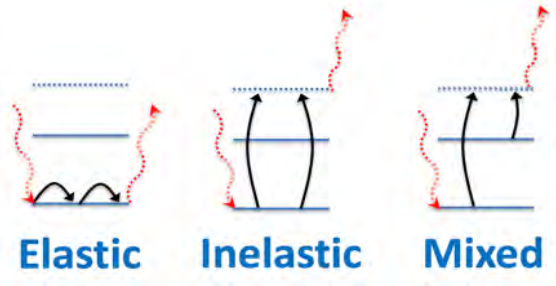


Figure 3.7: Schematic illustration of the components in X-ray scattering
Populated states are shown as solid horizontal lines, vacant electronic states are shown as horizontal dotted lines, with the scattering transitions shown as curved black arrows (one for each scattering matrix element) and incident and scattered photons as curly red arrows. Elastic (left) and inelastic (middle) scattering are well known, but coherent mixed scattering (right) constitutes a new predicted phenomenon that requires the coherence of XFELs to be observed.[100-103]

3.2.5 Conclusion and future outlook

The opportunities provided by a next-generation XFEL paint an exciting picture for the future of X-ray science. Advances in X-ray imaging will make it possible to accurately determine structure and structural dynamics of complex molecular machines across a large range of timescales (from femtoseconds to minutes), such as Photosystem II at sub-Abbe resolution, providing unprecedented insight into their workings. It is clear that imaging at XFELs will extend beyond the narrow definitions of imaging as a determination of the 3D structure of matter. Imaging experiments will be able to address specific atoms and atomic species, determine energetic properties of the system, probe electronic states and electronic motion, determine vibrational modes, and even probe subtle yet important quantum phenomena such as dispersion, interference and coherence.

Attosecond X-ray pulses with high repetition rate at tuneable energy, and with transform-limited bandwidth and high shot-to-shot reproducibility, will be needed. These must be coupled to high-performance detectors that are possibly energy-resolved. Advanced optical laser facilities must accompany the X-rays, with sub-femtosecond pump-probe synchronisation required to capture electronic coherences induced by optical pump pulses. It is expected that many of these auxiliary technologies will be developed over the next decade to be incorporated into next-generation XFEL facilities.

3.3 Attosecond science and non-linear X-ray spectroscopy

Electron dynamics, typically occurring on attosecond to femtosecond timescales, play a crucial role in a vast array of physical, biological and technological processes. This was recognised in the award of the 2023 Nobel Prize in Physics to attosecond physics and technology. High temporal resolution X-ray probes are essential to understanding and harnessing many of these processes, and will impact on knowledge and control of, for example, fast ionisation events, excitons in light harvesting systems, primary steps in photocatalysis, advanced photodetectors and photodynamic therapy.

3.3.1 Introduction to new attosecond XFEL capability

There has been a rapid advance in short pulse operation modes at XFELs since LCLS first started operation in 2009.[109] Low-bunch charge modes were soon found to produce self-amplified spontaneous emission (SASE) pulses as short as 3 fs[110]; emittance spoiler based methods followed,[111] and the two-colour fresh-slice mode[112] was developed and is now routinely used.[53] Two-pulse/two-colour X-ray modes are subject to orders of magnitude less inherent jitter (sub-femtosecond) than laser-X-ray experiments and so, at present, offer the highest temporal resolution pump-probe capabilities. When millijoule-level femtosecond duration SASE pulses are focused, high intensities ($> 10^{18}$ W cm^{-2}) are routinely attainable. Such high intensities are required to drive even relatively low order non-linear X-ray processes, since the relevant interaction strengths scale strongly with wavelength, leading to much diminished non-linear cross-sections in the X-ray range. Nevertheless, two-photon ionisation,[113] stimulated Raman[114] and stimulated emission[115] have previously been observed, as well as XFEL-pumped atomic X-ray lasers.[116] The challenge now is to go beyond multi-spiked stochastic SASE pulses, to permit more controllable non-linear interactions.

Enhanced SASE (eSASE) has been discussed for some time[117] as it offers a way to restrict the SASE lasing to a single SASE spike, with a field that much more closely approaches the *ideal* transform limit. This technique was first demonstrated[118] in 2019 with the generation of one- and two-colour eSASE isolated attosecond pulses and large coherent bandwidth. Using a circularly polarised laser field streaking method, these pulses were fully characterised in the 500 – 1000 eV range and found to give 200 – 500 attosecond pulse durations (**Figure 3.8**), with a relatively narrow distribution over multiple shots. Moreover, these short pulses were accompanied by a large coherent bandwidth in the 5 – 10 eV range, and the pulse energy was some nine orders of magnitude higher than that obtained by high harmonic generation (HHG) in the same photon energy range, the only other source of attosecond pulses.

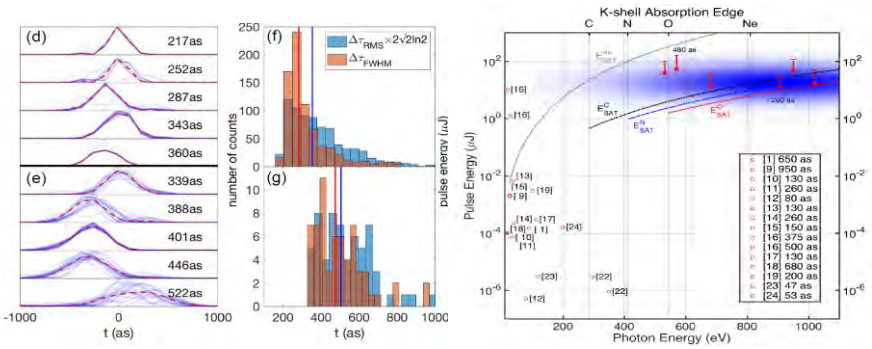


Figure 3.8: Results from LCLS showing (left) the measured 200 – 500 attosecond pulses in the SXR region, and (right) the comparison to HHG attosecond sources[118]

Figure reproduced with permission from J. Duris et al. "Tunable isolated attosecond X-ray pulses with gigawatt peak power from a free-electron laser" Nat. Phot. 14, 30-36 (2020), Springer Nature. DOI: 10.1038/s41566-019-0549-5

This breakthrough development is opening the path to important new opportunities in attosecond domain pump-probe measurements, and non-linear X-ray spectroscopy. It prompted the formation of an international collaboration led by SLAC scientists (Agostino Marinelli and James Cryan) that has proceeded to develop methodologies of attosecond measurement that will be further discussed in this section. Now both soft X-ray[119,120] and hard X-ray[121] isolated attosecond pulses, and pairs of attosecond

pulses of variable colour and delay, have been developed and made available to users at LCLS, LCLS II, the European XFEL[122] and Swiss FEL[123]. The rapid uptake of these capabilities by the user community is illustrated by the fact that the TMO end-station at LCLS II typically operates more than half of the time with attosecond modes.

The introduction of seeding[124] and echo-enabled seeding at FERMI[125] has shown that almost transform-limited (fully temporally coherent) femtosecond pulses can be delivered in the XUV and soft-X-ray range. These seeded pulses have enabled the first transient grating XUV FEL experiments[126] and prospects to scale these to higher photon energies look promising. Utilising phase-locked harmonics of the seeded FEL provides attosecond pulse train (APT) capabilities in the XUV spectral region.[127] The ability to control the relative harmonic amplitudes and phases in the APT is finding application in a range of coherent control experiments.

3.3.2 Attosecond science

The timescale of electronic dynamics in matter is naturally very fast; for example, the orbit time of an electron in the lowest Bohr level of the hydrogen atom is just 150 attoseconds. When superpositions of electronic valence states are formed, fast electronic dynamics are manifested as an observable effect, for example through the ultrafast time-dependent localisation of charge density. Given that the typical energy spacings of valence states can span several electron-volts or more, the resulting beating timescale is typically a few-femtoseconds to sub-femtosecond. The primary events of photoexcitation and radiolysis will intrinsically occur on such timescales when considered at the quantum level of a single system. The wider impact of this on science and technology is through the importance of photo-excitation/photoionisation in renewable energy (e.g. light harvesting technology), photocatalysis (e.g. photo-driven water splitting and biofuel generation), radiation damage of materials (e.g. in space and nuclear technology) and biomedicine (e.g. in radiation and photodynamic therapy, photoactivated fragmentation of biomolecules in mass spectrometry, and radiation damage and therapy).

The new X-ray attosecond pulse capability from eSASE provides the prospect of applying X-ray spectroscopic probes that allow, for the first time, the study of electron dynamics with full spatial resolution through atomically localised probing as well as the required temporal resolution. For example, in the X-ray ionisation of matter by a short pulse, the high kinetic energy of the outgoing electron leads to a “sudden ionisation” event that can project the resulting charged system into superposition of valence states, resulting in large amplitude charge density oscillation across the system with attosecond timescales. This “*charge migration*” situation has been widely studied theoretically, but can only now be realised in the context of true sudden ionisation. Ultrafast charge migration following sudden ionisation or excitation is believed to be a universal response of extended molecules, and is also likely to occur in some form in many condensed phase systems.[128] It is now understood that there is intrinsic coupling to the nuclear wavefunction through both zero-point geometry spread and subsequent rapid motion,[129] which will take place on a short (< 10 fs) timescale, so it is expected that coupling to nuclear modes will rapidly become important.[130] Understanding ultrafast electron-nuclear coupling poses an enormous challenge, requiring fully quantum dynamics calculations that go beyond the Born-Oppenheimer approximation, and experimental benchmarking is now vital.

Electron wavepackets excited by attosecond pulses lead to a new regime in photochemistry, where the electronic state dynamics drive the nuclear dynamics and the chemical reaction follows, in contrast to the usual case where nuclear dynamics drive the reaction and the electronic motion follows. Such charge directed reactivity has been suggested as a way to explain laser ionisation experiments in some molecules,[131] and may offer routes to control reactions in the future. Ultrafast hole evolution and motion is of critical importance to many aspects of photochemistry and photophysics, with little experimental data at these short timescales. At present, attosecond science relies heavily on the process of HHG as a means of generating attosecond pulses in the soft-X-ray photon energy range,[132,133] but, despite progress in the generation efficiency and shortness of the pulse duration,[134] the power levels are found to be very low (picojoules in the soft X-ray range). This has prohibited

applications to direct pump-probe measurements and instead techniques have been developed that use an intense IR field either as the pump[135] or the probe.[136 137] The strong IR field will, however, induce profound modifications to any extended multi-electron system[138] and so inhibit the ability to make measurements on the native charge migration process without unwanted strong field distortion.

Application of ultrafast X-ray spectroscopy with few-femtosecond XFEL pulses has already added insight. The prospect of following ultrafast hole dynamics resolved to specific atomic sites was predicted in 2014 and demonstrated in 2021[139] with the observation of a highly transient hole in isopropanol. This used a variant of X-ray absorption spectroscopy (XAS) where the detection channel was the observation of Auger-Meitner electrons from core excited final states, appearing when the probe was resonantly absorbed into a valence hole vacancy caused by a pump pulse. A further implementation of this methodology at the FLASH facility observed fast (~ 19 fs) period oscillatory hole dynamics in the amino acid glycine and evidence that the fast electronic motion then couples to vibronic motion on timescales ~ 40 fs, a first signature of attochemistry occurring[140]. Now that truly attosecond pump-probe capabilities are available at the European XFEL and LCLS/LCLS II, and attosecond pulse train and XUV field synthesis capabilities are available at FERMI, substantial scientific advances can be anticipated in the coming decade.

3.3.3 Attosecond measurement of hole dynamics and photoelectron delay

X-ray attosecond pulse pairs open up new routes for the pump-probe study of charge migration and other attosecond timescale electronic processes. A resonant core state to valence hole probing scheme enabled by attosecond X-ray pulses is far superior to current methods, in that the interaction ensures a non-perturbative measurement of the intrinsic electron dynamics, whilst also permitting atomically localised probing of the electronic state through the atomic specificity of core state spectroscopy.[141] In addition, attosecond streaking with circularly polarised fields is now being used to time-resolve the electron photoemission process and subsequent Auger cascades,[142] and such streaking based methods are being extended to measuring photoemission from XUV to hard X-ray pulses as new attosecond capabilities are developed.

As well as proving an invaluable tool for verifying the generation of attosecond pulses, angular streaking using a circularly polarised infra-red laser field has been directly applied to measurements of the dynamics of the photoionisation process. Two recent examples were conducted in the nitric oxide (NO) molecule. In the first of these, the attosecond pulse created a superposition of core-excited states near the O site; these gave rise to a clear quantum beat in the Auger-Meitner decay signal, indicating the first-time electronic coherence had been created with core electronic states.[143] In another study, the delay time of the photoelectron emitted from the O site was measured across a range of excitation energies and to probe the various contributions to the delay time, including transient trapping of the photoelectron owing to shape resonances, collisions with the Auger–Meitner electron that is emitted in the rapid non-radiative relaxation of the molecule and multi-electron scattering effects.[144] More recently the signature of core hole motion between two carbon sites within the 1,1-difluoroethylene ion was studied via angular streaking.[145] At the European XFEL, angular streaking was used to investigate the performance of soft X-ray attosecond generation modes and the dynamics of double core-hole formation.[146]

The ability to make two-colour attosecond pulses of variable delay is opening up new opportunities for probing hole dynamics in matter. This leverages the ability of XAS to probe sites within a material with atomic localisation and ~ 300 attosecond temporal resolution, opening the way to fully track hole and excitation dynamics at their natural timescales. The two-colour capabilities of the LCLS attosecond modes were demonstrated to have a controllable inter-pulse delay and were used to measure the dynamics of the double ionisation of aminophenol with better than 0.5 fs temporal resolution.[147] This controlled two-pulse sequence was then applied to measure hole dynamics in aminophenol using the Auger activated XAS methodology. This measurement captured the universal response of a molecule to attosecond ionisation that starts with fast decay of doubly excited states (in ~ 1 fs), and is followed by charge migration dynamics (1 – 10 fs) and then nuclear motion (> 10 fs)[148]. An XAS measured in

transmission was used to probe the photoionisation response of liquid water, with the probe delayed by 600 attoseconds after the ionisation triggering pulse. In this study, the fundamental was used to ionise a valence electron and the resulting hole was then populated by the second harmonic in a transition from the core O 1s state.[149] Unlike earlier X-ray emission spectroscopy (XES) studies, there was no evidence of a double peak structure in absorption spectrum corresponding to the $1b_1$ state. The XES results had been interpreted as being due to two separate structural motifs in liquid water, but these measurements had integrated the emission over the 4 fs core-hole lifetime. The attosecond XAS measurements instead allowed the transition to be probed within a frozen nuclear framework. Theoretical calculations indicated that the second peak observed in the XES was a result of ultrafast proton dynamics creating a different structural configuration in the water and was not a natural state under ambient conditions.[150]

With the new generation of eSASE capability likely to be extended across a wide photon energy range in a future light source, we will have the means to measure time-dependent information on the electron-hole evolution, and localisation in a wide range of situations in both gas and condensed phase systems. We also anticipate better synchronisation and better time-stamping (e.g. via circular streaking offering sub-femtosecond measurement resolution) between laser fields and X-rays in future facilities. Such advances will allow attosecond resolved measurements on excited state neutrals that will extend these X-ray probing methods to chemical excited state dynamics in gas and liquid phases and excitons in condensed phase materials, and open-up prospects for the control of photo-processes by manipulating the superposition of the electronic states.

3.3.4 Impulsive X-ray Raman interactions and non-linear X-ray optics

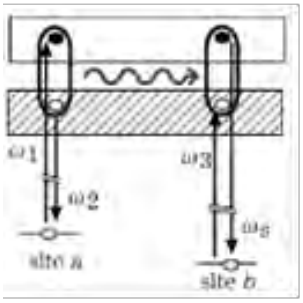
Concepts in nonlinear X-ray spectroscopy using attosecond pulses have been proposed and explored theoretically, including 1D[151] and 2D coherent X-ray Raman scattering.[152] One method already being realised is *impulsive* stimulated X-ray Raman scattering (ISXRS), which relies upon the large coherent bandwidth within a single attosecond X-ray pulse to provide both the pump and the Stokes transition frequencies required to excite a valence *electronic* state in the neutral. This is analogous to stimulated impulsive Raman in the optical domain (visible to UV), which primarily couples to *vibrational* states of matter. ISXRS offers unprecedented opportunities for creating localised coherent electronic wave packets in *un-ionised* states that can be employed to probe electronic couplings between atomic sites in a molecule or a condensed phase material.

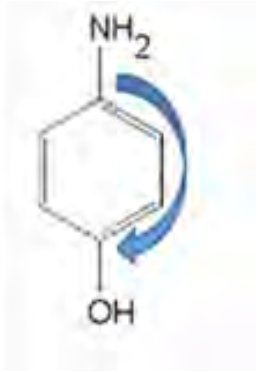
The use of ISXRS to generate valence electronic wavepackets was first achieved in NO using attosecond pulses at LCLS.[153] The 1s – $2\pi^*$ resonance in the oxygen atom was targeted using a pulse with a bandwidth of 5.5 eV, which impulsively excited several valence electronic states. Using a UV probe and theoretical simulations, production of an electronic wavepacket was confirmed. There was a further demonstration of this capability for a condensed phase system, when 400 as pulses were used for impulsive SXRS in liquid water.[154] In this case, a Stokes signature produced by stimulated emission was observed in the X-ray spectrum, thus demonstrating a *photon in – photon out* method suitable for probing condensed phase systems.

Tuning the X-ray photon energy resonances between inner shell and valence states in the molecule boosts the two-photon (Raman) excitation of excited state neutral atoms by a large factor. By strong resonance enhancement, the Raman process can select only atoms of a single species through a virtual transition to this core-excited intermediate state. The process can, therefore, lead to localised excitation at a specific site (site *a* in **Box 3.3**) within a neutral molecule, and it is possible to control which sites are excited by tuning the X-ray photon energy. A second delayed pulse, tuned to a different resonance, can then be used to induce a Raman transition at a nearby atomic site (site *b*). The electronic excitation transfer from site *a* to site *b* can then be determined through observation of changes to the stimulated X-ray emission spectrum induced in the second Raman transition. As a result, this process has the potential to provide the perfect tool to probe the transfer of electronic excitation within a molecule or a condensed phase system with atomic spatial and sub-fs temporal resolution, and is ultimately a *photon in – photon-out* method that lends itself to gas, solid and liquid

phase systems. The challenge for future experiments is to realise a different colour ISXRS probe of these dynamics, which would allow coherences at conical intersections and charge transfer within large molecules to be tracked using the site-specificity of the tuned XFEL pulses.[155] With the rapid progress underway in controlling the attosecond operation of XFELs, it is likely that these challenges will be met.

Box 3.3: New concepts to create and track coherent electronic wavepackets through materials





A double impulsive Raman sequence can excite a valence state wave-packet localised at one atomic site and probe at a second atomic site after a controlled delay.[151] This creates a unique opportunity for spatial/temporal resolved probing and quantum control. Such a flagship experiment is a stepping-stone to attosecond multi-dimensional spectroscopy, with creation and probing of localised electronic wave-packets in matter of all kinds.

Reprinted figure with permission from S. Tanaka and S. Mukamel, Phys. Rev. Lett. ***89****, 043001 (2002). Copyright (2002) The American Physical Society. DOI: 10.1103/PhysRevLett.89.043001.*

There has been much other progress in non-linear X-ray spectroscopy over the past decade, driven by the high brightness of SASE XFELs[156,157]. This includes stimulated X-ray Raman scattering driven by SASE, as well as attosecond pulses discussed above, where spectroscopic applications have been explored in the soft X-ray range[158] and also in the hard X-ray range[159]. Hard X-ray SXRS, using synchrotrons and XFELs, is seen as an important component in the spectroscopic investigation of chemical dynamics within dense media as it is possible to address, say, carbon, nitrogen or oxygen K-edge spectroscopy using more penetrating hard X-rays to drive appropriate Raman transitions that are sensitive to these much lower energy states[160,161]. Examples of SRXS have been reported in a number of systems using XFELs[162,163,164] and are now widely used (see, for example, the ChemRIXS endstation at LCLS and the SCS instrument at the European XFEL); applications are discussed further in **Chapters 5** and **6**.

Other promising non-linear X-ray methods that are now emerging include second harmonic generation (SHG) that offers a surface specific probe of great potential for studying chemistry at interfaces, for example in catalysis and batteries.[165] The first observations of SHG at 7.3 keV with a diamond crystal was made at SACLA[166] and then at the C K edge in graphite thin films at FERMI.[167] Recently soft X-ray SHG was used at LCLS to probe the surface structure of water in a liquid sheet microjet.[168] Because SHG can only occur in a non-centrosymmetric medium, the conditions for the generation are only met at an interface/surface where the symmetry is thus broken, leading to the high surface sensitivity of the technique.[169,170,171]

Four-wave mixing (FWM) also has much potential for studying matter at high spatial and temporal resolution. Experiments at FLASH using short wavelength and optical sources have, for instance, combined XUV from the XFEL with an infrared laser to study core excitons in LiF.[172] The development of transient grating FWM studies at FERMI has been a landmark in the application of non-linear X-ray methods to materials[173,174,175]. Transient grating (TG) spectroscopy has emerged as a powerful method that offers element specificity, smaller nanometre-scale grating periods and large momentum

transfers, such that it can map temporal information into the spatial domain where it can be observed against a zero background. It has proved of use in measuring phonon and thermal transport properties in materials on nanometre/femtosecond scales,[176,177] probing thermoelastic properties of materials[178] and the generation, control and probing of magnetic patterns[179,180], and detection of coherent nanoscale spin waves.[181] Transient grating methodology has also recently been demonstrated in the hard X-ray range.[182,183]

3.3.5 Conclusion and future directions

Building on these ideas, we can envision the development of new experimental techniques to probe electronic dynamics on femtosecond to attosecond timescales. In the future, with multi-pulse/multi-colour attosecond operation, it will become feasible to create a localised electronic excitation at one atomic site and then probe, with attosecond resolution, the motion of that excitation to *multiple* other atomic sites within the molecule or material, by observing stimulated emission at different X-ray frequencies (see **Box 3.3**). Further developments exploiting multi-colour attosecond pulses at high repetition rate will permit us to realise more elaborate X-ray four-wave mixing scenarios, currently at the level of theoretical investigation. These ideas promise to yield new types of multi-dimensional spectroscopy that can, in principle, examine the full range of nuclear, electronic and electronic-nuclear couplings in a material. Extension of the transient grating method to the X-ray range to investigate ultrafast transport in materials is one prospect, but this will require fully coherent broad-bandwidth pulses (such as those available with eSASE) with a high measure of phase coherence across a wide range of frequencies. With appropriate high repetition rate X-ray sources giving access to the measurement of weak signals at high fidelity, the extension of the methods to more complex materials, liquids and larger molecules is feasible.

Attosecond X-ray pulses, with provision for two- and multi-colour pulses, will be needed at high repetition rate. Each pulse will have ~ 10 eV of coherent bandwidth, and this capability will be needed across the soft X-ray to hard X-ray range to enable the full range of research. Hard X-ray attosecond pulses would enable impulsive Raman site-specific probing in bulk condensed phase materials that minimises damage to, and backgrounds from, the surrounding material. Optimal approaches to synchronise and time-sort the delay with external lasers will permit the development of a wide range of attosecond measurements, e.g. with an XUV pump (from HHG) and an X-ray probe or an optical pump and X-ray probe. New accelerator-based generation schemes for THz – optical – UV pulses perfectly synchronised with the X-rays (e.g. with an afterburner undulator) would permit attosecond probing of field dressed processes. It is likely that the full array of X-ray tools needed for these advanced spectroscopies can be developed over the next decade and incorporated into a next-generation XFEL facility.

3.4 Capturing conformational dynamics and rare thermo-dynamic states

Chemical reactions catalysed by biomolecules and transformations between states of matter, such as crystallisation or phase transitions, progress via complex trajectories across rare thermodynamic states. Many of the transitions and fluctuations critical to these processes happen at timescales too fast to be captured by any existing methods. XFEL imaging methods, coupled to advanced AI data sorting algorithms, offer a unique way to capture these changes essential to understanding how, for instance, biomolecules function in their native state and deliver improved control of matter for the benefit of material science.

3.4.1 Introduction

For many decades the key to our scientific understanding and control of matter in its various forms – molecules, polymers, solid materials (metals, semi-conductors, dielectrics) and biomolecules – has stemmed, in large part, from our ability to determine their atomic scale structure. In structural biology, the tight connection between structure and function is an underpinning paradigm that supports nearly all of biology and is responsible for the vast majority of new treatments linked to human health. Our scientific understanding of structure was delivered by the capability to use X-ray, neutron and electron diffraction, and imaging methods to determine the atomic scale arrangement of complex material. As successful as this picture has been, it nevertheless misses a key part of the story.

The challenge is that many processes in condensed phases, such as enzyme catalysis, crystallisation,[184,185] phase transitions,[186,187,188] or dynamic heterogeneity,[189] occur via rare states accessed via thermodynamic fluctuations. Yet, we only detect an ensemble averaged behaviour, strongly dominated by the stable endpoints of the process, rather than capturing the underlying transformational dynamics at a single molecule level. For example, in the context of biomolecules, scientists fit an atomic model to X-ray diffraction data from crystal comprising 10^6 copies of the macromolecule, each of which may include tens of thousands of atoms in a complex 3D arrangement. Functional information often comes from measuring the reaction kinetics and/or spectroscopic signals of an ensemble average reaction in solution. Overall reaction rates are typically rather slow (microseconds or longer) for biomolecules, although the dynamics of the critical sub-steps that manifest the functional processes nearly always happen on a much faster timescale (picosecond to nanosecond). Up until very recently, we have not had the appropriate tools to capture the atomic structures of dynamic systems engaged in performing their function. Thus, the ability to routinely measure the structure and function of macromolecules engaged in physiological processes, under physiological temperature and pressure, would be transformative.

If we can directly image key conformational steps, i.e. the rare thermodynamic states crucial to function, then the ensuing mechanistic insights will answer profound questions in condensed phase processes, including physics, biology and chemistry:

- How do enzyme-catalysed reactions occur in a living cell?
- How do molecular machines efficiently cross energy barriers to drive biological processes?
- What are the fluctuation dynamics of solvation networks in liquids?
- What are the initial steps in crystallisation and how do the initial crystal seeds grow?
- What are the mechanistic aspects that control phase transitions?
- How do spontaneous fluctuations and nanoscale heterogeneity relate in functional materials?

New X-ray diffraction and coherent diffraction imaging capabilities at XFELs enable single-shot structure determination/imaging, which exploit pulses short enough to capture individual conformations. For each single molecular or biomolecular assembly probed with femtosecond pulses,

we capture an instantaneous conformation that is not smeared by a long exposure time. This capability, combined with advanced data analysis techniques, offers a route to resolve the questions posed above and many others.[190,191] Using these methods, and with sufficient data, it is possible to map out the conformational trajectory through the free-energy landscape associated with a particular reaction path,[192] and address fundamental questions in statistical mechanics and rare events. In common with cryo-EM, this potential capability for single-particle imaging sets X-ray scattering data apart from ensemble-averaged methods, such as X-ray crystallography and NMR spectroscopy, that cannot capture the single-molecule conformations.

Whilst the most common technique to measure dynamics is by the pump-probe methodology, this is *not* viable for capturing the numerous reactions occurring at room temperature but driven by far from equilibrium transient conformational changes (e.g. barrier crossings). For instance, the molecular conformation(s) required by enzyme catalysis are very likely to be significantly different from the equilibrium structure of the macromolecule in its ground state. An alternative to pump-probe strategies is to take multiple short pulsed data points and then splice these together to create stop-motion views of the functional cycle. This often exploits either X-ray diffraction from a periodic array, as in serial micro-crystallography methods, or coherent diffraction imaging from non-regular specimens, as in single-particle imaging techniques, at high spatial localisation to avoid spatial averaging. Importantly, the density of the data sampling must be high enough that the rarely occupied high-energy states of the system are present within the data set. Moreover, the exposure time must be short enough to capture the various stages of these conformational changes without time averaging, scrambling or blurring. If these criteria are met, then the data techniques can in principle retrieve the structural dynamics of these critical events at high atomic and temporal resolution. With a **next-generation XFEL coupled to AI data analysis** methods this will become possible, as recent work is signposting.

3.4.2 Data driven approaches to structural dynamics

Pioneering work by the Ourmazd group [193] took pump-probe experimental data[194] that visualised the molecular rotational wavepacket in N_2 using Coulomb explosion. Despite the fact that the original data had 300 fs timing uncertainty, Ourmazd *et al*. were able to reconstruct the dynamics with a few femtosecond precision, including transient aligned states of the molecule. The key feature of this data-analysis method is that it does not require precise control of timing, as would be the case in a conventional pump-probe experiment. Instead, it uses random and essentially noisy data from the large dataset and applies advanced algorithms for sorting the data to reconstruct the rare events.

For some cases, such as cryo-EM, the relatively low temporal resolution available from freeze-quench methods (~ a millisecond) are adequate to capture the dynamics of slow processes. The ability to go to much faster timescales, however, corresponding to the actual inherent timescales of many intermediate states, and the opportunity to avoid artefacts from low temperature conditions, presses us to explore the possibilities available with ultrafast X-ray sources. Furthermore, cryo-EM data sets are typically rather small due to the time associated with the freeze-quench preparation and data collection, which limits the ability to "*see*" critical rate-limiting high-energy conformational states. Cryo-EM is, and will likely remain, the dominant method for single molecule conformational state determination with near atomic resolution. In contrast, lower resolution X-ray single-shot imaging may have a considerable role in uncovering the large conformational changes associated with high-energy, rate-limiting processes.

Another example, applied to single-molecule coherent diffractive imaging of the PR772 virus with low spatial resolution (in the 10 nanometre range), allowed Ourmazd *et al*. to visualise a rare event – the growth of a tubular structure from a portal vertex potentially associated with release of the virus genome, as shown in **Figure 3.9**.[195] This indicates the potential for application to X-ray snapshot imaging. The success of the technique was also demonstrated with cryo-EM data, where the conformational and energy landscape of the 80S ribosome extracted from yeast was mapped.[196]

More recently the same methodology has been applied to photo-chemical dynamics studied by time-resolved SFX of the photoactivated yellow protein (PYP)[197] and the de-excitation dynamics via a conical intersection was reported to have been revealed with few-femtosecond resolution[198].

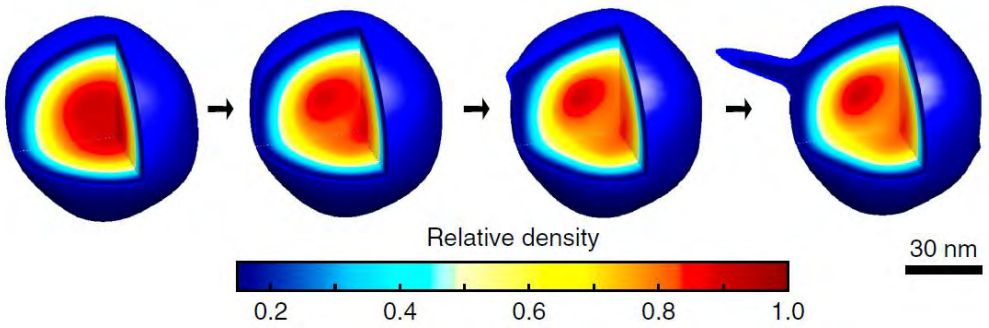


Figure 3.9: 3D structures revealed by conformational analysis of 37,550 single-particle X-ray snapshots of the PR772 virus grouped by conformational parameter. The rare tubular structure is captured in the rightmost conformer.[195]

*Reprinted by permission from Springer Nature from A. Hosseinizadeh et al. Nat. Methods **14,** 877–881. DOI: 10.1038/nmeth.4395 Copyright (2017)*

3.4.3 Developing methods for tracking conformational dynamics through the energy landscape

The further development of these methods will require some significant technical advances for which a next-generation XFEL facility can be optimised. Firstly, improved resolution of X-ray single-particle imaging is an important goal. The Single Particle Imaging Initiative at LCLS and other efforts globally have improved the methodology and resolution,[199] but it is believed there is still considerable scope for further improvement. This includes improved control of imaging conditions (X-ray intensity, spectrum, beam profile), an improved particle hit rate and higher precision positioning in the focus, less variation in the thickness of the hydrating water jacket around each sample, and further improvements on scattered background and on analysis algorithms. Evidence is emerging that the highest intensities are not required for imaging and that, if a nanometre resolution is sought, then soft or tender X-ray wavelengths rather than hard X-rays may be optimal.

The central advantage of the XFEL-based technique is the possibility of recording very large datasets. The probability of a specific conformer within the free energy landscape is determined by the Boltzmann factor, and hence the highest energy states furthest from equilibrium will also be the rarest. To be sure of sampling with sufficient numbers, *all* of the relevant conformers for a reaction with a high-energy transition state (as in processes driven by adenosine triphosphate (ATP) hydrolysis) will require billions of individual snapshots. This will remain very challenging for cryo-EM, but is well within reach of an XFEL, even one at a modest repetition rate of 10 kHz, which will require only hours under optimised conditions. Moreover, the very short pulses (few femtoseconds) of the XFEL will eliminate any possibility of temporal smearing, which remains a real issue given the freeze-quench time of cryo-EM.

It therefore appears that a high repetition rate seeded source operating at ~1 keV and with high flux harmonics (to 3 keV) may be a very appropriate source for furthering the method to sub-nanometre resolution. The seeding would ensure stable shot-to-shot conditions and a reproducible beam and spectrum. This would need to be coupled to the most innovative state-of-the-art sample delivery system. Another area where focused effort will be needed is in AI algorithm development to support the efficient conformational determination and sorting from the large data sets. For ultimate resolutions, a high repetition-rate hard X-ray source with some form of seeding could prove optimal. These capabilities are also likely to have impact in capturing the complex structural dynamics in

condensed phase systems and quantum materials, where fluctuations on the mesoscopic scale can play a critical role.

3.4.4 Future outlook

XFELs hold promise of bringing new insight into the rare events and thermodynamic states that underpin the function of enzyme catalysis, phase transitions, crystallisation (with its great importance for the properties of advanced materials), and the rate-controlling steps of many important processes in the chemical and biotech industries, food processing, and in the manufacture of materials. On a fundamental level, direct access to rare states and rare events will allow scientists to fine-tune their understanding of equilibrium and non-equilibrium thermodynamic processes. Single particle imaging and imaging of a wide range of thermodynamic states is likely to grow into an important technique that could benefit a wide range of research groups in the UK.

To advance this work, a high repetition-rate, seeded source operating at approximately 1 keV, with high flux harmonics up to 3 keV, would offer exciting opportunities. High repetition-rate hard X-ray pulses with high shot-to-shot stability would be even more transformative. These X-ray capabilities would need to be coupled to a state-of-the-art sample delivery system, and the most advanced detectors and AI driven analysis algorithms.

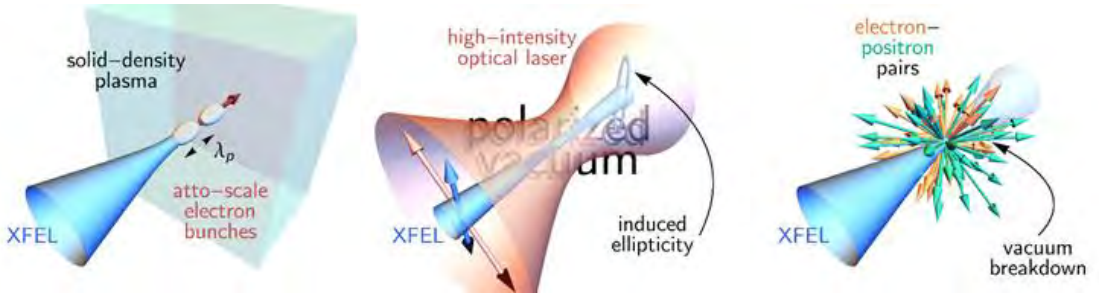
3.5 Non-linear X-ray physics and physics beyond the Standard Model with XFELs

With the development of high intensity X-ray lasers, it is possible to envisage new non-linear X-ray interaction physics in matter and with the quantum vacuum. The interaction physics of high intensity X-rays with matter is a largely unexplored problem. High intensity X-rays open the door to using multiphoton interaction in groundbreaking precision tests of observables that are normally manifest only in very high-energy collisions. This may allow tests for deviations from the Standard Model of particle physics, while being far below the Planck scale of 10^{19} GeV that is beyond the direct reach of any conceivable particle accelerator.

3.5.1 XFEL-driven non-linear dynamics in matter and vacuum

The combination of high photon frequency and high intensity means that XFELs are ideally suited to studying matter in extreme conditions, as discussed in **Section 4.2**. However, a future XFEL system that aimed for *relativistic intensity*, at XUV to soft X-ray wavelengths, could be used to explore new non-linear, X-ray propagation physics in matter, or even the vacuum itself.[200,201] The latter is possible because, according to quantum field theory, light can interact with transient electron-positron pairs, whose lifetime is restricted by the uncertainty principle. There are longstanding theoretical predictions that the vacuum, through this coupling, behaves as a non-linear, birefringent medium, and can even "decay" to electron-positron pairs.[202] The highly multiphoton nature of these processes means that they belong to the *non-perturbative* sector of QED. While the perturbative regime has been thoroughly explored with collider platforms, there have been only a few investigations of non-perturbative QED.[203] Neither vacuum birefringence nor vacuum breakdown have been observed with real photons. Here, we summarise three scientific opportunities, illustrated in **Box 3.4**, that would be available with XFEL pulses that are focused to high intensity.

Box 3.4: Example scientific opportunities available with XFEL pulses focused to high intensity



(Left) An XFEL drives a nonlinear plasma wake in a high-density plasma, accelerating atto-scale electron bunches at gradients of TeV/cm

(Centre) An XFEL probes the vacuum polarised by a high-power optical laser

(Right) An XFEL, focused to ultra-high intensity, sparks electron-positron pair creation from the vacuum

The propagation of a high-intensity optical laser through dense media is known to give rise to a wide range of non-linear effects: non-linear refractive index, ionisation, beam self-focusing and filamentation, as well as frequency conversion through self-phase modulation, harmonic generation and Raman and Brillouin scattering. Recent experiments have demonstrated the spectroscopic probing of warm dense matter[204] and attosecond lasing in the X-ray regime.[205] The basic physics of **non-linear X-ray interactions with solid density matter** have so far been little addressed, and a new facility with tightly focused, high energy pulses and a high repetition rate would allow these phenomena to be

explored. This is in part stimulated by the desire to understand how extremely intense X-rays propagate through matter. The properties of the plasma created by the excitation and acceleration of electrons in solids varies according the properties of the material: in a crystalline environment, for example, channelling and coherent bremsstrahlung give rise to radiation with novel properties.[206] Practical applications of such research include, for example, the development of extremely short pulse X-ray sources, a means of increasing the range of propagation of high intensity X-rays through matter, tailoring energy deposition for X-ray machining in bulk materials, and the possibility of developing time-resolved nanoscopic imaging with elemental sensitivity in dense systems.

One exciting possibility is using an XFEL beam to drive a wakefield in a solid-density plasma,[207] thereby scaling a laser-plasma accelerator[208] from optical to XUV or soft-X-ray wavelengths. This leverages the considerably higher frequency of an XFEL; as the plasma frequency of a medium increases with the electron density n_e, increasing the driver frequency renders higher density targets transparent. The plasma wavelength, λ_p [μm] = $n_e^{-0.5}$[10^{21} cm^{-3}], which controls the size of the accelerating structure and consequently the size of the electron bunches, is significantly reduced. For optical lasers, the use of a high-pressure gas jet 10^{18} – 10^{19} cm^{-3} yields a cavity size of 10 μm and therefore electron bunches that are tens of femtoseconds in duration. Driving a solid of density 10^{23} – 10^{25} cm^{-3} with X-rays, focused to an intensity ~ $10^{18}\,\lambda^{-2}$ [μm] W cm^{-2}, could yield electron bunch durations as short as 10^{-17} – 10^{-15} s. These could be used to generate secondary beams of gamma rays of comparable duration.

Non-linear behaviour occurs not only in matter, but also in the vacuum. While in classical electromagnetism, light does not interact with light, QED predicts that it is possible for photons to scatter off one another. In a collision between a high-intensity optical laser and an XFEL beam, this scattering manifests itself as **vacuum birefringence**. An initially linearly polarised XFEL beam would acquire a small ellipticity, as if it had passed through a birefringent medium. The difference is that the medium is not a material but the vacuum, which is polarised by the strong electromagnetic field of the optical laser. A lab-based measurement of vacuum birefringence is much in demand, as the same phenomenon should occur around highly magnetised compact objects, such as magnetars,[209] and claims of observation are disputed.[210,211] Furthermore, as the ellipticity change would be zero in Born-Infeld theory,[212] an experiment could rule out this alternative theory of non-linear electrodynamics.

The experimental challenge is the small size of the cross-section ($\sigma_{\gamma\gamma}$) for photon-photon scattering, and therefore the small size of the ellipticity change. Indeed, as $\sigma_{\gamma\gamma} = 10^{-31}\,(\hbar\omega^*/mc^2)^6\,cm^{-2}$ for centre-of-mass photon energies $\hbar\omega^*$, much smaller than the electron rest energy mc^2, the necessary photon fluxes are so high that light-by-light scattering has not yet been observed with real photons. The combination of an XFEL and a high-intensity optical laser leverages the strong scaling of $\sigma_{\gamma\gamma}$ with photon frequency: the cross-section is 11 orders of magnitude larger for XFEL-laser scattering than for laser-laser scattering, and 33 orders larger for XFEL-XFEL scattering (as attempted at SACLA[213]). The advantage of using a high-intensity optical laser is that signal is enhanced by coherence. The large separation in energy scales (keV versus eV) means that the X-ray photons primarily scatter forwards, with altered helicity rather than momentum. The ellipticity induced in the probe beam, $\delta = \omega L \Delta n/2$, is proportional to the *difference* in the refractive indices $\Delta n = 2\,\alpha\, I_{laser} / 15\, I_{crit}$. It is maximised by increasing the X-ray frequency ω and the laser intensity I_{laser} ($I_{crit} = 2 \times 10^{29}$ W cm^{-2}). As the ellipticity change is of order $\delta = 10^{-10}$, high initial polarisation purity and precision measurement capability are required.[214] Such experiments are already planned at the European XFEL as part of the HIBEF project; a next-generation XFEL has the potential to leverage new laser technology to reach higher optical field intensities and repetition rates, which will significantly enhance the signal statistics. A future possibility would be the probing of anomalous dispersion at higher X-ray energy, where the refractive indices become energy dependent.

At higher field strengths, these same vacuum non-linearities become strong enough to drive **Schwinger pair creation**, or **vacuum breakdown** to electron-positron pairs. This phenomenon, a landmark prediction of non-linear QED, becomes likely when the applied electromagnetic field can deliver work equal to $2mc^2$, i.e. twice the rest energy of an electron-positron pair, over a Compton length $\lambda_c = \hbar/(mc)$ which is ~ 386 fm. This process should be distinguished from the gamma-X-ray pair creation discussed

in **Section 4.3**, which occurs in the linear or weakly multiphoton regime and is therefore well described by perturbative QED. Schwinger pair creation is driven entirely by the field itself and cannot be described at any order of perturbation theory. Exponential suppression of the rate is overcome by fields that satisfy $E^2 - c^2B^2 > E^2_{cr}$, which requires either tight focusing or the overlap of two or more beams of extreme intensity. However, the characteristic field strength, $E_{cr} \sim 1.3 \times 10^{18}$ V m^{-1}, is so large that it is currently out of reach in a laboratory environment. In fields of critical strength, the electrons and positrons so created can be accelerated so strongly that they radiate hard gamma-rays, which stimulate further pair creation, radiation emission, and thus an electromagnetic cascade. It is speculated that triggering such a cascade is what limits the highest intensity that could ever be achieved with a tightly focused optical laser.[215,216] However, the higher photon frequency of an XFEL compared to an optical laser means that it is possible to reduce the volume of the focal region, suppressing cascade growth that could limit the largest field achievable It is predicted that a terawatt XFEL, focused close to the diffraction limit, could provide the first observation of Schwinger pair creation.[217] Here, capability for diffraction-limited focusing is essential: if the focal spot radius is 20 nm rather than 0.1 nm, the power requirements increase from 2 TW to 50 PW. Progress towards this goal would also allow for the study of higher order, multiphoton effects in gamma-X-ray pair creation (see **Section 4.3**); non-linear effects increase with the X-ray focused intensity I_X as $I_X^{3/2}$.

3.5.2 Physics beyond the Standard Model with XFELs

The Standard Model of particle physics allows for charge-parity (CP) violation in the electroweak and strong sectors. While the former is experimentally established, the latter is constrained by neutron electromagnetic dipole measurements to be negligibly small, with no natural explanation. This is known as the strong CP problem. One of the most well-motivated solutions to this problem is the axion proposal by Peccei and Quinn.[218] It has been subsequently noted that such models have a pseudo-Goldstone boson, the QCD axion,[219,220] which can make up a substantial fraction or the entirety of the dark matter abundance[221,222,223] of the Universe. Similar pseudoscalars, known as axion-like particles (ALPs), readily arise in the low-energy spectrum of string theory.[224] In the following, the term axion is used to refer to both the QCD axion and CP-conserving ALPs.

If the mass range around 1 eV is considered, the strongest bounds are placed by the CAST experiment,[225] a helioscope sensitive to the axion flux produced in the Sun. However, due to the astrophysical origin of the axions and the consequential lack of control over their production, the possibility of model dependence must seriously be taken into account. For example, the non-zero plasma frequency and high temperature conditions in the Sun affect the axion-photon effective coupling.[226] Similar arguments apply to stellar cooling bounds. In the lower mass range (<10 μeV), microwave-cavity searches (such as ADMX[227]) look for dark matter ALPs and achieve bounds very close to the QCD predictions, but, of course, these bounds are heavily dependent on the underlying assumptions of the local dark matter distribution.

As such, model-independent bounds given by purely terrestrial experiments can be attractive, particularly if they can be comparable to those provided by CAST or ADMX. With the development of high intensity laser beams, searches using the light-shining-through-walls (LSW) scheme[228] have become possible. These are based on the idea that a laser beam propagating in a magnetic field can spontaneously create axions that being weakly coupled, pass through an intervening wall. Behind the wall, any axions entering the reconversion magnetic field mix back into photons and are detected. Other laboratory axion searches include the PVLAS collaboration,[229] looking at induced birefringence as a polarised laser beam traverses a magnetic field. This effect receives contributions from both QED and axion interactions, with the leading QED contribution a one-loop process, which competes against the tree-level axion contribution. Because of this limitation, PVLAS bounds, even if they provide an enhancement from laser LSW searches, are still significantly above those provided by CAST.[230]

The above discussion suggests that XFEL searches could fill the gap in both exploring different mass ranges and in probing axion couplings below the PVLAS bounds. An XFEL facility could then be included in the worldwide effort of searches for dark matter, as synchrotrons have, in the past, been used in

LSW experiments, both at ESRF[231] and SPring-8[232]. The advantage of an XFEL in LSW searches is the $10^{17} – 10^{18}$ increase in the number of photons/s, implying a factor of 20 – 30 improvement in the predicted exclusion bounds (due to the very weak coupling of axions to ordinary matter).

A proof-of-principle experiment has recently been performed at the European XFEL facility. When using X-rays, it is possible to increase the detection sensitivity by exploiting the electric fields which are present within a crystalline material. These atomic electric fields can be as high as 10^{11} V m^{-1} which corresponds to magnetic field strengths of order 1 kT – much higher than the field strengths available using the best electromagnets – although the length scales accessible with crystal-based searches are smaller than for those with electromagnets, ~25 T m in the experiment of Halliday *et al*.[233] Furthermore, arranging atoms in a crystalline structure leads to a coherent effect analogous to Bragg scattering. Generation and reconversion can thus be carried out with a pair of X-ray crystals. This concept was first described by Buchmüller and Hoogeveen[234]. The setup used by the European XFEL experiment is shown in **Figure 3.10**.

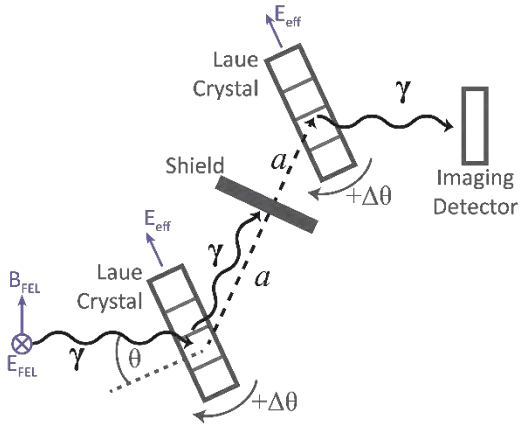


Figure 3.10: Diagram of the setup in the European XFEL experiment; the X-ray beam propagates from left to right. Here, B_{FEL} is the magnetic field in the XFEL beam, and E_{eff} is the crystalline electric field. Axion production and photon regeneration are expected to take place via the Primakoff effect within a pair of monolithic crystals, Ge(220) in Laue geometry. The shield is a 1 mm thick titanium sheet. The polarisation of the X-ray beam maximises the value of $B_{FEL} \cdot E_{eff}$ and thus the probability of axion production.

While similar experiments have also been performed at synchrotron facilities[235], there are two main advantages in using an XFEL compared to third generation light sources. First of all, because of the short pulse duration, it is possible to time-gate the signal and achieve nearly zero background. Secondly, for a short X-ray pulse the rocking curve of the crystal has a width dictated by the characteristic timescale of the scattering process. Because of the Borrmann effect, the extinction length of the X-rays is much longer than the X-ray photoelectric absorption, and therefore the characteristic timescale is given by the geometric time-delay due to scattering off multiple planes. This narrowing of the rocking curve may also be interpreted as a change in the effective index of refraction inside the crystal lattice, significantly increasing the interaction efficiency. Both of these effects are very difficult (if not impossible) to achieve at synchrotron facilities, hence the need to use an XFEL.

The sensitivity to heavy axions achieved in the European XFEL experiment is shown in **Figure 3.11**, outlining the competitiveness of this approach compared to other searches. In addition, these XFEL searches are scalable to much lower bounds, possibly approaching and surpassing what is needed to probe the QCD axion. This can be achieved using longer acquisition times and crystal lengths, leveraging the advantages of higher data rates from a next-generation XFEL. Taken together, these improvements would increase the sensitivity down to values unreachable by any other laboratory-based techniques in this mass range.

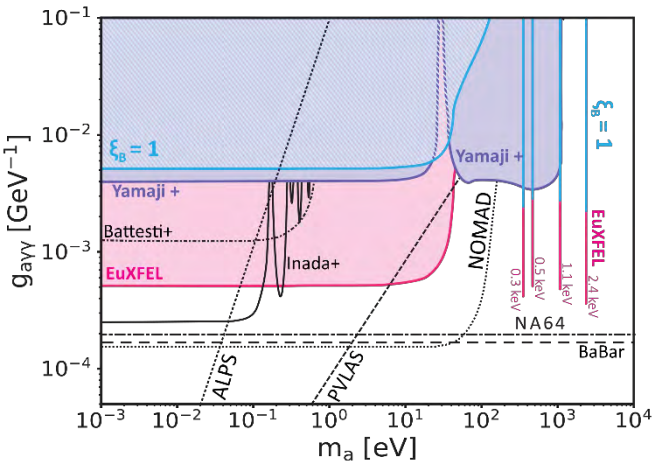


Figure 3.11: Bounds on the axion-photon coupling from the European XFEL experiment (pink) compared with those of other laboratory searches. See Halliday et al.[233] for references.

*Figure reproduced from J.W.D. Halliday et al. Phys. Rev. Lett. **134**, 055001 (2025) under the terms of a Creative Commons license. DOI: 10.1103/PhysRevLett.134.055001*

Note that recent studies have shown that when the Peccei-Quinn (PQ) symmetry breaks after cosmological inflation, axions are also produced by the decay of axion domain walls, and the preferred mass for axions to make up dark matter then exceeds 11 meV[236]. Axions in this mass range are associated with a low scale of the Peccei-Quinn (PQ) symmetry breaking, and so are theoretically preferred as being less susceptible to the 'axion quality problem,' i.e. the potential destabilising effects of quantum gravity on the PQ global symmetry[237]. A new axion production mechanism via isospin breaking has also been recently identified for all axion models that solve the strong CP problem; this requires m_a<53 meV for compatibility with supernova cooling constraints[238]. Thus, there is a "heavy axion window" that has remained relatively unexplored in the laboratory, and in which new experiments at XFEL facilities have the unique potential to make fundamental discoveries.

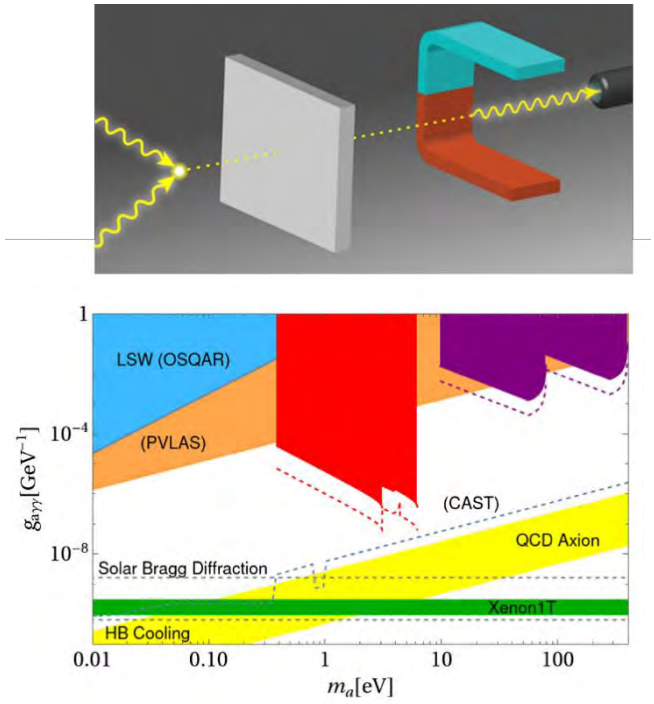


*Figure 3.12: Top: Probing production of dark matter with the coherent interaction of two laser beams (from Physics **13**, s59, 2020; APS/Alan Stonebraker). Bottom: Exclusion plot for axion parameter space. We included the mass interval which can be probed when considering frequency doubled beams. The dashed red line indicates the improvement for a 15 kJ laser. The purple region on the right shows the projected bounds for the collision of an optical and an XFEL[239].*

XFELs coupled to optical lasers can also contribute to these searches by extending the overall mass range. Recent work has shown that the collision of X-ray and optical laser photons may be able to circumvent the intrinsic limitation of laboratory-based searches using the LSW approach[240]. As shown in **Figure 3.12**, the collision of two beams can resonantly produce axions, with their presence inferred by a signal photon detected after magnetic reconversion, but with a much larger cross-section thanks to resonant excitation – achieving exclusion bounds comparable to CAST, but without any assumption on the axion generation in stars. The additional advantage of an XFEL-based search is the energy tunability, thus providing a natural means to scan across a broad energy range – which is needed, given that the ALP's mass is unconstrained by theory.

The proposed axion searches at an XFEL facility will be expected to further constrain the parameter space for axions and ALPs. Whilst a positive detection would be a significant discovery, with a long-lasting impact to our understanding of fundamental physics, a null experiment would also be extremely important, allowing the exclusion of theories and narrowing down the allowable mass range of these dark matter candidates. As we know, while cosmological and astrophysical evidence for dark matter is very compelling, attempts to identify the elusive particle itself have yet resulted in a null detection. Recent satellite observations with XMM-Newton and Chandra in the *Perseus* cluster have shown an unidentified emission line near 3.5 keV.[241,242] It has been suggested that this line may be the result of resonant excitation of dark matter particles. XFEL experiments could then provide an ideal experimental tool (because of the narrow bandwidth and high photon number) to resonantly excite dark matter particles and then measure their subsequent decay into X-ray photons. Initial calculations shows that it might be possible to detect of order 1 – 10 photons a week in this way, thereby potentially opening up a new search strategy for dark matter.[243]

In addition to the above-mentioned dark matter searches, XFELs could also be envisioned as a test of other fundamental physics processes, particularly when focused to high intensities. Ultra-short pulsed X-ray beams are expected to deliver unprecedented intensities at very short wavelength, already achieving values in excess of 10^{20} W/cm^2. An electron placed at the focus of such beams should experience enormous acceleration,[244] comparable to what it would feel if placed near the event horizon of a 6 x 10^{18} kg (= 3 x 10^{-12} M_{sun}) black hole. Indeed, for such low mass black holes, the surface gravity is strong enough that pairs of entangled photons can be produced from the vacuum, with one of the pair escaping to infinity. The black hole can then radiate, and the spectrum of such radiation is a blackbody at the so-called Hawking temperature.[245] This relation is at the foundation of quantum gravity phenomenology, since, by virtue of the equivalence principle, it is impossible to distinguish between an accelerated frame in flat space-time or gravitational effects. In flat space-time, the observation of thermal photons by an accelerated detector is called the Unruh effect.[246]

While the Unruh effect is well-established in the accelerated frame, its possible observation in the laboratory frame remains controversial.[247] This is because the calculation of what the observer sees in the rest frame involves non-trivial, non-equilibrium quantum field theory calculations, to the point that an experiment may be the only way to put the debate to rest.

Moreover, all proposals aimed at the observation of the Hawking/Unruh effect have so far been unable to reach the required conditions, but instead have focused on (classical) analogue systems.[248,249] Hawking radiation, information loss-paradox, as well as searches for dark-matter, are now within the grasp of new high intensity optical laser facilities.[250,251] But, while optical laser experiments are in principle able to achieve the required acceleration, they also need to separate the Unruh emission from any other classical or QED (e.g. radiation reaction) effect, which is very challenging.[252,253] Indeed, recent work has shown that, at tree level, the radiation emitted by an accelerated observer, in its instantaneous rest frame, is the same as Larmor radiation[254]. Hence, any effect related to acceleration radiation must focus to regimes where Larmor emission is minimised. A possibility would be to probe the effect of the Unruh thermal bath on electrons accelerated by a high intensity optical laser via Thomson scattering with an X-ray laser (see **Figure 3.13**)[255].

High-intensity, high-energy X-ray laser facilities thus offer a complementary approach that could provide a successful route towards the experimental validation of the Hawking/Unruh effect. For an electron accelerated by a 10^{19} W cm^{-2} laser, the Unruh temperature corresponds to the optical frequency band, and thus, it becomes much simpler to separate the Unruh emission from the X-ray background. In addition, at these high X-ray intensities, very light particles can also be created via similar mechanisms,[256] which then could complement the dark matter searches discussed above.

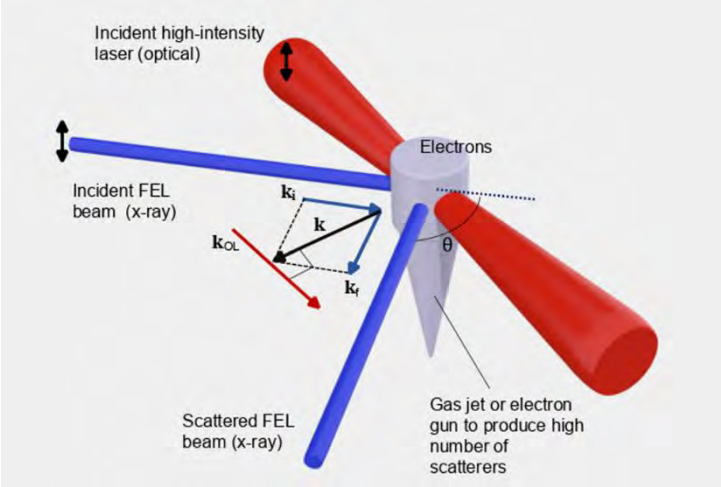


Figure 3.13: Schematic of the setup for the proposed experiment to detect Unruh radiation. The black arrows indicate the polarisation direction of the optical laser and XFEL beams (both vertical in the figure).

Figure reproduced from G. Gregori et al. Eur. Phys. J. C 84, 475 (2024) under the terms of a Creative Commons license.
DOI: 10.1140/epjc/s10052-024-12849-9

3.5.3 Conclusion and future outlook

The science outlined in this sub-section ranges from the basic science of non-linear high intensity X-ray matter interaction to tests of fundamental physics. Although all the research described will be very challenging, and at a range of risk levels from medium to high, the scientific rewards are correspondingly high. It is possible that this research could lead to a new understanding of the fundamental physics of the Universe. The high intensity X-rays required in the soft to hard X-ray range are feasible with current XFEL technology, and still higher intensities may be achieved as that technology, and that of X-ray optics, develops. As the limit, in many cases, will be that signals are weak, the use of high repetition rate (> 100 Hz to 100 kHz) is highly desirable. Here the restrictions may not be the XFEL itself, but rather the high-power optical lasers, which are needed to reach intensities as high as 10^{22} W cm^{-2} and for which scaling to higher repetition rates will be an important goal. That goal is synergistic with other high-power laser projects in the UK.

3.6 High brightness relativistic electron beam science

Monoenergetic relativistic electron beams with low emittance, in addition to driving the XFEL, can also be used directly for new research. This research includes electron beam-driven plasma wakefield acceleration (PWFA) and opportunities to use the electron beam for fundamental physics experiments. The incorporation of plasma photocathodes in PWFA can boost electron energy and brightness, which can have a transformative impact on photon pulses produced by the next generation of XFEL in the future. A second exciting opportunity comes from the possibility of developing a kaon physics experiment, offering unique prospects.

3.6.1 Introduction

At the heart of an XFEL is the low emittance relativistic electron beam that drives the X-ray production. Here we consider additional exciting science that uses that electron beam directly. The first example is the possibility of establishing an experimental end-station for the electron beam, accelerated to multiple GeV, that can be used to conduct research into the beam-driven plasma wakefield acceleration (PWFA) concept. In PWFA, a first electron bunch generates a wakefield that can accelerate a second trailing bunch to significantly higher energy. In this research, focus would be on the plasma photocathode concept, which uses a laser pulse to generate the second electron bunch directly in the wakefield at exactly the correct moment and location for optimal acceleration. This promises new ultra-low emittance electron beams of use in future accelerators and photon sources. Moreover, there are other potential scientific programmes that could be driven by the availability of the 8 GeV, short pulsed, high current beam most of which can be realised non-invasively to X-ray operation. A simulation study by SHINE recently demonstrated prospects for a high repetition-rate surface muon source driven by such a beam[257], with utility for material science and particle physics research programmes. We consider as an example, the possibility of using the electron beam directly in fundamental physics experiments by presenting the possibility of using the electron beam, after use in XFEL undulators and prior to dumping, to develop a leading kaon physics capability.

3.6.2 Plasma photocathode production of ultrabright electron beams

By transferring energy from a *driver* electron bunch to a following *witness* electron bunch via a plasma wave, the energy of witness beam electrons can be multiplied by a significant factor on a sub-metre-scale owing to the ~100 GV m^{-1} scale electric fields within the plasma wave.[258] Although accelerating witness bunches to GeV-scale energies has been demonstrated, achieving high quality (low energy spread and low emittance) bunches is difficult. Recently, PWFA-accelerated bunches have been used to demonstrate FEL gain at visible wavelengths[259,260], but extending this approach to the X-ray region will require significant improvements in the bunch quality.

Now, the plasma photocathode approach, invented,[261] and computationally[262] and experimentally[263] pioneered, by a UK-led collaboration, opens a transformative path towards the controlled production of electron beams of substantially improved quality compared to state-of-the-art. Here, electrons are released with minimal transverse momenta by laser-based ionisation directly within the plasma wave. Subsequent rapid acceleration and focusing in ~100 GV m^{-1} plasma fields then produces electron bunches that are intrinsically compressed to ultra-high brightness. This combination of plasma photogun, compressor and accelerator in a single, compact plasma accelerator stage allows generation of ultrashort (fs to sub-fs-scale), high-current (multi-kA) electron beams with extremely low emittance $\mathcal{E}_{nx,ny}$ down to the nm rad-scale – three orders of magnitude smaller than state-of-the-art levels. In addition to its superior emittance capability, the plasma photocathode process is decoupled from the shot-to-shot jitter of the electron driver beam,[262] which gives rise to potential for very high stability, and in turn an extremely wide parameter range of ultrabright electron bunches, including multi-colour trains with variable separation in energy and time.

The first demonstration of a plasma photocathode was achieved at SLAC's FACET facility in the "E-210: Trojan Horse" experiment[263] in 90° geometry between electron drive beam and plasma photocathode laser. **Figure 3.14** (to the right) shows 3D particle-in-cell (VSim) representations of this experiment (top) and improved versions in collinear geometry (bottom). The electron driver beam from the linac (green) sets up the plasma wave, and the plasma photocathode laser pulse (red) liberates electrons, which are then captured by the plasma wave and constitute the witness beam. R&D on improvement of electron beam quality from this concept is ongoing in the UK and the US, aiming to demonstrate electron beams with 10-nm-scale emittance, sub-fs duration and kA-scale currents.

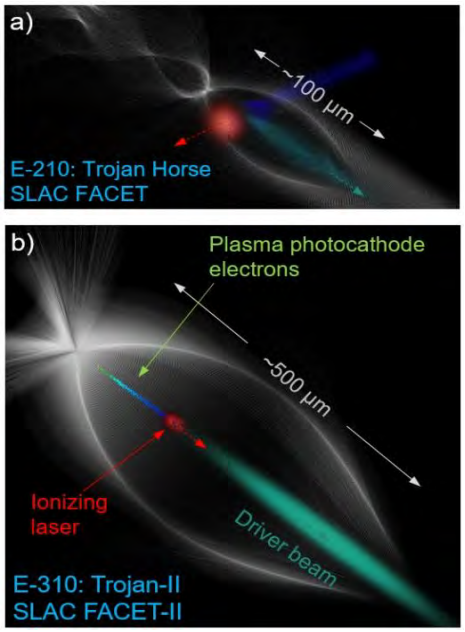


Figure 3.14: The"Trojan Horse" experiment scheme
Adapted from Ref. [263]

A further innovation enabled by plasma photocathodes can reduce the energy spread, from the typical few-%-level to relative energy spreads as low as the $\Delta W_{rms}/W < 0.01\%$ level already at $W \approx 3$ GeV witness beam energies. [262] This very small energy spread meets the requirement for FEL gain at even very hard X-ray wavelengths. It is also crucial for beam quality preservation during transport. Since the emittance of plasma photocathodes can yield nm rad-scale emittance levels in both planes ε_{nx} and ε_{ny}, the corresponding 5D-beam brightness $B_{5D} = 2I_p / (\varepsilon_{nx}\varepsilon_{ny})$, where I_p is the peak current, as well as the 6D-brightness $B_{6D} = B_{5D} / (0.1\% \Delta W_{rms}/W)$, are many orders of magnitude larger than achieved in state-of-the-art conventional accelerators. Recently, high-fidelity end-to-end simulation studies show that these ultra-high 6D brightness beams can be reliably produced and transported for lasing at soft[264] and hard X-ray wavelength[265].

While the experimental realisation and exploitation of plasma photocathode technology is still in its infancy, the experiments conducted to-date are in very good agreement with the expectations of theory and simulation, and the confidence level is therefore high that ultra-high beam qualities can be realised and harnessed[266]. The next generation of XFEL is in a symbiotic relation with PWFA: and the linac can be exploited to realise plasma photocathode PWFA and to produce increasingly bright electron beams that, in turn, can be harnessed for accessing fundamentally new photon science regimes.

3.6.3 Impact of ultrabright electron beams on photon science

The UK's STFC assumed leadership in the exploration of such ultrabright electron beams for photon science in the "PWFA-FEL" project ("Exploratory Study of PWFA-FEL at CLARA" 2019-2023), a UK-US collaboration that brought together plasma photocathode wakefield accelerator and XFEL experts.[267] Retroactive addition of PWFA-FEL capabilities into existing hard X-ray FEL facilities, such as LCLS[268] and/or LCLS-II, may be possible to some degree, but these ambitions would have to deal with existing facility layouts that may prevent full exploitation. The timing of a next-generation XFEL may offer an ideal balance between maturity of PWFA-FEL R&D, and timely provision of capacities to be able to fully harness the opportunities for novel electron beams and photon science. Provision of dedicated beamlines for plasma accelerator boosters would enable exciting R&D capabilities, ranging from photon science to high field/energy physics, without significantly increasing the spatial and financial footprint of the facility; it could even allow significant cost savings by reducing the electron energy and undulator length requirements (see below). Intriguingly, in addition to, or alternatively to, dedicated plasma accelerator beamline(s) directly powered by the linac, one could also accommodate the use of linac-generated electron beams *after* their passage through the undulators. When propagating through an undulator, the electron beam transfers only a fraction of its energy to the photon field, and the concomitant loss in electron beam quality does not significantly compromise its capability to drive

a PWFA. A particularly cost-effective and potentially 'high-gain' approach could therefore be integration of plasma wakefield brightness and energy afterburners into a linac-based next-generation XFEL after the undulator section, instead of only diagnosing and disposing the electron beam into a beam dump, as is usually done.

Figure 3.15 (left) summarises the scheme and potential parameters for a plasma-based accelerator stage driven by a linac-based next-generation XFEL. The plasma photocathode will substantially increase the electron beam parameter range, and will provide a strategic advantage compared with other XFEL facilities. The overarching impact from plasma photocathodes for photon science arises from their capability to produce ultrashort, high-current electron beams with superior emittances – the emittance improvement being at the root of this impact. **Figure 3.15** (right) highlights the boost in 6D brightness of the witness beam that may be realised from plasma photocathode PWFA stages. The plasma photocathode laser required needs to reach tunnel ionisation intensities for He (~ 10^{16} W cm^{-2}), which is compatible with commercially available kHz to MHz rep-rate laser systems generating ~ 1 mJ pulses.

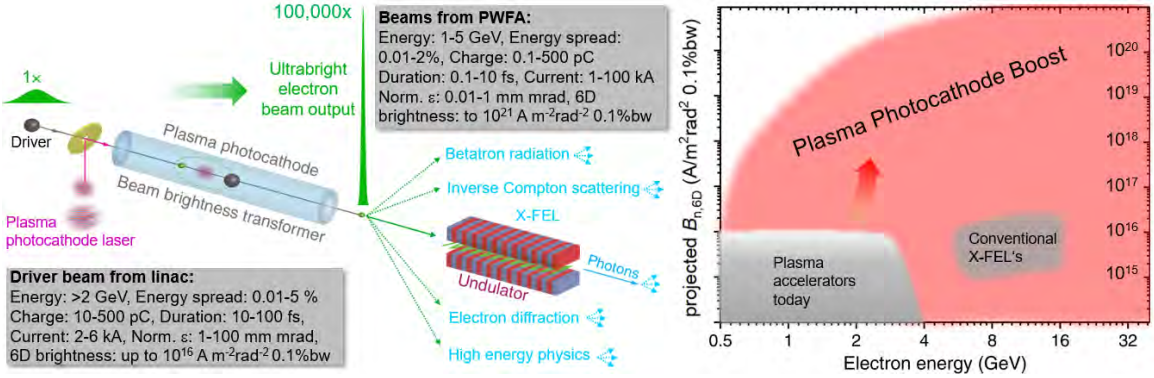


Figure 3.15: Layout for a plasma photocathode based PWFA (left) and the potential beam brightness boost (right)

Such ultrabright output electron beams potentially enable completely new photon science modalities to be explored. Two core requirements for coherent emission of X-ray photons are: (i) the energy spread threshold $\Delta W_{rms}/W < \eta$, where $\Delta W_{rms}/W$ is the relative energy spread, which reduces as $1/\gamma$ during the acceleration process, and $\eta \propto 1/\gamma$ is the FEL Pierce parameter; and (ii) the emittance threshold $\lambda_{min} \approx 4\pi\varepsilon_n/\gamma$ required to achieve saturation at X-ray wavelengths λ_{min}. First, the consequence of ultra-high brightness electron beams is a significant reduction in gain length in the undulator section, because the 1D gain length scales as $L_{1D} \propto B_{6D}^{-1/3}$. Second, such high gain leads to rapid growth of the photon field, and thus minimises slippage between the emerging radiation and the electron beam. This enables a potential route towards operation of the FEL in a single-spike regime for fully coherent ultrashort photon pulses.[264] Such photon pulses would enable novel scientific capabilities for femto-chemistry, materials science, and imaging of electronic distributions, their motion and ultrafast charge transfer, e.g. in biomolecules on their natural timescale. Beyond this, the dramatically reduced emittance opens a path towards hard X-ray wavelengths λ_{min} for electron energies of only a few GeV, or conversely there can be a push towards even harder photon energies.[265,269] Lower electron energies are particularly interesting in this connection, because the rate of mean energy loss to incoherent radiation scales as $\propto \gamma^2$, and an even more severe fundamental limitation towards harder photon energies arises from the quantum fluctuation of synchrotron radiation, which scales with γ^4. These scalings[270] entail dramatic growth of energy spread for high energy beams and impose insurmountable challenges for realisation of gamma-FELs with conventionally-accelerated electron beams. In contrast, low energy, ultralow emittance and high brightness beams from plasma photocathodes allow exploration of exciting possibilities towards gamma-ray FELs as well as for quantum FELs,[268] e.g. for precision studies of nuclear processes, and may allow realisation of photon-photon colliders, [265] e.g. for Breit–Wheeler electron-positron pair production.

Further tailored 'designer' electron beams can broaden the impact of plasma photocathode-generated electron beams on photon science at *a* next-generation XFEL, e.g. via synchronised and versatile multi-colour and pump-probe setups. Finally, as indicated in the *conceptual scheme* in **Figure 3.15** above (see also **Appendix 2**), ultralow emittance and ultra-high brightness beams also allow exploration of a range of wider opportunities, such as betatron and inverse Compton scattering sources, and ion channel lasers for photon science.[268] While experimental realisation of PWFA plasma photocathode-based production of ultra-high brightness beams is only beginning, the arising opportunities are potentially transformative. The integration of plasma wakefield accelerator beamlines for research and applications in next-generation XFEL*s* will allow full harnessing of this potential and will provide unique capabilities and a broad path to future-proof competitiveness and upgrade options.

Beyond photon science, a dedicated electron beamline in a next-generation XFEL facility will provide an ideal environment to demonstrate and validate technologies, critical not only for future plasma-XFELs and light sources but also for future plasma-based high-energy physics facilities. It will allow experimental exploration of multi-stage PWFA acceleration and testing of emittance preservation at the nm-rad level, and exploration of high transformer ratio PWFA stages to achieve energies relevant to high-energy physics. [265] Demonstration of in and out coupling of electron beams between PWFA stages can serve as precursor to a compact, high-average gradient PWFA accelerator facility for multi-GeV and ultra-high brightness electron beam generation for fundamental science and applications. At multi-GeV energies, combining ultra-high brightness beams with TW–PW-class, femtosecond-duration laser pulses open unprecedented opportunities to probe extreme regimes of modern physics. A particularly promising avenue is the integration of hybrid LWFA→PWFA acceleration in a collider geometry, enabling co-located ultra-high-brightness, multi-GeV electron beams, TW–PW lasers, and high-energy photon beams (X-ray to gamma-ray) in a single interaction region,[264,265] as illustrated in **Figure 3.16**. Such a configuration offers a unique gateway to fundamental physics investigations, including photon–photon collisions and SFQED, and particle physics experiments such as kaon physics exploration. By merging accelerator physics, laser science and photon science, the electron beamline stands as a cornerstone for developing and validating the advanced technologies that can define the future of light sources, colliders, and high-field research facilities.

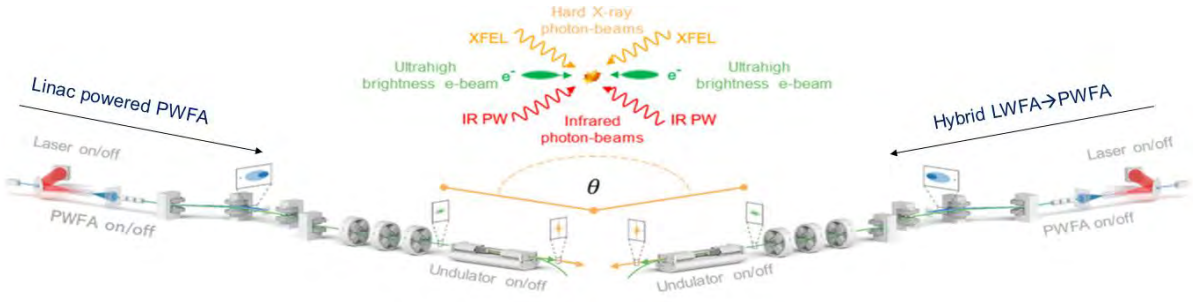


Figure 3.16: Future possibility of colliding extreme beams at a next-generation XFEL facility. Adapted from Ref. [264,265]

3.6.4 Kaon physics at a next-generation XFEL facility

With their unmatched potential to probe new physics beyond the Standard Model (SM) at the multi-TeV scale, ultra-rare kaon decays may soon unveil phenomena that redefine our understanding of the Universe. A concept for a non-invasive, synergistic, and relatively compact kaon experiment at a next-generation XFEL facility is presented here, offering a groundbreaking new opportunity in particle physics.

It is known that the SM, which has been carefully constructed and tested meticulously over the last 50 years, cannot provide the explanation for all phenomena we observe in the Universe, and this indicates that a more fundamental theory is waiting to be discovered.

Fermion (quarks and leptons) masses are the result of the Yukawa interactions between fermions and the Higgs boson. The origin of such interactions, and hence the pattern of fermion masses, called the

flavour problem, remains a puzzle of pivotal importance and can only be addressed with Physics Beyond the Standard Model (BSM). No matter if New Physics is at the TeV scale or well above, it is always very heavy compared to the energy scale of low-energy flavour experiments, making it impossible to directly excite it; therefore, rare and ultra-rare particle decays are the ideal environment for accessing very high-mass scales and identifying indirectly the presence of New Physics. As with all indirect probes of heavy new physics, the primary goal is to identify processes that are both highly suppressed and precisely predictable within the SM, while being exceptionally sensitive to physics beyond the SM.

The strange quark is a constituent of kaon particles (the electrically charged $K^{\pm}$, or neutral $K_{S,L}$). Kaons are unstable particles that are produced via the strong interaction, and decay via the weak interaction. Kaons may hold the key to finding BSM, since rare kaon decays give access to flavour-changing neutral-current transitions that are significantly suppressed within the SM framework, and exhibit heightened sensitivity to new particles and new interactions at higher mass scales than any other similar process.

The ultra-rare decay of a kaon (charged and neutral) to a pion and two neutrinos plays a very special role and is called the "golden-plated" mode, being largely unaffected by long-distance dynamics and therefore enabling the SM prediction to achieve remarkable theoretical precision. These transitions are sensitive to many well motivated BSM scenarios that are fully consistent with present high-energy data and would still give rise to large deviations from the SM in the golden-plated modes.[271–280] The branching ratios for K^+ and K_L are mutually constrained by an inequality, the Grossman-Nir bound[281], which, however, can be evaded in several BSM scenarios[282,283]. In particular, ultra-rare decays $K_L \rightarrow \pi^0\nu\nu$ are the theoretically most pristine channel to search for physics beyond the SM. The SM prediction of its branching ratio is[284] $2.87(7)(2)(23)[2.78(6)(2)(29)] \times 10^{-11}$ based on UTfit[285] [CKMfitter[286]] input, where the uncertainties are from short-distance, long-distance and parametric effects, respectively. The dominant uncertainties, currently at the level of 10%, are, hence, parametric in nature, and mainly due to the uncertainty in the determination of the CKM parameters[287]. Some New Physics models predict correlations between the charge and neutral golden modes, and with the direct CP violation parameter[288,289,290]. A precise measurement of $K_L \rightarrow \pi^0\nu\nu$ decay also constrains the CKM unitarity triangle from kaon observables alone[291], yielding a precision test of the SM complementary to the beauty physics programme.

Experimental status

The drive of the experimental effort in the kaon sector derives from the possibility of conducting precision measurements of rare processes, which may reveal the effects of New Physics. Kaon decay experiments are, in many ways, the quintessential intensity-frontier experiments because of the relatively small number of kaon decay modes and the relatively simple final states, combined with the relative ease of producing intense kaon beams.

Detection of the golden-plated kaon decays is challenging experimentally, due to the presence of two practically undetectable neutrinos and of background sources in excess of several orders of magnitude, and generally requires a dedicated setup, since the typical size and environment prevent multi-purpose collider experiments to select statistically significant clean samples of these processes. The neutral kaon decay $K_L \rightarrow \pi^0\nu\nu$ presents an even greater challenge than the charged kaon one, since neither the initial kaon nor the decay products carry electrical charge, preventing direct tracking or momentum measurement. As a result, this decay must be identified against a backdrop of much more common K_L decays – many of which are up to eleven orders of magnitude more frequent – and can easily mimic the signal, thereby contributing significantly to the background.

The detection of $\mathbf{K^+ \rightarrow \pi^+\nu\nu}$ has been recently proven to be possible. The NA62 experiment at CERN uses a proton beam impinging on a beryllium target to produce a hadron beam, from which positively charged kaons are selected. Since 2016, the NA62 experiment has largely been dedicated to the measurement of $K^+ \rightarrow \pi^+\nu\nu$ decays using a novel decay-in-flight technique.[292] After reporting evidence of the $K^+ \rightarrow \pi^+\nu\nu$ decay from data collected between 2016 and 2018,[293] the experiment has recently obtained the first 5σ observation of this decay by analysis of the data taken up until 2022[294]. NA62 is

scheduled to run until 2026 and researchers foresee collecting a factor of three-times more data than those analysed so far, pushing the relative uncertainty of the branching ratio down to 15%, assuming the same measured central value.

For **$K_L \rightarrow \pi^0\nu\nu$**, discriminating it from abundant backgrounds from other decays relies heavily on vetoing the presence of additional final-state particles. The most stringent direct experimental constraints on the $K_L \rightarrow \pi^0\nu\nu$ decay currently come from the KOTO experiment[295]. A neutral beam of photons, neutrons and K_L is extracted at 16 degrees from collisions of 30 GeV primary protons impinging on a gold target. Charged particles in the beamline are swept away with magnets, while a two-stage collimator is used to define a narrow neutral beam ("pencil" beam) that allows for transverse momentum reconstruction. In the KOTO detector, the two photons from a π^0 decay are detected with an electromagnetic calorimeter at the downstream end of a two-metre long signal decay volume. The decayed π^0 is reconstructed from two photons by assuming the pion mass and the decay point (vertex) being on the beam axis. Candidate events are defined in the plane of the vertex position and the π^0 transverse momentum. Backgrounds are reduced with a hermetic veto system consisting of counters surrounding the decay volume. Further background reduction is obtained using the kinematics of the π^0 and the cluster and pulse shapes in the calorimeter. The current KOTO upper limit is $B(K_L \rightarrow \pi^0\nu\nu) < 2.2 \times 10^{-9}$ (90% CL), with a single-event sensitivity of 9.33×10^{-10}.[296]

To significantly surpass the sensitivity of the SM prediction and enable the first observation of the $K_L \rightarrow \pi^0\nu\nu$ decay, the KOTO collaboration is advancing plans for a next-generation experiment – KOTO-II[297]. The goal is to improve sensitivity by over two orders of magnitude, reaching the $O(10^{-12})$ level. Still, KOTO-II relies on the same experimental technique as KOTO. We also note that NA62, KOTO and KOTO-II rely on a flat-top beam structure.

Future opportunities at a next-generation XFEL facility

In an experiment targeting the observation of the $K_L \rightarrow \pi^0\nu\nu$ decay, the primary strategy for background suppression is to ensure that no particles other than a single π^0 are produced, by vetoing any additional activity. The most challenging background to reject using this method is the $K_L \rightarrow \pi^0\pi^0$ decay, as relying exclusively on photon veto detectors would require an extremely high – and potentially impractical – detection efficiency.

A finely time-structured electron beam at a future XFEL facility could provide a unique opportunity for a next-generation kaon experiment, aiming for the first precise measurement of the $K_L \rightarrow \pi^0\nu\nu$ decay. In particular, it would offer an additional means of suppressing the dominant $K_L \rightarrow \pi^0\pi^0$ and other backgrounds: the determination of the K_L momentum p_K via the time-of-flight (ToF) technique. A conceptual illustration of the ToF method is shown in **Figure 3.17**.

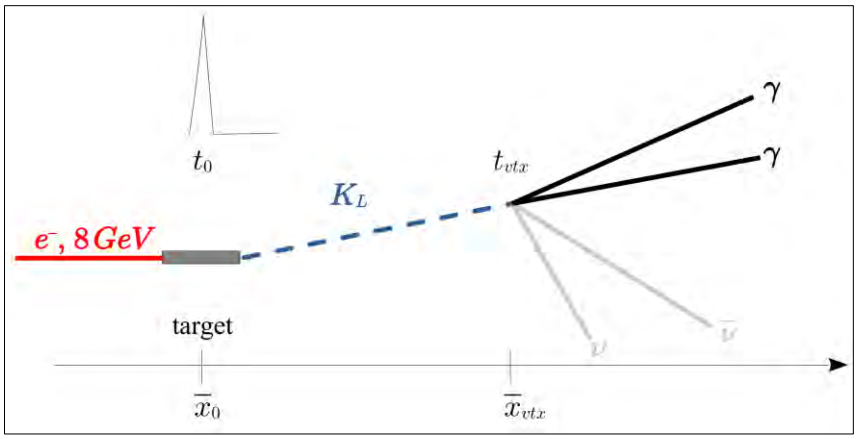


Figure 3.17: Conceptual illustration of the time-of-flight method

The bunched 8 GeV electron beam impinges on the production target positioned in x_0 and with size δx at a well-defined time t_0, with a temporal spread determined by the bunch length δt. Within the interval $[t_0 - \delta t/2, t_0 + \delta t/2]$, a K_L meson may be produced at a position within the target and

subsequently decay within the fiducial volume at x_{vtx}, at a time t_{vtx}, into a final state containing a π^0. By reconstructing the decay vertex x_{vtx} and the decay time t_{vtx} from the measured properties of the two photons from the π^0 decay, and using as the kaon production coordinates x_0 and t_0, the momentum of the K_L can be determined via the relation:

$$\vec{p}_K = \frac{\vec{x}_{vtx} - \vec{x}_0}{t_{vtx} - t_0} m_K,$$

where m_K is the K_L mass. With this method, the K_L momentum p_K can be determined with a relative precision given by

$$\frac{\sigma(p_K)}{p_K} \approx \sqrt{\frac{\sigma(|\vec{x}_{vtx}|)^2 + |\delta\vec{x}|^2}{|\vec{x}_{vtx} - \vec{x}_0|^2} + \frac{\sigma(t_{vtx})^2 + \delta t^2}{(t_{vtx} - t_0)^2}},$$

where $\sigma(|x_{vtx}|)$ and $\sigma(t_{vtx})$ are the spatial and temporal resolutions of the decay vertex, respectively. Assuming realistic values for the relevant parameters ($x_{vtx} - x_0$ = 10 m, $t_{vtx} - t_0$ = 30 ns, $\sigma(|x_{vtx}|)$ = 0.1 m, $\sigma(t_{vtx})$ = 500 ps, $|\delta x|$ = 0.1 m, and δt = 1 ps), a relative momentum resolution of approximately 2% can be achieved, serving as a representative benchmark for the performance of this technique. The choice of 0.1 m for $\sigma(|x_{vtx}|)$ is justified by existing benchmarks: KOTO, which lacks a projective calorimeter but benefits from a short 2 m decay volume, achieves a vertex resolution of 0.07 m, while KOTO-II, with a longer 20 m decay volume, expects a resolution of about 0.15 m. Crucially, as long as the electron bunch length δt is much smaller than the time resolution $\sigma(t_{vtx})$, the momentum resolution is not limited by the electron beam specifications.

With knowledge of the K_L momentum on an event-by-event basis, stringent kinematic constraints can be applied to better discriminate genuine $K_L \rightarrow \pi^0\nu\nu$ decays from background processes. A key variable that can be reconstructed is the squared missing mass, defined as

$$m^2_{\mathrm{miss}} = (P_K - P_{\pi^0})^2 = m^2_K + m^2_{\pi^0} + \sqrt{m^2_K + |\vec{p_K}|^2}\sqrt{m^2_{\pi^0} + |\vec{p}_{\pi^0}|^2} - \vec{p_K} \cdot \vec{p}_{\pi^0},$$

where m_K and $m_{\pi 0}$ are the masses of the K_L and π^0, and p_K and $p_{\pi 0}$ are their respective measured momenta.

Figure 3.18 shows the theoretical distribution of m^2_{miss} for the most common K_L decay modes containing a π^0, compared with the distribution expected for the $K_L \rightarrow \pi^0\nu\nu$ signal. No detector resolution effects are included in this illustration. It is evident that two distinct signal regions can be defined, separated by the prominent $K_L \rightarrow \pi^0\pi^0$ peak, as indicated in the figure. The precise boundaries of these regions will be determined based on the final experimental specifications, including the impact of resolution effects and the level of background suppression required.

The study of K_L decay kinematics through the m^2_{miss} variable – enabled by event-by-event reconstruction of the K_L momentum using the ToF technique – has the potential to suppress the dominant $K_L \rightarrow \pi^0\pi^0$ background, as well as the abundant $K_L \rightarrow \pi^0\pi\pi$ modes, by about three orders of magnitude. Considering that the $K_L \rightarrow \pi^0\pi^0$ decay has a branching ratio of order 10^{-4}, the three orders of magnitude obtained by the use of the ToF technique allows to limit the necessary π^0 rejection to a feasible 10^{-5}. Most of the other backgrounds from kaon decays have either another π^0 or a pair of charged particles missing; therefore, even assuming their branching ratios of order 1, an extra veto rejection of 10^{-4} is feasible. In conclusion, the use of the ToF technique significantly relaxes the performance requirements on the photon veto system. Furthermore, it allows the residual backgrounds to be directly measured from data, by defining dedicated control regions where these modes dominate. Overall, this approach not only enhances background suppression and validation strategies but also increases confidence that any observed signal genuinely originates from the rare $K_L \rightarrow \pi^0\nu\nu$ decay.

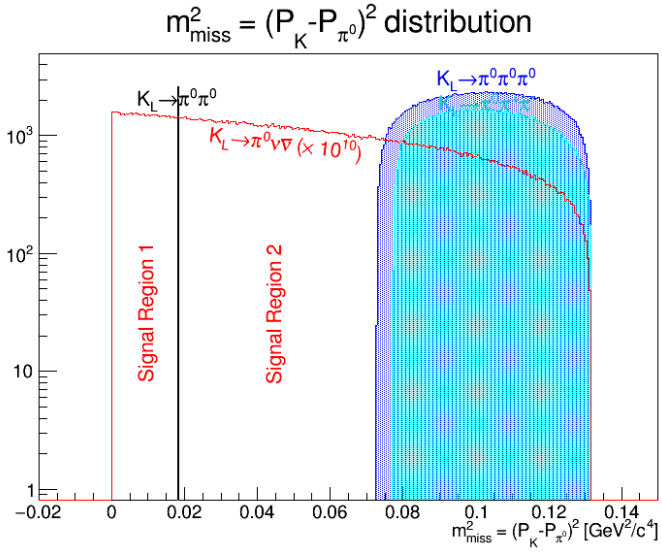


Figure 3.18: Missing mass distribution (arbitrary units vs GeV²/c²). Each component is scaled according to its branching ratio. The distribution of the $K_L \rightarrow \pi^0\nu\nu$ component is enhanced by 10^{10} for better visibility. No particle veto is applied.

Kaon yield

The total number $N_{\pi 0\nu\nu}$ of reconstructed $K_L \rightarrow \pi^0\nu\nu$ decays in a given period T can be estimated by the formula:

$$N_{\pi^0\nu\nu} = N_K^{bunch} f_{bunch}\, T\, \mathcal{B}(K_L \rightarrow \pi^0\nu\overline{\nu})\varepsilon_{reco},$$

where N_K^{bunch} is the number of K_L decays in the fiducial volume per bunch, f_{bunch} is the operating bunch frequency, $B(K_L \rightarrow \pi^0\nu\nu)$ is the $K_L \rightarrow \pi^0\nu\nu$ branching ratio and ε_{reco} is the reconstruction efficiency, which corresponds to the probability of reconstructing a $K_L \rightarrow \pi^0\nu\nu$ decay in the fiducial volume. The number N_k^{bunch} of K_L decays in the fiducial volume per bunch depends on the number N_e of incoming electrons per bunch, the kaon yield per incident electron ρ^e_K, the fraction ε_{coll} of the K_L selected by the collimation system, and the fraction ε_{FV} of selected K_L mesons that decay within the fiducial volume:

$$N_K^{bunch} = N_e\, \rho_K^e\, \varepsilon_{coll}\, \varepsilon_{FV}.$$

The number N_e depends on the operating beam current per bunch. A beam current of 150 pC per bunch corresponds to a number $N_e = 9 \times 10^8$ electrons per bunch. To estimate the kaon yield ρ^e_K, an 8 GeV electron beam incident on a tungsten target was simulated using BDSIM[298], considering various target thicknesses.

Figure 3.19 (left) shows the resulting kaon yield per incident electron for each simulated thickness. The yield increases with target thickness up to a maximum around 30 mm, after which it begins to decline. In the following, the maximum K_L yield—corresponding to the 30 mm target—of 8×10^{-6} kaons per electron will be used. **Figure 3.19 (right)** shows the distribution of the K_L momentum versus emission angle, for a target of 30 mm. The angle spans almost evenly a range between zero and 1.6 radians. Most of the momentum distribution lays between few MeV and 2.5 GeV, with a typical momentum of about 1 GeV and a tail reaching 7 GeV, for the forward angles.

The fraction ε_{FV} of K_L mesons decaying within the fiducial volume depends on the K_L momentum spectrum as well as, unsurprisingly, the definition of the fiducial volume itself – that is, its length and its distance from the target. Based on the K_L momentum spectrum shown in **Figure 3.19 (right)**, approximately 80% of K_L mesons decay within the first 100 meters from the target. **Figure 3.20** illustrates the fraction of K_L mesons decaying inside the fiducial volume for different combinations of starting position and length, both ranging from 0 to 50 m.

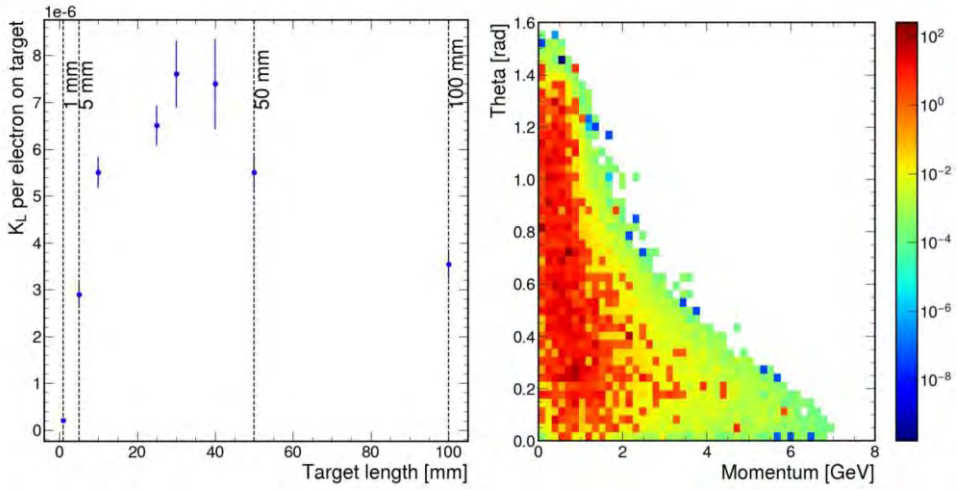


Figure 3.19: Left: number of K_L per electron impinging on target versus target length in mm. Right: distribution of K_L emission angle versus momentum for K_L produced from target

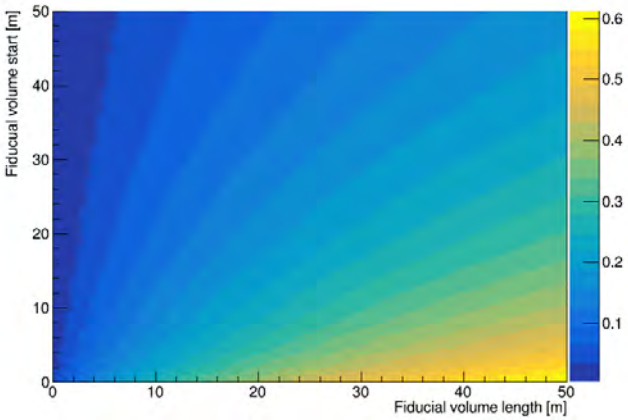


Figure 3.20: Fraction of K_L decays in fiducial volume, as a function of the start position (y-axis) and length (x-axis) of the fiducial volume

The operating bunch frequency f_{bunch} will be limited either by the maximum rate deliverable by the XFEL facility or by the highest frequency at which the ToF method can effectively be applied. For the ToF technique to work reliably, electron bunches must be spaced far enough apart to minimise the probability that a K_L meson from a previous bunch enters the fiducial volume during the detection window for K_L mesons from the current bunch. If such overlap occurs, K_L mesons from earlier bunches decaying in the fiducial volume during the current bunch's window will be assigned the wrong t_0, causing their time-of-flight to be systematically underestimated. This in turn leads to a systematic overestimation of the reconstructed p_K, degrading the accuracy of the kinematic reconstruction. To prevent this effect from limiting the ToF method's rejection power, the fraction η of K_L mesons from earlier bunches reaching the fiducial volume in the current bunch's detection window must remain well below the target level required for kinematic background suppression, which is typically around 10^{-3} – 10^{-4}. Besides the bunch frequency, several other factors play a role on the fraction η: the K_L momentum spectrum, the length of the fiducial volume, and its distance from the target. A larger fiducial volume or a volume positioned closer to the target both increase the probability of such overlaps. **Figure 3.21** shows how the fraction η of K_L decays within the fiducial volume assigned to the wrong bunch varies with the bunch frequency, for different fiducial volume configurations.

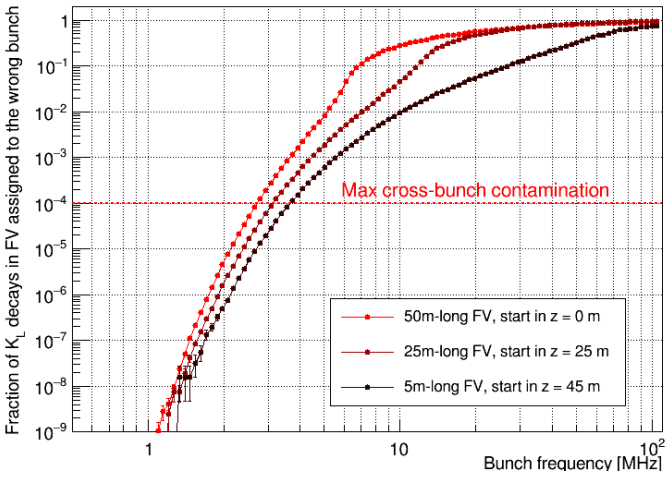


Figure 3.21: Fraction of K_L decays in fiducial volume assigned to the wrong bunch, as a function of bunch frequency in MHz, for three different definitions of fiducial volume. The maximum acceptable cross-bunch contamination is indicated by the red line.

The K_L momentum spectrum shown in **Figure 3.19 (right)** has been used for this evaluation. Even with the least favourable fiducial volume definition, a bunch frequency exceeding 2.5 MHz can still be used while keeping the fraction η at or below 10^{-4}. Therefore, the ToF technique can comfortably exploit the full potential of next-generation XFEL facilities, where the target bunch frequency is 1 MHz.

By combining all the factors, and assuming 270 days of data-taking per year with a conservative bunch repetition rate of 100 kHz, a rough estimate of the total number $N_{\pi 0\nu\nu}$ of reconstructed $K_L \to \pi^0\nu\nu$ decays over five years of running can be made:

$$N_{\pi^0\nu\nu} = 2.2 \times 10^5 \cdot \varepsilon_{coll} \cdot \frac{\varepsilon_{FV}}{0.3} \cdot \frac{\varepsilon_{reco}}{0.3}.$$

Typical values for ε_{FV} and ε_{reco} are expected to be of the order of 0.3. However, the value of ε_{coll} is highly dependent on the experimental strategy: it can range from approximately 10^{-6} for setups using tightly collimated beams, to values near 1 for configurations covering the full solid angle. As a result, ε_{coll} cannot be reliably estimated without a more detailed definition of the experimental layout. As discussed in the next section, multiple options for the experimental design are still under consideration. Given that achieving approximately O(100) reconstructed $K_L \to \pi^0\nu\nu$ decays would enable a precise measurement of the $K_L \to \pi^0\nu\nu$ branching ratio, a value of $\varepsilon_{coll} \gtrsim 4 \times 10^{-4}$ must be targeted. For comparison, an $\varepsilon_{coll} \sim 4 \times 10^{-4}$ could be obtained using a similar collimation system to the one of the KOPIO experiment[299], which had a solid angle of about 500 μsr.

Towards the experiment design

As shown in **Figure 3.19 (right)**, K_L particles are emitted from the target across the entire solid angle. Since the ToF technique requires knowledge of the K_L trajectory, two approaches are possible: one uses a collimator upstream of the experiment setup to allow only K_L mesons with a specific direction to pass, while the other uses the decay products to reconstruct the decay vertex.

The first option is illustrated in **Figure 3.22**, where a collimator with aperture of θ and length L is placed at a distance D from the target (θ is expected to be $\ll 1$ rad).

The angle does not necessarily need to be centred around the beam direction; for example, there might be advantages in centring off-axis if this helps with enhancing the ratio between the K_L and unwanted particles in the beam. Several combinations of the parameters have been considered; however, given the K_L emission angle, a significant reduction in the trajectory uncertainty leads inevitably to a significant signal reduction. Hence there is a tension between achieving a sufficiently precise position of the vertex and retaining a high K_L yield.

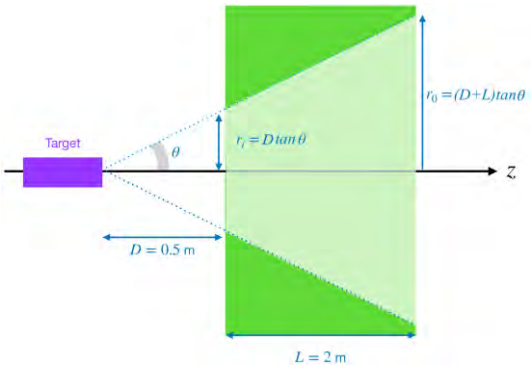


Figure 3.22: Conceptual illustration of a collimator device

A second approach is to use a detector design that is directly after the target and closer to it, and covers much (if not all) of the production solid angle. A key element of such a detector would be an electromagnetic calorimeter with projective capabilities, able to measure the direction of each photon precisely, as well as their energy and position, therefore reconstructing the full kinematic of each photon. Projective calorimetry is a technique that is already in use – for example by the KOTO experiment at JPARC[290] – and a fully projective calorimeter with an almost 4π coverage will be employed by the PIONEER[300] experiment at PSI. While the experimental technique is already well developed, the feasibility and cost will depend in this case on the size of the fiducial volume to ensure a significant yield of K_L decays.

Finally, there is the possibility of combining the two approaches, performing a first reduction of the solid angle region-of-interest with a collimator, and employing a projective calorimeter to achieve the necessary precision on the kaon trajectory. Ultimately, a detailed analysis of the complexity and costs versus the kaon decay yield will have to be performed, in order to create a realistic experimental design. A further consideration in the design is the resilience to the rate of unwanted particles from the neutral beam (photon, neutrons) as well as the result of photon interactions in the material (electrons). While detector high granularity can be employed to reduce the rate per single channel, this would enhance the cost and therefore a careful optimisation is again needed.

Any experimental design will also need to allow for a strong background suppression. This can be achieved with a combination of hermetic, high-efficiency photon veto detectors. Once photons are fully detected, two-body decays like $K_L \rightarrow \pi^0\pi^0$ can be clearly identified in the reconstructed K_L rest frame. Events missing low-energy photons – typically the hardest to detect – can be isolated and rejected. These two independent handles – precise kinematic reconstruction and photon vetoing – enable not only a strong suppression of $K_L \rightarrow \pi^0\pi^0$ backgrounds to levels well below the expected signal but also allow the residual background to be directly measured from data.

Conclusions

Flavour physics—and kaon physics, in particular—plays a prominent role in the ongoing update of the European Strategy. A kaon experiment at an XFEL facility would enable the continuation of this successful research program in Europe following the conclusion of the NA62 experiment. The XFEL characteristics would allow a substantial step change in the measurement of $K_L \rightarrow \pi^0\nu\nu$, which is recognised as one of the most interesting channels in flavour physics, and possibly the hardest to measure. The experiment presented here is more compact and relatively less expensive than typical kaon experiments, and it would exploit the XFEL's extreme bunching in a parasitic manner, without interfering with the facility's primary users.

3.7 References for Chapter 3

1 A. Valentini, D. Rivero, F. Zapata *et al.* "Optomechanical Control of Quantum Yield in Trans–Cis Ultrafast Photoisomerization of a Retinal Chromophore Model," *Angew. Chem. Int. Ed.* **56**, 3842 (2017) DOI: 10.1002/anie.201611265

2 L.A. Baker, S.E. Greenough and V.G. Stavros, "A Perspective on the Ultrafast Photochemistry of Solution-Phase Sunscreen Molecules," *J. Phys. Chem. Lett.* **7**, 22, 4655-4665 (2016) DOI: 10.1021/acs.jpclett.6b02104

3 E. Romero, R. Augulis, V. Novoderezhkin *et al.* "Quantum coherence in photosynthesis for efficient solar-energy conversion," *Nature Phys* **10**, 676-682 (2014) DOI: 10.1038/nphys3017

4 V.I. Prokhorenko, A. Picchiotti, M. Pola *et al.* "New Insights into the Photophysics of DNA Nucleobases," *J. Phys. Chem. Lett.* **7**, 22, 4445-4450 (2016) DOI: 10.1021/acs.jpclett.6b02085

5 P. Vasa and D. Mathur, "Ultrafast Quantum Mechanical Processes in Animals," *Springer, chapter in Ultrafast Biophotonics*, 145-157 (2016) DOI: 10.1007/978-3-319-39614-9_8

6 A.A. Lutman, J. MacArthur, M. Ilchen *et al.* "Polarization control in an X-ray free-electron laser," *Nature Photon* **10**, 468-472 (2016) DOI: 10.1038/nphoton.2016.79

7 L. Young *et al.* "Roadmap of ultrafast X-ray atomic and molecular physics," *J. Phys. B: At. Mol. Opt. Phys.* **51**, 032003 (2018) DOI: 10.1088/1361-6455/aa9735

8 P.M. Kraus, M. Zürch, S.K. Cushing *et al.* "The ultrafast X-ray spectroscopic revolution in chemical dynamics," *Nat Rev Chem* **2**, 82-94 (2018) DOI: 10.1038/s41570-018-0008-8

9 A. Kumar and M.D. Sevilla, "Proton-Coupled Electron Transfer in DNA on Formation of Radiation-Produced Ion Radicals," *Chem. Rev*. **110**, 12, 7002-7023 (2010) DOI: 10.1021/cr100023g

10 M. Durante, E. Bräuer-Krisch, M. Hill, "Faster and safer? FLASH ultra-high dose rate in radiotherapy" *Br J Radiol*. **91**(1082):20170628 (2018) DOI: 10.1259/bjr.20170628

11 K.S. Zinchenko *et al.* "Sub-7-femtosecond conical-intersection dynamics probed at the carbon K-edge" *Science* **371**, 489-494 (2021) DOI: 10.1126/science.abf1656

12 J. Duris *et al.,* "Tunable isolated attosecond X-ray pulses with gigawatt peak power from a free-electron laser." *Nature Photonics* **14**, 30-36 (2020) DOI:10.1038/s41566-019-0549-5.

13 E. Rodríguez-Cuenca, A. Picón, S. Oberl, A.I. Kuleff, & O. Vendrell, Core-Hole Coherent Spectroscopy in Molecules. *Physical Review Letters* **132**, 263202 (2024) DOI: 10.1103/PhysRevLett.132.263202

14 O. Gessner & M. Gühr, Monitoring Ultrafast Chemical Dynamics by Time-Domain X-ray Photo- and Auger-Electron Spectroscopy. *Accounts of Chemical Research* **49**, 138-145 (2016) DOI: 10.1021/acs.accounts.5b00361

15 N. Rohringer, "X-ray Raman scattering: a building block for nonlinear spectroscopy," *Philosophical Transactions of the Royal Society A: Mathematical, Physical and Engineering Sciences* **377**, 20170471 (2019) DOI: 10.1098/rsta.2017.0471

16 M. Kowalewski, K. Bennett, K.E. Dorfman & S. Mukamel, "Catching Conical Intersections in the Act: Monitoring Transient Electronic Coherences by Attosecond Stimulated X-Ray Raman Signals," *Physical Review Letters* **115**, 193003 (2015) DOI: 10.1103/PhysRevLett.115.193003

17 D. Keefer, T. Schnappinger, R. de Vivie-Riedle & S. Mukamel, "Visualizing conical intersection passages via vibronic coherence maps generated by stimulated ultrafast X-ray Raman signals," *Proceedings of the National Academy of Sciences* **117**, 24069-24075 (2020) DOI: 10.1073/pnas.2015988117

18 Y. Nam, *et al.* "Monitoring vibronic coherences and molecular aromaticity in photoexcited cyclooctatetraene with an X-ray probe: a simulation study," *Chemical Science* **14**, 2971-2982 (2023), DOI: 10.1039/D2SC04335A

19 M. Monti, L. Biancorosso, & E. Coccia, "Time-Resolved Circular Dichroism in Molecules: Experimental and Theoretical Advances," *Molecules* **29** (2024) DOI: 10.3390/molecules29174049

20 Y. Zhang, J. R. Rouxel, J. Autschbach, N. Govind & S. Mukamel, "X-ray circular dichroism signals: a unique probe of local molecular chirality," *Chemical Science* **8**, 5969-5978 (2017) DOI: 10.1039/C7SC01347G

21 J. Rouxel, M. Kowalewski and S. Mukamel, "Photoinduced molecular chirality probed by ultrafast resonant X-ray spectroscopy," *Structural Dynamics* **4**:4 (2017) DOI: 10.1063/1.4974260

22 L. Nahon *et al.* "Valence shell one-photon photoelectron circular dichroism in chiral systems," *J. El. Spect. Rel. Phen*., **204**, 322 (2015) DOI: 10.1016/j.elspec.2015.04.008

23 C. Lux, M. Wollenhaupt, T. Bolze *et al.* "Circular Dichroism in the Photoelectron Angular Distributions of Camphor and Fenchone from Multiphoton Ionisation with Femtosecond Laser Pulses," *Angew. Chem. Int. Ed*. **51**, 5001-5005 (2012) DOI: 10.1002/anie.201109035

24 A. Comby, E. Bloch, C.M.M. Bond *et al.* "Real-time determination of enantiomeric and isomeric content using photoelectron elliptical dichroism," *Nat Commun* **9**, 5212 (2018) DOI: 10.1038/s41467-018-07609-9

25 M. Tia, A. Knie *et al.* "Observation of Enhanced Chiral Asymmetries in the Inner-Shell Photoionisation of Uniaxially Oriented Methyloxirane Enantiomers," *J. Phys. Chem. Lett*. **8**, 13, 2780-2786 (2017) DOI: 10.1021/acs.jpclett.7b01000

26 S. Beaulieu *et al.* "Universality of photoelectron circular dichroism in the photoionisation of chiral molecules," *New J. Phys*. **18**, 102002 (2016) DOI: 10.1088/1367-2630/18/10/102002

[27] A. Comby *et al.,* "Relaxation Dynamics in Photoexcited Chiral Molecules Studied by Time-Resolved Photoelectron Circular Dichroism: Toward Chiral Femtochemistry," *J Phys Chem Lett* **7**, 4514-4519 (2016) DOI: 10.1021/acs.jpclett.6b02065

[28] V. Blanchet *et al.,* "Ultrafast relaxation investigated by photoelectron circular dichroism: an isomeric comparison of camphor and fenchone." *Phys Chem Chem Phys* **23**, 25612-25628 (2021) DOI: 10.1039/d1cp03569j

[29] V. Wanie *et al.,* "Capturing electron-driven chiral dynamics in UV-excited molecules," *Nature* **630**, 109-115, (2024) DOI: 10.1038/s41586-024-07415-y

[30] M. Ilchen *et al.,* "Site-specific interrogation of an ionic chiral fragment during photolysis using an X-ray free-electron laser," *Commun Chem* **4**, 119 (2021) DOI: 10.1038/s42004-021-00555-6

[31] D. Faccialà *et al.,* "Time-Resolved Chiral X-Ray Photoelectron Spectroscopy with Transiently Enhanced Atomic Site Selectivity: A Free-Electron Laser Investigation of Electronically Excited Fenchone Enantiomers," *Phys. Rev. X* **13**, 011044 (2023) DOI: 10.1103/PhysRevX.13.011044

[32] M.N. Pohl *et al.,* "Photoelectron circular dichroism in angle-resolved photoemission from liquid fenchone," *Phys. Chem. Chem. Phys.* **24**, 8081-8092 (2022) DOI: 10.1039/D1CP05748K)

[33] D. Stemer *et al.,* "Photoelectron Circular Dichroism of Aqueous-Phase Alanine," *arXiv:2412.08729* (2024) DOI: 10.48550/arXiv.2412.08729

[34] J.H. Both, A. Beliakouskaya. & K.-M. Weitzel, "Determination of the Molar Fraction and Enantiomeric Excess of Electrosprayed Amino Acid Anions Employing Photoelectron Circular Dichroism," *Analytical Chemistry* **97**, 4499-4504 (2025) DOI:10.1021/acs.analchem.4c05964

[35] S. Beaulieu *et al.* "Photoexcitation circular dichroism in chiral molecules," *Nature Physics* **14**, 484-489 (2018), DOI:10.1038/s41567-017-0038-z

[36] M. Waitz *et al.* "Imaging the square of the correlated two-electron wave function of a hydrogen molecule," *Nature Communications* **8**, 2266 (2017) DOI: 10.1038/s41467-017-02437-9

[37] M. Ilchen *et al.,* "Opportunities for gas-phase science at short-wavelength free-electron lasers with undulator-based polarization control," *Phys. Rev. Res.* **7**, 011001 (2025) DOI: 10.1103/PhysRevResearch.7.011001

[38] E. Ferrari *et al.* "Free electron laser polarization control with interfering crossed polarized fields," *Physical Review Accelerators and Beams* **22**, 080701 (2019), DOI: 10.1103/PhysRevAccelBeams.22.080701

[39] J. Morgan & B.W.J. McNeil, "Attosecond polarization modulation of X-ray radiation in a free-electron laser," *Physical Review Accelerators and Beams* **24**, 010701 (2021) DOI: 10.1103/PhysRevAccelBeams.24.010701

[40] S. Rozen, A. Comby, E. Bloch *et al.* "Controlling Subcycle Optical Chirality in the Photoionisation of Chiral Molecules," *Phys. Rev. X* **9**, 031004 (2019) DOI: 10.1103/PhysRevX.9.031004

[41] A.F. Ordonez & O. Smirnova, "Disentangling enantiosensitivity from dichroism using bichromatic fields," *Physical Chemistry Chemical Physics* **24**, 7264-7273 (2022), DOI:10.1039/D1CP05833A.

[42] D. Ayuso, O. Neufeld, A.F. Ordonez *et al.* "Synthetic chiral light for efficient control of chiral light–matter interaction," *Nat. Photonics* **13**, 866-871 (2019) DOI: 10.1038/s41566-019-0531-2

[43] A.M. Beckley, T.G. Brown and M.A. Alonso, "Full Poincaré beams II: partial polarization," *Opt. Express* **20**, 9357-9362 (2012) DOI: 10.1364/OE.20.009357

[44] P. Rebernik Ribič *et al.* "Extreme-Ultraviolet Vortices from a Free-Electron Laser," *Physical Review X* **7**, 031036 (2017), DOI:10.1103/PhysRevX.7.031036

[45] J.-L Bégin *et al.* "Nonlinear helical dichroism in chiral and achiral molecules," *Nature Photonics* **17**, 82-88 (2023), DOI:10.1038/s41566-022-01100-0

[46] G. De Ninno *et al.* "Photoelectric effect with a twist," *Nature Photonics* **14**, 554-558 (2020), DOI:10.1038/s41566-020-0669-y

[47] J. Ni *et al.* "Giant Helical Dichroism of Single Chiral Nanostructures with Photonic Orbital Angular Momentum," *ACS Nano* **15**, 2893-2900 (2021), DOI:10.1021/acsnano.0c08941

[48] J. R. Rouxel & S. Mukamel, "Molecular Chirality and Its Monitoring by Ultrafast X-ray Pulses," *Chemical Reviews* **122**, 16802-16838 (2022), DOI:10.1021/acs.chemrev.2c00115

[49] N. Fujii *et al.* "D-Amino acids in protein: The mirror of life as a molecular index of aging," *BBA - Proteins and Proteomics* **1866**:7, 840-847 (2018) DOI: 10.1016/j.bbapap.2018.03.001

[50] N. Berrah, "Molecular dynamics induced by short and intense X-ray pulses from the LCLS," *Phys. Scr*. **T169**, 014001 (2016) DOI: 10.1088/0031-8949/2016/T169/014001

[51] A. Rudenko, L. Inhester, K. Hanasaki *et al.* "Femtosecond response of polyatomic molecules to ultra-intense hard X-rays," *Nature* **546**, 129-132 (2017) DOI: 10.1038/nature22373

[52] L. Young, E. Kanter, B. Krässig *et al.* "Femtosecond electronic response of atoms to ultra-intense X-rays," *Nature* **466**, 56-61 (2010) DOI: 10.1038/nature09177

[53] N. Berrah, A. Sanchez-Gonzalez, Z. Jurek *et al.* "Femtosecond resolved observation of fragmentation of buckminsterfullerene following X-ray multiphoton ionisation," *Nat. Phys*. **15**, 1279-1283 (2019) DOI: 10.1038/s41567-019-0665-7

[54] S. Kuschel, P.J. Ho, A. Al Haddad *et al*. "Non-Linear Enhancement of Ultrafast X-Ray Diffraction through Transient Resonances," *Nat Commun* **16**, 847 (2025). DOI : 10.1038/s41467-025-56046-y

[55] C.S. Slater *et al.* "Coulomb-explosion imaging using a pixel-imaging mass-spectrometry camera," *Phys. Rev. A* **91**, 053424 (2015) DOI: 10.1103/PhysRevA.91.053424

[56] M. Pitzer, "How to determine the handedness of single molecules using Coulomb explosion imaging," *J. Phys. B: At. Mol. Opt. Phys.* **50** 153001 (2017) DOI: 10.1088/1361-6455/aa77a9

[57] H.V.S Lam. *et al.,* "Differentiating Three-Dimensional Molecular Structures Using Laser-Induced Coulomb Explosion Imaging," *Phys. Rev. Lett.* **132**, 123201 (2024) DOI:10.1103/PhysRevLett.132.123201

[58] E. Kukk, H. Myllynen, K. Nagaya *et al.* "Coulomb implosion of tetrabromothiophene observed under multiphoton ionisation by free-electron-laser soft-X-ray pulses," *Phys. Rev. A* **99**, 023411 (2019) DOI: 10.1103/PhysRevA.99.023411

[59] R. Boll *et al.* "X-ray multiphoton-induced Coulomb explosion images complex single molecules," *Nat. Phys.* **18**, 423-428 (2022) DOI:10.1038/s41567-022-01507-0

[60] M. Fisher-Levine *et al.* "Time-resolved ion imaging at free-electron lasers using TimepixCam*," J. Synchrotron Rad.* **25**, 336-345 (2018) DOI: 10.1107/S1600577517018306

[61] D. You *et al.* "Multi-particle momentum correlations extracted using covariance methods on multiple-ionisation of diiodomethane molecules by soft-X-ray free-electron laser pulses," *Phys. Chem. Chem. Phys*. **22**, 2648-2659 (2020) DOI: 10.1039/C9CP03638E

[62] T. Driver, R. Ayers, R. Pipkorn *et al.* "Partial covariance two-dimensional mass spectrometry for determination of biomolecular primary structure" (2019) DOI: 10.48550/arXiv.1904.05946

[63] Nobel Prize in Physiology or Medicine 1962 https://www.nobelprize.org/prizes/medicine/1962/summary/

[64] Nobel Prize in Chemistry 1962 https://www.nobelprize.org/prizes/chemistry/1962/summary/

[65] Nobel Prize in Physics 1915 https://www.nobelprize.org/prizes/physics/1915/summary/

[66] The Protein Data Bank (Wikipedia, 29 August 2019, https://tinyurl.com/y6f8lo4n) and the Cambridge Structural Database (Wikipedia, 29 August 2019, https://tinyurl.com/y62accha), with the number of structures in the latter surpassing 1 million in 2018

[67] R. Neutze, R. Wouts, D. van der Spoel *et al.* "Potential for biomolecular imaging with femtosecond X-ray pulses," *Nature* **406**, 752-757 (2000) DOI: 10.1038/35021099

[68] Z. Kam, "Determination of macromolecular structure in solution by spatial correlation of scattering fluctuations," *Macromolecules* **10**(5), 927-934 (1977) DOI: 10.1021/ma60059a009

[69] Z. Kam, M.H. Koch, J. Bordas, "Fluctuation X-ray scattering from biological particles in frozen solutions by using synchrotron radiation," *Proc Natl Acad Sci USA* **78**, 3559-3562 (1981) DOI: 10.1073/pnas.78.6.3559

[70] R.P. Kurta *et al.* "Correlations in Scattered X-Ray Laser Pulses Reveal Nanoscale Structural Features of Viruses," *Phys. Rev. Lett.* **119**, 158102 (2017) DOI: 10.1103/PhysRevLett.119.158102

[71] B. von Ardenne, M. Mechelke and H. Grubmüller, "Structure determination from single molecule X-ray scattering with three photons per image," *Nat Commun* **9**, 2375 (2018) DOI: 10.1038/s41467-018-04830-4

[72] T.B. Pittman *et al.* "Optical imaging by means of two-photon quantum entanglement," *Phys. Rev. A* **52**, R3429(R) (1995) DOI: 10.1103/PhysRevA.52.R3429

[73] R.S. Bennink *et al.* "Two-photon coincidence imaging with a classical source," *Phys. Rev. Lett*. **89**, 113601 (2002) DOI: 10.1103/PhysRevLett.89.113601

[74] A. Gatti *et al.* "Ghost imaging with thermal light: comparing entanglement and classical correlation," *Phys. Rev. Lett*. **93**, 093602 (2004) DOI: 10.1103/PhysRevLett.93.093602

[75] Y.Y Kim, I.A. Vartanyants *et al.* "Ghost Imaging at an XUV free-electron laser," *Phys. Rev. A* **101**, 013820 (2020) DOI: 10.1103/PhysRevA.101.013820

[76] T.J. Lane, D. Ratner, "What are the advantages of ghost imaging? Multiplexing for X-ray and electron imaging," **arXiv:1907.12178v2** (2019) DOI: 10.1364/OE.379503

[77] R.S. Aspden *et al.* "Photon-sparse microscopy: visible light imaging using infrared illumination," *Optica* **2**, 1049-1052 (2015) DOI: 10.1364/OPTICA.2.001049

[78] A.M. Kingston *et al.* "Ghost tomography," *Optica* **5**, 1516-1520 (2018) DOI: 10.1364/OPTICA.5.001516

[79] D. Ratner *et al.* "Pump-probe Ghost Imaging with SASE FELs," *Phys. Rev. X* **9**, 011045 (2019) DOI: 10.1103/PhysRevX.9.011045

[80] S. Asban, K.E. Dorfman, S. Mukamel, "Quantum phase-sensitive diffraction and imaging using entangled photons," *Proc Natl Acad Sci USA* **116**(24), 11673-11678 (2019) DOI: 10.1073/pnas.1904839116

[81] J.C. Goodrich, Ryan Mahon, Joseph Hanrahan, et al, "Quantum correlation imaging via X-ray parametric down-conversion," Optica 13, 135-142 (2026) DOI: 10.1364/OPTICA.574747

[82] Popova-Gorelova, Daria, David A. Reis, and Robin Santra. "Theory of X-Ray Scattering from Laser-Driven Electronic Systems". Physical Review B 98 (22): 224302 (2018) DOI: 10.1103/PhysRevB.98.224302

[83] A. Classen *et al.* "Superresolving imaging of arbitrary one-dimensional arrays of thermal light sources using multiphoton interference," *Phys. Rev. Lett*. **117**, 253601 (2016) DOI: 10.1103/PhysRevLett.117.253601

[84] A. Classen, J. von Zanthier *et al.* "Incoherent diffractive imaging via intensity correlations of hard X rays," *Phys. Rev. Lett*. **119**, 053401 (2017) DOI: 10.1103/PhysRevLett.119.053401

[85] R. Schneider, T. Mehringer, G. Mercurio *et al.* "Quantum imaging with incoherently scattered light from a free-electron laser," *Nature Phys* **14**, 126-129 (2018) DOI: 10.1038/nphys4301

[86] C. Thiel, J. von Zanthier *et al.* "Quantum imaging with incoherent photons," *Phys. Rev. Lett*. **99**, 133603 (2007) DOI: 10.1103/PhysRevLett.99.133603

[87] B. Stankus, H. Yong, N. Zotev *et al.* "Ultrafast X-ray scattering reveals vibrational coherence following Rydberg excitation," *Nat. Chem*. **11**, 716-721 (2019) DOI: 10.1038/s41557-019-0291-0

[88] M. Minitti, J.B. Hastings, P.M. Weber *et al.* "Imaging molecular motion: femtosecond X-ray scattering of an electrocyclic chemical reaction," *Phys. Rev. Lett*. **114**, 255501 (2015) DOI: 10.1103/PhysRevLett.114.255501

[89] H. Yong, X. Xu, J.M. Ruddock, B. Stankus, A. Moreno Carrascosa, N. Zotev, D. Bellshaw, *et al*. "Ultrafast X-Ray Scattering Offers a Structural View of Excited-State Charge Transfer". Proceedings of the National Academy of Sciences 118 (19): e2021714118 (2021) DOI: 10.1073/pnas.2021714118

[90] L. Ma, W. Du, H. Yong, B. Stankus, J.M. Ruddock, A.s Moreno Carrascosa, N. Goff, *et al*. 2025. "Revealing the Reaction Path of UVC Bond Rupture in Cyclic Disulfides with Ultrafast X-Ray Scattering". Science Advances 11 (3): eadp9175 (2025) DOI: 10.1126/sciadv.adp9175

[91] M.R. Ware *et al.* "On the limits of observing motion in time-resolved X-ray scattering," *Phil. Trans. R. Soc. A* **377**:20170477 (2019) DOI: 10.1098/rsta.2017.0477

[92] M.R. Ware *et al.* "Characterizing dissociative motion in time-resolved X-ray scattering from gas-phase diatomic molecules," *Phys. Rev. A* **100**, 033413 (2019) DOI: 10.1103/PhysRevA.100.033413

[93] H. Yong, A. Kirrander, P.M. Weber *et al.* "Determining Orientations of Optical Transition Dipole Moments Using Ultrafast X-ray Scattering," *J. Phys. Chem. Lett*. **9**, 22, 6556-6562 (2018) DOI: 10.1021/acs.jpclett.8b02773

[94] J.M. Glownia, P.H. Bucksbaum *et al.* "Self-referenced coherent diffraction X-ray movie of ångström- and femtosecond-scale atomic motion," *Phys. Rev. Lett*. **117**, 153003 (2016) DOI: 10.1103/PhysRevLett.117.153003

[95] A. Kirrander, P.M. Weber, "Fundamental Limits on Spatial Resolution in Ultrafast X-ray Diffraction," *Applied Sciences* **7**, 534 (2017) DOI: 10.3390/app7060534

[96] H. Yong, N. Zotev, J.M. Ruddock *et al.* "Observation of the molecular response to light upon photoexcitation," *Nat Commun* **11**, 2157 (2020) DOI: 10.1038/s41467-020-15680-4

[97] H. Yong, N. Zotev, J.M. Ruddock, B. Stankus, M. Simmermacher, A. Moreno Carrascosa, W. Du, *et al*. "Observation of the Molecular Response to Light upon Photoexcitation". Nature Communications 11 (1): 2157 (2020) DOI: 10.1038/s41467-020-15680-4

[98] A. Moreno Carrascosa, J.P. Coe, M. Simmermacher, M.J. Paterson, and A. Kirrander. "Towards High-Resolution X-Ray Scattering as a Probe of Electron Correlation". Physical Chemistry Chemical Physics 24 (39): 24542–52 (2022) DOI: 10.1039/D2CP02933B

[99] I. Gabalski, A. Green, P. Lenzen *et al.* "Imaging valence electron rearrangement in a chemical reaction using hard X-ray scattering." *Phys. Rev. Lett.* 135, 083001 (2025) DOI: 10.1103/53h3-vykl

[100] M. Simmermacher, N.E. Henriksen, K.B. Møller *et al.* "Electronic coherence in ultrafast X-ray scattering from molecular wave packets," *Phys. Rev. Lett*. **122**, 073003 (2019) DOI: 10.1103/PhysRevLett.122.073003

[101] G. Dixit, O. Vendrell and R. Santra, "Imaging electronic quantum motion with light," *Proc Natl Acad Sci USA* **109** (29), 11636-11640 (2012) DOI: 10.1073/pnas.1202226109

[102] M. Kowaleski *et al.* "Monitoring nonadiabatic avoided crossing dynamics in molecules by ultrafast X-ray diffraction," *Structural Dynamics* **4**, 054101 (2017) DOI: 10.1063/1.4984241

[103] K. Bennet *et al.* "Monitoring molecular nonadiabatic dynamics with femtosecond X-ray diffraction," *Proc Natl Acad Sci USA* **115** (26), 6538-6547 (2018) DOI: 10.1073/pnas.1805335115

[104] M. Simmermacher, K.B. Møller, A. Kirrander *et al.* "Theory of ultrafast X-ray scattering by molecules in the gas phase," *J. Chem. Phys*. **151**, 174302 (2019) DOI: 10.1063/1.5110040

[105] Y. Nam, H. Song, V.M. Freixas *et al*. "Monitoring Vibronic Coherences and Molecular Aromaticity in Photoexcited Cyclooctatetraene with an X-Ray Probe: A Simulation Study". ***Chem. Sci.***, **14**, 2971-2982 (2023) DOI: 10.1039/d2sc04335a

[106] D. Keefer, F. Aleotti, J.R. Rouxel *et al.* "Imaging Conical Intersection Dynamics during Azobenzene Photoisomerization by Ultrafast X-Ray Diffraction". *Proc. Natl. Acad. Sci. U.S.A.* **118** (3) e2022037118 (2021) DOI: 10.1073/pnas.2022037118

[107] G. Scholes, G. Fleming, L. Chen *et al.* "Using coherence to enhance function in chemical and biophysical systems," *Nature* **543**, 647-656 (2017) DOI: 10.1038/nature21425

[108] P.M. Kraus, H.J. Wörner *et al.* "Measurement and laser control of attosecond charge migration in ionised iodoacetylene," *Science* **350**, 790-795 (2015) DOI: 10.1126/science.aab2160

[109] P. Emma, R. Akre, J. Arthur *et al.* "First lasing and operation of an angstrom-wavelength free-electron laser," *Nature Photon* **4**, 641-647 (2010) DOI: 10.1038/nphoton.2010.176

[110] Y. Ding *et al.* "Measurements and Simulations of Ultralow Emittance and Ultrashort Electron Beams in the Linac Coherent Light Source," *Phys. Rev. Lett*. **102** 254801 (2009) DOI: 10.1103/PhysRevLett.102.254801

[111] Y. Ding *et al.* "Femtosecond X-Ray Pulse Characterization in Free-Electron Lasers Using a Cross-Correlation Technique" *Phys. Rev. Lett.* **109** 254802 (2012) DOI: 10.1103/PhysRevLett.109.254802

[112] A. Lutman, T. Maxwell, J. MacArthur *et al.* "Fresh-slice multicolour X-ray free-electron lasers10.1103/PhysRevA.92.040502," *Nature Photon* **10**, 745-750 (2016) DOI: 10.1038/nphoton.2016.201

[113] G. Doumy *et al.* "Nonlinear atomic response to intense ultrashort X-rays," *Phys. Rev. Lett*. **106**, 083002 (2011) DOI: 10.1103/PhysRevLett.106.083002

[114] C. Weninger, N. Rohringer *et al.* "Stimulated electronic X-ray Raman scattering," *Phys. Rev. Lett*. **111**, 233902 (2013) DOI: 10.1103/PhysRevLett.111.233902

[115] T. Kroll, C. Weninger, N. Rohringer, U. Bergmann *et al.* "Stimulated X-ray emission spectroscopy in transition metal complexes," *Phys. Rev. Lett*. **120**, 133203 (2018) DOI: 10.1103/PhysRevLett.120.133203

[116] N. Rohringer, D. Ryan, R. London *et al.* "Atomic inner shell X-ray laser at 1.46 nanometres pumped by an X-ray free-electron laser," *Nature* **481**, 488-491 (2012) DOI: 10.1038/nature10721

[117] A.A. Zholents and W.M. Fawley, "Proposal for intense Attosecond Radiation from an X-ray Free Electron Laser," *Phys. Rev. Lett*. **92**, 224801 (2004) DOI: 10.1103/PhysRevLett.92.224801

[118] J. Duris, S. Li, T. Driver *et al.* "Tunable isolated attosecond X-ray pulses with gigawatt peak power from a free-electron laser," *Nat. Photonics* **14**, 30-36 (2020) DOI: 10.1038/s41566-019-0549-5

[119] R.R. Robles, K.A. Larsen, D. Cesar *et al*., "Spectrotemporal Shaping of Attosecond X-Ray Pulses with a Fresh-Slice Free-Electron Laser," *Phys. Rev. Lett.* **134**, 115001 (2025) DOI: 10.1103/PhysRevLett.134.115001

[120] P. Franz, S. Li, T. Driver *et al*. "Terawatt-scale attosecond X-ray pulses from a cascaded superradiant free-electron laser," *Nat. Photonics* **18**, 698–703 (2024) DOI: 10.1038/s41566-024-01427-w

[121] S. Huang, Y. Ding, Y. Feng *et al*. "Generating single-spike hard X-ray pulses with nonlinear bunch compression in free-electron lasers," *Phys. Rev. Lett.* **119**, 154801 (2017) DOI: 10.1103/PhysRevLett.119.154801

[122] J. Yan, W. Qin, Y. Chen *et al*. "Terawatt-attosecond hard X-ray free-electron laser at high repetition rate," *Nat. Photon.* **18**, 1293–1298 (2024). DOI: 10.1038/s41566-024-01566-0

[123] E. Prat, A. Al Haddad, C. Arrell *et al*. "An X-ray free-electron laser with a highly configurable undulator and integrated chicanes for tailored pulse properties," *Nat Commun* **14**, 5069 (2023). DOI: 10.1038/s41467-023-40759-z

[124] E. Allaria, R. Appio, L. Badano *et al.* "Highly coherent and stable pulses from the FERMI seeded free-electron laser in the extreme ultraviolet," *Nature Photon* **6**, 699-704 (2012) DOI: 10.1038/nphoton.2012.233

[125] P. Rebernik Ribic, A. Abrami, L. Badano *et al.* "Coherent soft X-ray pulses from echo-enabled harmonic generation free-electron laser," *Nat. Photonics* **13**, 555-561 (2019) DOI: 10.1038/s41566-019-0427-1

[126] F. Bencivenga, R. Cucini, F. Capotondi *et al.* "Four-wave mixing experiments with extreme ultraviolet transient gratings," *Nature* **520**, 205-208 (2015) DOI: 10.1038/nature14341

[127] P.K. Maroju, C. Grazioli, M. Di Fraia *et al.* "Attosecond pulse shaping using a seeded free-electron laser," *Nature* **578**, 386-391 (2020) DOI: 10.1038/s41586-020-2005-6

[128] F. Remacle and R. D. Levine, "An electronic time scale in chemistry," *Proc Natl Acad Sci USA* **103** (18) 6793-6798 (2006) DOI: 10.1073/pnas.0601855103; J. Breidbach and L.S. Cederbaum, "Migration of holes: Formalism, mechanisms, and illustrative applications," *J. Chem. Phys.* **118**, 3983 (2003) DOI: 10.1063/1.1540618

[129] M. Vacher, M.A. Robb *et al.* "Electron dynamics upon ionisation of polyatomic molecules…," *Phys. Rev. Lett*. **118**, 083001 (2017) DOI: 10.1103/PhysRevLett.118.083001

[130] D. Mendive-Tapia, M. Vacher *et al.* "Coupled electron-nuclear dynamics: Charge migration and charge transfer initiated near a conical intersection," *J. Chem. Phys*. **139** 044110 (2013) DOI: 10.1063/1.4815914; M. Vacher. M.A. Robb *et al.* "Electron dynamics following photoionisation…," *Phys. Rev. A* **92**, 040502(R) (2015) DOI: 10.1103/PhysRevA.92.040502

[131] L.S. Cederbaum and J. Zobeley, "Ultrafast charge migration by electron correlation," *Chem. Phys. Lett.* **307** 205-210 (1999) DOI: 10.1016/S0009-2614(99)00508-4; R. Weinkauf *et al.* "Nonstationary Electronic States and Site-selective Reactivity," *J. Phys. Chem. A* **101**, 42, 7702-7710 (1997) DOI: 10.1021/jp9715742

[132] M. Drescher, F. Krausz *et al.* "X-ray Pulses Approaching the Attosecond Frontier," *Science* **291** 1923-1927 (2001) DOI: 10.1126/science.1058561

[133] F. Frank *et al.* "Technology for Attosecond Science," *Rev. Sci. Inst*. **83** 071101 (2012) DOI: 10.1063/1.4731658

[134] F. Calegari, F. Ferrari, M. Nisoli *et al.* "High-energy isolated attosecond pulses and applications to molecular physics," *Advances in Optical Materials, OSA Technical Digest (CD) (Optica Publishing Group, 2011)*, **paper HThB2** DOI: 10.1364/HILAS.2011.HThB2; T. Popmintchev, M. Chen, P. Arpin *et al.* "The attosecond nonlinear optics of bright coherent X-ray generation," *Nature Photon* **4**, 822-832 (2010) DOI: 10.1038/nphoton.2010.256

[135] E. Goulielmakis, Z. Loh, A. Wirth *et al.* "Real-time observation of valence electron motion," *Nature* **466**, 739-743 (2010) DOI: 10.1038/nature09212

[136] F. Calegari *et al.* "Ultrafast electron dynamics in phenylalanine intiated by attosecond pulses," *Science* **346**, 336-339 (2014) DOI: 10.1126/science.1254061

[137] A.L. Cavalieri, N. Müller, T. Uphues *et al.* "Attosecond spectroscopy in condensed matter," *Nature* **449**, 1029-1032 (2007) DOI: 10.1038/nature06229

[138] M. Lezius, V. Blanchet, M. Yu. Ivanov and A. Stolow, "Polyatomic molecules in strong laser fields: Nonadiabatic multielectron dynamics," *J. Chem. Phys.* **117**:4, 1575-1588 (2002) DOI: 10.1063/1.1487823

[139] T. Barillot, O. Alexander, B. Cooper *et al*. "Correlation-driven transient hole dynamics resolved in space and time in the isopropanol

molecule," *Phys. Rev. X* **11** 031048 (2021) DOI: 10.1103/PhysRevX.11.031048

140 D. Schwickert, M.Ruberti, P. Kolorenč *et al*. "Electronic quantum coherence in glycine molecules probed with ultrashort X-ray pulses in real time," *Science. Adv.* **8** eabn6848 (2022) DOI: 10.1126/sciadv.abn6848

141 B. Cooper *et al.* "Analysis of a measurement scheme for ultrafast hole dynamics…," *Faraday Discuss*. **171**, 93-111 (2014) DOI: 10.1039/C4FD00051J

142 N. Hartmann, G. Hartmann, R. Heider *et al.* "Attosecond time-energy structure of X-ray free-electron laser pulses," *Nature Photon* **12** 215-220 (2018) DOI: 10.1038/s41566-018-0107-6

143 S. Li *et al*. "Attosecond coherent electron motion in Auger-Meitner decay," *Science* **375**, 285 (2022) DOI: 10.1126/science.abj2096

144 T. Driver, M. Mountney, J. Wang *et al.* "Attosecond delays in X-ray molecular ionisation," *Nature* **632**, 762–767 (2024) DOI: 10.1038/s41586-024-07771-9

145 J. Wang, T. Driver, P.L. Franz *et al*. "Probing electronic coherence between core-level vacancies at different atomic sites," *Phys. Rev. X* **15**, 011008 (2025) DOI: 10.1103/PhysRevX.15.011008

146 L. Funke, M. Ilchen, K. Dingel *et al*. "Capturing Nonlinear Electron Dynamics with Fully Characterised Attosecond X-ray Pulses," arXiv preprint (2024) DOI: 10.48550/arXiv.2408.03858

147 Z. Guo, T. Driver, S. Beauvarlet *et al*. "Experimental demonstration of attosecond pump–probe spectroscopy with an X-ray free-electron laser," *Nat. Photon* **18**, 691–697 (2024) DOI: 10.1038/s41566-024-01419-w

148 T. Driver, Z. Guo, E. Isele *et al*. "Attosecond Coherent Electron Motion in a Photoionised Aromatic Molecule," arXiv (2024) DOI: 10.48550/arXiv.2411.01700 (accepted Nature Physics (2026))

149 S. Li *et al.* "Attosecond-pump attosecond-probe X-ray spectroscopy of liquid water," *Science* **383**, 1118-1122 (2024) DOI:10.1126/science.adn6059

150 O. Takahashi, R. Yamamura, T. Tokushima & Y. Harada, "Interpretation of the X-Ray Emission Spectra of Liquid Water through Temperature and Isotope Dependence," *Phys. Rev. Lett.* **128**, 086002 (2022) DOI:10.1103/PhysRevLett.128.086002

151 S. Tanaka and S. Mukamel, "Coherent X-Ray Raman Spectroscopy: A Nonlinear Local Probe for Electronic Excitations," *Phys. Rev. Lett*. **89**, 043001 (2002) DOI: 10.1103/PhysRevLett.89.043001;
S. Tanaka and S. Mukamel, "Probing exciton dynamics using Raman resonances in femtosecond X-ray four-wave mixing," *Phys. Rev. A* **67**, 033818 (2003) DOI: 10.1103/PhysRevA.67.033818

152 I.V. Schweigert and S. Mukamel, "Coherent Ultrafast Core-Hole Correlation Spectroscopy: X-Ray Analogues of Multidimensional NMR," *Phys. Rev. Lett*. **99**, 163001 (2007) DOI: 10.1103/PhysRevLett.99.163001;
J.D. Biggs, S. Mukamel *et al.* "Two-dimensional stimulated resonance Raman spectroscopy of molecules with broadband X-ray pulses," *J. Chem. Phys*. **136**, 174117 (2012) DOI: 10.1063/1.4706899

153 J.T. O'Neal *et al.* "Electronic Population Transfer via Impulsive Stimulated X-Ray Raman Scattering with Attosecond Soft-X-Ray Pulses," *Physical Review Letters* **125**, 073203 (2020), DOI: 10.1103/PhysRevLett.125.073203

154 O. Alexander *et al.* "Attosecond impulsive stimulated X-ray Raman scattering in liquid water," *Science Advances* **10**, eadp0841 (2024), DOI: 10.1126/sciadv.adp0841

155 Y. Zhang, J.D. Biggs, N. Govind & S. Mukamel, "Monitoring Long-Range Electron Transfer Pathways in Proteins by Stimulated Attosecond Broadband X-ray Raman Spectroscopy," *J. Phys. Chem. Lett.,* **5**, 21, 3656–3661 (2014) DOI: 10.1021/jz501966h

156 M. Chergui, M. Beye, S. Mukamel *et al.* "Progress and prospects in nonlinear extreme-ultraviolet and X-ray optics and spectroscopy,", *Nat. Rev. Phys*. **5**, 578–596 (2023) DOI: 10.1038/s42254-023-00643-7

157 C.P. Schwartz and W.S. Drisdell, "Nonlinear Soft X-Ray Spectroscopy," and Y. Kubota and K. Tamasaku, "Nonlinear X-Ray Spectroscopy," Chapter 5 in I. Matsuda and R. Arafune (eds.), Nonlinear X-Ray Spectroscopy for Materials Science, Springer Series in Optical Sciences, vol 246, Springer Singapore. DOI: 10.1007/978-981-99-6714-8_5

158 M. Beye, S. Schreck, F. Sorgenfrei *et al*. "Stimulated X-ray emission for materials science," *Nature* **501**, 191–194 (2013) DOI: 10.1038/nature12449

159 U. Bergmann, O.C. Mullins and S.P. Cramer, "X-ray Raman spectroscopy of carbon in asphaltene: Light element characterization with bulk sensitivity." *Anal. Chem*. **72**, 2609–2612 (2000) DOI: 10.1021/ac990730t

160 O.A. Paredes-Mellone, M.H. Nielsen, J. Vinson *et al*. "Investigating the electronic structure of high explosives with X-ray Raman spectroscopy," *Sci. Rep*. **12**, 19460 (2022). DOI: 10.1038/s41598-022-24066-z

161 K. Ledbetter, M.E. Reinhard, K. Kunnus *et al*. "Excited state charge distribution and bond expansion of ferrous complexes observed with femtosecond valence-to-core X-ray emission spectroscopy," *J. Chem. Phys*. **152**, 074203 (2020) DOI: 10.1063/1.5139441

162 T. Kroll, C. Weninger, R. Alonso-Mori *et al*. "Stimulated X-ray emission spectroscopy in transition metal complexes," *Phys. Rev. Lett.* **120**, 133203 (2018) DOI: 10.1103/PhysRevLett.120.133203

163 T. Kroll, C. Weninger, F.D. Fuller et al. "Observation of seeded Mn Kβ stimulated X-ray emission using two-color X-ray free-electron laser pulses," *Phys. Rev. Lett*. **125**, 037404 (2020) DOI: 10.1103/PhysRevLett.125.037404

164 K, Li, C. Ott, M. Agåker *et al*. "Super-resolution stimulated X-ray Raman spectroscopy," *Nature* **643**, 662–668 (2025) DOI: 10.1038/s41586-025-09214-5

165 C. Woodahl, S. Jamnuch, A. Amado *et al*. "Probing lithium mobility at a solid electrolyte surface," *Nat.*

Mater. **22**, 848–852 (2023) DOI: 10.1038/s41563-023-01535-y

166 S. Shwartz, M. Fuchs, J.B. Hastings *et al*. "X-ray second harmonic generation," *Phys. Rev. Lett*. **112**, 163901 (2014) DOI: 10.1103/PhysRevLett.112.163901

167 R.K. Lam, S.L. Raj, T.A. Pascal *et al*. "Soft X-ray second harmonic generation as an interfacial probe," *Phys. Rev. Lett*. **120**, 023901 (2018) DOI: 10.1103/PhysRevLett.120.023901

168 Hoffman, D.J., Devlin, S.W., Garratt, D. *et al.* Surface structure of water from soft X-ray second harmonic generation. *Nat Commun* **16**, 10522 (2025). https://doi.org/10.1038/s41467-025-65514-4

169 S. Yamamoto, T. Omi, H. Akai *et al*. "Element selectivity in second-harmonic generation of $GaFeO_3$ by a soft-X-ray free-electron laser," *Phys. Rev. Lett*. **120**, 223902 (2018) DOI: 10.1103/PhysRevLett.120.223902

170 E. Berger, S. Jamnuch, C.B. Uzandal *et al*. "Extreme ultraviolet second harmonic generation spectroscopy in a polar metal," *Nano Lett*. **21**, 6095–6101 (2021) DOI: 10.1021/acs.nanolett.1c01502

171 C.P. Schwartz, S.L. Raj, S. Jamnuch *et al*. "Angstrom-resolved interfacial structure in buried organic–inorganic junctions," *Phys. Rev. Lett*. **127**, 096801 (2021) DOI: 10.1103/PhysRevLett.127.096801

172 H. Rottke *et al*. "Probing electron and hole colocalization by resonant four-wave mixing spectroscopy in the extreme ultraviolet," *Sci. Adv*. **8**, eabn5127 (2022) DOI: 10.1126/sciadv.abn5127

173 F. Bencivenga, R. Cucini, F. Capotondi *et al*. "Four-wave mixing experiments with extreme ultraviolet transient gratings," *Nature* **520**, 205–208 (2015) DOI: 10.1038/nature14341

174 L. Foglia, F. Capotondi, R. Mincigrucci *et al*. "First evidence of purely extreme-ultraviolet four-wave mixing," *Phys. Rev. Lett*. **120**, 263901 (2018) DOI: 10.1103/PhysRevLett.120.263901

175 F. Bencivenga *et al*. "Nanoscale transient gratings excited and probed by extreme ultraviolet femtosecond pulses," *Sci. Adv*. **5**, eaaw5805 (2019) DOI: 10.1126/sciadv.aaw5805

176 A.A. Maznev, F. Bencivenga, A. Cannizzo *et al*. "Generation of coherent phonons by coherent extreme ultraviolet radiation in a transient grating experiment," *Appl. Phys. Lett*. **113**, 221905 (2018) DOI: 10.1063/1.5048023

177 A.A. Maznev, R. Mincigrucci, F. Bencivenga *et a*l. "Generation and detection of 50 GHz surface acoustic waves by extreme ultraviolet pulses," *Appl. Phys. Lett*. **119**, 044102 (2021) DOI: 10.1063/5.0060575

178 D. Naumenko *et al*. "Thermoelasticity of nanoscale silicon carbide membranes excited by extreme ultraviolet transient gratings: implications for mechanical and thermal management," *ACS Appl. Nano Mater.* **2**, 8, 5132–5139 (2019) DOI: 10.1021/acsanm.9b01024

179 D. Ksenzov *et al*. "Nanoscale transient magnetization gratings created and probed by femtosecond extreme ultraviolet pulses," *Nano Lett.* **21**, 7, 2905–2911 (2021) DOI: 10.1021/acs.nanolett.0c05083

180 K. Yao *et al*. "All-optical switching on the nanometer scale excited and probed with femtosecond extreme ultraviolet pulses," *Nano Lett*. **22**, 11, 4452–4458 (2022) DOI: 10.1021/acs.nanolett.2c01060

181 P.R. Meidaner *et al*. "Excitation and detection of coherent nanoscale spin waves via extreme ultraviolet transient gratings," *Sci. Adv*. **10**, eadp6015 (2024) DOI: 10.1126/sciadv.adp6015

182 J.R. Rouxel, D. Fainozzi, R. Mankowsky *et al*. "Hard X-ray transient grating spectroscopy on bismuth germanate," *Nat. Photon*. **15**, 499–503 (2021) DOI: 10.1038/s41566-021-00797-9

183 Ferrari, E., Ueda, H., Fainozzi, D. *et al.* All hard X-ray transient grating spectroscopy. *Commun Phys* **8**, 257 (2025). https://doi.org/10.1038/s42005-025-02178-y

184 H. Kulla *et al.* "Knowing When to Stop – Trapping Metastable Polymorphs in Mechanochemical Reactions," *Cryst. Growth Des*. **17**, 3, 1190-1196 (2017) DOI: 10.1021/acs.cgd.6b01572

185 A.J. Alexander and P.J. Camp "Non-photochemical laser-induced nucleation," *J. Chem. Phys*. **150**, 040901 (2019) DOI: 10.1063/1.5079328

186 G. Snyder and E. Toberer, "Complex thermoelectric materials," *Nature Mater*. **7**, 105-114 (2008) DOI: 10.1038/nmat2090

187 C. Xiao *et al.* "Superionic phase transition in silver chalcogenide nanocrystals realizing optimized thermoelectric performance," *J. Am. Chem. Soc*. **134**, 9, 4287-4293 (2012) DOI: 10.1021/ja2104476

188 S. Raoux, "Phase Change Materials," *Annu. Rev. Mater. Res*. **39**, 25-48 (2009) DOI: 10.1146/annurev-matsci-082908-145405

189 R. Pecora (Ed.), "Dynamic light scattering – applications of photon correlation spectroscopy," Plenum Press, New York and London (1985) DOI: 10.1007/978-1-4613-2389-1

190 A. Ourmazd, "Machine-learning Routes to Dynamics, Thermodynamics and Work Cycles of Biological Nanomachines" *in "X-ray free electron lasers: Applications in materials, chemistry, and biology," Energy and Environment Series. ed U. Bergmann et al. RSC*, **Chapter 22** 418-433 (2017) DOI: 10.1039/9781782624097-00418

191 A. Hosseinizadeh, A. Ourmazd *et al.* "Single-particle structural determination by X-ray FELs," *Structural Dynamics* **2**, 041601 (2015) DOI: 10.1063/1.4919740

192 A. Ourmazd, "Cryo-EM, XFELs and the structure conundrum in structural biology," *Nat Methods* **16**, 941-944 (2019) DOI: 10.1038/s41592-019-0587-4

193 R. Fung, A. Hanna, O. Vendrell *et al.* "Dynamics from noisy data with extreme timing uncertainty," *Nature* **532**, 471-475 (2016) DOI: 10.1038/nature17627

194 J. Glownia *et al.* "Time resolved pump-probe experiments at the LCLS," *Optics Express* **18**, 17620-17630 (2010) DOI: 10.1364/OE.18.017620

195 A. Hosseinizadeh, G. Mashayekhi, J. Copperman *et al.* "Conformational landscape of a virus by single

particle X-ray scattering," *Nat Methods* **14**, 877-881 (2017) DOI: 10.1038/nmeth.4395

196 A. Dashti, J. Frank, A. Ourmazd *et al.* "Trajectories of the ribosome as a Brownian nanomachine," *Proc. Natl. Acad. Sci. USA* **201419276** (2014) DOI: 10.1073/pnas.1419276111

197 K. Pande *et al*. "Femtosecond structural dynamics drives the *trans*/*cis* isomerization in photoactive yellow protein," *Science* **352**, 725–729 (2016) DOI: 10.1126/science.aad5081

198 A. Hosseinizadeh, N. Breckwoldt, R. Fung *et al.* "Few-fs resolution of a photoactive protein traversing a conical intersection," *Nature* **599**, 697–701 (2021). DOI: 10.1038/s41586-021-04050-9

199 A. Munke, J. Andreasson, A. Aquila *et al.* "Coherent diffraction imaging of single Dwarf Rice virus particles using hard X-rays at the LCLS," *Sci Data* **3**, 160064 (2016) DOI: 10.1038/sdata.2016.64

200 M. Marklund and P. Shukla, "Nonlinear collective effects in photon-photon and photon-plasma interactions," *Rev. Mod. Phys*. **78**, 591 (2006) DOI: 10.1103/RevModPhys.78.591

201 T. Tajima, "Laser acceleration in novel media," *Eur. Phys. J. Spec. Top.* **223**, 1037-1044 (2014) DOI: 10.1140/epjst/e2014-02154-6

202 J. Schwinger, "On Gauge Invariance and Vacuum Polarization," *Phys. Rev*. **82**, 664 (1951) DOI: 10.1103/PhysRev.82.664

203 D.L. Burke *et al.* "Positron Production in Multiphoton Light-by-Light Scattering," *Phys. Rev. Lett*. **79**, 1626 (1997) DOI: 10.1103/PhysRevLett.79.1626

204 L. Mercadier *et al*. "Nonlinear absorption of an X-ray pulse during the formation of warm dense matter," *Nat. Phys.* **20**, 1536–1537 (2024) DOI: 10.1038/s41567-024-02594-x

205 T.M. Linker, A. Halavanau, T. Kroll *et al*. "Attosecond Inner-Shell Lasing at Ångström Wavelengths," *Nature* **642**, 934–940 (2025) DOI: 10.1038/s41586-025-09105-9

206 U.I. Uggerhøj, "The interaction of relativistic particles with strong crystalline fields," *Rev. Mod. Phys*. **77**, 1131 (2005) DOI: 10.1103/RevModPhys.77.1131

207 B. Svedung Wettervik, A. Gonoskov and M. Marklund, "Prospects and limitations of wakefield acceleration in solids," *Phys. Plasmas* **25**, 013107 (2018) DOI: 10.1063/1.5003857

208 E. Esarey, C.B. Schroeder and W.P. Leemans, "Physics of laser-driven plasma-based electron accelerators," *Rev. Mod. Phys.* **81**, 1229 (2009) DOI: 10.1103/RevModPhys.81.1229

209 R.C. Duncan and C. Thompson, "Formation of very strongly magnetized neutron stars: Implications for gamma-ray bursts," *Astrophys. J. Lett.* **392**, L9 (1992) DOI: 10.1086/186413

210 R.P. Mignani, V. Testa, D. González Caniulef *et al.* "Evidence for vacuum birefringence from the first optical-polarimetry measurement of the isolated neutron star RX J1856.5–3754," *Mon.Not.Roy.Astron.Soc.* **465**, 1, 492-500 (2017) DOI: 10.1093/mnras/stw2798

211 L.M. Capparelli, A. Damiano, L. Maiani *et al.* "A note on polarized light from magnetars," *Eur. Phys. J. C* **77**, 754 (2017) DOI: 10.1140/epjc/s10052-017-5342-3

212 M. Born and L. Infeld, "Foundations of the new field theory," *Proc. R. Soc. Lond. A* **A144**, 425--451 (1934) DOI: 10.1098/rspa.1934.0059

213 T. Inada *et al.* "Search for photon-photon elastic scattering in the X-ray region," *Phys. Lett. B* **732**, 356-359 (2014) DOI: 10.1016/j.physletb.2014.03.054

214 H.-P. Schlenvoigt *et al.* "Detecting vacuum birefringence with X-ray free electron lasers and high-power optical lasers: a feasibility study," *Phys. Scr.* **91**, 023010 (2016) DOI: 10.1088/0031-8949/91/2/023010

215 A.M. Fedotov, N.B. Narozhny, G. Mourou, and G. Korn, "Limitations on the Attainable Intensity of High Power Lasers," *Phys. Rev. Lett*. **105**, 080402 (2010) DOI: 10.1103/PhysRevLett.105.080402

216 S.S. Bulanov, T.Zh. Esirkepov, A.G.R. Thomas, J.K. Koga, and S.V. Bulanov, "Schwinger Limit Attainability with Extreme Power Lasers," *Phys. Rev. Lett.* **105**, 220407 (2010) DOI: 10.1103/PhysRevLett.105.220407

217 A. Ringwald, "Pair production from vacuum at the focus of an X-ray free electron laser," *Phys. Lett. B* **510**, 107-116 (2001) DOI: 10.1016/S0370-2693(01)00496-8

218 R.D. Peccei and H.R. Quinn, "CP Conservation in the Presence of Pseudoparticles," *Phys. Rev. Lett*. **38**, 1440–1443 (1977) DOI: 10.1103/PhysRevLett.38.1440

219 S. Weinberg, "A New Light Boson?," *Phys. Rev. Lett.* **40**, 223 (1978) DOI: 10.1103/PhysRevLett.40.223

220 F. Wilczek, "Problem of Strong P and T Invariance in the Presence of Instantons," *Phys. Rev. Lett*. **40**, 279 (1978) DOI: 10.1103/PhysRevLett.40.279

221 J. Preskill, M.B. Wise, and F. Wilczek, "Cosmology of the invisible axion". *Phys. Lett. B* **120**, 127–132 (1983) DOI: 10.1016/0370-2693(83)90637-8

222 L.F. Abbott and P. Sikivie, "A cosmological bound on the invisible axion," *Phys. Lett. B* **120**, 133–136 (1983) DOI: 10.1016/0370-2693(83)90638-X

223 M. Dine and W. Fischler, "The not-so-harmless axion," *Phys. Lett. B* **120**, 137–141 (1983) DOI: 10.1016/0370-2693(83)90639-1

224 A. Arvanitaki, S. Dimopoulos, S. Dubovsky, N. Kaloper, and J. March-Russell, "String axiverse," *Phys. Rev. D* **81**, 123530 (2010) DOI: 10.1103/PhysRevD.81.123530

225 V. Anastassopoulos, S. Aune, K. Barth *et al.* "New CAST limit on the axion-photon interaction," *Nature Phys* **13**, 584-590 (2017) DOI: 10.1038/nphys4109

226 G. Raffelt and L. Stodolsky, "Mixing of the photon with low-mass particles," *Phys. Rev. D* **37**, 1237 (1988) DOI: 10.1103/PhysRevD.37.1237

227 N. Du *et al.* "Search for Invisible Axion Dark Matter with the Axion Dark Matter Experiment," *Phys. Rev. Lett.* **120**, 151301 (2018) DOI: 10.1103/PhysRevLett.120.151301

[228] P. Sikivie, "Experimental Tests of the Invisible Axion," *Phys. Rev. Lett*. **51**, 1415 (1983) DOI: 10.1103/PhysRevLett.51.1415

[229] F. Della Valle, A. Ejlli, U. Gastaldi *et al* "The PVLAS experiment: measuring vacuum magnetic birefringence and dichroism with a birefringent Fabry–Perot cavity," *Eur. Phys. J. C* **76**, 24 (2016) DOI: 10.1140/epjc/s10052-015-3869-8

[230] L.J. Rosenberg, "Dark-matter QCD-axion searches," *Proc Natl Acad Sci USA* **112** (40), 12278-12281 (2015) DOI: 10.1073/pnas.1308788112

[231] R. Battesti *et al.* "Photon Regeneration Experiment for Axion Search Using X-Rays," *Phys. Rev. Lett.* **105**(25):250405 (2010) DOI: 10.1103/PhysRevLett.105.250405

[232] T. Inada *et al.* "Results of a search for paraphotons with intense X-ray beams at SPring-8," *Phys. Lett. B* **722**, 301–304 (2013) DOI: 10.1016/j.physletb.2013.04.033

[233] J.W.D. Halliday, G. Marocco, K. A. Beyer *et al.* "Bounds on Heavy Axions with an X-Ray Free Electron Laser," *Phys. Rev. Lett.* **134**, 055001 (2025) DOI: 10.1103/PhysRevLett.134.055001

[234] W. Buchmüller, F. Hoogeveen, "Coherent production of light scalar or pseudoscalar particles in Bragg scattering," *Phys Lett B* **237**, 278–283 (1990) DOI: 10.1016/0370-2693(90)91444-G

[235] T. Yamaji, K. Tamasaku, T. Namba, T. Yamazaki, Y. Seino, "Search for Axion like particles using Laue-case conversion in a single crystal," *Phys Lett B* **782**, 523–527 (2018) DOI: 10.1016/j.physletb.2018.05.068

[236] K.A. Beyer, S. Sarkar, "Ruling out light axions: The writing is on the wall," *SciPost Phys.* **15**, 003 (2023) DOI: 10.21468/SciPostPhys.15.1.003

[237] M. Kamionkowski, J. March-Russell, "Planck-scale physics and the Peccei-Quinn mechanism," *Phys Lett B* **282**, 137–141 (1992) DOI: 10.1016/0370-2693(92)90492-M

[238] K Springmann *et al.* "A universal bound on QCD axions from supernovae," arXiv (2024) DOI: 10.48550/arxiv.2410.19902

[239] K.A. Beyer, G. Marocco, R. Bingham, G. Gregori, "Light-shining-through-wall axion detection experiments with a stimulating laser," *Phys Rev D* **105**, 035031 (2022) DOI: 10.1103/PhysRevD.105.035031

[240] K.A. Beyer, G. Marocco, R. Bingham and G. Gregori, "Axion detection through resonant photon-photon collisions," *Phys. Rev. D* **101**, 095018 (2020) DOI: 10.1103/PhysRevD.101.095018

[241] E. Bulbul *et al.* "Detection of an unidentified emission line in the stacked X-ray spectrum of galaxy clusters," *Astrophys. J*. **789**, 13 (2014) DOI: 10.1088/0004-637X/789/1/13

[242] A. Boyarsky, O. Ruchayskiy, D. Iakubovskyi and J. Franse, "Unidentified line in X-ray spectra of the Andromeda galaxy and Perseus galaxy cluster," *Phys. Rev. Lett*. **113**, 251301 (2014) DOI: 10.1103/PhysRevLett.113.251301

[243] F. Day and M. Fairbairn, "Detecting fluorescent dark matter with X-ray lasers," *Eur. Phys. J. C* **78**, 512 (2018) DOI: 10.1140/epjc/s10052-018-5994-7

[244] G.A. Mourou, T. Tajima, and S.V. Bulanov, "Optics in the relativistic regime," *Rev. Mod. Phys*. **78**, 309 (2006) DOI: 10.1103/RevModPhys.78.309

[245] S.W. Hawking, "Black hole explosions?," *Nature* **248**, 30-31 (1974) DOI: 10.1038/248030a0

[246] W.G. Unruh, "Notes on black-hole evaporation," *Phys. Rev. D* **14**, 870 (1976) DOI: 10.1103/PhysRevD.14.870

[247] G.W. Ford and R.F. O'Connell, "Is there Unruh radiation?," *Phys. Lett. A* **350**, 17–26 (2006) DOI: 10.1016/j.physleta.2005.09.068

[248] S. Weinfurtner, E.W. Tedford, M.C. Penrice, W.G. Unruh and G. Lawrence, "Measurement of stimulated Hawking emission in an analogue system," *Phys. Rev. Lett*. **106**(2):021302 (2011) DOI: 10.1103/physrevlett.106.021302

[249] J.R.M. de Nova, K. Golubkov, V.I. Kolobov, and J. Steinhauer, "Observation of thermal Hawking radiation and its temperature in an analogue black hole," *Nature* **569**, 688-691 (2019) DOI: 10.1038/s41586-019-1241-0

[250] P. Chen and T. Tajima, "Testing Unruh Radiation with Ultraintense Lasers," *Phys. Rev. Lett*. **83**, 256 (1999) DOI: 10.1103/PhysRevLett.83.256

[251] P. Chen and G. Mourou, "Accelerating Plasma Mirrors to Investigate the Black Hole Information Loss Paradox," *Phys. Rev. Lett.* **118**, 045001 (2017) DOI: 10.1103/PhysRevLett.118.045001

[252] G. Brodin *et al.* "Laboratory soft X-ray emission due to the Hawking–Unruh effect?," *Class. Quantum Grav*. **25**, 145005 (2008) DOI: 10.1088/0264-9381/25/14/145005

[253] I. Peña and D. Sudarsky, "On the possibility of measuring the Unruh Effect," *Found. Phys.* **44**, 689-708 (2014) DOI: 10.1007/s10701-014-9806-0

[254] G. Vacalis, A. Higuchi, R. Bingham, G. Gregori, "Classical Larmor formula through the Unruh effect for uniformly accelerated electrons," *Phys. Rev. D* **109**, 024044 (2024) DOI: 10.1103/PhysRevD.109.024044

[255] G. Gregori, G. Marocco, S. Sarkar, R. Bingham, C. Wang, "Measuring Unruh radiation from accelerated electrons," *Eur. Phys. J. C* **84**, 475 (2024) DOI: 10.1140/epjc/s10052-024-12849-9

[256] M.A. Wadud, B. King, R. Bingham and G. Gregori, "Axion particle production in a laser-induced dynamical spacetime," *Phys. Lett. B* **777**, 388-393 (2018) DOI: 10.1016/j.physletb.2017.12.039

[257] F. Liu, Y.Takeuchi, S.Chen *et al*, "Simulation studies of high-repetition rate electron driven surface muon beamline at SHINE" Phys. Rev. Accelerators and Beams **28**, 083401 (2025) DOI: 10.1103/t2d3-xqnp

[258] I. Blumenfeld, C. Clayton, F. Decker *et al.* "Energy doubling of 42 GeV electrons in a metre-scale plasma wakefield accelerator" *Nature* **445**, 741-744 (2007) DOI: 10.1038/nature05538

[259] R. Pompili, D. Alesini, M.P. Anania *et al.* "Free-electron lasing with compact beam-driven plasma

wakefield accelerator," *Nature* **605**, 659-662 (2022) DOI: 10.1038/s41586-022-04589-1

260 M. Galletti, D. Alesini, M.P. Anania *et al*. "Stable operation of a free-electron laser driven by a plasma accelerator," *Phys. Rev. Lett*. **129**, 234801 (2022) DOI: 10.1103/PhysRevLett.129.234801

261 B. Hidding, G. Pretzler, J. B. Rosenzweig, T. Königstein, D. Schiller and D. L. Bruhwiler, "Ultracold electron bunch generation via plasma photocathode emission and acceleration in a beam-driven plasma blowout," *Phys. Rev. Lett.* **108**, 035001 (2012) DOI: 10.1103/PhysRevLett.108.035001

262 G. Manahan, A. Habib, P. Scherkl *et al.* "Single-stage plasma-based correlated energy spread compensation for ultrahigh 6D brightness electron beams," *Nat Commun* **8**, 15705 (2017) DOI: 10.1038/ncomms15705

263 A. Deng, O.S. Karger, T. Heinemann *et al.* "Generation and acceleration of electron bunches from a plasma photocathode," *Nat. Phys.* **15**, 1156-1160 (2019) DOI: 10.1038/s41567-019-0610-9

264 L.H. Berman, D. Campbell, E. Hartmann *et al*. "Ultra-high-gain water-window X-ray laser driven by plasma photocathode wakefield acceleration," arXiv (2025) DOI: 10.48550/arXiv.2507.06403

265 A.F. Habib, G.G. Manahan, P. Scherkl *et al*. "Attosecond-Angstrom free-electron laser towards the cold beam limit," *Nat Commun* **14**, 1054 (2023) DOI:10.1038/s41467-023-36592-z

266 A.F. Habib *et al*. "Plasma Photocathodes," *Annalen der Physik* **535**, 2200655 (2023) DOI: 10.1002/andp.202200655

267 http://pwfa-fel.phys.strath.ac.uk/

268 A.F. Habib, P. Scherkl, G.G. Manahan *et al.* "Plasma accelerator-based ultrabright X-ray beams from ultrabright electron beams," *Proc. SPIE 11110, Advances in laboratory-based X-ray sources, Optics and Applications VII*, 111100A (2019) DOI: 10.1117/12.2530976

269 B.W.J. McNeil, N. R. Thompson, "X-ray free-electron lasers," *Nature Photon* **4,** 814-821 (2010) DOI: 10.1038/nphoton.2010.239

270 J. Rossbach, E.L. Saldin, E.A. Schneidmiller, M.V. Yurkov, "Fundamental limitations of an X-ray FEL operation due to quantum fluctuations of undulator radiation," *Nucl. Inst. Meth. A* **393**, 152-156 (1997) DOI: 10.1016/S0168-9002(97)00449-X

271 D.M. Straub, "Anatomy of flavour-changing Z couplings in models with partial compositeness," *J. High Energ. Phys*. **2013**, 108 (2013) DOI: 10.1007/JHEP08(2013)108

272 A.J. Buras, D. Buttazzo and R. Knegjens, "$K \to \pi$ and in simplified new physics models," *J. High Energ. Phys.* **2015**, 166 (2015) DOI: 10.1007/JHEP11(2015)166

273 K. Ishiwata, Z. Ligeti and M.B. Wise, "New vector-like fermions and flavor physics," *J. High Energ. Phys.* **2015**, 27 (2015). DOI: 10.1007/JHEP10(2015)027

274 M. Bordone, D. Buttazzo, G. Isidori *et al*. "Probing lepton-flavour universality with $K \to \pi$ decays," *Eur. Phys. J. C* **77**, 618 (2017) DOI: 10.1140/epjc/s10052-017-5202-1

275 S. Fajfer, N. Kosnik and L. Vale Silva, "Footprints of leptoquarks: from $K \to \pi$," *Eur. Phys. J. C* **78** 275 (2018) DOI: 10.1140/epjc/s10052-018-5757-5

276 R. Mandal and A. Pich, "Constraints on scalar leptoquarks from lepton and kaon physics," *J. High Energ. Phys.* **2019**, 89 (2019) DOI: 10.1007/JHEP12(2019)089

277 D. Marzocca, S. Trifinopoulos and E. Venturini, "From B-meson anomalies to Kaon physics with scalar leptoquarks," *Eur. Phys. J. C* **82**, 320 (2022) DOI: 10.1140/epjc/s10052-022-10271-7

278 O.L. Crosas, G. Isidori, J.M. Lizana, N. Selimovic and B.A. Stefanek, "Flavor non-universal vector leptoquark imprints in $K \to \pi$ and $\Delta F = 2$ transitions," *Phys. Lett. B* **835** (2022) 137525 DOI: 10.1016/j.physletb.2022.137525

279 G. D'Ambrosio, F. Mahmoudi and S. Neshatpour, "Beyond the Standard Model prospects for kaon physics at future experiments," *J. High Energ. Phys*. **2024**, 166 (2024) DOI: 10.1007/JHEP02(2024)166

280 G. D'Ambrosio, A.M. Iyer, F. Mahmoudi and S. Neshatpour, "Exploring scalar contributions with $K^+ \to \pi^+ \ell^+ \ell^-$," *Phys. Lett. B* **855** (2024) DOI: 10.1016/j.physletb.2024.138824

281 Y. Grossman and Y. Nir, "$K_L \to \pi^0 \nu\nu$ beyond the standard model," *Phys. Lett. B* **398** (1997) DOI: 10.1016/S0370-2693(97)00210-4

282 T. Kitahara, T. Okui, G. Perez, Y. Soreq and K. Tobioka, "New physics implications of recent search for $K_L \to \pi^0 \nu\bar{\nu}$ at KOTO," *Phys. Rev. Lett*. **124** 071801 (2020) DOI : 10.1103/PhysRevLett.124.071801

283 E. Goudzovski *et al*. "New physics searches at kaon and hyperon factories," Rep. Prog. Phys. 86 016201 (2023) DOI: 10.1088/1361-6633/ac9cee

284 G. Anzivino *et al*. "Workshop summary: Kaons@CERN 2023," *Eur. Phys. J. C* **84**, 4, 377 (2024) DOI: 10.1140/epjc/s10052-024-12565-4

285 M. Bona *et al.* "The 2004 UTfit collaboration report on the status of the unitarity triangle in the standard model," JHEP07(2005)028 DOI: 10.1088/1126-6708/2005/07/028

286 A. Hocker, H. Lacker, S. Laplace and F. Le Diberder, "A new approach to a global fit of the CKM matrix," *Eur. Phys. J. C* **21**, 225–259 (2001) DOI: 10.1007/s100520100729

287 J. Aebischer, A.J. Buras and J. Kumar, "On the importance of rare kaon decays: A Snowmass 2021 White Paper" arXiv (2022) DOI: 10.48550/arXiv.2203.09524

288 A.J. Buras, D. Buttazzo, J. Girrbach-Noe and R. Knegjens, "$K^+ \to \pi^+ \nu\bar{\nu}$ and $K_L \to \pi^0 \nu\bar{\nu}$ in the Standard Model: status and perspectives," *J. High Energ. Phys.* **2015**, 33 (2015) DOI: 10.1007/JHEP11(2015)033

289 J. Aebischer, A.J. Buras and J. Kumar, "Kaon physics without new physics in ε_K," *Eur. Phys. J. C* **83** 368 (2023) DOI: 10.1140/epjc/s10052-023-11474-2

290 R. Abbott *et al*. (RBC and UKQCD Collaborations) "Direct *CP* violation and the $\Delta I = ½$ rule in $K \to \pi\pi$ decay from the standard model," *Phys. Rev. D* **102** 054509 (2020) DOI: 10.1103/PhysRevD.102.054509

291 E. Lunghi and A. Soni, "Light quark loops in $K^{\pm} \to \pi^{\pm}\nu\bar{\nu}$ from vector meson dominance and update on the Kaon Unitarity Triangle," *J. High Energ. Phys.* **2024**, 97 (2024) DOI: 10.1007/JHEP12(2024)097

292 The NA62 collaboration, E. Cortina Gil, E. Minucci *et al*. "First search for $K^+ \to \pi^+\nu\bar{\nu}$ using the decay-in-flight technique," *Phys. Lett. B* **791** 156-166 (2019) DOI: 10.1016/j.physletb.2019.01.067

293 The NA62 collaboration, E. Cortina Gil, A. Kleimenova *et al*. "Measurement of the very rare $K^+ \to \pi^+\nu\bar{\nu}$ decay," *J. High Energ. Phys.* **2021**, 93 (2021). DOI: 10.1007/JHEP06(2021)093

294 The NA62 collaboration, E. Cortina Gil, J. Jerhot *et al*. "Observation of the $K^+ \to \pi^+\nu\bar{\nu}$ decay and measurement of its branching ration," *J. High Energ. Phys.* **2025**, 191 (2025). DOI: 10.1007/JHEP02(2025)191

295 J-PARC E14 Collaboration, J. Comfort *et al*. "Proposal for $K_L \to \pi^0\nu\bar{\nu}$ experiment at J-Parc," (2006) https://j-parc.jp/researcher/Hadron/en/pac0606/pdf/p14-Yamanaka.pdf

296 KOTO collaboration, J.K. Ahn, M. Farrington *et al.* "Search for the $K_L \to \pi^0\nu\bar{\nu}$ decay at the J-Parc KOTO experiment," *Phys. Rev. Lett*. **134**, 081802 (2025) DOI: 10.1103/PhysRevLett.134.081802

297 KOTO II preparation group, J.K. Ahn *et al*. "Proposal of the KOTO II experiment," arXiv (2025) DOI: 10.48550/arXiv.2501.14827

298 L.J. Nevay, S.T. Boogert, J. Snuverink *et al*. "BDSIM: An accelerator tracking code with particle-matter interactions," *Computer Physics Communications* **252** :1-17, 107200 (2020) DOI: 10.1016/j.cpc.2020.107200

299 I.-H. Chiang et al., BNL Proposal E926, Measurement of $K_L \to \pi^0\nu\nu$, September 1996.

300 PIONEER Collaboration, W. Altmannshofer, H. Binney, E. Blucher *et al*. "PIONEER: Studies of rare pion decays," arXiv (2022) DOI: 10.48550/arXiv.2203.01981

4. Science Opportunities for Matter in Extreme Conditions

Femtosecond X-ray pulses from XFELs enable the probing of the atomic and electronic structure of transiently produced extreme phases of matter in unprecedented detail. This provides new knowledge and understanding as to the behaviour and control of matter in widely diverse settings, including planetary interiors, stars, and inertial confinement fusion, and in shocked engineering materials.

Matter at extreme pressures and temperatures dominates the interiors of planets, exoplanets and stars and is a rich source of novel phenomena in condensed matter physics, materials science and plasma physics. Such matter can be created in the laboratory by compression and heating with high-powered optical lasers, but then only exists transiently. To probe the properties and structure of this matter under extreme conditions requires hard X-rays of ultrafast pulse duration, in order to achieve the required penetration of these highly opaque objects and to capture the rapidly evolving states.

Here we discuss this important area of science, with implications across clean energy, engineering, defence, astrophysics, planetary science and geophysics. In **Section 4.1**, we examine new science opportunities in studying shocked materials, in which high pressures are created using diamond anvil cells and high energy laser compression. The diverse phases of matter generated in these high pressure conditions are known to be highly complex and understanding them is vitally important to our knowledge of the Earth's interior and that of exoplanets. High energy density plasmas account for most of the visible universe and, in **Section 4.2**, we discuss how these states can be generated and probed using X-rays, providing fundamental new understandings of hot and warm dense matter, and resolving conundrums such as the X-ray opacity of stellar interiors. In **Section 4.3**, we discuss completely new science experiments that can be carried out if we interact laser accelerated electrons and protons with high intensity X-rays from an XFEL. Finally, in **Section 4.4**, we discuss the new science opportunities that would arise if we combined an XFEL with a kilojoule-class spherical compression facility.

4.1 Shocked materials and matter at extremes

The experimental study of matter at extreme density, where ion cores overlap significantly and the electronic structure is unique to the high-density regime, holds the promise of breakthroughs in our understanding of both solid and liquid phases. The creation and study of such matter will enable us to describe, understand and predict what electrons and ions will do in other condensed matter systems, with direct relevance to exoplanetary science. It will also enable us to determine how matter might be manipulated in the future, to design new and improved materials that cannot be predicted by more traditional "evolutionary" methods.

4.1.1 Introduction to Matter at Extremes

The study of materials at high energy densities, or equivalently very high pressures, is a rich source of novel phenomena in condensed matter physics and materials science, which offers a route to new phases and materials, and provides stringent tests of fundamental condensed matter theory, computation and simulation.[1] It is essential for understanding the interior of the Earth and exoplanets, and for developing models of material response in aerospace engineering and defence applications, and is increasingly making an impact in chemistry and materials science.[2]

Matter can be compressed and heated dynamically to extreme pressures and temperatures on nanosecond (or even sub-nanosecond) timescales via illumination by high energy optical lasers, a method that has been at the forefront of recent international efforts to achieve inertial confinement fusion (ICF). Laser compression offers the only means by which matter can be created at multi-megabar pressures and temperatures of 10^4 K in a laboratory environment,[3] the conditions that otherwise occur only deep within gas or ice-giant planets, such as Jupiter or Neptune, and within the very many exoplanets discovered by the likes of the Kepler space mission.

Understanding the internal structure of such planets relies on knowledge of the density and compressibility of the solid and liquid phases that make up their interior, and the crystalline structure adopted by the solid phases. For decades, these structures were assumed to be "simple" with the atoms packed closely together. The high density phases were also assumed to become free electron-like metals at high enough pressures, as a result of the kinetic energy of the electrons (which scales as $V^{-2/3}$) increasingly dominating over their potential energy (which scales as $V^{-1/3}$ for Coulomb interactions). There was, however, little experimental evidence to support these very broad assumptions.

4.1.2 The importance of X-ray studies

The arrival of third-generation synchrotron sources in the 1990s, combined with novel diamond anvil cell diffraction techniques and advances in electronic structure calculations, completely overturned these assumptions. The picture that emerged was one of complexity, where the structure of high-density matter was found to be as complex, if not more so, than that observed at ambient conditions. It was also found that materials might transform into semiconductors or insulators at high densities rather than into metals, and new forms of bonding, involving core electrons, were seen to enrich the structural landscape.

Key to these breakthroughs was the advent of advanced X-ray diffraction and spectroscopic techniques using diamond anvil cells. Even the most advanced synchrotrons, however, remain insufficiently bright to probe the very short-lived extreme states created as a result of laser irradiation and/or dynamic compression, which is the route to generate the highest pressures. The ultra-high brightness X-ray pulses from XFELs, on the other hand, can be focused to sub-micron dimensions, are extremely well collimated and are spatially coherent, and the sub-100 femtosecond pulse length is well-matched to probing the shortest-lived extreme states. Indeed, the pulse length is so short that even "smearing" of the data resulting from hydrodynamic motion can be removed.

XFELs thus enable us to study the structure and dynamics of extreme states of dense matter for the first time. Using the LCLS, UK researchers have: made the first measurement of material strength at

the same spatial (< 1 μm) and temporal (< 50 ps) scales as multimillion-atom molecular dynamics simulations;[4] shown that melting and solid-solid phase transitions in shocked compressed metals take place on nanosecond timescales,[5,6] and that complex, even incommensurate, forms are created on such timescales;[7,8] probed the equation of state and resolved the ionic interactions at atomic length scales in dense metals[9,10] and carbon;[11,12] and created and probed the absorption of solid-density plasmas (see **Section 4.2**). UK researchers also played leading roles in the first extreme conditions experiments in 2019 at the European XFEL.

Although much of the work above has focused on elemental materials, work on more complex systems is becoming commonplace. This includes deformation of brittle materials such as ceramics,[13] compression of hydrocarbons[14,15] including the observation of precipitation of diamond-like carbon under loading,[16] and planetary relevant compounds such as SiO_2[17,18] and water.[19] Recent advances using European XFEL pulses (see **Section 2.2.4**) to both heat and structurally probe polystyrene samples compressed in a diamond anvil cell have shown diamond-like carbon formation process occurs under lower pressure and temperature conditions than previously thought[20].

An example of the remarkable complexity present even in 'simple' elemental systems can be seen in **Figure 4.1**. This work on shock-compressed antimony (Sb) followed structural evolution from ambient conditions up to melt along the shock Hugoniot. This study demonstrates two of the key themes permeating the field. Firstly, it was able to access complex phase transitions into an incommensurate host-guest phase on nanosecond timescales. Such structures, observed at moderate pressures in static experiments, are expected to be common at TPa pressures and, as such, their observation in nanosecond timescale experiments is a critical validation of the potential of dynamic compression to access complex stable structures at astrophysically-relevant conditions (see **Box 4.1**).

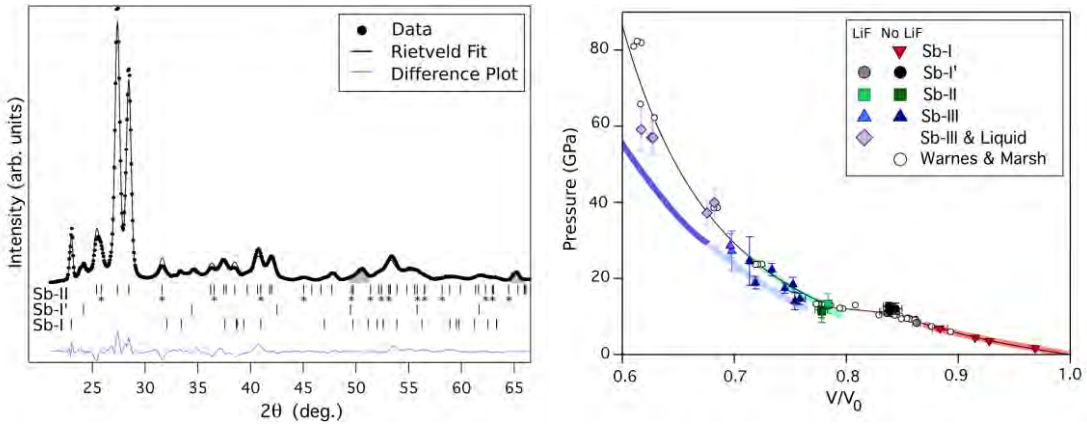


Figure 4.1: Examples of synchrotron quality diffraction data from an ordered incommensurate host-guest structure (left) and complex phase evolution with pressure (right) in shock compressed antimony[7]

Figure reproduced with permission from American Physical Society: A.L. Coleman et al. "Identification of Phase Transitions and Metastability in Dynamically Compressed Antimony Using Ultrafast X-Ray Diffraction" Phys. Rev. Lett 122, 255704 (2019), Copyright (2019). DOI: 10.1103/PhysRevLett.122.255704

Secondly, this work shows the formation of the previously unobserved phase Sb-I', which appears to be unique to dynamic loading conditions. This demonstrates the potential for the large shear stresses and restricted deformation timescales inherent to dynamic loading to lead to unique material behaviour, hitherto unseen in static compression studies. An understanding of these phenomena is important to the interpretation of data of planetary relevance and, more generally, to awareness of the dynamic compression and failure processes underlying key aeronautical and defence applications. It is therefore crucial to be able to explore and understand, at the microstructural level, the full sample journey through both compression and release.

The study of such systems has been made possible by the development of a suite of X-ray diagnostic capabilities. X-ray diffraction remains the workhorse of high energy density structural determination. This has been combined with imaging techniques to allow detailed probing of systems with complex multi-wave loading, and thus spatially inhomogeneous structures.[21,22] Experiments have been conducted to demonstrate X-ray absorption spectroscopy as a tool for probing the chemical

environment within high density matter.[23] Inelastic scattering techniques have been demonstrated that hold the potential to provide temperature measurements in the 0.1 – 1 eV range likely to be accessed in these experiments, completing our understanding of material equation of state.[24]

4.1.3 Opportunities for future study

Despite the rapid advances made in the study of dynamically compressed matter since the advent of XFELs, there is still considerable scope for growth and innovation in the field. In particular, there is still a significant range of pressure unexplored in XFEL science.

Current capabilities at LCLS only allow studies up to 3 Mbar,[9] with the majority of work being at no more than 1 – 2 Mbar. This compares to the 3.5 Mbar of the Earth's core, or the 40 – 50 Mbar estimated core pressure of Jupiter. Studies have been extended at the European XFEL since 2021, where the UK's £8M DiPOLE diode-pumped, 100 J, 10 Hz optical laser, has been installed. The DiPOLE laser is vastly superior to its LCLS equivalent, having three-times the energy, 2000-times the repetition rate and, crucially, the ability to fine tune the time-profile of the laser pulses it provides in almost real time, thereby allowing routine access to an extremely wide range of P-T states at unparalleled rates. Even here though, pressures will likely be limited to below 10 Mbar for most experiments. Use of DiPOLE has already yielded new science (see **Section 2.2.4**) with the observation of the structure of liquid carbon through the shock compression of a glassy carbon target by the DIPOLE100-X laser[25]. It should however be noted that both the LCLS and European XFEL facilities have planned upgrade paths to low repetition-rate kilojoule-scale optical lasers. In addition, plans for Fusion Energy research are being advanced at the European XFEL to harness the unique hard X-ray capabilities of that facility with a kilojoule-class laser system and new experimental infrastructure.

The potential of exploiting a wider range of pressures is significant. For example, in the same way that diamond is a familiar metastable high-pressure allotrope of carbon, a number of other high-pressure structures are predicted to be metastable at ambient conditions. One example is the proposed BC8 phase of carbon, which is notable for having a hardness comparable to – and potentially exceeding that of – diamond.[26] Any such metastability from a phase with a transition pressure above, or composition differing from, the Earth's mantle would potentially represent an entirely new material. The extreme structural and electronic properties of these phases means that such materials may exhibit extreme strength or density, have novel bandgaps suitable for exploitation in electronic or photovoltaic applications, or potentially exhibit superconductivity.[27]

Box 4.1: Super-Earths and Beyond – Probing the cores of planetary giants

(Figure right) Ab initio predictions of the solid phase and liquid (hatched) fields of stability in iron – a key core constituent for planets.[28]

Earth core conditions lie on the edge of current static technique capabilities, with five-times Earth-mass and Jupiter core lying in a regime accessible only to dynamic techniques with a multi-kilojoule class optical laser drivers. The two red lines denote the isentrope (lower) and the Hugoniot (upper). A next-generation XFEL could fully map this region via a combination of X-ray diffraction and spectroscopic techniques, determining the equation of state, phase and chemical properties key to understanding planetary structure and evolution.

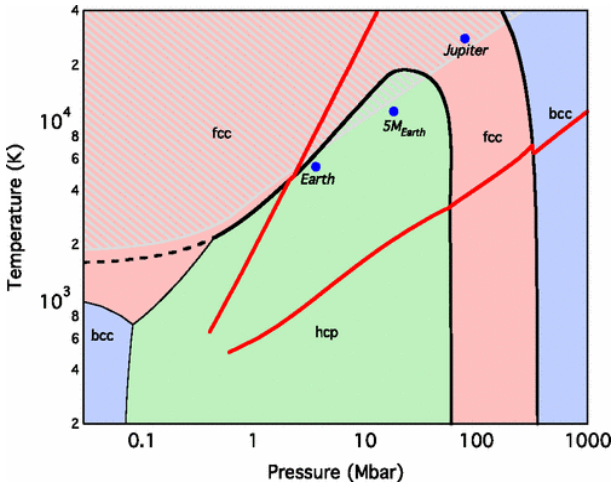


*Figure reprinted with permission from American Physical Society: L. Stixrude, "Structure of Iron to 1 Gbar and 40 000 K", Phys. Rev. Lett. **108**, 055505 (2012) DOI:10.1103/PhysRevLett.108.055505 Copyright (2012)*

In order to probe such materials, a full understanding of crystal and electronic structure *in situ* will be required. X-ray diffraction (XRD) as a structural probe, utilising 10 – 25 keV X-rays, is almost routine at XFELs, but accompanying spectroscopic techniques suitable for probing electronic properties often require quite disparate X-ray conditions. For example, techniques such as XANES[23] or XAS HEROS[29] require tuning to the vicinity of an absorption edge (typically <10 keV), which is usually avoided for scattering measurements. An XFEL capable of providing true two-colour modes of operation, allowing simultaneous structural and electronic probing, would open new avenues for comprehensive understanding of high-pressure states and potentially recoverable materials.

As discussed above, one key shortcoming of current experimental efforts is the inability to sample temperature, due to the optically opaque nature of the material and relatively low (typically sub eV) temperatures. One potential avenue for providing information on this final crucial component of equation of state is inelastic scattering, which employs high resolution (< 10 meV) X-ray scattering measurements to directly observe phonon (ion-acoustic) modes whose occupation is directly related to thermodynamic temperature.[24] However, the low efficiency of such scattering processes requires integration of the signal over a large number of shots and thus limits exploration of configuration space. This limitation could be alleviated by a self-seeded FEL with the inherent capability to reach ~10 meV bandwidth in the hard X-ray regime. Recently at LCLS, a bandwidth of ~ 30 meV was obtained by using self-seeding and an additional monochromator, enabling determination of the lattice temperature of laser heated gold[30] (see **Section 2.2.4**). Once again, with suitable machine capability, such a technique is potentially compatible with diffraction/spectroscopy approaches, for further broadening the information one can capture on these novel high pressure states.

4.1.4 Conclusions

The study of matter at extremes offers a window into the understanding of a wide range of phenomena from the astrophysical to fundamental material deformation. As a field experiencing rapid growth, there remains significant opportunity for discovery. Although both LCLS and the European XFEL have dedicated instruments for such studies, they are limited by the scale and ambition of the driver for compression, as well as the available X-ray parameters and thus the viability of X-ray techniques.

The UK has world-leading capability in many of the underpinning technological requirements for this science. STFC efforts in high repetition laser technology and microtarget assembly have already been foundational for the European XFEL's high energy density (HED) instrument and early experiments on LCLS.

A next-generation XFEL would offer unique opportunities to co-locate a world-class, large-scale laser compression platform alongside an advanced XFEL source. A high repetition rate, high energy (10 kJ class), temporally tunable laser system would allow access to numerous hitherto unexplored structures in a range of materials. This would go meaningfully beyond the scale envisaged for existing FELs, allowing such a system to access and explore a unique range of P-T states.

Coupled to this, a high photon energy, high pulse energy, narrow bandwidth, two-colour photon source would allow the full suite of X-ray diagnostic techniques to be brought to bear, to facilitate acquisition of the full structural, electronic and equation of state knowledge of the material. All of this would lead to unprecedented understanding of the high pressure and dynamic deformation regimes, and would also open routes to systematic searches for new metastable materials with potentially transformative scientific and industrial applications.

4.2 Quantum plasmas: warm and hot dense matter

The vast majority of the visible universe is in the plasma state, and extreme states of matter are routinely found in all astrophysical bodies from (exo)planets to stars. A comprehensive understanding of the structure and dynamics of such high energy density plasmas is thus of fundamental physical interest in its own right, but also forms the basis for progress in planetary physics, astrophysics, applications using laser-plasma interactions to generate compact radiation sources, and for providing the foundation to laboratory-based fusion energy. High temporal resolution X-ray probes, synchronised with high-energy drivers, will allow us to create these extreme conditions in a controlled laboratory setting and explore them on the fundamental temporal and spatial scales.

4.2.1 Introduction

Significant advances in X-ray science over the past decade have transformed our capability to study how matter behaves in extreme conditions of pressure, temperature and density. Of particular interest is the dense plasma regime, where quantum effects and correlations are important and dominate plasma dynamics. Matter in these conditions is prevalent across the universe in stellar[31] and (exo)planetary interiors,[32] is commonly encountered in most laser-plasma interactions,[33] and is of considerable interest within the context of inertial confinement fusion energy research.[34] In contrast to high-temperature classical plasmas that are well described by kinetic theory, the properties of quantum plasmas are governed by the complex interplay between Coulomb interactions, quantum correlations and kinetics, all comparable in size. This leads to a rich spectrum of plasma properties, albeit one that has proven highly challenging to model computationally and to investigate experimentally.

Since energies from quantum interactions are in competition with thermal energies, the domain where quantum effects dominate has historically been confined to low-temperature (i.e. cryogenic) systems at relatively high densities. However, quantum effects and correlations remain important in systems up to temperatures on the order of their Fermi energy. Since Fermi energies can exceed 10s of eV in high density systems (see **Figure 4.2**), quantum effects can remain important even at high temperatures. Matter in this regime cannot be described by classical plasma theory and is known as warm dense matter. Its equation of state has strong implications for planetary physics, as planetary cores are found in this regime, and its transport properties underly much of planetary formation and evolution. This research area is of growing interest in light of the observation of over a thousand exoplanet candidates, many of which do not have analogues within our own solar system.[35]

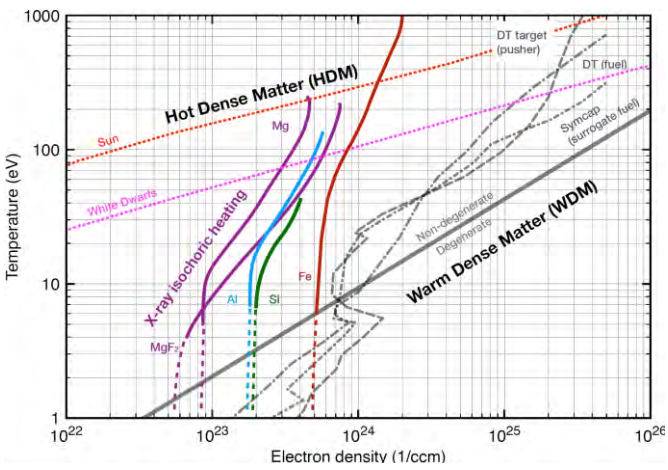
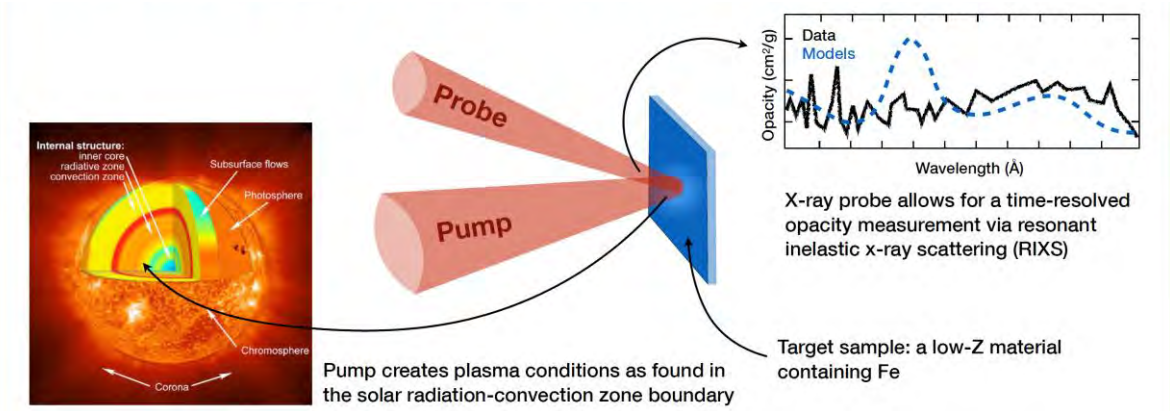


Figure 4.2: Temperatures and densities accessible in the laboratory using x-ray FEL isochoric heating: we can study a broad spectrum of extreme conditions, from planetary cores to stellar interiors. High energy compression drivers will allow us to investigate the unexplored regions at higher densities where quantum effects and correlations persist up to high temperatures.

While these observation-based discoveries are among the most exciting in a generation, they provide limited insight into the nature of these objects, i.e. their interior structure, evolutionary pathways, potential habitability, and physical and chemical processes that shape their geology and atmosphere. It is here that laboratory-based experiments can provide valuable insight into the behaviour of relevant high energy density (HED) systems, and guide future exploration. Similarly, our understanding of the structure, composition and evolution of stars also depends on a range of processes in the HED regime.

Standard solar models[36] using the revised element abundances were found to disagree with helioseismic observations that determine the internal solar structure using acoustic oscillations. Recent experimental work on the Z-pinch machine at Sandia from Bailey and collaborators[31,37] showed that the opacity of Fe in the boundary region between the convective and radiative zones in the sun could be partially responsible for this discrepancy. From this work, it emerges that the opacity of open L-shell mid-Z ions (Cr, Fe) are relatively poorly understood and cannot be explained by current state-of-the-art modelling efforts, while closed-shell ions (Ni) do not lead to similar difficulties. This emphasises the importance of benchmarking astrophysical data in the HED regime to guide developments, and highlights the role of well-characterised HED experiments in supporting this effort. An example experiment that could address some of this physics is shown for illustration in **Box 4.2**. Other work from the LCLS FEL has shown more generally that our overall understanding of the electronic structure of partially-ionised plasmas in the hot-dense conditions relevant to stellar envelopes remains incomplete,[38] and significant discrepancies remain between experiments and theoretical predictions of even fundamental quantities, such as degree of continuum lowering.[39,40,41]

Box 4.2: Time Resolved Iron Opacity Measurements in Stellar Envelopes



Schematic of an experimental platform to study the opacity of mid-Z elements such as Fe in stellar interior conditions. The plasma is generated isochorically by a soft X-ray pump and heated to the required conditions. After a time delay the system is probed at harder X-ray wavelengths and the L-shell opacity is determined via resonant inelastic X-ray scattering.

Illustration of the Sun courtesy of NASA/Goddard

4.2.2 HED science on XFELs to date

The first plasma experiments at FEL facilities[42] have successfully demonstrated the capability of X-rays to isochorically heat matter to temperatures between a few eV up to in excess of 100 eV (> 1 million K), providing access to the temperature-density conditions present in a range of stellar, white dwarf, and planetary interior conditions.[38,43,44] More recent work using nano-focused X-ray pulses suggests further isochoric heating of Fe to temperatures exceeding 1 keV at solid density, with electron densities well above 10^{24} cm^{-3}. The range of temperature-density conditions currently reachable via isochoric heating is schematically shown in **Figure 4.2**, alongside the temperature-density tracks for our sun and a typical white dwarf star. Such hot systems lend themselves well to be probed via X-ray emission spectroscopy, which has been successfully deployed to study the collisional dynamics of hot dense plasmas[45,46] and their opacity,[47,48] and shed light on the physics of ionisation potential depression,[39 - 41] all with unprecedented accuracy and control of experimental conditions. Investigations of warm dense plasmas relevant to planetary astrophysics has also yielded important new insights into the structure and equation of state of planetary interiors,[16,49,50] their transport properties,[51,52] opacity,[53] and degree of ionisation and continuum lowering.[54,55,56] To date, source limitations have constrained much of the high-temperature work to time-integrated experiments. Extending this research into the time domain and to much higher densities, while accurately controlling the HED conditions of the generated plasmas (and independently measuring the temperature, ionisation and density), remains among the most promising future research avenues in this area.

4.2.3 Future opportunities

XFELs coupled with energetic high-energy optical laser drivers provide a unique opportunity to investigate extreme states of matter. X-ray isochoric heating has already been shown to heat solid density systems to temperatures exceeding 1 keV on femtosecond timescales, while compression experiments on large-scale laser facilities have shown how we can tune the inter-atomic spacing in matter to the point where it becomes comparable to the de Broglie wavelength, providing access to a new quantum frontier in HED science, potentially pushing quantum behaviour to the macro-scale. While these extreme capabilities are separately available at select flagship facilities around the world today, no one facility can currently both create such extreme conditions and subsequently probe them using the range of cutting-edge X-ray techniques provided by X-ray FELs. In addition to this, high repetition-rate lasers and FELs will prove revolutionary to HED physics in that they will enable, for the first time, statistical analyses of many identical HED events, rather than the current norm based on isolated-event experiments. A next-generation XFEL with a capability to vary the pulse repetition rate delivered to experiments to best match target and laser will optimise available data rates. Access to insight into how rare events (e.g. nucleation of phases and dislocations, ejecta and detonation) lead to transformations will also enable new science.

Future developments in FEL technology may provide viable approaches to significantly increasing the energy output of a FEL from the millijoule level currently available towards 1 J. A joule-class X-ray FEL would have several transformative advantages to HED physics investigations, and would enable research opportunities unrivalled elsewhere. Firstly, it would allow us to access the ultra-high energy density regime via isochoric heating, generating dense plasmas at temperatures considerably in excess of those found in the centre of stars. It would further enable single-shot measurements of photon hungry diagnostics, such as inelastic or diffuse scattering, and would make it possible to apply novel non-linear spectroscopy techniques to HED investigations for the first time. A substantial increase in photons would also enhance the usefulness of beam-splitting techniques, and would, at least in principle, enable the generation of energetic X-ray comb pulse structures, which would provide new opportunities for multi-frame ultrafast time-resolved studies.

The main future scientific objectives will be linked to the ability to perform well-characterised, time-resolved studies to drive progress in HED science. Of particular interest will be experiments aimed at observing the real-time dynamics of dense plasmas, and of phase transitions of dynamically compressed materials. This includes studies into the transport of heat, charge and particles across interfaces, and the experimental characterisation of conductivity, diffusivity, viscosity, instabilities and plasma opacity. Transport properties, such as viscosity and thermal diffusivity in the warm dense matter regime in particular, are essential inputs for models of planetary evolution and nuclear fusion processes, and progress on this front will have an impact extending significantly beyond the realms of pure HED physics. Within this context, measurements of the opacity at the hot-dense conditions of relevance to the solar interior, performed in a well-characterised time-resolved experiment that demonstrates thermal equilibrium, may be possible for the first time, addressing key outstanding issues in solar modelling, as illustrated in **Box 4.2**.

The direct investigation of the electronic structure and excitation spectrum of highly compressed solids and dense plasmas is also of critical interest, not only because of its role in determining the overall partition functions and thermodynamics of extreme HED systems, but also because it will shed light on the mechanisms of core-electron interactions and how they give rise to the observed emergence of structural complexity at high pressures. At the highest pressures it may be possible that such mechanisms lead to the discovery of new states of matter, where quantum effects emerge and dominate material structure and dynamics even at very high temperatures. While access to such extreme regimes may already be possible on the largest facilities such as the National Ignition Facility, these facilities lack the key diagnostic techniques to probe fundamental excitation mechanisms and ultrafast electron dynamics in the most extreme conditions. These techniques, largely based on high-resolution inelastic X-ray scattering, necessitate a tunable, narrow-bandwidth, bright X-ray source, which is where an XFEL with these capabilities would prove transformative.

4.3 X-ray interactions with laser accelerated electrons

By utilising compact, laser-driven, plasma-based accelerators, we can generate X-ray and gamma ray sources synchronised with the X-rays available from the XFEL. Combining relativistic electron and XFEL sources would enable new science, for example allowing us to probe warm dense states, to access the extreme science of fundamental particle interactions, and to test the fundamental theories of quantum electrodynamics.

4.3.1 Laser wakefield accelerators

As described in more detail in **Appendix 2.2** in a laser wakefield accelerator (LWFA) an intense laser pulse drives a plasma wakefield, within which are generated electric fields of order 100 GV m^{-1} that can be used to accelerate charged particles. To date LWFAs have been used to generate electron beams with an energy up to 10 GeV from an accelerator stage only 30 cm long. The electron beams produced by LWFAs have been used to generate incoherent radiation from 100 eV to 100s of MeV via magnetic undulators, by betatron oscillations in the plasma wakefield, and by Compton scattering.

Since they are relatively compact and driven by the high power lasers that are necessarily part of an XFEL facility, LWFAs could be operated alongside an XFEL, greatly expanding the science that could be done on the facility, whilst also providing an opportunity to drive advances in LWFAs themselves. As shown schematically in **Figure 4.3**, one or more LWFAs could be driven by using the optical lasers required for HED science, as described in **Sections 4.1** and **4.2,** to pump a short-pulse (50 fs) laser driver for an LWFA.

4.3.2 Science combining relativistic electrons and an XFEL beam

Laser-accelerated electrons can generate bright, femtosecond-duration pulses of incoherent radiation. For example, betatron motion of the electron bunch in the LWFA itself generates forward-directed radiation in the keV range[57]. Alternatively, Compton scattering can generate narrow-band, tunable X-rays with photon energies into the multi-MeV range[58,59,60], which have sufficient brightness for single-shot radiography of dense material[61]. The Compton scattering beam can be supplied using a fraction of the LWFA drive beam or by using a plasma mirror to retro-reflect the LWFA drive laser[62], which provides a convenient, self-aligning geometry. The multi-keV X-rays produced by the betatron oscillations that occur within an LWFA are unique, in that they are both broadband and have a femtosecond duration. This makes them an ideal tool for X-ray absorption spectroscopy of rapidly evolving systems, such as those generated via laser compression or X-ray isochoric heating (see **Sections 4.1** and **4.2**). Work in this area has already started at the LCLS,[63] and is a focus of both UK[64] and international LWFA groups.[65] Recent work has also demonstrated the potential for single-shot "multi-messenger" imaging of dynamic systems, by using both the laser-accelerated electrons and the betatron radiation[66].

It should be noted that, in recent years, the first steps towards plasma-accelerator-driven FELs have been taken[67]. FEL gain at visible wavelengths has been reported for a beam-driven plasma accelerator. FEL gain at soft X-ray wavelengths, and seeded gain in the ultraviolet, have been produced from laser-accelerated electrons[68,69]. It is clear that significant further advances will be necessary before plasma-driven FELs could provide a user facility; nevertheless, with further development they could provide a future upgrade path, for example by providing compact, low-power auxiliary FEL beams.

The X-ray and gamma sources produced by these methods would be tightly synchronised both to each other and to the other lasers used at the XFEL (for example, to those used to compress matter), and of course with the XFEL itself. Hence LWFA-driven photon sources could provide additional, synchronised ultrafast probes for X-ray imaging, scattering and absorption measurements where they could be used to probe, for example, XFEL-generated warm-dense matter (WDM) and high-energy density (HED) states, as well as X-ray beam generated filaments and transient highly ionised states.

Likewise, a relativistic electron beam will interact with matter in highly novel ways that can then be probed by the XFEL with exceptional time resolution.

A laser capable of driving an LWFA is also capable of accelerating protons from thin foil targets, via a process called sheath acceleration[70]. Depending on the laser parameters these broadband protons extend up into the 10s of MeV range, with energies above 100 MeV recently enabled through the use of advanced targetry/acceleration mechanisms[71].These picosecond duration proton beams can be used to isochorically heat samples into the warm dense matter regime, which can then be interrogated by exploiting the full capabilities of the XFEL pulse. Conversely, laser-generated protons can be used to investigate the ion stopping power of WDM generated by the XFEL pulse, a topic of significant fundamental interest and of ICF relevance[72]. As described in the previous section, intense lasers can also be used to create warm dense matter directly, through the direct electron heating generated in a laser-solid interaction, or using the electron beams produced by a laser wakefield accelerator.

4.3.3 Probing fundamental physics

Combining LWFAs with an XFEL also offers some unique opportunities in fundamental science. One specific example is the study of photon-photon interactions. In 1934, Breit and Wheeler predicted that when two photons collide, they can produce an electron and a positron,[73] a process called "inelastic photon-photon scattering". This process is crucial in a range of astrophysical phenomena, and yet has never been observed in the laboratory. For example, extremely-high-energy gamma rays should not propagate across the universe due to their interaction with the cosmic microwave background,[74] and observations of TeV gamma rays are showing some tension with predictions based on the Breit-Wheeler process.[75]

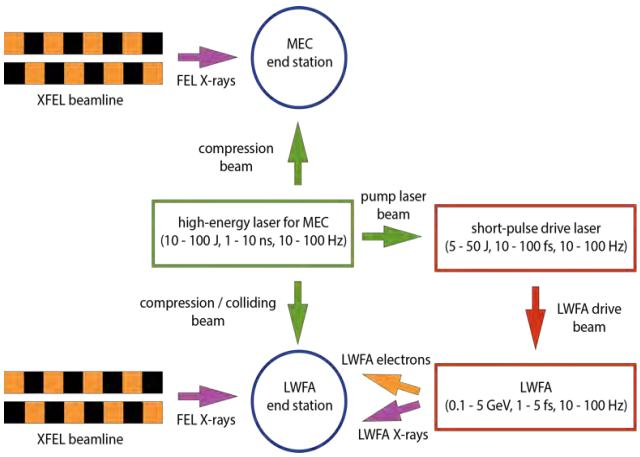


Figure 4.3: Schematic diagram illustrating how auxiliary lasers at an XFEL could drive a LWFA

Elastic photon-photon scattering, when two photons collide and change angle and energy, is one of the fundamental predictions of quantum electrodynamics, but it has never been observed with real photons. So far it has only been observed with very high-energy "virtual" photons.[76] In astrophysical scenarios, scattering of photons plays an important role in determining primordial abundances, and in the gamma-ray spectra we can observe from events early in the universe.[77] Attempts to measure low energy photon-photon scattering have not been successful (e.g. using keV photons from an XFEL[78] or eV photons using lasers) due to the very small cross-section at these low energies. Crucially, for both elastic and inelastic photon-photon scattering, the regime of relevance to astrophysics requires the invariant mass of the collision between two photons to be close to the rest mass of an electron-positron pair. With an XFEL pulse consisting of keV-range photons, this therefore requires collision with photon energies around a few hundred MeV. LWFAs are ideal sources of such photons, either through bremsstrahlung conversion or Compton back scattering.[79,80] Colliding 100 MeV photons with 1 - 10 keV XFEL photons will enable fundamental studies of photon-photon physics in the laboratory for the first time. Indeed, very recently, strongly non-linear Compton scattering from laser-accelerated electrons achieved a quantum non-linearity parameter as high as 0.46, opening a route to a new field of strong-field quantum electrodynamics[81].

4.3.4 Conclusion and future vision

Combining laser plasma accelerators with a next-generation XFEL would provide a unique capability that brings together a narrow energy spread relativistic electron beam with high brightness X-rays. This would be a cost-effective way of significantly broadening the science capabilities of a facility. Laser plasma accelerators would provide pulses of relativistic electrons, protons, gamma-rays and broad- and narrow-band X-rays that could be synchronised with the XFEL and other drivers, thereby allowing novel "multi-messenger" imaging, scattering and absorption measurements. These additional laser-generated beams would deliver new insights into the behaviour of matter compressed and heated to extreme conditions, could be used to provide additional isochoric heating, or could provide the photon beams needed to probe the fundamental physics of photon-photon interactions for the first time. The application of laser accelerated electrons, protons and neutrons to pulsed radiolysis investigations in Chemistry and Material Science is further discussed in **Section 6.3**.

The requirements for the XFEL would be the same as those required to deliver the other science described in this chapter – the ability to deliver high fluxes of high energy X-rays, ideally in the range 20 – 30 keV, but higher if possible. An LFWA requires a high-power optical drive laser. A focused intensity > 10^{19} W cm^{-2} with a repetition rate exceeding 10 Hz (eventually up to 100 Hz) would provide beyond-state-of-the-art capability for these combined X-ray-electron experiments. We note that these laser requirements are similar to those needed for other science in this Case (see **Section 3.5**).

4.4 Coupling an XFEL to a laser-driven spherical compression facility

The coupling of a laser-driven spherical-compression facility to a sufficiently hard and bright X-ray FEL would enable the diagnosis of extreme states of matter in unprecedented detail, leading to advances in both the pursuit of fusion energy and our understanding of the universe. This would be a transformative marriage of technologies that would be globally unique, enabling users to attain a leadership position in the associated science and technologies.

4.4.1 Introduction

Laser-driven spherical-compression enables the creation of temperature and density states otherwise inaccessible within the laboratory. These conditions are similar to those in the cores of stars, supernovae and giant planets. Historically, research in this area has been focused on two main areas: laser inertial confinement fusion[82] (one of two 'mainline' routes to fusion energy) and nuclear weapons research. In recent years, High Energy Density (HED) science research has become increasingly diverse, and now includes areas such as Laboratory Astrophysics, Nuclear Astrophysics, Planetary Physics, Plasma Physics, Matter at Extreme Conditions, Warm Dense Matter, Opacity, Equations of State, Laser-Plasma Interactions and Quantum Electrodynamics (QED).

International spherical compression facilities include the USA's National Ignition Facility (2.2 MJ of laser energy), France's Laser MegaJoule (similar to NIF), Russia's ISKRA-6 (2.8 MJ, under consideration), China's SG-III (180 kJ) and SG-II (320 kJ upgrade in progress), and the USA's Omega (30 kJ). However, due to the small spatial scales of the compressed plasma and the brief duration of peak compression, the limited precision of experimental diagnosis obstructs a detailed understanding of the physics of these extreme states of matter. Coupling a laser-driven spherical compression facility to a next-generation XFEL would enable a transformation in our understanding. For example, state-of-the-art experiments are typically limited to spatial resolutions of ~3 µm and temporal resolutions of 1 x 10^{-11} s (but usually significantly worse); in contrast, an XFEL can achieve spatial resolutions of ~30 nm and temporal resolutions of 1 x 10^{-14} s, an increase of 100- and 1000-fold respectively.

4.4.2 Applications

The key advantage of spherical compression is the capability to create and probe a far larger region of density and temperature parameter space than is possible with any other method, as illustrated in **Figure 4.4**.

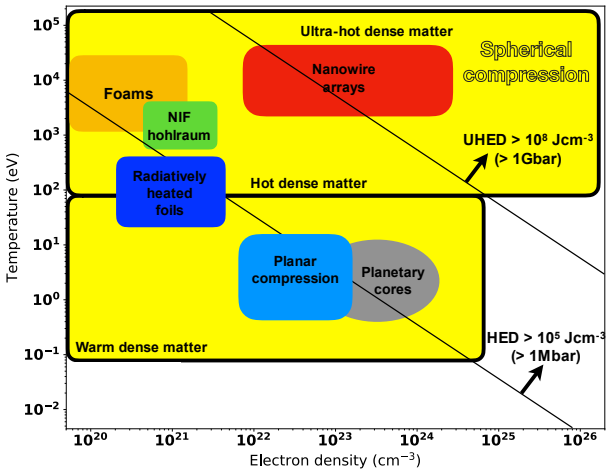


Figure 4.4: The region of density and temperature parameter space which can be explored via spherical compression (both yellow regions)

A laser-driven spherical compression facility sited alongside an XFEL would have a diverse range of applications in the fields from Laboratory Astrophysics to QED as listed in the introduction above. Rather than re-visiting these topics, which are detailed elsewhere within this chapter, we instead highlight that spherical compression would greatly increase the scope of these research areas by enlarging the accessible density and temperature parameter space.

Below we outline some areas where the coupling of a spherical compression facility to an XFEL would be truly transformative, creating a world-

leading, globally unique facility. This would enable these areas to be studied in unprecedented detail, with concomitant improvements in our understanding of the underlying science.

Laser driven inertial confinement fusion

Laser inertial fusion is one of two highly advanced, credible approaches to fusion energy, the second approach being magnetic confinement fusion. In December 2022, the USA's National Ignition Facility demonstrated the biggest breakthrough in all controlled fusion research to that date; more energy was output by the fusion reactions than was input to the experiment. This groundbreaking feat has since been repeated multiple times, and has re-invigorated research into Inertial Fusion Energy (IFE), which seeks to use laser inertial confinement fusion as a method of creating fusion energy.

In the quest for IFE, the unprecedented spatio-temporal resolution of an XFEL would enable ultra-high-resolution X-ray Compton scattering or phase contrast imaging of the implosion, with effectively no temporal blurring. While it is likely that at least 500 kJ of laser energy will be required for ignition, even with more energetically efficient implosion techniques such as Laser Direct Drive,[83,84] if a next-generation XFEL were coupled to a more modest (e.g. 100 kJ) spherical compression facility, this would transform our understanding of the implosion process, potentially accelerating IFE progress.

Fusion materials

A key challenge for fusion is the engineering of materials able to withstand the fast ion and neutron irradiation created by fusion reactions. The coupling of a spherical compression facility to an XFEL may enable the real-time evaluation of damage mechanisms caused by atomic displacements within the lattice.

The intensity frontier

Spherical compression requires quite significant laser energy, meaning that a system would likely need to be at least in the high tens of kilojoules in order to be globally competitive. Chirped Pulse Amplification (CPA, the subject of the 2018 Nobel Prize in Physics) enables this laser energy to be compressed in time. If the available laser energy were harnessed in this way, the achievable laser intensity would far exceed that of any existing or planned facility. Such a laser, when coupled to an XFEL, would enable the exploration of a raft of exotic fundamental physics (see **Section 3.5**).

Matter at extreme conditions

Studies of the mechanisms of deformation, melt, recrystallisation and polymorphic phase transitions in matter are currently limited to planar compression geometries, in which shear plays a significant role in the deformation dynamics, significantly complicating the interpretation of such experiments. A spherical implosion facility combined with an XFEL would enable hydrostatic (shear-free) compression to extreme states of matter to be studied in unprecedented detail, and to pressures and temperatures well beyond those currently accessible with planar compression.

Advanced manufacturing

The development of precision targetry for a spherical compression facility would greatly enhance existing cutting-edge UK manufacturing capabilities, such as those at Scitech Precision Ltd. Furthermore, the laser developments required for such a facility would consolidate the Central Laser Facility's position as world-leaders in the design and manufacture of high-energy, high repetition rate lasers, as recently demonstrated by the successful spin-out of DiPOLE Systems.[85] With these technologies in place, the UK would be excellently placed to capitalise on potential economic benefits if power production via laser fusion were to become a commercial reality.

Defence

The combination of spherical compression with an XFEL would enable Opacity and Equations of State studies to be performed with unprecedented fidelity at extreme densities and temperatures. Potentially such a facility could provide access to the burning plasma regime, unlocking a wealth of physics, the detailed understanding of which is critical in the nuclear test-ban era.

4.4.3 Facility needs

In terms of a next-generation XFEL facility characteristics, the key parameter is the ability to deliver high fluxes of high energy X-rays, ideally in the range 20 – 30 keV, higher if possible.

The cost of a laser-driven spherical compression facility is highly dependent on its design characteristics and in particular total laser energy. The largest international laser-compression facilities cost more than an XFEL; however, investment at this level would not be required to make a significant impact. A detailed examination of the optimal design characteristics of a laser-driven spherical compression facility is beyond the scope of this report. Instead, we briefly outline two approaches that might be considered to fund such a facility within a plausible funding envelope:

- a phased approach starting out at 1 – 10s kJ of laser energy, with a planned upgrade path;
- a combined energy, science and defence facility that could fulfil the requirements of three UK government departments, thereby leveraging additional funding.

Either way, given the scientific potential offered by such a facility, it is crucial at the FEL planning stage that sufficient physical space is left for the development of such a facility.

4.4.4 Conclusions and future vision

The coupling of a laser-driven spherical compression facility to an XFEL would be a transformative marriage of technologies. This globally unique capability would have the potential to revolutionise laser fusion research, accelerating the realisation of fusion energy, whilst enabling a diverse range of HED science, from Laboratory Astrophysics to Quantum Electrodynamics.

4.5 References for Chapter 4

1 R.J. Hemley and N.W Ashcroft, "The Revealing Role of Pressure in the Condensed Matter Sciences." *Phys. Today* **51**, 26-32 (1998) DOI: 10.1063/1.882374

2 P.F. McMillan, "New materials from high-pressure experiments." *Nat. Mater.* **1**, 19-25 (2002) DOI: 10.1038/nmat716

3 R.F. Smith, J. Eggert, R. Jeanloz *et al.* "Ramp compression of diamond to five terapascals." *Nature* **511**, 330-333 (2014) DOI: 10.1038/nature13526

4 D. Milathianaki *et al.* "Femtosecond visualization of lattice dynamics in shock-compressed matter." *Science* **342**, 220-223 (2013) DOI: 10.1126/science.1239566

5 M.G. Gorman *et al.* "Direct Observation of Melting in Shock-Compressed Bismuth With Femtosecond X-ray Diffraction." *Phys. Rev. Lett.* **115**, 095701 (2015) DOI: 10.1103/PhysRevLett.115.095701

6 E.E. McBride, A. Krygier, A. Ehnes *et al.* "Phase transition lowering in dynamically compressed silicon." *Nat. Phys.* **15**, 89-94 (2019) DOI: 10.1038/s41567-018-0290-x

7 A.L. Coleman *et al.* "Identification of Phase Transitions and Metastability in Dynamically Compressed Antimony Using Ultrafast X-Ray Diffraction." *Phys. Rev. Lett.* **122**, 255704 (2019) DOI: 10.1103/PhysRevLett.122.255704

8 R. Briggs *et al.* "Ultrafast X-Ray Diffraction Studies of the Phase Transitions and Equation of State of Scandium Shock Compressed to 82 GPa." *Phys. Rev. Lett.* **118**, 025501 (2017) DOI: 10.1103/PhysRevLett.118.025501

9 C.E. Wehrenberg, D. McGonegle, C. Bolme *et al.* "In situ X-ray diffraction measurement of shock-wave-driven twinning and lattice dynamics." *Nature* **550**, 496-499 (2017) DOI: 10.1038/nature24061

10 M. Sliwa, J.S. Wark *et al.* "Femtosecond X-Ray Diffraction Studies of the Reversal of the Microstructural Effects of Plastic Deformation during Shock Release of Tantalum." *Phys. Rev. Lett.* **120**, 265502 (2018) DOI: 10.1103/PhysRevLett.120.265502

11 D. Kraus *et al.* "The complex ion structure of warm dense carbon measured by spectrally resolved X-ray scattering." *Physics of Plasmas* **22** 056307 (2015) DOI: 10.1063/1.4920943

12 D. Kraus, A. Ravasio, M. Gauthier *et al.* "Nanosecond formation of diamond and lonsdaleite by shock compression of graphite." *Nat Commun* **7**, 10970 (2016) DOI: 10.1038/ncomms10970

13 S.J. Tracy *et al.* "In situ observation of a phase transition in silicon carbide under shock compression using pulsed X-ray diffraction." *Phys. Rev. B* **99**, 214106 (2019) DOI: 10.1103/PhysRevB.99.214106

14 N.J. Hartley, S. Brown, T.E. Cowan *et al.* "Evidence for Crystalline Structure in Dynamically-Compressed Polyethylene up to 200 GPa." *Sci Rep* **9**, 4196 (2019) DOI: 10.1038/s41598-019-40782-5

15 N.J. Hartley *et al.* "Liquid Structure of Shock-Compressed Hydrocarbons at Megabar Pressures." *Phys Rev Lett* **121**, 245501 (2018) DOI: 10.1103/PhysRevLett.121.245501

16 D. Kraus, J. Vorberger, A. Pak *et al.* "Formation of diamonds in laser-compressed hydrocarbons at planetary interior conditions." *Nat Astron* **1**, 606-611 (2017) DOI: 10.1038/s41550-017-0219-9

17 A.E. Gleason, C. Bolme, H. Lee *et al.* "Ultrafast visualization of crystallization and grain growth in shock-compressed SiO_2." *Nat Commun* **6**, 8191 (2015) DOI: 10.1038/ncomms9191

18 A.E. Gleason *et al.* "Time-resolved diffraction of shock-released SiO_2 and diaplectic glass formation." *Nat Commun* **8**, 1481 (2017) DOI: 10.1038/s41467-017-01791-y

19 A.E. Gleason *et al.* "Compression Freezing Kinetics of Water to Ice VII." *Phys. Rev. Lett.* **119**, 025701 (2017) DOI: 10.1103/PhysRevLett.119.025701

20 M. Frost, R.S. McWilliams, E. Bykova *et al.*, "Diamond precipitation dynamics from hydrocarbons at icy planet interior conditions." *Nat Astron* **8**, 174-181 (2024) DOI: 10.1038/s41550-023-02147-x

21 A. Schropp, R. Hoppe, V. Meier *et al.* "Imaging Shock Waves in Diamond with Both High Temporal and Spatial Resolution at an XFEL." *Sci Rep* **5**, 11089 (2015) DOI: 10.1038/srep11089

22 S.B. Brown *et al.* "Direct imaging of ultrafast lattice dynamics." *Sci Adv* **5**, eaau8044 (2019) DOI: 10.1126/sciadv.aau8044

23 M. Harmand *et al.* "X-ray absorption spectroscopy of iron at multimegabar pressures in laser shock experiments." *Phys. Rev. B* **92**, 024108 (2015) DOI: 10.1103/PhysRevB.92.024108

24 E.E. McBride *et al.* "Setup for meV-resolution inelastic X-ray scattering measurements and X-ray diffraction at the Matter in Extreme Conditions endstation at the Linac Coherent Light Source." *Rev. Sci. Instrum.* **89**, 10F104 (2018) DOI: 10.1063/1.5039329

25 D. Kraus, J. Rips, M. Schörner *et al.* "The structure of liquid carbon elucidated by in situ X-ray diffraction." *Nature* **642**, 351-355 (2025) DOI: 10.1038/s41586-025-09035-6

26 J. Sun, D.D. Klug and R. Martonák, "Structural transformations in carbon under extreme pressure: beyond diamond." *J. Chem. Phys.* **130**, 194512 (2009) DOI: 10.1063/1.3139060

27 A.P. Drozdov, M.I. Eremets, I.A. Troyan, V. Ksenofontov and S.I. Shylin, "Conventional superconductivity at 203 kelvin at high pressures in the sulfur hydride system." *Nature* **525**, 73-76 (2015) DOI: 10.1038/nature14964

28 L. Stixrude, "Structure of Iron to 1 Gbar and 40 000 K." *Phys. Rev. Lett.* **108**, 055505 (2012) DOI: 10.1103/PhysRevLett.108.055505

[29] W. Błachucki *et al.* "High energy resolution off-resonant spectroscopy for X-ray absorption spectra free of self-absorption effects." *Phys. Rev. Lett.* **112**, 173003 (2014) DOI: 10.1103/PhysRevLett.112.173003

[30] T.G. White, T.D. Griffin, D. Haden *et al.* "Superheating gold beyond the predicted entropy catastrophe threshold." *Nature* **643**, 950–954 (2025). DOI: 10.1038/s41586-025-09253-y

[31] J.E. Bailey, T. Nagayama, G. Loisel *et al.* "A higher-than-predicted measurement of iron opacity at solar interior temperatures." *Nature* **517**, 56-59 (2015) DOI: 10.1038/nature14048

[32] R.F. Smith, D.E. Fratanduono, D.G. Braun *et al.* "Equation of state of iron under core conditions of large rocky exoplanets." *Nat Astron* **2**, 452-458 (2018) DOI: 10.1038/s41550-018-0437-9

[33] P.K. Shukla and B. Eliasson, "Nonlinear aspects of quantum plasma physics." *Physics-Uspekhi* **53**, 51-76 (2010) DOI: 10.3367/UFNe.0180.201001b.0055

[34] J.A. Gaffney *et al.* "A Review of Equation-of-State Models for Inertial Confinement Fusion Materials." *High Energy Density Physics* **28**, 7-24 (2018) DOI: 10.1016/j.hedp.2018.08.001

[35] J.J. Lissauer, D.C. Fabrycky, E.B. Ford *et al.* "A closely packed system of low-mass, low-density planets transiting Kepler-11." *Nature* **470**(7332):53-58 (2011) DOI: 10.1038/nature09760

[36] J.N. Bahcall, W.F. Huebner, S.H. Lubow, P.D. Parker and R.K. Ulrich, "Standard solar models and the uncertainties in predicted capture rates of solar neutrinos." *Rev.Mod. Phys.* **54**, 767-799 (1982) DOI: 10.1103/RevModPhys.54.767

[37] T. Nagayama, J.E. Bailey, G.P. Loisel *et al.* "Systematic Study of L-Shell Opacity at Stellar Interior Temperatures." *Phys Rev Lett* **122**(23):235001 (2019) DOI: 10.1103/PhysRevLett.122.235001

[38] S.M. Vinko, O. Ciricosta, B.I. Cho *et al.* "Creation and diagnosis of a solid-density plasma with an X-ray free-electron laser." *Nature* **482**, 59-62 (2012) DOI: 10.1038/nature10746

[39] O. Ciricosta *et al.* "Direct Measurements of the Ionization Potential Depression in a Dense Plasma." *Phys. Rev. Lett.* **109**, 065002 (2012) DOI: 10.1103/PhysRevLett.109.065002

[40] S.M. Vinko, O. Ciricosta and J.S. Wark, "Density functional theory calculations of continuum lowering in strongly coupled plasmas." *Nat Commun* **5**, 3533 (2014) DOI: 10.1038/ncomms4533

[41] O. Ciricosta, S. Vinko, B. Barbrel *et al.* "Measurements of continuum lowering in solid-density plasmas created from elements and compounds." *Nat Commun* **7**, 11713 (2016) DOI: 10.1038/ncomms11713

[42] P. Emma, R. Akre, J. Arthur *et al.* "First lasing and operation of an ångstrom-wavelength free-electron laser." *Nature Photon* **4**, 641-647 (2010) DOI: 10.1038/nphoton.2010.176

[43] A. Lévy *et al.* "The creation of large-volume, gradient-free warm dense matter with an X-ray free-electron laser." *Phys. Plasmas* **22**, 030703 (2015) DOI: 10.1063/1.4916103

[44] O. Ciricosta *et al.* "Detailed model for hot-dense aluminum plasmas generated by an X-ray free electron laser." *Phys. Plasmas* **23**, 022707 (2016) DOI: 10.1063/1.4942540

[45] S.M. Vinko, O. Ciricosta, T. Preston *et al.* "Investigation of femtosecond collisional ionization rates in a solid-density aluminium plasma." *Nat Commun* **6**, 6397 (2015) DOI: 10.1038/ncomms7397

[46] Q.Y. van den Berg, E.V. Fernandez-Tello, T. Burian *et al.* "Clocking Femtosecond Collisional Dynamics via Resonant X-Ray Spectroscopy." *Phys Rev Lett* **120**(5):055002 (2018) DOI: 10.1103/PhysRevLett.120.055002

[47] T.R. Preston, S.M. Vinko, O. Ciricosta *et al.* "Measurements of the K-Shell Opacity of a Solid-Density Magnesium Plasma Heated by an X-Ray Free-Electron Laser." *Phys Rev Lett* **119**(8):085001 (2017) DOI: 10.1103/PhysRevLett.119.085001

[48] P. Hollebon, O. Ciricosta, M.P. Desjarlais *et al.* "Ab initio simulations and measurements of the free-free opacity in aluminum." *Phys Rev E* **100**(4-1):043207 (2019) DOI: 10.1103/PhysRevE.100.043207

[49] L.B. Fletcher, H. Lee, T. Döppner *et al.* "Ultrabright X-ray laser scattering for dynamic warm dense matter physics." *Nature Photon* **9**, 274-279 (2015) DOI: 10.1038/nphoton.2015.41

[50] D. Kraus, D.A. Chapman, A.L. Kritcher *et al.* "X-ray scattering measurements on imploding CH spheres at the National Ignition Facility." *Phys Rev E* **94**(1-1): 011202 (2016) DOI: 10.1103/PhysRevE.94.011202

[51] R.R. Faustlin *et al.* "Observation of ultrafast nonequilibrium collective dynamics in warm dense hydrogen." *Phys Rev Lett* **104**, 125002 (2010) DOI: 10.1103/PhysRevLett.104.125002

[52] P. Sperling, E.J. Gamboa, H.J. Lee *et al.* "Free-electron X-ray laser measurements of collisional-damped plasmons in isochorically heated warm dense matter." *Phys Rev Lett* **115**, 115001 (2015) DOI: 10.1103/PhysRevLett.115.115001

[53] G.O. Williams *et al.* "Tracking the ultrafast XUV optical properties of X-ray free-electron-laser heated matter with high-order harmonics." *Phys Rev A* **97**, 023414 (2018) DOI: 10.1103/PhysRevA.97.023414

[54] L.B. Fletcher *et al.* "X-ray Thomson scattering measurements of temperature and density from multi-shocked CH capsules." *Phys. Plasmas* **20**, 056316 (2013) DOI: 10.1063/1.4807032

[55] L.B. Fletcher *et al.* "Observations of continuum depression in warm dense matter with X-ray Thomson scattering." *Phys Rev Lett* **112**, 145004 (2014) DOI: 10.1103/PhysRevLett.112.145004

[56] D. Kraus *et al.* "Characterizing the ionization potential depression in dense carbon plasmas with high-precision spectrally resolved X-ray scattering." *Plasma Phys. Control. Fusion* **61** 014015 (2019) DOI: 10.1088/1361-6587/aadd6c

[57] S. Kneip, C. McGuffey, J. Martins *et al.* "Bright spatially coherent synchrotron X-rays from a table-

top source." *Nature Phys* **6**, 980-983 (2010) DOI: 10.1038/nphys1789

[58] N.D. Powers, I. Ghebregziabher, G. Golovin *et al.* "Quasi-monoenergetic and tunable X-rays from a laser-driven Compton light source." *Nature Photon* **8**, 28-31 (2014) DOI: 10.1038/nphoton.2013.314

[59] K. Khrennikov *et al.* "Tunable all-optical quasi-monochromatic thomson X-ray source in the nonlinear regime." *Phys Rev Lett* **114**, 195003 (2015) DOI: 10.1103/PhysRevLett.114.195003

[60] A. Döpp *et al.* "An all-optical Compton source for single-exposure X-ray imaging." *Plasma Phys. Control. Fusion* **58** 034005 (2016) DOI: 10.1088/0741-3335/58/3/034005

[61] A. Döpp *et al.* "An all-optical Compton source for single-exposure X-ray imaging." *Plasma Phys. Control. Fusion* **58** 034005 (2016) DOI: 10.1088/0741-3335/58/3/034005

[62] N. D. Powers *et al*., "*Quasi-monoenergetic and tunable X-rays from a laser-driven Compton light source*", Nature Photonics **8**, 28 (2013) DOI: 10.1038/nphoton.2013.314

[63] F. Albert, "Applications of Light Sources Driven by Laser-Wakefield Acceleration", presented at the 9th Int. Particle Accelerator Conf. (IPAC'18), Vancouver, BC, Canada (2018)

[64] B. Kettle. E. Gerstmayr, M.J.V. Streeter *et al.* "Single-Shot Multi-keV X-Ray Absorption Spectroscopy Using an Ultrashort Laser-Wakefield Accelerator Source." *Phys Rev Lett* **123**(25):254801 (2019) DOI: 10.1103/PhysRevLett.123.254801

[65] B. Mahieu, N. Jourdain, K. Ta Phuoc *et al.* "Probing warm dense matter using femtosecond X-ray absorption spectroscopy with a laser-produced betatron source." *Nat Commun* **9**, 3276 (2018) DOI: 10.1038/s41467-018-05791-4

[66] M. Balcazar *et al.* "Multi-messenger dynamic imaging of laser-driven shocks in water using a plasma wakefield accelerator." (2025) Preprint (Version 1) DOI: 10.21203/rs.3.rs-5811311/v1

[67] R. Pompili et al. "Free-electron lasing with compact beam-driven plasma wakefield accelerator." *Nature* **605**, 659 (2022) DOI: 10.1038/s41586-022-04589-1

[68] W. Wang et al. "Free-electron lasing at 27 nanometres based on a laser Wakefield accelerator." *Nature* **595**, 516 (2021) DOI: 10.1038/s41586-021-03678-x

[69] M. Labat et al. "Seeded free-electron laser driven by a compact laser plasma accelerator." *Nat Photonics* **17**, 150 (2023) DOI: 10.1038/s41566-022-01104-w

[70] A. Macchi, M. Borghesi and M. Passoni, "Ion acceleration by superintense laser-plasma interaction. " *Rev. Mod Phys*. **85**, 751-793 (2013) DOI: 10.1103/RevModPhys.85.751

[71] T. Ziegler, I. Göthel, S. Assenbaum *et al.* "Laser-driven high-energy proton beams from cascaded acceleration regimes." *Nat. Phys.* **20**, 1211–1216 (2024) DOI: 10.1038/s41567-024-02505-0; Y. Shou, X. Wu, K.H. Pae *et al.* "Laser-driven proton acceleration beyond 100 MeV by radiation pressure and Coulomb repulsion in a conduction-restricted plasma." *Nat Commun* **16**, 1487 (2025) DOI: 10.1038/s41467-025-56667-3

[72] B. Lahmann *et al.* "Measuring stopping power in warm dense matter plasmas at OMEGA." *Plasma Phys. Control. Fusion* **65** 095002 (2023) DOI: 10.1088/1361-6587/ace4f2

[73] G. Breit and J.A. Wheeler, "Collision of two light quanta." *Phys. Rev.* **46**, 1087 (1934) DOI: 10.1103/PhysRev.46.1087

[74] R.J. Gould and G.P. Schréder, "Pair production in photon-photon collisions." *Phys. Rev.* **155**, 1404-1407 (1967) DOI: 10.1103/PhysRev.155.1404

[75] M. Meyer, D. Horns and M. Raue, "First lower limits on the photon-axion-like particle coupling from very high energy gamma-ray observations." *Phys Rev D* **87**, 035027 (2013) DOI: 10.1103/PhysRevD.87.035027

[76] M. Aaboud, G. Aad, B. Abbott *et al*. ATLAS Collaboration, "Evidence for light-by-light scattering in heavy-ion collisions with the ATLAS detector at the LHC." *Nature Phys* **13**, 852-858 (2017) DOI: 10.1038/nphys4208

[77] R. Svensson and A. Zdziarski, "Photon-photon scattering of gamma rays at cosmological distances." *The Astrophysical Journal* **349**:415-428 (1990) DOI: 10.1086/168325

[78] T. Yamaji *et al.* "An experiment of X-ray photon–photon elastic scattering with a Laue-case beam collider." *Phys. Lett. B* **763**, 454-457 (2016) DOI: 10.1016/j.physletb.2016.11.003

[79] G. Sarri, K. Poder, J. Cole *et al.* "Generation of neutral and high-density electron-positron pair plasmas in the laboratory." *Nat Commun* **6**, 6747 (2015) DOI: 10.1038/ncomms7747

[80] K. Ta Phuoc, S. Corde, C. Thaury *et al.* All-optical Compton gamma-ray source. *Nature Photonics* **6**, 308-311 (2012) DOI: 10.1038/nphoton.2012.82

[81] M. Mirzaie, C.I. Hojbota, D.Y. Kim *et al.* "All-optical nonlinear Compton scattering performed with a multi-petawatt laser." *Nat. Photon.* **18**, 1212–1217 (2024) DOI: 10.1038/s41566-024-01550-8

[82] J. Nuckolls, L. Wood, A. Thiessen and G. Zimmerman, "Laser Compression of Matter to Super-High Densities: Thermonuclear (CTR) Applications." *Nature* **239**, 139-142 (1972) DOI: 10.1038/239139a0

[83] R.S. Craxton *et al.* "Direct-drive inertial confinement fusion: A review." *Physics of Plasmas* **22**, 110501 (2015) DOI: 10.1063/1.4934714

[84] V. Gopalaswamy, R. Betti, J.P. Knauer *et al.* "Tripled yield in direct-drive laser fusion through statistical modelling." *Nature* **565**, 581-586 (2019) DOI: 10.1038/s41586-019-0877-0

[85] https://dipolesystems.com/

5. Science Opportunities in Condensed Matter, Quantum and Nanomaterials

Condensed matter is at the core of modern physics, materials and technology. Already XFELs have demonstrated their capability to advance the field by revealing critical structural dynamics. Nowhere is this more apparent than with quantum and nanomaterials, which represent an exciting class of materials that contain fascinating new physics and have the potential to enable disruptive technologies for devices and in energy applications.

Quantum and nanomaterials have significant potential to deliver a wide range of new technologies. These materials can show drastically different behaviours – such as high temperature super-conductivity, exotic magnetism and high-speed phase transitions – from what is found in the more 'regular' materials that form the backbone of current technologies. However, one of the main challenges in fully exploiting their potential is that there is no clear consensus on why they possess the properties they do and how they can be exploited fully. XFELs have the potential to provide a transformational improvement in understanding how, and why, quantum and nanomaterials can be manipulated to induce advantageous new properties, shining light on new physics and deepening our understanding of how materials function.

Completely new approaches to how we measure materials can be brought about with XFELs. To date, Materials Physics has been dominated by the Fourier-domain. Material properties are measured as a function of frequency and momentum. Temporal and spatial dependences are inferred through Fourier inversion. This can be challenging, as most measurements lack the phase information, particularly in the X-ray regime, which generally hinders the inversion process. While this problem is particularly acute for real space imaging, the phase information can be vital for understanding the response of materials, particularly those that are not theoretically well understood.

Short pulse XFELs will allow us to make a breakthrough in this direction and measure materials in space and time. The high time-resolution and high-brightness of XFELs will allow us to capture fluctuations "in the act". For example, high temperature superconductivity emerges from a "strange metal" phase, where fluctuations between competing phases are believed to play a critical role in the material properties. Basic questions, such as whether these fluctuations compete against each other or enhance each other to determine the materials properties, are still unanswered. A real space and time approach will allow us to see if these fluctuations occur in the same regions of the sample and at the same time, or if they are pinned to specific defects and are essentially different processes – a property which is notoriously difficult to separate from the Fourier domain.

As well as answering existing questions, a time-domain approach will likely yield new opportunities. Most spectroscopic approaches measure two-body correlation functions. Intense and coherent laser-like XFELs may enable higher order correlation functions to be measured, which are vital for understanding spin-entanglement and the quantum properties of partially ordered spin phases. Fluctuations associated with quantum critical points could also be captured in "diffract-and-destroy" types of experiments, where conventional X-ray pulses would result in sample heating, moving the system away from the regime of quantum fluctuations.

In this section, we provide an overview of the major themes and opportunities provided by XFEL science in quantum and nanomaterials, with a summary of key experimental requirements.

5.1 Magnetic materials and control of ultrafast magnetisation

Ultrafast photo-excitation of quantum materials that exhibit intricate coupling between charge, spin and orbital degrees of freedom holds great promise for understanding and controlling the properties of non-equilibrium and hidden states. Here we discuss the state-of-the-art and introduce time-resolved resonant inelastic X-ray scattering (trRIXS) as a means of measuring charge, spin and orbital excitations. These excitations encode the correlations and interactions that determine the detailed properties of the generated states and may advance the technology of, for instance, fast, energy-efficient data storage.

5.1.1 Introduction to magnetic dynamics measured with FELs

Magnetism has fascinated mankind since its discovery over two thousand five hundred years ago. Although magnetic fields can be conceptualised using classical physics, the existence of magnetic materials can only be understood in terms of the fundamentally quantum mechanical nature of the world around us. Our ability to manipulate magnetism via ultrafast laser excitation has therefore attracted considerable excitement within the scientific community. In terms of applications, ultrafast magnetism provides routes to fast switching of electronic devices, which often store information in different magnetic states.[1] From a more fundamental point of view, ultrafast magnetism addresses the questions:

- What are the fundamental principles governing the interactions of photons with matter?[2]
- Can we use ultrafast excitations to generate magnetic states that are inaccessible in equilibrium?[3]

Magnetic or spin degrees of freedom are also intimately tied to many of the most interesting emergent electronic properties of materials, such as high temperature superconductivity quantum spin liquids, and colossal magnetoresistance.[4,5,6] Understanding quantum magnetism is therefore important to nascent efforts to realise and manipulate such states transiently.

Our current understanding of ultrafast magnetism tends to be based on simple magnetic order parameter ideas, of which the so-called three-temperature model is the most popular.[7] This involves defining effective temperatures for the lattice, electrons and spins, and constructing a phenomenological picture based on rates of energy-exchange between these degrees of freedom. This can, for example, capture the common phenomenology of a magnetic order being suppressed by high-fluence, high-energy optical pulses before it recovers slowly. This theoretical approach is rather natural in terms of the common tools for characterising transient magnetism, which are benchtop optical experiments that measure the net ferromagnetic order parameter using the Faraday or magneto-optical Kerr effects. Since most experiments measure simple order parameter dynamics, there is limited information and motivation to develop more sophisticated theories.

Working within this paradigm is, however, very limited, as it is most appropriate for states that are similar to those that are accessible via equilibrium thermal heating. This paradigm excludes many of the most interesting ideas such as magnetic switching,[8] generating transient superconductivity,[9] realising topological lattice or electronic structures[10,11] or rotating spin with terahertz or mid-infrared excitation.[12,13,14]

5.1.2 State-of-the-art in probing magnetic dynamics

Despite the increasing sophistication of table-top probes of magnetism, the information extracted tends to be held-back by the low energy of the beams. The wavelength of optical light is far longer than the atomic spacing and the length scales usually relevant to magnetism, meaning that a lot of the details of transient magnetic states are inaccessible to such experiments. This is perhaps the primary

reason why optical experiments tend to probe the net ferromagnetic order parameters. Using X-rays provides a direct way to access length scale-dependent properties and a more complete description. The most obvious way to do so is by studying spatially modulated states such as antiferromagnetism, orbital order or charge density waves.[15–19] These states have staggered order parameter as a function of position in the crystal lattice, which average to zero in spatially integrating probes.

Standard X-ray scattering with arbitrary X-ray energies interacts primarily via the Thompson cross-section and probes the atomic structure of the material. Resonant X-ray scattering, as illustrated in **Figure 5.1**, involves tuning the X-ray energy to excite a core hole resonance. This provides a means to couple X-rays to magnetic and orbital degrees of freedom and probe electronic order. Experiments where the momentum-dependence of the scattering is measured – so-called resonant diffraction – can probe electronic order parameters such as magnetic, charge, or orbital order. Going further, one can resolve both the energy and momentum change in the scattering process, which allows one to track the momentum-dependent dispersion of different electronic quasiparticles: this method is called resonant inelastic X-ray scattering or RIXS.[20] These quasiparticles encode the interactions that drive the novel electronic phases present in quantum materials and thus represents a powerful way to solve key problems in this major area of condensed matter physics.

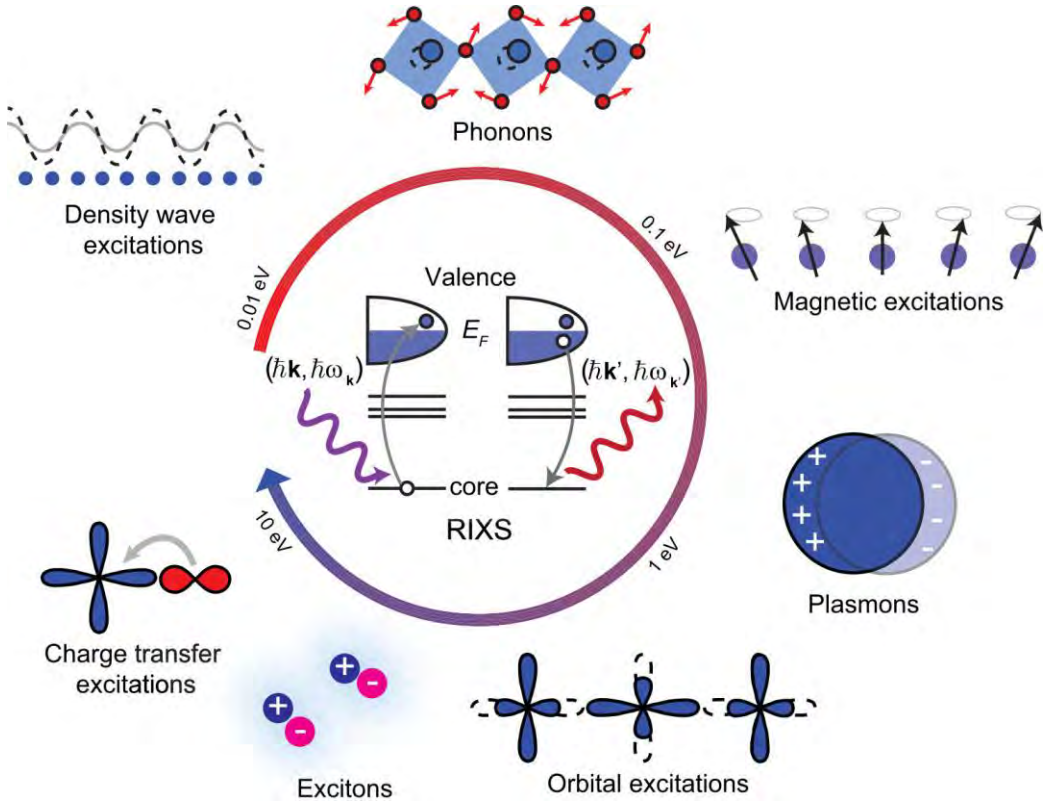


Figure 5.1: The resonant scattering process, shown in the centre, involves the resonant absorption of an X-ray photon, creating an intermediate state with a core hole and a valence excitation, before the hole is filled via the emission of another X-ray photon. Measuring the momentum-change of the scattering, in a so-called resonant diffraction experiment, can probe electronic order parameters such as magnetic order. By measuring the energy and momentum change of the X rays in a resonant inelastic X-ray scattering (RIXS) experiment, one can infer the properties of the excitations created in the material. The many different types of excitation that RIXS can probe are shown around the outside.[6]

Image reprinted with permission from Physical Review Journals: Image from M. Mitrano et al., Phys. Rev. X 14, 040501 (2024). DOI: 10.1103/PhysRevX.14.040501

Another important class of experiments probe the statistical distribution of magnetism with X-rays.[8,21,22,23] If one measures a ferromagnet with a characteristic domain size using X-ray resonant magnetic scattering, the diffraction pattern will be azimuthally symmetric, with a peak that reflects the

inverse domain size as seen in **Figure 5.2** (left).[8] Previous experiments have applied this approach at XFELs in order to probe magnetism, and have shown unique capabilities for separately probing different magnetic species at different length-scales.[8,21-23]

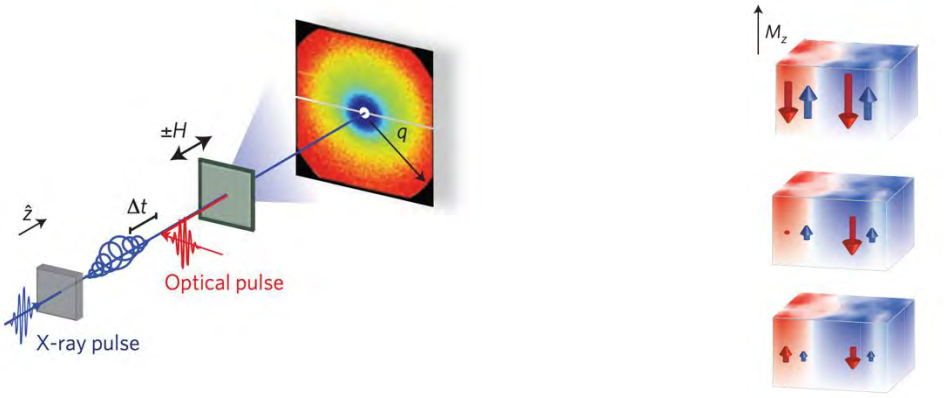


Figure 5.2: Magnetic domain dynamics. Left the experimental setup for magnetic diffraction from domains. Right an illustration of the evolution of iron and gadolinium moments out of equilibrium. [8]

Reprinted by permission from Springer Nature: C Graves et al. Nature Mater. ***12****, 293-298 (2013)*
DOI: 10.1038/nmat3597 Copyright (2013)

5.1.3 Future opportunities in magnetic dynamics

We identify three main categories of new experiments. The first involves more sophisticated and high time-resolution pump schemes, such as THz or mid-infrared excitation. This lower energy photo-excitation can couple more directly to magnetism or drive phonon modes in order to realise novel electronic states. Dedicated instrumentation for the pump and probe is highly desirable here, as the X-ray element of the experiment needs to be implemented in a more stable and straightforward way to allow more challenging photo-excitation schemes.

A very appealing but underexplored area is performing XFEL experiments in the perturbative regime, in which the ground state is only slightly disturbed and small changes are seen in the magnetic state. In this limit, the sample response can reflect the equilibrium dynamical susceptibility and coupling between different degrees of freedom. This scheme has been compellingly employed to provide parameter-free determination of electron-phonon coupling via the measurement of crystal structure and electronic band-structure after photo-excitation.[24] To the knowledge of the authors, this has not yet been applied to XFEL experiments of magnetism. Experiments involving small changes are especially well-suited to high-repetition-rate XFEL sources, as high average flux is needed to measure small changes in a weak magnetic order parameter signal.

Another area is the prospect of performing spectroscopy of collective excitations in transient states. Collective excitations encode key details about the interactions and short-range correlations in transient states. Time-resolved RIXS, as illustrated in **Figure 5.3**, has recently emerged as a practical means to probe such correlations and has measured magnons in photo-excited iridates.[17,25,26] Such a spectroscopy could answer some of the most profound questions, such as:

- How can we modify different components of the magnetic exchange on ultrafast timescales?
- Can we soften different components of the magnetic excitation spectra in order to transiently stabilise different magnetic ground states?
- How can we realise new quantum phases beyond those that can exist at equilibrium?[6]

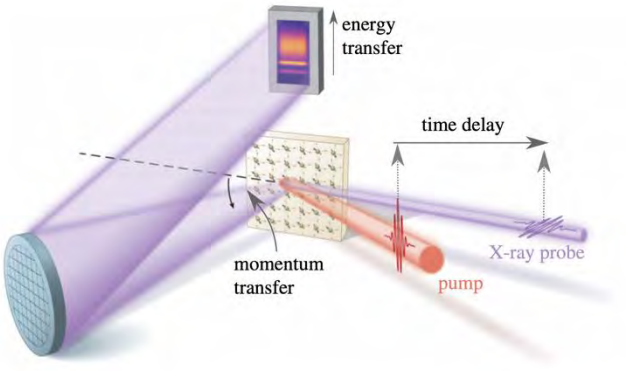


Figure 5.3: Time-resolved RIXS as recently realised in [17,25,27]. The momentum transfer is determined by the angle between the incident and scattered X-rays from the sample, along with the wavelength of the X-ray. The energy of the scattered photons is resolved by dispersing the X-rays with a grating or crystal analyser onto a two-dimensional detector. In tr-RIXS, a second pump laser pulse is used which arrives at a controllable time ahead of the incident X-rays.

*Figure reproduced from Y. Cao et al. "Ultrafast dynamics of spin and orbital correlations in quantum materials: an energy- and momentum-resolved perspective", Phil. Trans. R. Soc. A. **377** 20170480 (2019) DOI: 10.1098/rsta.2017.0480*

An XFEL with a dedicated spectrometer for such experiments would provide unique opportunities to help understand transient magnetism. In judging this progress, it is useful to consider that a typical order-of-magnitude temperature scale for phase transitions in many quantum materials is T ~ 100 K, which corresponds to an energy scale of k_BT ~ 10 meV and a timescale of $\hbar/k_BT$ ~ 100 fs (where kB is Boltzmann's constant). A key reason why RIXS is increasingly influential in the field of quantum materials is that its resolution is now approaching this important threshold. It is also important to perform experiments with adequate momentum resolution. However, since the typical quasiparticles have a dispersion over length-scale comparable to the unit cell, it is easily possible to achieve adequate momentum resolution for the vast majority of important problems. Illustrating the excitement in this area, several facilities (including the European XFEL, LCLS, SwissFEL, and SHINE) have active projects targeting high energy resolution RIXS of quantum materials. Breakthrough results, such as the observation of new non-equilibrium quantum states stabilised by the laser-modification of electronic hopping and laser-based tuning of hybridisation, are currently under submission in this nascent field.[28]

Looking to the future, the ability of XFELs to deliver multiple, phase-coherent pulses with controllable delay will facilitate new forms of higher-order spectroscopy. This would involve applying two (or more) phase coherent pump pulses prior to the probe pulse and corresponds to measuring a "three-point correlation function", as distinct from the "two-point correlation function" commonly measured by inelastic neutron scattering, inelastic X-ray scattering or, more recently, time-domain Fourier transform inelastic X-ray scattering at XFELs.[27] These correlation functions have direct signatures of fractional spin quasiparticles, such as Majorana fermions and fluxes,[29] which hold promise for realising robust quantum computers. This is in contrast to two-point correlation functions that can only couple to pairs of fractional excitations, leading to a broad continuum in energy. Such innovations have the potential to solve the decades-long quest to discover the quantum-correlations underlying putative spin liquid phases.[30]

5.2 Structural dynamics and light induced phases in quantum materials

The transient modification of structure in quantum materials by femtosecond pulses of laser light can induce new properties that do not appear in equilibrium. Coupling with an ultrafast X-ray probe can provide unprecedented insight into how electrons, phonons and spins interact to determine the properties of materials, such as magnetism, insulator-metal transitions and superconductivity. Here we discuss how light can be used to manipulate these interactions effectively and efficiently, in order to control material properties.

5.2.1 Introduction to the structural dynamics measured with FELs

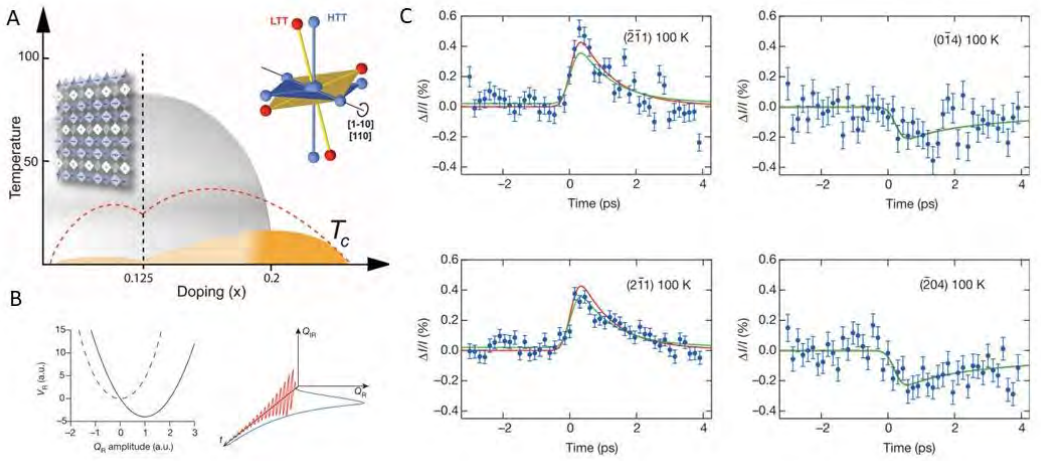
The atomic structure of quantum materials has a profound effect on the material's electronic and magnetic properties. Understanding the connection between the underlying atomic structure and the resulting functionality of the material is one of the key challenges in the physics of quantum materials. In many quantum materials, small – picometre – atomic displacements can result in materials with vastly different properties. These displacements are capable of changing a magnetic insulator into a metal or even a superconductor. The sensitivity to distortions represents significant challenges to understand quantum materials, as they intrinsically require highly accurate and precise measurements and theories[31] in order to accurately capture and characterise the subtle structural changes. However, this sensitivity also presents new opportunities for control. As only small atomic displacements are required to induce new electronic and magnetic properties, intense light pulses can distort the crystal structure of the lattice. This has led to a new field with the aim of controlling the properties of quantum materials "on demand".[4]

Several experiments have shown that light can transiently modify the structure of materials to induce new properties that do not appear in equilibrium in the host material. Light tuned to a structural resonance in order to shake specific bonds has been shown to induce insulator-metal,[32] magnetic[33] and superconducting[9] transitions. FELs are now enabling a step-change in our understanding of lattice dynamics, as they can probe the structural changes directly, capturing snapshots of the atomic configuration as it changes in real time (see **Box 5.1**).

FELs allow us to start looking at a new range of questions in quantum materials. Charge density wave instabilities are found in a whole range of quantum materials. The fluctuations of the charge and lattice may compete with, or complement, superconductivity, but we have not yet been able to observe these lattice fluctuations in real space. Short pulse coherent diffraction from the lattice may open up new options to image these processes, allowing us for the first time to study quantum materials in real space and real time, while diffract-and-destroy experiments could capture structural distortions and fluctuations that arise from quantum fluctuations at low temperatures, which are inaccessible to X-rays at the moment due to beam heating effects.

The new information obtained from FELs will enable completely new insights into both how small atomic displacements alter the functionality of quantum materials, and how light can manipulate these changes, which ultimately could lead to new paradigms in both our theoretical understanding of quantum materials and in future devices that can exploit the dynamic control of the material's phase.

Box 5.1: Light control of material properties



Light resonant to structural modes in quantum materials can be used to control the properties they exhibit. Some quantum materials exhibit high temperature superconductivity, but in others this can be suppressed due to a structural distortion (A). By using light resonant to a structural mode, the atomic positions can be controlled through phonon mode coupling (B). Recently, this process has been observed at LCLS using time-resolved X-ray diffraction to provide the first evidence for mode coupling. (Part A taken from [9]; B and C from [37]).

***Figure A** reprinted by permission from American Association for the Advancement of Science: D. Fausti et al. Science **331**, 189-191 (2011). DOI: 10.1126/science.1197294 Copyright (2011). **Figures B & C** reprinted by permission from Springer Nature: R. Mankowsky et al. Nature **516**, 71-73 (2014). DOI: 10.1038/nature13875 Copyright (2014)*

5.2.2 Structural dynamics in quantum materials

While femtosecond X-ray sources have enabled the study of aspects of light-induced phase transitions in quantum materials for some time,[34] the advent of ultrafast and ultra-bright FEL laser pulses has transformed our understanding of ultrafast structural transitions. Correcting for the intrinsic timing jitter between X-rays and the exciting laser has been key for much of the progress. Real-time jitter correction can time-stamp each measurement with a precision of 6 fs,[35] which is sufficient to observe most structural motion. Initial measurements on light-induced phase transitions focused on exploiting the time-resolution of XFELs to study vibrational coherences induced by optical excitation through Bragg scattering.[36] More recent advances have been driven by combining Bragg scattering with new methods to control the lattice, specifically mid-IR[37] and THz[38] excitation. By combining state-of-the-art X-ray sources with state-of-the-art laser-based methods to excite the system, new insights into how below-gap light can coherently modify the structures of materials is emerging and enabling new states of materials to form.

In addition to the advances that come from combining advanced pumping techniques with femtosecond X-rays, new techniques are beginning to emerge that can take advantage of the high photon flux. Phonons cause deviations from a perfect lattice by modulating the atomic structure on the length scale set by their wavelength. This transfers some scattered intensity from the 'ideal' Bragg peak into diffuse scattering between the peaks. As the phonon displacements are small, the intensity redistribution is weak and had been largely inaccessible to time-resolved studies. Ultra-bright XFELs, however, are intense enough to resolve this scattering with ease. Fourier Transform inelastic X-ray scattering[39] is a new technique that exploits this scattering to measure coherent phonon dynamics over the entire Brillouin zone for the first time (see **Figure 5.4 a**).[40] This time-domain approach is excellent for measuring low energy oscillations and sub-meV resolution phonon dynamics have already been reported,[40] making this technique competitive with inelastic X-ray scattering in terms of energy resolution.

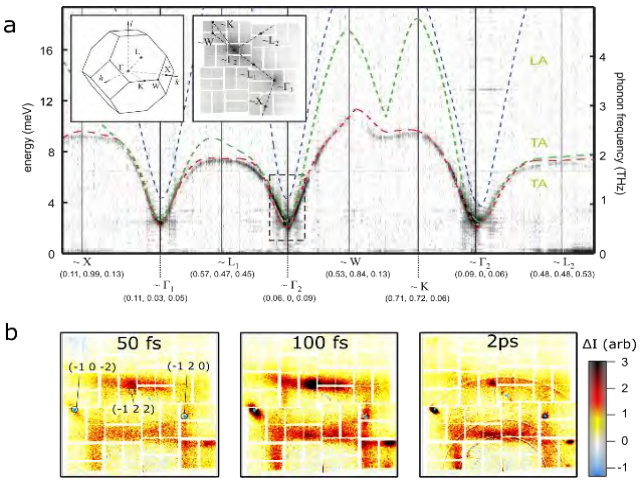


*Figure 5.4: Time-resolved diffuse X-ray scattering. **a** Fourier Transform inelastic X-ray scattering is now able to measure phonon dynamics in Ge throughout the entire Brillouin Zone with sub meV energy resolution.[40] **b** Time-resolved diffuse scattering changes during a structural phase transition in VO_2, showing that lattice disorder dominates at early timescales.[41]*

*Top image reprinted figure with permission from D. Zhu et al. Phys. Rev. B **92**, 054303 (2015), DOI: 10.1103/PhysRevB.92.054303.*
Copyright (2015) by the American Physical Society

*Bottom image reproduced from S. Wall et al. "Ultrafast disordering of vanadium dimers in photoexcited VO2", Science **362**, 6414 572-576 (2018) DOI: 10.1126/science.aau3873*

This technique can be used to examine how phonon populations change dynamically when the system is rapidly driven through a phase transition. This was performed for the first time on the prototypical quantum material VO_2 (**Figure 5.4 b**),[41] where it was observed that phonons are excited rapidly but incoherently throughout the entire Brillouin zone. This disorder-like process, only visible due to the high brightness and high momentum resolution of the FEL, overturned the previous description obtained from electron diffraction, that the transition was a coherent-like process resulting from well-defined regular atomic motions.[42] Further work has shown that there is a complex interaction between the photo-excited electrons and lattice that is not well captured by effective potential models based on elevated electronic temperature, and thus a greater understanding of the electron-phonon interaction will be needed to understand how material properties arise from non-equilibrium states.[43]

5.2.3 Future opportunities in structural dynamics

The study of structural dynamics and phase transitions with XFELs is rapidly developing. There are several directions in which future progress can be made, specifically combining state-of-the-art optical pump sources with the new probing techniques that are provided by short and intense X-ray pulses.

Recently, it was shown that light-induced phase transitions can be driven with a greater energy efficiency when multiple laser pulses are used. XFELs have been vital for understanding why this is the case. Ultrafast X-ray diffuse scattering measurements showed that local structural fluctuations, or polarons, are the reason for the improved efficiency.[44] Insight gained through the use of XFELs to probe light-induced polaronic phases can provide an opportunity to utilise local, as well as long-range, coherent distortions as a means of modifying the properties of quantum materials with greater energy efficiency. Future XFEL techniques, such as time-resolved PDF (see **Section 5.5**), will also become vital to understanding and optimising these processes.

In addition, interfaces and surfaces play a major role in determining the functionality of X-ray devices. X-rays typically penetrate deeply into materials and are less sensitive to surface effects, but the brightness of XFELs opens the opportunity to measure the X-ray scattering directly from the surface. The surface generates a form of scattering known as crystal truncation rods. Dedicated phase retrieval algorithms, such as Coherent Bragg Rod Analysis (COBRA), can then be used to reconstruct real-space images of the surface structure.[45] Given the intensity, brightness and coherence of XFELs it can be anticipated that the application of the COBRA technique will reveal depth-resolved dynamics in the material in the near future.

XFELs have many properties that make them the leading source for measuring the dynamics of quantum materials. X-rays have significantly higher q-resolution and the pulse durations can be an order of magnitude shorter than electron sources, which is a key competitor. These are crucial factors

for observing small and fast displacements but, most significantly, X-rays are insensitive to the mechanism used to excite the sample. X-rays are not directly perturbed by the pump pulse and only respond to the resulting changes in the material, whereas electrons are charged and can thus feel the electric field of the pump pulse during transit to the sample. This becomes particularly significant when the pump wavelength is increased, which increases the ponderomotive force applied on the electron beam.

There are, however, several technical drawbacks that X-rays face. In order to reconstruct a transient unit cell, i.e. to understand how the atoms re-arrange, at least as many Bragg peaks need to be measured as there are atoms in the unit cell, although this will only tell you the average motion, and more Bragg peaks are required to determine the Debye-Waller and disorder in the system. Quantum materials typically have tens of atoms in the unit cell, and thus many peaks need to be measured. MeV electron diffraction, for example, is ideal for this, as the high electron momentum makes it easy to measure 10s – 100s of Bragg peaks in a single geometry.

Currently, with X-rays we have to rotate the sample in order to access a sufficient number of Bragg peaks. While this is not a problem for static measurements, it introduces many challenges for dynamic measurements. Freely rotating samples while cooling and providing optical access have limited most experiments to temperatures above 100 K. In order to match pump and probe penetration depths, experiments must be performed in a near grazing geometry, which results in large spot sizes and limits the field strengths that can be reached. Furthermore, due to the large optical anisotropy of many quantum materials, rotating samples for X-ray diffraction can result in very different pumping configurations, which makes it challenging to compare results. There is an opportunity for the UK to leverage its expertise in cryogenics to design experimental stations that can access temperatures down to a few kelvin. As low temperature structural transitions are key to understanding quantum materials, this would put such effort in a world-leading position.

One way to overcome this limitation is a move to hard X-rays > 20 keV. If high quality free-standing samples can be obtained, a transmission Laue diffraction geometry would enable the measurement of multiple diffraction peaks in a single experimental geometry. These conditions are similar to those required for pair distributions measurements discussed in **Section 5.5**. This would also significantly simplify the experimental setup and cooling requirements, enabling much lower base temperatures to be reached than those achieved to date. Further benefits would arise from a ‘normal incident’ geometry, specifically high peak electric fields could be generated which could drive the sample into new regimes, while nanofocusing of the X-ray source could enable direct probing of macroscopic inhomogeneity.

While high repetition would be advantageous for experiments like time-resolved Fourier transform inelastic X-ray scattering, lower (kHz-rate) repetition rates can actually be advantageous. Free standing samples have poor thermal recovery and, if samples are in vacuum, repetition rates will have to be limited to kHz frequencies in order for the sample to be able to dissipate the heat. Experiments that aim to capture dynamic fluctuations, such as imaging real space CDW fluctuations, will potentially need to be measuring on a single shot basis.

5.2.4 Conclusions

From a structural point of view, a FEL with X-rays greater than 20 keV is highly desirable, as it would enable new experimental geometries that would generate much cleaner and more detailed information, with an option to access temperature ranges current machines cannot reach. The variable repetition rate capability of a next-generation XFEL will be advantageous; as while high repetition rates are sometimes beneficial, other experiments that are focused on low temperatures will need to work at reduced ~ kHz repetition rates, while experiments that are focused on imaging fluctuations are likely to work on a single shot basis.

5.3 Imaging dynamics in nanomaterials

The ability to directly image, in three-dimensions, time varying phenomena in nanoscale materials at the surface and in the bulk will greatly increase our understanding of how novel phases develop and how they influence the material properties. Coherent diffractive imaging (CDI) without lenses is a form of microscopy that can permit high resolution imaging, where the use of conventional optics is not feasible. When combined with ultrafast X-rays, time-resolved Bragg CDI provides a novel and robust means to image ordered material systems with sub-ångstrom sensitivity. Such insight will greatly aid our understanding of nanomaterials and will serve as a platform to develop next-generation materials and devices.

5.3.1 Introduction to nanomaterials imaging with XFELs

Nanomaterials are materials in which the defining characteristics of the material are size dependent. Technologies developed from nanomaterials are the subject of multidisciplinary research stemming from more traditional disciplines that routinely study the physical, chemical, biological, engineering and electronic aspects of materials. Nanomaterials have found use in a wide range of disciplines owing to their unique and often tuneable physical, chemical and biological properties, that often differ widely from the bulk material.[46]

When materials are reduced to the nanoscale, their behaviour is often very different from the bulk material due to quantum confinement effects and the increased surface-to-volume ratio that may result in behaviour that is dominated by surface properties.[47] It is for this reason that our ability to directly image materials in three-dimensions at the surface and in the bulk can greatly increase our understanding of how novel phases develop and influence the material properties. Progress in the study of nanomaterials will require tools to characterise the nanoscale structure in three-dimensions with atomic precision.

The dynamics of nanomaterials are governed by their quantum properties. Strong coupling between lattice, charge, spin and orbital degrees of freedom often gives rise to emergent behaviour and multi-functional properties.[48–51] Such materials are of great interest because the different properties may work together in uniquely different ways and lead to exciting new applications, if we could understand this better. For example, the coupling between magnetic spin and ferroelectric charge ordering can be utilised to develop magnetoelectronic devices where spin transport can be controlled electrically. This is advantageous for technological applications, including novel sensors and ultra-low power memory devices. As a result, there is a vibrant effort to understand the underlying mechanisms at work.[52,53,54]

Nanomaterials where degrees of freedom are strongly correlated can exhibit novel short-lived non-equilibrium phases that occur on the femtosecond timescale. They include light-induced superconductivity, terahertz-induced ferroelectricity and ultrafast solid-phase structural transformations.[9,55,56,57] Efforts to shed light on these hidden phases are further compounded by the limited theoretical framework that is able to adequately describe the spontaneous emergence of new phases of materials due to external excitation. In addition, few studies are dedicated to time-resolved measurements due to the limitations of adequate tools. For example, electron microscopes are able to resolve atomic scale features of sufficiently thin materials, but have poor time resolution.[58] In addition, femtosecond laser systems (excluding hard X-ray sources, treated here) have poor spatial resolution and cannot resolve atomic structural changes. The key to deciphering these phenomena lies in measuring time-dependent changes in the materials structure in three-dimensions. The ability to directly image these processes in three-dimensions at the surface and in the bulk will greatly increase our understanding of how the phase is initiated, how it proliferates and how it gives rise to emergent properties.

With the advent of fourth-generation XFEL facilities, it has become possible to study ultrafast structural dynamics in nanoscale materials for the first time.[59,60] This is enabled by the femtosecond coherent X-

ray pulses produced by the XFEL. Three-dimensional imaging at the surface and bulk of structural properties in nanoscale materials is made possible through lens-less imaging techniques, such as coherent X-ray imaging (CDI).[61] The following section provides an overview of the current state-of-the-art in imaging of dynamics in nanomaterials at XFEL facilities. Imaging of biological nano-materials is omitted and is instead treated in **Chapter 7**.

5.3.2 Ultrafast microscopy of nanomaterials

Traditional non-destructive methods for the study of nanomaterials, such as scanning electron microscopy (SEM), transmission electron microscopy (TEM), atomic force microscopy (AFM) and numerous spectroscopic techniques, can provide detailed information on the surface structure but do not directly probe the structure within the volume as a whole. Coherent diffraction imaging (CDI) is a powerful lens-less imaging technique for probing nanometre-sized crystalline materials with sub-ångstrom sensitivity. It is an attractive alternative to electron microscopy because of the better penetration of the electromagnetic waves in materials of interest, which are often less damaging to the sample than electrons.[61,62] There are a number of important variations on the conventional CDI method including forward scattering CDI, which is ideally performed on non-periodic structures, and Bragg Coherent X-ray diffraction Imaging (BCXDI).[63–66] Forward scattering CDI has found many uses, including serial crystallography and imaging extended objects (See **Sections 7.1** and **3.2**).

BCXDI is the reflection scattering variant of CDI.[62] BCXDI holds great promise for understanding transient phases in correlated nanomaterials (**Figure 5.5**). It is also largely non-destructive and provides structural information at the surface and throughout the bulk of a material. BCXDI was first applied to the study of gold nanocrystals.[63] Later it was shown that BCXDI also offers a means to determine in three-dimensions any structural changes due to strain, most likely to occur for nanocrystals that experience a structural distortion due to defects or external perturbation.[67]

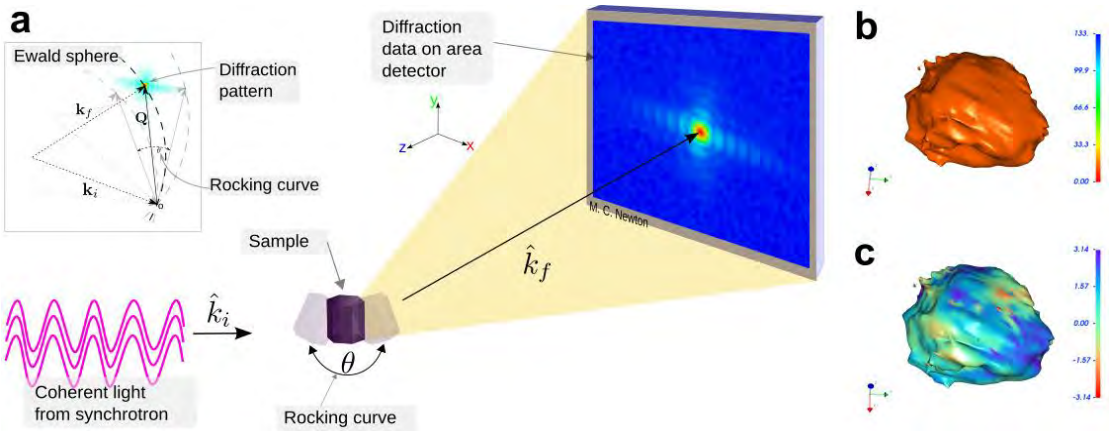


Figure 5.5: Illustration of the BCXDI imaging experiment. ***a:*** *Schematic of the BCXDI imaging experiment showing coherent X-ray illumination of a single perovskite bismuth ferrite nanocrystal in the Bragg geometry.[57] The inset illustrates Ewald sphere construction of the experimental geometry in reciprocal space.* ***b:*** *Reconstruction of the electron density amplitude of a single nanocrystal approximately 300 nm in length.* ***c:*** *Phase information shown at the surface of the nanocrystal in* ***b****.*

When coupled with an ultrafast coherent X-ray excitation source, BCXDI can be performed in a stroboscopic mode to provide time-resolved images in three-dimensions with nanometre resolution and ångstrom sensitivity. The spatial coherence of an XFEL beam ensures that BCXDI is feasible. The earliest example of time-resolved three dimensional imaging of nanomaterials was performed on gold nanocrystals at the LCLS.[68] By utilising femtosecond laser pulses to excite the nanomaterial, and femtosecond X-rays to probe in a 'pump-probe' experiment, it was possible to obtain three-dimensional images of the generation and subsequent evolution of coherent acoustic phonons on the picosecond timescale within a single gold nanocrystal, thus providing insights into the physics of the phenomenon (**Figure 5.6**). Further studies have focused on a broader range of materials systems such as ultrafast processes in complex transition metal-oxides.[57,69–71]

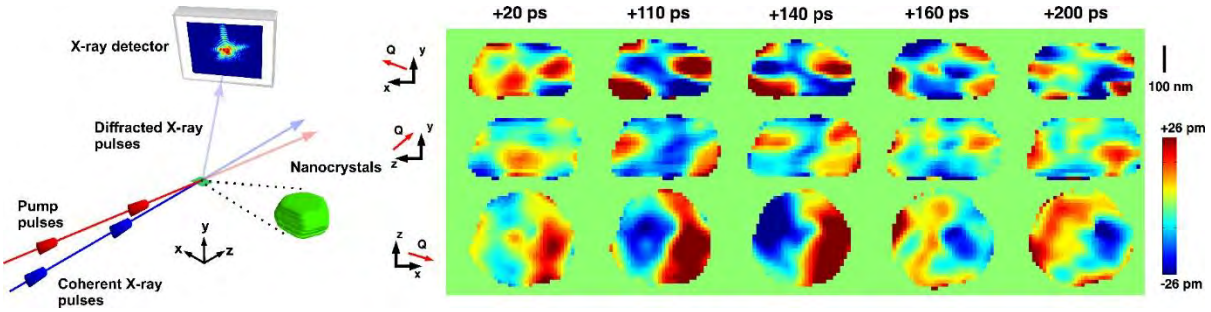


Figure 5.6: (Left) Schematic of the setup for ultrafast time resolved Bragg coherent diffraction imaging. Optical pulses (red) perturb the sample, generating phonons. Coherent X-ray pulses (generated from an XFEL) arrive a short time later where the diffracted pulses are recorded using an area detector. (Right) Imaging of acoustic phonons in a nanocrystal. Orthogonal cut planes through the nanocrystal showing the projected displacement as a function of delay time. For each delay time orthogonal slices taken from the centre of the nanocrystal are shown. The direction of the displacement field is given by the Q-vector in red.[68]

*Figure reprinted by permission from American Association for the Advancement of Science: J.N. Clark et al. Science **341**, 56–59 (2013). DOI: 10.1126/science.1236034 Copyright (2013)*

5.3.3 Future opportunities with XFELs

Ultrashort pulses of coherent X-ray beams hold the unique potential to record time-varying three-dimensional images of electronic, magnetic and crystalline structural properties in quantum materials on the nanoscale. The potential to image the inner workings of transient phenomena in and out of equilibrium including (multiferroic) phase-domain structures, dislocations, topological nanocrystals, strong-phase structures and structural phase transitions in three-dimensions will provide a potential route to solving long-standing problems that are driven by strong correlations. There remain a wide range of prototype quantum material systems that are not fully understood and yet lend themselves to XFEL experiments. These include multiferroic perovskite materials (e.g. $BiFeO_3$, $YMnO_3$, $La_xCa_{x-1}MnO_3$ (LCMO), $La_xSr_{x-1}FeO_3$ (LSFO), $La_xSr_{x-1}MnO_3$ (LSMO) and $PbVO_3$) for electronically mediated spin transport devices, structural phase change materials (e.g. $BaTiO_3$, VO_2) for femto-second ultrafast all optical switches, and ion diffusion in battery materials such as $LiCoO_2$.[34,57,72–74]

The remaining challenges for imaging quantum nanomaterial systems are two-fold. The first is the difficulty of measuring nanoscale materials using single extremely intense and short X-ray pulses before the onset of radiation damage (diffraction before destruction). For nanomaterials other than simple metals, this can pose a challenge when employed in a pump-probe measurement. The second is related to the ultimate resolution attainable by Bragg X-ray imaging methods, which is ~5 nm at present. Further development of XFEL facilities with increased X-ray brilliance will enable Bragg CDI methods to achieve atomic resolution and realise a long standing dream of an atomic-resolution X-ray microscope.[61,75] This would permit direct comparison of ab initio simulation with experiments and enable robust materials design with atomic precision.

5.3.4 Summary

The UK has significant strength in theoretical research into quantum materials and nanotechnology. There is also a strong global community in X-ray diffraction imaging techniques. For the UK's X-ray facilities to maintain world-class status, it is essential that important scientific questions are addressed and that emerging techniques, such as ultrafast CDI, are continuously developed and utilised. An XFEL that can reveal ultrafast processes that occur on the femtosecond timescale and beyond will prove an invaluable asset for the development of next-generation quantum technologies, and will provide world-leading ultrafast imaging of quantum materials.

5.4 Electronic dynamics in quantum materials

Ultrafast photoelectron spectroscopy (PES) is an enabling technique to provide insight into spin, orbital and charge degrees of freedom of chemical bonding characteristics in quantum materials. PES techniques combined with ultrafast X-rays will provide much needed answers to questions related to localised quantum state dynamic behaviour on the femto- and attosecond timescale, capturing electronic behaviour in real time.

5.4.1 Introduction

Correlating the structure and electronic structure of materials lies at the core of our understanding of functional materials. When moving from "regular" to quantum materials, we encounter a significant increase in complexity due to the particular nature and confinement of electronic states, e.g. at surfaces and interfaces. In many technologically relevant device systems, the overall electronic behaviour is dominated solely by interfaces rather than the surrounding extended structures. Even minute changes in the structure of a material can lead to significant differences in its electronic structure and the resulting electronic behaviour, determining whether a material is a metal, semimetal, semiconductor or insulator. The detailed nature of the electronic structure, including band structure, intrinsic and extrinsic charge carriers, and defect and trap states, is of great importance to the further development of future device generations.

To date, physical characterisation techniques have predominantly been confined to the study of the electronic structure in static, often bulk samples. Dynamic behaviour is often inferred by combining electrical measurements and physical characterisation at specific points that are "frozen in time". FELs provide an unmatched opportunity to study electronic structure dynamics in energy, space and time, providing a high level of understanding of quantum materials, which is essential to future application developments.

5.4.2 Background including earlier research at XFELs and by other methods

One of the key techniques used to study the electronic structure of matter is photoelectron spectroscopy (PES). Excitation sources from the UV to soft and hard X-rays are used to probe the occupied valence states and, in specific cases, occupied conduction states of materials including gases, liquids and solids. The technique is intrinsically referenced to the Fermi energy of the sample and can not only provide information on the chemical nature of bands in solids, but also on their overall alignment. The correlation of changes of the electronic structure of a material with both core level and valence spectra is immensely powerful to study local chemical environments, as well as the electron density and distribution of a system.

Standard PES is performed routinely in laboratories worldwide, but synchrotron sources are necessary for advanced studies. In particular, the probing of low occupation states, often vital to electronic behaviour, necessitates the high flux provided by synchrotrons to enable the detection of such low intensity features. In addition, the energy tunability of synchrotrons enables measurements under resonant conditions, and the associated discrimination between states of different orbital character enables the identification of specific contributions to the overall complex band structure. XFELs are expanding the dimensions that PES can explore from energy, space and spin to time, enabling multi-dimensional analysis of electronic structure dynamics.

The most important limitation for PES at FELs is the existence of vacuum space charge effects. The extremely brilliant FEL pulses can generate a dense cloud of photoelectrons at the sample surface and the Coulomb repulsion of the electrons leads to a strong distortion of the initial photoelectron energy distribution. This leads to shifting and overall broadening of spectra and therefore a loss in effective energy resolution. Both computational and experimental solutions to this challenge are being proposed, including amelioration by using very high repetition rate pulses of much lower intensity, and are at the core of current developments.[76–79]

A new area that XFELs have opened up is X-ray two-photon photoelectron spectroscopy (XTPPS). This technique exploits the femtosecond timescales provided at XFELs and follows the formation of single or two-site double core hole (ssDCH, tsDCH) states caused by the sequential absorption of two X-ray photons at a timescale matching the lifetime of Auger decay (below 10 fs). The DCH states have been shown to probe the local chemical environment more sensitively compared to single core hole (SCH) states, as they are directly coupled to any changes in valence electron structure of the two core hole atomic sites.[80–82] **Figure 5.7** shows a schematic of the different accessible core hole states. Access to this new regime in PES enables a detailed investigation of both core and valence structure of matter. XTPPS is developing rapidly, but is to date limited to molecular species.[83,84] Current and future developments towards its application to nano- and condensed matter systems will enable a new window into their electronic structure.

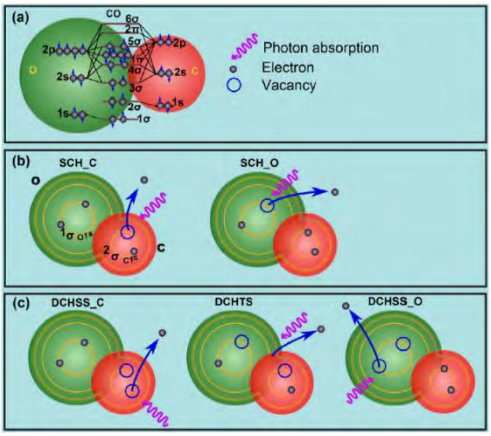


Figure 5.7: *Cartoon design of (a) the electronic structure of the CO molecule, (b) the SCH ionization at the C K-edge and the O K-edge, and (c) the ssDCH ionisation at the C K-edge, the ssDCH ionisation of the O K-edge and the tsDCH ionisation.* [85]

Figure reprinted from N. Berrah et al. Proc. Natl. Acad. Sci. USA. ***108****(41):16912-16915 (2011) DOI: 10.1073/pnas.1111380108*

Time-resolved PES (trPES) enables access to electronic state dynamics in quantum materials. To date, experiments have been performed using laboratory laser sources and synchrotrons[86,87] as well as XFELs.[76,88] Pioneering work by Hellmann and co-workers focused on understanding metal-insulator transitions, essential for so many electronic devices.[86,88,89] Their work focused on the Mott insulator 1*T*-TaS_2 and they successfully employed femtosecond time-resolved core-level photoelectron spectroscopy, as well as time-resolved angle-resolved PES (trARPES), to explore atomic-site specific charge-order dynamics of the charge-density wave and the relative contributions of electron-electron and electron-phonon interactions to electronic order in momentum space. **Figure 5.8** shows time-resolved ARPES spectra of a range of layered compounds.

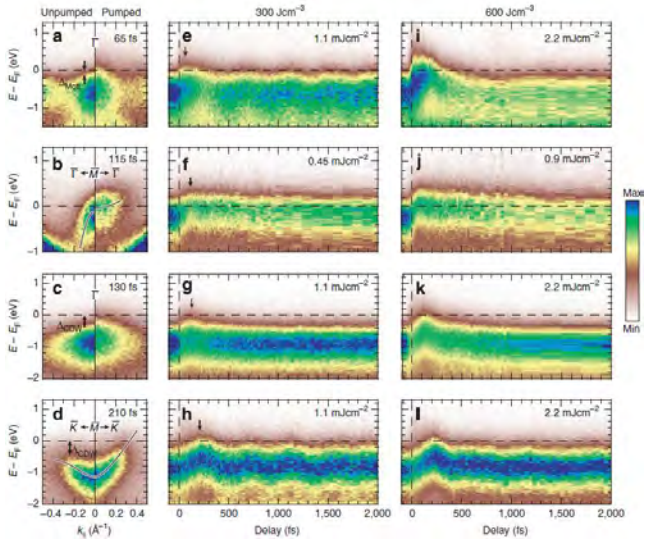


Figure 5.8: Time-resolved momentum-space view of the electronic structure in layered charge-density-wave compounds, including 1T-TaS_2, 1T-$TiSe_2$, and 1T-TaS_2.[86]*.*

Reprinted by permission from Springer Nature: S. Hellmann et al. Nat. Commun. ***3****, 1069 (2012). DOI: 10.1038/ncomms2078 Copyright (2012)*

Beyond soft X-ray PES, there has been considerable development of time-resolved hard X-ray PES (trHAXPES) setups and experiments in recent years.[90–92] The main advantage of HAXPES over XPS is the significant increase in probing depth, enabling the exploration of bulk systems and buried layers and interfaces, often crucial to material behaviour in a device context. Oloff and co-workers demonstrated that it is possible to resolve intrinsic charge-carrier recombination dynamics in electron-doped $SrTiO_3$, establishing trHAXPES as a well-placed technique to study intrinsic charge-carrier dynamics on ultrafast timescales.[91]

Recent work by Kutnyakhov and co-workers has laid the foundation for multi-dimensional PES using time-of-flight momentum microscopy (ToF-MM),[78] with the setup at FLASH that combines full-field momentum imaging and time-of-flight energy recording. Development and application of ToF-MM continue at pace,[93–96] enabling time-resolved experiments ranging from core-level to valence-band spectroscopy and photoelectron diffraction, exploiting the tunability of the photon energy to access varying probing depths.

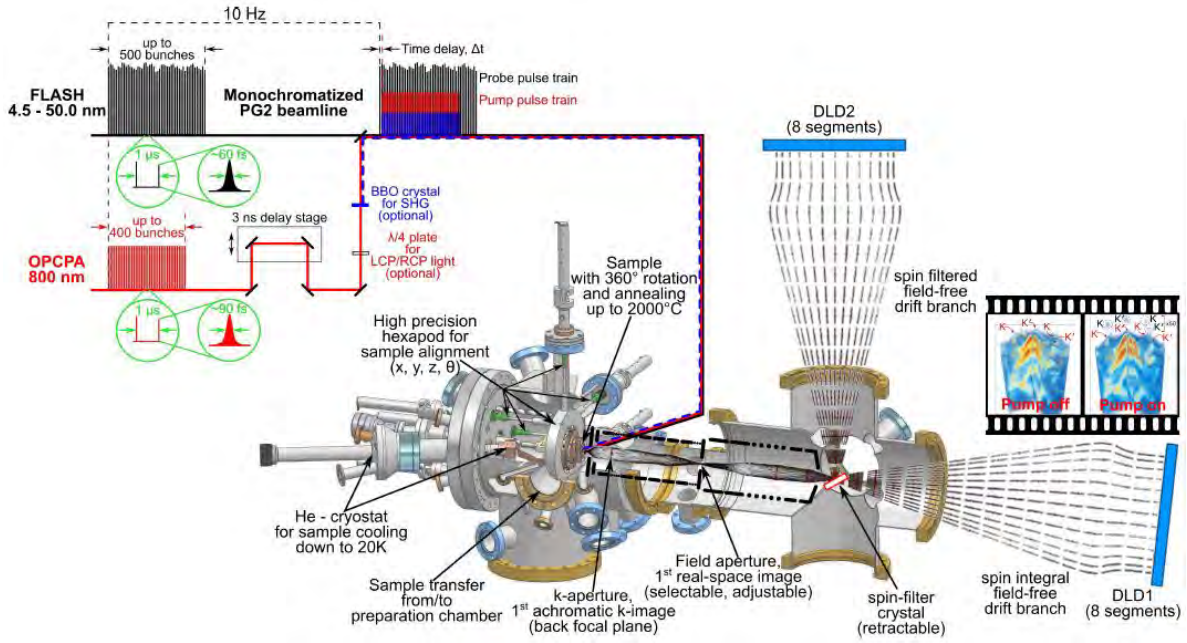


Figure 5.9: Simplified overview of the FLASH pulse structure, the PG2 beamline with synchronised pump laser (top left) and the experimental setup (middle) used to perform time-resolved momentum microscopy and acquire volumetric band-mapping movies (right inset) by means of a multidimensional recording scheme.[78]

Figure reproduced from D. Kutnyakhov et al. Rev. Sci. Inst. ***91****, 013109 (2020). DOI: 10.1063/1.5118777*

5.4.3 Energy efficient materials and devices

The need for energy efficient materials and devices is increasingly becoming an imperative necessity for developing advanced electronic components (transistors, LEDs, sensors, detectors and transducers) that consume exceptionally low amounts of energy whilst providing robust performance compared to existing technologies. The demand for such low energy and high performance materials and devices stems from the rapid growth in social media platforms, artificial intelligence (AI) and machine learning applications.

Since energy loss in materials is inversely proportional to the conductivity, accurate measurements of the conductivity and maximising its value is essential to controlling and reducing such losses in materials.[97] However, conductivity of materials and devices is dependent on scattering processes that occur at the micro- to nano-scales,[98] as well as temporal time-scales from atto- to nano-seconds.[99,100] Pump-probe XFEL based experiments are ideally suited to elucidating such processes, such as electron-electron, electron-phonon, electron-impurity scattering, phase transitions and ultrafast quasiparticle dynamics and hence energy dissipation in metals, semiconductors and superconductors.[101–103]

Recently, significant advances are emerging in graphene and 2D materials to understand mechanisms of energy dissipation in these new quantum materials using, for example, resonant inelastic X-ray (RIXS), time-resolved X-ray absorption spectroscopy (TR-XAS) and time-resolved/nano angle-resolved photoemission spectroscopy (TR-ARPES, NanoARPES).[104–106] These approaches allow probing of the fundamental mechanisms of energy transfer and dissipation in quantum materials with unprecedented detail.

5.4.4 Future opportunities with XFELs

XFELs already routinely provide access to femtosecond timescales, and first measurements with attosecond resolution have been reported. This provides access to electronically relevant timescales, allowing the probing of electron dynamics in real time. XFELs will enable going beyond static measurements of electronic structure, towards a full dynamic picture of the electronic behaviour of charge carriers. The ability of advanced PES setups to probe electronic, spin and crystal structure, coupled with the timescales accessible at future XFELs, will enable probing of band and defect populations dynamically and even under operando conditions. This will deliver unprecedented insights into how electronic materials function, providing vital knowledge for the development of future, disruptive device technologies and beyond.

Angle-resolved PES has already delivered a wealth of crucial insights into the electronic structure of materials.[107] The prospect of combining further ARPES variants with the time resolution delivered by an XFEL is promising for several reasons. Firstly, nanoARPES, which combines the information available from standard ARPES with a nano-focused X-ray beam, could explore a range of crucial questions regarding the electronic structure and dynamics in nanoscale systems.[108,109] Currently, X-ray spot sizes in nanoARPES are on the order of hundreds of nanometres, but future XFEL and synchrotron sources may enable spot sizes of only tens of nanometres to be delivered on the sample. Nanometre scale beams are moving towards matching the length scales of device relevant structures and future in operando setups, including the ability to bias a sample during measurement, this would enable the exploration of electron dynamics in both space and time, for example within advanced electronic devices.[97] A second exciting extension of ARPES uses hard X-rays (HARPES) and can be used to explore not just sample surfaces, but also bulk materials.[110] In the future, XFELs may be able to extend this to specific buried layers and interfaces whilst providing the high time resolution necessary to follow electron dynamics at interfaces, which are often crucial to final device behaviour and performance.[111]

Another exciting emerging area of study is multiple ionisation events and their use as chemical and electronic probes in PES, which promise new insights into both core and valence electronic nature of materials. Ongoing research is focusing on the extension of current work on small molecular species to more complex materials with the view of establishing this technique for quantum materials.

Several challenges remain when wanting to probe electronic structure both statically and dynamically in quantum materials. One of the biggest practical limitations to date has been the difficulty of obtaining useable signals from often small spectral features using short, extremely intense X-ray pulses without acquiring data influenced by radiation damage. Sample delivery and data acquisition systems for nanomaterials, as well as structured multilayer materials including buried interfaces, will need substantial further development to enable probing of low intensity contributions to, for example, density of states.

As mentioned above, space charge is a fundamental problem for PES, and high repetition rate sources combined with high efficiency electron detectors are necessary to combat its negative effects. Detector developments, e.g. the introduction of single-shot data acquisition systems that can be combined with existing high-resolution hemispherical electron energy analysers, are an integral part of future advances.[112] In parallel, ongoing development of powerful momentum microscope systems for both the soft and hard X-ray regimes is pushing towards three-dimensional data acquisition, collecting electron energies and their distribution in k-space on relevant timescales.[111,113–118]

XFEL pump-probe studies on 2D quantum materials and devices will enable fundamental insights and open future applications in energy efficient quantum computing, communications and sensors, as well as opto-electronics, energy storage and medical technologies. In particular, precise understanding of these 2D quantum materials using XFEL approaches could also open novel light-matter interaction applications in the future, i.e. lightwave electronics utilising oscillating electric fields of intense optical carrier waves as ultrafast biasing fields, enabling quantum operations that outpace the oscillation cycle of light. As illustrated in **Figure 5.10**, lightwave electronics can transport electrons coherently at petahertz (PHz) clock speeds – one million times faster than conventional electronics and 100 times faster than scattering occurs – and flip quantum states within a few femtoseconds under ambient conditions. Utilising a quasiparticle-electron collider setup, as shown in **Figure 5.10**, such quantum operations have been timed with attosecond precision to access delicate multi-electron interactions and correlations within 2D layered materials, providing direct access to electronic entanglement states. These breakthroughs have set the stage for meaningful quantum information advancements that will enable quantum technologies and augment classical electronic and photonic devices with entanglement capabilities. In order to utilise X-ray spectroscopy (including XAS and RIXS) to probe 2D quantum materials and devices, synchronisation to optical fields with better than 0.25 fs timing resolution is required and this may be achieved using either streaking based time tools or optical radiators (afterburner undulators) from the same electron bunch used to generate the X-rays.

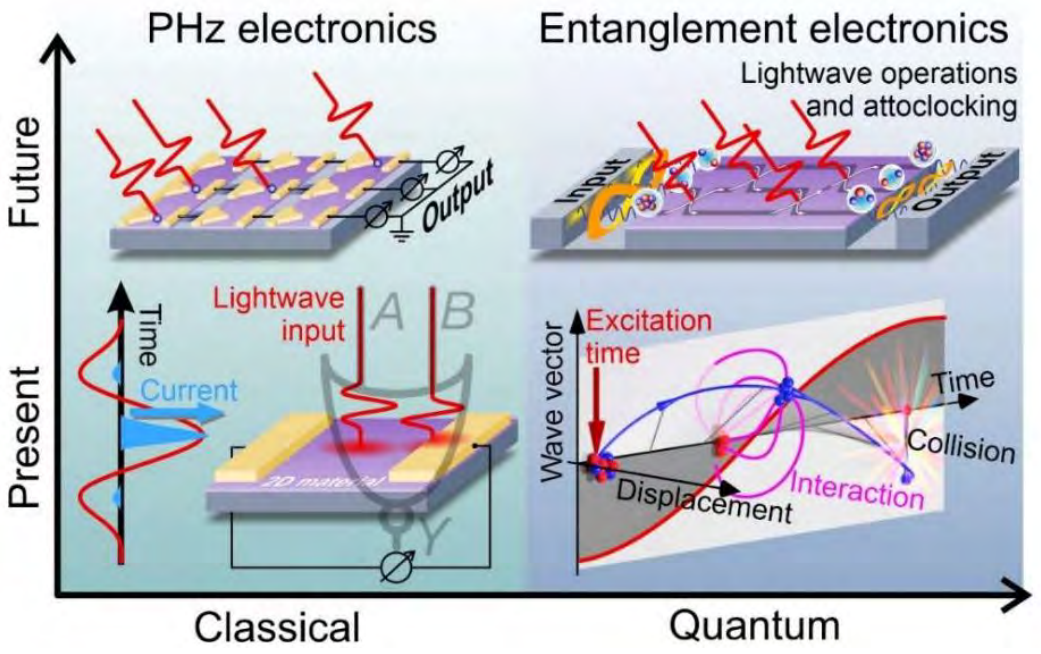


Figure 5.10: The emerging field of lightwave electronics
Strong light waves can non-linearly and coherently excite directional currents, following the main peak of few-cycle pulses (inset, lower left). This principle has enabled basic logic-gate operations (lower left, schematic) using the carrier-envelope phase of two pulses as inputs (A and B) and the output (Y) encoded in the current between electrodes, laying the groundwork for PHz electronics. Future directions could include building an entire PHz processor (top left) by integrating hybrid multi-electrode lightwave arrays. Lightwave operated quasiparticle-colliders can directly detect and drive multi-electron correlations (spheres) by atto-clocking excitation-to-collision timing (lower right). Advances could improve excitation, control, timing, and readout of multi- electron correlations in 2D layered materials (top right) by chaining multiple quantum-state operations within the lifetime of coherences for entanglement electronics.[119–122]

5.4.5 Summary

The UK has a strong, long-standing record in photoelectron spectroscopy and its application to study the electronic structure of matter. This is complemented by an outstanding theory community, supporting experimental efforts. The continuous development of experimental techniques at X-ray facilities is crucial to the understanding and development of future electronic materials and their applications.

The possibility of investigating ultrafast electron dynamics across a wide range of both chemical and physical systems using time-resolved PES is a game changer in the area of quantum technologies. The simultaneous detection of the electronic, spin and overall structure of a material on relevant timescales in the femto- and attosecond regime will open up a completely new way of directly probing the interactions between electronic, spin and lattice dynamics in quantum materials, enabling the emergence of new technological applications. Existing setups are generally limited to probing only one aspect of a system and can often not reach the attosecond timescales relevant for electron dynamics. This results in experiments providing only a partial view of the complete material system. However, the final behaviour of a material, either isolated or within a device application architecture, is an intricate interplay between electronic, spin and local structure. Therefore, future XFEL sources that combine energy tunability from the soft to the hard X-ray regime, high repetition rates to overcome space charge limitations, and attosecond time resolution to probe electron dynamics, would enable unprecedented insights into quantum materials for electronic applications and enable the conceptualisation and development of truly novel device concepts.

Electron transport and scattering as well as light-matter interactions in quantum materials, elucidated using XFEL-based pump-probe approaches, has the potential to lead to breakthroughs in science and technology in the future, with significant impact on energy efficient materials and their wide range of applications. Particularly exciting possibilities emerge for 2D quantum materials that have been optimised for their electron transport properties, using XFEL pump-probe techniques, to minimise dissipation and thereby open pathways to future petahertz lightwave and entanglement electronics.

5.5 Time resolved pair distribution functions

Persistent disorder in quantum materials can appear in various forms, including chemical, electronic, magnetic and geometric. Correlations present within the disorder often give rise to novel phases in the physical and chemical properties of quantum materials. Pair Distribution Function (PDF) measurements are able to probe disorder and, when combined with ultrafast X-rays, provide a potent method to identify the symmetry breaking transitions.

5.5.1 Introduction to pair distribution functions

There is a strong community in the UK using total scattering and Pair Distribution Function (PDF) techniques, and exploiting the dedicated X-ray and neutron instrumentation at the Diamond Light Source and STFC ISIS facilities. PDF is the Fourier transform of the total scattering intensity, which maps the probabilities of distances between all pairs of atoms.[123] Formally the Fourier transform must run from Q = 0 to infinity and so the maximum value of Q, Q_{max}, is a critical factor for high fidelity PDFs. Synchrotrons can use X-rays of 75 – 100 keV that allows Q_{max} to ~ 30 $Å^{-1}$, but with the ~ 10 – 20 keV available from current XFELs, Q_{max} is limited to around 10 $Å^{-1}$. Going to harder X-rays (perhaps in the beam harmonics) is important. The PDF function can be modelled precisely and shows specific information about local structure, so long as Q_{max} is high enough to separate the peaks. We expect there will be significant interest in developing the instrumentation and methodology needed to measure time-resolved X-ray PDFs at a future next-generation XFEL. Many of the problems of interest to this community will carry over into the time domain with the provision of a pump-probe methodology.

5.5.2 Orbital degeneracy lifting

One immediate application would be to address the important orbital degeneracy lifting (ODL) ideas, widespread in Quantum Materials, particularly those containing transition metal elements with partially filled d-orbitals.[124] The ability to access the femto- and picosecond time domain will enable a completely new dimension of understanding of ODL physics, by investigating the speed of its response to an ultrafast laser stimulus. ODL is a local state lacking long-range order, established to lift orbital degeneracies imposed by the high temperature crystal structure. Being electronic in nature and breaking crystal symmetry, it is expected both to fluctuate rapidly and to respond to a driving laser excitation. ODL leads to a subtle kind of local order that is invisible to most other X-ray analytical techniques, but can be clearly seen through the real-space PDF approach. ODL is hard to measure with X-ray Bragg diffraction, because it is a local effect within a crystal that does not change its overall symmetry; it therefore produces broad diffuse scattering in reciprocal space. ODL could be responsible for the local symmetry-breaking electronic nematicity found in a range of quantum materials, especially complex oxides and chalcogenides.[125,126]

5.5.3 Need for time-resolved Pair Distribution Function capabilities

PDF is a potent method to identify the symmetry breaking which, in extreme cases, leads to crystals with one lattice symmetry at large distances, and a completely different symmetry over the short range distance scale. A simple example of ODL explains the symmetry breaking found in FeSe.[127] PDF structural analysis of FeSe has revealed the presence of a local orthorhombic distortion (which lifts the degeneracy of d_{xz} and d_{yz} t_{2g} orbitals and which we have identified as an ODL state) with a correlation length of about 4 nm at temperatures where the average symmetry is tetragonal. The well-established lattice symmetry of FeSe is tetragonal above 90 K, with C_4 rotational symmetry about the c-axis. The low-temperature orthorhombic structure has C_2 symmetry. **Figure 5.11** shows that the C_4 structure fits the high-temperature PDF data at distances beyond 6 Å, but not below, where the C_2 structure is needed. This large local orthorhombic distortion in FeSe persists over wide ranges of temperatures, including into the nematic state at low temperatures, where the magnitude of the local distortion is much larger than the average crystallographic distortion, suggesting an imperfect long-range ordering

of the local state below Ts = 90 K. The results point to a model where ODL fluctuations, which persist up to at least 300 K, order at low temperature into the macroscopically orthorhombic phase.

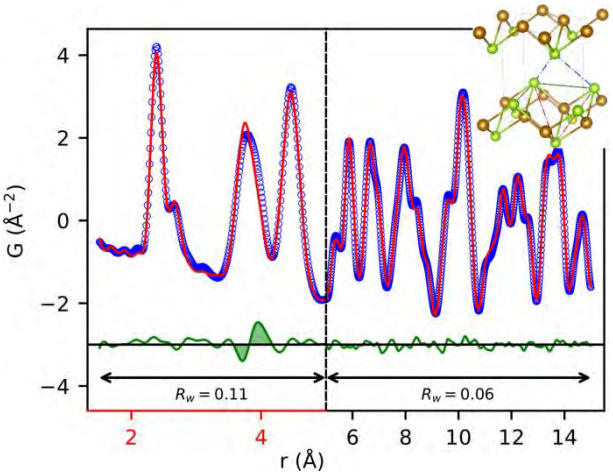


Figure 5.11: X-ray Pair Distribution Function measured from tetragonal FeSe at 300 K, well above its orthorhombic phase transition at 90 K. Local fluctuations are apparent in the second-neighbour peak at 3.9 Å, indicating local symmetry breaking. It is believed this is driven by local fluctuations in the d-orbitals, whose time-dependence could be tracked in a future tr-PDF experiment at a next-generation XFEL.[127]

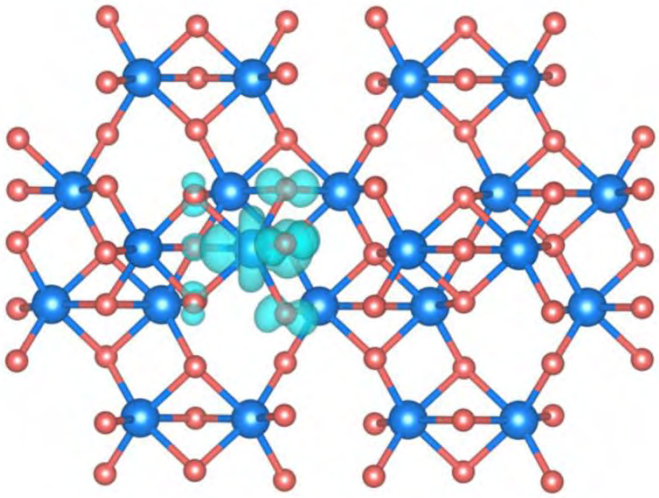
*Reprinted figure with permission from R.J. Koch et al. Phys. Rev. B **100**, 020501 (2019), DOI: 10.1103/PhysRevB.100.020501. Copyright (2019) by the American Physical Society*

The goal of a next-generation XFEL based time-resolved PDF measurement of FeSe would be to investigate the sequence of events following optical pumping into the valence band, followed by occupation of the Fe d-orbitals relevant to ODL and the subsequent local distortion of the lattice. Ultrafast electron diffraction (UED) studies of FeSe have already shown the sort of information that might be learned.[128]

Another class of materials that will be accessible by trPDF is the "relaxor ferroelectrics". This behaviour is typically found in perovskite complex oxide crystals, most famously in lead magnesium niobate, $PbMg_{1/3}Nb_{2/3}O_3$ (PMN), which shows unusual local structure and electrical properties. Conventional ferroelectrics exhibit a sharp first-order phase transition from a high temperature paraelectric state to a spontaneously polarised state at the Curie temperature, T_C. The phase transformation at T_C is unambiguously associated with a structural phase transition, which provides vital guidance to the design and scientific development of this class of materials. In comparison, relaxor ferroelectrics have a broader transition and never fully order below T_C, but simply slow down to form a glass-like low-temperature state with the same average crystal symmetry as at high temperature. The low-temperature state is called an ergodic relaxor (ER) state,[129] often explained by nanometre scale regions, called "polar nano regions" (PNRs), which possess randomly oriented dipole moments.

The existence of these PNRs has a dramatic effect on the electrical behaviour and shows a characteristic frequency dependence of the dielectric constant. Unlike conventional ferroelectrics, which exhibit a Curie-Weiss divergence of ε at T_C, PMN and other relaxors exhibit a rounded peak, which shifts to higher temperatures with frequency. The peak in ε depends very strongly on the measurement frequency, which indicates that there are relaxational dynamics with timescales that freeze out at different temperatures. The origin of this timescale, and its dependence on other experimental parameters, has been phenomenologically explained by a thermally-activated reconfiguration of the polarisation,[130] but this explanation is not microscopically understood despite extensive neutron[131] and X-ray diffuse scattering studies[132] and X-ray PDF investigation.[132,133]

Box 5.2: Bose-Einstein condensation in quantum materials



Proposed small polaron in hematite, α-Fe_2O_3.

The structure of "exotic" excited configurations in condensed matter systems, such as polarons, excitons and possibly Cooper pairs, are largely unknown. In each case, the structure of the excitation could be detected directly by small-angle scattering or else detected at large Q in a scattering experiment coupling to the small displacement of the atoms in the host crystal. These Bosonic excitations can undergo Bose–Einstein condensation (BEC) leading to a geometric assembly whose structure which could also be probed. For example, CdTe semiconductor microcavities, in which photons are confined and strongly coupled to electronic excitations, can create "exciton polaritons".[134]

The problem is that BEC is destroyed by thermal phonons and so occurs at millikelvin or microkelvin temperatures. A conventional X-ray diffraction experiment would destroy the delicate condensate, opening the opportunity for single-shot "diffract and destroy" approaches at an XFEL. Pump-probe single-shot methods will be effective for the photo-excited states. The density of excitons in the direct-gap semiconductor Cu_2O is seen to decay on the single nanosecond time scale.[135]

A possible structure of the "small polaron" delocalised electron-hole pair and its associated displacements has been proposed for hematite, a-Fe_2O_3. So long as a sufficient number of these can be generated with a pump laser, the tr-PDF method will be able to probe its role in the entire photocatalysis sequence of this and other solar energy storage technologies.[136]

*Figure reproduced from E. Pastor et al. Nat. Commun. **10**, 3962 (2019) under the terms of the Creative Commons Attribution 4.0 International License. DOI: 10.1038/s41467-019-11767-9*

5.5.4 Summary of tr-PDF Opportunities for a next generation XFEL

To develop the tr-PDF method at a next-generation XFEL will present some challenges. First and foremost, high energy X-rays are needed, ideally up to 50 keV. The one pump-probe X-ray PDF experiment published to date, studying the evolution of ODL in $CuIr_2S_4$ (with 23 keV X-rays at LCLS), employed a large area detector sensitive to these high energy X-rays, the Rayonix (MAR) MX340-XFEL.[137] To reach 50 keV, this will have to be augmented with a CdTe sensor. The lowest conceivable energy would be about 25 keV. This is needed to obtain a wide enough Q-range, with Q_{max} = 25 $Å^{-1}$ needed to fully resolve the peaks in the PDF in real space, as seen in **Figure 5.11**. New detector geometries, conceivably a wrap-around low-to-high 2θ layout, could be introduced to get to high Q_{max} with lower energy X-rays. PDF structure refinements and simulations can then be obtained with the existing PDFgui program suite[138] or RMCProfile codes.[139]

A general challenge in all pump-probe experiments is to obtain a good laser/X-ray overlap, to ensure that every part of the sample responds to the laser pump. For PDF experiments, we could use spin-coating to make thin layer samples of finely ground material on Si_3N_4 membrane windows, aiming for say 10 µm crystals in a close packed single layer. This design would allow every crystal to see the laser at normal incidence. The photo-stimulated electrons generated by the pump laser would traverse the grain quickly in the metallic state to provide overlap everywhere, not just within the electromagnetic skin depth. The X-ray beam will be spread over 100s of microns, even up to 1 mm^2. This helps the powder averaging and spreads the dose so we can stay below the sample damage threshold, but it is important to avoid “shadowing” of grains that would not see the laser.

The potential opportunities are huge: materials under high pressure, liquid structures, melting, recrystallisation, phase transitioning or super-cooled materials all have interesting changes in local structure. In **Box 5.2** we present, for example, the potential to use trPDF to probe Bose-Einstein condensation in quantum materials. Structural studies in the gas phase and Warm Dense Matter states would be new. Widespread application is expected in materials where disorder is intrinsic to function, such as photovoltaics, nanoparticle formation, and in battery/fuel cell materials.

5.6 Concluding remarks

The UK has a vibrant Quantum and Nano Materials community with experience in condensed matter theory, neutron scattering, synchrotron X-ray scattering, photoemission and laser spectroscopy of solid materials. Quantum materials are defined by the interactions of their populations of electrons and spins with the crystal lattice, often described out of equilibrium by using a “three-temperature” model and coupling rate constants. The timescales of the interactions range from femtosecond (electrons and spins) to pico- and nanosecond (acoustic lattice modes). Ultrafast techniques are needed to measure these coupling rates and elaborate the underlying theoretical picture.

Ultrafast excitations over a wide range of frequencies are needed, as well as sample environments to control pressure and temperature. Dedicated instrumentation is then required to measure the X-ray response in a pump-probe sequence. This chapter has described a number of advanced methods where the UK has significant capabilities:

- Resonant Inelastic X-ray Scattering (RIXS) is used to observe magnons, phonons and excited electronic states
- Time resolved measurements of X-ray Diffuse Scattering allow mapping of phonon dispersion curves and population densities
- Bragg Coherent Diffraction Imaging (BCDI) can locate the distribution of strain within nanocrystals
- Photoemission Spectroscopy (PES) can see the changes in electronic band structure with separated spin states
- X-ray Pair Distribution Functions (PDFs) can identify the local symmetry distortion of lattices.

Each of these methods, once developed for users of a future next-generation XFEL facility, would attract a wide range of material samples important to research, enabling the development of quantum devices and energy science applications. Here the amplification of beam time opportunities inherent at a next-generation XFEL, with the capacity for multiple simultaneous users, would be crucial to supporting a broad user community and diverse applications in the area of Quantum and Nano Materials.

5.7 References for Chapter 5

1 C.D. Stanciu, F. Hansteen, A.V. Kimel *et al.* "All-Optical Magnetic Recording with Circularly Polarized Light." *Phys. Rev. Lett*. **99**, 047601 (2007) DOI: 10.1103/PhysRevLett.99.047601

2 J. Bigot, M. Vomir and E. Beaurepaire, "Coherent ultrafast magnetism induced by femtosecond laser pulses." *Nature Phys* **5**, 515-520 (2009) DOI: 10.1038/nphys1285

3 Department of Energy Grand Challenges, https://science.osti.gov/bes/efrc/Research/Grand-Challenges

4 D.N. Basov, R.D. Averitt, and D. Hsieh, "Towards properties on demand in quantum materials." *Nature Mater **16**,* 1077-1088 (2017) DOI: 10.1038/nmat5017

5 J. Zhang and R. Averitt, "Dynamics and Control in Complex Transition Metal Oxides." *Annual Review of Materials Research* **44**, 19-43 (2014) DOI: 10.1146/annurev-matsci-070813-113258

6 M. Mitrano, S. Johnston, Young-June Kim, and M. P. M. Dean, "Exploring Quantum Materials with Resonant Inelastic X-Ray Scattering." Phys. Rev. X 14, 040501 (2024)

7 E. Beaurepaire, J. Merle, A. Daunois and J. Bigot, "Ultrafast Spin Dynamics in Ferromagnetic Nickel." *Phys. Rev. Lett*. **76**(22):4250-4253 (1996) DOI: 10.1103/PhysRevLett.76.4250

8 C. Graves, A. Reid, T. Wang *et al.* "Nanoscale spin reversal by non-local angular momentum transfer following ultrafast laser excitation in ferrimagnetic GdFeCo." *Nature Mater* **12**, 293-298 (2013) DOI: 10.1038/nmat3597

9 D. Fausti *et al.* "Light-Induced Superconductivity in a Stripe-Ordered Cuprate." *Science* **331**, 189-191 (2011) DOI: 10.1126/science.1197294

10 Y.H. Wang, H. Steinberg, P. Jarillo-Herrero, and N. Gedik, "Observation of Floquet-Bloch States on the Surface of a Topological Insulator." *Science* **342**, 453-457 (2013) DOI: 10.1126/science.1239834

11 E.J. Sie, C.M. Nyby, C.D. Pemmaraju *et al.* "An ultrafast symmetry switch in a Weyl semimetal." *Nature* **565**, 61-66 (2019) DOI: 10.1038/s41586-018-0809-4

12 S. Baierl, M. Hohenleutner, T. Kampfrath *et al.* "Nonlinear spin control by terahertz-driven anisotropy fields." *Nature Photon* **10**, 715-718 (2016) DOI: 10.1038/nphoton.2016.181

13 D. Afanasiev, J.R. Hortensius, B.A. Ivanov *et al.* "Ultrafast control of magnetic interactions via light-driven phonons." *Nat. Mater*. **20**, 607–611 (2021) DOI: 10.1038/s41563-021-00922-7

14 I. Radu, K. Vahaplar, C. Stamm *et al.* "Transient ferromagnetic-like state mediating ultrafast reversal of anti-ferromagnetically coupled spins." *Nature* **472**, 205-208 (2011) DOI: 10.1038/nature09901

15 P. Beaud, A. Caviezel, S. Mariager *et al.* "A time-dependent order parameter for ultrafast photoinduced phase transitions." *Nature Mater* **13**, 923-927 (2014) DOI: 10.1038/nmat4046

16 A. Kogar *et al.* "Light-induced charge density wave in $LaTe_3$." *Nat. Phys.* **16**, 159-163 (2020) DOI: 10.1038/s41567-019-0705-3

17 M.P.M. Dean, Y. Cao, X. Liu *et al.* "Ultrafast energy- and momentum-resolved dynamics of magnetic correlations in the photo-doped Mott insulator Sr_2IrO_4." *Nature Mater* **15**, 601-605 (2016) DOI: 10.1038/nmat4641

18 N. Thielemann-Kühn, D. Schick, N. Pontius *et al.* "Ultrafast and Energy-Efficient Quenching of Spin Order: Antiferromagnetism Beats Ferromagnetism." *Phys. Rev. Lett*. **119**, 197202 (2017) DOI: 10.1103/PhysRevLett.119.197202

19 L. Rettig, C. Dornes, N. Thielemann-Kühn *et al.* "Itinerant and Localized Magnetization Dynamics in Antiferromagnetic Ho", *Phys. Rev. Lett*. **116**, 257202 (2016) DOI: 10.1103/PhysRevLett.116.257202

20 M.P.M. Dean, "Insights into the high temperature superconducting cuprates from resonant inelastic X-ray scattering." *J. Magn. Magn. Mater* **376**, 3-13 (2015) DOI: 10.1016/j.jmmm.2014.03.057

21 E. Iacocca, T. Liu, A.H. Reid *et al.* "Spin-current-mediated rapid magnon localisation and coalescence after ultrafast optical pumping of ferrimagnetic alloys." *Nat Commun* **10**, 1756 (2019) DOI: 10.1038/s41467-019-09577-0

22 B. Pfau, S. Schaffert, L. Müller *et al.* "Ultrafast optical demagnetization manipulates nanoscale spin structure in domain walls." *Nat Commun* **3**, 1100 (2012) DOI: 10.1038/ncomms2108

23 B. Vodungbo, J. Gautier, G. Lambert *et al.* "Laser-induced ultrafast demagnetization in the presence of a nanoscale magnetic domain network." *Nat Commun* **3**, 999 (2012) DOI: 10.1038/ncomms2007

24 S. Gerber, S.L. Yang, D. Zhu *et al.* "Femtosecond electron-phonon lock-in by photoemission and X-ray free-electron laser." *Science* **357**(6346):71-75 (2017) DOI: 10.1126/science.aak9946

25 Y. Cao, D.G. Mazzone, D. Meyers *et al.* "Ultrafast dynamics of spin and orbital correlations in quantum materials: an energy- and momentum-resolved perspective." *Philos Trans A: Math Phys Eng Sci.* **377**(2145):20170480 (2019) DOI: 10.1098/rsta.2017.0480

26 D.G. Mazzone *et al.* "Laser-induced transient magnons in $Sr_3Ir_2O_7$ throughout the Brillouin zone." *Proc. Natl. Acad. Sci. U.S.A.* **118** (22) e2103696118 (2021) DOI: 10.1073/pnas.2103696118

27 D.M. Jonas, "Two-dimensional femtosecond spectroscopy." *Annu Rev Phys Chem*. **54,** 425 (2003) DOI: 10.1146/annurev.physchem.54.011002.103907

28 H. Padma, F. Glerean, S.F.R. TenHuisen *et al.* "Symmetry-protected electronic metastability in an optically driven cuprate ladder." *Nat. Mater.* (2025) DOI: 10.1038/s41563-025-02254-2

29 W. Choi, K.H. Lee, Y.B. Kim, "Theory of Two-dimensional Nonlinear Spectroscopy for the Kitaev Spin Liquid." *Phys. Rev. Lett.* **124**, 117205 (2020) DOI: 10.1103/PhysRevLett.124.117205

[30] L. Savery and L. Balents, "Quantum spin liquids: a review." *Rep. Prog. Phys*. **80** 016502 (2017) DOI: 10.1088/0034-4885/80/1/016502

[31] J. Varignon, M. Bibes and A. Zunger, "Origin of band gaps in 3d perovskite oxides." *Nat Commun* **10**, 1658 (2019) DOI: 10.1038/s41467-019-09698-6

[32] M. Rini, R. Tobey, N. Dean *et al.* "Control of the electronic phase of a manganite by mode-selective vibrational excitation." *Nature* **449**, 72-74 (2007) DOI: 10.1038/nature06119

[33] M. Först, A. Cavalleri *et al.* "Driving magnetic order in a manganite by ultrafast lattice excitation." *Phys. Rev. B* **84**, 241104 (2011) DOI: 10.1103/PhysRevB.84.241104

[34] A. Cavalleri *et al.* "Femtosecond Structural Dynamics in VO_2 during an Ultrafast Solid-Solid Phase Transition." *Phys. Rev. Lett*. **87**, 237401 (2001) DOI: 10.1103/PhysRevLett.87.237401

[35] M. Harmand, R. Coffee, M. Bionta *et al.* "Achieving few-femtosecond time-sorting at hard X-ray free-electron lasers." *Nature Photon* **7**, 215-218 (2013) DOI: 10.1038/nphoton.2013.11

[36] P. Beaud, A. Caviezel, S. Mariager *et al.* "A time-dependent order parameter for ultrafast photoinduced phase transitions." *Nature Mater* **13**, 923-927 (2014) DOI: 10.1038/nmat4046

[37] R. Mankowsky, A. Subedi, M. Först *et al.* "Nonlinear lattice dynamics as a basis for enhanced superconductivity in $YBa_2Cu_3O_{6.5}$." *Nature* **516**, 71-73 (2014) DOI: 10.1038/nature13875

[38] M. Kozina, M. Fechner, P. Marsik *et al.* "Terahertz-driven phonon upconversion in $SrTiO_3$." *Nat. Phys.* **15**, 387-392 (2019) DOI: 10.1038/s41567-018-0408-1

[39] M. Trigo, M. Fuchs, J. Chen *et al.* "Fourier-transform inelastic X-ray scattering from time- and momentum-dependent phonon- phonon correlations." *Nat. Phys* **9**, 790-794 (2013) DOI: 10.1038/nphys2788

[40] D. Zhu, M. Trigo *et al.* "Phonon spectroscopy with sub-meV resolution by femtosecond X-ray diffuse scattering." *Phys. Rev. B* **92**, 054303 (2015) DOI: 10.1103/PhysRevB.92.054303

[41] S. Wall, S. Yang, L. Vidas *et al.* "Ultrafast disordering of vanadium dimers in photoexcited VO_2." *Science* **362**, 572-576 (2018) DOI: 10.1126/science.aau3873

[42] P. Baum, D.-S. Yang and A.H. Zewail, "4D Visualization of Transitional Structures in Phase Transformations by Electron Diffraction." *Science* **318**, 788-792 (2007) DOI: 10.1126/science.1147724

[43] G.A. de la Peña Muñoz, A.A. Correa, S. Yang, S. *et al*. "Ultrafast lattice disordering can be accelerated by electronic collisional forces." *Nat. Phys*. **19**, 1489-1494 (2023) DOI: 10.1038/s41567-023-02118-z

[44] A.S. Johnson, E. Pastor, S. Batlle-Porro *et al*. "All-optical seeding of a light-induced phase transition with correlated disorder." *Nat. Phys*. **20**, 970–975 (2024) DOI: 10.1038/s41567-024-02474-4

[45] A.S. Disa, F.J. Walker, C.H. Ahn, "High-Resolution Crystal Truncation Rod Scattering: Application to Ultrathin Layers and Buried Interfaces." *Adv. Mater. Interfaces* **7**, 1901772 (2020) DOI: 10.1002/admi.201901772

[46] "Nanoscience and nanotechnologies: opportunities and uncertainties." *The Royal Society and The Royal Academy of Engineering* (2004) https://royalsociety.org/topics-policy/publications/2004/nanoscience-nanotechnologies/

[47] Y. Volokitin, J. Sinzig, L. de Jongh *et al.* "Quantum-size effects in the thermodynamic properties of metallic nanoparticles." *Nature* **384**, 621-623 (1996) DOI: 10.1038/384621a0

[48] E. Morosan, D. Natelson, A.H. Nevidomskyy and Q. Si, "Strongly Correlated Materials." *Advanced Materials* **24**, 4896-4923 (2012) DOI: 10.1002/adma.201202018

[49] E. Dagotto, "Complexity in Strongly Correlated Electronic Systems." *Science* **309**, 257-262 (2005) DOI: 10.1126/science.1107559

[50] "Multiferroics march on." *Nature Mater* **18**, 187 (2019) DOI: 10.1038/s41563-019-0310-y

[51] N.A. Spaldin, R. Ramesh, "Advances in magnetoelectric multiferroics." *Nature Mater* **18**, 203-212 (2019) DOI: 10.1038/s41563-018-0275-2

[52] E. Vogel, "Technology and metrology of new electronic materials and devices." *Nature Nanotech* **2**, 25-32 (2007) DOI: 10.1038/nnano.2006.142

[53] J. Yang, D. Strukov, and D. Stewart, "Memristive devices for computing." *Nature Nanotech* **8**, 13-24 (2013) DOI: 10.1038/nnano.2012.240

[54] D.H.S. Tan, A. Banerjee, Z. Chen and Y.S Meng, "From nanoscale interface characterization to sustainable energy storage using all-solid-state batteries." *Nat. Nanotechnol.* **15**, 170-180 (2020) DOI: 10.1038/s41565-020-0657-x

[55] W. Hu, S. Kaiser, D. Nicoletti *et al.* "Optically enhanced coherent transport in $YBa_2Cu_3O_{6.5}$ by ultrafast redistribution of inter- layer coupling." *Nature Mater* **13**, 705-711 (2014) DOI: 10.1038/nmat3963

[56] X. Li, T. Qiu, J. Zhang *et al.* "Terahertz field-induced ferroelectricity in quantum paraelectric $SrTiO_3$." *Science* **364**, 1079-1082 (2019) DOI: 10.1126/science.aaw4913

[57] M.C. Newton, M. Sao, Y. Fujisawa *et al.* "Time-Resolved Coherent Diffraction of Ultrafast Structural Dynamics in a Single Nanowire." *Nano Lett*. **14**, 5, 2413-2418 (2014) DOI: 10.1021/nl500072d

[58] H.S. Park, O.-H. Kwon, J.S. Baskin, B. Barwick and A.H. Zewail, "Direct observation of martensitic phase-transformation dynamics in iron by 4D single-pulse electron microscopy." *Nano Lett*. **9**, 3954-3962 (2009) DOI: 10.1021/nl9032704

[59] P. Emma, R. Akre, J. Arthur *et al.* "First lasing and operation of an ångstrom-wavelength free-electron laser". *Nature Photon* **4**, 641-647 (2010) DOI: 10.1038/nphoton.2010.176

[60] G. Margaritondo and P. Rebernik Ribic, "A simplified description of X-ray free-electron lasers." *J. Synchrotron Radiat.* **18**, 101-108 (2011) DOI: 10.1107/S090904951004896X

[61] J. Miao, T. Ishikawa, I.K. Robinson and M.M. Murnane, "Beyond crystallography: Diffractive

imaging using coherent X-ray light sources." *Science* **348**, 530-535 (2015) DOI: 10.1126/science.aaa1394

62 I. Robinson and R. Harder, "Coherent X-ray diffraction imaging of strain at the nanoscale." *Nature Mater* **8**, 291-298 (2009) DOI: 10.1038/nmat2400

63 M. Pfeifer, G. Williams, I. Vartanyants *et al.* "Three-dimensional mapping of a deformation field inside a nanocrystal." *Nature* **442**, 63-66 (2006) DOI: 10.1038/nature04867

64 H.N. Chapman, A. Barty, M. Bogan *et al.* "Femtosecond diffractive imaging with a soft-X-ray free-electron laser." *Nature Phys* **2**, 839-843 (2006) DOI: 10.1038/nphys461

65 G.J. Williams *et al.* "Fresnel Coherent Diffractive Imaging." *Phys. Rev. Lett*. **97**, 025506 (2006) DOI: 10.1103/PhysRevLett.97.025506

66 J.M. Rodenburg *et al.* "Hard-X-Ray Lensless Imaging of Extended Objects." *Phys. Rev. Lett*. **98**, 034801 (2007) DOI: 10.1103/PhysRevLett.98.034801

67 M.C. Newton, S.J. Leake, R. Harder and I.K. Robinson, "Three-dimensional imaging of strain in a single ZnO nanorod." *Nat Mater* **9**, 120-124 (2010) DOI: 10.1038/nmat2607

68 J.N. Clark, L. Beitra, G. Xiong *et al*, "Ultrafast three-dimensional imaging of lattice dynamics in individual gold nanocrystals." *Science* **341**, 6141 (2013) DOI: 10.1126/science.1236034

69 D. Rudolf, C. La-O-Vorakiat, M. Battiato *et al.* "Ultrafast magnetization enhancement in metallic multilayers driven by superdiffusive spin current." *Nature Communications* **3**, 1037 (2012) DOI: 10.1038/ncomms2029

70 A. Barty, S. Boutet, M. Bogan *et al, "*Ultrafast single-shot diffraction imaging of nanoscale dynamics." *Nature Photon* **2**, 415–419 (2008). DOI: 10.1038/nphoton.2008.128

71 J.-D. Nicolas, T. Reusch, M. Osterhoff *et al.* "Time-resolved coherent X-ray diffraction imaging of surface acoustic waves." *J Appl Crystallogr*. **47**, 1596-1605 (2014) DOI: 10.1107/S1600576714016896

72 T. Choi, S. Lee, Y.J. Choi, V. Kiryukhin and S.-W. Cheong, "Switchable Ferroelectric Diode and Photovoltaic Effect in $BiFeO_3$." *Science* **324**, 63-66 (2009) DOI: 10.1126/science.1168636

73 M. Bibes and A. Barthélémy, "Towards a magnetoelectric memory." *Nature Mater* **7**, 425-426 (2008) DOI: 10.1038/nmat2189

74 M. Nakano, K. Shibuya, D. Okuyama *et al.* "Collective bulk carrier delocalization driven by electrostatic surface charge accumulation." *Nature* **487**, 459-462 (2012) DOI: 10.1038/nature11296

75 I.A. Vartanyants *et al.* "Coherent X-ray scattering and lensless imaging at the European XFEL Facility." *J Synchrotron Rad.* **14**, 453-470 (2007) DOI: 10.1107/S0909049507037600

76 S. Hellmann *et al.* "Time-resolved X-ray photoelectron spectroscopy at FLASH." *New J. Phys*. **14**, 013062 (2012) DOI: 10.1088/1367-2630/14/1/013062

77 A. Pietzsch *et al.* "Towards time resolved core level photoelectron spectroscopy with femtosecond X-ray free-electron lasers." *New J. Phys*. **10**, 033004 (2008) DOI: 10.1088/1367-2630/10/3/033004

78 D. Kutnyakhov, R.P. Xian, M. Dendik *et al.* "Time- and momentum-resolved photoemission studies using time-of-flight momentum microscopy at a free-electron laser." *Rev Sci Instrum*. **91**, 013109 (2020) DOI: 10.1063/1.5118777

79 B. Schönhense *et al.* "Multidimensional photoemission spectroscopy-the space-charge limit." *New J. Phys*. **20**, 033004 (2018) DOI: 10.1088/1367-2630/aaa262

80 P. Salén *et al.* "Experimental Verification of the Chemical Sensitivity of Two-Site Double Core-Hole States Formed by an X-Ray Free-Electron Laser." *Phys. Rev. Lett*. **108**, 153003 (2012) DOI: 10.1103/PhysRevLett.108.153003

81 H. Fukuzawa *et al.* "Deep Inner-Shell Multiphoton Ionization by Intense X-Ray Free-Electron Laser Pulses." *Phys. Rev. Lett*. **110**, 173005 (2013) DOI: 10.1103/PhysRevLett.110.173005

82 Y. Zhang, U. Bergmann, R. Schoenlein, M. Khalil and N. Govind, "Double core hole valence-to-core x- ray emission spectroscopy: A theoretical exploration using time-dependent density functional theory." *J. Chem. Phys*. **151**(14): 144114 (2019) DOI: 10.1063/1.5111141

83 E. Pelimanni, A.E.A. Fouda, P.J Ho *et al.* "Observation of molecular resonant double-core excitation driven by intense X-ray pulses." *Commun Phys* **7**, 341 (2024) DOI: 10.1038/s42005-024-01804-5

84 A. Müller *et al*. "Double-K-hole resonances in single photoionization of He-like B^{3+} ions." *Phys. Rev. A* **110**, 062802 (2024) DOI: 10.1103/PhysRevA.110.062802

85 N. Berrah *et al.* "Double-core-hole spectroscopy for chemical analysis with an intense X-ray femtosecond laser." *Proc. Natl. Acad. Sci. USA*. **108**(41):16912-16915 (2011) DOI: 10.1073/pnas.1111380108

86 S. Hellmann, T. Rohwer, M. Kalläne *et al.* "Time-domain classification of charge-density-wave insulators." *Nat Commun* **3**, 1069 (2012) DOI: 10.1038/ncomms2078

87 F. Pressacco, V. Uhlíř, M. Gatti *et al.* "Laser induced phase transition in epitaxial FeRh layers studied by pump-probe valence band photoemission." *Structural Dynamics* **5**, 034501 (2018) DOI: 10.1063/1.5027809

88 S. Hellmann *et al.* "Ultrafast Melting of a Charge-Density Wave in the Mott Insulator $1T$ –TaS_2." *Phys. Rev. Lett.* **105**, 187401 (2010) DOI: 10.1103/PhysRevLett.105.187401

89 M. Dendzik *et al*. "Observation of an excitonic Mott transition through ultrafast core-cum-conduction photoemission spectroscopy." Phys. Rev. Lett. 125, 096401 (2020) DOI: 10.1103/PhysRevLett.125.096401

90 L.-P. Oloff *et al.* "Time-resolved HAXPES at SACLA: probe and pump pulse-induced space-charge

effects." *New J. Phys*. **16**, 123045 (2014) DOI: 10.1088/1367-2630/16/12/123045

[91] L.-P. Oloff, A. Chainani, M. Matsunami *et al.* "Time-resolved HAXPES using a microfocused XFEL beam: From vacuum space-charge effects to intrinsic charge-carrier recombination dynamics." *Sci Rep* **6**, 35087 (2016) DOI: 10.1038/srep35087

[92] T. Pincelli *et al.* "Transient quantum isolation and critical behavior in the magnetization dynamics of half-metallic manganites." *Phys. Rev. B* **100**, 045118 (2019) DOI: 10.1103/PhysRevB.100.045118

[93] D. Puntel, D. Kutnyakhov, L. Wenthaus et al. Out-of-equilibrium charge redistribution in a copper-oxide based superconductor by time-resolved X-ray photoelectron spectroscopy. *Sci Rep* **14**, 8775 (2024) DOI: 10.1038/s41598-024-56440-4

[94] P. Rosenberger et al. "Spin polarization of the two-dimensional electron gas at the EuO/SrTiO3(001) interface." *Phys. Rev. Materials* **9**, 064401 (2025) DOI: 10.1103/PhysRevMaterials.9.064401

[95] O. Karni, E. Barré, V. Pareek *et al.* "Structure of the moiré exciton captured by imaging its electron and hole." Nature 603, 247–252 (2022) DOI: 0.1038/s41586-021-04360-y

[96] K. Medjanik, O. Fedchenko, S. Chernov *et al.* "Direct 3D mapping of the Fermi surface and Fermi velocity." *Nature Mater* **16**, 615–621 (2017) DOI: 10.1038/nmat4875

[97] S.A. Awan *et al*. "Transport conductivity of graphene at RF and microwave frequencies." *2D Mater*. **3** 015010 (2016) DOI: 10.1088/2053-1583/3/1/015010

[98] K. Nakayama *et al*. "Nanomosaic of Topological Dirac States on the Surface of Pb5Bi24Si41 Observed by Nano-ARPES." *Nano Lett*. **19** (6): 3737–3742 (2019) DOI: 10.1021/acs.nanolett.9b00875

[99] S. Ulstrup *et al*. "Ultrafast electron dynamics in epitaxial graphene investigated with time- and angle-resolved photoemission spectroscopy." *J. Phys.: Condens. Matter* **27** 164206 (2015) DOI: 10.1088/0953-8984/27/16/164206

[100] A. Aeschlimann *et al*. "Direct evidence for efficient ultrafast charge separation in epitaxial WS_2/graphene heterostructures." *Sci. Adv*. **6**, eaay0761 (2020) DOI: 10.1126/sciadv.aay0761

[101] J. Moore, "The birth of topological insulators." *Nature* **464**, 194-198 (2010) DOI: 10.1038/nature08916

[102] M. Fiebig, T. Lottermoser, D. Meier *et al*. "The evolution of multiferroics." *Nat Rev Mater* **1**, 16046 (2016) DOI: 10.1038/natrevmats.2016.46

[103] C. Jozwiak, J. Sobota, K. Gotlieb *et al*. "Spin-polarized surface resonances accompanying topological surface state formation." *Nat. Commun*. **7**, 13143 (2016) DOI: 10.1038/ncomms13143

[104] F. Joucken *et al*. "Visualizing the Effect of an Electrostatic Gate with Angle-Resolved Photoemission Spectroscopy." Nano Lett. **19**, 4, 2682–2687 (2019) DOI: 10.1021/acs.nanolett.9b00649

[105] L. Broers and L. Mathey, "Detecting light-induced Floquet band gaps of graphene via trARPES." *Phys. Rev. Research* **4**, 013057 (2022) DOI: 10.1103/PhysRevResearch.4.013057

[106] F. Boschini *et al*. "Time-resolved ARPES studies of quantum materials." *Rev. Mod. Phys*. **96**, 015003 (2024) DOI: 10.1103/RevModPhys.96.015003

[107] H. Zhang, T. Pincelli, C. Jozwiak *et al.* "Angle-resolved photoemission spectroscopy." *Nat Rev Methods Primers* **2**, 54 (2022) DOI: 10.1038/s43586-022-00133-7

[108] A.J.H. Jones, R. Muzzio, P. Majchrzak *et al*. "Observation of Electrically Tunable van Hove Singularities in Twisted Bilayer Graphene from NanoARPES." *Advanced Materials* **32**, e2001656 (2020) DOI: 10.1002/adma.202001656

[109] D. Curcio. A.J.H. Jones, R. Muzzio *et al*. "Accessing the spectral function in a current-carrying device." Phys. Rev. Lett. 125, 236403 (2020) DOI: 10.1103/PhysRevLett.125.236403

[110] A. Gray, J. Minár, S. Ueda *et al*. "Bulk electronic structure of the dilute magnetic semiconductor Ga1-xMnxAs through hard X-ray angle-resolved photoemission." *Nature Mater* **11**, 957-962 (2012) DOI: 10.1038/nmat3450

[111] S. Babenkov, K. Medjanik, D. Vasilyev *et al.* "High-accuracy bulk electronic bandmapping with eliminated diffraction effects using hard X-ray photoelectron momentum microscopy." *Commun Phys* **2**, 107 (2019) DOI: 10.1038/s42005-019-0208-7

[112] M. Oura, T. Wagai, A. Chainani *et al.* "Development of a single-shot CCD-based data acquisition system for time-resolved X-ray photoelectron spectroscopy at an X-ray free-electron laser facility." *J. Synchrotron Rad*. **21**, 183-192 (2014) DOI: 10.1107/S1600577513028233

[113] C. Tusche, A. Krasyuk and J. Kirschner, "Spin resolved bandstructure imaging with a high resolution momentum microscope." *Ultramicroscopy* **159** Pt 3:520 - 529 (2015) DOI: 10.1016/j.ultramic.2015.03.020

[114] C. Tusche *et al.* "Multi-MHz time-of-flight electronic bandstructure imaging of graphene on Ir(111)." *Appl. Phys. Lett*. **108**, 261602 (2016) DOI: 10.1063/1.4955015

[115] K. Medjanik, O. Fedchenko, S. Chernov *et al.* "Direct 3D mapping of the Fermi surface and Fermi velocity." *Nat Mater*. **16**, 615-621 (2017) DOI: 10.1038/nmat4875

[116] K. Medjanik, S.V. Babenkov, S. Chernov *et al.* "Progress in HAXPES performance combining full-field k-imaging with time-of-flight recording." *J. Synchrotron Radiat*. **26**, 1996-2012 (2019) DOI: 10.1107/S1600577519012773

[117] O. Fedchenko, *et al.* "High-resolution hard-X-ray photoelectron diffraction in a momentum microscope-the model case of graphite." *New J. Phys.* **21**, 113031 (2019) DOI: 10.1088/1367-2630/ab51fe

[118] P. Grychtol *et al.* "The SXP instrument at the European XFEL." *J. Phys.: Conf. Ser*. **2380** 012043 (2022) DOI: 10.1088/1742-6596/2380/1/012043

[119] W. Ren *et al.* "The 2025 2D Materials Roadmap." https://doi.org/10.48550/arXiv.2503.22476

[120] J. Freudenstein, M. Bosch, M. Meierhofer *et al*. "Attosecond clocking of correlations between Bloch electrons." *Nature* **610**, 290-295 (2022) DOI: 10.1038/s41586-022-05190-2

[121] T. Boolakee, C. Heide, A. Garzón-Ramírez *et al*. "Light-field control of real and virtual charge carriers." *Nature* **605**, 251–255 (2022) DOI: 10.1038/s41586-022-04565-9

[122] M. Borsch, M. Meierhofer, R. Huber, M. Kira, "Lightwave electronics in condensed matter." *Nat Rev Mater*, 8, 668-687 (2023) DOI: 10.1038/s41578-023-00592-8

[123] D.A. Keen and A.L. Goodwin, "The crystallography of correlated disorder." *Nature* **521**, 303-309 (2015) DOI: 10.1038/nature14453

[124] E.S. Bozin, W.G. Yin, R.J. Koch *et al.* "Local orbital degeneracy lifting as a precursor to an orbital-selective Peierls transition." *Nat Commun* **10**, 3638 (2019) DOI: 10.1038/s41467-019-11372-w

[125] J. Wu, A.T. Bollinger, X. He and I. Božović, "Spontaneous breaking of rotational symmetry in copper oxide superconductors." *Nature* **547**, 432-435 (2017) DOI: 10.1038/nature23290

[126] S.A. Kivelson, E. Fradkin and V.J. Emery, "Electronic liquid-crystal phases of a doped Mott insulator." *Nature* **393**, 550-553 (1998) DOI: 10.1038/31177

[127] R.J. Koch *et al.* "Room temperature local nematicity in FeSe superconductor." *Phys. Rev. B* **100**, 020501 (2019) DOI: 10.1103/PhysRevB.100.020501

[128] T. Konstantinova *et al.* "Photoinduced dynamics of nematic order parameter in FeSe." *Phys. Rev. B* **99**, 180102(R) (2019) DOI: 10.1103/PhysRevB.99.180102

[129] A.A. Bokov and Z.-G. Ye, "Recent progress in relaxor ferroelectrics with perovskite structure." *J Mater Sci* **41**, 31-52 (2006) DOI: 10.1007/s10853-005-5915-7

[130] F.M. Jiang and S. Kojima, "Microheterogeneity and relaxation in $0.65Pb(Mg_{1/3}Nb_{2/3})O_3$-$0.35PbTiO_3$ relaxor single crystals." *Appl. Phys. Lett*. **77**, 1271-1273 (2000) DOI: 10.1063/1.1289909

[131] G. Xu, G. Shirane, J.R.D. Copley and P.M. Gehring, "Neutron elastic diffuse scattering study of $Pb(Mg_{1/3}Nb_{2/3})O_3$." *Phys. Rev. B* **69**, 064112 (2004) DOI: 10.1103/PhysRevB.69.064112

[132] A. Bosak, D. Chernyshov, S. Vakhrushev and M. Krisch, "Diffuse scattering in relaxor ferroelectrics: true three-dimensional mapping, experimental artefacts and modelling." A*cta Cryst. A* **68**, 117-123 (2012) DOI: 10.1107/S0108767311040281

[133] S. Vakhrushev, A. Nabereznov, S. Sinha, Y. Feng and T. Egami, "Synchrotron X-ray scattering study of lead magnoniobate relaxor ferroelectric crystals." *J. Phys. Chem. Solids*, **57**, 1517–1523 (1996), Proceeding of the 3rd Williamsburg Workshop on Fundamental Experiments on Ferroelectrics DOI: 10.1016/0022-3697(96)00022-4

[134] J. Kasprzak, M. Richard, S. Kundermann *et al.* "Bose-Einstein condensation of exciton polaritons." *Nature* **443**, 409 (2006) DOI: 10.1038/nature05131

[135] James P Wolfe and Joon I Jang, "The search for Bose–Einstein condensation of excitons in Cu_2O: exciton-Auger recombination versus biexciton formation." *New J. Phys*. **16**, 123048 (2014) DOI: 10.1088/1367-2630/16/12/123048

[136] E. Pastor, J. Park, L. Steier *et al.* "In situ observation of pico-second polaron self-localisation in α-Fe_2O_3 photoelectrochemical cells." *Nat Commun* **10**, 3962 (2019) DOI: 10.1038/s41467-019-11767-9

[137] J. Griffiths, A.F. Suzana, L. Wu *et al.* "Resolving Length Scale Dependent Transient Disorder Through an Ultrafast Phase Transition." *Nat. Mater*. **23** 1041-1047 (2024) DOI: 10.1038/s41563-024-01927-8

[138] C.L. Farrow *et al.* "PDFfit2 and PDFgui: computer programs for studying nanostructure in crystals." *J. Phys.:Condens. Matter* **19**, 335219 (2007) DOI: 10.1088/0953-8984/19/33/335219

[139] M.G. Tucker, D.A. Keen, M.T. Dove, A.L. Goodwin and Q. Hui, "RMCProfile: reverse Monte Carlo for polycrystalline materials." *J. Phys.:Condens. Matter* **19**, 335218 (2007) DOI: 10.1088/0953-8984/19/33/335218

6. Science Opportunities in the Chemical Sciences and Energy

All chemical reactions involve the movement of electrons and nuclei. One of the grand challenges in chemistry is to be able to predict exactly how a molecule will react, which is essential for designing new molecules and materials for any application. XFELs are unique in the information they can capture on the motion of electrons and nuclei and are an essential part of revolutionising our understanding of the fundamentals of reactivity, and designing future molecules and materials for a plethora of applications pertinent for all areas of modern life.

Two of the biggest open challenges in chemistry are to make any molecule and materials with the properties we need, and to do so in a sustainable way. XFELs have been playing a key role in tackling these challenges through advancing our understanding of the fundamental electron-nuclear dynamics and how it determines reaction mechanisms, on illuminating the first-most chemical events, and ways in which modification of a chemical structure influences the reaction outcome. This fundamental understanding is key to any 21st century applications, from harnessing energy of the Sun to precision medicine.

The next big opportunity for exploring and exploiting XFELs in the chemical sciences is the translation of these experimental techniques to ever more dilute systems, ever more complex mixtures, and ever more realistic conditions approaching those in the real world. One of the key considerations when studying chemistry is the multidimensional nature of the problems – molecules have many degrees of complexity in terms of the number of available electronic states, their conformational flexibility and the number of potential reaction pathways. Reconstructing clear 'molecular movies' from the experimental observations with atomic-scale precision requires particularly high data quality. Since chemical change occurs on the timescales of nuclear motion, femtosecond time resolution is a key requirement for relevant experimental techniques. The relatively low repetition rates, photon fluxes, and accessible energy ranges of current XFELs impose many technical barriers to achieving this key goal, limiting scientific and technological progress.

A next-generation XFELs will have a revolutionary impact on the chemical sciences, opening up new areas and broadening the scope of the scientific challenges that can be addressed with the step-change in technical capabilities. Several key aspects of the design that will be particularly beneficial to the chemical sciences are:

- High repetition rate (100 kHz or higher) and high brightness (> 10^{12} photons/pulse) to enable the required sensitivity and signal-to-noise ratio to be achieved
- A broad coverage of X-ray energies, from soft to hard (200 eV to 20 keV), making it possible to investigate most of the atomic absorption edges across the periodic table (**Figure 6.1**)
- The flexibility of joining multiple methods of reaction initiation and monitoring by combining X-rays, electron beams, and optical methods with femtosecond temporal resolution
- Extensive access enabled by a high efficiency multiplexed facility.

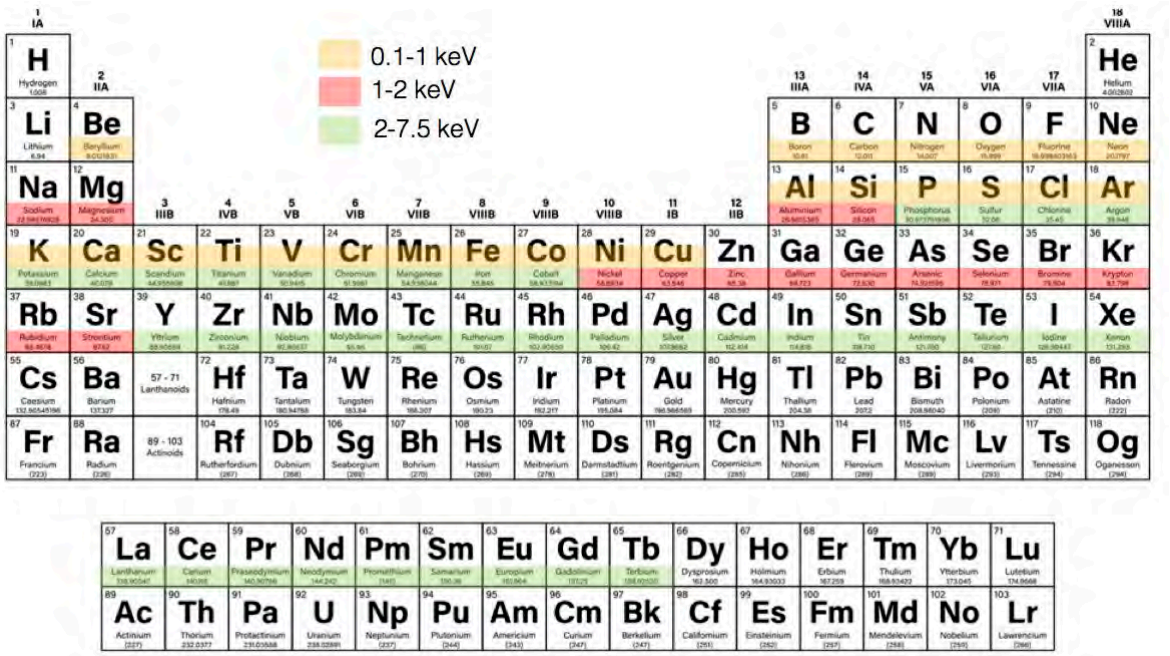


Figure 6.1: The Periodic Table showing energy ranges of X-rays for key absorption edges

To bring about a new level of understanding in areas as diverse as chemistry in space and the origin of life on Earth to photocatalysis or information storage, the processes involved need to be followed with atomic precision as they evolve along the multidimensional, multi-parameter landscape. A likely, and long-anticipated game-changer – ***a combination of high repetition rate X-ray pulses with optical VUV, UV, Vis, IR, THz excitation and detection pulses, which a researcher is able to mix and match on demand*** – is now within reach. Enhanced provision of all these capabilities will be an important feature at a next-generation XFEL.

Selected areas discussed in this Chapter include how XFELs are at the brink of enabling the next level of understanding of:

- Real-time molecular movies of reactions, transformations, and catalytic processes with atomic precision, on timescales from femtosecond upwards
- The interplay between fundamental nuclear, electronic, and spin dynamics, and their underpinning role in the rational design of photo-functional materials, materials for energy capture and storage, and novel catalytic approaches in all states of matter
- Atmospheric and environmental chemistry
- Chemistry in space
- Analytical chemistry and new diagnostics
- Therapies in medicine.

6.1 Fundamentals of reaction dynamics: Coupling between nuclear, electronic and spin degrees of freedom

Chemical dynamics encompasses the interplay of phenomena across multiple timescales, from femtoseconds (a vibrational period of a chemical bond) to seconds (full cycle of photosynthesis), involving structural, electronic and spin states evolving together. Next-generation XFELs will bring a combination of suitably short pulses of photons, with energies ranging from THz to X-ray, sufficiently high repetition rate of > 100 kHz, high spectral purity and high brightness of ~10^{12} photons/pulse, to enable a comprehensive interrogation of chemical reactions, non-equilibrium processes and transformations, "watching chemistry happen".

6.1.1 Introduction

The last decade has seen dramatic developments in our ability to use optical probes to interrogate phenomena in molecules and materials on ever shorter timescales, approaching the very act of breaking or formation of a chemical bond and reaching out into the attosecond domain.[1] Key questions that must still be answered include: *Can we possibly ever record a meaningful 'molecular movie', in which the convolved structural, electronic, vibrational, and spin dynamics are simultaneously resolved?*[2] *Can we now establish the role of coherent processes – both electronic and vibronic – in charge and energy transport on the nanoscale?*[3] *Can we achieve element-specific imaging of concurrent electronic, spin, and structural changes with femtosecond resolution?*[4-6] Unfortunately, methods based on the optical region of the electromagnetic spectrum cannot measure sub-ångstrom displacement and femtosecond motion in molecules, and therefore alternative and additional methods are urgently needed.

A powerful combination of the diverse range of femtosecond X-ray methods with the plethora of optical methods available could potentially answer the underlying questions, including:

- How long does it take the atoms to move?
- Where is the motion localised/delocalised within the molecule or material?
- What is the amplitude and the phase of this motion?
- What is (are) the reaction coordinate(s)?
- What is the role of coherence(s) in ultrafast transformations?
- Can we alter the outcome of a chemical reaction at will?

The XFEL and associated infrastructure of ultrafast optical methods will bring about a combination of short pulses of photons with energies ranging from THz to X-ray, high repetition rate of > 100 kHz, high spectral purity and high brightness, to finally enable a comprehensive interrogation of chemical reactions, non-equilibrium processes and transformations, in a real-time molecular movie. By combining multiple means of initiation and interrogation of reactions, it will be possible to extend our measurement capabilities. As a result, we will be able to, for example: determine the structure of excited and transition states with < 0.01 Å resolution; follow coherent vibrations in polyatomic molecules; and make direct observation of conical intersections, which are a key part to the mechanisms of ultrafast light-driven reactions yet remain elusive experimentally. *The existing methods of X-ray absorption* (that probe structure and unoccupied electronic density of states), *X-ray emission* (that probes occupied density of states), *resonant X-ray emission* (that enables high resolution experiments),[7] *X-ray Raman*[8] (that probes edges of light elements using harder X-rays), and *multiple emerging methods* must be combined to achieve a full and comprehensive picture of the system under study. It is also crucial that both light- and heavy-elements can be followed within the same experiment, as illustrated in the *Periodic Table with key X-ray energy ranges* (**Figure 6.1**), to simultaneously interrogate various metal centres and organic ligands, or multiple metal and/or light elements in molecules and materials. Key essential features needed from XFELs for the chemical

sciences include **simultaneous delivery of hard- and soft X-rays**, and the potential to **combine X-ray spectroscopic techniques with X-ray scattering methods**, such as X-ray diffraction, Coherent Diffractive Imaging (CDI) and X-ray photon correlation spectroscopy (XPCS). This combined approach is especially important for surface-related processes including heterogeneous catalysis, and for studies of advanced materials. For both applications (see **Chapters 5** and **8**), techniques for mapping dynamics, both locally and within heterogeneous domains, on the picosecond and even femtosecond timescale will need to be developed. Such approaches will finally enable us to visualise the dynamics in the form of "molecular movies", which will provide vital new insights into mechanisms of reactions and processes in physics, chemistry, and biology.

Since much of chemistry occurs in complex systems, we require the ability to make ultrafast X-ray measurements on systems of varying complexity, ranging from isolated gas phase molecules, nanoscale solvated clusters, and species adsorbed at metal and liquid interfaces, through to large molecular systems in solution. The ability to make ultrafast measurements in such dilute and diverse samples requires both high photon flux and high repetition rates (> 100 kHz). It is also of critical importance that the trigger and the probe pulses are synchronised or time-stamped to < 5 fs.

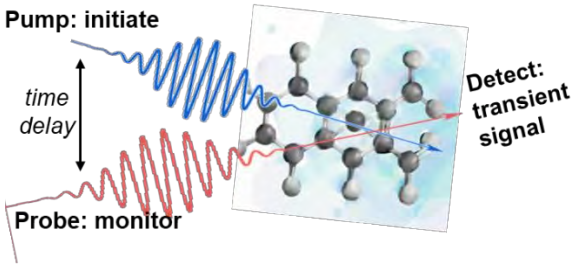


Figure 6.2: Generic pump-probe measurement configuration

It is important to acknowledge that only a small fraction of (bio)chemical reactions can be triggered with (visible) light, and therefore other means of triggering ultrafast reactions need to be coupled with X-ray interrogation techniques, for example a fast temperature jump (T-jump) triggered by an ultrafast laser pulse, vibrational (THz, IR) excitation, electron injection or even another X-ray pulse.

Many pioneering contributions of ultrafast X-ray spectroscopies that bring us closer to the "movie" goal have emerged in the last decade, such as resolving ligand dissociation in small metal complexes with relevance to catalysis,[9,10] vibrational wave-packet dynamics in an Fe-carbene photosensitiser determined via a combination of femtosecond X-ray emission and scattering,[11] the first demonstration of picosecond X-ray absorption spectroscopy to probe ligand binding to heme proteins *in physiological media*,[12] ultrafast spin-change in spin-crossover materials, and single-molecule molecular magnets for new methods of information storage. *Selected examples in which such studies can bring transformative change are discussed below.*

6.1.2 Ultrafast spin dynamics in molecules and biomolecules

The importance of deciphering the interplay of electronic and structural dynamics is well-illustrated in spin-crossover (SCO) molecules[13] containing, for example, $Fe^{2+/3+}$ or Co^{2+} which are able to change the spin-state in response to external perturbation, such as light,[14] temperature, or pressure. The change in spin-states is usually ultrafast, sub-100 fs, and accompanied by a dramatic change in properties: magnetic (ortho/para), optical or structural (one well known example is oxygen binding in heme; the associated changes in bond lengths can be several tenths of an ångstrom). The potential for targeted control of properties by external means opens up diverse applications of SCO in materials and devices, such as magnetic switching,[15] all-optical magnetic recording in iron garnet,[16] or photocatalytic CO_2 reduction (**Section 6.4**).

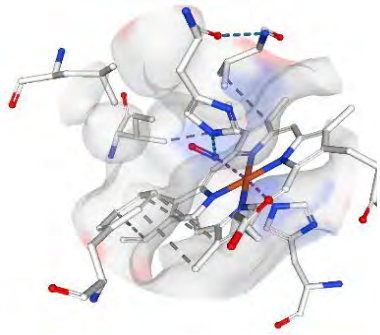


Figure 6.3: Nitrosyl Horse Heart Myoglobin. --- show bonds which reversibly form and break. Source: PDB 2FRJ

An example of the correlated spin and structural dynamics is the dissociation/recombination of NO from/to Fe-centre in Myoglobin.[12] Here, huge advances have been made in following the structures of the short-lived intermediates by XAS and WAXS whilst obtaining spin information by XES (K_β, 3p-1s and K_α, 2p-1s) by monitoring high spin/low-spin transition. For the next step in our understanding of the function of myoglobin (as just one example), we want to follow the formation and breaking of H-bonds (the dashed lines in **Figure 6.3**), and the changes of electron density, not only on and around the Fe centre, but of the ligand/protein itself, in real time. This major task calls for higher sensitivity, high repetition rate and, crucially, multiple detection, bringing in correlative XAS and XES methods, and RIXS to follow the changes in the ligand itself.[17]

In materials, the coupling between electronic and structural degrees of freedom is at the origin of the emergence of functions that can be triggered by direct or indirect excitation of various degrees of freedom, such as spin, electron, phonon, and lattice. These ultrafast phenomena affect various properties such as conductivity, magnetism and ferroelectricity. Understanding the complex out-of-equilibrium dynamics induced by light in these diverse systems requires both detailed calculations and molecular model compounds. Polynuclear metal complexes can serve as mimics of materials such as transition metal oxides, two-dimensional dichalcogenides, charge- and orbital-ordered manganites (anti-to-ferromagnetic phase transitions,[18] cyano-bridged photomagnets,[19] or mixed transition-metal/lanthanides).[20]

The fundamental understanding of the structure-function relationship requires the interplay between the oxidation states, the electron density distribution along the molecule or material, the spin-states, and the geometric changes to be resolved for (ideally) all atoms involved on ultrafast time-scales. The next-generation XFEL's high repetition rate and brightness will enable optimisation of new non-linear X-ray and optical/X-ray experiments. Together with the tunability, and the ability to track changes in several metal centres and organic components by simultaneous detection in several spectral regions, these experiments of the future will enable new hitherto inaccessible insights, principally into charge-transfer/electronic (such as change in oxidation state), structural and spin dynamics, and, ultimately, chemical reactivity.

6.1.3 Ground-state chemistry and solvent-solute interactions

A major challenge across chemical science is to understand molecular reorganisation in complex environments, in terms of both intra-molecular and environment dynamics. The reorganisation of a molecule's environment influences processes by solvation perturbations and outer-sphere molecular co-ordination, and often dictates transition states, chemical outcomes and product state distributions. However, addressing these problems is technologically challenging. One example is the current technological limitations of a powerful method of vibrational spectroscopy. Inter- and intramolecular vibrations underpin *any* chemical reaction, with low-frequency motions of a 10 – 400 cm^{-1} often postulated to be the key reaction coordinate. Current laser technology provides time-resolved IR capability, but with limited spectral coverage; at present, the region below ~ 800 cm^{-1} is inaccessible. An XFEL enables a fully temporally resolved 4000 – 1 cm^{-1} spectral coverage, which would open up the so far impossible studies, including: large collective motions of proteins, such as alpha helical stretches; hindered rotations of solvent molecules which influence solvent reorganisation dynamics in liquids; the direct probing of metal-carbon and metal-metal atom motions in surface science; and identification of key biologically active radical species during DNA strand breaks.



Figure 6.4: Different motions contributing to the solvation of species formed in 220 nm photolysis of BrCN in perfluorohexane.[26]

Reprinted with permission from Springer Nature: M. Grubb et al. Nat. Chem. 8, 1042-1046 (2016) DOI: 10.1038/nchem.2570 Copyright (2016)

The vast majority of chemical transformations are thermally activated, but how can one trigger it in order to resolve structural dynamics? The ability to trigger a reaction in the electronic ground state by, for example, ultrafast T-Jump, a THz or IR pulse, and to follow the accompanying structural, electronic, vibronic and spin changes on the ultrafast timescale *simultaneously* would be of tremendous fundamental and practical importance in understanding chemical reactivity. Ultrafast structural dynamics on the ground state potential energy surface can be investigated following photoexcitation and relaxation to the ground state, as shown by ultrafast X-ray scattering on a dinuclear Pt complex in solution,[21] a deep-UV triggered ground-state ring-opening dynamics of 1,3-cyclohexadiene in the gas phase,[22] or a reaction of sulfine in its hot ground state leading to as many as nine different products within < 1 ps.[23] *An XFEL coupled to an array of pump sources (THz – UV) and with high repetition rate, high brightness and broad spectral coverage, which will enable multiple-detection methods from the same sample, will open up such studies to multiple classes of chemical reactions in all states of matter.*

Photoinduced isomerisation reactions (a class of reactions that everyone is familiar with because of its role in vision), are one notable example of reactions with ultrafast structural changes. Recently, one sub-type of such reactions, ring-opening reactions, was investigated via time-resolved photoelectron spectroscopy with a seeded XUV FEL: the experiment traced the ultrafast ring opening of a thiophene molecule in the gas phase after 265 nm excitation, and showed that the initial ring opening and non-adiabatic coupling to the electronic ground state was driven by ballistic -S-C- bond extension within 350 fs.[24] These XFEL experiments provide unprecedented insights into both the electronic and the nuclear dynamics of this fundamental class of reactions, and illustrate how a similar approach can be used to follow almost any reaction. More complex systems will need X-ray spectroscopic probing at multiple atomic edges to fully follow and resolve all aspects of their complex and entangled dynamics.

The structure of solute species and the solvent around them is fundamental to the understanding of the multitude of chemical reactions that take place in solution, with various optical spectroscopies providing insight into inter-mode coupling and energy transfer.[25] Resolving contributions from rotational, vibrational, and translational modes into overall solvent-solute interactions (**Figure 6.4**) can

also help with understanding of interactions at interfaces and on surfaces.[26] This important field of fundamental research underpins vast areas of chemistry, biochemistry and medicine. X-ray absorption (EXAFS, XANES) is a particularly powerful technique here, owing to its element specificity, its wide-ranging applicability to the characterisation of the local environment of selected atoms in solids, liquids and even gases and its high sensitivity, which makes it applicable to local structural studies from ultra-dilute to pure substances.

The local environment is also of crucial importance in light-emitting materials – with a recent demonstration of ligand-mediated quantum yield enhancement in one-dimensional silver organothiolate metal-organic chalcogenolates, where exceptional brightness of XFELs permitted to resolve the role of Ag–O distance in emission enhancement using small molecule serial femtosecond X-ray crystallography (sm-SFX).[27]

The nature of vibrational energy redistribution in molecules and materials following an external perturbation, or within a product of a chemical reaction, is an important fundamental question. 2DIR-spectroscopy is now broadly used to answer this question, by following changes in vibrational frequencies, but it requires specific IR-reporting groups. Use of time-resolved X-ray spectroscopy on the sub-10 ps time-scale to directly detect changes associated with the movements of C, N, and O-atoms, in combination with 2DIR data, will allow "molecular movies" of ground state catalysts or proton transfer reactions to be delivered, or photoisomerisation pathways in proteins to be followed.[28]

6.1.4 Organic reactions, protein dynamics, DNA damage and photoprotection

Light elements, C, O, N and H, play a key role in all processes around us; in photosynthesis, in free radicals in biology and medicine, in DNA damage and photoprotection, enzyme catalysis or drug-target interactions, and in fundamental organic photochemistry in gas phase and solution-phase.[29] This prevalence of light elements represents one of the major challenges in investigations of ultrafast structural, electronic and spin dynamics, which makes it extremely important to have access to all organic molecules via C, N, and O-edges. We must deliver the "molecular movie" in this area of research without relying on heavy elements, an extremely challenging task which can be solved with the next-generation XFEL providing access to the $n\pi^*$ and $\pi\pi^*$ excited states that are present in virtually every organic molecule and building blocks of life.

An example of ultrafast molecular transformation involving light molecules is the dynamics of –S–S– bridges in proteins that respond to photoexcitation and oxidative stress. How does –S–S–bond cleave? What is the sequence of steps in radical/ion formation, and recombination? Is structural change following the primary photo-chemical event or vice versa? fs-TRXAS studies showed that a model molecule, dimethyl-disulfide $H_3C–S–S–CH_3$, undergoes direct dissociation to two $H_3C–S–$radicals within 120 fs upon UV-excitation.[30] This pioneering work on small molecules prepared the ground for investigating the dynamics of disulphide bridges in (photocaged) proteins, and under physiological conditions. However, translating this experiment to real biological systems is a big challenge: real systems will have orders of magnitude lower "concentration" of the –S–S–groups, are delicate, have only limited amounts of samples, and samples need to be interrogated before significant radiation damage occurs. These requirements demand high average photon flux and high, 10 – 100 kHz, repetition rate to ensure the necessary sensitivity, and can only be achieved at an XFEL.

High sensitivity and ~ 1 fs time resolution would enable direct mapping of structural changes as the system evolves through conical intersections (CIs), which are postulated but rarely[31] observed experimentally in the majority of reactions, occurring on the ultrafast timescale away from Born-Oppenheimer approximation. CIs dominate the pathways and outcomes of virtually all photophysical and photochemical molecular processes. Despite extensive experimental effort, CIs have not yet been directly observed, and the experimental evidence is being inferred from fast reaction rates and some vibrational signatures. Theoretical work by Mukamel *et al.* proposes that short X-ray (rather than optical) pulses can directly detect the passage through a CI with adequate temporal and spectral sensitivity.[32] To precisely time the CI and map the energy differences, a molecular system has to pass a CI that is in close vicinity to the Franck-Condon point. The work suggests that transient

redistribution of ultrafast electronic coherences in attosecond Raman signals (TRUECARS), a novel extension of time-domain coherent anti-Stokes Raman spectroscopy (CARS), commonly used to probe vibrational coherence, is an ideal tool to investigate ultrafast, photophysical system dynamics. The experimental parameters required – broadband sub-femtosecond X-ray pulses with spectral widths of several eV – can only be realised from state-of-the-art XFELs.

Recent pioneering work on organic excited states[33] demonstrated how a combination of time-resolved Auger electronic spectroscopy with TR-NEXAFS resolve structural and electronic changes induced by UV-excitation in the nucleobase thymine (**Figure 6.5**), establishing the elongation of –C–O bond and non-adiabatic transition from ππ* to the "dark" nπ* state. Such direct observation of non-adiabatic dynamics in small molecules is unprecedented, whilst detecting dark states is intrinsically hard in optical spectroscopy. The ultrafast soft X-ray capability at a next-generation XFEL will enable the next step of this research: moving from individual nucleo-bases to DNA, understanding DNA damage. One step further will be real-time imaging of DNA damage/repair in living cells, and watching the action of light-activated therapy, such as PDT or antimicrobial treatment, in real time.

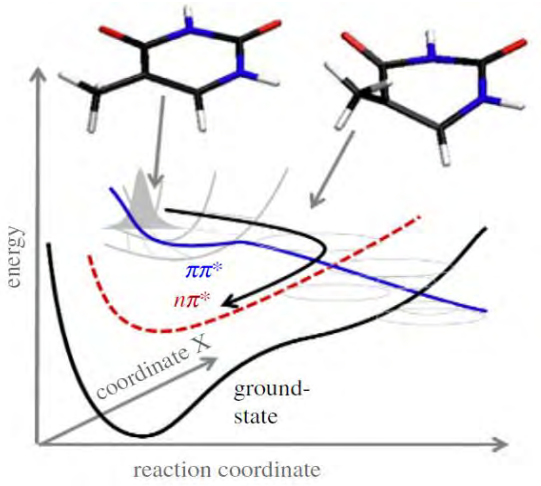


Figure 6.5: Photochemistry of DNA
TR-AES and TR-NEXAFS reveals possible relaxation paths a ππ state of thymine populated by UV-pulse, to the dark nπ* state and to the ground state via conical intersections.[29]*

Figure reproduced from T.J.A. Wolf et al. "Probing ultrafast ππ/nπ* internal conversion in organic chromophores via K-edge resonant absorption". Nat. Commun. 8, 29, (2017), licensed under Creative Commons CC BY 4.0*

With regard to extending the power of XFELs to investigating light elements and protein dynamics, recent groundbreaking work with femtosecond crystallography at XFEL of the phytochrome from *Deinococcus radiodurans* demonstrated that ultrafast proton transfer may act as a relay to channel photoexcitation energy to the protein matrix, thus giving a "remote control" mechanism to transduce cofactor signals to their hosting enzymes.[34] The structures reveal a space-conserving mechanism for rotation of the D-ring in the excited state, in which a rearrangement of a conserved hydrogen bond network occurs within 300 fs, which precedes the isomerisation reaction of the chromophore.

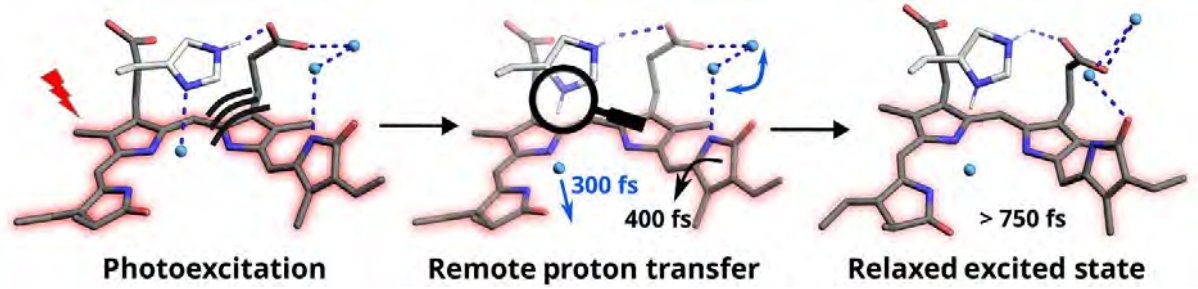


Figure 6.6: Scheme of remote-controlled proton transfer and rotation of D-ring
Photoexcitation of the biliverdin chromophore (in sticks) leads to an ultrafast change of protonation at His^{260} (left side: with epsilon hydrogen bond; middle and right side: with both epsilon and delta position with hydrogen atoms), which is not part of the photoexcited π-system. This change in configuration is the driving force behind the movement of the key pyrrole water molecule in the binding pocket and occurs within 300 fs, while the rotation of the D-ring takes 400 fs. The right side shows the relaxed excited state structure, which is observed after 750 fs.

Reproduced from: M.K. Shankar et al. Science Advances, 2025, 11 (42), DOI: 10.1126/sciadv.ady0499

6.1.5 Fundamental dynamics of energy and charge, coherent and optical control of reactivity

The development of new chemical processes relies on the advancement of our mechanistic understanding of chemical change in complex systems. Ultrafast chemical reactions are often mediated by the complex non-adiabatic couplings between electronic and nuclear motions that occur when the Born-Oppenheimer approximation breaks down. As already mentioned above, since chemical change occurs on the timescales of nuclear motion, femtosecond time resolution is a key requirement for relevant experimental techniques. Combining non-linear methods, multi-pulse optical and X-ray spectroscopies, on the femtosecond scale will enable tracking of the evolving spin structural, and electronic landscape following the trigger.[35]

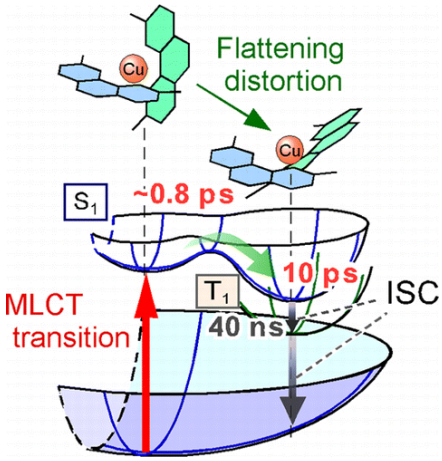


Figure 6.7: Light-triggered distortion in a Cu-complex. Ultrafast nuclear, spin and electronic, dynamics are convolved.[37]

Reprinted with permission from the American Chemical Society: M. Iwamura et al. Acc. Chem. Res. 48, 782, (2015) DOI: 10.1021/ar500353h. Copyright (2015)

Transition metal complexes, differently to organic entities, often undergo ultrafast intersystem crossing (ISC), leading to long-lived triplet excited states which determines their applications in photocatalysis (the prime examples are Re(I) and Ru(II) complexes for CO_2 reduction, or Ir(III) complexes for H_2 production), in Phosphorescent Organic Light Emitting Diodes (PhLEDs), or in photodynamic therapies (Pt, Ir, Ru). As excited states evolve, ultrafast structural, electronic, spin and vibrational dynamics occur simultaneously. To follow such simultaneous processes requires multi-pulse experiments, where each parameter can be probed independently after a common trigger. For example, the mechanism of ultrafast ISC is likely to involve spin-vibronic effects, as spin-orbit and vibrational coupling occur on a similar ultrafast timescale.[36]

Time-resolved X-ray studies, using a variety of available methods, have been conducted on e.g. Cu-complexes which exhibit huge structural change in the excited state (**Figure 6.7**),[37,38] on di-nuclear Pt(II) photocatalysts,[39,40] and on a multitude of Fe complexes (see ***Spin dynamics***, **Section 6.1.2**), all of which demonstrated complex dynamics. It is hoped that ultrafast multi-pulse X-ray studies with optical triggering, combined with linear and non-linear spectroscopies in the THz – UV range, will allow the identification of the reaction coordinates responsible for the ISC in transition metal complexes, as well as in photo-functional materials. Here, an XFEL will bring in element-specific information, for several elements at the same time, and the ability to interrogate the same sample with multiple methods (structural and spectroscopic) simultaneously. The ability to perform ultrafast (fs) X-ray studies with multicolour X-rays, combining for example detection of two metal edges, or a metal and the ligand, in the same experiment, will allow for a reliable understanding of photochemical dynamics – as, for example, in the recent work which utilised ultrafast two-colour X-Ray emission spectroscopy to reveal excited state landscape in an Fe–Co metal dyad, in which the iron part acts as a photosensitiser, powering up the cobaloxime catalyst.[41]

The ability to control chemical reactivity is one of the holy grails of chemistry. Diverse methods have been designed to achieve this goal (some of which are covered in ***Attosecond science***, **Section 3.3**), such as coherent control[35,42] or bond-specific perturbation in molecules undergoing photoinduced electron transfer[43] and in organic PV materials.[44] Various degrees of control of chemical reactivity have been achieved, yet the mechanisms of such controls remain elusive, especially in the condensed phase. Ultrafast multi-pulse and nonlinear structural methods will enable us to resolve vibrational and vibronic coupling in charge and energy transfer reactions, identify reaction coordinates, follow energy transfer from one vibronic mode to another, and visualise where exactly the energy and charge are distributed along the molecules, in space and time, and which reaction pathways are driven by what vibrations. Long-term, it may also bring about rational control and design not only of new classes of molecules, for example, as single-molecule magnets or molecular conductors, but of yet unimagined photo-functional materials, bringing us one step closer to fulfilling the dream of “reactivity at will”.

6.1.6 Conclusions and future vision

Our vision for chemical dynamics is to open new horizons in science and technology, which rely on the currently hidden understanding of chemical change at a molecular level on the ångstrom scale with femtosecond precision.

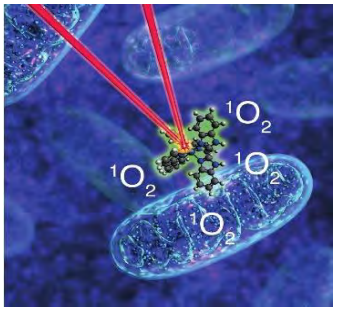


Figure 6.8: NIR two-photon activated killing of cells with a metal complex.[45] Could we follow the PDT action in real time?
Figure reproduced from L.K. McKenzie et al. Chem. Eur. J. 23 (2017) DOI: 10.1002/chem.201780262

The open questions in chemical dynamics range from rare events in gases to energy propagation in condensed media, the intermolecular mechanisms that control DNA damage and organic reactivity, and the drug-target interactions. Resolving electron-, spin-, and structural dynamics simultaneously is essential to answer these questions. An exciting example of future research, which is currently consigned to science-fiction, would be real-time observation of anti-cancer or antibacterial drugs in action at the interface with medicine and structural biology (see **Chapter 7**). Recent advances of transition metal complexes as anti-cancer PDT[45] (**Figure 6.8**), and antibacterial agents[46] started a whole new area in photomedicine and antimicrobial sciences. Using Cryo-EM, correlative microscopy or AFM,[47] it has so far been possible to determine the action of such agents only on fixed samples. The ability to track each step and electronic and structural changes of the agent and the sub-cellular structures in real time, in live objects, will bring an entirely new perspective to our understanding, treatment, and potentially even prevention, of diseases.

An XFEL will also facilitate a step-change in time-resolved ambient pressure photoemission of light elements, most notably including C, N and O, which are the backbone of organic and biological molecular systems. Developing a sustainable economy will rely on deep understanding of their natural genesis and control of chemical and physical transformations to commodities and value-added products. Reaction engineering with homogeneous and heterogeneous catalysis is expected to play an important role here, and XFEL insight to the real-time dynamics in solutions and at interfaces will facilitate a transformative advance, with research spanning the whole range of Life, Physical and Engineering Sciences. An example of research into high value-added applications is solar energy conversion devices, including hybrid organic/inorganic perovskites and their interfaces with transition metal oxides. Understanding the dynamics of element- and functional group-specific recombination paths is paramount for improving efficiency, i.e. we need to determine the polaron dynamics in the metal oxide,[48] as well as electron and hole transport to the electron- and hole collectors.

Another application area is in the broad range of catalytic processes associated with metal-oxide surfaces. Taking photocatalysis as a flagship example, application of ARPES (see **Section 5.4**) to the oxygen evolution reaction on an oxide surface will enable one to follow the decomposition of water and the formation of intermediates on a fs-ps timescale by monitoring the chemical shift of the O 1s ARPES peak. At 4 keV the escape depth of O 1s photoelectrons in water is approximately 9 nm, allowing bulk-like liquid films to be used to study photocatalysis, electrocatalysis, or corrosion. The information from ARPES is complementary to that obtained by X-ray absorption spectroscopy, because it is sensitive to the element specific chemical state near the surface, enabling a complete mechanism of interface processes to be resolved for the first time. The capability to perform time-resolved ARPES at > 3 keV will be unique. Critically it will benefit from the high repetition rate of an XFEL to allow sufficient data rates whilst limiting distortions from space charge. One scenario is to use the 3rd or 5th harmonic of a high-repetition rate seeded XFEL to provide the required high spectral purity, high data rate and moderate pulse energy needed for these measurements.

The key facility features that will enable these breakthroughs include seeded/transform-limited high-repetition-rate operation (>100 kHz), high brightness, broad spectral coverage, THz-IR-Vis-VUV laser sources synchronised to sub-5 fs, and the ability to simultaneously interrogate the process of interest with multiple methods, combining spectroscopic (local information) and structural methods. These capabilities will allow us to understand and control chemical dynamics and tailor it to our needs.

6.2 Exploring complex energy landscapes through chemical activation

Physical, chemical and biological processes are governed by interactions across complex potential energy surfaces. Understanding these surfaces is fundamentally important for everything from chemical reactivity and protein folding, through to crystal structure prediction and developing new materials and pharmaceuticals. To understand these surfaces in ever greater detail, across multiple length and time scales, we need new experimental tools that can demonstrate control over the electronic, spin and vibronic degrees of freedom of a material, to engineer novel transient states of matter with exotic properties only achievable in an out-of-equilibrium regime, and explore new phases and types of materials.

6.2.1 Introduction

All chemical processes are governed by dynamics that occur across complex energy landscapes. These landscapes need to be understood across multiple length and timescales. Ultrafast events, that happen on the shortest timescale, ultimately control changes and reaction outcomes on the much longer timescales, hence understanding of such ultrafast processes is critical for any chemical understanding. To understand the mechanisms behind, for example, chemical reactions, ultrafast magnetisation, phonon-triggered changes in structure, photoinduced processes within materials and at interfaces, we need to be able to measure these ultrafast changes in real time on the timescales from a few femtoseconds to tens of picoseconds. The ultrafast X-ray methods enabled by an XFEL are perfect tools for probing this diverse range of processes at molecular, supramolecular and bulk level, as they capture all the timescales of changes in any complex matter system while providing a probe that is sensitive to both the structural and the electronic change, making an experimental survey of such complexes energy landscapes uniquely possible. However, applying these extremely powerful XFEL-based techniques to a diverse range of molecules, materials and devices also requires a versatile range of synchronised ultrafast pump sources in order to initiate the process of interest. Such pump sources include optical pump fields from the THz to XUV and pulse electron beams, as each such pump sets in motion unique dynamics and consequently, leads to a unique chemical and material change. A powerful combination of XFEL capabilities with the diverse initiation techniques will drive significant advances in the diversity of systems that can be studied as well as of the types of reactions and processes. Of critical importance is that the pump (event trigger) and probe pulses are sufficiently well synchronised to permit temporal resolution approaching the sub-5 fs limit. This, in turn, would enable complex pulse sequences to be used to build on the more established multidimensional optical techniques[43,49-51] with the inclusion of a single (or multiple) X-ray probe(s) over a range of energies (see **Section 6.1**), which will provide time-resolved structural information that is often only inferred by other measurement techniques. Thus, we emphasize that it is essential that any new light source will provide an array of pump-probe and multidimensional capabilities that will collectively resolve the ultrafast structure and dynamics in a wide range of chemical and material processes.

A number of possible pumping options have been specifically highlighted throughout this Science Case, including THz and IR (**Sections 5.1** and **5.2**), UV (**Sections 6.1**, **6.5** and **7.2**) and X-ray (**Section 3.3**). This section highlights two important options – THz and UV (pulsed elections are discussed in **Section 6.3**) – that provide opportunities for exciting chemical science by providing unique capabilities at an XFEL.

6.2.2 Intense THz excitation combined with ultrafast X-ray measurement techniques

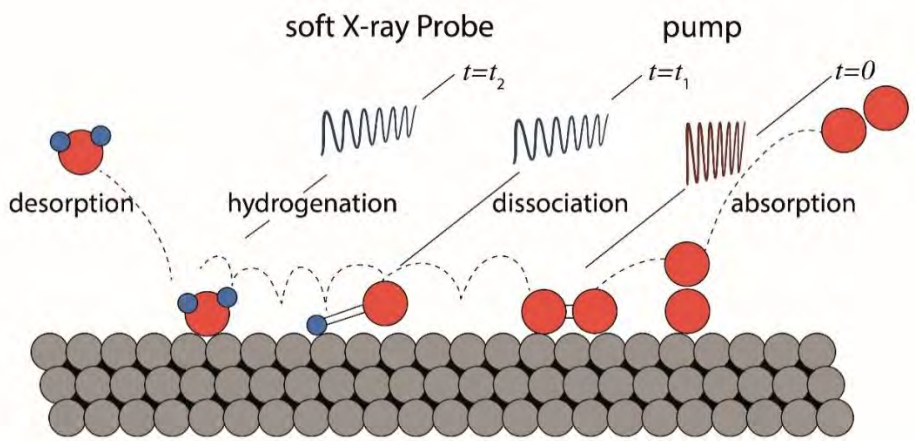
Absorption at THz frequencies (0 – 30 THz) can be complex and is governed by many different physical mechanisms that are fundamentally important to understand. In simple crystalline materials, the absorption is dominated by strongly coupled phonons,[52-54] while in complex crystalline systems, these are mixed with low-frequency internal motions.[55,56] In amorphous materials,[57,58] a large number of

overlapping bands often give rise to a featureless spectral vibrational density of states that is very difficult to interpret — even for apparently simple systems, such as water.[59] THz absorption, however, has shown exceptional sensitivity to long-range order and dynamics, whether in polymorph formation,[60] structural formation in solutions[61] or ionic liquids,[62] as well as sensitivity to enzyme functional dynamics.[63,64]

THz frequency normal modes are particularly interesting because they have been linked to reaction pathways and dynamics in the majority of reactions, with specific examples including the initiation of energetic materials,[57] enzymatic reactions (in particular proton tunnelling[64]), probing solution phase dynamics,[65] solid-state phase transitions in metal-organic frameworks (MOFs),[66-69] materials that exhibit solid-state phase transitions,[51,55,70] and catalytic surface chemistry.[71]

The recent development of a range of methods able to generate intense THz pulses has led to a dynamic research field aimed to manipulate matter.[72,73] Examples relevant to the chemical sciences include the orientation of OCS molecules in the gas phase,[74] THz-induced crystallisation of carbamazepine and indomethacin from an amorphous phase to different polymorphic phases in comparison to temperature-induced crystallisation[75] while recent calculations propose the use of THz pulses for molecular isomerisation control.[76] This has obvious implications in the study of the relative stability of pharmaceutical compounds, but also has the potential to provide a new insight into the important processes of nucleation and crystallisation, which in turn may provide new perspectives to aid first-principles structure prediction – one of the grand challenges of the chemical sciences which is discussed in relation to industry-relevant research in **Section 8.3**.[77]

Box 6.1: Controlling catalytic reactions with THz excitations



An initial intense THz pump pulse can be used to manipulate a molecule adsorbed to a catalytic surface. This initiates a reaction that is then probed by a series of time-delayed optical and X-ray pulses, which can be used to provide both spectroscopic and structural information of all the active species involved in the entire catalytic reaction pathway, in real time. This is crucial information to aid the design of next-generation efficient and sustainable catalytic materials.[71]

Figure reproduced from A. Nilsson et al. "Catalysis in real time using X-ray lasers." Chem. Phys. Lett. 675, 145-173 (2017) under the terms of a Creative Commons Attribution 4.0 International License. DOI: 10.1016/j.cplett.2017.02.018

Measurements have also demonstrated that high-field THz pulses can promote specific reaction pathways on a catalytic surface, by strongly interacting with molecules adsorbed on a surface or with the electron bath of the catalytic surface; for instance, selectively inducing CO oxidation on a Ru(0001) surface (see **Box 6.1**, on controlling catalytic reactions).[71,78] Similarly, more recent work shows the use of a resonant THz/IR pulse to achieve tunable surface wettability with the potential to control surface catalysis.[79] There are also a number of studies that show the manipulation of lattice and spin dynamics, including the discovery of novel phases through the direct manipulation of phonons and magnons using high-field THz pulses (**Figure 6.9**).[50,52,53,80]

In this context, several measurements have used ultrafast X-ray pulses to probe this THz electric-field driven manipulation of dynamics (see **Figure 6.9**) in materials. In $BaTiO_3$, the modulations of the ferroelectric polarisation[81] were detected, while in $SrTiO_3$ coupling of phonon modes[53] a metastable ferroelectric phase,[52] multiferroicity[82] and polarization density waves[83] have all been observed. These studies are, however, limited by the range of accessible Bragg reflections, and by the signal-to-noise at current XFELs. Extensions to higher energy (> 25 keV), using PDF approaches, or to higher repetition rate (for both XFEL and THz sources), would provide the first direct visualisations of these local atomic-scale motions — a crucial step in making these experimental tools useful for practical exploration of increasingly complex materials.

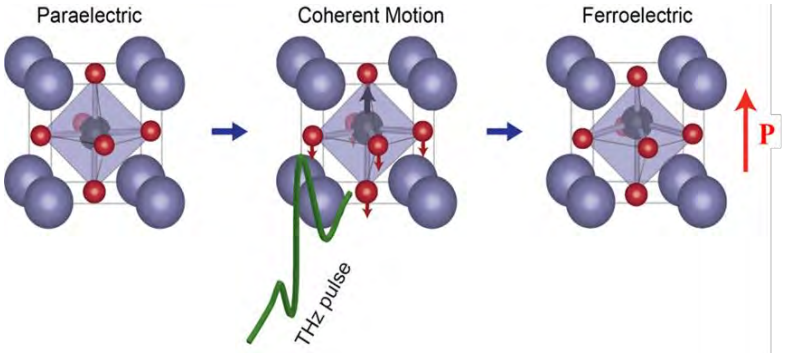


Figure 6.9: A single-cycle THz electric field which moves all the ions it encounters toward their positions in a new ferroelectric crystalline phase. In STO, the initial high-symmetry configuration around each Ti^{4+} ion has no dipole moment and the crystal is paraelectric. The incident field drives the "soft" lattice vibrational mode, moving the ions along the directions indicated into a lower-symmetry geometry with a dipole moment.[52] This ion movement can be probed directly with X-rays.

Figure reproduced from X. Li et al. "Terahertz field–induced ferroelectricity in quantum paraelectric $SrTiO_3$." Science 364, 1079-1082 (2019) DOI:10.1126/science.aaw4913

What is particularly exciting is that, in all these studies and more, THz pumping has enabled the exploration of the complex energy landscapes that underpin reactivity and dynamics. These systems do not require the chromophores needed for most optical excitation, suggesting that the THz excitation could become a universal pumping source for the majority of materials. Importantly, the low energy of THz radiation, coupled with the high peak electric (< 100 MV cm^{-1}) and magnetic fields (< 33 T) that can be generated, may provide a universal way to manipulate matter without the excess energy associated with optical excitation.[71,78]

Revolutionary advances in THz generation make the prospect of THz-manipulated chemistry even more appealing, and within reach.[84] THz radiation has the ability to manipulate matter on an ultrafast timescale and provides the capability to achieve insight into the fundamental dynamics of processes, which in turn can be used to underpin the future rational design of materials with tailored physical and chemical properties.

6.2.3 Magnetic fields enable new generation data storage

Magnetism in novel nanoscale materials is a key ingredient in modern information technology. Manipulating magnetic materials is the cornerstone of hard drive technology, where binary digital information is recorded by aligning the direction of the magnetic poles in the hard drive. New technologies are urgently needed, in large part due to growth in AI and data centres. The recent forecast from the International Energy Agency (IEA) predicts an increase of the electricity demand by the data centres from 206 TWh in the period 2020-2025, to 465 TWh in the period 2025-2030 (cf. approx. 5500 TWh total demand in this period).[85] With the ever-increasing use of big data for driverless cars, robots, video surveillance, artificial intelligence etc, there is a coupled need to develop new generation data storage devices.

Recent developments in ultrafast magnetism have resulted in photo-magnetic recording in materials which has the distinct advantage of faster sequential switching rates due to the non-thermal

mechanism.[86] These experiments make use of specific optical transitions, exciting the electrons from one atomic orbital to another, which in turn changes the magneto-crystalline anisotropy.[86] However, the microscopic mechanisms responsible for such behaviour are difficult to understand because they involve a high density of electronically excited states, vibrational motion, and different spin states, which are all highly coupled (see **Section 6.1**). At present, this lack of detailed understanding is hindering the development of new materials to achieve fast, energy-efficient operation and also miniaturising the magnetic grains towards the nanoscale.

The capability of fs X-ray spectroscopy will facilitate unprecedented new insights into the mechanism of action in emerging photo-magnetic materials, such as the trinuclear single-molecule magnets $[Mn^{III}_3O(Et\text{-}sao)_3(\beta\text{-}pic)_3(ClO_4)]$,[87] as performed for light-induced excited spin-state trapping (LIESST) systems.[17,88] In this case, the excitation of a vibrational wavepacket, closely associated to the Jahn-Teller distortion (**Figure 6.10)** was found to be closely linked to the magnitude and orientation of the magnetic anisotropy. These results highlight the strong coupling between electronic and nuclear degrees of freedom, and the strong electron correlation between electrons on several Mn sites in the polynuclear molecule, important for the photo-magnetic properties. The ability to probe the electronic (XAS, XES), structural (XAS) and spin (XES) dynamics of these complex materials and related analogues on the timescale upon which they operate, i.e. femtoseconds, will enable fine control of the magnetic properties and coherence times of these materials, and provide crucial new insights urgently required to develop new storage materials.

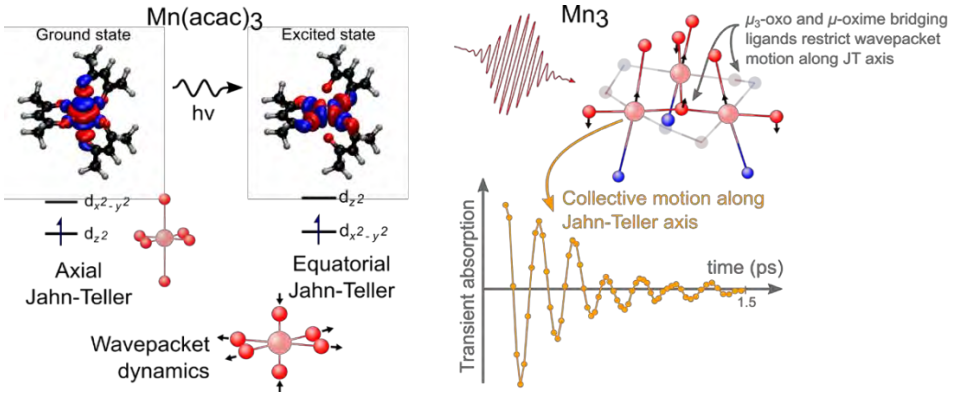


Figure 6.10: Photophysics of Mn^{3+} complexes. The antibonding nature of the e_g orbitals lead to a rapid switch of the JT distortion in the excited state of $Mn(acac)_3$ (left). In Mn_3, the strong bonds in the triangle prevent equatorial expansion and the Mn ion (right).[87]

*Figure courtesy of Thomas Penfold, reproduced from F. Liedy et al. "Vibrational coherences in manganese single-molecule magnets after ultrafast photoexcitation" Nat. Chem. **12**, 452-458 (2020), Springer Nature. DOI: 10.1038/s41557-020-0431-6*

Light-induced spin-state switching in so-called Single Ion Magnets (SIM) has been recently investigated on the prototypical complex $[Co(terpy)_2]^{2+}$ (terpy = 2,2′:6′,2″-terpyridine) in solution phase. A combination of ultrafast optical absorption spectroscopy and X-ray emission spectroscopy allowed for tracking the photoinduced processes: the complex undergoes a spin-state transition from a tetragonally elongated doublet state to a tetragonally compressed quartet state on the femtosecond timescale, i.e. it sustains ultrafast Jahn-Teller (JT) photoswitching between the states of two different spin multiplicities. This discovery greatly widens the possibilities for implementing magnetic multifunctionality and eventually controlling ultrafast magnetisation with optical photons.[89]

A comprehensive insight into ultrafast dynamics of photo-switchable materials is desired for efficient control of material properties through light excitation.[90] Recently, advances in femtosecond diffraction methods (**Figure 6.11**) enabled capturing ultrafast molecular motions and lattice dynamics in spin crossover films. The study followed a polycrystalline spin crossover thin film as a prototypical example and reveal the sequential photo-switching dynamics, from local molecular rearrangement to global lattice deformation. On the earliest femtosecond timescale, the local molecular structural rearrangement occurs within a constant unit-cell volume through a two-step process, involving initial Fe–ligand bond elongation followed by ligand rotation. The highly-oriented structure of the

nanocrystalline films and the experimental geometry enables resolving the full anisotropic lattice structural dynamics in and out of the sample plane separately. While both molecular switching and lattice heating influence lattice volume, they exert varying degrees of impact at disparate timescales following photoexcitation. This work highlighted the opportunities provided by MeV electron and X-ray free electron laser to advance the understanding of ultrafast dynamics of photo-switchable materials, moving one step closer to applications in photo-functional materials and information storage devices.

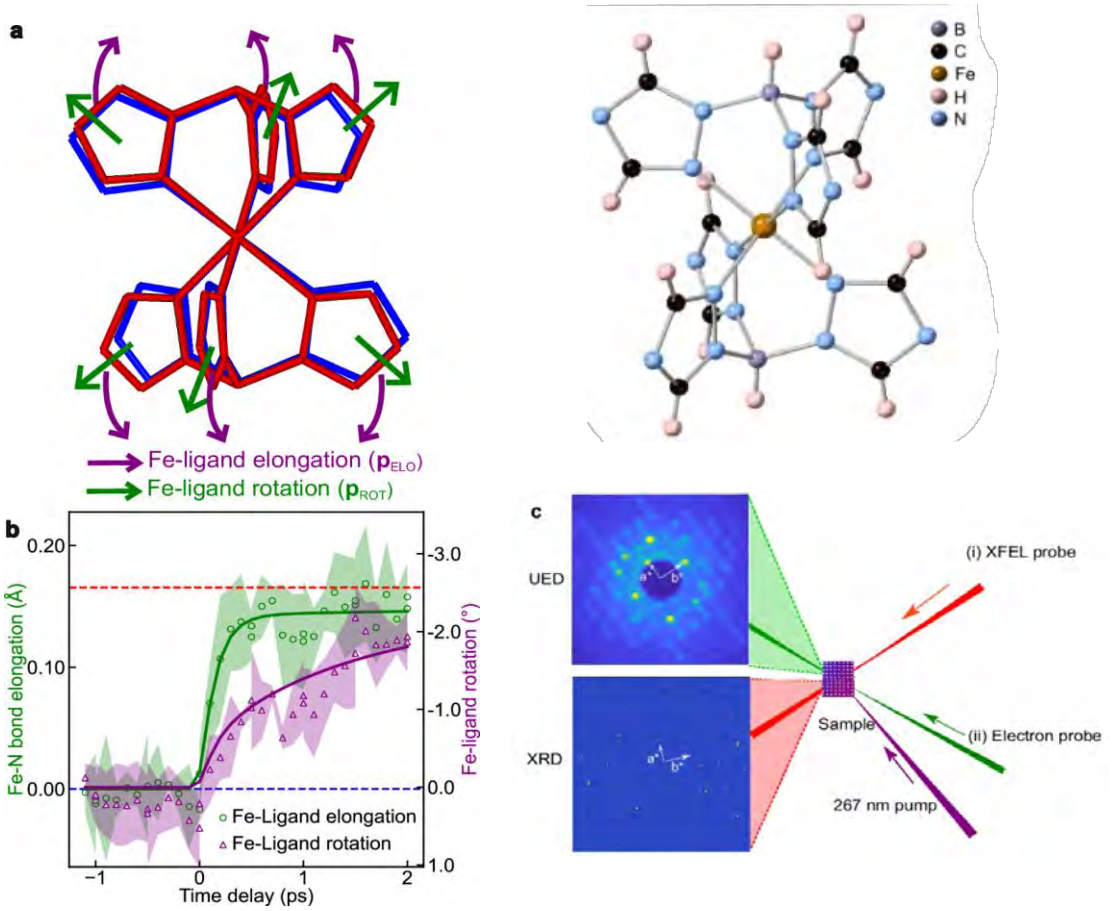


Figure 6.11: Capturing ultrafast molecular motions and lattice dynamics in spin crossover film using femtosecond diffraction methods

Top right – structure of the SOC Fe complex (1). a Structures of the molecule in the LS state (in the LT unit cell) (blue smooth lines) and in the HS state (converted into the same LT unit cell) (red fluted lines). The atomic motions are decomposed into two structural dynamics groups schematised by arrows: symmetric Fe–ligand elongation with the rigid ligands (pELO) and ligand rotation toward the HS structure (pROT), b Temporal evolution of the Fe–ligand distance (average length of the Fe–N coordination bonds, green open circles) and of the ligand rotation (average N–Fe–N angles, purple open circles) in the ultrafast timescale (from −1 to + 2 ps). Solid lines show the fitting curves using multi-exponential decay functions. Horizontal dashed lines correspond to the structural parameters in the HT phase (373 K) and LT phase (300 K), respectively. Error bars represent the full-width at half-maximum (FWHM) of the global maximum peaks of the Pearson correlation coefficient in reaction coordinate space. C. Schematic of the experimental setup and representative diffraction images. After photoexcitation with 267-nm pump pulses, the structural response of 1 was measured separately by (i) ultrafast XRD at an XFEL and (ii) MeV-UED.

*Reproduced from Vinci, D., Ridier, K., Qi, F. et al. Capturing ultrafast molecular motions and lattice dynamics in spin crossover film using femtosecond diffraction methods. Nat Commun **16**, 2043 (2025), under the terms of a Creative Commons Attribution 4.0 International License. DOI: 10.1038/s41467-025-57202-0.*

6.2.4 Conclusion and future vision

While the recent science enabled by the development of pumping sources is ground-breaking, the introduction of high-field THz, IR and optical/UV sources at high repetition rates (up to 100 KHz), available at the X-ray interaction point (with > 10^{12} X-ray photons per pulse) for complex multi-pulse experiments, is unprecedented. An accelerator-based THz source in particular would provide unparalleled control of bandwidth, pulse width and field in a spectral region that has been underutilised to date. This, in combination with a range of synchronised laser-driven, optical, infrared, THz and HHG based sources, will be a world-first, enabling a vast amount of new science by exploration of potential energy landscapes for increasingly complex materials using novel experimental tools that combine these pump sources with multiple, in-situ spectroscopic probes, simultaneously. However, the nature of these complex multi-pulse measurements means that the importance of sample environment and delivery should never be underestimated, with some important points discussed further in **Section 9.2**.

One future exciting research direction that a facility of this kind could enable would be the use of intense THz excitation to manipulate biological systems. An example of this approach is the potential disruption of H-bonding in a solvent network surrounding a protein whose structure has already been probed by low-intensity THz radiation.[61,108] Another example is through the THz pumping of enzymatic promoting modes[63] which have long been suggested as directly linked to the reaction coordinate in complex enzymatic reactions, particularly where electric field controlled catalytic mechanism are thought to be involved and these high peak THz-fields could be used to resonantly (and non-resonantly) influence the reaction pathway in these complex bio-materials. All the examples discussed here, and more, require a high-field (> 100 MV/cm), narrowband and tunable THz pump source that could be used to selectively excite specific modes in a material, combined with a plethora of broadly tunable XFEL and laser-based sources for providing ultrafast spectroscopic and structural information as the material changes. This research would require a tunable accelerator-based THz source (> 10 μm) combined with laser-based systems to achieve shorter wavelengths.

6.3 Pulse radiolysis and radiation damage mechanisms

A next-generation XFEL equipped with synchronised electron, proton and neutron beams coupled with ultrafast X-ray pulse pairs will provide a powerful new tool for the study of the mechanisms of radiolysis and radiation damage in materials. It has the power to fully resolve the complex multi-timescale chain of events from the initial physical processes (attosecond – femtosecond) through to the longer time-scale chemical transformations (picosecond – microsecond) of radiolysis and radiation damage.

6.3.1 Introduction

Radiolysis of a material, either directly by electron beams, ion beams (including protons), or high-energy photons (e.g., x-rays), or indirectly by neutron beams, is important both scientifically – by providing a means to excite a sample beyond optical and electrochemical routes that will also make underlying mechanisms tractable to ultrafast measurement, and technologically – because radiation damage in matter has a pervasive importance across multiple settings where ionising radiation is present, for example radio-medicine and radiobiology, nuclear industry, defence, or space technology and exploration. In contrast to the photochemical dynamics that are the emphasis of most of this chapter, where the primary event is absorption of a photon by the subject molecule, the primary event in radiolysis is ionisation of the solvent/matrix in which a molecule is located, while in very concentrated samples, direct ionisation of the molecule/site itself can also occur to some extent.

The primary event of electron removal in this ionisation trigger will invariably be very fast (femtosecond or attosecond), as is discussed in **Section 3.3** in the context of the impulsive ionisation of gas phase molecules. X-ray attosecond pump pulses that can drive fast core and valence shell ionisation are a viable proxy for fast charged particles, and leverage the use of X-ray pump-probe channels to measure the fastest processes in the chain of events. For instance, it is possible that attochemical processes, driven by the oscillatory forces established by charge migration, may play a role on these fast timescales; the extent to which this is the case remains an open research question – and XFELs are now providing us with the attosecond-resolved pump-probe tools to be able to address this. The fastest steps of the physics of radiolysis including electron solvation, solute-solvent charge transfer and formations of radicals can be captured by such X-ray based methods, with the advantage that they can be captured at the high repetition rate of a next-generation XFEL. Chemical and structural changes occurring on a longer timescale can then be tracked using a combination of X-ray scattering and spectroscopy methods.

The planned provision of synchronised charged particle beams, driven by the PW laser (e.g. at the ES 12 end-station) opens up new prospects to initiate radiation damage exactly analogous to that caused by fast protons/ions in space, and even neutrons in the nuclear industry. Charged particle laser-driven sources, electrons, protons and ions are discussed in **Section 4.3**. Recently, progress has been made towards high intensity laser-driven pulsed neutron sources [91,92] that, combined with an XFEL, would allow unique opportunities to time-resolve neutron damage mechanisms in materials.

6.3.2 Current state of research

The importance of pulse radiolysis in chemistry, established since the early 1960s, was originally due to the complementary nature of the way it activates solutes compared to flash photolysis and electrochemistry. Radiolysis acts primarily by ionising the solvent, with around 2 MeV of energy being deposited per cm for electrons with an energy of ~10 MeV in a medium with a density of 1 g/mL. The resulting charged species (solvated electrons and/or solvent cations) can be rapidly scavenged by the solute.

The importance of solvated electrons was recognised early[93,94] and remains a key part of the mechanistic chain in most situations. Radiolysis is a complex chain of processes occurring over multiple timescales from femtoseconds to many years. Modelling these processes is vitally important as is accurate data to test these models. The early physical and physio-chemical processes happen on attosecond to femtosecond and picosecond to nanosecond temporal scales respectively, with chemical processes then following with inferred (ensemble averaged) rates in the nanosecond to multiple seconds range.

For example, at Brookhaven National Laboratory, USA, the 9 MeV electron accelerator at the Laser Electron Accelerator Facility (LEAF) generates picosecond pulses of electrons. LEAF couples such initiation with time-resolved UV-vis-NIR and mid-IR detection, which allows one to study fast, radiolysis-triggered chemistry.[95,96] Reaching to an even faster domain, a facility in Osaka, Japan, has reported a time resolution to 240 fs with pulse radiolysis.

Radiolysis/radiation damage by ions, protons and neutrons is of importance in many areas including nuclear energy (security of long-term storage), defence, space (resilience of space hardware, astro-data interpretation), fusion (resilience of materials in a reactor) and healthcare (radiotherapy and nuclear medicine) sectors. The Dalton Cumbria Facility (DCF)[97] in the UK seeks to research these issues and is equipped with several continuous beam particle accelerators which are compatible with samples relevant to the nuclear industry, medicine and defence. Currently, DCF has two ion accelerators (5 MV Tandem and 2.5 MV single), that can accelerate protons (10 MeV), α-particles (15 MeV) and $^{6}C^{+}$ to 35 MeV, whilst acceleration of $^{7}Li^{+}$ is used in interaction with a plastic target to provide a 13 MeV neutron beam at low flux. Some opportunities for nanosecond science will be opened up with the planned 70 ns pulse kicker. The XFEL will move this strategically important research into the femtosecond domain.

The importance of radiation biology in medicine has long been established owing to various therapeutic approaches using ionising radiation. From a medical research perspective, there are large differences between the use of photons and ions in destroying tumour cells. The difference in energy deposition between X-rays and protons/ions – with the energy deposition of the former being relatively uniform through the tissue whereas protons have a strong Bragg peak where energy loss leads to very enhanced cross-section. The Laser Hybrid Accelerator for Radiological Applications (LhARA) project seeks to construct an optimised proton source for proton beam therapy applications. High power lasers will generate protons at a 10 Hz repetition rate by target normal sheath acceleration (TNSA), which will then be collimated by an electrostatic lens and accelerated up to 127 MeV in a fixed field accelerator. The operational specification is 10 Hz rep-rate with ion pulses of 10–40 ns duration. For the applications to therapeutics, it is currently believed that delivery of the dose in a shorter time ("FLASH") will ameliorate healthy tissue damage issues. There is evidence that the high dose rate not only spares healthy tissue but is also as effective as the conventional low dose rate at tumour control.

There is considerable activity on TNSA in the UK at the CLF and collaborating universities (University of Strathclyde, Queen University Belfast, and Imperial College London). Based on current results, TNSA may reach ~100 MeV protons with higher energies maybe available from relativistic induced transparency methods. It is anticipated that the proton beam pulse durations will be of the order of ~3 ps. The DiPOLE lasers used in these studies currently operate at 10 Hz, but it is anticipated that the repetition rate will be increased (with some loss in peak power) to 100 Hz in due course. For operating at higher repetition-rates, the use of liquid sheet targets to overcome sample damage is planned. Likewise, ion and neutron beams are anticipated from the same lasers. TNSA has proven to be a robust method with a current maximum energy of ~85 MeV. Relativistic transparency methods that render the target transparent, rather than opaque, to the interaction can boost energy and are currently being investigated, with the promise of delivering proton beams with up to ~150 MeV energy.

These proton sources are being used, for example, in the radiolysis of SiO_2.[98,99] The samples are exposed to protons and probed from the side by a chirped optical beam to build a temporal map of transmission. There is evidence of formation of electrons in the conduction band with < 0.5 ps lifetime. Protons have also been applied to water where solvated electrons are activated by the protons but with solvation time increased compared to photolysis, it is believed the protons may induce cavities by "pushing" water molecules aside.[100] This work is leading to real time analysis of evolving concentrations of radiolytic species.[101] The central tenet of this approach relies on a) the absolute timing fiducial provided by the prompt X-ray pulse from high power lasers interacting with solid targets to b) probe the low momentum transfer for proton interactions in liquid/solid density in real time. The current Gemini laser at the CLF is supporting a range of activity in this area and it is anticipated that EPAC will greatly boost this research.

Regarding short-pulse-duration high-flux neutron sources, the laser-driven methods take the leading role, using a two-step process where electrons are accelerated to relativistic energies via laser wakefield acceleration (LWFA), and subsequently generate neutrons through Bremsstrahlung emission followed by photonuclear reactions in a tungsten converter. This method achieved (in 2025) total neutron yield of 3.9×10^8 neutrons per shot, outperforming the TNSA scheme by several orders of magnitude.[102] With the additional prospect of further enhancements of pulsed neutron sources, there are good prospects for combining a wide range of charged particle interactions with excellent synchronisation to the X-rays at a next-generation XFEL, propelling the field towards higher sensitivity and orders of magnitude better time resolution.

6.3.3 Future opportunities

The application of XFELs to the study of the radiolysis of water has begun with several landmark experiments from the Young group at Argonne National Laboratory, USA. Recent experiments were performed at LCLS with multiphoton ionisation of the valence states of water [103,104] to study the lifetime of the $^1b_1$ hole state. The importance of the processes around the molecular cation: proton transfer, recombination and vibrational relaxation were investigated. In subsequent experiments, attosecond X-ray induced hole dynamics were studied in an attosecond pump-probe measurement with a single time delay (0.6 fs) [105] (see **Section 2.2.3**). Future plans related to the IDREAM (Ion Dynamics in Radioactive Environments and Materials) US DOE Energy Frontier Research Center programme aim to apply these measurements to processes in liquid nuclear waste storage.

Attosecond pump-probe measurements enabled with both hard and soft-X-ray pulses will allow both spectroscopic and structural investigations of the primary events of radiolysis and radiation damage. These methodologies can be applied to gas and liquid phase molecules as well as condensed phase systems (see **Section 9.4 Flagship Programme II).** As the radiolysis is driven by fast X-ray ionisation of the sample the full repetition rate of the end-stations (~ 100 kHz) should be achievable for these measurements significantly increasing sensitivity for the detection of short lived and rare transient species. Both gas and condensed phase studies would be enabled by this capability with the possibility to resolve the mechanisms over temporal ranges from attoseconds to milliseconds.

Future perspectives for electron triggered processes at a next generation XFEL include the study of: electron solvation, pre-solvated electron and/or solvent cation capture, solvent cation fragmentation, and dissociative electron capture. Structural probes will also be of value for establishing metal oxidation states in catalysis.[106] X-ray spectroscopy would be important for characterisation of short-lived catalytic intermediates.[107] The electron beams required are typically in the ~10s of MeV range and so could be provided by a compact RF gun synchronised to the facility or from the laser acceleration method. The former methodology may support multi-kHz measurement repetition rates. This would enable research in both liquid and condensed phase materials and potentially to directly probe both electronic and structural changes in real time, in operando conditions, with temporal resolution from femtoseconds to milliseconds.

Heavier charged and neutral particles can be well synchronised to the X-rays of a next-generation XFEL through laser acceleration methods, driven by the petawatt laser at the MEC end-station. Synchronisation to the ~100 fs level (with possibilities to develop cross-correlating time tools to timestamp each shot at the 10 fs level) should be readily achievable, permitting sub-picosecond to femtosecond temporal resolution of the induced radiolysis measured through time-resolved X-ray spectroscopic and scattering channels. Repetition rates would scale with those of the DiPOLE technology and so we might anticipate to readily achieve a 100 Hz repetition rate for these measurements in the longer term. Extension of studies from liquids and condensed phase materials to biological tissue to address mechanisms at work in proton therapy would be enabled by this capability. The further development of laser-driven pulsed neutron sources will open the opportunity to study in real-time the mechanisms of neutron damage in materials.

6.4 Understanding catalysis

Although catalysts are often the key to invaluable chemical and biochemical processes, their complex and elusive nature has by and large defied our current abilities to characterise and understand their microscopic action. This situation has partly arisen from the very fast timescales involved in their role as agents of chemical action, which are faster than conventional characterisation capabilities. The recent developments in femtosecond XFEL technology and instrumentation have finally opened the door on this fascinating research area, and we now have an unprecedented opportunity to capture the behaviour of catalysts in their active state. These developments are now expected to deliver on the long-standing dream of catalyst by design, as opposed to trial and error.

6.4.1 Introduction to catalysis

Catalysis is fundamental for the sustainability of our modern way of life. Most of the products that we use regularly, such as medicines, fuels, fertilisers, perfumes and products designed for the purification of air and water, make use of a catalyst at some point during their manufacture. Catalysts can also be found in nature, where they facilitate critical reactions. It is estimated that 90% of all chemical processes involve the use of a catalyst.[108] From an economic point of view, the chemical manufacturing and pharmaceutical industry accounted for £39.7 billion of the UK economy's Gross Value Added (GVA)[109] (2025) and approx. 136,000 direct jobs.[110]

The discovery of new and improved catalysts is becoming ever more important to produce sustainable materials as efficiently as possible. Typical methods that are used in catalyst development are often based on a trial and error approach, where a catalyst is exposed to several types of substrates and analysed, and the process is repeated with adjusted design and operational parameters.[111] Although this approach is often successful, and efficiency is ever improving,[112] it is heavily resource-intensive both in terms of researcher time and of materials, which are often rare and precious metals, whilst still effectively being very narrow in scope. The rational development of catalysts is the alternative approach, but it needs deep understanding of a catalyst's specific functionality and reaction mechanisms. Effective progress by this route can only be achieved by knowing the detailed geometrical structure of the catalyst's atomic and molecular environments, as well as their active electronic structure, and how all these factors change during chemical processes.

Most catalytic studies focus on either the structural characterisation of the product outcome or the low energy intermediates formed long after the activation period. However, most catalytic mechanisms require an activation point from where a low energy state material, or pre-catalyst, needs to be 'pumped' to form the true catalyst that exists in a highly reactive state. This true catalyst can then undergo chemistry that either could not otherwise be performed, or with a high selectivity towards the generation of one product type. The characterisation of either the activation route or the properties of the activated species is a challenging prospect, as by its very nature the complex is highly unstable and often short-lived; but despite this difficulty, this issue is critical to address as it clearly pre-determines the future catalyst's operational ability. To produce a major shift forward in the field of catalysis, the focus must therefore shift from the analysis of product distribution and kinetic outlooks to a direct method of experimental characterisation of the active species paired with advanced computational theory.

Nowadays, XFELs are capable of providing intense and short X-ray pulses, presenting an exciting opportunity to determine the nature of transient catalytic intermediates and the dynamics with which they are formed, so we can understand, predict and control the resulting chemical processes. X-ray Absorption Near Edge Structure (XANES) spectroscopy, X-ray Emission Spectroscopy (XES), X-ray Scattering (XS) and Resonant Inelastic X-ray Scattering (RIXS) are some of the techniques that have successfully been used in XFELs for the study of catalytic reactions. **Chapter 8** will consider practical industrial applications of XFELs in catalysis. Here, we will briefly introduce fundamental aspects of catalysis and how next-generation XFELs can address the existing challenges.

6.4.2 Revealing fundamentals of catalysis

Photocatalysts are set to become some of the most important materials in terms of sustainability, looking to harness the Sun's energy in order to perform high energy transformations, such as water splitting or fuel production.[113,114] Laser pump/X-ray probe studies are proving to be a truly unique characterisation tool for these materials, identifying the highly active species and key excited state chemistry. Many pump-probe studies in catalysis have been performed using the temporal probe capabilities of third-generation synchrotron sources, enabling investigations on timescales of hundreds of picoseconds.[115-118] Although time resolutions below the picosecond have been achieved at synchrotron sources using original timing schemes, such as laser-electron slicing, this has been attained at a significantly reduced flux.[119,120] The emergence of XFEL sources has enabled studies in femtosecond timescales with high flux, that have subsequently allowed the electron and nuclear movements to be followed in real time far from thermal equilibrium, both in the soft and hard X-ray regimes. Here we will review the most significant catalysis studies performed at XFEL facilities.

Most of the catalytic system studies on femtosecond timescales in the hard X-ray regime have been focused on understanding the photochemistry of transition metal complexes, as they play essential roles as photosensitisers for hydrogen evolution[121] or for solar energy conversion.[122] Transition metal complexes are widely used for photochemical application owing to their ability to absorb visible light, and subsequently create energetic excited states with holes and electrons that are well separated between the metal centre and the ligands. XANES spectroscopy is ideally suited to investigate the electronic and geometric structure of transition metal centres, taking advantage of the element specificity of the technique to provide access to the d-d electronic transitions in the excited state that cannot be directly detected by optical spectroscopy. The first femtosecond time-resolved XANES (TR-XANES) experiment in the hard X-ray regime was carried out in 2010 at the Linac Coherent Light Source (LCLS)[123] achieving a time-resolution of 500 fs, limited by the instability of the XFEL pulses in arrival time. Since then, the situation has been enormously improved upon, using several technological advances,[124-127] enabling numerous femtosecond XANES investigations.

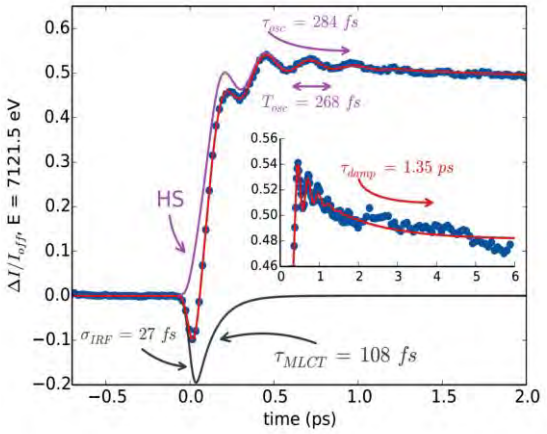


Figure 6.12: Fit to the femtosecond transient XANES of $[Fe(bpy)_3]^{2+}$ measured at 7121.5 eV, showing the contribution of the MLCT and of the oscillating high spin state.[14]

*Figure reproduced from H.T. Lemke et al. "Coherent structural trapping through wave packet dispersion during photoinduced spin state switching". Nat. Commun. **8** (2017), licensed under Creative Commons CC BY 4.0*

One example by Lemke *et al*.[14] used TR-XANES to investigate nuclear wavepacket oscillations of the solvate iron (II) bipyridine complex for the first time, extracting valuable information of the Fe–N breathing vibrational mode (**Figure 6.12**). The system was previously studied using the time resolution available at synchrotron sources,[128,129] and although the structural dynamics of the spin crossover was revealed, the molecular breathing was not observed owing to the insufficient signal-to-noise ratio. A similar experiment[37] managed to track multiple components of the coherent nuclear wavepacket dynamics in a copper(I) phenanthroline complex, showing that the amplitude of the identified vibration modes can be modified by changing the incident X-ray energy. The increased stability of the XFELs has facilitated the performance of X-ray Absorption Spectroscopy experiments in an extended energy range. Following the publication of the first steady-state Extended X-ray Absorption Fine Structure (EXAFS) spectrum acquired at the LCLS,[130] Britz *et al*.[131] collected a full range time-resolved EXAFS spectrum up to 500 eV above the absorption edge on an Fe(II) polypyridine complex in solution.

While XANES is used to provide information about the empty electronic states of transition metal centres, XES is used to provide information about the occupied density of states projected on the

absorbing atom. Although time-resolved XES (TR-XES) has been performed in synchrotron sources to determine the spin state of transition elements with picosecond time resolution,[132] the technique has benefitted greatly from the high pulse intensity and high time resolution of XFEL sources. Many investigations have been performed on the study of the K_α and K_β emission lines of 3d transition metals in molecules, taking advantage of the sensitivity of these emission lines to the oxidation state and the number of unpaired electrons of the transition.[16]

The valence electronic structure of transition metal complexes in solution has also been studied with X-ray spectroscopy in the soft X-ray range with femtosecond time resolution at XFEL sources.[8,133] Time-resolved RIXS (TR-RIXS) at the Fe L_3 edge has been performed to study the ligand exchange dynamics of $Fe(CO)_5$, concluding that the photoinduced removal of CO generates a 16-electron $Fe(CO)_4$ species in an excited singlet state, that either converts to the triplet ground state or combines with a solvent molecule to regenerate a penta-coordinated low spin singlet state Fe species (**Figure 6.13**). It can also recombine with a CO molecule to regenerate the initial state.

Femtosecond soft X-ray pulses have also been used to probe the real-time dynamic evolution of the adsorbate electronic structure of different transient species during chemical reactions using TR-XANES and TR-XES. These studies are important to increase our microscopic understanding of surface reactions, a long-standing goal in heterogeneous catalysis, where chemical reactions occur at the solid surface. In these studies, the optical laser is used to start the reaction, while the XFEL pulse is used to follow the changes in the electronic structure of the adsorbate.[134] Several studies have been focused on the investigation of the desorption of a CO molecule from a Ru(0001) surface[135,136] at both the O and the C K-edge.[137] Ultrafast X-ray spectroscopy has also been used to identify the short-lived intermediates that are formed during reaction of CO with O_2 on a ruthenium surface (see **Box 6.1** where THz pump pulses were used to alter the dynamics of the same reaction) .[138] In this study, the optical laser pulse excites motions of CO and O_2 on the surface, allowing the reactants to collide, while new electronic states are shown in the oxygen TR-XANES spectrum.

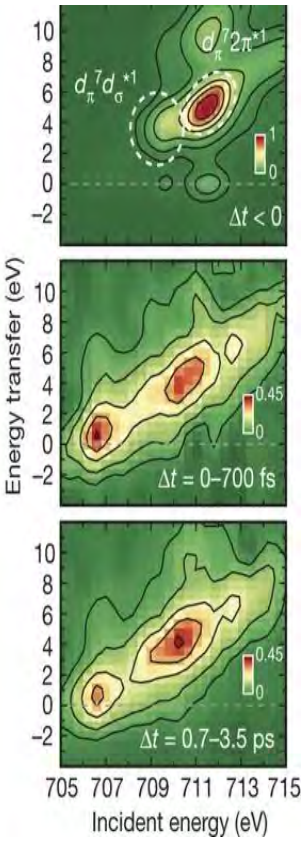


Figure 6.13: Time-resolved RIXS at the Fe L_3 edge sheds light on the ligand exchange dynamics of $Fe(CO)_5$. Measured Fe L3-RIXS intensities versus energy transfer and incident photon energy. Top: ground-state $Fe(CO)_5$. Middle and bottom: difference intensities for delay intervals of 0–700 fs and 0.7–3.5 ps, respectively.[9]

Reprinted by permission from Springer Nature:
*P. Wernet et al. Nature **520**, 78 (2015)*
DOI: 10.1038/nature14296
Copyright (2015)

The ability to perform time-resolved XS (TR-XS) in solution with XFEL sources is also widely used for the study of catalytically relevant systems, as it provides information on the structural changes in the system under study, including the changes in the solvent cage and the dynamics of the bulk solvent after excitation. Thus, TR-XS has been used to extract information of the excited state dynamics in iridium-based dimeric complexes in acetonitrile solution[139] with 100 fs time resolution using a 9.5 keV X-ray pulse. TR-XS has also been used to study the ultrafast structural dynamics of bond formation in $[Au(CN)_2^-]_3$ in solution.[140,141]

As the experimental requirements for TR-XES and in-solution TR-XS are very similar, requiring the use of a fixed incident energy, several investigations have been performed combining both techniques at XFEL sources, illustrating the complementary nature of the techniques: while XES provides information on the changes of the electronic structure, XS provides information on the structural changes. This combination of methods has been used for the study of photocatalytic dyads,[142] and of the solvent-solute interactions that occur simultaneously to the spin transition on aqueous Fe(II) bipyridine.[143]

6.4.3 XFELs enable understanding of natural, artificial and hybrid catalysts

Vitamin B12 – cobalamin – continues to fascinate researchers, as despite its vital role in our function, it is not yet clear how it works. Recent ultrafast X-ray studies reveal that excited state dynamics of B12 coenzyme is controlled by the axial base,[144] whist a combination of optical and X-ray probes helped follow the light-induced dynamics of its close relatives – Aquocobalamin and Hydroxobalamin.[145] In further exciting developments, ultrafast X-ray studies focussed on CarH – a protein photoreceptor that uses a form of B12, adenosylcobalamin (AdoCbl), to sense light via formation of a metastable excited state. Aside from AdoCbl bound to CarH, methylcobalamin (MeCbl) is the only other example – to date – of photoexcited cobalamins forming metastable excited states with lifetimes of nanoseconds or longer. A recent study used transient Co K-edge X-ray absorption and X-ray emission spectroscopies in conjunction with transient absorption spectroscopy in the UV-visible region to characterise the excited states of MeCbl. These data show that the metastable excited state of MeCbl has a slightly expanded corrin ring and increased electron density on the cobalt, but only small changes in the axial bond lengths (**Figure 6.14**).[146] These recent breakthroughs highlight how a combination of ultrafast X-ray and optical methods can help one understand the very first steps of catalysis and biocatalysis.

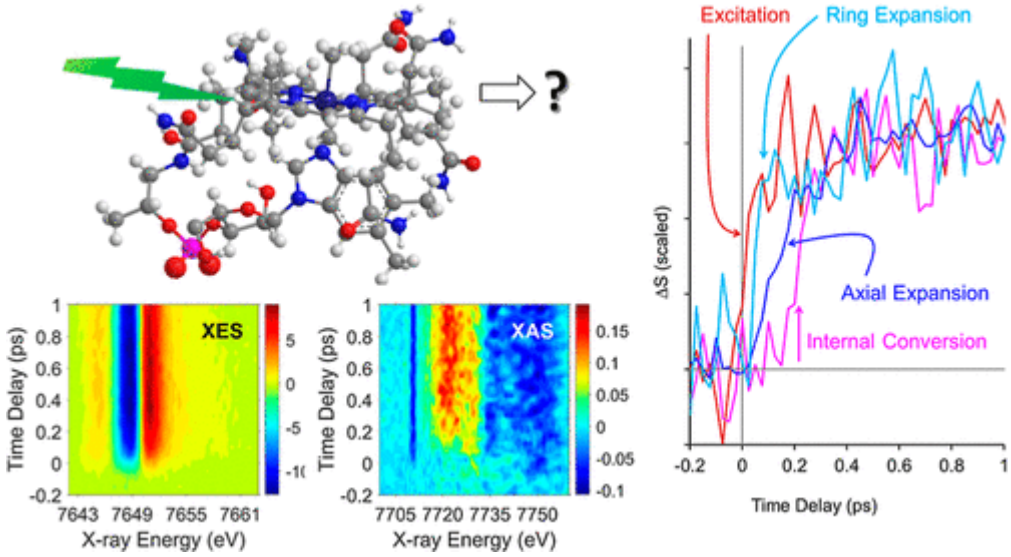


Figure 6.14: Structural evolution of photoexcited methylcobalamin towards a CarH-like metastable state: Evidence from Time-Resolved X-ray Absorption and X-ray Emission

Reproduced with permission from the American Chemical Society: R.J. Sension et al, J. Phys. Chem. B 2024, 128, 34, 8131–8144 (2024) DOI: 10.1021/acs.jpcb.4c03729 Copyright (2024)

The performance of photocatalytic materials strongly depends on the processes occurring after photoexcitation. In situ pump-flow-probe XAFS study of photoexcited electron transfer over single atom-Pt/CoOOH photocatalysts can serve as a further example of recent advances in heterogeneous photocatalysis enabled by X-ray methods.[147] The PFP-XAFS spectroscopy followed photoexcited electron transfer from semiconductor to cocatalyst in a single atom(SA)-Pt/CoOOH photocatalyst: upon photoirradiation, photoexcited electrons in the CoOOH semiconductor are found to transfer into Pt 5d orbitals, reaching a maximum population at 10 μs delay time – here, there is a clear need for femtosecond sources to follow the first steps of electron injection.

In solid state photocatalysis, a thorough understanding of the decay pathways of photoexcited charge carriers within the host material can help explain the observed increase in activity induced by light absorption and guide the development of strategies to optimise conversion efficiency. In particular, the interaction between photoexcited charge carriers and lattice induces a distortion, which in turn generates a potential that self-traps the excited charges, limiting performance. The quasiparticle associated with the charge-lattice interaction is called a polaron. Polaron formation in the ground state, arising from the incorporation of additional electronic charges into the lattice, is frequently

observed in many oxides, where the interaction between the added charge and the associated lattice distortion limits mobility by confining carriers in band-gap polaronic states, leading to electrical conduction being limited to thermally induced hopping of trapped charge carriers. In photocatalysis, the formation of polarons after photoexcitation has been identified as a key factor limiting the photoactivity of compounds such as hematite and other oxides. On the other hand, extrinsic polaronic states originating from defects can broaden the absorption range of oxides, decrease the recombination rate, and enhance photoactivity.

Extreme ultra-violet and X-ray-based ultrafast spectroscopies have been demonstrated to be able to provide detailed information on the dynamics of photoexcitation and decay processes in various materials. For example, in hematite, a small polaron formation after photoexcitation was inferred from the observed sub-100 fs splitting of the Fe $M_{2,3}$ edge,[148] whilst tungsten trioxide, WO_3 – a catalyst for water splitting – was shown to form a metastable state associated with a structural change that forms within a few hundred picoseconds.[149,150]

Recent studies using ultrafast X-ray methods at EU XFEL focussed on a well-known photocatalytic material – cerium oxide (**Figure 6.15**). In cerium oxide, the localisation of extra charges in 4f states significantly limits the electron-based conductivity, which occurs through polaron hopping. Theoretical calculations have shown that polaron formation leads to an expansion of the Ce–O bond length by ~ 0.1 Å. Such changes are expected to have a positive impact on cerium oxide-based photocatalysts by weakening the bond between the cation and oxygen, thereby reducing the energy required for oxygen vacancy formation, which is crucial for the material's functionality. At the same time, it can extend the lifetime of the photoexcited carriers.

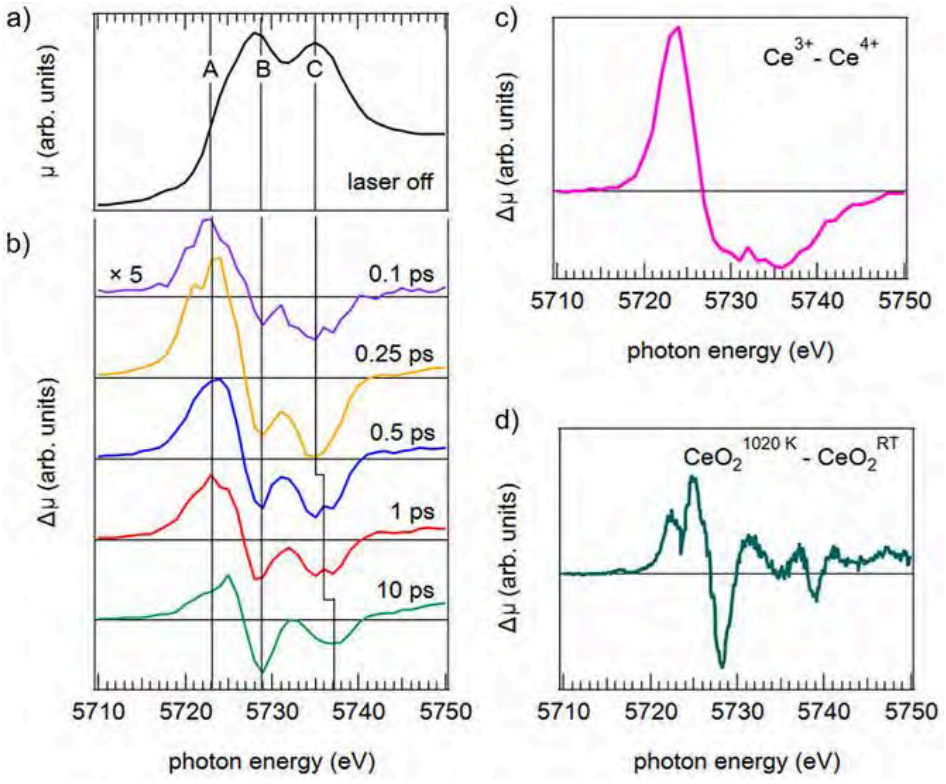


Figure 6.15: Ultrafast dynamics of electronic and structural modifications induced by photoexcitation in cerium oxide.

Ce L_3-edge XANES: a) steady-state spectrum; b) transient spectra at different delay times; c) difference between spectra measured on Ce^{3+} and Ce^{4+} reference samples; d) difference between two steady–state Ce L_3 -edge HERFD-XANES spectra measured at 1020 K and at RT.

Reproduced from S. Pelatti et al, Adv. Electron. Mater. e00429 (2025) under the terms of a Creative Commons Attribution 4.0 License DOI: 10.1002/aelm.202500429

The recent study of ultrafast dynamics of electronic and structural modifications induced by photoexcitation in cerium oxide correlates the dynamics of the evolution of the Ce-related electronic structure, obtained through pump-probe XANES, with the evolution of the local atomic structure around Ce ions, analysed via pump-probe EXAFS at the Ce L_3 edge.[151] The research takes advantage of the capabilities of XFELs, unique facilities that provide ultrashort, high intensity coherent X-ray pulses, tuneable in energy, that can be synchronised with ultrashort optical laser pulses with variable delay.

The analysis of pump-probe Ce L_3-edge XANES and EXAFS spectra reveals modifications in both the electronic and local atomic structure of a cerium oxide film following photoexcitation. It was established that within the response time of the experiment (a few tens of femtoseconds), the electronic structure exhibits ultrafast changes consistent with transient occupation of Ce 4f states. This is followed by a partial relaxation into a metastable photoexcited state, characterised by a time constant of 0.45 ps. Concurrently, a structural expansion of ~ 0.14 Å occurs in the first shell of oxygen atoms surrounding the excited Ce ion – consistent with values predicted by DFT – indicating the formation of a photoinduced polaronic state. Both the electronic and structural modifications persist for over 300 ps after the photoexcitation. The observed time correlation between the photoinduced electronic and structural changes further reinforces the hypothesis of photoinduced polaron formation – and sheds a new light on the photocatalytic performance of metal oxides.

6.4.4 Future opportunities in catalysis

As seen in the previous section, XFEL sources are now beginning to make a significant impact on the way that we understand chemical processes. The examples demonstrate that the short duration and high flux of XFEL pulses can be used effectively to observe atomic motions and electronic transitions in real time, moving from the scenario where experiments were limited to study only thermally relaxed transient states. The ultimate goal in catalysis is to be able to record movies of chemical processes, where electronic and nuclear structural dynamics are acquired, and XFEL sources are well along the path to delivering this capability. The resulting insights will ultimately bring control of reactions at the electronic and atomic level, when they are initiated by light or other stimuli.

Although spectroscopy and scattering techniques are currently being used with success at XFEL sources to help understand catalytic systems, especially in the field of photocatalysis, most of these studies have so far only been performed on model molecular systems, far from real conditions of concentration. It is expected that, in future, it will become possible for more challenging systems to be studied at XFEL sources under more realistic conditions of concentration and within complicated sample environments, profiting from technological developments that will deliver pulses with higher repetition rates and brightness. The development of spectrometers covering larger solid angles with even higher energy resolution will also contribute to the study of more demanding experiments. Such developments are of considerable interest in catalysis, where often low amounts of the active species are used, and reactions are often performed under harsh conditions of high temperature with toxic and/or flammable gas atmospheres.

It is, however, important to note that the more complicated the system to study, the more difficult it will be to obtain a complete picture of the chemical process with a single structural technique, and the application of multiple techniques simultaneously is going to be necessary to obtain the comprehensive insight required for knowledge guided process optimisation. Chemical studies at synchrotrons reflect this, as multichannel methods under realistic conditions are nowadays routinely used to deliver the full hierarchical characterisation of materials. The study of chemical processes at XFEL sources is not an exception, and many XFEL end-stations now offer the instrumentation needed to perform both spectroscopy and scattering. XES and in-solution XS are frequently used simultaneously, providing complementary information: XES providing information on the electronic configuration dynamics through probing the unoccupied density of states, and in-solution XS providing information on the nuclear motion and changes in the solvent structure. Both methods need a fixed wavelength to be performed and there is no need for scanning the incident beam, and they both profit from the pulse nature of the XFEL source, collecting the entire spectrum in a single acquisition.

XANES is often available together with XES and XS, providing complementary information about the occupied density of states of the absorbing element, traditionally requiring the scanning of the incident energy. One could envisage being able to get information about the occupied density of states using the pulse nature of the XFEL sources using alternative methods such as High Energy Resolution Off-Resonant Spectroscopy (HEROS). This method, when performed using an X-ray spectrometer operating in a dispersive geometry, allows measurements of a scattered X-ray spectrum in a single acquisition using monochromatic incident beam. The feasibility of the method was first demonstrated at the Swiss Light Source (SLS), but owing to the extremely weak scattering cross section of the off-resonant signal, it has not been exploited at synchrotron sources.[152] More recently, HEROS has been used at the LCLS to record the static spectra of copper and copper oxide with femtosecond time resolution, taking advantage of the brightness of the XFEL pulses.[153] The next step will be to use this method to study the electronic dynamics of ultrafast chemical processes and combine it with the simultaneous collection of XS data to get structural information, as it is nowadays possible to do when combining XES and XS.

An additional method that will be able to provide complementary spectroscopy information in the hard X-ray regime is X-ray Raman Scattering (XRS). The technique uses hard X-rays for performing XANES spectroscopy of light elements, such as O, C, N, etc. The use of hard X-rays makes this method a bulk sensitive probe that can be used with a broad range of sample environments, removing the experimental difficulties of working in the soft X-ray regime. Providing access to the study of the electronic structure of low Z materials in the bulk is of significant interest in the study of catalytic reactions, particularly in the field of heterogeneous catalysis, where most systems are composed of an active support that is used for the conversion of small molecules consisting of C, O, N and H (see **Section 6.1**). The Raman cross-section is orders of magnitude smaller than that of the photoelectric absorption, so this method will benefit greatly from the high flux available in XFEL sources, as experiments will be feasible at more realistic concentration conditions than those currently achievable at synchrotron sources. The combination of XRS with other techniques, such as XES and XS, will provide a more complete picture of the catalytic process.

Sometimes in catalysis, the 'one-pot' approach, in which more than one catalyst is used in a single reactor to perform sequential transformations, is used instead of the more traditional stepwise-mediated synthetic approaches. In other cases, the catalytic species contains more than one active site, each catalysing a different step in a chemical process, as is the case of mixed metal photocatalysts. The determination of the electronic and structural dynamics of all the active species involved in the catalytic process is necessary in both scenarios in order to elucidate the reaction mechanism, and to understand how the changes of one active site correlate to the others during the reaction. Element-sensitive techniques, such as X-ray spectroscopies, are an ideal way to acquire this understanding, allowing the disentanglement of the role of the different sites by tuning the energy to the selected element. These sorts of studies have traditionally been performed in a sequential manner, both at synchrotron and XFEL sources, focusing on one active site after another. Very recently, a novel experiment has been performed at the European XFEL in a Fe-Co dyad, where the iron centre acts as the photosensitiser while the cobalt centre catalyses the reaction once the intra-molecular charge transfer has occurred.[154] The experiment used two dispersive emission spectrometers simultaneously, one aligned to collect the emission spectrum of the iron centre, and the other, the Co centre. By measuring the two sites simultaneously, the authors of that study managed to correlate the electronic dynamics of both active sites within the photocatalyst. Although this pioneering experiment represents an important step forward towards the understanding of the electronic dynamics of mixed metal catalysts, the system was chosen carefully so that the absorption edges of the two active sites were close enough in energy to allow the simultaneous collection of the emission spectra. It is not, however, easy to extend this methodology to other systems where the absorption edges of the elements of interest are at very different energies, but this restriction could be overcome by using two X-ray beams impinging in the sample simultaneously, in a similar fashion to what has been done at Diamond Light Source, where a soft and a hard X-ray beam are used for electron spectroscopy.[155]

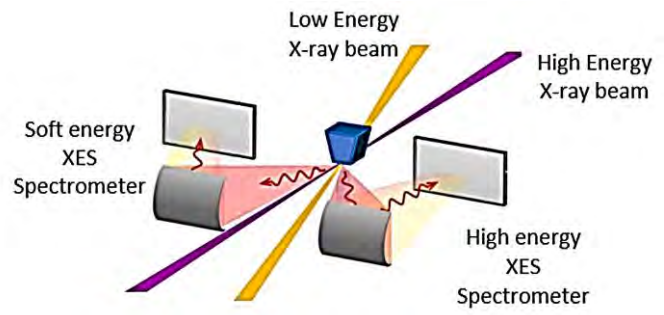


Figure 6.16: Schematic of a XES experiment performed in the soft and the hard X-ray regime simultaneously (adapted from [127]).

*Figure adapted from Y. Kayser et al. Nat. Commun. **10**, 4761 (2019) under the terms of a Creative Commons Attribution 4.0 International License. DOI: 10.1038/s41467-019-12717-1*

Such a development would make the collection of simultaneous XES for more than one element much more generally applicable, including the possibility of studying elements with absorption edges in the hard and soft X-ray energy regimes (**Figure 6.16**). In these cases, not only can mixed catalysts be studied, but also metal transition catalysts with low Z ligands, i.e. the hard X-ray beam will be used to study the electronic dynamics of the transition metal active site, while the soft X-ray beam will be used to study the electronic changes in the ligand donor. This methodology will provide unprecedented insight into electronic movements from two or more atomic sites simultaneously.

6.4.5 Conclusion

Catalysis is critical to all areas of modern life. To develop new and improved catalysts to produce materials in a more efficient and sustainable manner, we need a deep understanding of the chemical processes. This information can be obtained by solving the electronic and geometrical structures of the catalytic species and following how these characteristics change during reactions.

XFEL sources are already playing an important role in increasing our understanding of catalytic processes. The high temporal resolution of these sources is opening avenues that allow the study of atomic motions and electronic transitions in real time, recording movies of the chemical reactions, and the simultaneous combination of several structural techniques, such as XANES, XES, RIXS and XS, has often proven essential for fully resolving the subtle but vitally important aspects of catalytic processes.

Higher repetition rates and brightness will enable the study of catalytic reactions under operando conditions, when low concentrations and complicated sample environments are used. Furthermore, the addition of techniques such as HEROS and XRS to the suite of spectroscopy tools available at XFEL sources will have a major impact on our ability to advance our understanding of the field. The long-term goal would be to simultaneously record the electronic and geometrical changes in two centres in the catalyst by using two colour X-ray pulses.

This brief overview is intended to provide a background to applications of XFEL in industrial catalysis, outlined in **Chapter 8**.

6.5 Chemistry and the environment: Aerosols, atmospheric, space chemistry, combustion, corrosion

The chemistry of complex mixtures – inherent in astrochemical, environmental and industrial situations – is amongst the most challenging to study. The multiscale nature of the problems, combined with random mixing and complex kinetics of competing chemical processes, makes accurate measurements vital for producing the quantitative models of reactivity in the gas phase, or at gas/liquid and gas/solid interfaces required to understand these problems. Current technological approaches are insufficient to achieve the required sensitivity. The ability of experiments employing a high repetition rate XFELs to provide temporally, spatially and chemically specific maps of reaction mixtures during the processes of interest will provide mechanistic detail far beyond current capabilities. The resulting information-rich data will provide new perspectives on the chemical and physical properties and processes that control efficiency and material degradation, providing new routes to process optimisation, control and environmental reform.

6.5.1 Chemistry and the environment

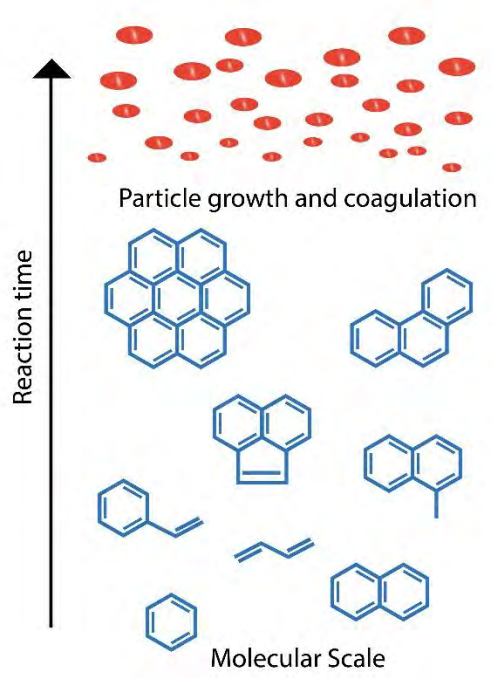
Chemistry in the environment covers a broad range of astrochemical, atmospherically and industrially important processes. The key feature that links these aspects together is the complex interplay between the chemical changes occurring and the inhomogeneous mixing, driven by complex gas or fluid dynamics.[156] These combined effects lead to localised chemical changes, with almost chaotic spatial and temporal characteristics in some circumstances. This combination of multiscale (in both length and time) characteristics combined with inherent spatial inhomogeneities means that accurate measurements remain a significant challenge for conventional light sources. The ability of XFELs to measure spectra with a single pulse, enabling chemical specificity (through linear and non-linear X-ray spectroscopies) and particle detection (through diffractive imaging), is potentially game changing for the study of the chemistry of these complex mixtures and materials.

In all cases, the ability to initiate chemical transformation with a variety of pump sources (i.e. THz, IR, UV, VUV, e-Beam) provides routes to studying different reaction types of relevance to diverse environmental areas. Combining different mechanisms of initiation (see **Section 6.1, 6.2** and **6.3**) with ultrafast and hyper-sensitive methods of detection of various types of short-lived molecular reactive intermediates (i.e. ions, radicals etc) will provide a multiplexed approach to complex chemical problems that would be impossible to solve with a single technique alone.

6.5.2 Combustion

As well as driving the development of next-generation energy production and storage materials (**Section 8.6**), the XFEL can continue to drive efficiency savings in the energy sector through increased understanding of combustion dynamics. Combustible fuels form an integral, and currently irreplaceable, part of our energy portfolio. They represent a high energy density material that is easily stored and transported, making them a key commodity for the foreseeable future. While the UK has committed to banning the sale of new petrol and diesel vehicles from 2035, the use of combustible fuels in other areas is set to continue (e.g. in aviation), such that the challenges associated with driving ever increasing efficiencies should continue to be met. As an example of the impact of efficiency savings, around 80% of energy used within the UK still derives from combustion sources. Despite a growing population leading to an increase in energy demands and the UK's continued reliance on combustible fuels, UK emissions continue to fall and in 2018 were 44% below 1990 levels,[157] in large part driven by increased efficiency. Reaching the UK target of net zero emissions by 2050 will require the combined effect of new technologies and an increase in energy efficiency, both of which are areas where the capabilities of an XFEL source can address open questions.

Intelligent routes to increasing the efficiency of combustion sources require temporally (femto- to microseconds) and spatially resolved, species-specific measurements of the complex chemistry occurring. These data are a prerequisite for the development of predictive models that can direct next-generation system development. For combustion, this means that detailed and accurate measurements of the dynamic chemical distribution within the flames are required. Optical and fluorescence measurements have limited applicability owing to the highly scattering environments and variability in pressure creating spatially-dependent quenching rates, limiting data reliability and availability.[158] Synchrotron based methods can provide time averaged speciation maps through soft X-ray absorption and fluorescence measurements,[159,160] but currently miss the temporal changes in species and how these link to gas dynamics and time dependent local changes in density, pressure and temperature. The unique capabilities of an XFEL in providing high X-ray fluxes at potentially high repetition rates would allow single shot spectral measurements across large spatial areas, providing temporally and spatially resolved species specific maps during the combustion process. Spatially tracking the production, distribution, growth and loss of polycyclic aromatic hydrocarbons (PAHs), for example, will provide details of the early stages of particulate formation and reveal how the local physical characteristics, as well as the chemical environment, either enhance or inhibit their formation (see **Box 6.2**). This has further links to the chemistry of hot and cold plasmas in planetary atmospheres and to the chemistry of space (**Section 6.5.4**), where PAHs form around 20% of all galactic carbon, but questions remain over whether their formation is a "top-down" process starting at the breakup of soot from carbon stars, or are they (also) formed in a "bottom-up" synthesis from small unsaturated chemical species.



Box 6.2: Tracking particle formation in combustion from the molecular level to macroscopic scales

A high intensity optical pump seeds particulate formation through the localised generation of small radical species. By combining X-ray spectroscopies, specifically XANES and XES, with scattering measurements, XFEL probes can map all stages from the molecular growth and formation of PAHs through to particle size distribution via scattering. Extra information on the surface chemistry and structure of the particles can subsequently be obtained through X-ray surface second harmonic generation. The combination of techniques covers time and length scales, from femtoseconds and ångstroms at the molecular level, through to 100s of nanometres and microseconds for the particulate formation.

This ability becomes increasingly important as we move to higher efficiency engine types, such as those based on Homogeneous Charge Compression Ignition (HCCI). HCCI engines provide much higher fuel efficiency than other internal combustion engines, achieving both CO_2 and NO_x reduction.[161] In HCCI engines, fuel ignition is driven by compression leading to autoignition. The much higher pressure and much lower temperature make the resulting chemistry quite different[162] from that occurring inside a standard engine. Developing sample environments that create analogous conditions is a challenge. As a first step, mechanical compression provides opportunities to exploit stroboscopic imaging that will utilise the high brightness and high repetition rate of the XFEL. Subsequent development in initiating the combustion through pressure waves could lead to robust pump-probe methodologies that allow for a truly molecular-scale measurements of these new combustion environments. Both approaches

will require the high brightness, ultrashort pulse duration and high-repetition rate of a modern XFEL source for dynamic imaging of the combustion process. By moving beyond state-averaged quantities, such as mixing fractions, to tracking of real time and spatially resolved chemical changes, fully correlative analysis of the turbulent reaction mixtures can be performed. Optical laser-derived perturbations, e.g. laser filaments, can then drive changes in processes such as particle formation,[163] allowing for measurements covering timescales from femto- to micro-seconds. Species-specific probing can be further enhanced through the use of stimulated X-ray Raman probes to monitor changing bonding character in specific reactive intermediates and stable molecules through the flame.[164] The highly detailed and information-rich data will provide detail far beyond the current state-of-the-art, allowing for new insights into the complex interplay of chemistry, fluid dynamics, nucleation and particulate formation that define the fundamental chemical and physical processes that affect energy conversion efficiency.

6.5.3 Corrosion and biofilms

Material suitability and lifetime is often defined by the corrosion processes that degrade material quality over time. Our molecular level understanding of the chemical processes and mechanisms that drive material degradation is limited, which means that our ability to design and manage materials over extended periods is far from optimal. Typical corrosion prevention methods rely on sacrificial layers or the control of diffusion through the use of structured surfaces and coatings. Mechanistic information could lead to a breakthrough technology that impedes the chemistry that drives corrosion, helping to reduce the trillion-pound cost of corrosion to global economies and preserve precious material resources.[165]

To develop these controls requires a molecular level understanding of the degradation pathways and of how the surface-level interactions are affected by the coatings and structures currently used. Such studies require detailed structural information of the surface topography and chemical state. Recent developments in operando measurements have utilised synchrotron sources for X-ray diffraction measurements, performed in conjunction with mass spectrometry. The combination of techniques allows for studies of oxidation processes that can be linked to changes on particular facets of complex nanostructures, with a sensitivity to changes occurring over the minutes-to-hours timeframe.[166] Extending such measurement to localised oxidation state changes, and the identification of deposits and corrosion products, requires high sensitivity and rapid spectral data collection. Similar to the combustion studies, the ability to map spatial regions in a single shot removes state averaging and allows for correlative analysis of the changes across all aspects. In electrochemically driven processes, this could include information on the etching and structuring of the surface combined with oxidation state changes and chemical product formation, providing the multivariable analysis required to understand the interplay between physical, chemical and structural effects.

Another pressing concern of material suitability and corrosion surrounds the development of biofilms. Biofilms form owing to the collective growth of microorganisms over surfaces. While this presents material opportunities, their growth over implants and in fuel and chemical storage containers causes bacterial infections, corrosion of surfaces and degradation of stored material.[167] Large-scale investment into the prevention, detection and management of biofilms is driven by the needs of wide-ranging industries affected by these issues. There are fundamental questions surrounding the composition and dynamics of biofilm growth, and how adaptions to the molecular framework could be used to direct growth and control activity for potentially beneficial applications. For this to become reality, standardised models need to be developed which must be based on detailed experimental data.

Probes that are sensitive to surface properties and reactions are required for both corrosion and biofilm studies. Newly emerging techniques that are only possible at high intensity XFEL facilities are moving non-linear optical probes, developed in the visible and infrared, into the X-ray regime. In recent experiments at the FERMI XFEL, soft X-ray second harmonic generation experiments were performed on graphite surfaces and showed surface level sensitivity with element specificity.[12] These non-linear

X-ray techniques will play a key role in understanding these surface driven processes, and will have strong links to the catalysis experiments (**Section 6.4**). The increased penetration depth and atom specificity of the X-ray second harmonic generation experiments will detail active site information and molecule-specific kinetics, even at buried layers and interfaces.[168] Moreover, by simultaneously following biofilm growth, the activity of bacteriophages at controlling and removing biofilms can be integrated at the molecular level, impacting on the boundary between chemistry, life sciences and industry.

6.5.4 Atmospheric and space sciences

The fields of atmospheric chemistry and astrochemistry share many of the experimental challenges associated with studies of low temperature combustion. In the Earth's atmosphere, the generation of radical and other reactive species through photochemical and exothermic reactions leads to local heating and pressure changes that redistribute the reactive species, initiating chemical reaction networks that depend on the local chemical composition. The ever-expanding range and complexity of chemical species present within the atmosphere is increasingly challenging to characterise,[169] with a wide variety of homogeneous and heterogeneous gas-phase and aerosol/particulate chemistry to consider. Insights into the chemical behaviour of the Earth's atmosphere have relevance across all planetary atmospheres, complemented by increasing amounts of available data from detailed observations of 'alien' atmospheres both within our solar system (Titan, Jupiter, etc) and further afield.

Gas-phase atmospheric chemistry

Atmospheric reactions often proceed over multiple multi-welled potential energy surfaces, with large reaction networks featuring multiple branching points and complex kinetics.[162] As an example, **Figure 6.17** outlines the currently identified reactions of isoprene,[170] a naturally occurring volatile organic compound (VOC) and trace atmospheric species found in green spaces. A huge molecular branching space arises from this single molecule, and identifying and quantifying the resulting species and characterising their reactivity with atmospheric oxidants plays a major role in understanding our environment. Other important examples include the reactions of alkenes with ozone and the formation of Criegee intermediates,[171-173] and the ozonolysis of alkenes. A high-repetition-rate XFEL offers the opportunity to perform sheet or line imaging of X-ray absorption or emission in order to monitor the time and position-resolved dynamics associated with complex formation and reaction. Additional mechanistic information is accessible via XFEL probes combined with photoelectron and photoion coincidence detection. Such experiments will provide detailed mechanistic and kinetic information that can be used to improve atmospheric models.

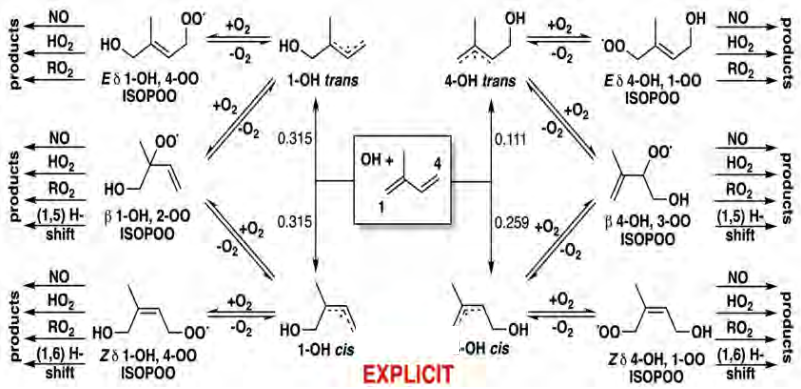


Figure 6.17: Reaction scheme for isoprene highlighting the complex branching space and kinetics required in understanding atmospheric composition and chemistry.[170]

Figure reproduced from K.H. Bates and D.J. Jacob "A new model mechanism for atmospheric oxidation of isoprene: global effects on oxidants, nitrogen oxides, organic products, and secondary organic aerosol" ACP, 19, 9613–9640 (2019) under the terms of a Creative Commons Attribution 4.0 License. DOI: 10.5194/acp-19-9613-2019

Aerosol and interfacial chemistry

Aerosols play a key role in atmospheric chemistry, and are of particular importance owing to the impact of aerosol and particulate concentrations on human health and climate change.[174,175] The adverse effects of breathing in small particulates in polluted atmospheres are well documented, and reducing particulates is a major focus of the UK's clean air strategy. The effects of atmospheric aerosols and particulates in relation to climate change are less well understood.[176] This is partly a result of the fact that in atmospheric science, as in combustion, the processes by which aerosols and particulates form are unclear. The uncertainty lies not only in the nucleation and growth processes (see also **Section 8.2**), but also in the chemical composition and surface activity of the resulting aerosols and particulates as they grow. These properties affect reactivity and atmospheric lifetime, knowledge of which is needed for accurate climate modelling.

A variety of techniques employing XFEL radiation can shed light on these phenomena. Hard X-ray scattering can provide information on particle growth, size, and morphology, while linear and non-linear soft and hard X-ray spectroscopies such as XANES, XES, and XCARS (**Section 3.3.4**), can probe composition and functionality. The high flux and intensity generated by an XFEL also promises surface-sensitive probes such as X-ray second-harmonic generation and, with the proposed two-colour operation, the ability to perform surface sum-frequency generation in the X-ray regime for the first time.

An important region of the Earth's atmosphere is the air-sea interface, where the oceans and the atmosphere form a coupled system. The exchange of heat, momentum, water, and a large variety of chemical species at the interface exerts a considerable and complex influence on climate, with local effects on regional air quality and marine biological productivity. Key to gaining insight into the emission and deposition of trace chemical species at the air-sea interface is an understanding of the structure, composition, and chemistry of the sea-surface microlayer (SSM) that comprises the uppermost tens to hundreds of microns of the ocean. The SSM has considerable chemical and biological complexity, with enriched concentrations of amphiphiles, colloids, aggregates, halogenated VOCs, and phytoplankton. As a result, the important interactions bridge the fields of biology, chemistry, physics, and oceanography, with the potential to impact the environment across almost all scales.

Ubiquitous nanoscopic and microscopic aerosol particles and cloud droplets suspended in the air play crucial roles in Earth's climate and the formation of air pollution. Surfaces are a prominent part of aerosols and droplets, owing to the high surface area to bulk volume ratios, but very little is known about their specific properties. Many atmospheric compounds are surface-active, leading to enhanced surface concentrations in aqueous solutions. Their distribution between the surface and bulk may determine heterogeneous chemistry and many other properties of aerosol and cloud droplets, however, this has not been directly observed. X-ray photoelectron spectroscopy (XPS) is used to obtain direct molecular-level information on the surface composition and structure of aqueous solutions of surface-active organics as model systems for atmospheric aerosol and cloud droplets – the high brightness of the X-ray beam at XFELs will enable a much higher sensitivity to understand how pollutants work.[177]

Experiments with high-flux XFEL sources on laboratory analogues of the SSM provide opportunities to monitor the coupled reactions involved in environmentally important processes, for example the production and subsequent reaction of molecular iodine, as a function of parameters such as temperature, humidity, pH, sea-salt concentrations, ozone levels, and nature of microalgae. XFEL radiation can be used with liquid microjet model systems to monitor concentrations of reactants, reaction intermediates and products with both time and spatial resolution. Gas-phase studies using X-ray photoelectron spectroscopy and photoelectron-photoion coincidence spectroscopy (PEPICO) can be combined with methods that take advantage of the highly penetrating nature of hard X-rays to probe processes deeper in the solution with atomic and oxidation-state specificity.

Astrochemistry

The ultrashort, extremely intense X-ray pulses generated by an XFEL represent a powerful tool for use in the investigation of fundamental processes relevant to interstellar environments.

A large number of chemical systems are now being identified based on data from space-based observing platforms tuned to the mid- and far-IR regions (James Webb Space Telescope) and focussed on star forming-regions. The data yield insights into icy dust (IceAge Project[178]) and help identification of small molecular coolants (small hydrides, water etc.) as well as more chemically complex systems.

At the more extreme end of the use case, XFELs can mimic the intense X-ray radiation fields found near black holes, neutron stars, or young stellar objects, allowing the study of matter under extreme conditions (see Chapter 4) and perhaps probing nuclear and high energy processes that occur in stellar interiors and supernovae, shedding light on the origin of elements. They can also ionise materials to generate plasmas similar to those found in stellar atmospheres or interstellar shock waves.

Many of the reactions of relevance to the interstellar medium occur on ice grain boundaries and can lead to much more complex chemical species than may otherwise be expected.[179] At lower energies, but still in the X-ray regime, XFELs enable time-resolved pump-probe studies into the photofragmentation, photoionisation, and photoinduced chemistry of interstellar molecules (e.g. water, methanol, PAHs) when exposed to cosmic X-ray radiation. Determination of fundamental parameters such as photoionisation cross-sections, rate constants, and accessible fragmentation pathways through such studies will feed into the development of improved astrochemical models. Techniques such as X-ray absorption and emission spectroscopy (and a variety of other spectroscopies) can reveal electronic structure and bonding in exotic and transient species relevant to astrochemistry, potentially assisting with the identification of previously undiscovered interstellar molecules through assignment of spectral signatures from astronomical observations.

Gas-phase chemistry in the interstellar medium is complemented by chemistry occurring on the surface of dust grains seeded from SiO_2 and TiO_2 formed in the outflows of aging stars.[179] Many molecules in the interstellar medium are frozen into icy mantles on these dust grains. XFEL radiation can be used to probe how exposure to high-energy photons alters the chemistry of these ices, producing radicals and complex organic molecules including polycyclic aromatic hydrocarbons (PAHs), thought to be the primary carriers of the diffuse interstellar bands as well as playing a key role in maintaining charge balance within the ISM. Similar to the studies on aerosols mentioned above, X-ray scattering methods can be used to monitor dust grain growth in laboratory simulations, as well as to probe the morphology and composition of the resulting particles. A detailed understanding of these processes is critical for models of star and planet formation.

As noted in the earlier section, the next-generation XFEL provides opportunities to study reaction mechanisms through the use of THz to XUV ultrafast light sources synchronised with ultrafast X-ray probes. The high energy pump sources create the short-lived radicals involved, while THz or X-ray probes provide chemical identification and track changes in bonding and structure. Combining this with non-linear X-ray probes that provide site-specific detail of the chemical changes promises to provide the most detailed insight into a wide range of reactions identified to occur in astrochemical environments, and may also provide opportunities (including through the use of X-ray probes of chirality, **Section 3.1.3**) to test tentative theories regarding formation of biological molecules in such inhospitable environments.[180]

6.5.5 Conclusion and future vision

The availability of a next-generation XFEL will enable the studies above that will provide new insight into a wide variety of complex, multiscale chemical dynamics, leading to the development of new computational models that provide understanding and drive the innovative design of future systems. A key challenge to successful implementation will be the production of stable and reproducible sample environments, equivalent to the real reactors, fuel injectors, liquid jets, droplets, interstellar ice surfaces etc. that we wish to study. Such development will require innovation and attention during the design and development stages of any future XFEL. These are challenging technical problems but, once solved, the promise of a highly stable, high repetition rate XFEL facility to make fully correlative measurements of key criteria offers unprecedented advantages over current methodologies. The broad range of unique capabilities will enable studies of gas-phase systems, reactions on surfaces and across interfaces, where sensitivity is key. In particular, the combination of X-ray spectroscopies that offer atomic and/or molecular sensitivity in isolated systems (XANES, XES, XCARS, etc) and on surfaces (X-ray second harmonic generation), combined with information on particle growth, size, morphology and the rare events (**Section 3.4**) that drive growth and formation, obtained through hard X-ray scattering and CDI measurements, will allow for detailed comparisons across systems and environments.

6.6 Conclusions and vision: XFEL and chemical sciences

XFELs enable a wealth of research areas spanning all aspects of the chemical sciences, from the fundamentals of photochemistry and catalysis, through to the device and material properties of batteries and photovoltaics, and further into biochemistry and medicine. Owing to the ultrafast timescales of XFEL measurements combined with molecule and atom-specific probes, a state-of-the-art XFEL facility could revolutionise our understanding of chemical processes across all these areas. An XFEL can open-up new horizons in chemical sciences and at the interface with materials, physics, biology and medicine. It will offer an unprecedented degree of scrutiny of reactions happening in gases, liquids, solids and at interfaces, yielding real-time spatially resolved "molecular movies" with atomic precision and femtosecond resolution, paving the way for new photoactive materials. Examples of real-world impact may include photoactive materials for harnessing solar energy and magnetic information storage, light-driven Earth-abundant catalysts for conversion of CO_2 into value-added chemicals, anticancer drugs, and antimicrobial compounds which can help bring clean water to all.

The unique capability of a high repetition rate of over 100 kHz, high brightness XFEL with $>10^{12}$ photons to measure chemically-specific, and even atom-specific maps, on the intrinsic time (towards attoseconds) and length scale (ångstroms) of molecular processes, will offer unprecedented detail of the molecular-scale changes that enable molecular- or macroscopic function, and control efficiency across many orders of magnitude, from molecular level to whole-organism or device. Crucially, the new technological advances of the XFEL will also have the potential to capture the rare events that initiate chemical change, thus providing routes to understanding and controlling material degradation and fouling. Knowledge of the molecular level processes that control chemical and material properties will provide new understanding and real-world impacts that will inspire and deliver next-generation technology.

Such a broad and bold vision also demands a significant provision of diverse auxiliary light sources to act as pump and/or probe. These sources should cover the VUV, UV, Vis, IR, and THz regimes to allow for interrogation of the complex energy landscapes across systems where different modes of activation are required. Synchronisation (~ 5 fs) of multiple pump-probe sources, and the ability to interrogate the same sample by a multitude of X-ray spectroscopic (XES, XAS) and scattering methods (CDI, XPCS) simultaneously is another key requirement of the proposed X-ray plug-and-play combinatorial approach. Active development of novel sample delivery methods will be essential to take full advantage of the XFEL capabilities; particularly where materials are potentially delicate (e.g. batteries and solar cells), contain complex, sometime heterogeneous, mixtures and structures (e.g. combustion), or are both delicate and extremely precious (e.g. cells, proteins, or DNA). Achieving these challenging targets will provide the routes to increased impact across industrial sectors, enable sustainability targets to be met, guide environmental reform, and drive innovation for a prosperous and resilient society.

6.7 References for Chapter 6

1 T. Elsaesser. "Introduction: Ultrafast Processes in Chemistry." *Chem. Rev.* **117**, 10621 (2017) DOI: 10.1021/acs.chemrev.7b00226

2 R.J.D. Miller. "Femtosecond Crystallography with Ultrabright Electrons and X-rays: Capturing Chemistry in Action." *Science* **343**, 1108-1116 (2014) DOI: 10.1126/science.1248488

3 G.D. Scholes, G. Fleming, L. Chen *et al. "*Using coherence to enhance function in chemical and biophysical systems." *Nature* **543**(7647) 647-656 (2017) DOI: 10.1038/nature21425

4 G.D. Scholes, C. Smyth, "Perspective: Detecting and measuring exciton delocalization in photosynthetic light harvesting." *J. Chem. Phys.* **140**, 110901 (2014) DOI: 10.1063/1.4869329

5 F. Fassioli, D.G. Oblinsky, G.D. Scholes, "Designs for molecular circuits that use electronic coherence." *Faraday Discuss.* **163**, 341-351 (2013) DOI: 10.1039/c3fd00009e

6 C. Consani, S. Ruetzel, P. Nuernberger, T. Brixner, "Quantum control spectroscopy of competing reaction pathways in a molecular switch." *J. Phys. Chem. A* **118**, 11364-72 (2014) DOI: 10.1021/jp509382m

7 M. Maiuri, M. Garavelli, G. Cerullo, "Ultrafast Spectroscopy: State of the Art and Open Challenges." *J. Am. Chem. Soc.* **142**, 3-15 (2020) DOI: 10.1021/jacs.9b10533

8 V. Kimberg, N. Rohringer, "Stochastic stimulated electronic x-ray Raman spectroscopy." *Struct. Dyn.* **3**, (2016) DOI: 10.1063/1.4940916

9 P. Wernet, K. Kunnus, I. Josefsson *et al.* "Orbital-specific mapping of the ligand exchange dynamics of $Fe(CO)_5$ in solution." *Nature* **520**, 78, (2015) DOI: 10.1038/nature14296

10 P. Wernet. "Chemical interactions and dynamics with femtosecond X-ray spectroscopy and the role of X-ray free-electron lasers *Phil. Trans. R. Soc. A.* **377:** 20170464 (2019) DOI: 10.1098/rsta.2017.0464

11 M. Levantino *et al.* "Observing heme doming in myoglobin with femtosecond X-ray absorption spectroscopy." *Struct. Dyn.* **2**, 041713 (2015) DOI: 10.1063/1.4921907

12 R. Monni *et al.* "Tryptophan-to-heme electron transfer in ferrous myoglobins." *Proc. Natl. Acad. Sci.* 201423186, (2015) DOI: 10.1073/pnas.1423186112

13 N. Huse *et al.* "Femtosecond Soft X-ray Spectroscopy of Solvated Transition-Metal Dynamics." *J. Phys. Chem. Lett.* **2**, 880-884 (2011) DOI: 10.1021/jz200168m

14 H.T. Lemke, K. Kjær, R. Hartsock *et al.* "Coherent structural trapping through wave packet dispersion during photoinduced spin state switching." *Nat. Commun.* **8**, 15342 (2017) DOI: 10.1038/ncomms15342

15 C-H. Lambert, S. Mangin, B.S.D.Ch.S. Varaprasad *et al.* "All-optical control of ferromagnetic thin films and nanostructures." **345**, 1337-1340 (2014) DOI: 10.1126/science.1253493

16 A. Stupakiewicz, K. Szerenos, M.D. Davydova *et al.* "Selection rules for all-optical magnetic recording in iron garnet." *Nat. Commun.* **10**, 612 (2019) DOI: 10.1038/s41467-019-08458-w

17 W. Zhang, R. Alonsi-Mori, U. Bergmann *et al.* "Tracking excited-state charge and spin dynamics in iron coordination complexes.." *Nature* **509**, 345 (2014) DOI: 10.1038/nature13252

18 T. Li, A. Patz, L. Mouchiliadis *et al.* "Femtosecond switching of magnetism via strongly correlated spin–charge quantum excitations." *Nature* **496**, 69 (2013) DOI: 10.1038/nature11934

19 S. Ohkoshi, K. Imoto, Y. Tsunobuchi *et al.* "Light-induced spin-crossover magnet." *Nat. Chem.* **3**, 564-569 (2011) DOI: 10.1038/nchem.1067

20 A.R. Khorsand, M. Savoini, A. Kirilyuk *et al.* "Element-Specific Probing of Ultrafast Spin Dynamics in Multisublattice Magnets with Visible Light." *Phys. Rev. Lett.* **110**, 107205 (2013) DOI: 10.1103/physrevlett.110.107205

21 K. Haldrup, G. Levi, E. Biasin *et al.* "Ultrafast X-Ray Scattering Measurements of Coherent Structural Dynamics on the Ground-State Potential Energy Surface of a Diplatinum Molecule." *Phys. Rev. Lett.* **122**, 63001 (2019) DOI: 10.1103/physrevlett.122.063001

22 J.M. Ruddock, H. Yong, B. Stankus *et al.* "A deep UV trigger for ground-state ring-opening dynamics of 1,3-cyclohexadiene." *Sci. Adv.* **5**, eaax6625 (2019) DOI: 10.1126/sciadv.aax6625

23 B. Mignolet, B.F.E. Curchod, T.J. Martínez, "Rich Athermal Ground-State Chemistry Triggered by Dynamics through a Conical Intersection." *Angew. Chemie Int. Ed.* **55**, 14993 (2016) DOI: 10.1002/anie.201607633

24 S. Pathak, L.M. Ibele, R. Boll *et al.* "Tracking the Ultraviolet Photochemistry of Thiophenone During and Beyond the Initial Ultrafast Ring Opening." arXiv preprint arXiv: 1912.00531v2 (2020)

25 J.A. Borek, F. Perakis, P. Hamm, "Azide-water intermolecular coupling measured by 2-color 2D IR spectroscopy." *EPJ Web Conf.* **41**, 6005 (2013) DOI: 10.1051/epjconf/20134106005

26 M.P. Grubb, P. Coulter, H. Marroux *et al.* "Translational, rotational and vibrational relaxation dynamics of a solute molecule in a non-interacting solvent." *Nat. Chem.* **8**, 1042-1046 (2016) DOI: 10.1038/nchem.2570

27 M. Aleksich, Y. Cho, D.W. Paley *et al*. "Ligand-Mediated Quantum Yield Enhancement in 1-D Silver Organothiolate Metal–Organic Chalcogenolates." *Adv. Funct. Mater*. **35**, 2414914 (2025) DOI: 10.1002/adfm.202414914

28 M.G. Romei, C-Y. Lin, I.I. Mathews, S.G. Boxer, "Electrostatic control of photoisomerization pathways in proteins." *Science* **367**, 76-79 (2020) DOI: 10.1126/science.aax1898

29 T.J.A. Wolf, R.H. Myhre, J.P. Cryan *et al.* "Probing ultrafast $\pi\pi^*/n\pi^*$ internal conversion in organic chromophores via K-edge resonant absorption." *Nat. Commun.* **8**, 29 (2017) DOI: 10.1038/s41467-017-00069-7

30 K. Schnorr, A. Bhattacherjee, K.J. Oosterbaan *et al.* "Tracing the 267 nm-Induced Radical Formation in Dimethyl Disulfide Using Time-Resolved X-ray Absorption Spectroscopy." *J. Phys. Chem. Lett.* **10**, 1382 (2019) DOI: 10.1021/acs.jpclett.9b00159

31 A.J. Musser, M. Liebel, C. Schnedermann *et al.* "Evidence for conical intersection dynamics mediating ultrafast singlet exciton fission." *Nat. Phys.* **11** (2015) DOI: 10.1038/nphys3241

32 M. Kowalewski, K. Bennett, K.E. Dorfman, S. Mukamel, "Catching Conical Intersections in the Act: Monitoring Transient Electronic Coherences by Attosecond Stimulated X-Ray Raman Signals." *Phys. Rev. Lett.* **115** (2015) DOI: 10.1103/physrevlett.115.193003

33 T.J.A. Wolf and M. Gühr, "Photochemical pathways in nucleobases measured with an X-ray FEL." *Phil. Trans. R. Soc. A* **377**: 20170473 (2019) DOI: 10.1098/rsta.2017.0473

34 M.K. Shankar *et al*. "Ultrafast, remote-controlled protonation reaction enables structural changes in a phytochrome." *Sci. Adv*. **11**, eady0499 (2025) DOI:10.1126/sciadv.ady0499

35 M. Först, R. Mankowsky, A. Cavalleri, "Mode-Selective Control of the Crystal Lattice." *Acc. Chem. Res.* **48**, 2, 380-387 (2015) DOI: 10.1021/ar500391x

36 T.J. Penfold, E. Gindensperger, C. Daniel, C.M. Marian, "Spin-Vibronic Mechanism for Intersystem Crossing." *Chem. Rev.* **118**, 6975 (2018) DOI: 10.1021/acs.chemrev.7b00617

37 M. Iwamura, S. Takeuchi, T. Tahara, "Ultrafast Excited-State Dynamics of Copper(I) Complexes." *Acc. Chem. Res.* **48**, 782 (2015) DOI: 10.1021/ar500353h

38 T. Katayama, T. Northey, W. Gawelda *et al.* "Tracking multiple components of a nuclear wavepacket in photoexcited Cu(I)-phenanthroline complex using ultrafast X-ray spectroscopy." *Nat. Commun.* **10**, 3606 (2019) DOI: 10.1038/s41467-019-11499-w

39 R.M. van der Veen, A. Cannizzo, F. van Mourik *et al.* "Vibrational relaxation and intersystem crossing of binuclear metal complexes in solution." *J. Am. Chem. Soc.* **133**, 305-315 (2011) DOI: 10.1021/ja106769w

40 M. Chergui, E. Collet, "Photoinduced Structural Dynamics of Molecular Systems Mapped by Time-Resolved X-ray Methods." *Chem. Rev.* **117**, 11025-11065 (2017) DOI: 10.1021/acs.chemrev.6b00831; P. Kim, A. J. S. Valentine, S. Roy *et al.* "Ultrafast branching in intersystem crossing dynamics revealed by coherent vibrational wavepacket motions in a bimetallic Pt(II) complex", *Faraday Discuss.* **237**, 259-273 (2022) DOI: 10.1039/D2FD00009A

41 M. Nowakowski, M. Huber-Gedert, H. Elgabarty *et al*. "Ultrafast Two-Color X-Ray Emission Spectroscopy Reveals Excited State Landscape in a Base Metal Dyad." *Adv. Sci.* **11**(38):e2404348 (2024) DOI: 10.1002/advs.202404348

42 D. Meshulach and Y. Silberberg, "Coherent quantum control of two-photon transitions by a femtosecond laser pulse." *Nature* **396**, 239-242 (1998) DOI: 10.1038/24329

43 M. Delor. P.A. Scattergood, I.V. Sazanovich *et al.* "Toward control of electron transfer in donor-acceptor molecules by bond-specific infrared excitation." *Science* **346**, 1492 (2014) DOI: 10.1126/science.1259995

44 A.A. Bakulin, A. Rao, V.G. Pavelyev *et al.* "The Role of Driving Energy and Delocalized States for Charge Separation in Organic Semiconductors." *Science* **335**, 1340-1344 (2012) DOI: 10.1126/science.1217745

45 L.K. McKenzie, I.V. Sazanovich, E. Baggaley *et al.* " Frontispiece: Metal Complexes for Two-Photon Photodynamic Therapy: A Cyclometallated Iridium Complex Induces Two-Photon Photosensitization of cancer Cells under Near-IR LIght." *Chem. Eur. J.* **23** (2017) DOI: 10.1002/chem.201780262

46 K.L. Smitten, H.M. Southam, J.B. de la Serna *et al.* "Using Nanoscopy To Probe the Biological Activity of Antimicrobial Leads That Display Potent Activity against Pathogenic, Multidrug Resistant, Gram-Negative Bacteria." *ACS Nano*. **13**(5), 5133-5146 DOI: 10.1021/acsnano.8b08440

47 L. Pasquina-Lemonche, J. Burns, R.D. Turner *et al.* "The architecture of the Gram-positive bacterial cell wall." *Nature* **582**, 294-297 (2020) DOI: 10.1038/s41586-020-2236-6

48 Y. Zhang, D.T. Payne, C.L. Pang, C. Cacho. R.T. Chapman. E. Springate, H.H. Fielding, G. Thornton, "State-selective dynamics of TiO_2 charge-carrier trapping and recombination." *J. Phys. Chem. Lett.*, **10**, 5265-5270 (2019) DOI: 10.1021/acs.jpclett.9b02153

49 N.T. Hunt, "2D-IR spectroscopy: ultrafast insights into biomolecule structure and function." *Chem. Soc. Rev*. **38**, 1837 (2009) DOI: 10.1039/B819181F

50 J. Lu, X. Li *et al.* "Two-dimensional spectroscopy at terahertz frequencies*"* in: T. Buckup, J. Leonard (eds) Multidimensional Time-Resolved Spectroscopy. *Top Curr Chem (Z)* **376**, 6 (2018) DOI: 10.1007/s41061-018-0185-4

51 M. Delor, T. Keane, P.A. Scattergood *et al.* "On the mechanism of vibrational control of light-induced charge transfer in donor–bridge–acceptor assemblies." *Nat. Chem*. **7**(9):689-695 (2015) DOI: 10.1038/nchem.2327

52 X. Li, T. Qiu, J. Zhang *et al.* "Terahertz field–induced ferroelectricity in quantum paraelectric $SrTiO_3$." *Science* **364**, 1079 (2019) DOI: 10.1126/science.aaw4913

53 M. Kozina, M. Fechner, P. Marsik *et al.* "Terahertz-driven phonon upconversion in $SrTiO_3$." *Nat. Phys*. **15**, 387 (2019) DOI: 10.1038/s41567-018-0408-1

54 R.J.D. Miller, "Mapping atomic motions with ultrabright electrons: The chemists' gedanken experiment enters the lab frame." *Annu. Rev. Phys. Chem*. **65**, 583 (2014) DOI: 10.1146/annurev-physchem-040412-110117

55 A.D. Burnett, J. Kendrick, C. Russell *et al.* "Effect of molecular size and particle shape on the terahertz absorption of a homologous series of tetraalkylammonium salts." *Anal. Chem*. **85**, 16, 7926-7934 (2013) DOI: 10.1021/ac401657r

56 S. Ye, K. Tonokura, M. Koshi, "Energy transfer rates and impact sensitivities of crystalline explosives." *Combust. Flame* **132**, 240-246 (2003) DOI: 10.1016/S0010-2180(02)00461-3

57 J. Sibik, J. Axel Zeitler, "Terahertz response of organic amorphous systems: experimental concerns and perspectives." *Philos. Mag*. **96**, 842 (2016) DOI: 10.1080/14786435.2015.1111528

58 K.A. Niessen, M. Xu, A.G. Markelz, "Terahertz optical measurements of correlated motions with possible allosteric function." *Biophys. Rev*. **7**, 201 (2015) DOI: 10.1007/s12551-015-0168-4

59 A. Beneduci, "Which is the effective time scale of the fast Debye relaxation process in water?." *J. Mol. Liq*. **138**, 55 (2008) DOI: 10.1016/j.molliq.2007.07.003

60 E.P. Parrott, J. Axel Zeitler, "Terahertz time-domain and low-frequency Raman spectroscopy of organic materials." *Appl. Spectrosc*. **69**, 1 (2015) DOI: 10.1366/14-07707

61 V. Conti Nibali, M. Havenith, "New insights into the role of water in biological function: Studying solvated biomolecules using terahertz absorption spectroscopy in conjunction with molecular dynamics simulations." *J. Am. Chem. Soc.* **136**, 12800 (2014) DOI: 10.1021/ja504441h

62 C. Roth, T. Peppel, K. Fumino *et al.* "The importance of hydrogen bonds for the structure of ionic liquids: Single-crystal X-ray diffraction and transmission and attenuated total reflection spectroscopy in the terahertz region." *Angew. Chem. Int. Ed*. **49**, 10221 (2010) DOI: 10.1002/anie.201004955

63 S. Hay, N. Scrutton, "Good vibrations in enzyme-catalysed reactions." *Nat. Chem*. **4**, 161 (2012) DOI: 10.1038/nchem.1223

64 K.A. Niessen, M. Xu, D.K. George *et al.* "Protein and RNA dynamical fingerprinting." *Nat Commun* **10**, 1026 (2019) DOI: 10.1038/s41467-019-08926-3

65 S. Pezzotti, W. Chen, F. Novelli *et al*. "Terahertz calorimetry spotlights the role of water in biological processes." *Nat. Rev. Chem*. **9**, 481–494 (2025) DOI: 10.1038/s41570-025-00712-8

66 M.R. Ryder, B. Civalleri, T.D. Bennett *et al.* "Identifying the role of terahertz vibrations in metal-organic frameworks: from gate-opening phenomenon to shear-driven structural destabilization." *Phys. Rev. Lett*. **113**, 215502 (2014) DOI: 10.1103/PhysRevLett.113.215502

67 N.Y. Tan, M.T. Ruggiero, C. Orellana-Tavra *et al.* "Investigation of the terahertz vibrational modes of ZIF-8 and ZIF-90 with terahertz time-domain spectroscopy." *Chem. Commun*. **51**, 16037 (2015) DOI: 10.1039/c5cc06455d

68 T. Itakura, H. Matsui, T. Tada *et al.* "The role of lattice vibration in the terahertz region for proton conduction in 2D metal–organic frameworks." *Chem. Sci*. **11**, 1538-1541(2020) DOI: 10.1039/c9sc05757a

69 S.A. Ajibade, L. Catalano, J. Kölbel *et al*. "Terahertz Spectroscopy Unambiguously Determines the Orientation of Guest Water Molecules in a Structurally Elusive Metal–Organic Framework." *J. Phys. Chem. Lett*. **15** (20) 5549-5555 (2024) DOI: 10.1021/acs.jpclett.4c00706

70 L. Catalano, R. Sharma, D.P Karothu *et al*. "Toward on-demand polymorphic transitions of organic crystals via side chain and lattice dynamics engineering." *J. Am. Chem. Soc*. **146** (46) 31911-31919 (2024) DOI: 10.1021/jacs.4c11289

71 A. Nilsson, J. LaRue, H. Öberg *et al.* "Catalysis in real time using X-ray lasers." *Chem. Phys. Lett*. **675**, 145-173 (2017) DOI: 10.1016/j.cplett.2017.02.018

72 P. Salén, M. Basini, S. Bonetti *et al.* "Matter manipulation with extreme terahertz light: Progress in the enabling THz technology." *Physical Reports* **836-837**, 1-74 (2019) DOI: 10.1016/j.physrep.2019.09.002

73 T. Kampfrath, K. Tanaka and K. Nelson, "Resonant and nonresonant control over matter and light by intense terahertz transients." *Nature Photon* **7**, 680-690 (2013) DOI: 10.1038/nphoton.2013.184

74 S. Fleischer, Y. Zhou, R.W. Field, K.A. Nelson, "Molecular orientation and alignment by intense single-cycle THz pulses." *Phys. Rev. Lett*. **107**, 163603 (2011) DOI: 10.1103/PhysRevLett.107.163603

75 M.T. Ruggiero, M. Krynski, E.O. Kissi *et al.* "The significance of the amorphous potential energy landscape for dictating glassy dynamics and driving solid-state crystallisation." *Phys. Chem. Chem. Phys.* **19**, 30039 (2017) DOI: 10.1039/c7cp06664c

76 Z. Zhu, S. Gu, C. Chang *et al*. "Computational study of terahertz-driven controllable molecular isomerization." *Nat Commun* **16**, 7081 (2025) DOI: 10.1038/s41467-025-62521-3

77 S.L. Price, "Control and prediction of the organic solid state: a challenge to theory and experiment." *Proc. R. Soc. London, Ser. A* **474**, 20180351 (2018) DOI: 10.1098/rspa.2018.0351

78 J.L. Larue, T. Katayama, A. Lindenberg *et al.* "THz-pulse-induced selective catalytic CO oxidation on Ru." *Phys. Rev. Lett*. **115**, 036103 (2015) DOI: 10.1103/PhysRevLett.115.036103

79 Z. Zhu, J. Zhu C. Chang *et al*. "Tunable Surface Wettability via Terahertz Electrowave Controlled Vicinal Subnanoscale Water Layer." *Nano Lett*. **24**, (10) 3243–3248 (2024) DOI: 10.1021/acs.nanolett.4c00248

80 J. Lu, X. Li, H.Y. Hwang *et al.* "Coherent two-dimensional terahertz magnetic resonance spectroscopy of collective spin waves." *Phys. Rev. Lett*. **118**, 207204 (2017) DOI: 10.1103/PhysRevLett.118.207204

81 F. Chen *et al.* "Ultrafast terahertz-field-driven ionic response in ferroelectric $BaTiO_3$." *Phys. Rev. B: Condens. Matter* **94**, 180104 (2016) DOI: 10.1103/PhysRevB.94.180104

82 M. Basini, M. Pancaldi, B. Wehinger *et al*. "Terahertz electric-field-driven dynamical multiferroicity in $SrTiO_3$." *Nature* **628**, 534–539 (2024) DOI: 10.1038/s41586-024-07175-9

83 G. Orenstein, V. Krapivin, Y. Huang *et al*. "Observation of polarization density waves in SrTiO3." *Nat. Phys*. **21**, 961–965 (2025) DOI: 10.1038/s41567-025-02874-0

84 M. Krasilnikov, Z. Aboulbanine, G. Adhikari *et al*. "First high peak and average power single-pass THz free-electron laser in operation." *Phys. Rev. Accel. Beams* **28**, 030701 (2025) DOI: 10.1103/PhysRevAccelBeams.28.030701

85 https://www.iea.org/reports/electricity-2026

86 A. Stupakiewicz, K. Szerenos, D. Afanasiev *et al.* "Ultrafast nonthermal photo-magnetic recording in a transparent medium." *Nature* **542**, 71-74 (2017) DOI: 10.1038/nature20807

87 F. Liedy, J. Eng, R. McNab *et al.* "Vibrational coherences in manganese single-molecule magnets after ultrafast photoexcitation." *Nat. Chem*. **12**, 452-458 (2020) DOI: 10.1038/s41557-020-0431-6

88 G. Auböck, M. Chergui, "Sub-50-fs photoinduced spin crossover in $[Fe(bpy)_3]^{2+}$." *Nat Chem*. **7**(8):629-633 (2015) DOI: 10.1038/nchem.2305

89 S.E. Canton, M. Biednov, M. Pápai *et al*. "Ultrafast Jahn-Teller Photoswitching in Cobalt Single-Ion Magnets." *Adv Sci* **10**(21):e2206880 (2023) DOI: 10.1002/advs.202206880

90 D. Vinci, K. Ridier, F. Qi *et al*. "Capturing ultrafast molecular motions and lattice dynamics in spin crossover film using femtosecond diffraction methods." *Nat Commun* **16**, 2043 (2025) DOI: 10.1038/s41467-025-57202-0

91 M. Roth, D. Jung, K. Falk *et al*. "Bright Laser-Driven Neutron Source Based on the Relativistic Transparency of Solids." *Phys Rev Lett* **110**(4):044802 (2013) DOI: 10.1103/PhysRevLett.110.044802

92 M.M. Günther, O.N. Rosmej, P. Tavana *et al.* "Forward-looking insights in laser-generated ultra-intense γ-ray and neutron sources for nuclear application and science." *Nat Commun* **13**, 170 (2022) DOI: 10.1038/s41467-021-27694-7

93 W. Weyl, "Ueber Metallammonium-Verbindungen." *Pogg. Ann. Phys*. **123**, 350-367 (1864) DOI: 10.1002/andp.18641970407

94 E.J. Hart, J.W. Boag, "Absorption Spectrum of the Hydrated Electron in Water and in Aqueous Solutions." *J. Am. Chem. Soc*. **84**, 4090-4095 (1962) DOI: 10.1021/ja00880a025

95 M.J. Bird *et al*. "Pushing the limits of the electrochemical window with pulse radiolysis in chloroform." *Phys. Chem. Chem. Phys*. **22**, 14660-14670 (2020) DOI: 10.1039/d0cp01948h

96 N.A. Till *et al*. "The Application of Pulse Radiolysis to the Study of Ni(I) Intermediates in Ni-Catalyzed Cross-Coupling Reactions." *J Am Chem Soc*. **143**(25):9332-9337 (2021) DOI: 10.1021/jacs.1c04652.

97 https://www.dalton.manchester.ac.uk/research/

98 B. Dromey, M. Coughlan, L. Senje *et al.* "Picosecond metrology of laser-driven proton bursts." *Nat Commun* **7**, 10642 (2016) DOI: 10.1038/ncomms10642

99 S. Kar, H. Ahmed, R. Prasad *et al.* "Guided post-acceleration of laser-driven ions by a miniature modular structure." *Nat Commun* **7**, 10792 (2016) DOI: 10.1038/ncomms10792

100 A. Prasselsperger, M. Coughlan, N. Breslin *et al*. "Real-Time Electron Solvation Induced by Bursts of Laser-Accelerated Protons in Liquid Water." *Phys Rev Lett*. **127**(18):186001 (2021) DOI: 10.1103/PhysRevLett.127.186001

101 J.P. Kennedy *et al.* "Real-Time Observation of Frustrated Ultrafast Recovery from Ionization in Nanostructured SiO_2 Using Laser-Driven Accelerators." *Phys. Rev. Lett*. **133**, 135001 (2024) DOI: 10.1103/PhysRevLett.133.135001

102 S. Vallières, F. Fillion-Gourdeau, S. Fourmaux *et al*. "High average-flux laser-driven neutron source." *Nat Commun* **16**, 11498 (2025) DOI: 10.1038/s41467-025-66535-9

103 Z.H. Loh, G. Doumy, C. Arnold *et al.* "Observation of the fastest chemical processes in the radiolysis of water." *Science*, **367**(6474):179-182 (2020) DOI: 10.1126/science.aaz4740

104 L. Kjellsson, K.D. Nanda, J.E. Rubensson *et al*. "Resonant Inelastic X-Ray Scattering Reveals Hidden Local Transitions of the Aqueous OH Radical." *Phys Rev Lett*. **124**(23):236001 (2020) DOI: 10.1103/PhysRevLett.124.236001

105 S. Li *et al*. "Attosecond-pump attosecond-probe x-ray spectroscopy of liquid water." *Science* **383**, 1118-1122 (2024) DOI: 10.1126/science.adn6059

106 M. Kudisch, R.X. Hooper, L.K. Valloli *et al*. "Photolytic activation of Ni(II)X2L explains how Ni-mediated cross coupling begins." *Nat Commun* **16**, 5530 (2025) DOI:10.1038/s41467-025-60729-x

107 D.C. Grills *et al.* "Mechanistic aspects of CO_2 reduction catalysis with manganese-based molecular catalysts." *Coordination Chemistry Reviews* **374**, 173-217 (2018) DOI: 10.1016/j.ccr.2018.05.022

108 G. Ertl *et al* (Eds), *Handbook of Heterogeneous Catalysis*. (Wiley-VCH, Weinheim, 2008). DOI: 10.1002/9783527610044

109 "GDP(O) Low Level Aggregates National Accounts." *ONS, 2025*

110 "UK Employee Jobs by Industry." *ONS, September 2025*

111 Q. Zhao, G. Meng, S.P. Nolan, M. Szostak, "N-Heterocyclic Carbene Complexes in C-H Activation Reactions." *Chemical Reviews* **120** 1981 (2020) DOI: 10.1021/acs.chemrev.9b00634

112 C.J. Taylor, A. Pomberger, K.C. Felton *et al*. "A Brief Introduction to Chemical Reaction Optimization." *Chem. Rev*. **123** (5) 3089-3126 (2023) DOI: 10.1021/acs.chemrev.2c00798

113 J.K. McCusker, "Photocatalysis: Fuel from photons." *Science* **293** 1599 (2001) DOI: 10.1126/science.1064112

114 M. Grätzel, "Solar energy conversion by dye-sensitized photovoltaic cells." *Inorg. Chem.* **44**, 6841 (2005) DOI: 10.1021/ic0508371

115 L.X. Chen, X. Zhang, "Photochemical processes revealed by X-ray transient absorption spectroscopy." *J. Phys. Chem. Lett.* **4**, 4000 (2013) DOI: 10.1021/jz401750g

116 S.A. Bartlett, N.A. Besley, A.J. Dent *et al.* "Monitoring the Formation and Reactivity of Organometallic Alkane and Fluoroalkane Complexes with Silanes and Xe Using Time-Resolved X-ray Absorption Fine Structure Spectroscopy." *J. Am. Chem. Soc.* **141**, 11471 (2019) DOI: 10.1021/jacs.8b13848

117 L.X. Chen, X. Zhang, E.C. Wasinger *et al.* "Tracking electrons and atoms in a photoexcited metalloporphyrin by X-ray transient absorption spectroscopy." *J. Am. Chem. Soc.* **129**, 9616 (2007) DOI: 10.1021/ja072979v

118 L.X. Chen, X. Zhang, E.C. Wasinger *et al.* "X-ray snapshots for metalloporphyrin axial ligation." *Chem. Sci.* **1**, 642-650 (2010) DOI: 10.1039/c0sc00323a

119 R.W. Schoenlein, S. Chattopadhyay, H.H. Chong *et al.* "Generation of femtosecond pulses of synchrotron radiation." *Science* **287**, 2237-2240 (2000) DOI: 10.1126/science.287.5461.2237

120 P. Beaud, S.L. Johnson, A. Streun *et al.* "Spatiotemporal stability of a femtosecond hard-X-ray undulator source studied by control of coherent optical phonons." *Phys. Rev. Lett.* **99**, 174801 (2007) DOI: 10.1103/physrevlett.99.174801

121 J.I. Goldsmith, W.R. Hudson, M.S. Lowry, T.H. Anderson. S. Bernhard, "Discovery and high-throughput screening of heteroleptic iridium complexes for photoinduced hydrogen production." *J. Am. Chem. Soc.* **127**, 7502-10 (2005) DOI: 10.1021/ja0427101

122 H.B. Gray, A.W. Maverick, "Solar chemistry of metal complexes." *Science* **214**, 1201-5 (1981) DOI: 10.1126/science.214.4526.1201

123 H.T. Lemke, C. Bressler, L.X. Chen *et al.* "Femtosecond x-ray absorption spectroscopy at a hard x-ray free electron laser: Application to spin crossover dynamics." *J. Phys. Chem. A* **117**, 735-740 (2013) DOI: 10.1021/jp312559h

124 T. Katayama, Y. Inubushi, Y. Obara *et al.* "Femtosecond x-ray absorption spectroscopy with hard x-ray free electron laser." *Appl. Phys. Lett.* **103**, 131105 (2013) DOI: 10.1063/1.4821108

125 T. Katayama, S. Owada, T. Togashi *et al.* "A beam branching method for timing and spectral characterization of hard X-ray free-electron lasers." *Struct. Dyn.* **3**, 034301 (2016) DOI: 10.1063/1.4939655

126 K. Nakajima, Y. Yoti, T. Katayama *et al.* "Software for the data analysis of the arrival-timing monitor at SACLA." *J. Synchrotron Radiat.* **25**, 592-603 (2018) DOI: 10.1107/s1600577517016654

127 Y. Kayser, C. Milne, P. Juranić *et al.* "Core-level nonlinear spectroscopy triggered by stochastic X-ray pulses." *Nat. Commun.* **10**, 4761 (2019) DOI: 10.1038/s41467-019-12717-1

128 W. Gawelda, V.T. Pham, M. Benfatto *et al.* "Structural determination of a short-lived excited iron(II) complex by picosecond X-ray absorption spectroscopy." *Phys. Rev. Lett.* **98**, 6 (2007) DOI: 10.1103/physrevlett.98.057401

129 Ch. Bressler, C. Milne, V.T. Pham *et al.* "Femtosecond XANES study of the light-induced spin crossover dynamics in an iron(II) complex." *Science* **323**, 489-492 (2009) DOI: 10.1126/science.1165733

130 R. Chatterjee, C. Weninger, A. Loukianov *et al.* "XANES and EXAFS of dilute solutions of transition metals at XFELs." *J. Synchrotron Radiat.* **26**, 1716-1724 (2019) DOI: 10.1107/s1600577519007550

131 A. Britz, B. Abraham, E. Biasin *et al.* "Resolving structures of transition metal complex reaction intermediates with femtosecond EXAFS." *Phys. Chem. Chem. Phys.* **22**, 2660-2666 (2020) DOI: 10.1039/c9cp03483h

132 G. Vankó, P. Glatzel, V.T. Pham *et al.* "Picosecond time-resolved X-ray emission spectroscopy: Ultrafast spin-state determination in an iron complex." *Angew. Chemie - Int. Ed.* **49**, 5910-5912 (2010) DOI: 10.1002/anie.201000844

133 K. Kunnus, I. Josefsson, I. Rajkovic *et al.* "Identification of the dominant photochemical pathways and mechanistic insights to the ultrafast ligand exchange of $Fe(CO)_5$ to $Fe(CO)_4EtOH$." *Struct. Dyn.* **3** 043204 (2016) DOI: 10.1063/1.4941602

134 T. Katayama, T. Anniyev, M. Beye *et al.* "Ultrafast soft X-ray emission spectroscopy of surface adsorbates using an X-ray free electron laser." *J. Electron Spectros. Relat. Phenomena* **187**, 9-14 (2013) DOI: 10.1016/j.elspec.2013.03.006

135 M. Dell'Angela, T. Anniyev, M. Beye *et al.* "Real-Time Observation of Surface Bond Breaking with an X-ray Laser." *Science* **339**, 1302-1305 (2013) DOI: 10.1126/science.1231711

136 M. Beye, T. Anniyev, R. Coffee *et al.* "Selective ultrafast probing of transient hot chemisorbed and precursor states of CO on Ru(0001)." *Phys. Rev. Lett.* **110**, 186101 (2013) DOI: 10.1103/physrevlett.110.186101

137 H.-Y. Wang, S. Schreck, M. Weston *et al.* "Time-resolved observation of transient precursor state of CO on Ru(0001) using carbon K-edge spectroscopy." *Phys. Chem. Chem. Phys.* **22**, 2677 (2020) DOI: 10.1039/c9cp03677f

138 H. Öström, H. Öberg, H. Xin *et al.* "Surface Chemistry: Probing the transition state region in catalytic CO oxidation on Ru." *Science* **347**, 978-982 (2015) DOI: 10.1126/science.1261747

139 T.B. van Driel, K. Kjær, R. Hartsock *et al.* "Atomistic characterization of the active-site solvation dynamics of a model photocatalyst." *Nat. Commun.* **7**, 13678 (2016) DOI: 10.1038/ncomms13678

140 K.H. Kim, J. Kim. S. Nozama *et al.* "Direct observation of bond formation in solution with femtosecond X-ray scattering." *Nature* **518**, 385-389 (2015) DOI: 10.1038/nature14163

141 K.H. Kim, J.G. Kim, K.Y. Oang *et al.* "Femtosecond X-ray solution scattering reveals that bond formation mechanism of a gold trimer complex is independent of excitation wavelength." *Struct. Dyn.* **3**, 043209 (2016) DOI: 10.1063/1.4948516

142 S.E. Canton, K. Kjær, G. Vankó *et al.* "Visualizing the non-equilibrium dynamics of photoinduced intramolecular electron transfer with femtosecond X-ray pulses." *Nat Commun* **6**, 6359 (2015) DOI: 10.1038/ncomms7359

143 K. Haldrup, W. Gawelda, R. Abela *et al.* "Observing Solvation Dynamics with Simultaneous Femtosecond X-ray Emission Spectroscopy and X-ray Scattering." *J. Phys. Chem. B* **120**, 1158-1168 (2016) DOI: 10.1021/acs.jpcb.5b12471

144 T. Chung et al. "Ultrafast X-ray Absorption Spectroscopy Reveals Excited-State Dynamics of B_{12} Coenzymes Controlled by the Axial Base." *J. Phys. Chem. B* **128**, 6, 1428–1437 (2024) DOI: 10.1021/acs.jpcb.3c07779

145 R.J. Sension *et al.* "Watching Excited State Dynamics with Optical and X-ray Probes: The Excited State Dynamics of Aquocobalamin and Hydroxocobalamin." *J. Am. Chem. Soc*. **145**, 25, 14070–14086 (2023) DOI: 10.1021/jacs.3c04099

146 R.J. Sension *et al.* "Structural Evolution of Photoexcited Methylcobalamin toward a CarH-like Metastable State: Evidence from Time-Resolved X-ray Absorption and X-ray Emission." *J. Phys. Chem. B* **128**, 34, 8131–8144 (2024) DOI: 10.1021/acs.jpcb.4c03729

147 W. Cheng *et al.* "In situ pump-flow-probe XAFS study of photoexcited electron transfer over single atom-Pt/CoOOH photocatalysts." *Chemistry Letters* **53**:1, upae012 (2024) DOI: 10.1093/chemle/upae012

148 L. Carneiro, S. Cushing, C. Liu *et al*. "Excitation-wavelength-dependent small polaron trapping of photoexcited carriers in α-Fe_2O_3." *Nature Mater* **16**, 819–825 (2017) DOI: 10.1038/nmat4936

149 A. Koide *et al*. "Photoinduced anisotropic distortion as the electron trapping site of tungsten trioxide by ultrafast W L_1-edge X-ray absorption spectroscopy with full potential multiple scattering calculations." *Phys. Chem. Chem. Phys*. **22**, 2615-2621 (2022) DOI: 10.1039/C9CP01332F

150 D. Kido *et al*. "Metastable Structure of Photoexcited WO_3 Determined by the Pump-probe Extended X-ray Absorption Fine Structure Spectroscopy and Constrained Thorough Search Analysis." *Chemistry Letters* **51**:11, 1083-1086 (2022) DOI: 10.1246/cl.220381

151 S. Pelatti, E. Spurio, D. Catone *et al.* " Ultrafast Dynamics of Electronic and Structural Modifications Induced by Photoexcitation in Cerium Oxide." *Adv. Electron. Mater*.: e00429. (2025) DOI: 10.1002/aelm.202500429

152 J. Szlachetko, M. Nachtegaal, J. Sá *et al.* "High energy resolution off-resonant spectroscopy at sub-second time resolution: (Pt(acac)2) decomposition." *Chem. Commun.* **48**, 10898 (2012) DOI: 10.1039/c2cc35086f

153 J. Szlachetko, C.J. Milne, J. Hoszowska *et al.* "Communication: The electronic structure of matter probed with a single femtosecond hard x-ray pulse." *Struct. Dyn.* **1**, 021101 (2014) DOI: 10.1063/1.4868260

154 M. Bauer. "*Private Communication*"

155 T-L. Lee and D.A. Duncan, "A Two-Color Beamline for Electron Spectroscopies at Diamond Light Source." *Synchrotron Radiat. News* **31**, 16 (2018) DOI: 10.1080/08940886.2018.1483653

156 J.B. Bell, M.S. day, M.J. Lijewski, "Simulation of nitrogen emissions in a premixed hydrogen flame stabilized on a low swirl burner." *Proceedings of the Combustion Institute* **34**(1):1173-1182 (2013) DOI: 10.1016/j.proci.2012.07.046

157 UK Greenhouse Gas Emissions National Statistics. Available from https://www.gov.uk/government/collections/final-uk-greenhouse-gas-emissions-national-statistics

158 M.J. Evans and P.R. Medwell. "Understanding and Interpreting Laser Diagnostics in Flames: A Review of Experimental Measurement Techniques." *Front. Mech. Eng*. **5**, 65 (2019) DOI: 10.3389/fmech.2019.00065

159 J.H. Frank, A. Shavorskiy, H. Bluhm *et al.* "In situ soft X-ray absorption spectroscopy of flames." *Appl. Phys. B* **117**, 493-499 (2014). DOI: 10.1007/s00340-014-5860-8

160 J. Dunnmon, S. Sobhani, T.W Kim *et al.* "Characterization of scalar mixing in dense gaseous jets using X-ray computed tomography." *Exp Fluids* **56**, 193 (2015) DOI: 10.1007/s00348-015-2057-9

161 M.R. Kamesh *et al.* "Approaches and solutions to HCCI – a review energy systems: fuel and combustion, injection and atomization" *IOP Conf. Series: Materials Science and Engineering* **402**, 012204 (2018) DOI:10.1088/1757-899X/402/1/012204

162 D.L. Osborn. "Reaction Mechanisms on Multiwell Potential Energy Surfaces in Combustion (and Atmospheric) Chemistry." *Annu. Rev. Phys. Chem*. **68**, 233 (2017) DOI: 10.1146/annurev-physchem-040215-112151

163 H. Zang, Y. Fu, M. Hou *et al.* "Ultrafast swelling and shrinking of soot in alkanol–air flames induced by femtosecond laser filamentation."

Combust. Flame, **212**, 345 (2020), DOI: 10.1016/j.combustflame.2019.11.009

164 S. Tanaka and S. Mukamel, "Coherent X-ray Raman spectroscopy: A nonlinear local probe for electronic excitation," *Phys. Rev. Lett*. **89**, 043001 (2002) DOI: 10.1103/PhysRevLett.89.043001

165 G. Koch, "Cost of Corrosion." in "Trends in Oil and Gas Corrosion Research and Technologies" ed. A.M. El-Sherik, Woodhead Publishing, 1st edn, 2017, ch. 1, pp 3-30, DOI: 10.1016/B978-0-08-101105-8.00001-2

166 U. Hejral, D. Franz, S. Volkov, S. Francoual, J. Strempfer, and A. Stierle, "Identification of a Catalytically Highly Active Surface Phase for CO Oxidation over PtRh Nanoparticles under Operando Reaction Conditions." *Phys. Rev. Lett.* **120**, 126101 (2018) DOI: 10.1103/PhysRevLett.120.126101

167 H. Koo, R. Allan, R. Howlin *et al.* "Targeting microbial biofilms: current and prospective therapeutic strategies." *Nat. Rev. Microbiol*. **15**, 740-755 (2017) DOI: 10.1038/nrmicro.2017.99

168 R.K. Lam *et al.* "Soft X-Ray Second Harmonic Generation as an Interfacial Probe." *Phys. Rev. Lett*. **120**, 023901 (2018). DOI: 10.1103/PhysRevLett.120.023901

169 B.I. Escher, H.M. Staleton, E.L. Schymanski, "Tracking Complex Mixtures of Chemicals in our Changing Environment." *Science* **367**, 388392 (2020) DOI: 10.1126/science.aay6636

170 K.H. Bates and D.J. Jacob, "A new model mechanism for atmospheric oxidation of isoprene: global effects on oxidants, nitrogen oxides, organic products, and secondary organic aerosol." *Atmos. Chem. Phys*. **19**, 9613 (2019) DOI:10.5194/acp-19-9613-2019

171 C.A. Taatjes, O. Welz, A.J. Eskola *et al.* "Direct Measurements of Conformer-Dependent Reactivity of the Criegee Intermediate CH_3CHOO " *Science* **340**, 177-180 (2013) DOI: 10.1126/science.1234689

172 C.A. Taatjes, D.E. Shallcross and C. Percival, "Intermediates just want to react." *Nature Chem* **6**, 461-462 (2014) DOI: 10.1038/nchem.1966

173 C.A. Taatjes, D.E. Shallcross and C. Percival, "Research frontiers in the chemistry of Criegee intermediates and tropospheric ozonolysis." *Phys. Chem. Chem. Phys.* **16**, 1704-1718 (2014) DOI: 10.1039/C3CP52842A

174 U. Pöschl, "Atmospheric Aerosols: Composition, Transformation, Climate and Health Effects." *Angew. Chem. Int. Ed*. **44**, 7520-7540 (2005). DOI: 10.1002/anie.200501122

175 D. Yang, H. Zhang and J. Li, "Changes in anthropogenic PM2.5 and the resulting global climate effects under the RCP4.5 and RCP8.5 scenarios by 2050." *Earth's Future* **8**, e2019EF001285 (2020). DOI: 10.1029/2019EF001285

176 T.C. Bond, S.J. Doherty, D.W. Fahey *et al.* "Bounding the role of black carbon in the climate system: A scientific assessment." *J. Geophys. Res. Atmos.* **118**, 5380 (2013) DOI:10.1002/jgrd.50171

177 N.L. Prisle, "Surfaces of Atmospheric Droplet Models Probed with Synchrotron XPS on a Liquid Microjet." *Acc. Chem. Res*. **57**, 2, 177–187 (2024) DOI: 10.1021/acs.accounts.3c00201

178 M. McClure *et al*. James Webb Space Telescope IceAge Project, http://jwst-iceage.org/

179 A. Belloche, R.T. Garrod, H.S.P. Müller, K.M. Menten, "Detection of a branched alkyl molecule in the interstellar medium: iso-propyl cyanide." *Science* **345**, 1584 (2014) DOI: 10.1126/science.1256678

180 R.I. Kaiser *et al.* "On the formation of dipeptides in interstellar model ices." *Astrophys. J.* **765**, 111 (2013) DOI: 10.1088/0004-637X/765/2/111

7. Science Opportunities in the Life Sciences

The strongest current cases of XFEL use in the life sciences include serial femtosecond crystallography (SFX), time-resolved SFX, time-resolved X-ray spectroscopy and time-resolved single particle imaging. The SFX methods exploit slurries of nano- to micro-crystalline samples, at near-physiological temperature and pressure, to generate atomic resolution models and probe authentic function from the same sample. Reaction cycles for time-resolved SFX are initiated by light or mixing strategies and many are generalisable across all of biology. Thus, dynamic structural biology and molecular movies of macromolecular function will become routine. In many cases, especially with metal-dependent systems, complementary spectroscopic information can also be collected from the same samples and X-ray pulses (e.g. X-ray emission spectroscopy, XES), providing even more detailed mechanistic insights. Structure-functional results will translate into better drugs and treatments impacting human health, and better catalysis for clean energy and agriculture. A frontier opportunity that remains particularly challenging is to extend single particle imaging methods to biomolecules in solution, so that nearly all dynamic processes in biology can be studied with high temporal and spatial resolution. A next-generation XFEL with the greatest impact and benefit to many life science research groups in the UK and abroad will deliver evenly spaced X-ray pulses to the end station at 10k – 100 kHz, all day and every day of facility operation. Reliable, robust and regular access will make a big difference for both routine and cutting-edge R&D programmes.

Sixty years ago, at the dawn of structural biology, Nobel laureate Max Perutz attempted to measure the structural impact of O_2 binding to haemoglobin crystals. His large crystals did not survive O_2 exposure, because it triggered significant and functionally relevant conformational changes in each protein within the crystal lattice.[1,2] When Perutz conducted his experiments, he used a weak, lab-based X-ray source that required large crystals to collect as much diffraction data as possible from a small number of samples at room temperature. One hypothesis is that the crystal lattice, which is held together by weak interactions, builds up strain across a large crystal and breaks into smaller and smaller fragments – essentially dissolving. Importantly, the lattice also did not prevent the dynamic and functional consequences of O_2 binding; although considering the instrumentation at the time, there was nothing useful left for structural analysis.

XFELs offer new opportunities in structural biology, especially for samples at near-physiological conditions and for time-resolved studies that link together the analysis of structure and function with the same samples.[3-9] The unparalleled XFEL intensity reduces the crystal size requirements, such that even submicron crystals can yield high quality diffraction data collected at room temperature.[10,11] The fs pulse duration also provides sharp temporal resolution, without sufficient time for radiation-induced alterations in most cases. These characteristics prompted the following statement from Tetsuya Ishikawa (Director, RIEKEN SPring-8 Center, Sayo, Hyoga, Japan) at SLAC National Accelerator Laboratory, Menlo Park CA USA on 2 May 2014:

> *The basis of science is observation. The most fundamental way of observation is by light. X-rays are a form of light that can probe atoms and molecules. X-ray lasers can probe atoms and molecules on their fundamental time scales, femtoseconds. X-ray lasers are therefore one of the fundamentally most powerful tools for science.*

More than 99% of all organisms that have ever lived on the Earth are now extinct.[12] Thus, it is perhaps unsurprising that the consensus of the life science community is to promote research and development for peaceful and humane purposes only. This is consistent with existing policies at Diamond Light Source, the European XFEL and the European Synchrotron Radiation Facility, among others.

Despite seven previous mass extinctions across the geologic timescale, the current diversity of life is staggering. With lifespans that range from hours to dozens of millennia, organisms exist that can tolerate temperatures from about –15°C to 125°C, pressures from the vacuum of space up to 1,100

atmospheres, pH values between 0 and 12.5, visible light conditions ranging from full sun to 5 x 10^6 fold attenuation and UV and/or ionising radiation up to ≥1,000 J/m^2 or 50 Gy/hr (12,000 Gy in an acute dose).[13] Despite these taxonomic characteristics, modern biology today is often defined and underpinned by genomic analyses (**Figure 7.1**).

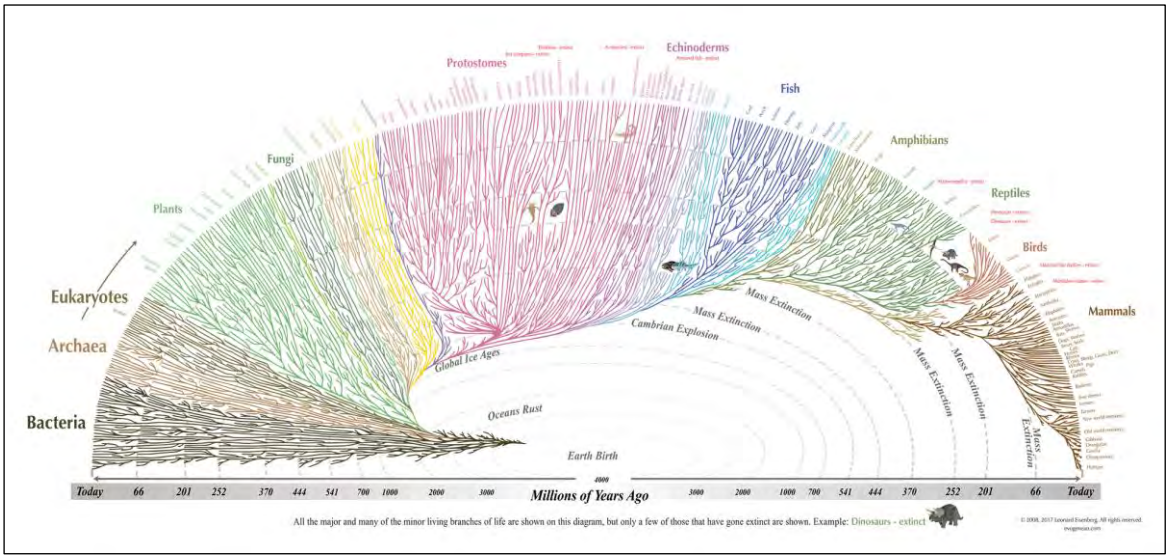


Figure reproduced from the Evogeneao Tree of Life.
© 2008, 2017 Leonard Eisenberg (evogeneao.com)
(https://www.evogeneao.com/en/explore/tree-of-life-explorer)

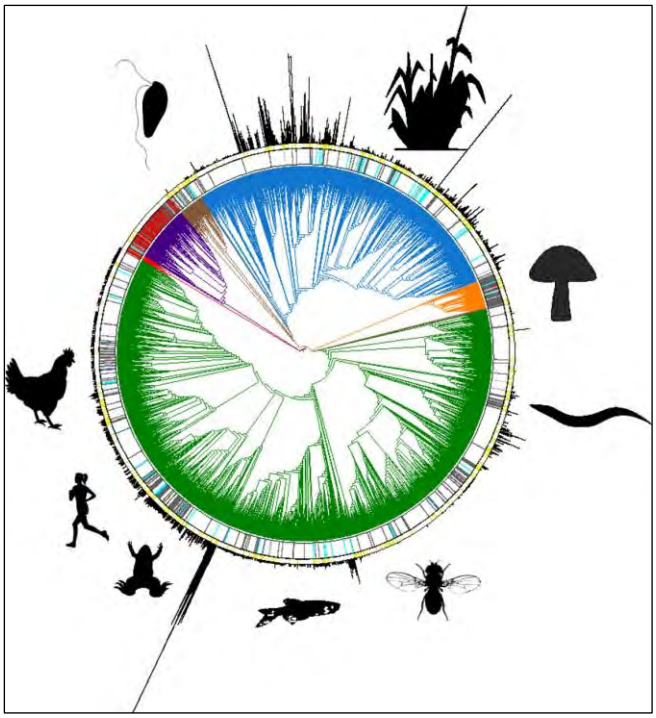


*Figure reproduced from H.A. Lewin et al. Proc. Natl. Acad. Sci. USA **115**, 4325-4333. Copyright (2018) National Academy of Sciences DOI: 10.1073/pnas.1720115115*

Figure 7.1: The evolution and status of the sequencing of life on Earth

(Top) The Evogeneao Tree of Life diagram, and the explorer generation counting technique, provide an easy-to-understand illustration of the core evolution principle. All the major and many minor living branches of life are shown, but only a few that have gone extinct (e.g. dinosaurs). Humans are "new to Earth" (lower right) and related not only to every living thing today, but also to everything that has ever lived on Earth.

(Left) Current status of the sequencing of life. Open Tree of Life (opentreeoflife.org) synthesis of phylogeny for all of life with resolution to the genus level, and showing phylogenetic information for Archaea (red), Bacteria (purple), Fungi (orange), Plantae (blue), Protista (brown) and Animalia (green). The current state of genomic information available from NCBI's GenBank is shown in the inner circle, with complete genomes colored in red, chromosome level in blue, scaffolds in dark gray and contigs in light gray. The second circle shows the transcriptomes from the NCBI Transcriptome Shotgun Assembly Sequence Database (www.ncbi.nlm.nih.gov/genbank/tsa/). Genome size as C value is displayed in bars around the outer circle. Data for animals is from the Animal Genome Size Database (www.genomesize.com/), data for plants is from the Royal Botanic Gardens, Kew (cvalues.science.kew.org/) and data for fungi is from the Fungal Genome Size Database (www.zbi.ee/fungal-genomesize/).

Indeed, the impact of the human genome project is enormous as suggested by the statement from Battelle (Columbus, Ohio) and the United for Medical Research[1] coalition:[14,15]

> *The reference human genome is to biology what the periodic table is to chemistry: a fundamental platform for understanding and advancing science for generations.*

Genomes derive from "individuals," whereas in contrast, metagenomic analyses help reveal complex relationships amongst organisms and their environments.[16-19] As of October 2025, the Kyoto Encyclopaedia of Genes and Genomes (KEGG) database lists genomes from 1,234 Eukaryotes, 9,980 Prokaryotes, 9,527 Bacteria, 453 Archaea and 14,382 viruses, as well as metagenomes listed by the National Center for Biotechnology Information (NCBI, Bethesda, Maryland, USA) from environmental sources including 848 marine, 954 fresh water, 2,461 soil and 712 organismal samples.[20-24] **Table 7.1** indicates millions of genomes, genes and macromolecular atomic models that exhibit massive diversity and cover all enzyme classes. About half of the gene products have also been mapped or linked to metabolic or signalling pathways, or many other important biological functions. **Interactions between organisms range from benign to symbiotic to pathogenic; deciphering the fundamental principles that dictate the scale, scope and consequence(s) of these interactions remains a grand challenge in biology.** Answering this challenge will have profound implications to human health, renewable energy sources and climate change, species extinction versus survival, and food production for a human population expected to reach 11.2 billion by the end of the century.[25]

The answers will not come exclusively from genomic analyses but rather are greatly influenced by structural biology and many complementary methods (see **Figure 7.2**, **Figure 10.1** and also **Appendix 1**). X-ray macromolecular crystallography (MX)[3,4,6,10,26-28] and cryo-Electron Microscopy (cryo-EM)[29-35] are essential and well established experimental tools for structural biologists worldwide. Indeed, as indicated in **Table 7.1** and **Figure 10.1**, the ratio of newly released atomic models by the wwPDB determined X-ray crystallography to cryo-EM is likely to reach parity soon.[36-38] For instance, 57% of new experimental models released by wwPDB in 2025 were based upon X-ray diffraction data and 41% were based upon cryo-EM data.

Table 7.1: Comparison of statistics for experimental atomic models released by the PDB in 2025

Method	Number	Growth in 2025	Avg. # Residues / Model	Resolution Range (Å)	Average Resolution (Å ± SD)	Subset Better Than		
						resolution (Å)	number	fraction
X-ray Diff.	10,083	9.4%	998	0.8 - 9.96	2.03 ± 0.02	1.5	1,859	18.4%
Cryo-EM	7,204	25%	4,403	1.3 - 35	3.28 ± 1.05	2.5	652	9.1%
Source: Public domain data provided by the Worldwide Protein Data Base (wwPDB) https://www.wwpdb.org								

Part of the impact of the field to the scientific community is highlighted by 31 Nobel Prizes related to crystallography to date. Of critical importance to the life science community, the 2024 Nobel Prize in Chemistry was awarded 50% to Demis Hassabis and John Jumper (Google DeepMind) "for protein structure prediction" and 50% to David Baker (University of Washington) "for computational protein design". Their major scientific breakthroughs accurately predict the three-dimensional (3D) structure of proteins from the corresponding amino acid sequences.[39-44] They used machine learning and artificial intelligence algorithms to leverage vast amounts of data in the public domain, including about 160,000 atomic models curated by the wwPDB. They also paired the structural analysis with

[1] The coalition consists of the American Association for Cancer Research, American Cancer Society Cancer Action Network, American Diabetes Association, American Heart Association, Association of American Universities, Association of Public and Land Grant Universities, BD, Biotechnology Industry Organization, Boston University, Corning, FasterCures, Harvard University, Johns Hopkins University, Life Technologies, Massachusetts Institute of Technology, Melanoma Research Alliance, Northwestern University, Pancreatic Cancer Action Network, Partners Healthcare, PhRMA, Research!America, Stanford University, The Endocrine Society, Thermo Fisher Scientific, University of Pennsylvania, University of Southern California, Vanderbilt University, and Washington University in St. Louis.

complementary gene and genomic sequences, to identify 3D spatial relationships through co-variance of protein mutations across species and in some cases evolution. The laureates released AlphaFold2 and RoseTTAfold as open-source code and deposited over one million computational atomic models of single chain proteins with the wwPDB (**Table 7.2**). Moreover, the AlphaFold DB developed by Google DeepMind and EMBL-EBI[2] now provides open access to over 200 million protein structure predictions.[45] The original programs and strategies have been quickly followed-up and include AlphaFold3 along with similar approaches to predict ligand binding to proteins and protein-protein interactions.[45,49-55] AlphaFill predicts protein-cofactor complexes and AlphaFold3 predicts macromolecular complexes between proteins and their partners, including other proteins, nucleic acids and ligands.[55,56]

This has profoundly changed the research and development landscape in life sciences. These powerful new tools are used by the community in many ways, but most importantly as "hypothesis generators" to support ongoing R&D efforts in new and novel ways, including solving crystallographic problems in phasing.[46-48] It remains to be seen how many time-resolved experimental datasets will be needed to support another generation of programs that predict function and dynamics as well.[57]

Table 7.2: NCBI genomes, KEGG genes and wwPDB statistics (compiled 5 Oct 2025)

Category	NCBI genomic datasets [a]			KEGG genes [b]		Atomic models in wwPDB [c]	
	Total	Reference	Annotated	All	Functional orthologs [d]	Exper.	Comp.
All organisms	3,146,599	42,178	2,355,231	62,348,162	27,839	242,874	1,068,577
Archaea	31,147	765	16,801	25,323		6,394	19,588
Bacteria	2,787,800	21,419	2,319,374	127,681		80,007	380,286
Escherichia coli	360,336	2	337,799	4,288	3,044	14,327	23,125
Eukaryota	54,966	19,994	9,602			135,221	668,506
Arabidopsis thaliana	344	1	8	29,446		2,610	27,491
Brassica napus	16	1	5	102,151	4,330	15	155
Homo sapiens	1,839	1	8	24,684	12,566	78,806	28,277
Mus musculus	74	1	2	26,125		10,286	21,679
Sacch. cerevisiae	1,688	1	420	6,449	3,357	6,580	8,962
Viruses	245,535	0	8,523	688,601		23,998	197
Metagenomes	1,926	0	3			191	
Ecological / mixed	10,349	0	894				
Seawater / marine	918	0	3				
Fresh water	954	0	438				
Sediments	558	0	1				
Soil	2,461	0	298				
Human gut	3,396	0	3				
Mouse gut	486	0	0				
Plant	78	0	20				

[a] **Source: https://www.ncbi.nlm.nih.gov/datasets/genome**

[b] **Source: https://www.kegg.jp/kegg/docs/statistics.html - Protein and/or RNA genes**

[c] **Source: https://www.wwpdb.org - based upon experimental data (e.g. X-ray or EM), or computational methods (e.g. AlphaFold)**

[d] **Annotated with the KEGG Orthology (KO) system; the basis for cross-species annotation in KEGG. The set of genes in the genome that can be mapped to KEGG reference pathways and BRITE reference hierarchies to generate organism-specific pathways and hierarchies.**

[2] https://alphafold.ebi.ac.uk

Synchrotron X-ray sources or cryo-EM were vital to the R&D efforts in each of the recent Nobel laureates' laboratories. Synchrotron facilities also serve the entire structural biology community, who now leverage these capabilities on a daily basis.[26,27] As a result, more than 242,000 atomic models are currently curated by the Protein Data Bank (PDB), with an estimated economic value of more than $24B.[58-60] Furthermore, structural biology remains critical to more than 90% of all drugs approved by the US FDA since 2010.[61-66]

Despite these impressive experimental and computational results, and the important biological insights derived from them, the known genes summarised in **Table 7.2** are tallied in the tens of millions, with the number of genes per organism ranging from a few thousand for microbes to about 20,000 for humans to over 100,000 for some plants. Although there are more than 62 million annotated protein or RNA genes listed in the KEGG databases, enzymes typically account for about 20% of the genes in most organisms. Because enzymes "do the work" of life, it is the overall level of homology and structural/functional differences that account for the diversity we observe in life today.

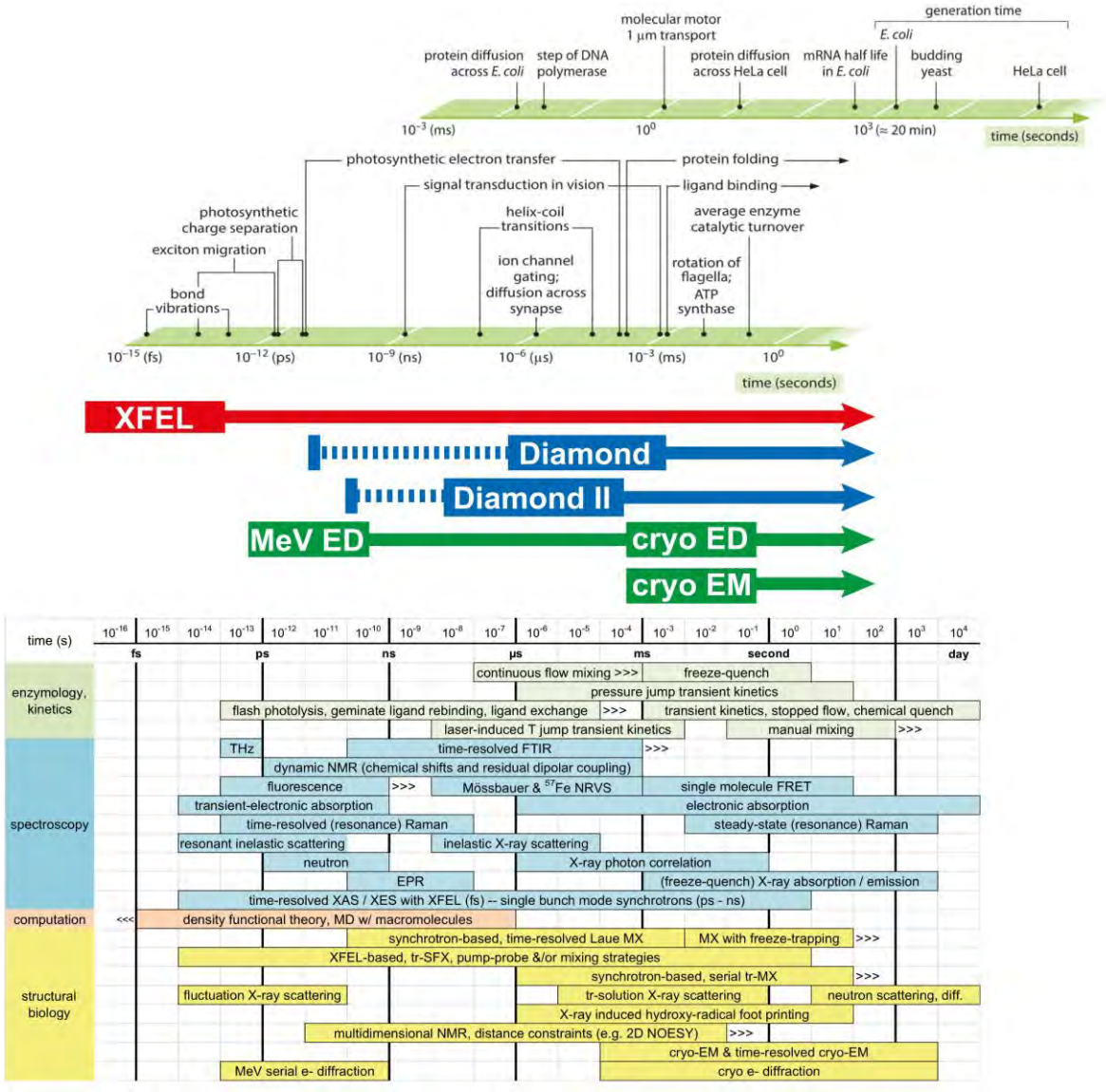


Figure 7.2: A comparison of X-ray sources and types of phenomena they are used to study Biochemical processes span orders of magnitude in time (top). The X-ray dose and time required to elicit a spectroscopic change and an X-ray diffraction pattern to high resolution at a modern synchrotron or XFELs range from μs to fs at synchrotrons and XFELs, respectively. For comparison, examples of complementary methods are shown along the bottom. Biologists will often use many of these methods in their research.

Top figure reproduced from "Cell Biology by the Numbers", by Ron Milo, Rob Phillips. Copyright 2015, Taylor and Francis Group LLC

Thus, one might conclude that we are incredibly ignorant with respect to an atomic level understanding of biology on a global scale, and that there is a tremendous amount of new information still to be discovered. To these ends, structural biology results via any and all experimental methods are critical to our comprehensive understanding of life (**Table 7.2**, **Figure 7.1** and **Figure 7.2**). High resolution structures – mainly obtained to date by X-ray crystallography, NMR spectroscopy and cryo-EM – are also complemented by electron diffraction from micron to submicron-size crystals,[67-73] neutron diffraction and small angle scattering,[74-77] macromolecular structure prediction,[78-81] small and wide angle X-ray scattering of biomolecules in solution,[82-86] super resolution fluorescence microscopy,[87] optogenetics,[88,89] DNA and RNA sequencing and multimodal data analysis technologies applied to single cells,[90,91] cryo-electron tomography,[92-94] X-ray microscopy, tomography and ptychography,[95-100] and a variety of methods to establish interaction networks between biomolecules.[101] As a result, most biologists analyse integrated structural, functional and dynamic data from different techniques, samples and conditions. This applies to macromolecules in pure states, to increasing complexity of heterogenous samples, and ultimately to physiological conditions such as within whole cells or tissues.

The vast majority of the MX datasets are collected from one to a few crystal(s) measuring ~ 10s - 100s μm^3, held at 100 K in a cryostream and rotated about one or more axis during data collection.[103] Indeed, in 2025 only 7.5% (754) of the atomic models released were derived from X-ray diffraction data collected above 100 K. All of the cryo-EM atomic models are collected from samples at ~ 100 K. But life is dynamic and function is not compatible with the cryogenic conditions. Indeed, dynamics and timescales in biology (**Figure 7.2**) range from femtoseconds for electronic transitions and bond vibrations, to picoseconds for light-induced charge separation, photoisomerization and amino acid side chain rotation, to microseconds for domain motion and ion transport and fast enzyme reactions, to milliseconds for most enzyme reaction rates and fast protein folding, to seconds for protein synthesis and DNA or RNA replication/synthesis.

We are experiencing a step-change in macromolecular crystallography that is very nicely captured in a recent book by Moffat and Lattman.[102] It derives from serial MX and time-resolved functional studies that are directly linked to XFELs and the use of micron-size samples.[3,4,6,9] One important hypothesis is that micron-sized crystals minimise or eliminate barriers to relieving strain that builds up when conformational changes propagate across molecules and unit cells. A dramatic case in point is an aptamer of messenger RNA, a riboswitch that binds adenosine and undergoes a large conformational change that ultimately regulates gene expression.[104-106] Using a slurry of micron-size RNA crystals and mix-and-inject methods, Stagno *et al.* reported time-resolved SFX results that demonstrate ligand binding-induced conformational changes so significant that the crystals changed symmetry, but they did not shatter.[107,108] This remarkable result has also recently been observed via atomic force microscopy wherein the probe-tip is scanned across the outer layers of microcrystals. These experiments demand the intensity and tight focus of the XFEL beam; without either, these experiments would not be feasible.

Finally, we must recognise advances in measurement methodologies under development at XFELs that may have substantial impact on the life sciences in the future. In **Chapter 3** we highlight how advances in the realm of physics are foreseen to have high impact across the sciences. In **Section 3.2.2** we introduce advances that harness quantum correlation to overcome the phase problem and radically reduce radiation damage issues. In **Section 3.4** we introduce how data driven approaches, combined with single particle imaging, may be able to uncover the full conformational dynamics and capture rare states in biological molecules and assemblies with exceptional temporal resolution without the need for using pump-probe methods. Driven by the needs of imaging engineering materials in operation and matter at extreme conditions there have been recent advances in wide angle dynamic imaging at LCLS and European XFEL. It is anticipated, that enabled by the exceptional average brightness of a next generation XFEL, that this may lead to volumetric imaging strategies over > 1 cm^3 with nm resolution, an example of this is discussed in **Chapter 9.4 Flagship Programme XI: Nanobioimaging in tissues and organs – wiring diagrams for whole brains.**

7.1 Serial femtosecond crystallography enabled by XFELs and adopted by synchrotrons – a new era in structural biology

Serial crystallography presents a revolutionary opportunity to solve structures from slurries of nano- to micron-size crystals. The high brightness and tight focus of the XFEL beam enables a diffract-before-destroy methodology that rapidly reveals structures from samples at physiological conditions.

7.1.1 Introduction

Crystallographers frequently observe microcrystal showers, measuring only a few microns on a side, that arise from initial sparse matrix screens used early in most projects. These conditions are then "optimised" to yield large single crystals typically measuring ~ 25 - 100s µm or more on at least two sides. During typical data collection at 100 K, the X-ray dose is distributed throughout the entire crystal volume, by combinations of rotation and translation.[109-116] And so, although microcrystals are ubiquitous, they are frequently overlooked because they can be difficult to use and/or perceived to be inappropriate for structural analysis.[117,118] However, the characteristics of XFELs change the sample requirements for MX. Showers of microcrystals are ideal for XFELs that deliver hard X-rays with high flux density in a very well-focused fs-long pulse. Microcrystals of membrane proteins – an under-represented class in the Protein Data Bank (PDB) – are often produced and well-suited for serial femtosecond crystallography (SFX) methods.[119-124] Moreover, SFX strategies have translated to analogous serial MX methods at synchrotrons (typically abbreviated as SSX) around the world including Diamond, and are anticipated for Diamond-II, as well as to cryoEM too.[125,126,127]

SFX is a relatively new technique developed to exploit the fs pulses from XFELs and to use thousands of micron-size crystals or smaller.[3,4,6,9,117,118,128] It is the dominant method in life sciences at all five XFELs since it was first reported in 2011 by Chapman and colleagues at the LCLS.[129,130] The impact of SFX is summarised in **Table 7.3** and **Figure 7.3**, wherein atomic models released by the wwPDB and their associated publications are a clear measure of impact. These atomic models are almost always accompanied by a primary citation. Over the years, 16.9% of the primary citations were in the high-profile publications *Science*, *Nature*, or *Cell*. The Field Weighted Citation Impact (FWCI) is largest for LCLS (4.82), followed by SwissFEL (3.06), SACLA (2.84), the European XFEL (2.24) and PAL-XFEL (1.13). These results often highlight the unique characteristics of SFX methods afforded by XFEL facilities. This includes an almost complete lack of radiation-induced alterations in the atomic models, exploitation of micron to sub-micron size crystals and exquisitely sharp temporal resolution in time-resolved studies. These are impressive advances in only a few years of operations and the biology community is very eager for more XFEL access to expand the experimental use cases.

Another measure of XFEL impact relates to technology transfer, wherein the life science community is encouraging and developing serial approaches at nearly all synchrotron facilities. Comparisons between SFX at XFELs and MX results from approximately comparable beamlines at synchrotrons reveal that the combined XFEL impact is a bit less than one synchrotron MX beamline (**Table 7.3**). Considering that each XFEL facility dedicates only a fraction of its beamtime to field SFX experiments, the comparison appears reasonably valid. However, the average percentage of high-profile publications and the FWCI for 4/5 XFEL facilities are higher for the XFELs. For instance, the number of publications in *Science*, *Nature* and *Cell* for the synchrotron beamlines averages about 5.5% over the same period. The highest FWCI for the synchrotron beamlines is SSRL (1.95) followed by SLS (1.90), SSRF (1.75), Diamond (1.68), APS (1.62), SPring-8 (1.5) and ESRF (1.42).

Table 7.3: Publications and their associated macromolecular atomic models released by the wwPDB linked to data collected at an XFEL or selected synchrotron beamlines

XFEL SFX Publications	Total	*Science*	*Nature*	*Cell*	*PNAS*	*JACS*	Nat ___	Sci ___	Avg. days to PDB
all five	225	14	22	2	20	5	55	21	972
SLAC - LCLS	112.50	9.00	15.67	2.00	13.00	3.50	29.83	5.83	913
SACLA	71.32	2.50	3.83	-	6.00	1.00	11.33	10.83	998
SwissFEL	10.83	2.50	2.50	-	-	-	3.33	-	1164
PAL-XFEL	15.83	-	-	-	-	0.50	3.00	4.33	915
European XFEL	14.50	-	-	-	1.00	-	7.50	-	585
XFEL SFX PDB Atomic Models	**Total**	***Science***	***Nature***	***Cell***	***PNAS***	***JACS***	**Nat ___**	**Sci ___**	**# to be published**
all five	846	88	128	2	53	16	231	62	72
SLAC - LCLS	335	33	48	2	36	7	94	19	14
SACLA	274	28	25	-	13	8	80	32	15
SwissFEL	157	27	55	-	-	-	28	-	37
PAL-XFEL	40	-	-	-	-	1	8	11	5
European XFEL	40	-	-	-	4	-	21	-	1

Synchrotron Crystallography	Totals		*Science*		*Nature*		*Cell*		Avg. days to PDB
Synch. beamline	**Pub.**	**PDB**	**Pub.**	**PDB**	**Pub.**	**PDB**	**Pub.**	**PDB**	per beamline
Diamond I24	1047	1703	14	21	33	43	9	12	1009
ESRF ID29	1289	2104	18	26	17	24	8	19	1154
SLS X10SA	1007	3278	21	41	24	44	12	24	1850
APS ID-19 (SBC)	929	2885	14	23	16	25	13	27	867
SSRL BL12-2	819	1762	33	87	16	18	20	36	777
SPring-8 BL41XU	622	1133	13	20	29	53	8	12	1138
SSRF BL17U1	813	1672	2	3	15	24	7	11	1094

These public domain data include atomic models released by the wwPDB[3] between 02 Feb 2011 and 02 April 2025. Publication abbreviations include PNAS, Proc. Nat. Acad. Sci U.S.A.; JACS, J. Am. Chem. Soc.; Nat___ are the various journals in the Nature family, e.g. Nature Methods, Nature Comms, etc; Sci___ are the various journals in the Science family, e.g. Science Advances, etc. The average number of days to PDB indicates the time between data collection and release of the atomic model, which often, but not always, corresponds to the publication date. Synchrotron beamlines include I24 at Diamond Light Source; ID29 at the European Synchrotron Radiation Facility (ESRF); beamline X10SA at Swiss Light Source (SLS); ID-19 (SBC-CAT) at Advanced Photon Source (APS); beamline BL12-2 at the Stanford Synchrotron Radiation Lab (SSRL); beamline BL41XU at the Super Photon Ring – 8 GeV (SPring-8); beamline BL17U1 at the Shanghai Synchrotron Radiation Facility (SSRF.)

[3] www.rcsb.org

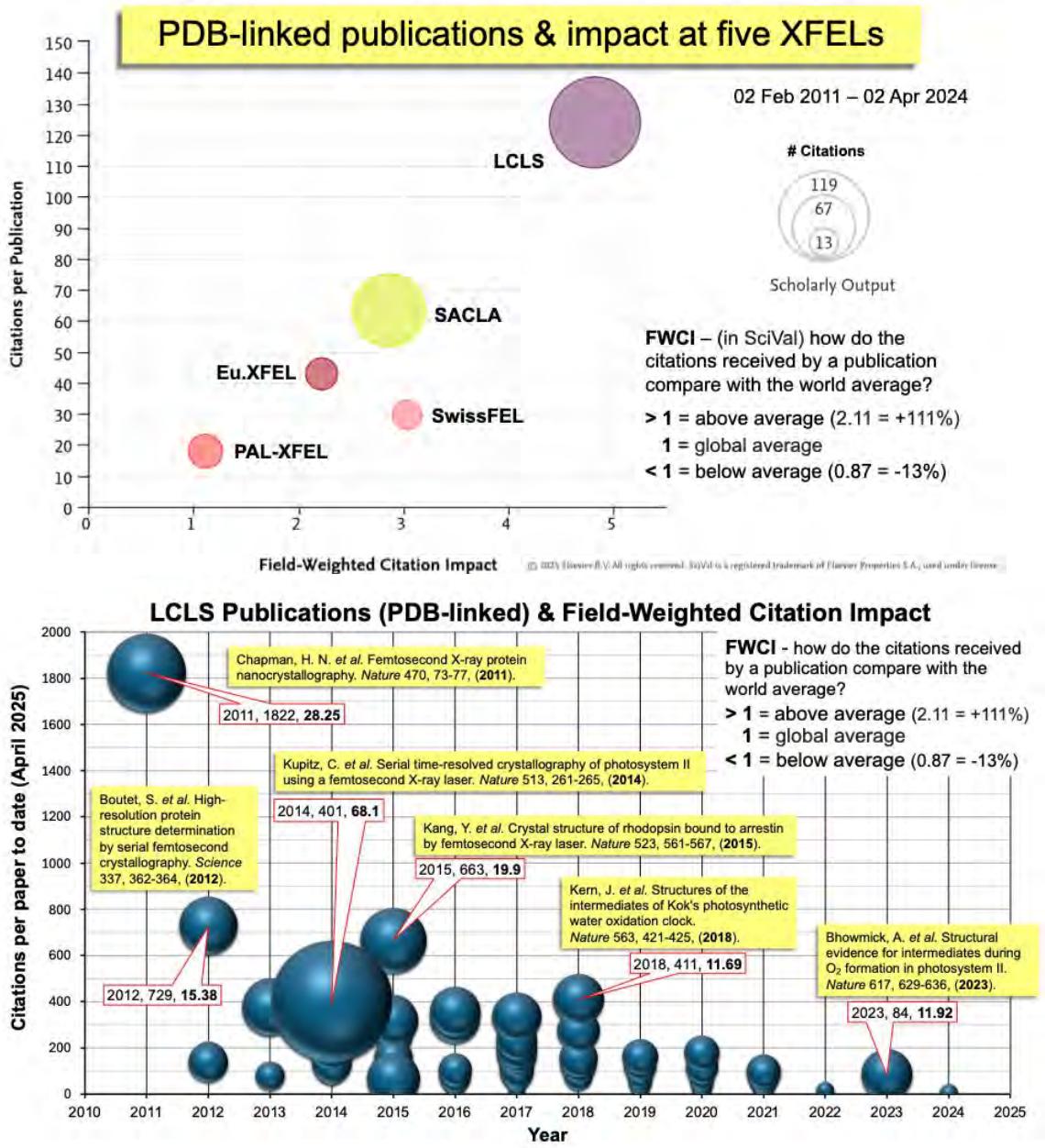


Figure 7.3: Macromolecular atomic models linked to data collected at an XFEL released by the PDB

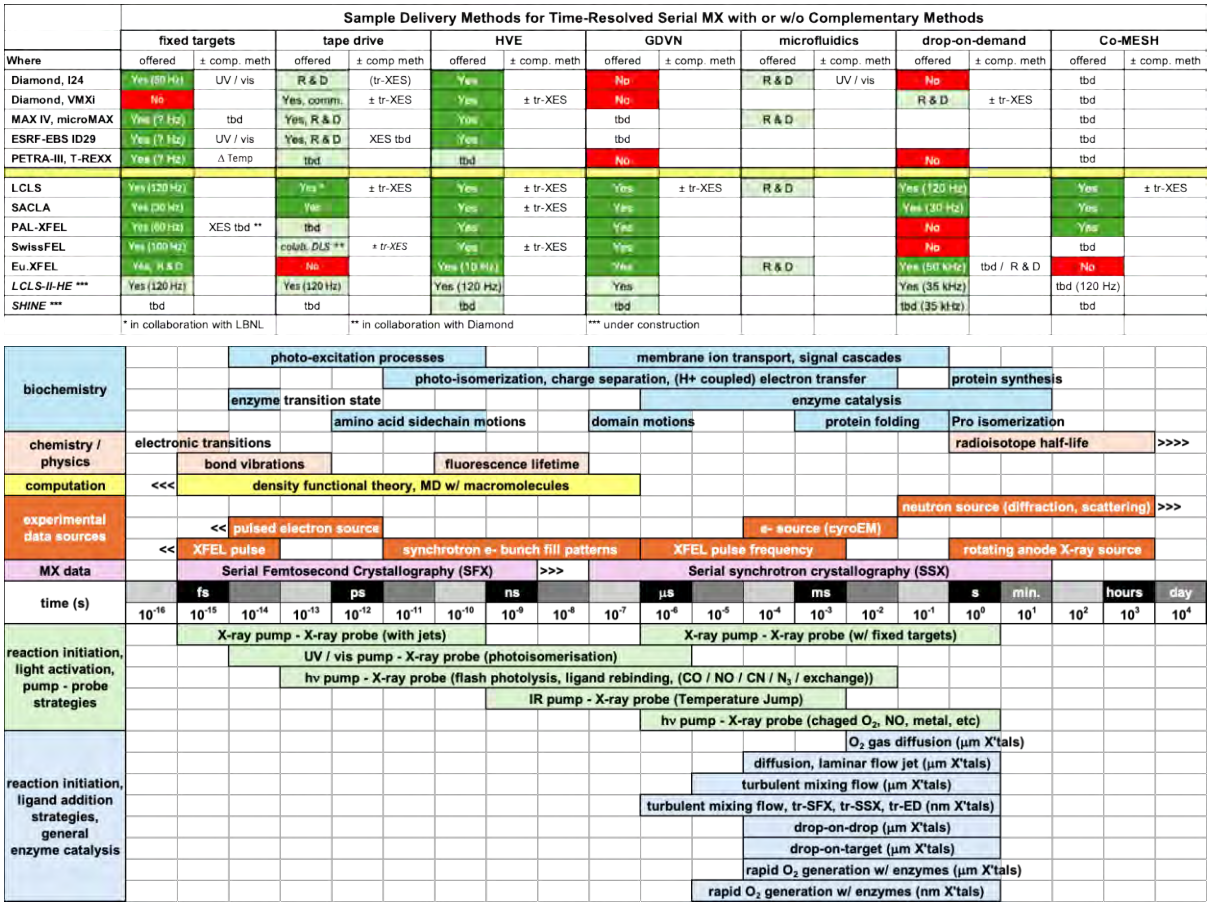
(Top) The number of citations per publication versus the Field Weighted Citation Impact (FWCI) indicates the largest impact at LCLS. This is consistent with the entire SFX field emerging from this facility.
(Bottom) An evaluation of impact of the LCLS publications linked to SFX methods clearly highlights the first SFX result, a G-coupled protein receptor (GCPR) result, and several time-resolved studies of photosystem II.

These data are from https://www.rcsb.org and apply to atomic models released between 02 Feb 2011 and 02 Apr 2025.

7.1.2 Sample delivery and efficiency

SFX studies are very often conducted at room temperature, from which one still diffraction pattern is recorded from each microcrystal in a random orientation. XFEL beams are typically well-focused to deliver submicron or 1 - 3 µm spot size at the sample and are about nine orders of magnitude brighter than synchrotrons like Diamond Light Source. Because so much energy is deposited into the sample, it explodes.[131] Consequently, SFX methods require a unique sample for each diffraction pattern and the whole dataset is merged from thousands of still images. To this end, sample delivery methods for serial MX is a very active R&D effort in the field. The aim is to rapidly and efficiently deliver samples, without wasting precious material, at a rate that matches the XFEL pulse frequency and/or the detector characteristics.

A variety of methods have been developed to deliver a slurry of microcrystals into the XFEL interaction region (**Figure 7.4**), which include liquid flow-focusing gas dynamic virtual nozzles (ff-GDVN) or viscous media jets and extruders (HVE),[123,129,132-138] a concentric-flow electrokinetic injector (Co-MESH),[11,139,140] on-demand micro-droplets (drop-on-demand) that may be coupled to a conveyor belt transport system (tape drive),[141-150] fixed targets that raster a sample array through the X-ray beam,[146,151-164] goniometer-based methods,[165-169] and microfluidic devices.[128,170-173] Many of these methods are readily adaptable to time-resolve studies in MX and/or cryo-EM and dictated in part by how the reaction is triggered by either light or mixing, as discussed below.[1]



Sample Delivery Methods for Time-Resolved Serial MX with or w/o Complementary Methods																
	fixed targets		tape drive		HVE		GDVN		microfluidics		drop-on-demand		Co-MESH	
Where	offered	± comp. meth	offered	± comp meth	offered	± comp. meth	offered	± comp. meth	offered	± comp. meth	offered	± comp. meth	offered	± comp. meth
Diamond, I24	Yes (60 Hz)	UV / vis	R & D	(tr-XES)	Yes		No		R & D	UV / vis	No		tbd	
Diamond, VMXi	No		Yes, comm.	± tr-XES	Yes	± tr-XES	No				R & D	± tr-XES	tbd	
MAX IV, microMAX	Yes (? Hz)	tbd	Yes, R & D		Yes		tbd		R & D				tbd	
ESRF-EBS ID29	Yes (? Hz)	UV / vis	Yes, R & D	XES tbd	Yes		tbd						tbd	
PETRA-III, T-REXX	Yes (? Hz)	Δ Temp	tbd		tbd		No				No		tbd	
LCLS	Yes (120 Hz)		Yes *	± tr-XES	Yes	± tr-XES	Yes	± tr-XES	R & D		Yes (120 Hz)		Yes	± tr-XES
SACLA	Yes (30 Hz)		Yes		Yes	± tr-XES	Yes				Yes (30 Hz)		Yes	
PAL-XFEL	Yes (60 Hz)	XES tbd **	tbd		Yes		Yes				No		Yes	
SwissFEL	Yes (100 Hz)		coupl. DLS **	± tr-XES	Yes	± tr-XES	Yes				No		tbd	
Eu.XFEL	Yes, R & D		No		Yes (10 Hz)		Yes		R & D		Yes (50 kHz)	tbd / R & D	No	
LCLS-II-HE ***	Yes (120 Hz)		Yes (120 Hz)		Yes (120 Hz)		Yes				Yes (35 kHz)		tbd (120 Hz)	
SHINE ***	tbd		tbd		tbd		tbd				tbd (35 kHz)		tbd	

* in collaboration with LBNL ** in collaboration with Diamond *** under construction

Figure 7.4: Sample delivery methods for time-resolved serial crystallography at XFELs (tr-SFX) or synchrotrons (tr-SSX) and how they map to timescales important to biology

(Top) Seven common tr-SFX sample delivery methods and whether they are compatible with complementary spectroscopic analysis. In some cases, the technique is in commissioning (comm.), still to be determined (tbd), or under active research and development (R & D) at the facility.

(Bottom) The lower portion shows the time domains accessible to some key sample delivery methods for tr-SFX or tr-SSX, with light activated systems typically (light green) responding faster than those that require substrate mixing (light blue). These map to the upper portion listing facility characteristics, and several dynamic features important to biology.

SFX data collection times are driven by a combination of the X-ray pulse frequency, the detector capabilities and the hit ratio, defined as the number of indexed lattice(s) divided by the total number of X-ray pulses delivered. Crystal hit ratios range from much less than 1% to greater than 100% in some fixed target systems with more than one crystal in a fraction of the wells. Ideally each crystal lattice will be in a random orientation and thus, the whole SFX dataset is built up in a stochastic process. **Table 9.1** in **Section 9.2.4** compares the typical data collection times required at different XFEL facilities in operation now and anticipated at those currently under construction. It shows that a 25,000 indexed lattice dataset can take significantly more than a 12-hour shift with a low hit ratio and a slow detector or pulse frequency. In contrast, only a few seconds are needed under conditions that yield a high indexing ratio with a fast detector. It is important to point out that in the fastest cases to date, the detector becomes a limiting factor rather than the X-ray pulse frequency. Moreover, in every case, the scientists must evaluate each SFX dataset in as near to real time as possible. This is clearly

more challenging with faster data collection, larger image files and larger unit cells with many more reflections that must be merged. Consequently, highly parallelised algorithms will be critical as well as access to large clusters and/or supercomputer centres for the most intensive calculations.[174-179]

Although SFX was first demonstrated in 2011 at the LCLS,[129,130] serial MX methods are now also available at nearly all major synchrotron facility around the world.[27,180-189] Moreover, beamlines dedicated to serial MX are often identified as a flagship capability at facilities undergoing upgrades to diffraction-limited lattice configurations, including Diamond-II (see **Appendix 1**).[190-192] Thus, room-temperature, serial MX methods that couple dynamics and functional studies with structural analysis will become routine around the world. This trend will continue to expand and impact all of life sciences.

7.1.3 Membrane proteins

About 30% of the human genome codes for membrane proteins.[120,193-195] Because they are located and function at the interface between cells or organelles, they are critical mediators/sensors of environmental conditions, nutrient transport and cell communication and signalling. Not surprisingly then, membrane proteins are targets for more than 50% of all drugs available worldwide.[196,197] The PDB currently curates more than 29,000 "membrane protein" atomic models, of which more than 18,500 were determined by X-ray diffraction and more than 9,300 by cryo-EM. Furthermore, SFX methods at three XFELs facilities were used for more than 85 of the early XFEL atomic models released by the PDB. Because membrane proteins are hard to crystallise and often only yield microcrystals, they are ideally suited to structural analysis at XFELs.[120,121,195,198]

Significant progress has been made crystallising membrane proteins using lipidic cubic phase (LCP) methods.[119,124,199] In addition, viscous media and LCP extruders (see **Section 8.5**) are highly efficient methods for delivering membrane protein crystals into the X-ray interaction region.[123,200,201] The high viscosity of LCP makes it unsuitable for mix-inject style time-resolved studies. However, LCP is amenable to ligand exchange under equilibrium conditions, which is an emerging strategy for drug discovery, especially in the G Protein-coupled Receptor (GPCR) family.[120,121,202,203] To date approved drugs that target GPCRs impact to the central nervous, cardiovascular, immune, metabolic and reproductive systems, as well as many human cancers. The importance of GPCRs was the recognised by the 2012 Nobel Prize in Chemistry to Lefkowitz and Kobilka "for studies of G-protein-coupled receptors."

7.1.4 Future directions

Serial MX will continue to expand at synchrotrons and XFELs around the world. This will benefit from hard X-rays with tight focus and XFEL pulse frequencies from kilohertz to megahertz. Data collection from samples at near-physiological conditions, especially compared to cryogenic conditions, will provide new strategies for drug discovery (see **Section 8.5**). However, no single method can solve all scientific problems, so it is essential that a next-generation XFEL is fully integrated into the wider UK science infrastructure. In the life sciences, several complementary methods exploiting X-rays and electrons will yield atomic level structural and functional insights with increasing temporal resolution, which can be applied to individual macromolecules through to whole cells and tissues. This is addressed and expanded upon in **Section 10.4**, which highlights synergies between facilities.

Membrane proteins, including a wide range of important GPCR family members, will be a strong use case for academic and industrial XFEL users in the coming decades. In biology, samples are often scarce and, therefore, on-demand sample delivery methods will always be important to the community. Some of the current methods for on-demand sample delivery can operate at up to 50 kHz, but further developments are needed to achieve 0.5 MHz or faster. For megahertz pulse frequencies, fast GDVN-type jets are likely to be essential (see **Section 7.3** below). It is also clear that future SFX experiments will tax computational resources by generating very large datasets that may require varying degrees of image triage, and will need merging as fast as possible so that scientists can make the most effective use of XFEL beamtime.

Light source characteristics that include essentially super-conducting linac CW high repetition rate and increased stability parameters will allow the further development of the accuracy of stationary serial MX. Post-refinement is being developed to improve the quality of the retrieved amplitudes.[204-212] With the necessary increased frame rate of area detectors, orders of magnitude improvement in data collection rates relative to current 'warm linac' hard X-ray FELs will be achieved (see also **Section 9.2.4** and **Table 9.1**). For example, the European XFEL fields AGPIDs [213-215] and JUNGFRAU [216,217] detectors, wherein the former can collect 3520 data frames per second overall out of the 27,000 pulses per second delivered in 4.5 MHz trains lasting no more than 600 µs; by comparison, warm linac machines deliver pulses at up to 120 Hz. In addition, increased stability will allow a more accurate X-ray geometry determination to improve post-refinement methods, for further enhancements of the structure factor amplitude determination. A discussion of the crystallographic signal-to-noise and the new molecular physics that may be probed in such a regime has been presented.[218] These include the detection and analysis of vibrational coherence dynamics, in addition to resolving reactive mode displacements on ultrafast timescale.

The structural biology community desires a next-generation XFEL with fast kickers that delivers a fractional share of the X-ray pulses to a life science end station every day of facility operations, probably for at least 12 hours per day, and with pulses delivered at evenly distributed rates commensurate with the state-of-the-art detectors (*e.g.* 35,000 Hz using an ePixUHR 16M detector under development for LCLS-II-HE, or better).[219] Moreover, fast sources and detectors reduce the total time needed to collect typical SFX datasets to only a few seconds (see **Table 9.1**). This puts significant pressure on facilities to automate on-demand sample delivery and machine alignment strategies that rapidly optimize overlap between sample delivery and X-ray pulse. Solutions to this multivariable problem are likely to come from Machine Learning / AI algorithms that leverage fast and accurate beam position monitors and feedback loops that link to motion controls. The strategies may also include quasi-real time data analysis methods leveraging results from complex and escalating analysis and interdependencies. An example pipeline should assess and triage "blank" images whereas diffraction images are processed and saved. Moreover, the analysis pipeline(s) could extend to include assessment(s) of ligand occupancy via interrogation of electron density maps and/or spectroscopic methods. The evolution of various tools will likely converge on sophisticated, integrated and automated systems that steer the beamline and end station components without significant human intervention. These advances should significantly reduce the access barriers to XFEL beamtime for most researchers. This could lead to various Block Allocation Groups (BAGs) awarded some fraction of the total beamtime that take responsibility for executing ground state and time-resolved experiments; analogous to the popular BAG access mode at most synchrotron facilities. BAG applications and cutting-edge experiments will probably still be peer reviewed and the beam time split between the best scoring applications. Some fraction of the XFEL beamtime will also probably be devoted to remote and unattended SFX data collection strategies. This would be analogous to the popular unattended data collection (UDC) access mode pioneered in 2014 by the MASSIF-1 beamline at ESRF [220-222] and now offered by several synchrotrons including Diamond. Indeed, many of the collaborators of the XFEL Hub at Diamond use UDC that is applied to standard size crystals and exploits traditional, rotation-based diffraction at 100 K as vital preparatory steps for tr-SSX and/or tr-SFX experiments. Thus, lower-barrier access at most facilities is a synergistic effort across them all.

7.2 Dynamic structural biology: Photosensitive systems

A remaining frontier challenge of structural biology is to determine time-resolved structures at atomic resolution directly from systems engaged in function, at physiological temperatures and pressures. XFEL methods coupled with pump-probe strategies are making important advances towards this goal.

7.2.1 Introduction

Time-resolved serial MX naturally blends functional and structural analyses into the same sample and experiment. This is sometimes described as *Dynamic Structural Biology.* It exploits slurries of microcrystals at room temperature and is increasingly prevalent at XFELs and synchrotrons. Light-activated systems are relatively rare in biology but are easier to initiate and many have the potential to probe isomerisation rates from femtoseconds and slower. General time-resolved structural biology is separated from ultrafast applications by fundamental timescales of decoherence, which is typically completed within few picoseconds. Coherent dynamics are separately discussed in **Section 7.3**, while pure population dynamics at slower timescales are the focus of biochemistry applications discussed here.

Heretofore the *status quo* in structural biology has been to use many separate samples, from which different types of data are collected under different conditions. Some of the experimental conditions may be very far from physiological. For example, traditional MX or cryo-EM methods usually provide insightful atomic models of a particular ground state or a trapped intermediate state molecule from a sample held at 100 K. In contrast, most functional studies are conducted in solution, at room temperature, and often include binding, conformational changes and/or other types of dynamics.

Some contextual background

The earth orbits our sun in the so-called, "habitable zone," favouring temperate conditions and liquid water.[223,224,225] The solar chromosphere exhibits blackbody radiation consistent with a temperature of about 5800 K (**Figure 7.5**) and bathes our planet in photons ranging from the ultraviolet (180 – 380 nm) to more than 2,500 nm. The solar spectrum has a broad peak at ~ 500 nm and these photons have an equivalent energy of 57.1 kcal/mol (239 kJ/mol), thus the energy from visible light photons supported the evolution of biological systems that capture and convert visible light photons into chemical potential energy and/or mechanical work. For instance, as illustrated below (**Section 7.2.3**) photosystem II (PS-II) evolved to produce O_2 from two H_2O (water) molecules. The bond dissociation energy of O_2 is 119 kcal/mol (498 kJ/mol) and chlorophylls absorb photons in the 400 nm range that provide about 71 kcal/mol (299 kJ/mol). Given that PS-II is about 60% efficient[226] and light is quantized into photons, it takes 4 photons to split water and generate O_2. The evolution of photosynthesis transformed the earth's environment from reducing to oxidizing conditions that challenged many life forms and precipitated ferrous iron out the oceans, which is visible in the geologic record. [227,228,229]

Moreover, the chemical potential energy in dioxygen (O_2) and its exothermic reaction to accept four electrons to form two water molecules powered the evolution of complex life.[229,230,231] Fortunately, O_2 is kinetically inert because its triplet ground state is spin forbidden for reactions with organic molecules in a singlet ground state – otherwise reduced carbon molecules (*e.g.* methane CH_4) would spontaneously combust. Thus, enzymes evolved to activate O_2 for "desirable" reactions, while avoiding many dangerous side reactions potentiated by reactive oxygen species (ROS) such as superoxide, hydrogen peroxide, hydroxy radicals, ozone (O_3) and singlet O_2.[232 – 247] For instance, methanotrophic bacteria evolved to use methane (CH_4) as a sole source of carbon and energy. The first enzyme in the CH_4 to CO_2 catabolic pathway, methane monooxygenase (MMO), uses 2 electrons and either copper or iron metallocentres to activate O_2 to facilitate breaking the C–H bond (105 kcal/mol; 439 kJ/mol) to form methanol (CH_3OH) and water (H_2O).[248 – 254] MMO controls the reaction by only generating highly reactive species after all the reagents are safely sequestered within the active site that also prevent the undesired oxidation of active site residues.

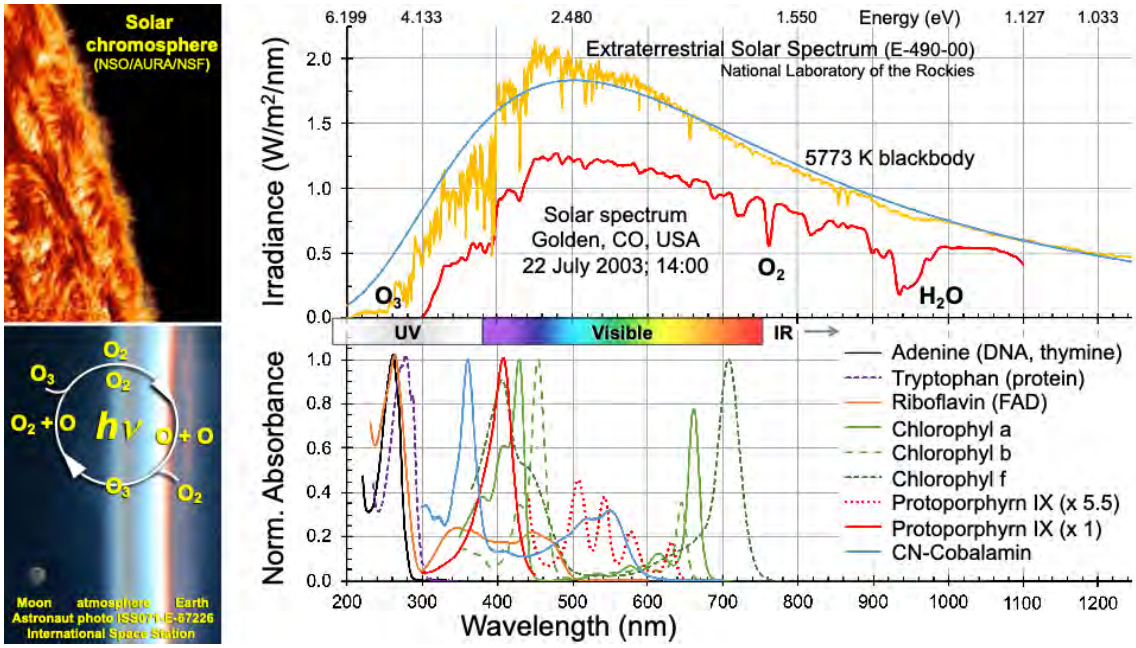


Figure 7.5: The solar irradiance spectra (top) compared to absorption spectra of some biomolecules (bottom)

*Ozone (O_3) is generated from oxygen (O_2) in atmospheric photochemical reactions (inset lower left). Proteins and nucleic acids (DNA) exhibit absorption peaks at 280 and 260 nm, respectively, and these photons have sufficient energy to damage most biomolecules. O_3 absorbs photons with a peak at 250 nm (the highest energy in the solar spectrum) and thereby protects all life on earth. Photosynthetic organisms evolved to use chlorophylls to absorb four visible light photons that together provide enough energy to make O_2 from two water molecules (**Section 7.2.3**). Use of cobalamin is reported in Rios-Santacruz, R. et al. "Integrated structural dynamics uncover a new B12 photoreceptor activation mode." Nature **650**, 1045-1052, (2026) DOI:10.1038/s41586-025-10074-2. Examples of some photoreactions in biology that exploit tryptophan and/or FADH- (~ riboflavin) are discussed below.*

Images from NASA in the public domain. Solar spectra created with data in the public domain provided by the US National Laboratory of the Rockies. Normalised absorption spectra plotted with data in the public domain provide by PhotochemCAD (www.photochemcad.com).

How enzymes work is fundamentally important to life on earth and to mechanistic enzymology in general. For instance, the MMO reaction is so close to the limit energetically, that the enzyme struggles to cleave the C–D (^{2}H) bond in CD_4 (107 kcal/mol, 449 kJ/mol), causing the reaction to slow down so much that the observed primary kinetic isotope effect (KIE) is between 50 – 100 (more typically, the semiclassical KIE limit is on the order of 7–10).[255-259] The critical reactive intermediate in MMO almost never cleaves the C–T (^{3}H) bond in a chiral ethane molecule, CHDT-CH_3.[260] An implication of a large KIE is that MMO operates via **quantum tunnelling**.[261-268] Deuterium (^{2}H, or D) with larger mass, has a lower vibrational frequency and lower zero point energy compared to hydrogen (^{1}H) and therefore has a higher activation energy (*E*a) over the transition state, which results in a slower reaction rate. Tritium (T, ^{3}H; 106.4 kcal/mol, 445 kJ/mol) has an even lower zero point energy than deuterium. The lower mass of hydrogen also yields a higher probability to tunnel through a potential energy barrier. Together these effects intensify the magnitude of the KIE. Quantum tunnelling arises from wave-particle duality and follows the rules of wave mechanics requiring overlapping waveforms. Consequently, tunnelling has reduced temperature sensitivity compared to conventional chemical reactions. However, the tunnelling barrier width is linearly related to the H/D-atom donor-acceptor distance, with smaller distances and lighter atoms more likely to exhibit tunnelling behaviour. Hence, the C–T bond has two strikes against its reaction with MMO. The atomic distances of quantum tunnelling are thereby linked with macromolecular structure, dynamics and temperature. The characteristics of the temperature dependence of the KIE, $\Delta Ea = Ea(D) - Ea(H)$, serve as a critical descriptor of the C–H/D bond making and breaking events. These types of reactions are ubiquitous across biology. Enzymes that activate O_2, exhibit large KIEs and/or exploit quantum tunnelling are under investigation using XFELs (if/when they are awarded beamtime, and only if the R&D projects are funded), many of which benefit from tr-SFX ± tr-XES capabilities developed by the XFEL Hub at Diamond and others.

7.2.2 Time-resolved studies of light-sensitive proteins

So, our modern "*Goldilocks* zone" is also a rough neighbourhood. In addition to the perils of reactive oxygen species, solar irradiation includes photons in the ultraviolet range with sufficient energy to excite biomolecules leading to damage and the introduction of mutations into genomes. Most biological tissues scatter light and appear opaque because of the difference between the refractive index (RI) of different components; *e.g.* low RI for water phases like cytosol and high RI for protein, lipid phases and organelles like mitochondria or chloroplasts.[269] The extremes range from bones that are opaque to the eye lens that is transparent. Moreover, the eye lens must function for decades under oxidizing (aerobic) conditions and the presence of sunlight.

Human γ-D-crystallin (HGD) is a major structural protein of the human eye lens, the transparent, ellipsoid tissue that focuses light into a sharp image on the retina (**Figure 7.6**).[270] Because lens cells lose their organelles during development *in utero*, HGD must retain its native structure for decades. However, ageing under aerobic conditions replete with reactive oxygen species and exposure to UV irradiation eventually leads to protein aggregation that scatters light (a symptom of cataract formation).[271] Cataract impacts about 50% of the global population over age 50 and caused blindness in 15.2 million cases in 2020.[272] The structural basis of a cataract pathogenicity emerged from an Arg36 to Ser (R36S) variant of the HGD protein that produced crystals in the eye lens, and analysis of one of them yielded a 2.25 Å resolution crystal structure.[273] HGD contains 174 amino acids, of which 6 are Cys (3.4%) and 4 are tryptophan (2.3%) residues; both tallies are significantly above the average for human proteins. Although long regarded as a passive structural protein, growing evidence indicates that HGD participates actively in light-driven redox chemistry that involves the Cys and Trp residues. Previous synchrotron serial crystallography performed at Diamond Light Source and EMBL at PETRA III allowed identification of photo-driven structural changes linked to protein repair and glutathione recycling. [274]

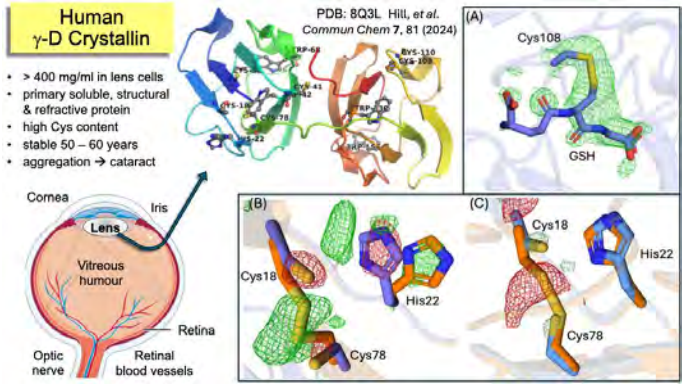


Figure 7.6: Anatomy and protein of the eye lens

*Crystal structures and unpublished data from Briony Yorke et al. support the hypothesis and suggest mechanisms to reverse oxidative and light-induced damage to maintain native folded state of γ-D crystallin. (**A**) Native reducing agent glutathione (GSH) bound to surface cysteine C108 in aged HGD. (**B**) Further aging results in the formation of a strained internal disulfide bond between C18 and C78. (**C**) Internal disulfide cleavage occurs within 5 ns of 308 nm laser pulse eventually resulting in loss surface disulfide adducts on millisecond timescale.*

Source: Public domain and unpublished data from B. Yorke

Ongoing time-resolved experiments at XFEL facilities, including SACLA and SwissFEL, have revealed a multi-step redox pathway in HGD wherein transient disulfide bond formation precedes light-driven structural changes. These XFEL measurements have established a mechanistic framework for understanding how crystallins manage oxidative stress through controlled redox transitions. Complementary femtosecond X-ray absorption spectroscopy measurements at the European XFEL and SwissFEL have revealed the timescales and identities of intermediate sulphur radical and ionic intermediates formed upon UV illumination of disulfides, which are essential for decoding the underlying photochemical mechanisms in proteins.[275] Together, structural and spectroscopic measurements can provide full characterisation of light-induced redox pathways. By resolving early intermediates, researchers are advancing fundamental insight into protein photochemistry and oxidative ageing, while providing a structural basis of strategies that stabilise crystallins to prevent or reverse cataract formation. Thus, HGD maintains transparency while it also executes essential "repairs" to preserve vision.

DNA Photolyase: UV light-induced alterations to DNA, including generation of cyclobutane pyrimidine dimers (CPDs), pose a significant risk to every genome exposed to sunlight on earth (**Figure 7.7**). As Dr T. J. Lane said during his talk at the Royal Society on 30 July 2023, *"It's been estimated that about 50 to 100 of these lesions form per second per cell at the surface of the skin."* Dr Aziz Sancar said during his Nobel Lecture on 08 Dec. 2015, "*Photolyase is a photon-powered nanomachine that uses blue light photons to repair thymine dimers that are induced in DNA by UV. ... Decades before the discovery of photolyase, it had been known that UV kills bacteria very efficiently. In 1949 Albert Kelner, of Cold Spring Harbor, made the interesting observation that if bacteria killed by UV were exposed to visible light, the dead bacteria were miraculously brought back to life."* DNA Photolyase, a blue enzyme when isolated, is responsible for these observations.[276-279] Photoreactivation using UV to visible light photons is a highly conserved strategy from bacteria to vertebrates (except for placental mammals, which use DNA excision repair strategies) for preserving the integrity of the genome after sunlight exposure. It is arguably one of the most important enzymes in the evolution of life on our sunny, planet earth. How DNA photolyase works was recently revealed by tr-SFX using XFELs.

The two studies of Maestre-Reyna *et al.* and Christou *et al.* published independently in 2023 in *Science* reported tr-SFX results of the DNA photolyase from the archaea *Methanosarcina mazei* (**Figure 7.7**) after leveraging beamtime awarded over a few years by several synchrotrons and XFELs (LCLS, SACLA, European XFEL and SwissFEL).[280-285] They observed that the synchrotron data was typically "plagued" by X-ray induced photoelectrons flooding the exposed crystal volume that complicated the analysis. In contrast, the XFEL data avoided these issues due to the femtoseconds pulse length used to obtain each tr-SFX diffraction pattern; consequently, data from SACLA and SwissFEL are acknowledged in the two papers. Both groups used a high-viscosity extruder (HVE) to deliver the water-soluble enzyme in microcrystal slurries and collected at 30, or 100 Hz at SACLA or SwissFEL, respectively. Their laser illumination schemes were in the multiphoton regime, whereas $\lesssim 1$ photon per chromophore is typical for members of the enzyme superfamily that often exhibit a high quantum yield for the DNA repair reaction. Overall, these R&D projects highlight the importance of regular access to large scale facilities and the iterative nature of time-resolved crystallography studies.

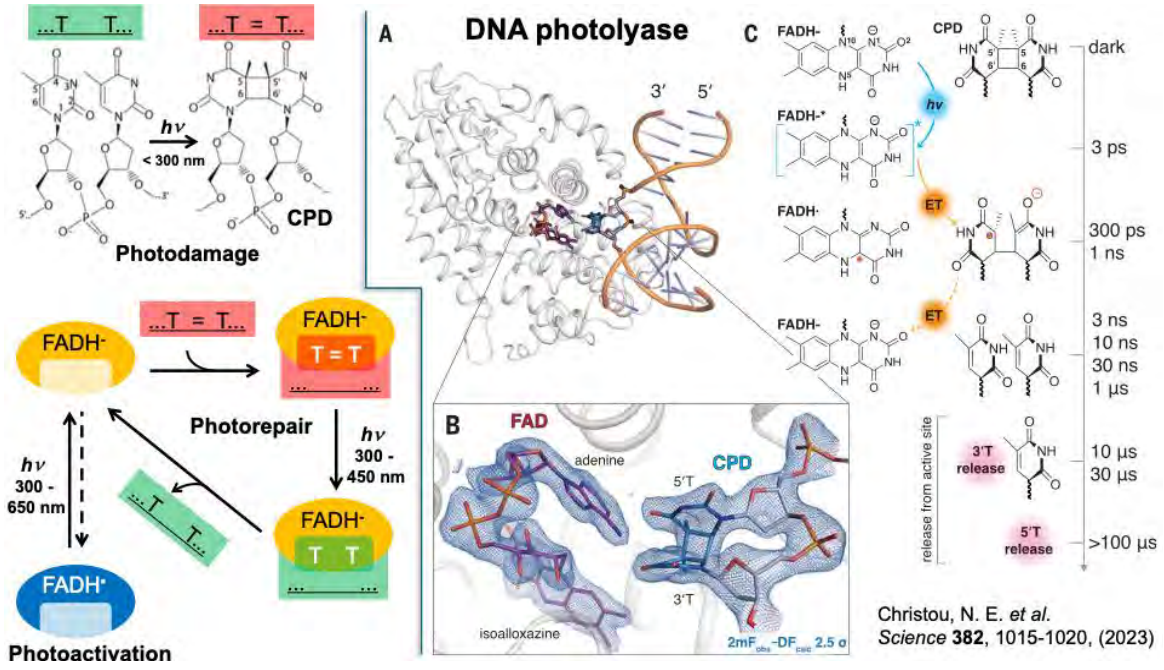


Figure 7.7: Time-resolved crystallography captures light-driven DNA repair

*(**Left**) UV light induced damage to DNA and a repair cycle of CPD-photolyase with its cofactor regeneration cycle. (**Right**) (**A**) Structure of photolyase from M. mazei co-crystallised with a dsDNA 14-mer containing a CPD. (**B**) Region of interest showing the CPD binding mode with respect to FAD. (**C**) Schematic of the reaction mechanism, including FAD states (left), the corresponding thymine dimer states (middle), and the pump-probe delays acquired in this study (right). The blue line indicates photon absorption (h ν) and the orange line, electron transfer (ET), with dashes representing the possibility of electron loss resulting in a mixture of states. At the longest time point studied (100 µs), the 5′ thymine was only partially released, as indicated by the time axis.*

Right-hand portion reproduced with permission from the American Association for the Advancement of Science.

CPD photolyase genes within the DNA photolyase superfamily are present and remain highly conserved in blind, cave-dwelling fish, *e.g. Phreatichthys andruzzii* isolated from sunlight for 3 million years beneath the Somalian desert.[286,287] Although swimming in the total darkness, the aerobic fish still experience oxidative stress *i.e.* reactive oxygen species (ROS), which generates many types of DNA damage, including 8-hydroxydeoxyguanosine (8-OHdG) and CPDs. The analysis shows that the enzyme evolved to function in the light independent repair of ROS-induced 8-OHdG and CPD. The molecular mechanism has not been deciphered but is likely to include the FAD and H_2O_2 and could benefit from future tr-SFX studies.

The DNA photolyase superfamily also includes **cryptochromes**, falvoproteins acting as photoreceptors involved in circadian rhythms and cell signalling. Recent pump-probe tr-SFX results from SACLA using the cryptochrome from the single-cell, green alga *Chlamydomonas reinhardtii* documented the structural changes associated with absorption of 450 nm light at 19 timepoints ranging from 10 ns to 233 ms.[288] The results show that light generates a [$FAD^{\bullet-}$ / $Tyr373^{\bullet}$] radical pair, and at longer timepoints, starts a series of much larger conformational changes that lead to C-terminal unfolding. In cryptochromes, the diradical pair is thought to function in sensing earth's magnetic field in birds [289,290,291], and the C-terminal unfolding is linked to important to downstream signalling cascades. Large conformational changes that effect DNA binding affinity and physiological impact are also part of the photoactivation in the prototypical cobalamin B12 photoreceptor CarH.[292,293] XFELs have also been critical to SFX studies of resting and ligand complexes of human MT1 and MT2 melatonin receptors that are G-protein-coupled receptors (GPCRs) involved in regulating circadian rhythms. [202,294,295]

(Photo)decarboxylases – potential impact to renewable energy: More than one billion years ago, terrestrial plants evolved from green algae (phylum *Chlorophyta*), a diverse and often unicellular group of photosynthetic eukaryotes.[296] Genomic analysis of *Chlorella variabilis* NC64A, reveals an evolution that included genomic interplay with viruses and symbiosis between eukaryotes.[297] Of particular note, the symbiotic microalga expresses a flavin-dependent photoenzyme involved in lipid metabolism called **fatty acid photodecarboxylase (*Cv*FAP)**, a member of the large glucose-methanol-choline (GMC) superfamily of oxidoreductases. *Cv*FAP uses blue light with a quantum yield >80% to produce n-alkanes or -alkenes (*i.e.* gasoline or petrol) from fatty acids. A detailed and comprehensive light driven reaction mechanism was revealed by interdisciplinary methods including biochemical, static and tr-SFX and spectroscopy, and computational approaches.[298-302] The time-resolved R&D programme reported in *Science* was executed at the ESRF in Grenoble via its in-house research programme, including the *in-crystallo* Optical Spectroscopy (icOS) laboratory, and at the LCLS. The enzyme uses a "remarkably complex mechanism" that includes $FADH^-$ photoexcitation and a unique example of a hydrated electron within a protein cavity.

The algae and plants that lived and died in shallow seas millions of years ago sank to the seafloor and were buried with other sediments. Under high pressure and temperature, the reduced carbon slowly transformed over millions of years into fossil fuel deposits. Today we mine for coal and drill for oil. The oil and chemical industries transform their spoils into gasoline, diesel, and jet fuel that are burned to provide energy for industrial civilisations, and/or to produce many high value chemical feedstocks. These activities produce CO_2 on a sufficient scale that we are both responsible for, and witness to, **global climate change** – a problem of profound importance to humanity.

Fortunately, fatty acid decarboxylases like *Cv*FAP clearly expand our **green chemistry options for renewable liquid biofuels**. Indeed, biology has many examples of enzymes that produce alkanes and alkenes from fatty acids and/or aldehydes.[303-306] XFELs will help support these kinds of R&D programmes, especially those that include or are inspired by enzymes that use heme and nonheme iron metallocentres to facilitate catalysis. For instance, cyanobacteria produce a soluble aldehyde-deformylating oxygenase (ADO, formerly known as aldehyde decarbonylase) that uses a dinucelar nonheme iron active site homologous to MMO, to transform a free fatty aldehyde into its corresponding n-1 alkane. The XFEL Hub at Diamond uses tr-SFX ± tr-XES methods in an R&D collaboration that focuses on the *Staphylococcus aureus* cytochrome P450 decarboxylase that directly converts a fatty acid and H_2O_2 into a corresponding n-1 alkene and CO_2.

Ultrafast time-resolved spectroscopic experiments performed on photo-active proteins in solution have provided many important insights into the very early events after absorbing a photon. Because XFELs are relatively new, analogous time-resolved SFX experiments are still emerging. In most reports, authors compare time-resolved SFX and spectroscopic results; although they may have used similar pump-probe delay times, the comparisons frequently do not yield one-to-one correlations. One possible explanation is that the crystal versus solution conditions are sufficiently different that ultrafast spectroscopic experiments have not been performed at, for example, the same pH, viscosity, or ionic strength, among many other potential variables that were present in the SFX experiments. Furthermore, the desire of structural biologists to observe and maximise illumination-dependent differences in electron density maps has often pushed experimental conditions into the multi-photon regime. Recently it has become clear that visible light power dependence studies are critically important to nearly all light-activated time-resolved SFX experiments. Unfortunately, in part because beamtime is so rare, scientists may under-prioritise these "control" experiments, and as a result these types of data may be sacrificed under time-pressure situations. Fortunately, several recent reports are addressing some of these challenges.[307-312]

Examples of XFEL experiments involving light-activated systems include photosystem I [130,313-317], photosystem II [139,141,143,144,167,318-329], photoactive yellow protein [330-332] , human rhodopsin [200,333-337], bacteriorhodopsins [135,338-345], jumping spider rhodopsin [346,347], light-activated ion channels [348,349], fluorescent proteins [350-353], several phytochromes [143,354-356], DNA photolyase [283,284,285], gamma-D crystallin [274], and photo-dissociation studies of myoglobin-CO [309,357] or cytochrome c oxidase-CO.[358-361] Of these systems, photosystems I and II have evolved mechanisms to diffuse the excess energy absorbed in multiphoton events through the network of internal chromophores, and are therefore less susceptible to the impact of single versus multiphoton time-resolved SFX studies. The photo-dissociation of CO from metalloproteins can be considered outside their normal function and less constrained by illumination conditions. The remaining systems evolved to react to visible photons, and single photon methods are likely to be most physiological. Moreover, many of these systems experience photo-driven conformational changes that are often linked to photoisomerization of the chromophore. Such events are often very fast and require timing tools to help coordinate the pump-probe experiment.[362-365]

Optogenetics refers to the ability to control a biological outcome through illumination with light.[89,366-372] The field has grown with our understanding of how various organisms sense and respond to ambient light through the action of one or more photoreceptors. These types of proteins evolved to absorb visible light photons, which drives photoisomerization event(s), that consequently trigger conformational change(s) and ultimately elicit an output response most likely through signalling cascades or a change in pH or ion concentration. Thus, optogenetics combines biophysics, structural biology, genetics and cell biology. But it all starts with a fundamental, atomic level understanding of structure, function, and dynamics of photosensor proteins — of which there are many. Their function relies upon chromophores that often exhibit extreme radiation sensitivity.

A promise of optogenetics in cell biology is to advance the field from observing or describing molecules (even at atomic level detail) to controlling them in real time. Indeed, doing so will clearly demonstrate critical mechanistic understanding for how cells work individually and/or in larger "collaborations" such as tissues and organs.[373-378] In addition, photopharmacology, or the combination of photochemistry and pharmacology is most often applied to small molecules to trigger desirable transformation(s), which is highly complementary to optogenetics.[379-384] Sensory macromolecules include the Light-Oxygen-Voltage (LOV), blue-light sensitive domains harbouring a flavin chromophore and found in bacteria to higher plants.[385-388] A variety of rhodopsins and channelrhodopsins are widely used optogenetic tools to trigger many types of physiological changes. [339,349,389-392]

An illustrative example is the phytochrome superfamily of proteins that are generally divided into two functional regions (**Figure 7.8**).[393-395] For instance, an N-terminal photosensory module houses a covalently-bound bilin, or bilin-derived chromophore within a central domain, followed by a C-terminal output module that usually contains one or more protein kinase domains that transfers

the signal to various downstream phosphorylation signalling cascades. Typically, phytochromes act as red/far-red photoswitches that are activated/deactivated by absorption of red or far-red light, respectively, by means of a covalently bound bilin chromophore. However, using a similar bilin cofactor but different protein-ligand covalent linkages, these proteins photoswitch between other colours of light, e.g. blue/green for Te-PixJ. Moreover, the spectroscopic analysis of the photoconversion reaction typically identify several intermediates formed with kinetic rate constants ranging from fs - ps - µs - ms - seconds. The photoisomerization effects are the fastest events, and the slowest events relate to larger conformational changes propagating throughout the protein that have the largest biological impact. The structural basis and dynamics for these proteins is still poorly understood and several groups are persuing time-resolved SFX programmes and synchrotron-based studies with various pump-probe strategies.[143,354,355,396-408]

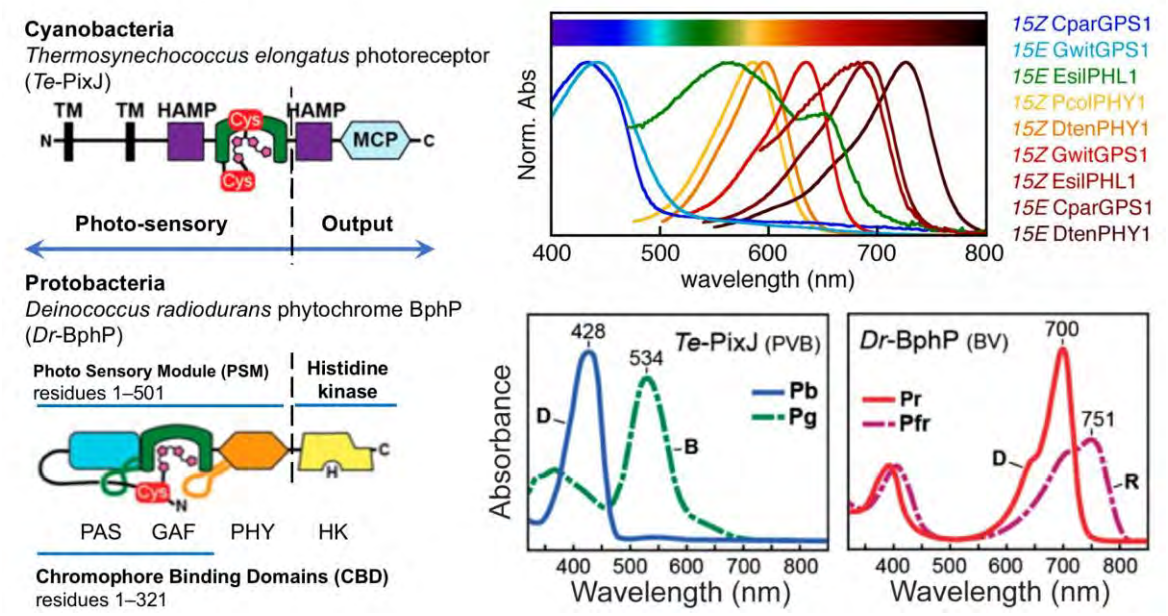


Figure 7.8: Protein domain organisation and spectral properties of two phytochrome photosensors (top, right) Normalised absorption peaks for several algal phytochromes. (bottom, right) Absorption spectra of the dark-adapted (D) and photoactivated states after blue (B) or red (R) illumination of Te-*PixJ or* Dr-*BphP. (left) The domain architecture of two phytochromes; abbreviations are: TM, predicted transmembrane region; HAMP, histidine kinase/adenylyl cyclase/methyl binding protein/phosphatase; MCP methyl-accepting chemotaxis protein; PAS, Period/Arnt/Single-Minded; GAF, cGMP phosphodiesterase / adenylyl cyclase / FhlA doain with chromophore binding residues; PHY, phytochrome-specific region; HK, histidine kinase.*

Left and lower right figures adapted with permission from E.S. Burgie and R.D. Vierstra, The Plant Cell ***26*** *(12) 4568-4583 (2014) DOI: 10.1105/tpc.114.131623; Upper right figure reproduced from N.C. Rockwell et al. Proc. Natl. Acad. Sci. USA* ***111****, 3871-3876 Copyright (2018) National Academy of Sciences DOI: 10.1073/pnas.1401871111*

7.2.3 Photosystem II: a benchmark system

Photosystem II (PS-II) is a high-value, benchmark system for time-resolved SFX studies with results coming principally from three international teams of researchers in the USA, Asia, and Europe.[141,314,318-320,322-324,326,327,409-422] The enzyme is responsible for the "great oxidation event" approximately 2.4 billion years ago ("Oceans Rust" in **Figure 7.1**), which transformed the earth from an anaerobic reducing atmosphere to the oxygen-rich and oxidising atmosphere it is today. PS-II is a large integral membrane protein expressed in all plant and most photosynthetic microorganisms. The protein uses four photons to catalyse the four-electron oxidation of two water molecules that form one O_2 molecule plus four H^+ that help establish a proton gradient used for ATP generation by ATP synthase. The PS-II reaction is driven by visible light photons that initiate very rapid charge separation events (femtoseconds to picoseconds), and much slower electron-transfer events (hundreds of milliseconds) to reduce the quinone pool.

Thus, PS-II is an ideal system for time-resolved SFX studies; but the entire reaction cycle spans more than 12 orders of magnitude in time, which creates experimental challenges. A large collaborative group developed an on-demand, acoustic droplet ejection onto tape system (**Figure 7.9**).[141,143,145,146,

[324,328,329,410,411,413-415,423,424] It transports discrete nL droplets across a laser illumination platform before they reach the X-ray interaction region. This allows for multiple illumination/equilibration perturbations to advance the reaction cycle for time-resolved SFX experiments. An added benefit of the design is that the region between the droplet ejection and the X-ray interaction region can also be fitted with either an O_2 reaction chamber or a second pL droplet ejector system, both of which enable a wide range of mixing based time-resolved reactions.

O_2 bond formation within PS-II is catalysed by the oxygen evolving complex (OEC) that include a Mn_4O_5Ca cluster (**Figure 7.10**).[425,426] When a photon is absorbed by the P680 chromophore, it results in charge separation and electron transfer to the quinone site. The oxidised P680 is then reduced by the OEC, which advances one oxidation state with each photon absorption event. In the Kok cycle, the first photon promotes the S_1 to S_2 transition, the second photon S_2 to S_3, and the third photon from S_3 to S_4. The S_4 state catalyses the conversion of two water molecules into O_2 resulting in the S_0 state of the OEC. Absorption of a fourth photon produces the stable S_1 starting state.

The Mn atoms within the cluster act as a redox "buffer" and each oxidation state has a unique $K\beta_{1,3}$ X-ray emission spectrum (XES). Consequently, time-resolved XES collected simultaneously with time-resolved SFX provides complementary data on the electronic and atomic structures of the catalytic centre.[141,324,326-329,427] Groups working principally at the LCLS and LBNL developed methods to simultaneously collect time-resolved SFX data in the forward direction and time-resolved X-ray emission spectroscopy (XES) at 90°, from each sample and each X-ray pulse.[141,143, 144 ,324,325,327-329,427-429] Some of the results for PS-II are shown in **Figure 7.10** for the OEC poised in the S_3 state where µs time-resolved structures demonstrate motion of the Mn atoms and entry of a new solvent atom (label O6

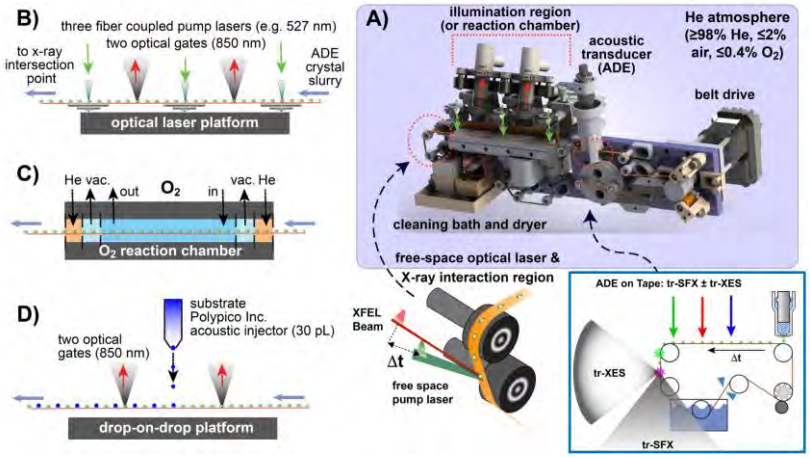


*Figure 7.9: Acoustic tape drive system for pump-probe time-resolved SFX and XES measurements of PS-II (A & B) and options for O_2 dependent reactions (C) or drop-on-drop ligand additions (D). See also Fuller et al. (2017) Nature Methods **14**, 443-449.*

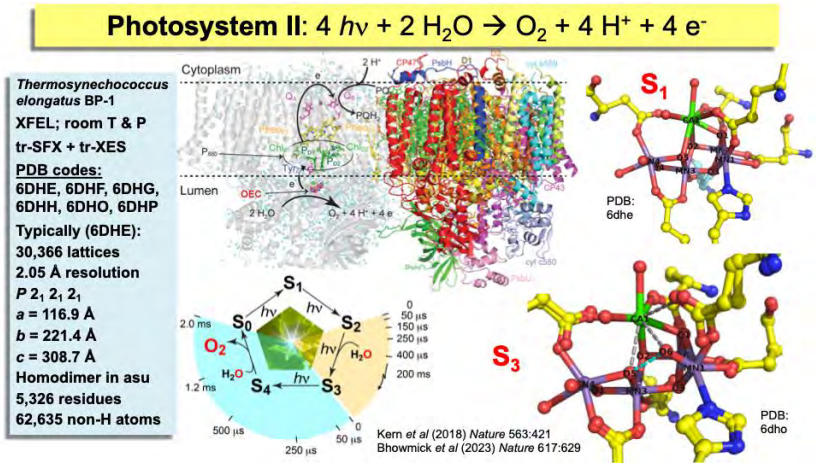


Figure 7.10: Correlated time-resolved SFX and XEX results from PS-II (left) Some of the characteristics of PS-II crystal structures. (middle), the overall structure of PS-II and the Kok's water oxidising clock (OEC) with tr-SFX + tr-XES datapoints indicated. (right) atomic models for OEC Mn_4O_5Ca cluster in S1 ground and S3 intermediate states.

*Right top and bottom reproduced from J. Kern et al. "Structures of the intermediates of Kok's photosynthetic water oxidation clock", Nature **563**, 421–425 (2018), Springer Nature. DOI: 10.1038/s41586-018-0681-2*

in the image).[141] The atomic model is correlated with oxidation of the Mn atoms within the OEC and the O_2 generation assays from crystal slurries. Details for the time-resolved reaction that forms the O_2 molecule remain ill-defined; however, the deepest mechanistic insights will likely depend upon correlated studies and benefit from XFEL sources.

7.2.4 Caged compound and proteins

Light-driven strategies to initiate catalysis in systems that are not naturally light sensitive include: a) caged compounds, b) caged proteins, c) ligand exchange, or d) temperature jump methods.[321,430-450] Each of these must satisfy the requirements of high selectivity, high quantum yield and temporal resolution. To these ends, *o*-nitrobenzyl moieties are among the most common photocaging groups for substrates and amino acids, but their decaging photochemistry may not be as fast nor as clean as *p*-hydroxyphenacyl or coumarylmethyl derivatives. Caged substrates are either co-crystallised with the target macromolecule or soaked into slurries of microcrystals. Incorporation of non-natural amino acids that convert a given protein into a caged protein is more difficult (e.g. **Figure 7.11**). Consequently, caged protein approaches typically include a computational evaluation stage, followed by protein translation using *amber* TAG codon-suppression methods, or post-translational modification strategies. The photo-active moiety is most often linked to thio, amino, carboxy or hydroxy groups of proteins or substrate ligands, and is then cleaved by irradiation with UV to visible light. Photo-cleavage of the caging group varies in rate (ps – µs) and quantum yield (<0.2 – 1), which then generates: *i)* authentic substrate in the active site vicinity, *ii)* a rapid pH shift, *iii)* a temperature jump, *iv)* removes an active site barrier and enables substrate binding, or *v)* eliminates a dynamic or conformational restraint required for catalysis. Ligand exchange methods include photolabile metal-CO or NO complexes that mimic a metal-O_2 intermediates in a reaction cycle. Photodissociation of the blocking diatomic molecules then allows for O_2 binding and the ensuing reaction. All of these methods are experiencing a resurgence of R&D activity and provide important opportunities for time-resolved structural biology at XFELs. Some of these techniques will require careful coordination of the timing between the visible light pump laser and the XFEL probe pulse.

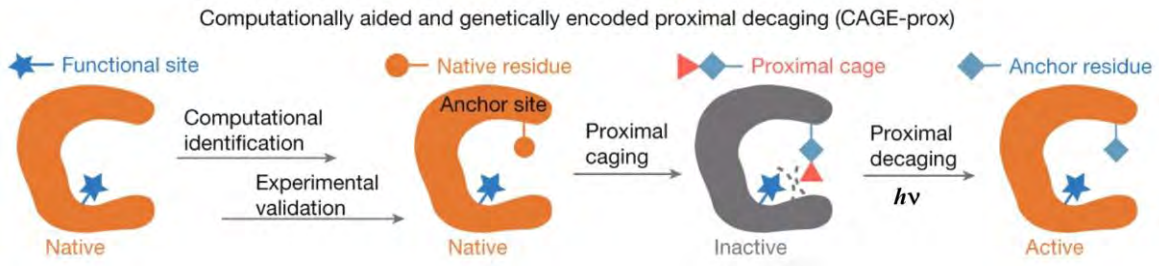


Figure 7.11: Schematic concept of the CAGE-prox strategy

A proximal cage can be genetically incorporated at an anchor site in close proximity to the protein functional site for temporal blockage of its activity. Proximal decaging can lead to rapid rescue of protein functions, as long as the decaged anchor residue has negligible influence on protein activity.

Reprinted by permission from Springer Nature: J. Wang et al. Nature 569, 509–513 Copyright (2019) DOI: 10.1038/s41586-019-1188-1

7.2.5 Future directions

Time-resolved serial MX studies of light-activated proteins will continue to expand at synchrotrons and XFELs around the world. This R&D effort will benefit from hard X-rays with tight focus and XFEL pulse frequencies from kHz to MHz. A variety of illumination schemes must be well integrated into the sample delivery and data collection strategies. For instance, some systems will need fs time resolution, whereas other more complex dynamic process may require seconds to evolve. Moreover, short pulse duration visible laser illumination schemes should be complemented with longer exposure strategies, potentially from CW lasers and/or diodes with triggering. Since many chromophore containing proteins are radiation sensitive, XFELs offer clear advantages for obtaining diffraction data before deleterious effects destroy the samples. Data processing to provide near-to-real time analysis is critical and will burden computational resources.

A second opportunity for data analysis of stationary diffraction is the explicit retrieval of ultrafast population information through application of optical crystallography theory.[218,451-453] This is an important example that provides one of several strong cases for high-repetition rate and increased sensitivity of time resolved SFX.

Specifically, for all crystal classes of uniaxial and biaxial symmetries (trigonal, tetragonal, hexagonal, triclinic, monoclinic and ortho-rhombic crystal classes) the resulting birefringence connects the orientation dependence of electric field decomposition to the explicit analysis of power density dependent population transfer. Inversion of an indexing matrix for a stationary diffraction image from time-resolved SFX data will allow a calculation of orthogonal field directions in the X-ray crystallo-graphic coordinate frame from solving Maxwell's polarised wave equations in anisotropic media (**Figure 7.12**). While this requires explicit knowledge of the intrinsic birefringence value and wavelength dependence depending on the point group symmetry, opportunities for population analysis specifically exploit the high repetition rate regime. With knowledge of linear and non-linear optical cross sections, the time-resolved SFX data can be separated in data bins according to the calculated photo-selection of linear and non-linear population under intense femtosecond optical excitation. With currently available signal-to-noise and crystallographic statistics, time-resolved studies effectively average the full Debye-Scherrer range of individual reflections, while high repetition rate studies will separate the population difference that exist within (**Figure 7.12**). This provides additional compelling motivation for the development of high repetition rate, increased stability and high accuracy crystallography. It is evident that such applications will be possible and successful with the availability of many more stationary diffraction observations. A second compelling motivation for increased sensitivity is the control and observation of small amplitude coherent motion, discussed in **Section 7.4**.

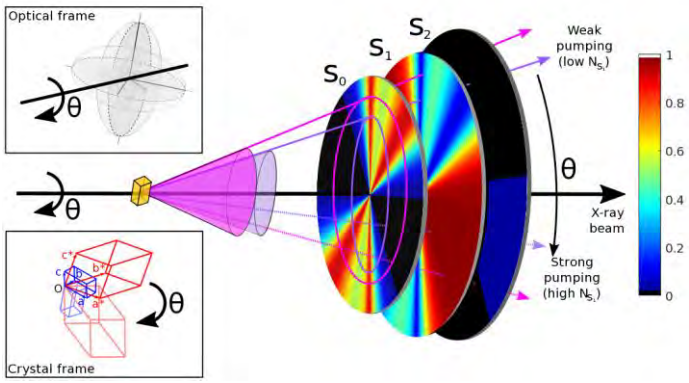


Figure 7.12: Illustration of the analysis of orientation dependence of photoinduced populations with reference to both the optical orientation and the X-ray crystallographic orientation

Tracing a Debye-Scherrer ring in revolution, the polarisation directions are modified according to the solutions to Maxwell's polarised wave equations. Therefore, population transfer may be analysed radially in the detector plane, as illustrated with a physical calculation example for a uniaxial case.

*Figure reproduced with permission from C.D.M. Hutchison and J.J. van Thor, Phil. Trans. R. Soc. A. **377** 20170474 DOI: 10.1098/rsta.2017.0474*

7.3 Dynamic structural biology: Molecular movies of enzyme catalysis

Dynamic structural biology is as much a philosophy as a set of tools to collect as much data as possible, from every sample and every X-ray pulse, at physiological temperature and pressure, with an aim to create time-resolved molecular movies of macromolecules engaged in function. Time-resolved SFX studies exploiting mixing methods are generalisable and have significant potential for revealing the dynamics of enzyme catalysis in broad context across biology.

7.3.1 Introduction

The concept of dynamic structural biology is illustrated in **Figure 7.13** and links reaction dynamics with sample preparation, reaction triggering and data collection. Diffusion-triggered methods for time-resolved crystallography experiments were proposed in 2000 by the LCLS Scientific Advisory Committee, in 'First Scientific Experiments for LCLS' (http://www.slac.stanford.edu/pubs/slacreports/reports03/slac-r-611.pdf). [454]

> *Time-resolved structural studies on diffusive processes in crystalline enzymes are difficult due to problems with mixing enzyme and reactant in the crystal. With submicron-sized samples, the vast majority of solution techniques and methodologies will suddenly become available for time-resolved structural investigations at the LCLS.*

Macromolecular crystals are typically about 50% protein and 50% solvent, which is similar to the 65% fraction of water within human cells. Analyzing more than 36,000 enzymes listed in the *BRENDA* database reveals that *a)* the median turnover time for catalysis in solution is about 70 ms, *b)* more than 60% exhibiting a k_{cat} value between 1 – 100 s^{-1}, and *c)* enzymes catalyzing reactions related to secondary metabolism are typically 30-fold slower than those of central metabolism.[455-459]

Dynamics play important but often ill-defined roles in enzyme catalysis.[458-467] A driving hypothesis for time-resolved serial MX is that because small molecule substrates diffuse relatively fast (*e.g.* molecules in water at 310 K: O_2 (32 g/mol) = 2 $\mu m^2/ms$; glycine (75 g/mole) = 1 $\mu m^2/ms$; glucose (180 g/mole) = 0.6 $\mu m^2/ms$; sucrose (342 g/mole) = 0.52 $\mu m^2/ms$), enzyme microcrystals will equilibrate with substrates faster than catalytic turnover.[313,468-476] This implies that time-resolved structural biology methods are generalisable when exploiting micron-size crystals or smaller. With 6,029,364 enzyme genes and tens of thousands of enzyme types listed in the KEGG databases (**Table 7.2**), there is an enormous reaction landscape to be explored. However, due to the very limited availability of XFEL beamtime, relatively few time-resolved SFX experiments exploiting mixing strategies have been conducted at fully commissioned XFEL facilities.[9,107,143,475,477-483]

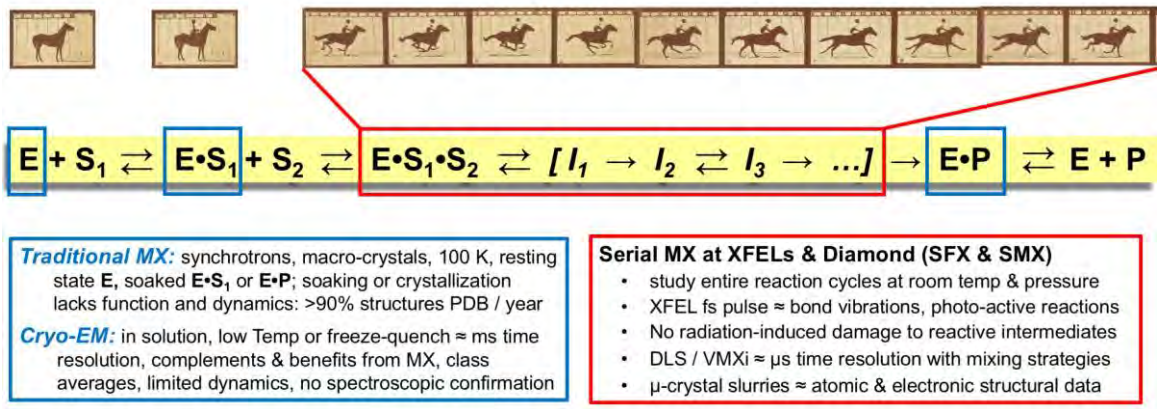


Figure 7.13: Concepts of time-resolved structural biology.
Snap-shots of data inspired by Muybridge's "horse in motion" photographs (Palo Alto CA, June 1878, 500 µs shutter speed). Stable, ground-state complexes are studied by traditional MX and cryo-EM methods, most often at 100 K. Time-resolved cryo-EM methods use freeze-quench techniques, typically with ms time resolution. Serial MX methods with microcrystals and monochromatic X-rays at synchrotrons or XFELs collect still diffraction images at room temperature with µs - fs exposures, respectively, at different Δt intervals after optical laser flash(es) or ligand mixing.

7.3.2 Mix-inject sample delivery for time-resolved SFX

To date, most time-resolved SFX studies that exploit mixing methods used liquid gas dynamic virtual nozzle (GDVN) style jets or microfluidic devices that have been developed by several groups.[107,108,133,134,313,475,477-486] For the majority of cases, GDVNs typically achieve sample injection speeds of 10 – 30 m s^{-1} and are suitable for 10 – 120 Hz repetition rate XFEL sources. Many of these mixing-injectors are slow and need on the order of seconds to fully mix substrate with crystals. Other types of devices mix on the ms timescale but require high-dilution ratios to infuse substrate into the crystal slurry stream. These types consume large amounts of substrate or ligand and dilute the crystal concentration, which also reduces the overall SFX data collection rates. All of the GDVN nozzle methods are prone to clogging or freezing when used in vacuum chambers and benefit from cleaning between samples.

For MHz sources, sample injection speeds need to be on the order of 50 – 100 m s^{-1} so that fresh material is presented to each XFEL pulse.[131,315,487-490] Mixing injectors that produce such high jet velocities must have very small orifices and therefore can only accommodate microcrystals. This matches the desire to use less than ~3 µm crystals and is consistent with rapid equilibration of ligands throughout the crystal. These constraints also impact GDVN nozzle fabrication. For instance, a recent example developed for MHz data collection at the European XFEL used a high-end 3D printer (Nanoscribe GmbH) and two-photon stereolithography methods to achieve free-form geometries with submicron precision.[133] Devices like those illustrated in **Figure 7.14** produce 50 – 225 µm jet lengths, diameters as low as 536 ± 35 nm with a liquid flow rate of 2.4 ± 0.12 µl min^{-1} and a gas flow rate of 22.5 ± 0.2 mg min^{-1}. At the SPB/SFX instrument at the European XFEL, a similar design with a gas and liquid orifice size of 60 and 50 µm diameter, respectively, was used to inject microcrystals of up to 6 to 8 µm in size at velocities of up to 100 m s^{-1}.[489,490] The delay timepoint(s) achievable for high velocity mix-inject jets is principally a function of the flow rate and the distance the sample-ligand mixture travels to the nozzle exit; the time of flight to the beam will only be ~ 1 – 3 µs and thus very short compared to most enzyme reaction times (average turnover time of ~ 70 ms).

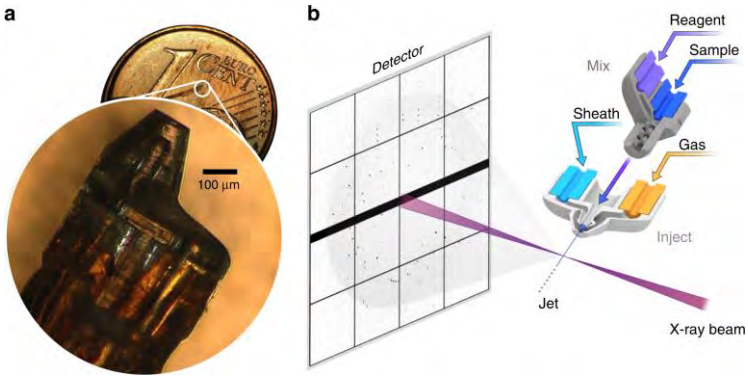


Figure 7.14: A microfluidic device for time-resolved SFX. ***a)*** *Through micro-3D-printing Knoška et al fabricate microfluidic devices of a few 100 µm in size. Magnified view of a nozzle placed on a 1 cent coin for scale reference.* ***b)*** *This technique can realise integrated nozzle assemblies to jet protein crystal suspension into the X-ray interaction region for diffractive imaging.*

Figure reproduced from J. Knoska et al. Nat. Comms. ***11****, 657 (2020) under the terms of the Creative Commons Attribution 4.0 International License.*

7.3.3 '*Multimessenger techniques*' help reduce ambiguity in time-resolved SFX experiments

Time-resolved SFX that is correlated with time-resolved XES has been used extensively to study PS-II.[141,143,324-329,429] This strategy provides data relevant to the electronic and atomic structures of metal centres. For these types of experiment, it is important to evaluate the impact of the XEFL pulse intensity and duration upon the metal centre since the measurement itself will alter the electronic structure of the centre. Under some circumstances non-linear excitation processes may disturb the spectroscopic signature of the metalloenzyme without significantly altering the recorded diffraction pattern.

The acoustic tape drive system described above can also be used for mixing-based studies from metalloenzyme reactions, including those that react with O_2 or water-soluble ligands (see **Figure 7.9**).[356,419,491-497] For example, iron-dependent enzymes are ubiquitous in biology, but it is difficult to study oxygen-Fe intermediates by traditional, synchrotron-based MX methods, because their reactivity also makes them very sensitive to photoreduction by the X-ray beam. In many cases an Fe(IV)=O intermediate is produced in the reaction cycle; therefore, it is also important to include X-ray emission spectroscopy to help differentiate it from Fe(II)–OH_2, and Fe(III)–OH species. The electron density maps for these three moieties are nearly identical except at extraordinarily high resolution. These types of compounds are also very sensitive to X-ray radiation-induced artifacts, but the spectroscopic signatures are very different. This strategy provides critical correlations between atomic and electronic structures (especially first row transition metal centres) from the same sample and X-ray pulse. For instance, this also represents an opportunity to include time-resolved XES measurements into the time-resolved SFX data processing pipelines so that only diffraction patterns that also exhibit the appropriate spectroscopic signature are merged into a timepoint dataset. Such a strategy will provide more confidence in the electron density map interpretation and in the resulting atomic models deposited to the PDB that are released to the whole structural biology community.

The electronic structure of a metal centre is an essential factor in reactivity and is profoundly influenced by its first and second shell coordination geometry, as well as the local electrostatic environment.[498-501] X-ray absorption spectroscopy (XAS) techniques complement crystallography, especially the analysis of the X-ray absorption near-edge structure (XANES) and the extended X-ray absorption fine structure (EXAFS) regions of the spectrum. The XANES portion provides insights into the oxidation state and coordination geometry, whereas XAFS region provides accurate measurements of metal-metal and metal-ligand distances. Indeed, the metric parameters that come from fits to the XAFS spectral region are often far more accurate than the errors in crystallographic methods will allow.

Nearly all types of spectroscopic measurement, including XES and XAS, record a signal from all of the particular metal atoms in the sample, whether they are ordered in the crystal lattice and/or enzyme active site (likely catalytically relevant) or disordered in the surrounding mother liquor (probably not mechanistically important). Thus, spectral overlap can be a challenge and is particularly difficult for enzymes that contain multinuclear metal clusters wherein each metal atom may have a discreet redox and electronic structure (**Figure 7.15**). An emerging method to resolve this ambiguity is to measure the XAS edge in the crystallographic diffraction data; a technique referred to as **spatially-resolved anomalous dispersion (SPREAD)**.[502-505] The method typically includes a series of complete diffraction datasets collected at several monochromatic energies across the K-absorption edge of the particular metal of interest. The electronic structure is then assigned to each individual metal centre by refining the wavelength-dependent anomalous correction parameters in the datasets. This data collection strategy has been attempted at LCLS beamtime using seeded beam and SASE mode; and the preliminary results suggest that it is possible. In the meantime, recent theoretical calculations using 50,000 – 100,000 simulated diffraction patterns with *nanoBragg* demonstrate that SASE-based XFEL pulses with a 30 eV bandpass are suitable for analysis by SPREAD analysis of the [2Fe:2S] reduced ferredoxin containing an Fe(III)-Fe(II) centre.[502] The simulations also indicate that the incident spectrum for each XFEL pulse must also be included in the analysis.[506] Furthermore, radial streaks are observed in Bragg reflections collected with a long crystal to detector distance and derive from the combined effects of the broad XFEL bandpass, crystal mosaicity, and energy-dependent structure factors.[507]

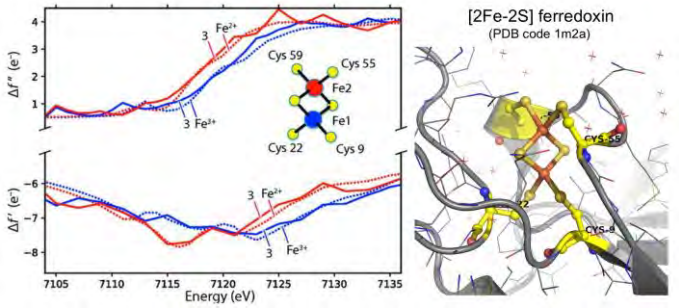


Figure 7.15: Spatially resolved anomalous dispersion (SPREAD) and crystal structure enable redox assignment to metal ions.

(left) Simulated anomalous scattering curves for the two iron centres converge to the ground truth showing that the oxidation state difference between Fe^{2+} and Fe^{3+} is clearly revealed by the refined 3-macrocycle models. (right) The 1.5 Å resolution crystal structure of the [2Fe-2S] ferredoxin from Aquifex aeolicus reveals the atomic position, but not the redox status of the metal atoms.

*Left-hand figure reproduced from N.K. Sauter et al. Acta Cryst. D **76**, 176-192 (2020) under the terms of a Creative Commons Attribution License. DOI: 10.1107/S2059798320000418*

In parallel and complementary to XFEL efforts, time-resolved MX methods are also under development at synchrotron facilities, especially those that provide pink-beam and microfocus capabilities.[182,183,185,508-511] At XFEL or synchrotron facilities, the reactions in crystals must be synchronised throughout all unit cells in order to observe high resolution diffraction from reaction cycle intermediates. For mixing strategies this will depend upon viscosity and the size of the substrate molecules traversing channels within the crystal lattice and macromolecules themselves.[512-514] Therefore, best practices dictate that when possible scientists should measure reactivity in the solid state and from more than one space group with different lattice packing. The homogeneity of the microcrystal slurry is also an important optimisation parameter for mixing-based time-resolved SFX experiments.[515,516]

7.3.4 Future directions

Time-resolved serial MX using nano- to micro-crystals and triggered with substrate diffusion is potentially generalisable across all of biochemistry. Therefore, it will continue to expand at synchrotrons and XFELs around the world. This effort will benefit from hard X-rays with tight focus and XFEL pulse frequencies from kHz to MHz. The quality and homogeneity of the crystal slurry with respect to size and morphology impact diffusion of substrate(s) into the crystal lattice and enzyme active sites – this is an active area of R&D by several groups. Datasets with two or more complementary types of information will continue to yield deeper mechanistic insights on more

metalloenzyme systems. Spatially-resolved anomalous dispersion (SPREAD) analysis shows promise for assigning redox status to individual metal atoms from highly-redundant SFX datasets collected with SASE mode,[502] and should be further evaluated with seeded and monochromatic XFEL methods. Data processing to provide near-to-real time analysis is critical and will burden computational resources.

Electron diffraction (ED) also generates high resolution atomic models from slurries of microcrystals (see **Appendix 1**; however, the crystal thickness is restricted to several hundred nanometres because electrons interact with matter more strongly than X-rays.[68,69,71,72] Sub-micron size samples reduce problems associated with inelastic scatter, multiple scattering events, or simply diminishing returns of information. A pulsed electron source, coupled with sub-micron size crystals that are injected into the interaction regions, is a perfect match for time-resolved dynamic structural biology; provided that various challenges are overcome.[517-519] Many of these issues are synergistic with time-resolved SFX at XFELs, and include sample delivery with mixing strategies and data processing pipelines with near-real time feedback.

In the future, time-resolved serial crystallography experiments will happen at XFELs and at synchrotrons, with very similar sample delivery and reaction initiation strategies. This will greatly increase reliability and access by many more scientists. Scientists will routinely study enzyme reaction coordinates with a variety of complementary reporters such as spectroscopy correlated with atomic structures. It will be possible to test the hypothesis that reactions and dynamics are druggable! Hence, there is significant potential for early-stage drug discovery at physiological temperature that explore compound binding to almost any point along a reaction pathway … and that will provide extra specificity. Exploiting the dynamics of reactions opens the potential to drugging cryptic sites that may not be accessible from ground state and/or low-temperature studies. Vertex' new sodium pump inhibitor, suzetrigine, is an example of the potential impact.[520-523] It was the first truly novel analgesic to be licensed for over 20 years when it received FDA approval in the USA in January 2025. A key to their success was understanding the dynamics of the ion channel amongst various sodium pump family members. It demonstrates that drugging the dynamics of a system is a viable strategy.

7.4 Controlling and measuring nuclear and electronic coherence within biological systems

Some photo-induced biochemical processes are so fast that nuclear and electronic quantum coherence are believed to have a role. XFELs are offering a new incisive window into this behaviour.

7.4.1 Introduction

The current and future abilities for ultrafast protein X-ray crystallography hold great potential for the development of methods and new approaches to interrogate protein dynamics. The field of ultrafast spectroscopy has traditionally used indirect methods for observation of structural dynamics, such as spectral shift analysis. Direct ultrafast crystal structure determination and electron density dynamics will allow many advances in structural dynamics that are not directly possible with spectroscopy. The development of time-resolved SFX at XFEL facilities has enabled the detection of nuclear coherent motions with application of ultrafast pump-probe techniques. For such applications, access to the ultrafast time scale is necessary and needs the ability to combine a femtosecond optical laser excitation pump with an X-ray probe from an XFEL pulse at ångstrom wavelength, femtosecond duration and delay time(s), and high X-ray photon flux.

A number of successful time-resolved protein X-ray crystallography experiments have been reported which included delays in the sub-picosecond timescale that includes vibrational coherence dynamics.[331,340,357] For time-resolved macromolecular crystallography, the combination of large unit cell dimensions, light atoms having small cross-section, and often small isomorphous differences, dictate the X-ray source requirements.[129,130,314,318,490,524,525] The photoinduced differences for protein crystals are analysed in real space from the electron density differences obtained by inverse Fourier transform, rather than on the level of $\Delta I/I$ of individual Bragg diffraction spots.[526] This requires strict isomorphism, which is maintained on ultrafast timescale in protein crystals.

Because the atomic cross-section, which dominates the valence electron density contribution, determines the measurements of protein structural dynamics by X-ray crystallography, it is rapidly dominated by displacements and order-disorder transitions through the analysis of isomorphous differences. It is well established from the ultrafast vibrational spectroscopy field that the typical dephasing timescale measured for protein samples is on the order of $\sim 1-2$ ps depending on the system of interest.[527-531] The ultrafast time-resolved SFX of proteins thus must include contributions from coherent vibrational dynamics.[218,526] This is a relatively new experimental ability that has been demonstrated in recent years, but has opened up a new field of application. Electronic coherence properties may not be readily available from X-ray crystallography, but a new type of application can be proposed to apply phase-locked two-pulse femtosecond excitation for time-resolved SFX experiments that would in principle provide a frequency correlation measurement from the coherence time alteration. [218]

7.4.2 'Blending' ultrafast spectroscopy and ultrafast time-resolved SFX

The emerging area of ultrafast time-resolved SFX can exploit and build on decades of ultrafast vibrational spectroscopy research and coherence theory.[218,526] A close analogy can be made between the technique of impulsive Raman spectroscopy, which is an ultrafast time-domain technique, and the ultrafast time-resolved SFX observation.[527,529] The comparison additionally identifies clear and obvious opportunities for future development of time-resolved SFX, particularly with emphasis of growing the experimental bandwidth and improving the signal-to-noise ratio. Impulsive Raman spectroscopy can achieve observation of vibrational wavepacket motion at frequencies exceeding 3000 cm^{-1} employing few-femtosecond laser pulses.[532] The detection in transmission resolves the four-wave mixing signals which modulate the population dynamics signals with typically very small amplitudes, from the transition probability modification of coherent motion in the ground and excited state. In the pump-probe time-resolved SFX experiment the creation of ground and excited state wavepackets are

population and displacement driven, respectively, and result from the field-dipole interaction with rank of two, which is sufficient to create interstate coherence.[218,533] Their properties have been evaluated on the basis of theoretical considerations.[218] In the case of protein crystallography, which lacks the atomic and subatomic information, charge density analysis is typically not available and detection of electron density differences are primarily caused by atomic displacements. This places limits on the frequency range of nuclear coherence that can be expected to contribute to the measurements, judged from the calculation of displacements and reduced masses for harmonic frequency calculations of proteins.[526] In addition, the Huang-Rhys factors, as well as anharmonicities, must be evaluated in order to analyse their real-space displacements. Therefore, currently the explicit measurement of fingerprint modes in the ~800 – 1800 cm^{-1} frequency range, which have few pm characteristic displacements, are currently not accessible. Similarly, high frequency hydrogen stretching modes (3000 – 3500 cm^{-1}) are not accessible for reasons of small displacement and experimental bandwidth, and additionally from the small cross-section of hydrogen.

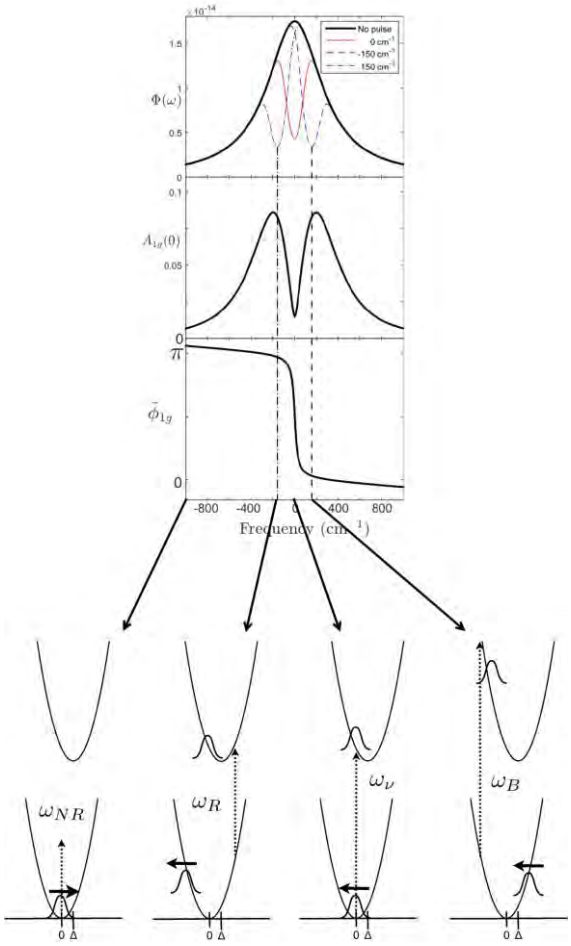


Figure 7.16: Illustration of the lineshape theory treatment of ground and excited state vibrational coherence calculation using additional wavepacket representations.
Laser excitation of a homogeneously broadened line Φ(ω) with carrier frequency below (ω_R), on (ω_ν), or above (ω_B) resonance creates a total impulsive ground state coherence A_{1g} with phase φ_{1g}. The resulting ground coherence is shown for the high temperature case (300 K).

*Figure reproduced from J.J. van Thor, Struct. Dyn. **6**, 050901 (2019) under the terms of a Creative Commons Attribution (CC-BY) License. DOI: 10.1063/1.5110685*

The Raman spectroscopy literature includes ample evidence that the study of fingerprint modes is particularly desirable for the functional analysis of protein dynamics. In contrast, current time-resolved SFX capabilities include measurements that can only be strongly dominated by low frequency modes (below few-hundred wavenumbers) which have large displacement as the result of significant associated reduced mass.[529,532] An additional reason that the frequency range is limited to low frequency modes is a physical limit to the crystallographic signal-to-noise that arises from the current sub-KHz repetition rate and source and detector capabilities. In this regime it is shown that very intense femtosecond optical excitation is a requirement, or otherwise no light induced differences will be resolved. Practically, this requires the stretching of optical pulses in the range of 100 – 200 fs. A detailed discussion of non-linear optical transformation in this regime has been presented previously.[2,218, 526,534,535]

7.4.3 Future directions

The case for development of increased experimental bandwidth and signal-to-noise is particularly compelling. Since the experimental bandwidth for pump-probe application of SFX is currently dominated by the optical pulse rather than the XFEL pulse duration, increased sensitivity of the pump-induced difference measurements will allow improvement of the time resolution. This would be achieved through increased repetition rate of a hard X-ray FEL light source, as well as the area detector frame-rate to achieve orders of magnitude improvement in data rate. In addition, the improvement

of source stability will significantly contribute. The latter includes pulse intensity, carrier frequency, spectral distribution and bandwidth stabilisation on a shot-to-shot basis. Such future capabilities will increase the ability to resolve ground and excited state coherent vibrational motion at frequencies higher than the current $\sim$300 cm^{-1} limit, by time-resolved SFX from crystallographic coordinates directly (**Figure 7.16**). The novel capabilities will significantly develop results from decades of ultrafast Raman spectroscopy methods and theory.

For ultrafast diffraction studies, a compelling case is made for precise control of XFEL pulse parameters and stability. Time-resolved crystallography studies require highly accurate determination of structure factor amplitudes and their temporal differences.[218,364,451,526] Beyond the formal limit of the time resolution in pump-probe applications, a proposal for chirped-pulse experiments has evaluated an alternative for extracting and analysing ultrafast dynamics.[536] A broadband energy-chirped hard X-ray pulse has been demonstrated at the SwissFEL with up to 4% bandwidth.[537-539] Characteristic parameters for analysing the time dependence of stationary protein diffraction with energy-chirped pulses have been reported.[536] Depending on crystal mosaic spread, convergence and recordable resolution, individual reflections are expected to spend at least ≈ 50 attoseconds and up to ≈ 8 femtoseconds in reflecting condition. The maximum theoretical time resolution achievable to be on the order of 50 – 200 as from the instantaneous bandwidth of a chirped SASE pulse. High repetition rate XFEL experiments with high flux will maximise the achievable time resolution and potentially allow an optical excitation shorter than the sweep of a chirped XFEL pulse, and coinciding within its temporal envelope, such that internal 'dark' structure factor referencing can be extracted.[536] This demonstrates very promising experimental approaches for dynamical studies using energy-chirped XFEL diffraction. Since the high resolution information is associated with the highest time resolution, small molecule experiments that allow recording of sub-atomic resolution, providing transition charge density information[218] are of particular interest, in addition to protein dynamics studies.

7.5 Capturing biological function in single molecules

If enough diffraction patterns from single particles at random orientations can be collected with a sufficient signal-to-noise ratio, then the ab initio three-dimensional electron density for the molecule can be calculated. Current theoretical calculations and experiments suggest that high repetition rate XFELs and efficient sample delivery methods will generate the > 100,000 images needed to produce approximately 3 Å resolution models. Thus, the potential for near atomic resolution of macromolecular dynamics under physiological conditions remains a driver for XFEL-based coherent diffraction imaging of single particles.

7.5.1 Introduction

Among the important science drivers for the development of the LCLS was the potential to observe structures of macromolecules from close to physiological conditions, without requiring crystals.[454] The concepts of single particle imaging (SPI) were supported by timely theoretical considerations by Hadju and Neutze *et al*.[468,540,541] However, as discussed in the sections above, SFX methods succeed "easily" because they depend upon collecting Bragg reflections from nano- to micron-size crystals; in essence a strongly diffracting sample with data originating from a strong, well-focused X-ray beam. In a way, Gati *et al.* and Tetreau *et al.* approached the SPI goal by using extremely small crystals that consist of only few thousand unit cells.[10,11] Based upon their analysis, Gati *et al.* conclude, "It should be possible, under ideal experimental conditions, to obtain data from protein crystals with only 100 unit cells in volume [and] that single-molecule imaging of individual biomolecules could almost be within reach."

These SPI efforts are complementary to fluctuation X-ray scattering (FXS), an emerging experimental technique in which X-ray solution scattering data are collected from particles in solution using XFELs.[86] Traditional synchrotron-based solution scattering methods, such as SAXS/WAXS, suffer from a very low data-to-parameter ratio because the exposure time is much longer the particle rotation rate. This produces an angularly isotropic scattering signal. In contrast, each SAXS/WAXS measurement at an XFEL is collected much faster than the particle rotational diffusion times. As a result, the signal contains authentic angular fluctuations and consequently orders of magnitude more information when extracted by calculating the angular correlations in the dataset. With brighter and faster XFEL facilities, it will be possible to collect much larger volumes of higher-quality correlation data outside the water window, thereby extending the resolution of the data, and allowing high-throughput studies on smaller biomolecules at sub-nanometre resolution.

7.5.2 The single particle imaging (SPI) initiative

Single particle imaging, in contrast to SFX, demands that one measure a weak signal from a strong beam that is further complicated or obscured by any and all other scattering structures in the beam. Experience and recent theoretical calculations demonstrate that more images of high quality are always better.[542] Moreover, newly emerging manifold-based machine learning algorithms when applied to large datasets are able to reveal the rare events and dynamic changes exercised by the sample (see **Section 3.4**).[543]

Some recent progress in SPI has exploited the high repetition rate of the European XFEL.[544-551] For example, gold nanoparticles in two morphologies and sizes (octahedra of 30 and 40 nm sizes; cubes of 42 and 17 nm sizes) were used to generate SPI datasets with more than 564,000 images to more than 1,430,000 images[552]. These were derived from "good" hits of the X-ray beam on the different high-Z particles and of sufficient quality to reproduce models to between 21 to 53 Å resolution. Sample delivery remains a critically important challenge for low-Z particles in biology, wherein aerosol injectors inspired by mass spectroscopy show promise.[553-555] Nevertheless, as the European XFEL delivers 3520 pulses per second with images collected with the AGIPD and assuming a 1% hit ratio, then scientists should anticipate more than 1.5 million images in a single 12-hour shift. Even more data will come faster at MHz XFELs with 10 – 20 kHz detectors.

The challenges have been extreme and originating from many perspectives, ranging from sample delivery all the way through to data processing. To address the challenges, an international collaboration, the SPI initiative,[556,557] formed to coordinate activities amongst groups. For SPI experiments, the typical LCLS pulse energy is about 2 - 5 mJ, which at the CXI instrument equals about 1.78 to 4.46 x 10^{12} photons/pulse at 7.0 keV, and at the AMO instrument equals 7.80 x 10^{12} to 1.95 x 10^{13} photons/pulse at 1.6 keV. To date, at the LCLS they have achieved about 6 Å resolution with hard X-rays at the CXI instrument, and about 10 Å resolution with soft X-rays at the AMO instrument. Thus, the potential to study macromolecular dynamics in near-physiological conditions, and to capture (ultrafast) biological, chemical and physical processes remains a grand challenge for XFEL facilities.

As alluded to in **Appendix 1**, cryo-EM has overtaken single particle X-ray imaging as the dominant method for macromolecular structure determination from non-crystalline, frozen hydrated samples. Nevertheless, Chapman states:[3]

> *The promise of more photons per atom recorded in a diffraction pattern than electrons per atom contributing to an electron micrograph may enable diffraction measurements of single molecules, although challenges remain.*

Some of the challenges include:

- developing methods to introduce homogenous macromolecules into the interaction region, with high and sustainable overlap between sample stream and X-ray pulses
- delivering high enough X-ray intensity in a tightly focused beam (need > 10^{14} photons μm^{-2} of 4 – 10 keV photons focused into tens of nm^{-2} size)
- eliminating background scattering, or limiting it to no more than about 100 photon counts per diffraction pattern
- delivering a stream of reproducible and uncontaminated particles (perhaps at variable delay time(s) after initiating a reaction via mixing or pump-probe strategies)
- acquiring tens of thousands to millions of patterns per dataset
- interpreting the noisy diffraction data.

In **Section 3.4** it was pointed out that the density of the data sampling must be high enough that the rarely occupied high-energy states of the system are present within the dataset. Moreover, the exposure time must be short enough to capture the various stages of these conformational changes without time averaging, scrambling or blurring. If these criteria are met, then the data techniques can in principle retrieve the structural dynamics of these critical events at high atomic and temporal resolution.

Thus, XFEL facility repetition rate and detector frame rate both impact the quality and quantity of SPI data that can be collected in a given time (**Table 7.4**). To date, the main limitation has been achieving adequate and sustainable sample hit rates. However, to realise higher resolution single particle imaging, the field needs faster detectors with lower noise such that it is easier to differentiate single scattered photons from the sample compared to those from the various sources of background noise.

Thus, a faster X-ray source does not necessarily translate into a faster detector. Indeed, a 100 kHz detector is a distant R&D objective, and yet MHz sources are available now.

Table 7.4: Main detector characteristics used at several XFEL facilities

	AMO / LCLS	CXI / LCLS	TXI / LCLS-II	SPB/SFX / Eu.XFEL	BL2 / SACLA	SwissFEL
Detector	pnCCD	CSPAD [b]	ePix10k	AGIPD [d]	MPCCD	JUNGFRAU [f]
Pixel Size (μm^{-2})	75 x 75	110 x 110	100 x 100	200 x 200	50 x 50	75 x 75
Single Photon Sensitivity	Yes	Yes	yes	yes	yes [e]	yes
Quantum Efficiency	> 80% @ 0.3~12 keV	~97% @ 8 keV	~85% @ 5 keV	> 80% @ 0.3~25 keV	~ 85% @ 5.5 keV	Up to 85% @ 12 keV
Dynamic Range	10^3 @ 2 keV	3.5 x 10^2 @ 8 keV	~ 10^4 @ 8 keV	> 10^4 @ 12.5 keV	1.2 x 10^3 @ 6 keV	>10^4 @ 12 keV
Noise (e^-)	20 / 2 [a]	300	120	265	300	100
Pulse Rate (kHz)	0.12	0.12	0.48 / 2~4 / 10~20 [c]	4500	0.06	0.1~2.4

Taken from Sun, Z.B., Fan, J.D., Li, H.Y., and Jiang, H.D. (2018) Current Status of Single Particle Imaging with X-ray Lasers, Appl Sci-Basel 8 doi: ARTN 132; 10.3390/app8010132.

[a] For pnCCD, the readout noise is 20 e^- for low gain, 2 e^- for high gain.

[b] The dynamic range and ASIC noise for CSPAD under high gain mode are 350 photons @ 8 keV and 300 e^- r.m.s. For low gain mode, they're 2700 photons @ 8 keV and 1000 e^- r.m.s.

[c] The current version is about 480 Hz. For digital domain multiplexing, the frame rate will be 2~4 kHz. For fast ADCs, the frame rate will be 10~20 kHz.

*[d] See D. Greiffenberg, J. Instrum. 2012, **7**, C0110 and A. Allahgholi, et al J. Instrum. 2015, **10**, C01023 for information.*

[e] Keeping the single photon detection capability for X-ray photon energy higher than 6 keV.

*[f] See J.H. Jungmann-Smith, et al J. Synchrotron Radiat. 2016, **23**, 385–394 for detailed information.*

7.5.3 Future directions

Significant challenges still need to be overcome, but solutions to many of these are on the horizon. The overall quality of the SPI reconstruction depends heavily upon the number of diffraction patterns in the dataset. Assuming realistic conditions for a) experimental sample delivery conditions, b) X-ray fluences in a well-focused beam at 4 – 10 keV, c) MHz repetition rate sources with at least kHz or faster detectors, then scientists anticipate collecting tens of millions of snapshots during a single productive shift. Theoretical calculations estimate that at least 66,000 to > 500,000 images are needed to generate an electron density map to about 3 Å resolution.[542]

7.6 Conclusion and summary

Ilme Schlichting said at the Royal Society in London on 29 July 2024, "In biology, the sample is the science!" Indeed, biology is a large and high-impact area at all synchrotron and XFEL facilities. About 50% of the total user community at Diamond focuses on life sciences; although they frequently rely upon highly automated data collection strategies and use a smaller overall fraction of Diamond beamlines. The number of important biological targets is staggering, as illustrated by the KEGG databases statistics listed in **Table 7.2**. Moreover, new and novel threats to human health are always emerging. For example, proteins from the COVID-19 virus were recently used for cryo-EM structures and MX-based ligand screening at the XChem facility at Diamond Light Source.[558-567] Those are prime examples of high-throughput data collection and analysis that is enabled by mature and optimised facilities.

Structure-based drug discovery and fragment-based screening are major strategies used by all pharmaceutical companies to bring new drugs to market. And yet, most new drugs fail because they lack efficacy. These strategies often rely upon ground-state crystal structures determined at 100 K. An emerging alternative, that de-risks new therapeutic avenues, is to study the whole dynamic reaction cycle, which will reveal and mediate changes that are focused upon particular function. Indeed, XChem is expanding capabilities to probe ground-state ligand complexes at room-temperature using the VMXi beamline at Diamond. These activities are currently driving the K04 flagship project at Diamond II. It is also integrated into OpenBind, a pioneering initiative creating the world's largest open-access dataset of drug–protein interactions – to accelerate the development of new treatments (https://openbind.uk/). An important next step will be to drug enzyme reaction cycles using time-resolved serial MX approaches executed at physiological temperatures, which will benefit from additional funding for R&D efforts.

To meet these challenges, there is strong consensus in the UK, and the wider life science community, that anything that can be done to improve XFEL access and training would be very useful. To these ends, there is a need in the intermediate term to widen the applications of XFELs in life sciences especially by:

- Providing stable funding for the XFEL Hub at Diamond for life science (as well as the Physical Sciences XFEL Hub at the Central Laser Facility) to help support UK research groups executing experiments granted time at international XFEL facilities. Moreover, without funding, new sample-efficient delivery and reaction initiation methods will emerge too late (or not at all) to fully leverage new capabilities under development at LSLC-II-HE, European XFEL, and/or anticipated for a next-generation XFEL. These efforts cost a small fraction of a new facility, need to happen now, and will prepare the community for new experimental capabilities.
- Making SFX and time-resolved SFX methods more accessible to smaller groups through automation in sample delivery and data processing
- Coordinating training of expertise, building capacity, and engagement with the XFEL Hub at Diamond by the UK community, to make best use of the five existing XFEL facilities
- Establishing a XFEL Doctoral Training Centre for studying biological dynamics should be a *Priority Theme* for EPSRC/BBSRC, as well as providing short-term training courses
- Increasing industry involvement – dynamics of enzymes and protein-ligand interactions will have major implications in drug discovery.

High impact life science is being generated by XFELs. The current situation has been reached after only 15 years of operation, with most of that time being restricted to a couple of low repetition rate facilities. Over the next 10 years we must anticipate further advances in capability, understanding and techniques that may open new doors to go far beyond the opportunities outlined above. The impact of a next-generation XFEL facility optimised for high repetition rate data collection would present a very significant future capability and capacity increase, that would doubtless be of substantial benefit to the UK life sciences community.

7.7 References for Chapter 7

1 M.F. Perutz, M.G. Rossmann, A.F. Cullis *et al*. "Structure of haemoglobin: a three-dimensional Fourier synthesis at 5.5-Å resolution, obtained by X-ray analysis." *Nature* **185**, 416-422 (1960) DOI: 10.1038/185416a0

2 M.F. Perutz, W. Bolton, R. Diamond *et al*. "Structure of Haemoglobin. An X-Ray Examination of Reduced Horse Haemoglobin." *Nature* **203**, 687-690 (1964)DOI: 10.1038/203687a0

3 H.N. Chapman, "X-Ray Free-Electron Lasers for the Structure and Dynamics of Macromolecules." *Annu Rev Biochem* **88**, 35-58 (2019) DOI: 10.1146/annurev-biochem-013118-110744

4 I. Schlichting, "Serial femtosecond crystallography: the first five years." *IUCrJ* **2**, 246-255 (2015) DOI: 10.1107/S205225251402702X

5 U. Bergmann, V. Yachandra and J. Yano (Eds), "X-Ray Free Electron Lasers: Applications in Materials, Chemistry and Biology." The Royal Society of Chemistry, London, UK (2017) DOI: 10.1039/9781782624097

6 P. Fromme, "XFELs open a new era in structural chemical biology." *Nat Chem Biol* **11**, 895-899 (2015) DOI: 10.1038/nchembio.1968

7 S. Boutet, P. Fromme and M.S. Hunter (Eds), "X-ray Free Electron Lasers; A Revolution in Structural Biology." 1 ed., Springer International Publishing, Springer Nature Switzerland AG (2018) DOI: 10.1007/978-3-030-00551-1

8 T.R.M. Barends, B. Stauch, V. Cherezov *et al.* "Serial femtosecond crystallography."*Nat Rev Methods Primers* **2**, 59 (2022) DOI: 10.1038/s43586-022-00141-7

9 J.C.H. Spence, "XFELs for structure and dynamics in biology." *IUCrJ* **4**, 322-339 (2017) DOI: 10.1107/S2052252517005760

10 C. Gati, D. Oberthuer, O. Yefanov *et al*."Atomic structure of granulin determined from native nanocrystalline granulovirus using an X-ray free-electron laser." *Proc Natl Acad Sci U S A* **114**, 2247-2252 (2017) DOI: 10.1073/pnas.1609243114

11 G. Tetreau, A. Banneville, E.A. Andreeva *et al*. "Serial femtosecond crystallography on in vivo-grown crystals drives elucidation of mosquitocidal Cyt1Aa bioactivation cascade." *Nat Commun* **11**, 1153 (2020) DOI: 10.1038/s41467-020-14894-w

12 A. Barnosky, N. Matzke, S. Tomiya *et al.* "Has the Earth's sixth mass extinction already arrived?." *Nature* **471**, 51-57 (2011) DOI: 10.1038/nature09678

13 C.P. McKay, "Requirements and limits for life in the context of exoplanets." *Proc Natl Acad Sci U S A* **111**, 12628-12633 (2014) DOI: 10.1073/pnas.1304212111

14 Battelle, "The Impact of Genomics on the U.S. Economy." Battelle Memorial Institute (2013) http://unitedformedicalresearch.org/wp-content/uploads/2013/06/The-Impact-of-Genomics-on-the-US-Economy.pdf, access date 26 Feb 2020

15 M. Wadman, "Economic return from Human Genome Project grows." *Nature* (2013) DOI: 10.1038/nature.2013.13187

16 B. Methé, K. Nelson, M. Pop *et al.* "A framework for human microbiome research." *Nature* **486**, 215-221 (2012) DOI: 10.1038/nature11209

17 J.A. Gilbert and S.V. Lynch, "Community ecology as a framework for human microbiome research." *Nat Med* **25**, 884-889 (2019) DOI: 10.1038/s41591-019-0464-9

18 H.A. Lewin, G.E. Robinson, W.J. Kress *et al*. "Earth BioGenome Project: Sequencing life for the future of life." *Proc Natl Acad Sci U S A* **115**, 4325-4333 (2018) DOI: 10.1073/pnas.1720115115

19 J.A. Gilbert, J. K. Jansson and R. Knight, "The Earth Microbiome project: successes and aspirations." *BMC Biol* **12**, 69 (2014) DOI: 10.1186/s12915-014-0069-1

20 J. Du, Z. Yuan, Z. Ma, J. Song, X. Xie and Y. Chen, "KEGG-PATH: Kyoto encyclopedia of genes and genomes-based pathway analysis using a path analysis model." *Mol Biosyst* **10**, 2441-2447 (2014) DOI: 10.1039/c4mb00287c

21 E. Altermann and T.R. Klaenhammer, "PathwayVoyager: pathway mapping using the Kyoto Encyclopedia of Genes and Genomes (KEGG) database." *BMC Genomics* **6**, 60 (2005) DOI: 10.1186/1471-2164-6-60

22 M. Kanehisa and S. Goto, "KEGG: Kyoto Encyclopedia of Genes and Genomes." *Nucleic Acids Res* **28**, 27-30 (2000) DOI: 10.1093/nar/28.1.27

23 M. Kanehisa, Y. Sato, M. Furumichi, K. Morishima and M. Tanabe, "New approach for understanding genome variations in KEGG." *Nucleic Acids Res* **47**, D590-D595 (2019) DOI: 10.1093/nar/gky962

24 M. Kanehisa, M. Furumichi, Y. Sato, Y. Matsuura, and M. Ishiguro-Watanabe, "KEGG: biological systems database as a model of the real world." *Nucleic Acids Res* **53**, D672-D677 (2025) DOI: 10.1093/nar/gkae909

25 M. Roser, "Future Population Growth" (2020) https://ourworldindata.org/future-population-growth, access date 26 Feb 2020

26 R.L. Owen, J. Juanhuix and M. Fuchs, "Current advances in synchrotron radiation instrumentation for MX experiments." *Arch Biochem Biophys* **602**, 21-31 (2016) DOI: 10.1016/j.abb.2016.03.021

27 J.M. Grimes, D.R. Hall, A.W. Ashton *et al*. "Where is crystallography going?." *Acta Crystallogr D Struct Biol* **74**, 152-166 (2018) DOI: 10.1107/S2059798317016709

[28] S.M. Gruner and E.E. Lattman, "Biostructural Science Inspired by Next-Generation X-Ray Sources." *Annu Rev Biophys* **44**, 33-51 (2015) DOI: 10.1146/annurev-biophys-060414-033813

[29] "Method of the Year 2015." *Nature Methods* **13**, 1 (2016) DOI: 10.1038/nmeth.3730

[30] R. Fernandez-Leiro and S.H. Scheres, "Unravelling biological macromolecules with cryo-electron microscopy." *Nature* **537**, 339-346 (2016) DOI: 10.1038/nature19948

[31] D. Elmlund and H. Elmlund, "Cryogenic electron microscopy and single-particle analysis." *Annu Rev Biochem* **84**, 499-517 (2015) DOI: 10.1146/annurev-biochem-060614-034226

[32] Y. Cheng, N. Grigorieff, P.A. Penczek and Walz, T. "A primer to single-particle cryo-electron microscopy." *Cell 161*, 438-449 (2015) DOI: 10.1016/j.cell.2015.03.050

[33] P.S. Shen, "The 2017 Nobel Prize in Chemistry: cryo-EM comes of age." *Anal Bioanal Chem* **410**, 2053-2057(2018) DOI: 10.1007/s00216-018-0899-8

[34] S. Subramaniam, "The cryo-EM revolution: fueling the next phase." *IUCrJ* **6**, 1-2 (2019) DOI: 10.1107/S2052252519000277

[35] R.M. Glaeser, "How Good Can Single-Particle Cryo-EM Become? What Remains Before It Approaches Its Physical Limits?." *Annu Rev Biophys* **48**, 45-61 (2019) DOI: 10.1146/annurev-biophys-070317-032828

[36] A. Patwardhan *et al*. "Extending the reach of single-particle cryoEM." *Current Opinion in Structural Biology* **92**, 103005 (2025) DOI: 10.1016/j.sbi.2025.103005

[37] H. Berman, K. Henrick and H. Nakamura, "Announcing the worldwide Protein Data Bank." *Nat Struct Biol* **10**, 980 (2003) DOI: 10.1038/nsb1203-980

[38] wwPDB Consortium, "Protein Data Bank: the single global archive for 3D macromolecular structure data." *Nucleic Acids Res* **47**, D520-D528 (2019) DOI: 10.1093/nar/gky949

[39] M. Baek *et al.* "Accurate prediction of protein structures and interactions using a three-track neural network." *Science* **373**, 871-876 (2021) DOI: 10.1126/science.abj8754

[40] S.L. Lovelock *et al.* "The road to fully programmable protein catalysis." *Nature* **606**, 49-58 (2022) DOI: 10.1038/s41586-022-04456-z

[41] M. Varadi *et al.* "AlphaFold Protein Structure Database: massively expanding the structural coverage of protein-sequence space with high-accuracy models." *Nucleic Acids Res* **50**, D439-D444 (2022) DOI: 10.1093/nar/gkab1061

[42] J. Jumper and D. Hassabis, "Protein structure predictions to atomic accuracy with AlphaFold." *Nat Methods* **19**, 11-12 (2022) DOI: 10.1038/s41592-021-01362-6

[43] K. Tunyasuvunakool *et al.* "Highly accurate protein structure prediction for the human proteome." *Nature* **596**, 590-596 (2021) DOI: 10.1038/s41586-021-03828-1

[44] J. Jumper *et al.* "Highly accurate protein structure prediction with AlphaFold." *Nature* **596**, 583-589 (2021) DOI: 10.1038/s41586-021-03819-2

[45] M. Varadi *et al.* "AlphaFold Protein Structure Database in 2024: providing structure coverage for over 214 million protein sequences." *Nucleic Acids Res* **52**, D368-D375 (2024) DOI: 10.1093/nar/gkad1011

[46] T.C. Terwilliger, D. Liebschner, T.I. Croll *et al.* "AlphaFold predictions are valuable hypotheses and accelerate but do not replace experimental structure determination." *Nat Methods* **21**, 110–116 (2024) DOI: 10.1038/s41592-023-02087-4

[47] A.J. McCoy, M.D. Sammito and R.J. Read, "Implications of AlphaFold2 for crystallographic phasing by molecular replacement." *Acta Crystallogr D Struct Biol* **78**, 1-13 (2022) DOI: 10.1107/S2059798321012122

[48] W. Wang, Z. Gong and W.A. Hendrickson, "AlphaFold-guided molecular replacement for solving challenging crystal structures." *Acta Crystallogr D Struct Biol* **81**, 4-21 (2025) DOI: 10.1107/S2059798324011999

[49] X. Dai *et al*. "predicting metal-binding proteins and structures through integration of evolutionary-scale and physics-based modeling." *J Mol Biol* **437**, 168962 (2025) DOI: 10.1016/j.jmb.2025.168962

[50] X. Lin, Z. Su, Y.L. Liu *et al.* "SuperMetal: a generative AI framework for rapid and precise metal ion location prediction in proteins." *J Cheminform* **17**, 107 (2025) DOI: 10.1186/s13321-025-01038-9

[51] D.P. Kiouri *et al*. "Structure-based approaches for protein-protein interaction prediction using machine learning and deep learning." *Biomolecules* **15** (2025) DOI: 10.3390/biom15010141

[52] F. Offensperger *et al.* "Large-scale chemoproteomics expedites ligand discovery and predicts ligand behavior in cells." *Science* **384**, eadk5864 (2024) DOI: 10.1126/science.adk5864

[53] T.F. Huddy, Y. Hsia, R.D. Kibler *et al.* "Blueprinting extendable nanomaterials with standardized protein blocks." *Nature* **627**, 898-904 (2024) DOI: 10.1038/s41586-024-07188-4

[54] S.L. Lovelock, R. Crawshaw, S. Basler *et al.* "The road to fully programmable protein catalysis." *Nature* **606**, 49-58 (2022) DOI: 10.1038/s41586-022-04456-z

[55] J. Abramson, J. Adler, J. Dunger *et al.* "Accurate structure prediction of biomolecular interactions with AlphaFold 3." *Nature* **630**, 493-500 (2024) DOI: 10.1038/s41586-024-07487-w

[56] Hekkelman, M. L., de Vries, I., Joosten, R. P. & Perrakis, A. "AlphaFill: enriching AlphaFold models with ligands and cofactors." *Nat Methods* **20**, 205-213, doi:10.1038/s41592-022-01685-y (2023).

[57] A.E. Paton, D.A. Boiko, J.C. Perkins *et al.* "Connecting chemical and protein sequence space to predict biocatalytic reactions." *Nature* **646**, 108-116 (2025) DOI: 10.1038/s41586-025-09519-5

[58] H.M. Berman, G.J. Kleywegt, H. Nakamura and J.L. Markley, "The Protein Data Bank at 40: reflecting on the past to prepare for the future." *Structure* **20**, 391-396 (2012) DOI: 10.1016/j.str.2012.01.010

[59] K.P. Sullivan, P. Brennan-Tonetta and L.J. Marxen, "Economic Impacts of the Research Collaboratory for Structural Bioinformatics (RCSB) Protein Data Bank." Office of Research Analytics, Rutgers New Jersey Agricultural Experiment Station, New Brunswick, NJ (2017) https://cdn.rcsb.org/rcsb-pdb/general_information/about_pdb/Economic%20Impacts%20of%20the%20PDB.pdf, access date 06 October 2018; DOI: 10.2210/rcsb_pdb/pdb-econ-imp-2017

[60] C. Markosian, L. Di Costanzo, M. Sekharan *et al*. "Analysis of impact metrics for the Protein Data Bank." *Sci Data* **5**, 180212 (2018) DOI: 10.1038/sdata.2018.212

[61] D.S. Goodsell, C. Zardecki, L. Di Costanzo *et al*. "RCSB Protein Data Bank: Enabling biomedical research and drug discovery." *Protein Sci* **29**, 52-65 (2020) DOI: 10.1002/pro.3730

[62] C. Zardecki, J. Westbrook and S.K. Burley, "PDB Structure Data Impacted Discovery and Development of Recently FDA-Approved Drugs." *The FASEB Journal* **33**:1_supplement, 779.53-779.53 (2019) DOI: 10.1096/fasebj.2019.33.1_supplement.779.53

[63] J.D. Westbrook and S.K. Burley, "How Structural Biologists and the Protein Data Bank Contributed to Recent FDA New Drug Approvals." *Structure* **27**, 211-217 (2019) DOI: 10.1016/j.str.2018.11.007

[64] J.D. Westbrook, R. Soskind, B.P. Hudson and S.K. Burley, "Impact of the Protein Data Bank on antineoplastic approvals." *Drug Discov Today* S1359-6446(20)30070-2 (2020) DOI: 10.1016/j.drudis.2020.02.002

[65] S.K. Burley, "Protein data bank: From two epidemics to the global pandemic to mRNA vaccines and Paxlovid." *Curr Opin Struct Biol* **90**, 102954 (2025) DOI: 10.1016/j.sbi.2024.102954

[66] S.K. Burley, A. Wu-Wu, S. Dutta *et al*. "Impact of structural biology and the protein data bank on us fda new drug approvals of low molecular weight antineoplastic agents 2019-2023." *Oncogene* **43**, 2229-2243 (2024) DOI: 10.1038/s41388-024-03077-2

[67] B.L. Nannenga and T. Gonen, "MicroED opens a new era for biological structure determination." *Curr Opin Struct Biol* **40**, 128-135 (2016) DOI: 10.1016/j.sbi.2016.09.007

[68] R. Bücker, P. Hogan-Lamarre, P. Mehrabi *et al*. "Serial protein crystallography in an electron microscope." *Nat Commun* **11**, 996 (2020) DOI: 10.1038/s41467-020-14793-0

[69] H. Xu, H. Lebrette, M.T. Clabbers *et al*. "Solving a new R2lox protein structure by microcrystal electron diffraction." *Sci Adv* **5**, eaax4621 (2019) DOI: 10.1126/sciadv.aax4621

[70] K.P. Khakurel, B. Angelov and J. Andreasson, "Macromolecular Nanocrystal Structural Analysis with Electron and X-Rays: A Comparative Review." *Molecules* **24**(19):3490 (2019) DOI: 10.3390/molecules24193490

[71] A.M. Wolff, I.D. Young, R.G. Sierra *et al*. "Comparing serial X-ray crystallography and microcrystal electron diffraction (MicroED) as methods for routine structure determination from small macromolecular crystals." *IUCrJ* **7**, 306-323 (2020) DOI: 10.1107/S205225252000072X

[72] M. Martynowycz, W. Zhao, J. Hattne, G.J. Jensen and T. Gonen, "Qualitative Analyses of Polishing and Precoating FIB Milled Crystals for MicroED." *Structure* **27**, 1594-1600 (2019) e1592 DOI: 10.1016/j.str.2019.07.004

[73] B.L. Nannenga, "MicroED methodology and development." *Struct Dyn* **7**, 014304 (2020) DOI: 10.1063/1.5128226

[74] J.R. Helliwell, "Fundamentals of neutron crystallography in structural biology." *Methods Enzymol* **634**, 1-19 (2020) DOI: 10.1016/bs.mie.2020.01.006

[75] G.C. Schröder, W.B. O'Dell, D.A.A. Myles, A. Kovalevsky and F. Meilleur, "IMAGINE: neutrons reveal enzyme chemistry." *Acta Crystallogr D Struct Biol* **74**, 778-786 (2018) DOI: 10.1107/S2059798318001626

[76] E. Mahieu and F. Gabel, "Biological small-angle neutron scattering: recent results and development." *Acta Crystallogr D Struct Biol* **74**, 715-726 (2018) DOI: 10.1107/S2059798318005016

[77] H. Kwon, P.S. Langan, L. Coates, E.L. Raven and P.C.E. Moody, "The rise of neutron cryo-crystallography." *Acta Crystallogr D Struct Biol* **74**, 792-799 (2018) DOI: 10.1107/S205979831800640X

[78] J. Yang, I. Anishchenko, H. Park, Z. Peng, S, Ovchinnikov and D. Baker, "Improved protein structure prediction using predicted interresidue orientations." *Proc Natl Acad Sci U S A* **117**(3): 1496-1503 (2020) DOI: 10.1073/pnas.1914677117

[79] S. Ovchinnikov, H. Park, D.E. Kim, F. DiMaio and D. Baker, "Protein structure prediction using Rosetta in CASP12." *Proteins* **86**: 113-121 (2018) DOI: 10.1002/prot.25390

[80] H. Deng, Y. Jia and Y. Zhang, "Protein structure prediction." *Int J Mod Phys B* **32**(18):1840009 (2018) DOI: 10.1142/S021797921840009X

[81] D. Baker and A. Sali, "Protein structure prediction and structural genomics." *Science* **294**, 93-96 (2001) DOI: 10.1126/science.1065659

[82] M. Levantino, B.A. Yorke, D.C. Monteiro, M. Cammarata and A.R. Pearson, "Using synchrotrons and XFELs for time-resolved X-ray crystallography and solution scattering experiments on

biomolecules." *Curr Opin Struct Biol* **35**, 41-48 (2015) DOI: 10.1016/j.sbi.2015.07.017

83 S.P. Meisburger, W.C. Thomas, M.B. Watkins and N. Ando, "X-ray Scattering Studies of Protein Structural Dynamics." *Chem Rev* **117**(12): 7615-7672 (2017) DOI: 10.1021/acs.chemrev.6b00790

84 M. Cammarata, M. Levantino, F. Schotte *et al*. "Tracking the structural dynamics of proteins in solution using time-resolved wide-angle X-ray scattering." *Nat Methods* **5**, 881-886 (2008) DOI: 10.1038/nmeth.1255 https://www.nature.com/articles/nmeth.1255#supplementary-information

85 K. Pande, J.J. Donatelli, E. Malmerberg *et al*. "Free-electron laser data for multiple-particle fluctuation scattering analysis." *Sci Data* **5**, 180201 (2018) DOI: 10.1038/sdata.2018.201

86 K. Pande, J.J. Donatelli, E. Malmerberg *et al*. "Ab initio structure determination from experimental fluctuation X-ray scattering data." *Proc Natl Acad Sci U S A* **115**, 11772-11777 (2018) DOI: 10.1073/pnas.1812064115

87 "Method of the Year 2008." *Nat Methods* **6**, 1 (2009) DOI: 10.1038/nmeth.f.244

88 "Method of the Year 2010." *Nat Methods* **8**, 1 (2011) DOI: 10.1038/nmeth.f.321

89 K. Deisseroth, "Optogenetics." *Nat Methods* **8**, 26-29 (2011) DOI: 10.1038/nmeth.f.324

90 "Method of the Year 2013." *Nat Methods* **11**, 1 (2014) DOI: 10.1038/nmeth.2801

91 "Method of the Year 2019: Single-cell multimodal omics." *Nat Methods* **17**, 1 (2020) DOI: 10.1038/s41592-019-0703-5

92 R. Strack, "Structures in situ." *Nat Methods* **17**, 21 (2020) DOI: 10.1038/s41592-019-0704-4

93 M. Schaffer, S. Pfeffer, J. Mahamid *et al*. "A cryo-FIB lift-out technique enables molecular-resolution cryo-ET within native Caenorhabditis elegans tissue." *Nat Methods* **16**, 757-762 (2019) DOI: 10.1038/s41592-019-0497-5

94 F.K. Schur, "Toward high-resolution in situ structural biology with cryo-electron tomography and subtomogram averaging." *Curr Opin Struct Biol* **58**, 1-9 (2019) DOI: 10.1016/j.sbi.2019.03.018

95 M. Du and C. Jacobsen, "Relative merits and limiting factors for x-ray and electron microscopy of thick, hydrated organic materials." *Ultramicroscopy* **184**, 293-309 (2018) DOI: 10.1016/j.ultramic.2017.10.003

96 S.D. Rawson, J. Maksimcuka, P.J. Withers and S.H. Cartmell, "X-ray computed tomography in life sciences." *BMC Biol* **18**(1):21 (2020) DOI: 10.1186/s12915-020-0753-2

97 S. Sala, V.S.C. Kuppili, S. Chalkidis, D.J. Batey, X. Shi, C. Rau and P. Thibault, "Multiscale X-ray imaging using ptychography." *J Synchrotron Radiat* **25**, 1214-1221 (2018) DOI: 10.1107/S1600577518007221

98 M. Do, S.A. Isaacson, G. McDermott, M.A. Le Gros and C.A. Larabell, "Imaging and characterizing cells using tomography." *Arch Biochem Biophys* **581**, 111-121 (2015) DOI: 10.1016/j.abb.2015.01.011

99 J. Guo and C.A. Larabell, "Soft X-ray tomography: virtual sculptures from cell cultures." *Curr Opin Struct Biol* **58**, 324-332 (2019) DOI: 10.1016/j.sbi.2019.06.012

100 A.A. Ekman, J.H. Chen, J. Guo *et al*. "Mesoscale imaging with cryo-light and X-rays: Larger than molecular machines, smaller than a cell." *Biol Cell* **109**, 24-38 (2017) DOI: 10.1111/boc.201600044

101 J.S. Hawe, F.J. Theis and M. Heinig, "Inferring Interaction Networks From Multi-Omics Data." *Front Genet* **10**, 535 (2019) DOI: 10.3389/fgene.2019.00535

102 Moffat, K. & Lattman, E. E. *Dynamics and Kinetics in Structural Biology: Unravelling Function Through Time-Resolved Structural Analysis*. (Wiley, 2023).

103 H.M. Berman, S.K. Burley, G.J. Kleywegt, J.L. Markley, H. Nakamura and S. Velankar, "The archiving and dissemination of biological structure data." *Curr Opin Struct Biol* **40**, 17-22 (2016) DOI: 10.1016/j.sbi.2016.06.018

104 R.R. Breaker, "Riboswitches and Translation Control." *Cold Spring Harb Perspect Biol* **10**(11):a032797 (2018) DOI: 10.1101/cshperspect.a032797

105 R.R. Breaker, "Riboswitches and the RNA world." *Cold Spring Harb Perspect Biol* **4**(2):a003566 (2012) DOI: 10.1101/cshperspect.a003566

106 Y.R. Bhandari, L. Fan, X. Fang *et al*. Topological Structure Determination of RNA Using Small-Angle X-Ray Scattering, *J Mol Biol* **429**(23):3635-3649 (2017) DOI: 10.1016/j.jmb.2017.09.006

107 J. Stagno, Y. Liu, Y. Bhandari *et al*. Structures of riboswitch RNA reaction states by mix-and-inject XFEL serial crystallography, *Nature* **541**, 242-246 (2017) DOI: 10.1038/nature20599

108 J.R. Stagno, Y. R. Bhandari, C.E. Conrad, Y. Liu and Y.X. Wang, "Real-time crystallographic studies of the adenine riboswitch using an X-ray free-electron laser." *FEBS J* **284**(20): 3374-3380 (2017) DOI: 10.1111/febs.14110

109 R. Henderson, "The potential and limitations of neutrons, electrons and X-rays for atomic resolution microscopy of unstained biological molecules." *Q Rev Biophys* **28**, 171-193 (1995) DOI: 10.1017/s003358350000305x

110 R. Henderson, "Cryoprotection of Protein Crystals against Radiation-Damage in Electron and X-Ray-Diffraction." *P Roy Soc B-Biol Sci* **241**, 6-8 (1990) DOI: 10.1098/rspb.1990.0057

111 E. de la Mora, N. Coquelle, C.S. Bury *et al*. "Radiation damage and dose limits in serial synchrotron crystallography at cryo- and room temperatures." *Proc Natl Acad Sci U S A* **117**(8): 4142-4151 (2020) DOI: 10.1073/pnas.1821522117

[112] C.S. Bury, J.C. Brooks-Bartlett, S.P. Walsh and E.F. Garman, "Estimate your dose: RADDOSE-3D." *Protein Sci* **27**, 217-228 (2018) DOI: 10.1002/pro.3302

[113] E.F. Garman and M. Weik, "Radiation Damage in Macromolecular Crystallography." In: A. Wlodawer, Z. Dauter, M. Jaskolski (eds) *Protein Crystallography. Methods in Molecular Biology,* **1607**, 467-489 (2017). Humana Press, New York, NY. DOI: 10.1007/978-1-4939-7000-1_20

[114] O.B. Zeldin, S. Brockhauser, J. Bremridge, J.M. Holton and E.F. Garman, "Predicting the X-ray lifetime of protein crystals." *Proc Natl Acad Sci U S A* **110**, 20551-20556 (2013) DOI: 10.1073/pnas.1315879110

[115] J.M. Holton and K.A. Frankel, "The minimum crystal size needed for a complete diffraction data set." *Acta Cryst.* D**66**, 393-408 (2010) DOI: 10.1107/S0907444910007262

[116] J.M. Holton, "A beginner's guide to radiation damage." *J Synchrotron Radiat* **16**, 133-142 (2009) DOI: 10.1107/S0909049509004361

[117] R.L. Shoeman, E. Hartmann and I. Schlichting, "Growing and making nano- and microcrystals." *Nat Protoc* **18**, 854-882 (2023) DOI: 10.1038/s41596-022-00777-5

[118] C.J. Tremlett *et al.* "Small but mighty: the power of microcrystals in structural biology." *IUCrJ* **12**, 262-279 (2025) DOI: 10.1107/S2052252525001484

[119] D. Li and M. Caffrey, "Structure and Functional Characterization of Membrane Integral Proteins in the Lipid Cubic Phase." *J Mol Biol* (2020) DOI: 10.1016/j.jmb.2020.02.024

[120] Q. Zhang and V. Cherezov, "Chemical tools for membrane protein structural biology." *Curr Opin Struct Biol* **58**, 278-285 (2019) DOI: 10.1016/j.sbi.2019.06.002

[121] A. Mishin, A. Gusach, A. Luginina, E. Marin, V. Borshchevskiy and V. Cherezov, "An outlook on using serial femtosecond crystallography in drug discovery." *Expert Opin Drug Dis* **14**:9, 933-945 (2019) DOI: 10.1080/17460441.2019.1626822

[122] R. Neutze, G. Branden and G.F. Schertler, "Membrane protein structural biology using X-ray free electron lasers." *Curr Opin Struct Biol* **33**, 115-125 (2015) DOI: 10.1016/j.sbi.2015.08.006

[123] U. Weierstall, D. James, C. Wang *et al*. "Lipidic cubic phase injector facilitates membrane protein serial femtosecond crystallography." *Nat Commun* **5**, 3309 (2014) DOI: 10.1038/ncomms4309

[124] M. Caffrey, "A comprehensive review of the lipid cubic phase or in meso method for crystallizing membrane and soluble proteins and complexes." *Acta Cryst.* F**71**, 3-18 (2015) DOI: 10.1107/S2053230X14026843

[125] A. Banari, A.K. Samanta, A. Munke *et al.* "Advancing time-resolved structural biology: latest strategies in cryo-EM and X-ray crystallography." *Nat Methods* **22**, 1420–1435 (2025) DOI: 10.1038/s41592-025-02659-6

[126] Schulz, E. C. *et al.* 'Probing the modulation of enzyme kinetics by multi-temperature, time-resolved serial crystallography." *Nat Commun* **16**, 6553, (2025) DOI:10.1038/s41467-025-61631-2.

[127] Khusainov, G., Standfuss, J. & Weinert, T. "The time revolution in macromolecular crystallography." *Structural Dynamics* **11**, (2024) DOI:10.1063/4.0000247.

[128] J. Stubbs *et al.* "Droplet microfluidics for time-resolved serial crystallography." *IUCrJ* **11**, 237-248 (2024) DOI: 10.1107/S2052252524001799

[129] S. Boutet, L. Lomb, G.J. Williams *et al*. High-resolution protein structure determination by serial femtosecond crystallography, *Science* **337**(6092): 362-364 (2012) DOI: 10.1126/science.1217737

[130] H.N. Chapman, P. Fromme, A. Barty, *et al*. "Femtosecond X-ray protein nanocrystallography." *Nature* **470**, 73-77 (2011) DOI: 10.1038/nature09750

[131] C. Stan, D. Milathianaki, H. Laksmono *et al*. "Liquid explosions induced by X-ray laser pulses." *Nature Phys* **12**, 966-971 (2016) DOI: 10.1038/nphys3779

[132] D. Kim, A. Echelmeier, J. Cruz Villarreal *et al*. "Electric Triggering for Enhanced Control of Droplet Generation." *Anal Chem* **91**(15): 9792-9799 (2019) DOI: 10.1021/acs.analchem.9b01449

[133] J. Knoska, L. Adriano, S. Awel *et al*. "Ultracompact 3D microfluidics for time-resolved structural biology." *Nat Commun* **11**, 657 (2020) DOI: 10.1038/s41467-020-14434

[134] D. Oberthuer, J. Knoška, M. Wiedorn *et al*. "Double-flow focused liquid injector for efficient serial femtosecond crystallography." *Sci Rep* **7**, 44628 (2017) DOI: 10.1038/srep44628

[135] P. Nogly, V. Panneels, G. Nelson *et al*. "Lipidic cubic phase injector is a viable crystal delivery system for time-resolved serial crystallography." *Nat Commun* **7**, 12314 (2016) DOI: 10.1038/ncomms12314

[136] D.P. DePonte *et al*. "Gas dynamic virtual nozzle for generation of microscopic droplet streams." *J. Phys. D: Appl. Phys.* **41** 195505 (2008) DOI: 10.1088/0022-3727/41/19/195505

[137] G. Kovácsová, M.L. Grünbein, M. Kloos *et al*. "Viscous hydrophilic injection matrices for serial crystallography." *IUCrJ* **4**, 400-410 (2017) DOI: 10.1107/S2052252517005140

[138] C.E. Conrad, S. Basu, D. James *et al*. "A novel inert crystal delivery medium for serial femtosecond crystallography." *IUCrJ* **2**, 421-430 (2015) DOI: 10.1107/S2052252515009811

[139] R.G. Sierra, C. Gati, H. Laksmono *et al*. "Concentric-flow electrokinetic injector enables serial crystallography of ribosome and photosystem II." *Nat Methods* **13**, 59-62 (2016) DOI: 10.1038/nmeth.3667

[140] E.H. Dao, F. Poitevin, R.G. Sierra *et al*. "Structure of the 30S ribosomal decoding complex at ambient

temperature." *RNA* **24**, 1667-1676 (2018) DOI: 10.1261/rna.067660.118

141 J. Kern, R. Chatterjee, I.D. Young *et al*. "Structures of the intermediates of Kok's photosynthetic water oxidation clock." *Nature* **563**, 421-425 (2018) DOI: 10.1038/s41586-018-0681-2

142 A.M. Orville, CHAPTER 18 "Acoustic Methods for On-demand Sample Injection into XFEL Beams." In *X-Ray Free Electron Lasers: Applications in Materials, Chemistry and Biology*, pp 348-364, (2017) The Royal Society of Chemistry. DOI: 10.1039/9781782624097-00348

143 F.D. Fuller, S. Gul, R. Chatterjee *et al*. "Drop-on-demand sample delivery for studying biocatalysts in action at X-ray free-electron lasers." *Nat Methods* **14**, 443-449 (2017) DOI: 10.1038/nmeth.4195

144 C.G. Roessler, R. Agarwal, M. Allaire *et al*. "Acoustic Injectors for Drop-On-Demand Serial Femtosecond Crystallography." *Structure* **24**, 631-640 (2016) DOI: 10.1016/j.str.2016.02.007

145 A.S. Soares, M.A. Engel, R. Stearns *et al*. "Acoustically mounted microcrystals yield high-resolution X-ray structures." *Biochemistry* **50**, 4399-4401 (2011) DOI: 10.1021/bi200549x

146 B. Davy, D. Axford, J.H. Beale *et al*, "Reducing sample consumption for serial crystallography using acoustic drop ejection." *J Synchrotron Radiat.* **26**, 1820-1825 (2019) DOI: 10.1107/S1600577519009329

147 P. Wu, C. Noland, M. Ultsch *et al*. "Developments in the Implementation of Acoustic Droplet Ejection for Protein Crystallography." *J Lab Autom* **21**, 97-106 (2016) DOI: 10.1177/2211068215598938

148 F. Mafuné, K. Miyajima, K. Tono *et al*. "Microcrystal delivery by pulsed liquid droplet for serial femtosecond crystallography." *Acta Crystallogr D Struct Biol* **72**, 520-523 (2016) DOI: 10.1107/S2059798316001480

149 B. Hadimioglu, R. Stearns and R. Ellson, "Moving Liquids with Sound: The Physics of Acoustic Droplet Ejection for Robust Laboratory Automation in Life Sciences." *J Lab Autom* **21**, 4-18 (2016) DOI: 10.1177/2211068215615096

150 S. Perrett *et al.* "Kilohertz droplet-on-demand serial femtosecond crystallography at the European XFEL station FXE." *Struct Dyn* **11**, 024310 (2024) DOI: 10.1063/4.0000248

151 M.S. Hunter, B. Segelke, M. Messerschmidt *et al*. "Fixed-target protein serial microcrystallography with an x-ray free electron laser." *Sci Rep* **4**, 6026 (2014) DOI: 10.1038/srep06026

152 R.B. Doak, G.N. Kovacs, A. Gorel *et al*. "Crystallography on a chip - without the chip: sheet-on-sheet sandwich." *Acta Crystallogr D Struct Biol.* **74**, 1000-1007 (2018) DOI: 10.1107/S2059798318011634

153 S. Oghbaey, A. Sarracini, H.M. Ginn *et al*. "Fixed target combined with spectral mapping: approaching 100% hit rates for serial crystallography." *Acta Crystallogr D Struct Biol* **72**, 944-955 (2016) DOI: 10.1107/S2059798316010834

154 D.A. Sherrell, A.J. Foster, L. Hudson *et al*. "A modular and compact portable mini-endstation for high-precision, high-speed fixed target serial crystallography at FEL and synchrotron sources." *J Synchrotron Radiat* **22**, 1372-1378 (2015) DOI: 10.1107/S1600577515016938

155 C. MuellerA. Marx, S.W. Epp *et al*. "Fixed target matrix for femtosecond time-resolved and in situ serial micro-crystallography." *Struct Dyn* **2**, 054302 (2015) DOI: 10.1063/1.4928706

156 P. Aller, J. Sanchez-Weatherby, J. Foadi *et al*. "Application of in situ diffraction in high-throughput structure determination platforms." *Methods Mol Biol* **1261**, 233-253 (2015) DOI: 10.1007/978-1-4939-2230-7_13

157 J. Lieske, M. Cerv, S. Kreida *et al*. "On-chip crystallization for serial crystallography experiments and on-chip ligand-binding studies." *IUCrJ* **6**, 714-728 (2019) DOI: 10.1107/S2052252519007395

158 P. Roedig, H.M. Ginn, T. Pakendorf *et al*. "High-speed fixed-target serial virus crystallography." *Nat Methods* **14**, 805-810 (2017) DOI: 10.1038/nmeth.4335

159 P. Roedig, R. Duman, J. Sanchez-Weatherby *et al*. "Room-temperature macromolecular crystallography using a micro-patterned silicon chip with minimal background scattering." *J Appl Crystallogr* **49**, 968-975 (2016) DOI: 10.1107/S1600576716006348

160 P. Roedig, I. Vartiainen, R. Duman *et al*. "A micro-patterned silicon chip as sample holder for macromolecular crystallography experiments with minimal background scattering." *Sci Rep* **5**, 10451 (2015) DOI: 10.1038/srep10451

161 R.B. Doak *et al.* "Sheet-on-sheet fixed target data collection devices for serial crystallography at synchrotron and XFEL sources." *Journal of Applied Crystallography* **57**, 6 1725-1732 (2024) DOI: 10.1107/S1600576724008914

162 R. Bosman *et al.* "A systematic comparison of Kapton-based HARE chips for fixed-target serial crystallography." *Cell Reports Physical Science* **5**, 101987 (2024) DOI: 10.1016/j.xcrp.2024.101987

163 G. Gotthard *et al.* "Fixed-target pump-probe SFX: eliminating the scourge of light contamination." *IUCrJ* **11**, 749-761 (2024) DOI: 10.1107/S2052252524005591

164 R.L. Owen *et al*. "A standard descriptor for fixed-target serial crystallography." *Acta Crystallogr D Struct Biol* **79**, 668-672 (2023) DOI: 10.1107/S2059798323005429

165 M.L. Shelby, D. Gilbile, T.D. Grant *et al*. "A fixed-target platform for serial femtosecond crystallography in a hydrated environment." *IUCrJ* **7**, 30-41 (2020) DOI: 10.1107/S2052252519014003

166 G. Chreifi, E.L. Baxter, T. Doukov *et al*. "Crystal structure of the pristine peroxidase ferryl center

and its relevance to proton-coupled electron transfer." *Proc Natl Acad Sci U S A* **113**, 1226-1231 (2016) DOI: 10.1073/pnas.1521664113

167 E.L. Baxter, L. Aguila, R. Alonso-Mori *et al*. "High-density grids for efficient data collection from multiple crystals." *Acta Crystallogr D Struct Biol* **72**, 2-11 (2016) DOI: 10.1107/S2059798315020847

168 A.E. Cohen, S.M. Soltis, A. Gonzale *et al*. "Goniometer-based femtosecond crystallography with X-ray free electron lasers." *Proc Natl Acad Sci U S A* **111**, 17122-17127 (2014) DOI: 10.1073/pnas.1418733111

169 U. Zander, G. Bourenkov, A.N. Popov *et al*. "MeshAndCollect: an automated multi-crystal data-collection workflow for synchrotron macromolecular crystallography beamlines." *Acta Crystallogr D Biol Crystallogr* **71**, 2328-2343 (2015) DOI: 10.1107/S1399004715017927

170 D. Doppler *et al.* "Modular droplet injector for sample conservation providing new structural insight for the conformational heterogeneity in the disease-associated NQO1 enzyme." *Lab on a chip* **23**, 13 3016-3033 (2023) DOI: 10.1039/d3lc00176h

171 D. Doppler *et al.* "Co-flow injection for serial crystallography at X-ray free-electron lasers." *J Appl Crystallogr* **55**, 1 1-13 (2022) DOI: 10.1107/S1600576721011079

172 A. Echelmeier, J. Cruz Villareal, M. Messerschmidt *et al.* "Segmented flow generator for serial crystallography at the European X-ray free electron laser." *Nat Commun* **11**, 4511 (2020) DOI: 10.1038/s41467-020-18156-7

173 D. Kim *et al.* "Electric Triggering for Enhanced Control of Droplet Generation." *Anal. Chem.* **91**, 15, 9792-9799 (2019) DOI: 10.1021/acs.analchem.9b01449

174 N.K. Sauter, J.P. Rose and T.N. Bhat, "Transactions from the 69th Annual Meeting of the American Crystallographic Association: Data best practices-current state and future needs." *Struct Dyn* **7**, 021301 (2020) DOI: 10.1063/4.0000011

175 H.J. Bernstein, L.C. Andrews, J.A. Diaz Jr *et al*. "Best practices for high data-rate macromolecular crystallography (HDRMX)." *Struct Dyn* **7**, 014302 (2020) DOI: 10.1063/1.5128498

176 F. Leonarski, A. Mozzanica, M. Brückner *et al.* "JUNGFRAU detector for brighter x-ray sources: Solutions for IT and data science challenges in macromolecular crystallography." *Struct Dyn* **7**, 014305 (2020) DOI: 10.1063/1.5143480

177 S.P. Meisburger, D.A. Case and N. Ando, "Diffuse X-ray scattering from correlated motions in a protein crystal." *Nat Commun* **11**, 1271 (2020) DOI: 10.1038/s41467-020-14933-6

178 A. Förster and C. Schulze-Briese, "A shared vision for macromolecular crystallography over the next five years." *Struct Dyn* **6**, 064302 (2019) DOI: 10.1063/1.5131017

179 J.R. Helliwell, B. McMahon, J.M. Guss and L.M.J. Kroon-Batenburg, "The science is in the data." *IUCrJ* **4**, 714-722 (2017) DOI: 10.1107/S2052252517013690

180 F.Z. Zhao, B. Zhang, E.K. Yan *et al*. "A guide to sample delivery systems for serial crystallography." *FEBS J* **286**, 4402-4417 (2019) DOI: 10.1111/febs.15099

181 I. Martiel, H.M. Muller-Werkmeister and A.E. Cohen, "Strategies for sample delivery for femtosecond crystallography." *Acta Crystallogr D Struct Biol* **75**, 160-177 (2019) DOI: 10.1107/S2059798318017953

182 A. Meents, M.O. Wiedorn, V. Srajer *et al*. "Pink-beam serial crystallography." *Nat Commun* **8,** 1281 (2017) DOI: 10.1038/s41467-017-01417-3

183 P. Mehrabi, E.C. Schulz, M. Agthe *et al*. "Liquid application method for time-resolved analyses by serial synchrotron crystallography." *Nat Methods* **16**, 979-982 (2019) DOI: 10.1038/s41592-019-0553-1

184 J.M. Martin-Garcia, C.E. Conrad, G. Nelson *et al*. "Serial millisecond crystallography of membrane and soluble protein microcrystals using synchrotron radiation." *IUCrJ* **4**, 439-454 (2017) DOI: 10.1107/S205225251700570X

185 J.M. Martin-Garcia, L Zhu, D. Mendez *et al*. "High-viscosity injector-based pink-beam serial crystallography of microcrystals at a synchrotron radiation source." *IUCrJ* **6**, 412-425 (2019) DOI: 10.1107/S205225251900263X

186 J. Orlans, S.L. Rose, G. Ferguson *et al.* "Advancing macromolecular structure determination with microsecond X-ray pulses at a 4th generation synchrotron." *Commun Chem* **8**, 6 (2025) DOI: 10.1038/s42004-024-01404-y

187 E.C. Schulz, B.A. Yorke, A.R. Pearson, and P. Mehrabi, "Best practices for time-resolved serial synchrotron crystallography." *Acta Cryst.* **D78**, 14-29 (2022) DOI: 10.1107/S2059798321011621

188 M.A. Hough and R.L. Owen, "Serial synchrotron and XFEL crystallography for studies of metalloprotein catalysis." *Curr Opin Struct Biol* **71**, 232-238 (2021) DOI: 10.1016/j.sbi.2021.07.007

189 A.R. Pearson and P. Mehrabi, "Serial synchrotron crystallography for time-resolved structural biology." *Curr Opin Struct Biol* **65**, 168-174 (2020) DOI: 10.1016/j.sbi.2020.06.019

190 D. Chenevier and A. Joly, "ESRF: Inside the Extremely Brilliant Source Upgrade." *Synchrotron Radiation News* **31**, 32-35 (2018) DOI: 10.1080/08940886.2018.1409562

191 L.C. Chapon, I. Boscaro-Clarke, A.J. Dent, A. Harrison, M. Launchbury, D.I. Stuart and R.P. Walker (Eds), "Diamond-II — Conceptual Design Report." Harwell Science & Innovation Campus, Didcot, Oxfordshire, OX11 0DE, UK, Diamond Light Source Ltd. (2019) https://www.diamond.ac.uk/dam/jcr:ec67b7e1-

fb91-4a65-b1ce-f646490b564d/Diamond-II%20Conceptual%20Design%20Report.pdf, access date 12 May 2020

192 I. Boscaro-Clarke, L.C. Chapon, A.J. Dent *et al*. "Diamond-II — Advancing Science." Harwell Science & Innovation Campus, Didcot, Oxfordshire OX11 0DE, UK, Diamond Light Source Ltd. (2019) https://www.diamond.ac.uk/dam/jcr:2ddff8c5-80fe-43aa-8a00-321be9c02cc6/Diamond%20II%20Science%20Interactive%20_%20Dec%202019%20Update.pdf, access date 12 May 2020

193 L. Fagerberg, K. Jonasson, G. von Heijne, M. Uhlen and L. Berglund, "Prediction of the human membrane proteome." *Proteomics* **10**, 1141-1149 (2010) DOI: 10.1002/pmic.200900258

194 M.S. Almen, K.J. Nordström, R. Fredriksson and H.B. Schiöth, "Mapping the human membrane proteome: a majority of the human membrane proteins can be classified according to function and evolutionary origin." *BMC Biol* **7**, 50 (2009) DOI: 10.1186/1741-7007-7-50

195 A. Ishchenko, E.E. Abola and V. Cherezov, "Crystallization of Membrane Proteins: An Overview." *Methods Mol Biol* **1607**, 117-141 (2017) DOI: 10.1007/978-1-4939-7000-1_5

196 M.A. Yildirim, K.I. Goh, M.E. Cusick *et al*. "Drug-target network." *Nat Biotechnol* **25**, 1119-1126 (2007) DOI: 10.1038/nbt1338

197 Z. Wu, W. Li, G. Liu and Y. Tang, "Network-Based Methods for Prediction of Drug-Target Interactions." *Front Pharmacol* **9**, 1134 (2018) DOI: 10.3389/fphar.2018.01134

198 B. Stauch and V. Cherezov, "Serial Femtosecond Crystallography of G Protein-Coupled Receptors." *Annu Rev Biophys* **47**, 377-397 (2018) DOI: 10.1146/annurev-biophys-070317-033239

199 A. Zabara, T.G. Meikle, R. Trenker *et al*. "Lipidic Cubic Phase-Induced Membrane Protein Crystallization: Interplay Between Lipid Molecular Structure, Mesophase Structure and Properties, and Crystallogenesis." *Cryst. Growth Des.* **17**, 11, 5667-5674 (2017) DOI: 10.1021/acs.cgd.7b00519

200 Y. Kang, X.E. Zhou, X. Gao *et al*. "Crystal structure of rhodopsin bound to arrestin by femtosecond X-ray laser." *Nature* **523**, 561-567 (2015) DOI: 10.1038/nature14656

201 W. Liu, D. Wacker, C. Gati *et al*. "Serial femtosecond crystallography of G protein-coupled receptors." *Science* **342**, 1521-1524 (2013) DOI: 10.1126/science.1244142

202 R.M. Stein, H.J. Kang, J.D. McCorvy *et al*. "Virtual discovery of melatonin receptor ligands to modulate circadian rhythms." *Nature* **579**, 609-614 (2020) DOI: 10.1038/s41586-020-2027-0

203 A. Ishchenko, B. Stauch, G.W. Han *et al.* "Toward G protein-coupled receptor structure-based drug design using X-ray lasers." *IUCrJ* **6**, 1106-1119 (2019) DOI: doi:10.1107/S2052252519013137

204 T.A. White, V. Mariani, W. Brehm *et al*. "Recent developments in *CrystFEL*." *J Appl Cryst* **49**, 680-689 (2016) DOI: 10.1107/S1600576716004751

205 T.A. White, "Post-refinement method for snapshot serial crystallography." *Phil Trans R Soc B* **369**: 20130330 (2014) DOI: 10.1098/rstb.2013.0330

206 G. Winter, D.G. Waterman, J.M. Parkhurst *et al*. "DIALS: implementation and evaluation of a new integration package." *Acta Cryst D***74**, 85-97 (2018) DOI: 10.1107/S2059798317017235

207 A.S. Brewster, D.G. Waterman, J.M. Parkhurst *et al*. "Improving signal strength in serial crystallography with DIALS geometry refinement." *Acta Cryst D***74**, 877-894 (2018) DOI: 10.1107/S2059798318009191

208 D.G. Waterman, G. Winter, R.J. Gildea *et al*. "Diffraction-geometry refinement in the DIALS framework." *Acta Cryst D***72**, 558-575 (2016) DOI: 10.1107/S2059798316002187

209 N.K. Sauter, "XFEL diffraction: developing processing methods to optimize data quality." *J Synchrotron Radiat* **22**, 239-248 (2015) DOI: 10.1107/S1600577514028203

210 O. Yefanov, C. Gati, G. Bourenkov *et al*. "Mapping the continuous reciprocal space intensity distribution of X-ray serial crystallography." *Philos Trans R Soc Lond B Biol Sci* **369**, 20130333 (2014) DOI: 10.1098/rstb.2013.0333

211 H.M. Ginn, A.S. Brewster, J. Hattne *et al.* "A revised partiality model and post-refinement algorithm for X-ray free-electron laser data." *Acta Cryst D***71**, 1400-1410 (2015) DOI: 10.1107/S1399004715006902

212 Y. Gevorkov, O. Yefanov, A. Barty *et al*. "XGANDALF - extended gradient descent algorithm for lattice finding." *Acta Cryst A***75**, 694-704 (2019) DOI: 10.1107/S2053273319010593

213 A. Allahgholi, J. Becker, A. Delfs *et al*. "The Adaptive Gain Integrating Pixel Detector at the European XFEL." *J Synchrotron Radiat* **26**, 74-82 (2019) DOI: 10.1107/S1600577518016077

214 A. Allahgholi, J. Becker, L. Bianco *et al*. "AGIPD, a high dynamic range fast detector for the European XFEL." *JINST* **10** C01023 (2015) DOI: 10.1088/1748-0221/10/01/C01023

215 D. Greiffenberg, "The AGIPD detector for the European XFEL." *JINST* **7** C01103(2012) DOI: 10.1088/1748-0221/7/01/C01103

216 F. Leonarski, A. Mozzanica, M. Brückner *et al*. "JUNGFRAU detector for brighter x-ray sources: Solutions for IT and data science challenges in macromolecular crystallography." *Struct Dyn* **7**, 014305 (2020) DOI: 10.1063/1.5143480

217 F. Leonarski, S. Redford, A. Mozzanica *et al*. "Fast and accurate data collection for macromolecular crystallography using the JUNGFRAU detector." *Nat Methods* **15**, 799-804 (2018) DOI: 10.1038/s41592-018-0143-7

218 J.J. van Thor, "Advances and opportunities in ultrafast X-ray crystallography and ultrafast

structural optical crystallography of nuclear and electronic protein dynamics." *Struct Dyn* **6**, 050901 (2019) DOI: 10.1063/1.5110685

[219] Mous, S., Hunter, M. S., Poitevin, F., Boutet, S. & Gee, L. B. "Macromolecular crystallography and biology at the Linac Coherent Light Source." *Journal of Synchrotron Radiation* **32**, 548-566, (2025) DOI:10.1107/S1600577525002735

[220] Svensson, O., Gilski, M., Nurizzo, D. & Bowler, M. W. "A comparative anatomy of protein crystals: lessons from the automatic processing of 56 000 samples." *IUCrJ* **6**, 822-831, (2019) DOI:10.1107/S2052252519008017

[221] Nurizzo, D. *et al.* "RoboDiff: combining a sample changer and goniometer for highly automated macromolecular crystallography experiments." *Acta Crystallographica Section D* **72**, 966-975, (2016) DOI:10.1107/S205979831601158X

[222] Bowler, M. W. *et al.* "MASSIF-1: a beamline dedicated to the fully automatic characterization and data collection from crystals of biological macromolecules." *Journal of Synchrotron Radiation* **22**, 1540-1547, (2015) DOI:10.1107/S1600577515016604

[223] Bohl, A., Lawrence, L., Lowry, G. & Kaltenegger, L. "Probing the limits of habitability: a catalogue of rocky exoplanets in the habitable zone." *Monthly Notices of the Royal Astronomical Society* **547**, (2026) DOI:10.1093/mnras/stag028

[224] Cockell, C. S. *et al.* "Sustained and comparative habitability beyond Earth." *Nature Astronomy* **8**, 30-38, (2024) DOI:10.1038/s41550-023-02158-8

[225] Schwieterman, E. W. *et al.* "Exoplanet Biosignatures: A Review of Remotely Detectable Signs of Life." *Astrobiology* **18**, 663-708, (2018) DOI:10.1089/ast.2017.1729

[226] Yang, X.-L. *et al.* "Modeling light response of effective quantum efficiency of photosystem II for C3 and C4 crops." *Frontiers in Plant Science* Volume 16 - 2025, (2025) DOI:10.3389/fpls.2025.1478346

[227] Wang, H. *et al.* "Two-billion-year transitional oxygenation of the Earth's surface." *Nature* **645**, 665-671, (2025) DOI:10.1038/s41586-025-09471-4

[228] Johnson, J. E., Present, T. M. & Valentine, J. S. "Iron: Life's primeval transition metal." Proceedings of the National Academy of Sciences 121, e2318692121, (2024) DOI:10.1073/pnas.2318692121

[229] Fischer, W. W., Hemp, J. & Valentine, J. S. "How did life survive Earth's great oxygenation?" *Current Opinion in Chemical Biology* **31**, 166-178, (2016) DOI:10.1016/j.cbpa.2016.03.013

[230] Reinhard, C. T., Planavsky, N. J., Olson, S. L., Lyons, T. W. & Erwin, D. H. "Earth's oxygen cycle and the evolution of animal life." *Proc Natl Acad Sci USA* **113**, 8933-8938, (2016) DOI:10.1073/pnas.1521544113

[231] Raymond, J. & Segre, D. The effect of oxygen on biochemical networks and the evolution of complex life. *Science* **311**, 1764-1767, doi:10.1126/science.1118439 (2006)

[232] Braun, A. & Solomon, E. I. "Electronic Structure Contributions to the Reactivity of Mononuclear FeIV-Oxo Intermediates." *Accounts of Chemical Research* **59**, 209-220, (2026) DOI:10.1021/acs.accounts.5c00655

[233] Stańczak, A. *et al.* "Coupled binuclear copper sites in biology: An experimentally-calibrated computational perspective." *Coordin Chem Rev* **525**, 216301, (2025) DOI: 10.1016/j.ccr.2024.216301

[234] Rousseau, D. L., Ishigami, I. & Yeh, S.-R. "Structural and functional mechanisms of cytochrome c oxidase." *J Inorg Biochem* **262**, 112730, (2025) DOI:10.1016/j.jinorgbio.2024.112730

[235] Phintha, A. & Chaiyen, P. "Unifying and versatile features of flavin-dependent monooxygenases: Diverse catalysis by a common C4a-(hydro)peroxyflavin." *J Biol Chem* **299**, 105413, (2023) DOI:10.1016/j.jbc.2023.105413

[236] Robinson, R. M., Klancher, C. A., Rodriguez, P. J. & Sobrado, P. "Flavin oxidation in flavin-dependent N-monooxygenases." *Protein Sci* **28**, 90-99, (2019) DOI:10.1002/pro.3487

[237] Lingappa, U. F., Monteverde, D. R., Magyar, J. S., Valentine, J. S. & Fischer, W. W. "How manganese empowered life with dioxygen (and vice versa)." *Free Radical Biology and Medicine* **140**, 113-125, (2019) DOI:10.1016/j.freeradbiomed.2019.01.036

[238] Meier, K. K. *et al.* "Oxygen Activation by Cu LPMOs in Recalcitrant Carbohydrate Polysaccharide Conversion to Monomer Sugars." *Chemical Reviews* **118**, 2593-2635, (2018) DOI:10.1021/acs.chemrev.7b00421

[239] Piano, V., Palfey, B. A. & Mattevi, A. "Flavins as Covalent Catalysts: New Mechanisms Emerge." *Trends Biochem Sci* **42**, 457-469, (2017) DOI:10.1016/j.tibs.2017.02.005

[240] Solomon, E. I. *et al.* "Copper Active Sites in Biology." *Chemical Reviews* **114**, 3659-3853, (2014) DOI:10.1021/cr400327t

[241] Huijbers, M. M., Montersino, S., Westphal, A. H., Tischler, D. & van Berkel, W. J. "Flavin dependent monooxygenases." *Arch Biochem Biophys* **544**, 2-17, (2014) DOI:10.1016/j.abb.2013.12.005

[242] Sheng, Y. *et al.* "Superoxide Dismutases and Superoxide Reductases." *Chemical Reviews* **114**, 3854-3918, (2014) DOI:10.1021/cr4005296

[243] Neidig, M. L. & Solomon, E. I. "Structure-function correlations in oxygen activating non-heme iron enzymes." *Chem Commun (Camb)*, 5843-5863, (2005) DOI:10.1039/b510233m

[244] Costas, M., Mehn, M. P., Jensen, M. P. & Que, L., Jr. "Dioxygen activation at mononuclear nonheme iron active sites: enzymes, models, and intermediates." *Chem Rev* **104**, 939-986, (2004) DOI:10.1021/cr020628n

[245] Valentine, J. S. *et al.* "The dark side of dioxygen biochemistry." *Curr Opin Chem Biol* **2**, 253-262, (1998) DOI:10.1016/s1367-5931(98)80067-7

[246] Holm, R. H., Kennepohl, P. & Solomon, E. I. "Structural and Functional Aspects of Metal Sites in Biology." *Chem Rev* **96**, 2239-2314, (1996) DOI:10.1021/cr9500390

[247] Ingraham, L. L. & Meyer, D. L. *Biochemistry of Dioxygen*. (Springer New York, NY, 1985)

[248] Tucci, F. J. & Rosenzweig, A. C. "Direct Methane Oxidation by Copper- and Iron-Dependent Methane Monooxygenases." *Chem Rev* **124**, 1288-1320, (2024) DOI:10.1021/acs.chemrev.3c00727

[249] Zhu, Y. et al. "Structure and activity of particulate methane monooxygenase arrays in methanotrophs." *Nat Commun* **13**, 5221, (2022) DOI:10.1038/s41467-022-32752-9

[250] Koo, C. W. & Rosenzweig, A. C. "Biochemistry of aerobic biological methane oxidation." *Chem Soc Rev* **50**, 3424-3436, (2021) DOI:10.1039/d0cs01291b

[251] Srinivas, V. et al. "High-Resolution XFEL Structure of the Soluble Methane Monooxygenase Hydroxylase Complex with its Regulatory Component at Ambient Temperature in Two Oxidation States." *J Am Chem Soc* **142**, 14249-14266, (2020) DOI:10.1021/jacs.0c05613

[252] Banerjee, R., Jones, J. C. & Lipscomb, J. D. "Soluble Methane Monooxygenase." *Annu Rev Biochem* **88**, 409-431, (2019) DOI:10.1146/annurev-biochem-013118-111529

[253] Ruscic, B. "Active Thermochemical Tables: Sequential Bond Dissociation Enthalpies of Methane, Ethane, and Methanol and the Related Thermochemistry." *The Journal of Physical Chemistry A* **119**, 7810-7837, (2015) DOI:10.1021/acs.jpca.5b01346

[254] Sazinsky, M. H. & Lippard, S. J. in Sustaining Life on Planet Earth: Metalloenzymes Mastering Dioxygen and Other Chewy Gases (eds Peter M. H. Kroneck & Martha E. Sosa Torres) 205-256 (Springer International Publishing, 2015)

[255] Luo, Y. R. Comprehensive Handbook of Chemical Bond Energies. (CRC Press, 2007)

[256] Zheng, H. & Lipscomb, J. D. "Regulation of Methane Monooxygenase Catalysis Based on Size Exclusion and Quantum Tunneling." *Biochemistry* **45**, 1685-1692, (2006) DOI:10.1021/bi051605g

[257] Shu, L. et al. "An $Fe_2(IV)O_2$ diamond core structure for the key intermediate Q of methane monooxygenase." *Science* **275**, 515-518, (1997) DOI:10.1126/science.275.5299.515

[258] Nesheim, J. C. & Lipscomb, J. D. "Large kinetic isotope effects in methane oxidation catalyzed by methane monooxygenase: evidence for C-H bond cleavage in a reaction cycle intermediate." *Biochemistry* **35**, 10240-10247, (1996) DOI:10.1021/bi960596w

[259] Lee, S. K., Nesheim, J. C. & Lipscomb, J. D. "Transient intermediates of the methane monooxygenase catalytic cycle." *J Biol Chem* **268**, 21569-21577 (1993)

[260] Priestley, N. D. et al. "Cryptic stereospecificity of methane monooxygenase." *J Am Chem Soc* **114**, 7561-7562, (1992) DOI:10.1021/ja00045a037

[261] Klinman, J. P., Miller, S. M. & Richards, N. G. J. A "Foundational Shift in Models for Enzyme Function." *J Am Chem Soc* **147**, 14884-14904, (2025) DOI:10.1021/jacs.5c02388

[262] Hammes-Schiffer, S. "Explaining Kinetic Isotope Effects in Proton-Coupled Electron Transfer Reactions." *Accounts of Chemical Research* **58**, 1335-1344, (2025) DOI:10.1021/acs.accounts.5c00119

[263] Arcus, V. L., van der Kamp, M. W., Pudney, C. R. & Mulholland, A. J. "Enzyme evolution and the temperature dependence of enzyme catalysis." *Current Opinion in Structural Biology* **65**, 96-101, (2020) DOI:10.1016/j.sbi.2020.06.001

[264] Arcus, V. L. & Mulholland, A. J. "Temperature, Dynamics, and Enzyme-Catalyzed Reaction Rates." *Annu Rev Biophys* **49**, 163-180, (2020) DOI:10.1146/annurev-biophys-121219-081520

[265] Klinman, J. P. & Offenbacher, A. R. "Understanding Biological Hydrogen Transfer Through the Lens of Temperature Dependent Kinetic Isotope Effects." *Accounts of Chemical Research* **51**, 1966-1974, (2018) DOI:10.1021/acs.accounts.8b00226

[266] Arcus, V. L. et al. "On the Temperature Dependence of Enzyme-Catalyzed Rates." *Biochemistry* **55**, 1681-1688, (2016) DOI:10.1021/acs.biochem.5b01094

[267] Klinman, J. P. & Kohen, A. "Hydrogen tunneling links protein dynamics to enzyme catalysis." *Annu Rev Biochem* **82**, 471-496, (2013) DOI:10.1146/annurev-biochem-051710-133623

[268] Kohen, A. & Klinman, J. P. "Hydrogen tunneling in biology." *Chem Biol* 6, R191-198, (1999) DOI:10.1016/s1074-5521(99)80058-1

[269] Ou, Z. et al. "Achieving optical transparency in live animals with absorbing molecules." *Science* **385**, eadm6869, (2024) DOI:10.1126/science.adm6869

[270] Cheng, C. "Tissue, cellular, and molecular level determinants for eye lens stiffness and elasticity." *Front Ophthalmol (Lausanne)* **4**, 1456474, (2024) DOI:10.3389/fopht.2024.1456474

[271] Truscott, R. J. W. "Age-related nuclear cataract—oxidation is the key." *Experimental Eye Research* **80**, 709-725, (2005) DOI:10.1016/j.exer.2004.12.007

[272] Blindness, Global Burden of Diseases, "Vision Impairment, C. & Vision Loss Expert Group of the Global Burden of Disease, S. Causes of blindness and vision impairment in 2020 and trends over 30 years, and prevalence of avoidable blindness in relation to VISION 2020: the Right to Sight: an analysis for the Global Burden of Disease Study." *Lancet Glob Health* **9**, e144-e160, (2021) DOI:10.1016/S2214-109X(20)30489-7

[273] Kmoch, S. *et al.* "Link between a novel human γD-crystallin allele and a unique cataract phenotype explained by protein crystallography." *Human Molecular Genetics* **9**, 1779-1786, (2000) DOI:10.1093/hmg/9.12.1779

[274] Hill, J. A., *et al.* and Yorke, B. A. "An ultraviolet-driven rescue pathway for oxidative stress to eye lens protein human gamma-D crystallin." *Commun Chem* **7**, 81, (2024) DOI:10.1038/s42004-024-01163-w

[275] Ochmann, M. *et al.* "UV photochemistry of the L-cystine disulfide bridge in aqueous solution investigated by femtosecond X-ray absorption spectroscopy." *Nat Commun* **15**, 8838, (2024) DOI:10.1038/s41467-024-52748-x

[276] Kelner, A. "Effect of Visible Light on the Recovery of *Streptomyces griseus conidia* from Ultra-violet Irradiation Injury." *Proc Nat Acad Sci USA* **35**, 73-79, (1949) DOI:10.1073/pnas.35.2.73

[277] Sancar, A. "Structure and Function of DNA Photolyase and Cryptochrome Blue-Light Photoreceptors." *Chemical Reviews* **103**, 2203-2238, (2003) DOI:10.1021/cr0204348

[278] Tan, C. *et al.* "Direct Determination of Resonance Energy Transfer in Photolyase: Structural Alignment for the Functional State." *J Phys Chem A* **118**, 10522-10530, (2014) DOI:10.1021/jp504349b

[279] Banerjee, S. K., Christensen, R. B., Lawrence, C. W. & LeClerc, J. E. "Frequency and spectrum of mutations produced by a single cis-syn thymine-thymine cyclobutane dimer in a single-stranded vector." *Proc Nat Acad Sci USA* **85**, 8141-8145, (1988) DOI:10.1073/pnas.85.21.8141

[280] Moffat, K. "Dynamics and kinetics in structural biology: the example of DNA photolyase." *Q Rev Biophys* **58**, e8, (2025) DOI:10.1017/S0033583524000222

[281] He, Y., Barone, M., Meech, S. R., Lukacs, A. & Tonge, P. J. "Light-Driven Enzyme Catalysis: Ultrafast Mechanisms and Biochemical Implications." *Biochemistry* **64**, 2491-2505, (2025) DOI:10.1021/acs.biochem.5c00039

[282] Vos, M. H. "Filming DNA repair at the atomic level." *Science* **382**, 996-997, (2023) DOI:10.1126/science.adl3002

[283] Christou, N. E. et al. "Time-resolved crystallography captures light-driven DNA repair." *Science* 382, 1015-1020, (2023) DOI:10.1126/science.adj4270

[284] Maestre-Reyna, M. et al. "Visualizing the DNA repair process by a photolyase at atomic resolution." *Science* 382, eadd7795, (2023) DOI:10.1126/science.add7795

[285] Maestre-Reyna, M. et al. "Serial crystallography captures dynamic control of sequential electron and proton transfer events in a flavoenzyme." *Nat Chem* 14, 677-685, (2022) DOI:10.1038/s41557-022-00922-3

[286] Hong, Y., Huang, Y. & Huang, Z. "DNA repair in darkness: evolutionary conservation of photolyase function beyond light." *Communications Biology* **9**, 328, (2026) DOI:10.1038/s42003-026-09750-4

[287] Li, H. *et al.* "Conservation of dark CPD photolyase function in blind cavefish." *Nature Communications* **16**, 7377, (2025) DOI:10.1038/s41467-025-62795-7

[288] Maestre-Reyna, M. *et al.* "Capturing structural intermediates in an animal-like cryptochrome photoreceptor by time-resolved crystallography." *Science Advances* **11**, eadu7247, (2025) DOI:10.1126/sciadv.adu7247

[289] Xu, J. *et al.* "Magnetic sensitivity of cryptochrome 4 from a migratory songbird." *Nature* **594**, 535-540, (2021) DOI:10.1038/s41586-021-03618-9

[290] Hore, P. J. & Mouritsen, H. "The Radical-Pair Mechanism of Magnetoreception." *Annual Review of Biophysics* **45**, 299-344, (2016) DOI:10.1146/annurev-biophys-032116-094545

[291] Ritz, T., Thalau, P., Phillips, J. B., Wiltschko, R. & Wiltschko, W. "Resonance effects indicate a radical-pair mechanism for avian magnetic compass." *Nature* **429**, 177-180, (2004) DOI:10.1038/nature02534

[292] Rios-Santacruz, R. *et al.* "Integrated structural dynamics uncover a new B12 photoreceptor activation mode." *Nature* **650**, 1045-1052, (2026) DOI :10.1038/s41586-025-10074-2

[293] Poddar, H. *et al.* "Redox driven B(12)-ligand switch drives CarH photoresponse." *Nat Commun* **14**, 5082, (2023) DOI:10.1038/s41467-023-40817-6

[294] Stauch, B. *et al.* "Structural basis of ligand recognition at the human MT1 melatonin receptor." *Nature* **569**, 284-288, (2019) DOI:10.1038/s41586-019-1141-3

[295] Johansson, L. C. *et al.* "XFEL structures of the human MT2 melatonin receptor reveal the basis of subtype selectivity." *Nature* **569**, 289-292, (2019) DOI:10.1038/s41586-019-1144-0

[296] Heckman, D. S. *et al.* "Molecular Evidence for the Early Colonization of Land by Fungi and Plants." *Science* **293**, 1129-1133, (2001) DOI:10.1126/science.1061457

[297] Blanc, G. *et al.* "The *Chlorella variabilis* NC64A Genome Reveals Adaptation to Photosymbiosis, Coevolution with Viruses, and Cryptic Sex." *The Plant Cell* **22**, 2943-2955, (2010) DOI:10.1105/tpc.110.076406

[298] Vos, M. H., Balduzzi, E., Sorigué, D. & Aleksandrov, A. "Ultrafast photooxidation of semireduced flavin in fatty acid photodecarboxylase." *Science Advances* **11**, eadz1904, (2025) DOI:10.1126/sciadv.adz1904

[299] Sorigue, D. et al. "Mechanism and dynamics of fatty acid photodecarboxylase." *Science* **372**, (2021) DOI:10.1126/science.abd5687

[300] Sorigue, D. et al. "An algal photoenzyme converts fatty acids to hydrocarbons." *Science* **357**, 903-907, (2017) DOI:10.1126/science.aan6349

[301] Hadjidemetriou, K. et al. "Time-resolved serial femtosecond crystallography on fatty-acid

photodecarboxylase: lessons learned." *Acta Crystallogr D Struct Biol* **78**, 1131-1142, (2022) DOI:10.1107/S2059798322007525

302 Li, F. et al. "Photo-driven decarboxylation for sustainable biofuel production: a review on harnessing the potential of fatty acid decarboxylases." *Chemical Communications* **61**, 18273-18288, (2025) DOI:10.1039/D5CC02448J

303 Williams, L. J. et al. "The cytochrome P450 decarboxylase from Staphylococcus aureus can produce a diene from a C18 monounsaturated fatty acid: A spectroscopic, structural and kinetic characterisation." *J Inorg Biochem* 275, 113117, (2026) DOI:10.1016/j.jinorgbio.2025.113117

304 Tseliou, V. et al. "Stereospecific radical coupling with a non-natural photodecarboxylase." *Nature* 634, 848-854, (2024) DOI:10.1038/s41586-024-08004-9

305 Schirmer, A., Rude, M. A., Li, X., Popova, E. & del Cardayre, S. B. "Microbial biosynthesis of alkanes." *Science* 329, 559-562, (2010) DOI :10.1126/science.1187936

306 Andre, C., Kim, S. W., Yu, X.-H. & Shanklin, J. "Fusing catalase to an alkane-producing enzyme maintains enzymatic activity by converting the inhibitory byproduct H_2O_2 to the cosubstrate O_2." *Proc Nat Acad Sci USA* 110, 3191-3196, (2013) DOI:10.1073/pnas.1218769110

307 A. Vallejos, G. Katona and R. Neutze, "Appraising protein conformational changes by resampling time-resolved serial x-ray crystallography data." *Struct Dyn* **11**, 044302 (2024) DOI: 10.1063/4.0000258

308 R. Neutze and R.J.D. Miller, "Energetic laser pulses alter outcomes of X-ray studies of proteins." *Nature* **626**, 720-722 (2024) DOI: 10.1038/d41586-024-00233-2

309 T.R.M. Barends, A. Gorel, S. Bhattacharyya *et al.* "Influence of pump laser fluence on ultrafast myoglobin structural dynamics." *Nature* **626**, 905-911 (2024) DOI: 10.1038/s41586-024-07032-9

310 A. Gorel, I. Schlichting and T.R.M. Barends, "Discerning best practices in XFEL-based biological crystallography - standards for nonstandard experiments." *IUCrJ* **8**, 532-543 (2021) DOI: 10.1107/S205225252100467X

311 J.M. Baxter, J. M. *et al.* "Power Density Titration of Reversible Photoisomerization of a Fluorescent Protein Chromophore in the Presence of Thermally Driven Barrier Crossing Shown by Quantitative Millisecond Serial Synchrotron X-ray Crystallography." *J. Am. Chem. Soc.* **146**, 16394-16403 (2024) DOI: 10.1021/jacs.3c12883

312 G. Brändén and R. Neutze, "Advances and challenges in time-resolved macromolecular crystallography." *Science* **373**, 6558 (2021) DOI: 10.1126/science.aba0954

313 A. Aquila, M.S. Hunter, R.B. Doak *et al*. "Time-resolved protein nanocrystallography using an X-ray free-electron laser." *Opt Express* **20**, 2706-2716 (2012) DOI: 10.1364/Oe.20.002706

314 L.C. Johansson, D. Arnlund, G. Katona *et al*. "Structure of a photosynthetic reaction centre determined by serial femtosecond crystallography." *Nat Commun* **4**, 2911 (2013) DOI: 10.1038/ncomms3911

315 M.O. Wiedorn, S. Awel, A.J. Morgan *et al.* "Rapid sample delivery for megahertz serial crystallography at X-ray FELs." *IUCrJ* **5**, 574-584 (2018) DOI: 10.1107/S2052252518008369

316 A. Echelmeier, D. Kim, J. Cruz Villarreal *et al*. "3D printed droplet generation devices for serial femtosecond crystallography enabled by surface coating." *J Appl Cryst* **52**, 997-1008 (2019) DOI: 10.1107/S1600576719010343

317 C. Gisriel, J. Coe, R. Letrun *et al*. "Membrane protein megahertz crystallography at the European XFEL." *Nat Commun* **10**, 5021 (2019) DOI: 10.1038/s41467-019-12955-3

318 C. Kupitz, S. Basu, I. Grotjohann *et al.* "Serial time-resolved crystallography of photosystem II using a femtosecond X-ray laser." *Nature* **513**, 261-265 (2014) DOI: 10.1038/nature13453

319 K. Ayyer, O.M. Yefanov, D. Oberthür *et al.* "Macromolecular diffractive imaging using imperfect crystals." *Nature* **530**, 202-206 (2016) DOI: 10.1038/nature16949

320 M. Suga, F. Akita, M. Sugahara *et al.* "Light-induced structural changes and the site of O=O bond formation in PSII caught by XFEL." *Nature* **543**, 131-135 (2017) DOI: 10.1038/nature21400

321 M. Suga, A. Shimada, F. Akita *et al*. "Time-resolved studies of metalloproteins using X-ray free electron laser radiation at SACLA." *Biochim Biophys Acta Gen Subj* **1864**, 129466 (2020) DOI: 10.1016/j.bbagen.2019.129466

322 M. Suga, F. Akita, K. Yamashita *et al.* "An oxyl/oxo mechanism for oxygen-oxygen coupling in PSII revealed by an x-ray free-electron laser." *Science* **366**(6463):334-338 (2019) DOI: 10.1126/science.aax6998

323 M. Suga, F. Akita, K. Hirata *et al*. "Native structure of photosystem II at 1.95 Å resolution viewed by femtosecond X-ray pulses." *Nature* **517**, 99-103 (2015) DOI: 10.1038/nature13991

324 I. Young, M. Ibrahim, R. Chatterjee *et al.* "Structure of photosystem II and substrate binding at room temperature." *Nature* **540**, 453-457 (2016) DOI: 10.1038/nature20161

325 J. Kern, V.K. Yachandra and J. Yano, "Metalloprotein structures at ambient conditions and in real-time: biological crystallography and spectroscopy using X-ray free electron lasers." *Curr Opin Struct Biol* **34**, 87-98 (2015) DOI: 10.1016/j.sbi.2015.07.014

326 J. Kern, R. Tran, R. Alonso-Mori *et al.* "Taking snapshots of photosynthetic water oxidation using femtosecond X-ray diffraction and spectroscopy."

Nat Commun **5**, 4371 (2014) DOI: 10.1038/ncomms5371

[327] J. Kern, R. Alonso-Mori, R. Tran *et al.* "Simultaneous femtosecond X-ray spectroscopy and diffraction of photosystem II at room temperature." *Science* **340**(6131), 491-495 (2013) DOI: 10.1126/science.1234273

[328] R. Alonso-Mori, J. Kern, R. Gildea *et al*. "Energy-dispersive X-ray emission spectroscopy using an X-ray free-electron laser in a shot-by-shot mode." *Proc Natl Acad Sci U S A* **109** (47) 19103-19107 (2012) DOI: 10.1073/pnas.1211384109

[329] T. Fransson, R. Chatterjee, F.D. Fuller *et al*. "X-ray Emission Spectroscopy as an in Situ Diagnostic Tool for X-ray Crystallography of Metalloproteins Using an X-ray Free-Electron Laser." *Biochemistry* **57**, 4629-4637 (2018) DOI: 10.1021/acs.biochem.8b00325

[330] J. Tenboer, S. Basu, N. Zatsepin *et al*. "Time-resolved serial crystallography captures high-resolution intermediates of photoactive yellow protein." *Science* **346**, 1242-1246 (2014) DOI: 10.1126/science.1259357

[331] K. Pande, C.D. Hutchison, G. Groenhof *et al*. "Femtosecond structural dynamics drives the trans/cis isomerization in photoactive yellow protein." *Science* **352**, 725-729 (2016) DOI: 10.1126/science.aad5081

[332] S. Pandey, R. Bean, T. Sato *et al*. "Time-resolved serial femtosecond crystallography at the European XFEL." *Nat Methods* **17**, 73-78 (2020) DOI: 10.1038/s41592-019-0628-z

[333] X.E. Zhou, X. Gao, A. Barty *et al*. "X-ray laser diffraction for structure determination of the rhodopsin-arrestin complex." *Sci Data* **3**, 160021 (2016) DOI: 10.1038/sdata.2016.21

[334] R. Bosman, G. Ortolani, S. Ghosh *et al.* "Structural basis for the prolonged photocycle of sensory rhodopsin II revealed by serial synchrotron crystallography." *Nat Commun* **16**, 3460 (2025) DOI: 10.1038/s41467-025-58263-x

[335] A. Krishnamoorthi, D. Salom, A. Wu, K. Palczewski and P.M. Rentzepis, "Ultrafast transient absorption spectra and kinetics of human blue cone visual pigment at room temperature." *Proc Natl Acad Sci U S A* **121**, e2414037121 (2024) DOI: 10.1073/pnas.2414037121

[336] T. Gruhl, T. Weinert, M.J. Rodrigues *et al.* "Ultrafast structural changes direct the first molecular events of vision." *Nature* **615**, 939–944 (2023) DOI: 10.1038/s41586-023-05863-6

[337] D. Dhankhar, D. Salom, K. Palczewski and P.M. Rentzepis, "Ultrafast spectra and kinetics of human green-cone visual pigment at room temperature." *Proc Natl Acad Sci U S A* **120**, e2214276120 (2023) DOI: 10.1073/pnas.2214276120

[338] T. Nakane, S. Hanashima, M. Suzuki *et al*. "Membrane protein structure determination by SAD, SIR, or SIRAS phasing in serial femtosecond crystallography using an iododetergent." *Proc Natl Acad Sci U S A* **113**, 13039-13044 (2016) DOI: 10.1073/pnas.1602531113

[339] E. Nango, A. Royant, M. Kubo *et al*. "A three-dimensional movie of structural changes in bacteriorhodopsin." *Science* **354**, 1552-1557 (2016) DOI: 10.1126/science.aah3497

[340] P. Nogly, T. Weinert, D. James *et al*. "Retinal isomerization in bacteriorhodopsin captured by a femtosecond x-ray laser." *Science* **361** (2018) DOI: 10.1126/science.aat0094

[341] C. Wickstrand, P. Nogly, E. Nango, S. Iwata, J. Standfuss and R. Neutze, "Bacteriorhodopsin: Structural Insights Revealed Using X-Ray Lasers and Synchrotron Radiation." *Annu Rev Biochem,* **88**, 59-83 (2019) DOI: 10.1146/annurev-biochem-013118-111327

[342] T. Weinert, P. Skopintsev, D. James *et al*. "Proton uptake mechanism in bacteriorhodopsin captured by serial synchrotron crystallography." *Science* **365**, 61-65 (2019) DOI: 10.1126/science.aaw8634

[343] V. Panneels, W. Wu, C.J. Tsai *et al*. "Time-resolved structural studies with serial crystallography: A new light on retinal proteins." *Struct Dyn* **2**, 041718 (2015) DOI: 10.1063/1.4922774

[344] G. Nass Kovacs, J.P. Colletier, M.L. Grünbein *et al*. "Three-dimensional view of ultrafast dynamics in photoexcited bacteriorhodopsin." *Nat Commun* **10**, 3177 (2019) DOI: 10.1038/s41467-019-10758-0

[345] Q. Bertrand, P. Nogly, E. Nango *et al.* "Structural effects of high laser power densities on an early bacteriorhodopsin photocycle intermediate." *Nat Commun* **15**, 10278 (2024) DOI: 10.1038/s41467-024-54422-8

[346] N. Varma, E. Mutt, J. Mühle *et al*. "Crystal structure of jumping spider rhodopsin-1 as a light sensitive GPCR." *Proc Natl Acad Sci U S A* **116**, 14547-14556 (2019) DOI: 10.1073/pnas.1902192116

[347] T. Nagata, M. Koyanagi, H. Tsukamoto *et al*. "The counterion-retinylidene Schiff base interaction of an invertebrate rhodopsin rearranges upon light activation." *Commun Biol* **2**, 180 (2019) DOI: 10.1038/s42003-019-0409-3

[348] J.H. Yun, X. Li, J.H. Park *et al*. "Non-cryogenic structure of a chloride pump provides crucial clues to temperature-dependent channel transport efficiency." *J Biol Chem* **294**, 794-804 (2019) DOI: 10.1074/jbc.RA118.004038

[349] S. Mous *et al.* "Dynamics and mechanism of a light-driven chloride pump." *Science* **375**, 6583:845-851 (2022) DOI: 10.1126/science.abj6663

[350] C.D.M. Hutchison, V. Cordon-Preciado, R.M.L. Morgan *et al*. "X-ray Free Electron Laser Determination of Crystal Structures of Dark and Light States of a Reversibly Photoswitching Fluorescent Protein at Room Temperature." *International Journal of Molecular Sciences* **18**(9): 1918 (2017) DOI: 10.3390/ijms18091918

[351] J. Woodhouse, G. Nass Kovacs, N. Coquelle *et al*. "Photoswitching mechanism of a fluorescent protein revealed by time-resolved crystallography and transient absorption spectroscopy." *Nat Commun* **11**, 741 (2020) DOI: 10.1038/s41467-020-14537-0

[352] J.P. Colletier, M. Sliwa, F.X. Gallat *et al*. "Serial Femtosecond Crystallography and Ultrafast Absorption Spectroscopy of the Photoswitchable Fluorescent Protein IrisFP." *J Phys Chem Lett* **7**, 882-887 (2016) DOI: 10.1021/acs.jpclett.5b02789

[353] N. Coquelle, M. Sliwa, J. Woodhouse *et al*. "Chromophore twisting in the excited state of a photoswitchable fluorescent protein captured by time-resolved serial femtosecond crystallography." *Nat Chem* **10**, 31-37 (2018) DOI: 10.1038/nchem.2853

[354] P. Edlund, H. Takala, E. Claesson *et al*. "The room temperature crystal structure of a bacterial phytochrome determined by serial femtosecond crystallography." *Sci Rep* **6**, 35279 (2016) DOI: 10.1038/srep35279

[355] E. Claesson, W.Y. Wahlgren, H. Takala *et al*. "The primary structural photoresponse of phytochrome proteins captured by a femtosecond X-ray laser." *Elife* **9**:e53514 (2020) DOI: 10.7554/eLife.53514

[356] L. Sauthof *et al.* "Serial-femtosecond crystallography reveals how a phytochrome variant couples chromophore and protein structural changes." *Science Advances* **11**, 22:eadp2665 (2025) DOI: 10.1126/sciadv.adp2665

[357] T.R. Barends, L. Foucar, A. Ardevol *et al*. "Direct observation of ultrafast collective motions in CO myoglobin upon ligand dissociation." *Science* **350**(6259): 445-450 (2015) DOI: 10.1126/science.aac5492

[358] I. Ishigami, N.A. Zatsepin, M. Hikita *et al*. "Crystal structure of CO-bound cytochrome c oxidase determined by serial femtosecond X-ray crystallography at room temperature." *Proc Natl Acad Sci U S A* **114**, 8011-8016 (2017) DOI: 10.1073/pnas.1705628114

[359] A. Shimada, M. Kubo, S. Baba *et al*. "A nanosecond time-resolved XFEL analysis of structural changes associated with CO release from cytochrome c oxidase." *Sci Adv* **3**, e1603042 (2017) DOI: 10.1126/sciadv.1603042

[360] Safari, C. *et al.* "Time-resolved serial crystallography to track the dynamics of carbon monoxide in the active site of cytochrome c oxidase." *Sci Adv* **9**, eadh4179, (2023) DOI:10.1126/sciadv.adh4179

[361] Rousseau, D. L., Ishigami, I. & Yeh, S.-R. "Structural and functional mechanisms of cytochrome c oxidase." *J Inorg Biochem* **262**, 112730, (2025) DOI:10.1016/j.jinorgbio.2024.112730

[362] K. Nakajima, Y. Joti, T. Katayama *et al*. "Software for the data analysis of the arrival-timing monitor at SACLA." *J Synchrotron Radiat* **25**, 592-603 (2018) DOI: 10.1107/S1600577517016654

[363] T. Katayama, S. Owada, T. Togashi *et al*. "A beam branching method for timing and spectral characterization of hard X-ray free-electron lasers." *Struct Dyn* **3**, 034301 (2016) DOI: 10.1063/1.4939655

[364] A. Sanchez-Gonzalez, A.S. Johnson, A. Fitzpatrick *et al*. "Coincidence timing of femtosecond optical pulses in an X-ray free electron laser." *J Appl Phys* **122**, 203105 (2017) DOI: 10.1063/1.5012749

[365] T. Yabuuchi, A. Kon, Y. Inubushi *et al*. "An experimental platform using high-power, high-intensity optical lasers with the hard X-ray free-electron laser at SACLA." *J Synchrotron Radiat* **26**, 585-594 (2019) DOI: 10.1107/S1600577519000882

[366] H. Kandori, "Biophysics of rhodopsins and optogenetics." *Biophys Rev* **12**(2): 355-361 (2020) DOI: 10.1007/s12551-020-00645-0

[367] D. Krueger, E. Izquierdo, R. Viswanathan, J. Hartmann, C. Pallares Cartes and S. De Renzis, "Principles and applications of optogenetics in developmental biology." *Development* **146** (2019) DOI: 10.1242/dev.175067

[368] A. Losi, K.H. Gardner and A. Moglich, "Blue-Light Receptors for Optogenetics." *Chem Rev* **118**, 10659-10709 (2018) DOI: 10.1021/acs.chemrev.8b00163

[369] E.G. Govorunova, O.A. Sineshchekov, H. Li and J.L. Spudich, "Microbial Rhodopsins: Diversity, Mechanisms, and Optogenetic Applications." *Annu Rev Biochem* **86**, 845-872 (2017) DOI: 10.1146/annurev-biochem-101910-144233

[370] K.G. Chernov, T.A. Redchuk, E.S. Omelina and V.V. Verkhushaa, "Near-Infrared Fluorescent Proteins, Biosensors, and Optogenetic Tools Engineered from Phytochromes." *Chem Rev* **117**, 6423-6446 (2017) DOI: 10.1021/acs.chemrev.6b00700

[371] K. Moffat, "Time-resolved crystallography and protein design: signalling photoreceptors and optogenetics." *Philos Trans R Soc Lond B Biol Sci* **369**, 20130568 (2014) DOI: 10.1098/rstb.2013.0568

[372] A. Moglich and K. Moffat, "Engineered photoreceptors as novel optogenetic tools." *Photochem Photobiol Sci* **9**, 1286-1300 (2010) DOI: 10.1039/c0pp00167h

[373] Airan, R. D., Thompson, K. R., Fenno, L. E., Bernstein, H. & Deisseroth, K. "Temporally precise *in vivo* control of intracellular signalling." *Nature* **458**, 1025-1029, (2009) DOI:10.1038/nature07926

[374] Deisseroth, K. "Optogenetics: 10 years of microbial opsins in neuroscience." *Nature Neuroscience* **18**, 1213-1225, (2015) DOI:10.1038/nn.4091

[375] Wittmann, T., Dema, A. & van Haren, J. "Lights, cytoskeleton, action: Optogenetic control of cell dynamics." *Current Opinion in Cell Biology* **66**, 1-10, (2020) DOI:10.1016/j.ceb.2020.03.003

[376] Emiliani, V. et al. "Optogenetics for light control of biological systems." *Nature Reviews Methods Primers* **2**, 55, (2022) DOI:10.1038/s43586-022-00136-4

[377] Vlasova, A. D. et al. "Intracellular microbial rhodopsin-based optogenetics to control metabolism and cell signaling." *Chemical Society Reviews* **53**, 3327-3349, (2024) DOI:10.1039/D3CS00699A

[378] Charette, M., Rosenblum, C., Shade, O. & Deiters, A. "Optogenetics with Atomic Precision–A Comprehensive Review of Optical Control of Protein Function through Genetic Code Expansion." *Chemical Reviews* **125**, 1663-1717, (2025) DOI:10.1021/acs.chemrev.4c00224

[379] Hüll, K., Morstein, J. & Trauner, D. "*In Vivo* Photopharmacology." *Chemical Reviews* **118**, 10710-10747, (2018) DOI:10.1021/acs.chemrev.8b00037

[380] Wranik, M. et al. "Watching the release of a photopharmacological drug from tubulin using time-resolved serial crystallography." *Nat Commun* 14, 903, (2023) DOI:10.1038/s41467-023-36481-5

[381] Glover, H. *et al.* "Photoswitch dissociation from a G protein-coupled receptor resolved by time-resolved serial crystallography." *Nature Communications* **15**, 10837, (2024) DOI:10.1038/s41467-024-55109-w

[382] Santini, R. et al. "Targeted Covalent Photoswitch for Two-Photon Control of Endogenous Receptors." *J Am Chem Soc* **148**, 12708-12716, (2026) DOI:10.1021/jacs.5c19954

[383] Miyazaki, T. et al. "*De novo* chemo-optogenetics through the rational design of photoresponsive molecules and selection of their artificial protein binding pairs." *Nature Chemistry*, (2026) DOI:10.1038/s41557-026-02121-w

[384] Stipp, R. *et al.* "Structural Mechanism of an Efficacy Photoswitch Targeting the beta(2)-adrenergic Receptor." *Angew Chem Int Ed Engl*, e17995, (2026) DOI:10.1002/anie.202517995

[385] Gotthard, G. *et al.* "Capturing the blue-light activated state of the Phot-LOV1 domain from *Chlamydomonas reinhardtii* using time-resolved serial synchrotron crystallography." *IUCrJ* **11**, 792-808, (2024) DOI:10.1107/S2052252524005608

[386] Gotthard, G. *et al.* "Fixed-target pump-probe SFX: eliminating the scourge of light contamination." *IUCrJ* **11**, 749-761, (2024) DOI:10.1107/S2052252524005591

[387] Konold, P. E. *et al.* "Microsecond time-resolved X-ray scattering by utilizing MHz repetition rate at second-generation XFELs." *Nature Methods* **21**, 1608-1611, (2024) DOI:10.1038/s41592-024-02344-0

[388] Flores-Ibarra, A. et al. "Light-Oxygen-Voltage (LOV)-sensing Domains: Activation Mechanism and Optogenetic Stimulation." *J Mol Biol* 436, 168356, (2024) DOI:10.1016/j.jmb.2023.168356

[389] Deisseroth, K. & Hegemann, P. "The form and function of channelrhodopsin." *Science* **357**, eaan5544, (2017) DOI:10.1126/science.aan5544

[390] Skopintsev, P. *et al.* "Femtosecond-to-millisecond structural changes in a light-driven sodium pump." *Nature* **583**, 314-318, (2020) DOI:10.1038/s41586-020-2307-8

[391] Mulder, M. *et al.* "Structural Insights Into the Opening Mechanism of C1C2 Channelrhodopsin." *J Am Chem Soc* **147**, 1282-1290, (2025) DOI:10.1021/jacs.4c15402

[392] Dixit, N., Pyari, G. & Roy, S. "Theoretical analysis of low-power optogenetic suppression of action potentials in human ventricular cardiomyocytes expressed with potassium-selective channelrhodopsins." Scientific Reports 16, 9765, (2026) DOI:10.1038/s41598-026-40578-4

[393] E.S. Burgie and R.D. Vierstra, "Phytochromes: an atomic perspective on photoactivation and signaling." *Plant Cell* **26**, 4568-4583 (2014) DOI: 10.1105/tpc.114.131623

[394] N.C. Rockwell, D. Duanmu, S.S. Martin *et al*. "Eukaryotic algal phytochromes span the visible spectrum." *Proc Natl Acad Sci U S A* **111**, 3871-3876 (2014) DOI: 10.1073/pnas.1401871111

[395] M.E. Auldridge and K.T. Forest, "Bacterial phytochromes: more than meets the light." *Crit Rev Biochem Mol Biol* **46**, 67-88 (2011) DOI: 10.3109/10409238.2010.546389

[396] E.S. Burgie, J.A. Clinger, M.D. Miller *et al*. "Photoreversible interconversion of a phytochrome photosensory module in the crystalline state." *Proc Natl Acad Sci U S A* **117**, 300-307 (2020) DOI: 10.1073/pnas.1912041116

[397] F.Li, E.S. Burgie, T. Yu *et al*. "X-ray radiation induces deprotonation of the bilin chromophore in crystalline D. radiodurans phytochrome." *J Am Chem Soc* **137**, 2792-2795 (2015) DOI: 10.1021/ja510923m

[398] A. Schmidt, L. Sauthof, M. Szczepek *et al*. "Structural snapshot of a bacterial phytochrome in its functional intermediate state." *Nat Commun* **9**, 4912 (2018) DOI: 10.1038/s41467-018-07392-7

[399] H. Takala, A. Björling, O. Berntsson *et al*. "Signal amplification and transduction in phytochrome photosensors." *Nature* **509**, 245-248 (2014) DOI: 10.1038/nature13310

[400] A. Ulijasz, G. Cornilescu, C. Cornilescu *et al*. "Structural basis for the photoconversion of a phytochrome to the activated Pfr form." *Nature* **463**, 250-254 (2010) DOI: 10.1038/nature08671

[401] E.S. Burgie, J.M. Walker, G.N. Phillips Jr and R.D. Vierstra, "A photo-labile thioether linkage to phycoviolobilin provides the foundation for the blue/green photocycles in DXCF-cyanobacteriochromes." *Structure* **21**, 88-97 (2013) DOI: 10.1016/j.str.2012.11.001

[402] A. Björling, O. Berntsson, H. Lehtivuori *et al*. "Structural photoactivation of a full-length bacterial phytochrome." *Sci Adv* **2**, e1600920 (2016) DOI: 10.1126/sciadv.1600920

[403] D.J. Heyes, S.J.O. Hardman, M.N. Pedersen *et al*. "Light-induced structural changes in a full-length cyanobacterial phytochrome probed by time-

resolved X-ray scattering." *Commun Biol* **2**, 1 (2019) DOI: 10.1038/s42003-018-0242-0

[404] X. Yang, Z. Ren, J. Kuk and K. Moffat, "Temperature-scan cryocrystallography reveals reaction intermediates in bacteriophytochrome." *Nature* **479**, 428-432 (2011) DOI: 10.1038/nature10506

[405] X. Yang, E.A. Stojković, W.B. Ozarowski, J. Kuk, E. Davydova and K. Moffat, "Light Signaling Mechanism of Two Tandem Bacteriophytochromes." *Structure* **23**, 1179-1189 (2015) DOI: 10.1016/j.str.2015.04.022

[406] N.C. Woitowich, A.S. Halavaty, P. Waltz *et al*. "Structural basis for light control of cell development revealed by crystal structures of a myxobacterial phytochrome." *IUCrJ* **5**, 619-634 (2018) DOI: 10.1107/S2052252518010631

[407] S. Bhattacharya, M.E. Auldridge, H. Lehtivuori, J.A. Ihalainen and K.T. Forest, "Origins of fluorescence in evolved bacteriophytochromes." *J Biol Chem* **289**, 32144-32152 (2014) DOI: 10.1074/jbc.M114.589739

[408] M.E. Auldridge, K.A. Satyshur, D.M. Anstrom and K.T. Forest, "Structure-guided engineering enhances a phytochrome-based infrared fluorescent protein." *J Biol Chem* **287**, 7000-7009 (2012) DOI: 10.1074/jbc.M111.295121

[409] R. Hussein *et al.* "Cryo-electron microscopy reveals hydrogen positions and water networks in photosystem II." *Science* **384**, 1349-1355 (2024) DOI: 10.1126/science.adn6541

[410] J. Yano, J. Kern and V.K. Yachandra, "Structure Function Studies of Photosystem II Using X-Ray Free Electron Lasers." *Annu Rev Biophys* **53**, 1:343-365 (2024) DOI: 10.1146/annurev-biophys-071723-102519

[411] M.D. Doyle, A. Bhowmick, D.C. Wych *et al.* "Water Networks in Photosystem II Using Crystalline Molecular Dynamics Simulations and Room-Temperature XFEL Serial Crystallography." *J Am Chem Soc* **145**, 14621-14635 (2023) DOI: 10.1021/jacs.3c01412

[412] A. Bhowmick, P.S. Simon, I. Bogacz *et al.* "Going around the Kok cycle of the water oxidation reaction with femtosecond X-ray crystallography." *IUCrJ* **10**, 642-655 (2023) DOI: 10.1107/S2052252523008928

[413] A. Bhowmick, R. Hussein, I. Bogacz *et al.* "Structural evidence for intermediates during O_2 formation in photosystem II." *Nature* **617**, 629-636 (2023) DOI: 10.1038/s41586-023-06038-z

[414] M. Ibrahim, N.W. Moriarty, J. Kern *et al.* Reply to Wang *et al*. "Clear evidence of binding of Ox to the oxygen-evolving complex of photosystem II is best observed in the omit map." *Proc Natl Acad Sci U S A.* **118**(24):e2102342118 (2021) DOI: 10.1073/pnas.2102342118

[415] R. Hussein, M. Ibrahim, A. Bhowmick *et al.* "Structural dynamics in the water and proton channels of photosystem II during the S_2 to S_3 transition." *Nat Commun* **12**, 6531 (2021) DOI: 10.1038/s41467-021-26781-z

[416] L. Shen *et al.* "Structure and function of a huge photosystem I–fucoxanthin chlorophyll supercomplex from a coccolithophore." *Science* **389**, eadv2132 (2025) DOI: 10.1126/science.adv2132

[417] R. La Rocca *et al.* "Structure of a photosystem II-FCPII supercomplex from a haptophyte reveals a distinct antenna organization." *Nat Commun* **16**, 4175 (2025) DOI: 10.1038/s41467-025-59512-9

[418] L. Shen *et al.* "Structure of a unique PSII-Pcb tetrameric megacomplex in a chlorophyll d-containing cyanobacterium." *Sci Adv* **10**, eadk7140 (2024) DOI: 10.1126/sciadv.adk7140

[419] A.M. Orville *et al.* in *Ultrafast Electronic and Structural Dynamics* (ed Kiyoshi Ueda) 439-476, Springer Nature Singapore, 2024

[420] Z. Mao *et al.* "Structure and distinct supramolecular organization of a PSII-ACPII dimer from a cryptophyte alga Chroomonas placoidea." *Nat Commun* **15**, 4535 (2024) DOI: 10.1038/s41467-024-48878-x

[421] H. Li, Y. Nakajima, E. Nango *et al.* "Oxygen-evolving photosystem II structures during S_1–S_2–S_3 transitions." *Nature* **626**, 670-677 (2024) DOI: 10.1038/s41586-023-06987-5

[422] H. Li, Y. Nakajima, T. Nomura *et al.* "Capturing structural changes of the S_1 to S_2 transition of photosystem II using time-resolved serial femtosecond crystallography." *IUCrJ* **8**, 431-443 (2021) DOI: 10.1107/S2052252521002177

[423] C.G. Roessler, A. Kuczewski, R. Stearns *et al*. "Acoustic methods for high-throughput protein crystal mounting at next-generation macromolecular crystallographic beamlines." *J Synchrotron Radiat* **20**, 805-808 (2013) DOI: 10.1107/S0909049513020372

[424] I. Bogacz, H. Makita, P.S. Simon *et al.* "Room temperature X-ray absorption spectroscopy of metalloenzymes with drop-on-demand sample delivery at XFELs." *Pure Appl Chem* **95**(8):891-897 (2023) DOI: 10.1515/pac-2023-0213

[425] J. Yano and V. Yachandra, "Mn_4Ca cluster in photosynthesis: where and how water is oxidized to dioxygen." *Chem Rev* **114**, 4175-4205 (2014) DOI: 10.1021/cr4004874

[426] W. Hillier and T. Wydrzynski, "^{18}O-Water exchange in photosystem II: Substrate binding and intermediates of the water splitting cycle." *Coordin Chem Rev* **252**, 306-317 (2008) DOI: 10.1016/j.ccr.2007.09.004

[427] R. Alonso-Mori, D. Sokaras, D. Zhu *et al*. "Photon-in photon-out hard X-ray spectroscopy at the Linac Coherent Light Source." *J Synchrotron Radiat* **22**, 612-620 (2015) DOI: 10.1107/S1600577515004488

[428] R. Alonso-Mori, K. Asa, U. Bergmann *et al*. "Towards characterization of photo-excited electron transfer and catalysis in natural and artificial systems using

XFELs." *Faraday Discuss* **194**, 621-638 (2016) DOI: 10.1039/c6fd00084c

[429] S.C. Jensen, B. Sullivan, D.A. Hartzler *et al*. "X-ray Emission Spectroscopy at X-ray Free Electron Lasers: Limits to Observation of the Classical Spectroscopic Response for Electronic Structure Analysis." *J Phys Chem Lett* **10**, 441-446 (2019) DOI: 10.1021/acs.jpclett.8b03595

[430] T. Tosha, T. Nomura, T. Nishida *et al*. "Capturing an initial intermediate during the P450nor enzymatic reaction using time-resolved XFEL crystallography and caged-substrate." *Nat Commun* **8**, 1585 (2017) DOI: 10.1038/s41467-017-01702-1

[431] Monteiro, D. C. F., Amoah, E., Rogers, C. & Pearson, A. R. "Using photocaging for fast time-resolved structural biology studies." *Acta Crystallogr D Struct Biol* **77**, 1218-1232, (2021) DOI:10.1107/S2059798321008809.

[432] Sandelin, E. et al. "Characterization and evaluation of photolabile (μ-peroxo)(μ-hydroxo)bis[bis(bipyridyl)cobalt caged oxygen compounds to facilitate time-resolved crystallographic studies of cytochrome c oxidase." *Photochemical & Photobiological Sciences* **23**, 839-851, (2024) DOI:10.1007/s43630-024-00558-x

[433] Smyth, P. et al. "Time-resolved serial synchrotron and serial femtosecond crystallography of heme proteins using photocaged nitric oxide." *IUCrJ* **12**, (2025) DOI:10.1107/S2052252525006645

[434] A. Deiters, D. Groff, Y. Ryu, J. Xie and P.G. Schultz, "A genetically encoded photocaged tyrosine." *Angew Chem Int Ed Engl* **45**, 2728-2731 (2006) DOI: 10.1002/anie.200600264

[435] J. Wang, Y. Liu, Y. Liu *et al*. "Time-resolved protein activation by proximal decaging in living systems." *Nature* **569**, 509-513 (2019) DOI: 10.1038/s41586-019-1188-1

[436] R.S. Givens, M. Rubina and J. Wirz, "Applications of p-hydroxyphenacyl (pHP) and coumarin-4-ylmethyl photoremovable protecting groups." *Photochem Photobiol Sci* **11**, 472-488 (2012) DOI: 10.1039/c2pp05399c

[437] L.N. Johnson, "Time-resolved protein crystallography." *Protein Sci* **1**, 1237-1243 (1992) DOI: 10.1002/pro.5560011002

[438] R.H. Austin, K.W. Beeson, L. Eisenstein, H. Frauenfelder and I.C. Gunsalus, "Dynamics of ligand binding to myoglobin." *Biochemistry* **14**, 24, 5355-5373 (1975) DOI: 10.1021/bi00695a021

[439] P. Mondal and M. Meuwly, "Solvent Composition Drives the Rebinding Kinetics of Nitric Oxide to Microperoxidase." *Sci Rep* **8**, 5281 (2018) DOI: 10.1038/s41598-018-22944-z

[440] Y. Murakawa, M. Nagai and Y. Mizutani, "Differences between protein dynamics of hemoglobin upon dissociation of oxygen and carbon monoxide." *J Am Chem Soc* **134**, 1434-1437 (2012) DOI: 10.1021/ja209659w

[441] D. Beece, L. Eisenstein, H. Frauenfelder *et al*. "Dioxygen replacement reaction in myoglobin." *Biochemistry* **18**, 3421-3423 (1979) DOI: 10.1021/bi00582a032

[442] J.C. Flanagan and C.R. Baiz, "Ultrafast pH-jump two-dimensional infrared spectroscopy." *Opt Lett* **44**, 4937-4940 (2019) DOI: 10.1364/OL.44.004937

[443] S. Abbruzzetti, S. Sottini, C. Viappiani and J.E. Corrie, "Kinetics of proton release after flash photolysis of 1-(2-nitrophenyl)ethyl sulfate (caged sulfate) in aqueous solution." *J Am Chem Soc* **127**, 9865-9874 (2005) DOI: 10.1021/ja051702x

[444] Thompson, M. C. "Combining temperature perturbations with X-ray crystallography to study dynamic macromolecules: A thorough discussion of experimental methods." *Methods Enzymol* **688**, 255-305, (2023) DOI:10.1016/bs.mie.2023.07.008

[445] M.C. Thompson, B.A. Barad, A.M. Wolff *et al*. "Temperature-jump solution X-ray scattering reveals distinct motions in a dynamic enzyme." *Nat Chem* **11**, 1058-1066 (2019) DOI: 10.1038/s41557-019-0329-3

[446] D.A. Keedy, L.R. Kenner, M. Warkentin *et al*. "Mapping the conformational landscape of a dynamic enzyme by multitemperature and XFEL crystallography." *Elife* **4**:e07574 (2015) DOI: 10.7554/eLife.07574

[447] M.J. Reddish, R. Callender and R.B. Dyer, "Resolution of Submillisecond Kinetics of Multiple Reaction Pathways for Lactate Dehydrogenase." *Biophys J* **112**, 1852-1862 (2017) DOI: 10.1016/j.bpj.2017.03.031

[448] M.B. Winter, M. A. Herzik Jr, J. Kuriyan and M.A. Marletta, "Tunnels modulate ligand flux in a heme nitric oxide/oxygen binding (H-NOX) domain." *Proc Natl Acad Sci U S A* **108**, E881-889 (2011) DOI: 10.1073/pnas.1114038108

[449] N. Alberding, H. Frauenfelder and P. Hanggi, "Stochastic theory of ligand migration in biomolecules." *Proc Natl Acad Sci U S A* **75**, 26-29 (1978) DOI: 10.1073/pnas.75.1.26

[450] N. Alberding, R.H. Austin, S.S. Chan *et al*. "Fast reactions in carbon monoxide binding to heme proteins." *Biophys J* **24**, 319-334 (1978) DOI: 10.1016/S0006-3495(78)85380-6

[451] C.D.M. Hutchison and J.J. van Thor, "Optical control, selection and analysis of population dynamics in ultrafast protein X-ray crystallography." *Philos Trans A Math Phys Eng Sci* **377**, 20170474 (2019) DOI: 10.1098/rsta.2017.0474

[452] C.D.M. Hutchison, S. Perrett and J.J. van Thor, "XFEL Beamline Optical Instrumentation for Ultrafast Science." *J Phys Chem B.* **128**(37):8855-8868 (2024) DOI: 10.1021/acs.jpcb.4c01492

[453] C.D.M. Hutchison, J.M. Baxter, A. Fitzpatrick *et al.* "Optical control of ultrafast structural dynamics in a fluorescent protein." *Nat. Chem.* **15**, 1607-1615 (2023) DOI: 10.1038/s41557-023-01275-1

454 G.K. Shenoy, J. Stöhr, R.R Freeman *et al*. "LCLS The First Experiments." *SSRL-SLAC Report R-611*, Stanford Linear Accelerator Center, Stanford University (2003) https://www.slac.stanford.edu/pubs/slacreports/reports03/slac-r-611.pdf, access date February 2020

455 D. Davidi, L.M. Longo, J. Jablonska, R. Milo, D.S. Tawfik, "A Bird's-Eye View of Enzyme Evolution: Chemical, Physicochemical, and Physiological Considerations." *Chem Rev.* **118**, 8786-8797 (2018) DOI: 10.1021/acs.chemrev.8b00039

456 A. Bar-Even, E. Noor, Y. Savir *et al*. "The moderately efficient enzyme: evolutionary and physicochemical trends shaping enzyme parameters." *Biochemistry* **50**, 4402-4410 (2011) DOI: 10.1021/bi2002289

457 L. Jeske, S. Placzek, I. Schomburg, A.Chang, D. Schomburg, "BRENDA in 2019: a European ELIXIR core data resource." *Nucleic Acids Res* **47**, D542-D549 (2019) DOI: 10.1093/nar/gky1048

458 C. Walsh, "Enabling the chemistry of life." *Nature* **409**, 226-231 (2001) DOI: 10.1038/35051697

459 S.J.Benkovic and S. Hammes-Schiffer, "A perspective on enzyme catalysis." *Science* **301**, 1196-1202 (2003) DOI: 10.1126/science.1085515

460 G.G. Hammes, "Multiple conformational changes in enzyme catalysis." *Biochemistry* **41**, 26, 8221-8228 (2002) DOI: 10.1021/bi0260839

461 A. Warshel and R.P. Bora, "Perspective: Defining and quantifying the role of dynamics in enzyme catalysis." *J Chem Phys* **144**, 180901 (2016) DOI: 10.1063/1.4947037

462 P.K. Agarwal, "A Biophysical Perspective on Enzyme Catalysis." *Biochemistry* **58**, 6, 438-449 (2019) DOI: 10.1021/acs.biochem.8b01004

463 K.A. Henzler-Wildman, V. Thai, M. Lei *et al*. "Intrinsic motions along an enzymatic reaction trajectory." *Nature* **450**, 838-844 (2007) DOI: 10.1038/nature06410

464 K.A. Henzler-Wildman, M. Lei, V. Thai *et al*. "A hierarchy of timescales in protein dynamics is linked to enzyme catalysis." *Nature* **450**, 913-916 (2007) DOI: 10.1038/nature06407

465 A. Kohen, "Role of dynamics in enzyme catalysis: substantial versus semantic controversies." *Acc Chem Res* **48**, 2, 466-473 (2015) DOI: 10.1021/ar500322s

466 H. Frauenfelder, G. Chen, J. Berendzen *et al*. "A unified model of protein dynamics." *Proc Natl Acad Sci U S A* **106**, 5129-5134 (2009) DOI: 10.1073/pnas.0900336106

467 H. Frauenfelder, S.G. Sligar and P.G. Wolynes, "The energy landscapes and motions of proteins." *Science* **254**, 1598-1603 (1991) DOI: 10.1126/science.1749933

468 R. Milo, P. Jorgensen, U. Moran, G. Weber, M. Springer, "BioNumbers--the database of key numbers in molecular and cell biology." *Nucleic Acids Research* **38**, D750-753 (2010) DOI: 10.1093/nar/gkp889

469 M. Schmidt, "Reaction Initiation in Enzyme Crystals by Diffusion of Substrate." *Crystals* **10**(2) 116 (2020) DOI: 10.3390/cryst10020116

470 M. Schmidt and D.K. Saldin, "Enzyme transient state kinetics in crystal and solution from the perspective of a time-resolved crystallographer." *Struct Dyn* **1**, 024701 (2014) DOI: 10.1063/1.4869472

471 M. Schmidt, "Mix and Inject: Reaction Initiation by Diffusion for Time-Resolved Macromolecular Crystallography." *Advances in Condensed Matter Physics* 2013 (5-6):1-10 (2013) DOI: 10.1155/2013/167276

472 J. Hajdu, R. Neutze, T. Sjögren *et al*. "Analyzing protein functions in four dimensions." *Nat Struct Mol Biol* **7**, 1006-1012 (2000) DOI: 10.1038/80911

473 M. Schmidt, "Time-Resolved Macromolecular Crystallography at Pulsed X-ray Sources." *Int J Mol Sci* **20**(6): 1401 (2019) DOI: 10.3390/ijms20061401

474 M. Schmidt, "Time-Resolved Macromolecular Crystallography at Modern X-Ray Sources." *Methods Mol Biol* **1607**, 273-294 (2017) DOI: 10.1007/978-1-4939-7000-1_11

475 C. Kupitz, J.L. Olmos Jr, M. Holl *et al.* "Structural enzymology using X-ray free electron lasers." *Struct Dyn* **4**(4):044003 (2017) DOI: 10.1063/1.4972069

476 H. van den Bedem and J.S. Fraser, "Integrative, dynamic structural biology at atomic resolution--it's about time." *Nat Methods* **12**, 307-318 (2015) DOI: 10.1038/nmeth.3324

477 J.L. Olmos, S. Pandey, J.M. Martin-Garcia, M. Schmidt *et al. "*Enzyme intermediates captured "on the fly" by mix-and-inject serial crystallography." *BMC Biol* **16**, 59 (2018) DOI: 10.1186/s12915-018-0524-5

478 P. Mehrabi, E.C. Schulz, R. Dsouza *et al*. "Time-resolved crystallography reveals allosteric communication aligned with molecular breathing." *Science* **365**, 1167-1170 (2019) DOI: 10.1126/science.aaw9904

479 I. Ishigami, A. Lewis-Ballester, A. Echelmeier *et al*. "Snapshot of an oxygen intermediate in the catalytic reaction of cytochrome c oxidase." *Proc Natl Acad Sci U S A* **116**, 3572-3577 (2019) DOI: 10.1073/pnas.1814526116

480 S. Horrell, D. Kekilli, K. Sen *et al*. "Enzyme catalysis captured using multiple structures from one crystal at varying temperatures." *IUCrJ* **5**, 283-292 (2018) DOI: 10.1107/S205225251800386X

481 S. Horrell, S.V. Antonyuk, R.R. Eady *et al*. "Serial crystallography captures enzyme catalysis in copper nitrite reductase at atomic resolution from one crystal." *IUCrJ* **3**, 271-281 (2016) DOI: 10.1107/S205225251600823X

482 Y. Fukuda, K.M. Tse, T. Nakane *et al*. "Redox-coupled proton transfer mechanism in nitrite reductase revealed by femtosecond crystallography." *Proc Natl Acad Sci U S A* **113**, 2928-2933 (2016) DOI: 10.1073/pnas.1517770113

[483] S.P, Muench, S.V. Antonyuk, S.S. Hasnain, "The expanding toolkit for structural biology: synchrotrons, X-ray lasers and cryoEM." *IUCrJ* **6**, 167-177 (2019) DOI: 10.1107/S2052252519002422

[484] G.D. Calvey, A.M. Katz and L. Pollack, "Microfluidic Mixing Injector Holder Enables Routine Structural Enzymology Measurements with Mix-and-Inject Serial Crystallography Using X-ray Free Electron Lasers." *Anal Chem* **91**, 7139-7144 (2019) DOI: 10.1021/acs.analchem.9b00311

[485] G.D. Calvey, A.M. Katz, C.B. Schaffer and L. Pollack, "Mixing injector enables time-resolved crystallography with high hit rate at X-ray free electron lasers." *Struct Dyn* **3**, 054301 (2016) DOI: 10.1063/1.4961971

[486] D.C.F. Monteiro, M. Vakili, J. Harich *et al*. "A microfluidic flow-focusing device for low sample consumption serial synchrotron crystallography experiments in liquid flow." *J Synchrotron Radiat* **26**, 406-412 (2019) DOI: 10.1107/S1600577519000304

[487] M.L. Grünbein and G. Nass Kovacs, "Sample delivery for serial crystallography at free-electron lasers and synchrotrons, *Acta Crystallogr D Struct Biol* **75**, 178-191 (2019) DOI: 10.1107/S205979831801567X

[488] M.L. Grünbein, R.L. Shoeman and R.B. Doak, "Velocimetry of fast microscopic liquid jets by nanosecond dual-pulse laser illumination for megahertz X-ray free-electron lasers." *Opt Express* **26**, 7190-7203 (2018) DOI: 10.1364/OE.26.007190

[489] M.L. Grünbein, J. Bielecki, A. Gorel *et al*. "Megahertz data collection from protein microcrystals at an X-ray free-electron laser." *Nat Commun* **9**, 3487 (2018) DOI: 10.1038/s41467-018-05953-4

[490] M.O. Wiedorn, D. Oberthür, R. Bean *et al*. "Megahertz serial crystallography." *Nat Commun* **9,** 4025 (2018) DOI: 10.1038/s41467-018-06156-7

[491] J.J.A.G. Kamps, R. Bosman, A.M. Orville and P. Aller in *Method Enzymol* Vol. 709 (eds Peter Moody & Hanna Kwon) 57-103 (Academic Press, 2024)

[492] R.C. Nguyen *et al.* "In Situ Structural Observation of a Substrate- and Peroxide-Bound High-Spin Ferric-Hydroperoxo Intermediate in the P450 Enzyme CYP121." *J Am Chem Soc* **145**, 25120-25133 (2023) DOI: 10.1021/jacs.3c04991

[493] H. Makita, P.S. Simon, J. Kern, J. Yano and V.K. Yachandra, "Combining on-line spectroscopy with synchrotron and X-ray free electron laser crystallography." *Curr Opin Struct Biol* **80**, 102604 (2023) DOI: 10.1016/j.sbi.2023.102604

[494] H. Lebrette, V. Srinivas, J. John *et al.* "Structure of a ribonucleotide reductase R2 protein radical." *Science* **382**, 109-113 (2023) DOI: 10.1126/science.adh8160

[495] J. John, O. Aurelius, V. Srinivas *et al.* "Redox-controlled reorganization and flavin strain within the ribonucleotide reductase R2b–NrdI complex monitored by serial femtosecond crystallography." *eLife* **11**, e79226 (2022) DOI: 10.7554/eLife.79226

[496] P. Rabe *et al.* "X-ray free-electron laser studies reveal correlated motion during isopenicillin N synthase catalysis." *Science Advances* **7**, eabh0250 (2021) DOI: 10.1126/sciadv.abh0250

[497] A. Butryn *et al.* "An on-demand, drop-on-drop method for studying enzyme catalysis by serial crystallography." *Nat Commun* **12**, 4461 (2021) DOI: 10.1038/s41467-021-24757-7

[498] M.W. Mara, R.G. Hadt, M.E. Reinhard *et al*. "Metalloprotein entatic control of ligand-metal bonds quantified by ultrafast x-ray spectroscopy." *Science* **356**, 1276-1280 (2017) DOI: 10.1126/science.aam6203

[499] R.H. Holm and E.I. Solomon, "Introduction: Bioinorganic enzymology II." *Chem Rev* **114**, 4039-4040 (2014) DOI: 10.1021/cr5001332

[500] E.I. Solomon, R.K. Szilagyi, S. DeBeer George and L. Basumallick, "Electronic structures of metal sites in proteins and models: contributions to function in blue copper proteins." *Chem Rev* **104**, 419-458 (2004) DOI: 10.1021/cr0206317

[501] R.H. Holm, P. Kennepohl and E.I. Solomon, Structural and Functional Aspects of Metal Sites in Biology, *Chem Rev* **96**, 2239-2314 (1996) DOI: 10.1021/cr9500390

[502] N.K. Sauter, J. Kern, J. Yano and J.M. Holton, "Towards the spatial resolution of metalloprotein charge states by detailed modeling of XFEL crystallographic diffraction." *Acta Crystallogr D Struct Biol* **76**, 176-192 (2020) DOI: 10.1107/S2059798320000418

[503] O. Einsle, S.L. Andrade, H. Dobbek, J. Meyer and D.C. Rees, "Assignment of individual metal redox states in a metalloprotein by crystallographic refinement at multiple X-ray wavelengths." *J Am Chem Soc* **129**, 8, 2210-2211 (2007) DOI: 10.1021/ja067562o

[504] T. Spatzal, J. Schlesier, E.M. Burger *et al*. Nitrogenase FeMoco investigated by spatially resolved anomalous dispersion refinement, *Nat Commun **7***, 10902 (2016) DOI: 10.1038/ncomms10902

[505] L. Zhang, J.T. KaiserG. Meloni *et al*. "The sixteenth iron in the nitrogenase MoFe protein." *Angew Chem Int Ed Engl 52*, 10529-10532 (2013) DOI: 10.1002/anie.201303877

[506] D.L. Zhu, M. Cammarata, J.M. Feldkamp *et al*. "A single-shot transmissive spectrometer for hard x-ray free electron lasers." *Appl Phys Lett* **101**, 034103 (2012) DOI: 10.1063/1.4736725

[507] J. Hattne, N. Echols, R. Tran *et al*. "Accurate macromolecular structures using minimal measurements from X-ray free-electron lasers." *Nat Methods* **11**, 545-548 (2014) DOI: 10.1038/nmeth.2887

[508] J. Sanchez-Weatherby, J, Sandy, H. Mikolajek *et al*. "VMXi: a fully automated, fully remote, high-flux in

situ macromolecular crystallography beamline." *J Synchrotron Radiat* **26**, 291-301 (2019) DOI: 10.1107/S1600577518015114

509 Klureza, M. A. *et al.* "Multiplexing methods in dynamic protein crystallography." *Methods Enzymol* **709**, 177-206, (2024) DOI:10.1016/bs.mie.2024.10.009

510 Yorke, B. A., Beddard, G. S., Owen, R. L. & Pearson, A. R. "Time-resolved crystallography using the Hadamard transform." *Nature Methods* **11**, 1131, (2014) DOI:10.1038/nmeth.3139

511 Laxmi, S., Jaho, S., Myers, W. K., Vincent, K. A. & Carr, S. B. "Crystallise, poise, capture: a multimodal platform for correlated structural and spectroscopic characterisation of redox enzymes." *J Biol Inorg Chem,* (2026) DOI:10.1007/s00775-026-02148-x

512 L. Pravda, K. Berka, R. Svobodová Vařeková *et al.* "Anatomy of enzyme channels." *BMC Bioinformatics* **15**, 379 (2014) DOI: 10.1186/s12859-014-0379-x

513 D.H. Juers and J. Ruffin, "MAP_CHANNELS: a computation tool to aid in the visualization and characterization of solvent channels in macromolecular crystals." *J Appl Crystallogr* **47**, 2105-2108 (2014) DOI: 10.1107/S160057671402281

514 R.G. Coleman and K.A. Sharp, "Finding and characterizing tunnels in macromolecules with application to ion channels and pores." *Biophys J* **96**, 632-645 (2009) DOI: 10.1529/biophysj.108.135970

515 M. Heymann, A. Opthalage, J.L. Wierman *et al.* "Room-temperature serial crystallography using a kinetically optimized microfluidic device for protein crystallization and on-chip X-ray diffraction." *IUCrJ* **1**(Pt 5), 349-360 (2014) DOI: 10.1107/S2052252514016960

516 B.G. Abdallah, N.A. Zatsepin, S. Roy-Chowdhury *et al*. "Microfluidic sorting of protein nanocrystals by size for X-ray free-electron laser diffraction." *Struct Dyn* **2**, 041719 (2015) DOI: 10.1063/1.4928688

517 P.F. Zhu *et al*. "Femtosecond time-resolved MeV electron diffraction." *New J Phys* **17** 063004 (2015) DOI: 10.1088/1367-2630/17/6/063004

518 T. Vecchione, P. Denes, R.K. Jobe *et al*. "A direct electron detector for time-resolved MeV electron microscopy." *Rev Sci Instrum* **88**, 033702 (2017) DOI: 10.1063/1.4977923

519 J.P.F. Nunes, K. Ledbetter, M. Lin *et al*. "Liquid-phase mega-electron-volt ultrafast electron diffraction." *Struct Dyn* **7**, 024301 (2020) DOI: 10.1063/1.5144518

520 Kingwell, K. "Na(V)1.8 inhibitor poised to provide opioid-free pain relief." *Nat Rev Drug Discov* 24, 3-5, (2025) DOI:10.1038/d41573-024-00203-3

521 Broadfoot, M. "A New Type of Pain Pill: A novel drug blocks pain signals before they reach the brain, and it doesn't carry the addiction potential of opioids." *Sci Am* 331, 56, (2024) DOI:10.1038/scientificamerican092024-1N1UgwhFnhAK4VKi2kb6rv

522 Jones, J. *et al.* "Selective Inhibition of Na(V)1.8 with VX-548 for Acute Pain." *N Engl J Med* **389**, 393-405, (2023) DOI:10.1056/NEJMoa2209870

523 Huang, X. *et al.* "Structural basis for high-voltage activation and subtype-specific inhibition of human Na(v)1.8." *Proc Natl Acad Sci USA* **119**, e2208211119, (2022) DOI:10.1073/pnas.2208211119

524 A. Barty, C. Caleman, A. Aquila *et al*. "Self-terminating diffraction gates femtosecond X-ray nanocrystallography measurements." *Nature Photon* **6**, 35-40 (2012) DOI: 10.1038/nphoton.2011.297

525 R.A. Kirian, T. A. White, J.M. Holton *et al*. "Structure-factor analysis of femtosecond microdiffraction patterns from protein nanocrystals." *Acta Crystallogr A* **67**, 131-140 (2011) DOI: 10.1107/S0108767310050981

526 C.D.M. Hutchison and J.J. van Thor, "Populations and coherence in femtosecond time resolved X-ray crystallography of the photoactive yellow protein." *Int Rev Phys Chem* **36**, 117-143 (2017) DOI: 10.1080/0144235x.2017.1276726

527 A.T.N. Kumar, F. Rosca, A. Widom and P.M. Champion, "Investigations of ultrafast nuclear response induced by resonant and nonresonant laser pulses." *J Chem Phys* **114**, 6795-6815 (2001) DOI: 10.1063/1.1356011

528 A.T.N. Kumar, F. Rosca, A. Widom and P.M. Champion, "Investigations of amplitude and phase excitation profiles in femtosecond coherence spectroscopy." *J Chem Phys* **114**, 701-724 (2001) DOI: 10.1063/1.1329640

529 F. Rosca, A.T.N. Kumar, X. Ye, T. Sjodin, A.A. Demidov and P.M. Champion, "Investigations of coherent vibrational oscillations in myoglobin." *J Phys Chem A* **104**, 18, 4280-4290 (2000) DOI: 10.1021/jp993617f

530 C.J. Bardeen, Q. Wang and C.V. Shank, "Femtosecond chirped pulse excitation of vibrational wave packets in LD690 and bacteriorhodopsin." *J Phys Chem A* **102**, 17, 2759-2766 (1998) DOI: 10.1021/jp980346k

531 A. McClelland, A. Demidov, A. Benabbas *et al*. "Direct Observations of Low Frequency Vibrational Coherences in wt-GFP." *AIP Conference Proceedings* **1267**, 674-675 (2010) DOI: 10.1063/1.3482744

532 H. Kuramochi, S. Takeuchi and T. Tahara, "Femtosecond time-resolved impulsive stimulated Raman spectroscopy using sub-7-fs pulses: Apparatus and applications." *Review of Scientific Instruments* **87**(4): 043107 (2016) DOI: 10.1063/1.4945259

533 J.J. van Thor, "Coherent two-dimensional electronic and infrared crystallography." *J Chem Phys* **150**(12): 124113 (2019) DOI: 10.1063/1.5079319

[534] C.D.M. Hutchison, M. Kaucikas, J. Tenboer *et al*. "Photocycle populations with femtosecond excitation of crystalline photoactive yellow protein." *Chem Phys Lett* **654**, 63-71 (2016) DOI: 10.1016/j.cplett.2016.04.087

[535] C.N. Lincoln, A.E. Fitzpatrick and J.J. van Thor, "Photoisomerization quantum yield and non-linear cross-sections with femtosecond excitation of the photoactive yellow protein." *Phys Chem Chem Phys* **14**, 15752-15764 (2012) DOI: 10.1039/c2cp41718a

[536] A. Fadini, S. Reiche, K. Naas and J.J. van Thor, "Applications and Limits of Time-to-Energy Mapping of Protein Crystal Diffraction Using Energy-Chirped Polychromatic XFEL Pulses." *Appl. Sci.* **10**(7), 2599 (2020) DOI: 10.3390/app10072599

[537] E. Prat, M. Calvi and S. Reiche, "Generation of ultra-large-bandwidth X-ray free-electron-laser pulses with a transverse-gradient undulator." *J Synchrotron Radiat* **23**, 874-879 (2016) DOI: 10.1107/S1600577516007177

[538] A.S. Hernandez, E. Prat, S. Bettoni, B. Beutner and S. Reiche, "Generation of large-bandwidth x-ray free-electron-laser pulses." *Phys Rev Accel Beams* **19**, 090702 (2016) DOI: 10.1103/PhysRevAccelBeams.19.090702

[539] E. Prat, P. Dijkstal, E. Ferrari and S. Reiche, "Demonstration of Large Bandwidth Hard X-Ray Free-Electron Laser Pulses at SwissFEL." *Phys Rev Lett* **124**(7):074801 (2020) DOI: 10.1103/PhysRevLett.124.074801

[540] R. Neutze, R. Wouts, D. van der Spoel *et al*. "Potential for biomolecular imaging with femtosecond X-ray pulses." *Nature* **406**, 752-757 (2000) DOI: 10.1038/35021099

[541] R. Neutze and J. Hajdu, "Femtosecond time resolution in x-ray diffraction experiments." *Proc Natl Acad Sci U S A* **94**(11): 5651-5655 (1997) DOI: 10.1073/pnas.94.11.5651

[542] I. Poudyal, M. Schmidt and P. Schwander, "Single-particle imaging by x-ray free-electron lasers-How many snapshots are needed?." *Struct Dyn* **7**(2): 024102 (2020) DOI: 10.1063/1.5144516

[543] A. Hosseinizadeh, G. Mashayekhi, J. Copperman *et al*, "Conformational landscape of a virus by single particle X-ray scattering." *Nat Methods* **14**, 877-881 (2017) DOI: 10.1038/nmeth.4395

[544] E. Sobolev, S. Zolotarev, K. Giewekemeyer *et al*. "Megahertz single-particle imaging at the European XFEL." *Commun Phys* **3**, 97 (2020) DOI: 10.1038/s42005-020-0362-y

[545] J. Bielecki, F. Maia and A.P. Mancuso, "Perspectives on single particle imaging with x rays at the advent of high repetition rate x-ray free electron laser sources." *Struct Dyn* **7**, 040901 (2020) DOI: 10.1063/4.0000024

[546] T. You, J. Bielecki and F. Maia, "Impact of gas background on XFEL single-particle imaging." *Sci Rep* **15**, 29559 (2025) DOI: 10.1038/s41598-025-15092-8

[547] M. Stransky *et al.* "Computational study of diffraction image formation from XFEL irradiated single ribosome molecule." *Sci Rep* **14**, 10617 (2024) DOI: 10.1038/s41598-024-61314-w

[548] Z. Shen *et al.* "Resolving Nonequilibrium Shape Variations among Millions of Gold Nanoparticles." *ACS Nano* **18**, 15576-15589 (2024) doi:10.1021/acsnano.4c00378

[549] J. E, M. Stransky, Z. Shen *et al.* "Water layer and radiation damage effects on the orientation recovery of proteins in single-particle imaging at an X-ray free-electron laser." *Sci Rep* **13**, 16359 (2023) DOI: 10.1038/s41598-023-43298-1

[550] A. Round *et al.* in *Advanced Technologies for Protein Complex Production and Characterization: Volume II* (eds M. Cristina Vega & Francisco J. Fernández) 141-162, Springer Nature Switzerland, 2024

[551] T. Ekeberg *et al.* "Observation of a single protein by ultrafast X-ray diffraction." *Light Sci Appl* **13**, 15 (2024) DOI: 10.1038/s41377-023-01352-7

[552] K. Ayyer, P.L. Xavier, J. Bielecki *et al*. "3D diffractive imaging of nanoparticle ensembles using an X-ray laser" (2020) arXiv:2007.13597 [physics.app-ph]

[553] C. Uetrecht, K. Lorenzen, M. Kitel *et al*. "Native mass spectrometry provides sufficient ion flux for XFEL single-particle imaging." *J. Synchrotron Rad.* 2b6, 653-659 (2019) DOI: 10.1107/S1600577519002686

[554] K. Giewekemeyer, A. Aquila, N.D. Loh *et al*. "Experimental 3D coherent diffractive imaging from photon-sparse random projections." *IUCrJ* **6**, 357-365 (2019) DOI: 10.1107/S2052252519002781

[555] J. Bielecki, M.F. Hantke, B.J. Daurer *et al*. "Electrospray sample injection for single-particle imaging with x-ray lasers." *Sci Adv.* **5**, eaav8801 (2019) DOI: 10.1126/sciadv.aav8801

[556] A. Aquila, A. Barty, C. Bostedt *et al*. "The linac coherent light source single particle imaging road map." *Struct Dyn* **2**, 041701 (2015) DOI: 10.1063/1.4918726

[557] Z.B. Sun, J.D. Fan, H.Y. Li and H.D. Jiang, "Current Status of Single Particle Imaging with X-ray Lasers." *Appl Sci* **8**(1), 132 (2018) DOI: 10.3390/app8010132

[558] R. Yan, Y. Zhang, Y. Li, L. Xia, Y. Guo and Q. Zhou, "Structural basis for the recognition of the SARS-CoV-2 by full-length human ACE2." *Science* **367**(6485): 1444-1448 (2020) DOI: 10.1126/science.abb2762

[559] D. Wrapp, N. Wang, K.S. Corbett *et al.* "Cryo-EM structure of the 2019-nCoV spike in the prefusion conformation." *Science* **367**, 1260-1263 (2020) DOI: 10.1126/science.abb2507

[560] A.C. Walls, Y.J. Park, M.A. Tortorici, A. Wall, A.T. McGuire and D. Veesler, "Structure, Function, and Antigenicity of the SARS-CoV-2 Spike Glycoprotein." *Cell* (2020) DOI: 10.1016/j.cell.2020.02.058

[561] T.P. Velavan and C.G. Meyer, "The COVID-19 epidemic." *Trop Med Int Health* **25**(3): 278-280 (2020) DOI: 10.1111/tmi.13383

[562] Z. Shen, Y. Xiao, L. Kang *et al.* "Genomic diversity of SARS-CoV-2 in Coronavirus Disease 2019 patients." *Clin Infect Dis*. **ciaa203** (2020) DOI: 10.1093/cid/ciaa203

[563] S.E. Thomas, P. Collins, R.H. James *et al.* "Structure-guided fragment-based drug discovery at the synchrotron: screening binding sites and correlations with hotspot mapping." *Philos Trans A Math Phys Eng Sci* **377**, 20180422 (2019) DOI: 10.1098/rsta.2018.0422

[564] D. Zhang, M.S. Markoulides, D. Stepanovs *et al*. "Structure activity relationship studies on rhodanines and derived enethiol inhibitors of metallo-β-lactamases." *Bioorg Med Chem* **26**(11): 2928-2936 (2018) DOI: 10.1016/j.bmc.2018.02.043

[565] P.M. Collins, A. Douangamath, R. Talon *et al*. "Achieving a Good Crystal System for Crystallographic X-Ray Fragment Screening." *Methods Enzymol* **610**, 251-264 (2018) DOI: 10.1016/bs.mie.2018.09.027

[566] D. Bowkett, R. Talon, C. Tallant *et al*. "Identifying Small-Molecule Binding Sites for Epigenetic Proteins at Domain-Domain Interfaces." *ChemMedChem* **13**(10), 1051-1057 (2018) DOI: 10.1002/cmdc.201800030

[567] P.M. Collins, J.T. Ng, R. Talon *et al*. "Gentle, fast and effective crystal soaking by acoustic dispensing." *Acta Crystallogr D Struct Biol* **73**, 246-255 (2017) DOI: 10.1107/S205979831700331X

8. Opportunities for Technology and Applications

Measurement of processes at their essential lengths and timescales is immensely important to advancing technology, as well as to science. Key sectors of industry and manufacturing, such as engineering, advanced manufacturing and materials, chemicals, medicines/pharmaceuticals, consumer/household products, food, automotive, energy, agriculture and electronics, will substantially benefit from these advances, with societal impact in growth, healthcare, environment, transport and defence.

The case presented so far has emphasised science opportunities, but there always have been clear connections to technology and the broader application of the methods and knowledge afforded by XFEL science. As discussed in **Chapter 2**, the capability to measure matter at the quantum scales of both *time* and *space* inevitably connects to advanced technologies and manufacturing. A further example is the Chemicals sector, which in 2022 had an annual turnover in the UK of £70 billion, representing 1.2% of UK GDP and accounting for 15% of UK exports and 12% of imports.[1] It generated £21.9 billion of Gross Value Added (GVA) for the UK economy, comparable to the contributions of the life sciences, automotive and aerospace sectors[1]. The Chemicals sector underpins other industries, including pharmaceuticals, agriculture and manufacturing[1]. As discussed in **Section 6.4.1**, from a societal point of view, the chemical manufacturing and pharmaceutical industry accounted for around 136,000 direct jobs in 2025 and an additional 500,000 in its supply chain.[1] Any deep understanding of materials and matter, including their genesis, transformations and performance under conditions of applications, opens up new innovation routes to high value-added products.

This section explicitly addresses some of the opportunities foreseen for UK Industry. This survey is not complete, as myriad industrial and broader societal impacts are anticipated, but the ones that are highlighted are illustrative of the broad potential. In **Chapter 10**, the impact of a next-generation XFEL is discussed in the context of the key sectors identified in the UK government's Industrial Strategy, and connected to the emerging UKRI themes. Here we examine a sample of areas that we see as having high potential impact: shocked materials, crystallisation and nucleation in soft materials, dynamic processes in advanced manufacturing, catalysis, materials for energy generation, and life sciences in pharma and bio-tech. The cases explored include:

- The behaviour of shocked materials relevant to diverse applications, ranging from turbines to explosives, and feeding into UK engineering and defence
- The fundamental understanding and measurement capabilities to track the formation of solid phases from liquids, which is relevant to situations ranging from food processing to lubrication of engines to drug discovery and medicines manufacturing
- Development of a quantitative understanding of mechanisms in advanced manufacturing in order to optimise processes such as friction welding, additive manufacturing and laser processing, and even to develop new concepts in X-ray lithography for beyond the next generation chip manufacture
- Probing compression and instability formation in inertial confined fusion energy and probing materials and radiation damage mitigation, e.g. in the first wall region of a fusion energy plant, to support fusion energy regardless of confinement method
- Building on SFX structural biology and time-resolved methods to use insights from life sciences to address the most pressing questions in drug discovery, human health and agriculture.

The applications of XFELs to solving industrial and societal problems are at the heart of the strategic case for a next-generation XFEL. Such applications feature in our **Flagship Research Programmes** (**Section 9.4**), where eight of the 11 cases presented address real world problems ranging across Green Chemistry, Batteries, Fusion Energy, Advanced Electronics and Brain Imaging at the Nanoscale.

8.1 Properties of shocked materials for engineering and defence

The properties of materials under shock loading conditions are of both fundamental scientific interest and importance across a wide range of engineering domains, from aerospace through to defence.[2] XFEL technology is driving rapid progress in the underpinning science in this area, and represents an accelerated pathway for the manufacturing and qualification of the next generation of engineering materials and processes.

8.1.1 New understanding of materials response at multiple scales

With the advent of high-brilliance, femtosecond duration hard X-ray FEL sources, an understanding of the rich array of the underlying microscopic processes, which govern the macroscopic response of heterogenous engineering-relevant materials to rapid loading and unloading, is now within reach. The routes by which materials deform and respond to external stresses are complex, as they depend not only on the underlying structure (the particular crystal phase), but also on the evolution of the population of defects within the system that mediate plastic flow. Given that defect density itself is strain and strain-rate dependent, a comprehensive understanding of material strength, and response to impact, all the way from the microscale of the lattice dynamics to the macroscale of system response on engineering length-scales remains largely elusive. XFELs are starting to have significant impact in bridging this important gap in our knowledge, with large angle diffraction techniques (that measure structure, lattice spacings and orientations) and small angle scattering (which can measure void evolution) and developing dynamic imaging approaches (see **Section 9.4 Flagship Science and Technology Programmes VI and VII**) combining to provide hitherto inaccessible insights into the pertinent physics on the atomic scale. Furthermore, the femtosecond nature of the X-ray beam ensures that all measurements are free from motional blurring, with the diffraction signals being recorded on a timescale even shorter than that of the oscillation period of atomic vibrations.

Importantly, these measurements can also now be augmented with computer simulations on precisely the same length scales (several microns) and timescales (spanning picoseconds to nanoseconds). Multi-million (or billion) atom molecular dynamics simulations can now be performed, from which simulated diffraction patterns (linking the micro and macro properties) can be extracted and compared with experiment. The fidelity of these simulations itself relies on a good knowledge of the interatomic potentials between atoms, but here a feedback loop engendered by a comparison of experimental results and theoretical prediction will play an increasingly important role in verifying the development of the potentials themselves.

An understanding of material flow under rapid impact is important in both fundamental and applied sciences. At the fundamental level, impact phenomena have played an important part in the evolution and modification of our own and other planets, and the resultant flow of material can be seen at the extremes of the macroscale in geological features such as the Chicxulub crater in Mexico, or are readily apparent from a casual glance upwards at our moon. In the applied sciences arena, the applications in the defence industry are obvious, whilst the response of matter to high velocity impact is also important in design of protection for satellites, space stations, future space habitats and their electronics from impact with high velocity grains of dust of even few micron dimension.[3] What is perhaps less known is that laser-ablative impact treatment of materials via so-called ‘laser-peening’ can induce residual compressive stresses in the surface of materials, which can retard crack initiation and growth, thus increasing the fatigue strength of important engineering components.[4, 5] However, very little in situ experimental data exists on the underpinning evolution of the defect landscape and microstructure during this process, and enhanced physical understanding could well lead to improved material-properties outcomes.

Progress to date in using XFELs to reveal lattice-level information has already been spectacular. As noted above, both structure and strain rate play important roles in the dynamic response of materials.

At extremely high strain rates, it had long been predicted that the initial response of a material would be purely elastic until its ultimate yield strength limit (hundreds of times greater than realised in practice) was reached, as even pre-existing defects and dislocations would not have time to relieve plastic flow under high-velocity impact for the first few tens of picoseconds.[6] Such 'super-elastic' response, reaching the ultimate compressive strength of a pure crystal but within an initially defective sample, has been demonstrated and observed via such femtosecond diffraction in copper samples.[7] It is also now known that some of the most complex phase transitions that a single element can undergo can be induced and observed within samples compressed for just a few nanoseconds, with the transitions in both scandium[8] and antimony[9] exhibiting the change from regular crystalline matter to a complex incommensurate 'host-guest' phase under rapid compression.

The opportunity to study the relative importance of plasticity mechanisms within a given sample has also been demonstrated. The femtosecond pulses of X-rays not only afford information on structure and lattice spacing, but also on the orientation of the lattice planes during deformation, allowing us to distinguish between the amount of impact damage internalised as twinning, as opposed to direct dislocation motion – such proof of principle experiments have been conducted in tantalum samples.[10] Importantly, the defective nature of the sample was monitored during the release of the shock pressure from the sample, and the microstructural changes induced by the shock (that is to say the density of both twins and lattice rotation due to other defects) was shown to be largely annihilated upon rarefaction:[11] the state of the sample (in terms of its microstructure) during impact is very different from that which one would observe in a sample that was recovered and analysed after the event itself. This observation highlights the imperative of performing such in situ real-time experiments that X-ray lasers make possible.

In other experiments, small-angle X-ray scattering has been used to diagnose the details of cavitation underlying spall failure and excellent agreement was obtained with molecular dynamics simulations.[12] These experiments typically employ a sample thickness on the order of a few microns and X-ray photon energy on the order of 10 keV, although an FEL with higher photon energies would allow study of thicker samples approaching engineering length scales, as well as provide for greater exploration of reciprocal space, which would be especially useful in elucidating complex structures formed under shock and ramp compression.

At the mesoscale, the relationship between material response and microstructural parameters, such as grain size distribution and orientation (texture), must be understood. With this understanding, the opportunity for new engineering materials with designed-in properties arises.[13] Molecular dynamics calculations of the role of individual and idealised collections of grains under impact has started to be studied,[14] affording opportunities for transferring the lessons learnt from the modelling to the design of specific FEL-based experiments to learn about grain-grain interactions, and the dependence of material response on grain size as well as texture.

It should be noted that the methods described above are not limited to metals and metal alloys but are applicable to a wide range of engineering materials which include polymers, ceramics and their composites. These systems too have outstanding fundamental questions surrounding their responses to impact loading. Explosives for example, are heterogeneous systems containing grains, pores and cracks,[15] and consequently exhibit complex physical phenomena over multiple length scales[16] (see **Figure 8.1**) which underpin performance and safety. Recently, XFEL experiments employing explosive samples have studied phase changes under shock compression and the role of micron-scale inhomogeneities in detonation initiation.[17]

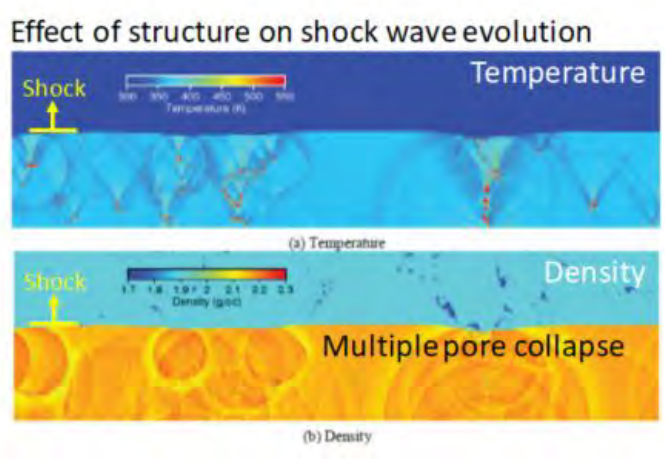


Figure 8.1: Shock propagation in an explosive (from Ref. [15])

(Ministry of Defence © Crown Owned Copyright 2020/AWE)

*Reproduced from B. Lambourn and C. Handley, AIP Conference Proceedings **1793**, 120025 (2017), DOI: 10.1063/1.4971707, with the permission of AIP Publishing*

At the macroscale, the sample size is representative of components used in applications, and so engineering processes can be studied and optimised. These include (as noted above) laser peening,[4,5] foreign object damage to turbine blades,[18] laser powder additive manufacturing (AM) (reference,[19] and **Section 8.3**) and explosive initiators.[20] At the typical operating scale of several millimetres, X-ray energies up to ~ 100 keV are required for single-shot imaging and X-ray diffraction studies.[21] Although these processes occur on relatively slow timescales (< 100 ns), the fast time resolution offered by an XFEL can help to elucidate dynamics occurring very early in time.

8.1.2 Future opportunities

In order to access the high-pressure shock conditions of interest in samples with thickness of a few microns, an optical driver is necessary, and this would also be a requirement for a next generation XFEL facility. The newly developed UK (CLF) DiPOLE laser system,[22] for example, can access multi-Mbar pressures at a 10 Hz repetition rate (**Section 4.1**) and we anticipate increasing both energy and repetition rate. Such a laser would also find application in laser peening and particle impact studies (in the latter case by using the laser to propel a particle off a surface towards a target), but a higher energy (multi-kJ) system would allow us to access even higher pressures, taking us into the regime of relevance for planetary science. Opportunities exist for overlap with interests in a laser-driven compression facility (see **Section 4.4**). It is anticipated that wide-angle dynamic imaging with sub-micron resolution alongside scattering will play a crucial role in fully interrogating processes at all relevant length and time scales.

For studies at longer length-scales and loading durations, a bespoke precision impact system, analogous to a single- or multiple-stage gas gun, will be required. Such a system will enable sustained loading over several 10s of nanoseconds in samples ranging from 10s – 100s of micrometres, thereby bridging the gap between crystal physics and the mesoscale, permitting study of cumulative deformation and damage processes such as adiabatic shear, spallation, jetting and fragmentation, and potentially the study of samples of shape and geometry that are analogous to those in real engineering applications. We note that the coupling of such a mechanical driver to a short-pulse X-ray source has already been proven at the Advanced Photon Source synchrotron,[23] albeit with X-ray pulses of much longer duration (100 ps) than can be produced at a FEL. As we move up in length scale and Z, the photon energies required will increase, and further studies of the flux of the higher harmonics of any FEL design will need to be taken into consideration. Finally, we note that as well as shock drivers specifically tailored for the FEL, this branch of science will also require state-of-the-art secondary shock diagnostics to understand the states generated, including, velocimetry, pyrometry, and imaging. For other applications, specialised equipment is required – such as a process replicator for Additive Manufacturing studies.[19]

8.2 Multiphase-multicomponent formulated products

Consumer product, chemical and pharmaceutical manufacturing are part of the chemistry-using industries and make a gross value-added (GVA) annual contribution of more than £65 billion to the UK economy. The properties of organic solids in particular present enormous industrial R&D challenges, because key interactions and transformations are poorly understood at the molecular level. These include, for example, solubilisation, nucleation, crystal growth, dissolution and agglomeration. For decades, the science of these phenomena has progressed slowly due to the experimental challenges associated with localised spatiotemporally rare events. The time and imaging capabilities afforded by XFEL scattering and spectroscopies open up a realistic perspective to progress in this area.

Control of phase separations, such as nucleation, solidification and crystallisation, is essential for the manufacture of formulated products across virtually all industry sectors involving chemicals, for example medicines, foods, detergents, lubricants and agrochemicals. Practical bottlenecks in chemical product design and manufacture arise from the challenging properties of crystalline solids and their interfacial interactions (both solid-solid and solid-liquid interactions). Especially for organic materials, crystal structure, size, morphology, mechanical properties, solubility and surface properties of particles combine to create complex manufacturing challenges. The predictive design of multi-phase multi-component products requires a deeper understanding of key transformations (e.g. nucleation, crystal growth, dissolution, agglomeration solubilisation), including the impact of process conditions (temperature, pressure, composition, mixing). They result in what is typically a product with multi-scale structure that nucleates through localised rare events at the molecular level. Understanding the ultrafast structural and electronic dynamics of the transition states associated with these events is the prerequisite for the establishment of predictive relationships between multiphase-multi-component formulation conditions, product structure and product performance.

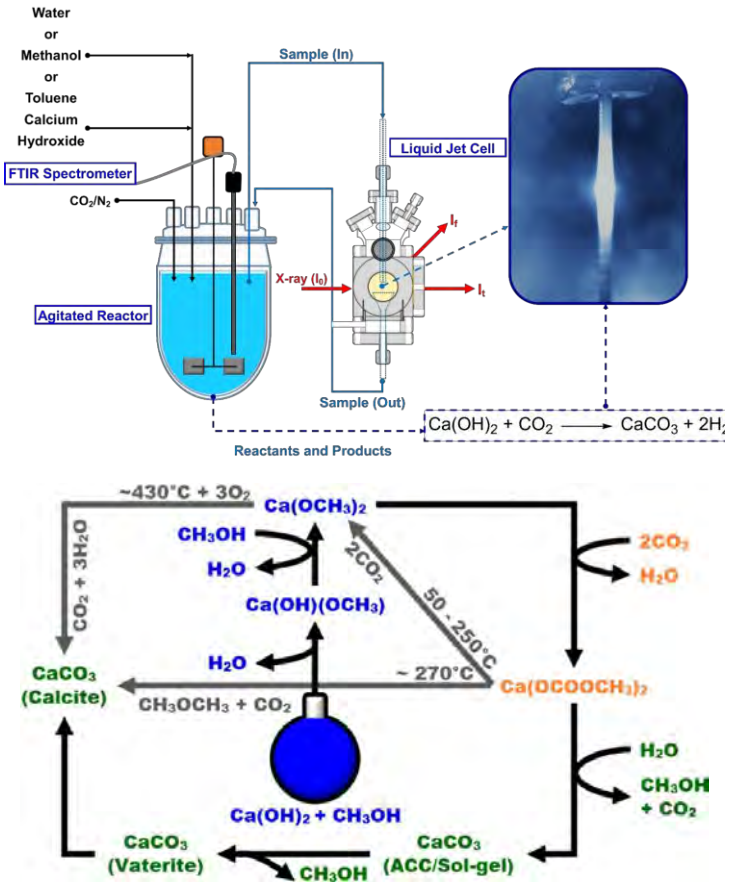


Figure 8.2: (Top) Liquid-jet time-resolved XAS operando probing of the multiphase-multicomponent synthesis of surfactant-stabilised $CaCO_3$ detergent particles.

Reproduced from Kathyola et al.[24] Ind. Eng. Chem. Res. 62, 40, 16198–16206 (2023) under the terms of a CC-BY 4.0 license

DOI: 10.1021/acs.iecr.3c02540

(Bottom) Network of competing reactions detected by the XAS analysis of the process

Reproduced unchanged from Kathyola et al.[25] ACS physical chemistry Au, 4,5 555-567 (2024) under the terms of a CC-BY 4.0 license

DOI: 10.1021/acsphyschemau.4c00041

The keys to making progress in this area are *in situ* and *operando* studies of the actual industrial process. For example, the multiphase multicomponent manufacture of sulphonate-stabilised calcium

carbonate nanoparticles, which are widely used as detergents in engine lubricant formulations, has been studied using a scaled down version of the industrial process by *operando* Ca K edge (~4 keV) XAS at Diamond Light Source[24]. These studies revealed a complex network of reactive nucleation and phase transformation processes that determine the final product structure.[25,26] Each pathway is associated with its own activation barrier that determines the structure of the resulting $CaCO_3$ product. Understanding the dynamic of these barrier crossing events will be essential for the predictive control of product properties and would be accessible by XFEL studies with a liquid jet.

Another example is organic lubricant additives for reducing friction whose performance depends on the tribochemistry and structure of the resulting tribofilms in the boundary regime,[27] which would benefit from X-ray reflectivity studies of self-assembly dynamics at interfaces. The mechanistic basis for the performance of friction modifiers is critical for product design. Ultrafast dynamics studies with XFELs could lead to a step change in understanding and could involve, for example, the construction of a tribometer permitting operando studies, building on neutron and synchrotron X-ray research[28]. Finally, insight into the molecular dynamics of component interactions, e.g. detergents and dispersants, is crucial for formulated product design. Current stopped flow methods for neutron studies at ILL achieve time resolution of ~ 0.03 s but XFELs will be required for understanding the molecular basis for kinetics through systems characterisation by ultrafast spectroscopy and imaging.

Generally, scientific progress in this area of applied science has been slow due to the experimental challenges of localised spatiotemporally rare events in complex chemical systems. The molecular nature of self-assembled nuclei of new phases, their dynamics and relationship to observable rates of formation remain uncertain.[29–31] Nucleation events create structure from the molecular and nanoscale all the way up to the colloidal domain that are characterised by complex interfacial energetics involving electrostatics, covalent and non-covalent interactions. Crystallisation from homo-geneous solution is believed to start with a nucleus (or nuclei) of interacting solute molecules, which initiate phase-separation.[30 – 32] Classical Nucleation Theory (CNT), widely used in describing these phenomena,[29,33] poses that in supersaturated solutions nuclei of a critical size are formed, whose structure matches that of the final product.[34,35] Dynamic equilibria (fluctuations) in super-saturated phases create unstable small clusters ('sub-critical nuclei') and other transient aggregates.[33,35] The experimental challenge is to detect the relevant nucleation event(s) at the nanoscale, which are stochastic in time and in space. It is also believed that alternative molecular pathways to those predicted by CNT exist (**Figure 8.3**). Localisation of homogeneous events by, e.g. use of liquid-liquid interfaces[36] and small volume electron microscopy imaging,[37] are a viable way forward, but they also interfere with the nucleation dynamics through interface formation or radiolysis.

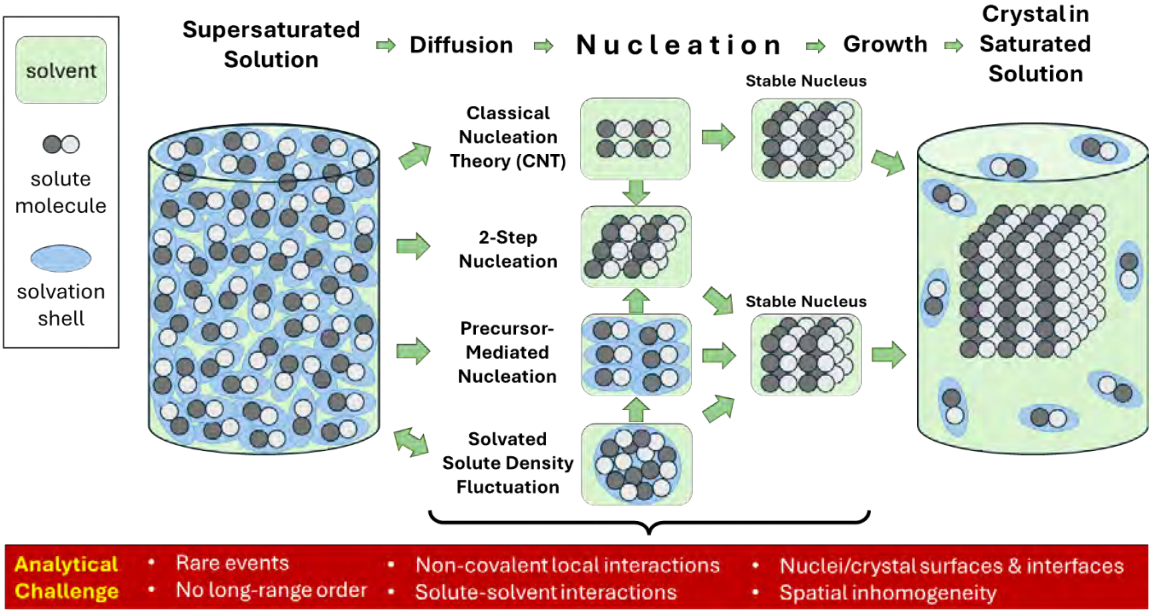


Figure 8.3: Classical nucleation theory and alternative mechanistic pathways in crystallisation, highlighting the experimental challenges in nucleation science

XFEL scattering and spectroscopy methodologies will for the first time provide the required multiscale combination of time and spatial resolution to overcome these challenges, through high experiment repetition rate, multi-detector probing and molecular level imaging taking snapshots of small sample volumes under nucleation conditions. Advanced synchrotron and neutron characterisation, with core level spectroscopies, PDF (see also **Section 5.5**), scattering and diffraction methods, has indicated that, in combination with modelling, these techniques can provide the required deep structural understanding. For taking this field of hybrid fundamental and applied research in small molecule crystallography forward, we can take cues from the already fledgling field of time-resolved serial femtosecond crystallography (SFX) of proteins. Indeed, SFX studies of enzyme reactions are one of the major use cases for XFELs in the life sciences (see **Chapter 7**).[38 – 42] Just as in applied particle research, R&D efforts are significantly impacted by crystal size and size-distribution within the slurry (homogeneity).[42 –45] The principal reason is because the fraction of macromolecules on the surface of a crystal increases with smaller crystals. Consider, for example, a cubic crystal with 150 Å unit cell dimensions (**Figure 8.4**), which is a typical size for enzymes. A slurry comprised of 1 µm crystals will have just under 10% of the unit cells on the exterior layer of each crystal, but the exterior surface layer of 0.3 µm crystals includes 30% of the unit cells. Substrates must diffuse throughout the mother liquor and the microcrystals to initiate enzyme reactions. Macromolecular crystals are about 50% solvent/ mother liquor and 50% protein.[46 – 49] Enzymes on the surface of the crystal will bind substrates faster than those buried inside. Typical substrate molecules diffuse at roughly 1 $\mu m^2\ \mu s^{-1}$ and the rate depends upon viscosity as well as the size, shape and electrostatics of the intermolecular solve channels within the crystal lattice.[50 – 55] Diffusion through micron-size crystals is significantly faster than the average 70 ms reaction time for enzyme catalysis. A variety of mix and inject sample delivery methods are available and there is significant R&D activity in this area.[53 – 59] Therefore, time-resolved SFX is generalisable; however, cleaner results will be derived from more homogenous microcrystal slurries.

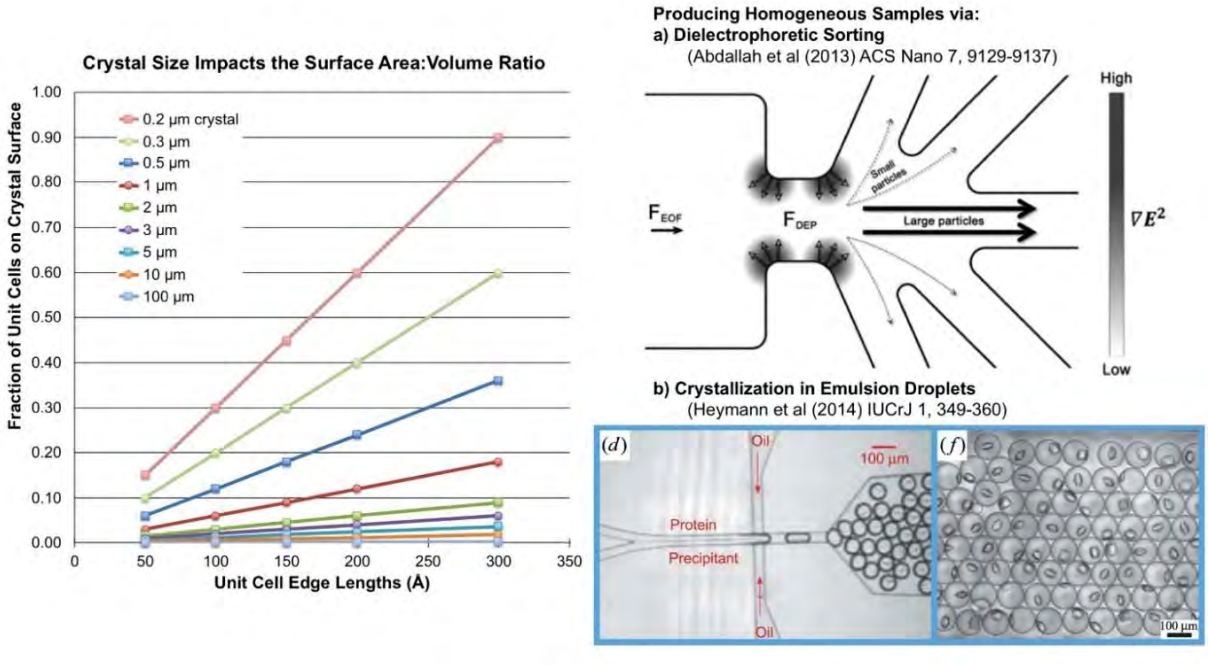


Figure 8.4: (Left) The fraction of unit cells on the surface of a crystal increases with smaller crystal size. (Right) Some methods to produce uniform slurries of microcrystal that are suitable for time-resolved SFX studies.

*Top right (a): Reprinted with permission from American Chemical Society: B.G. Abdallah et al. ACS Nano **7**, 9129-9137. Copyright (2013). DOI: 10.1021/nn403760q; Bottom right (b): Reproduced from M. Heymann et al. IUCrJ **1**, 349-360 (2014) under the terms of a Creative Commons Attribution International License. DOI: 10.1107/S2052252514016960*

The influences of the homogeneity of the slurry, crystal size, morphology, lattice packing and solvent content upon the reaction rates have not been quantified. These should be measured for each system of interest and include more than one space group and/or crystal morphology whenever possible. For example, the ratio of surface area to volume changes as a function of crystal size and becomes pronounced in samples of submicron crystals composed of macromolecules in large unit cells (cf. **Chapter 7**). This may impact the overall k_{cat} measured from a slurry, especially if the molecules on the outside catalyse reactions with a different rate than those buried within the interior. If so, this suggests that lattice constraints may impact the reaction of interest, which may be alleviated in an alternative space group with different crystal packing. To date, microcrystal slurries are often grown in batch mode with relatively few constraints that do not always produce homogenous results. Therefore, heterogeneous microcrystal slurries can be filtered through pores of known size and/or sorted with microfluidic methods and dielectrophoresis (DEP) focusing.[60 – 62] In contrast, producing homogenous slurries of microcrystals often benefits from the use of microfluidic methods to grow individual crystals of predefined dimensions based upon nucleation in nL volume drops encapsulated in oil.[63] Using the SFX approach we can therefore realistically hope to also unravel sequences of events in the nucleation and crystal growth processes in small molecule systems. Moreover, the applied science community in the UK can build on a rich existing knowledge transfer network in the field of small molecule particle science with an engrained culture of industrial collaborations, exemplified by UKRI manufacturing hubs. These existing dissemination and collaboration relationships can be built on seamlessly for creating economic impact.

Finally, going beyond studies of supramolecular interactions in small molecule crystallisation, femtosecond X-ray scattering also offers opportunities to study the dynamics in more complex systems, including self-assembly of larger molecules, for example in peptide and protein folding.[64 – 66] Peptide and protein *mis-folding* into amyloid structures, such as fibrils, is well established as the origin of Alzheimer's disease,[67] but amyloidosis is now believed to be associated with other pathological conditions, for example Parkinson's disease.[68] A fundamental challenge to progress is polymorphism, which can be overcome using an ultrafast X-ray diffraction imaging approach that provides information on individual fibrils. In a recent study, graphene was used as a support, realising low background scattering from the support.[66] Using nanofocused femtosecond X-ray pulses, diffraction from amyloid protofibrils was obtained with resolution down to 2.4 Å in single diffraction patterns. The ability to focus on fibril dynamics with high spatiotemporal resolution could open new technological developments towards rapid point-of-care diagnosis as well as therapeutics.

8.3 Dynamic processes in additive manufacturing, laser machining and photolithography

Various advanced technologies vital to the manufacturing base, including friction welding, additive manufacturing and laser machining, require an understanding of microstructural phenomena frequently occurring at fast timescales. XFELs offer probing capabilities that surpass the current state-of-the-art and allow these processes to be followed from milliseconds to sub-picosecond timescales. Soft X-ray/extreme UV pulses of high brightness from a high repetition rate XFEL may lead to new prospects in matching Moore's law with nanometre scale resolution photolithography.

8.3.1 Rapid events in materials science and advanced manufacturing

During various novel manufacturing processes (e.g. friction welding, laser micro-machining, additive manufacturing, forging, etc.), metallic materials experience rapid microstructural events due to the high temperatures and stresses during these processes, especially when accompanied by both high strain rate deformation ($\sim 10^3$/s) and high heating rates ($10^6 - 10^9$ K/s). These microstructural phenomena need to be understood and controlled in order to achieve the required quality and performance. This has raised the need for experimental tools that enable real-time observation of the microstructural development and phase transformations (PTs) during these manufacturing processes. Synchrotron X-ray diffraction (XRD) and in situ high temperature microscopy (Attallah *et al*.) have been successfully used in several studies to in situ investigate the phase evolution during melting and solidification, as well as the solid-to-solid phase transformations. However, more research is needed within an X-ray (synchrotron and XFEL) context, and higher temporal resolution demanded to capture all of the timescales of these processes.

Friction welding: high strain rate thermo-mechanical deformation and rapid heating

During friction welding or forging operations, the material experiences rapid thermomechanical deformation (typically in a shear deformation mode). Friction welding is a high integrity welding process that is employed in welding aero-engine components; notably the bladed disk (BLISK) structures. Spatially resolving high speed synchrotron X-ray diffraction has been demonstrated to identify the solid phases formed during the complex thermomechanical deformation process of forming the weld (**Figure 8.5**). Future faster investigations can develop dynamic material models for the rapid thermal and thermomechanical conditions associated with friction welding, taking into consideration microstructural development in addition to the flow stress/strain behaviour at these rapid rates. This will address the limitation in the current models, which rely on thermomechanical and thermodynamic/phase transformation data

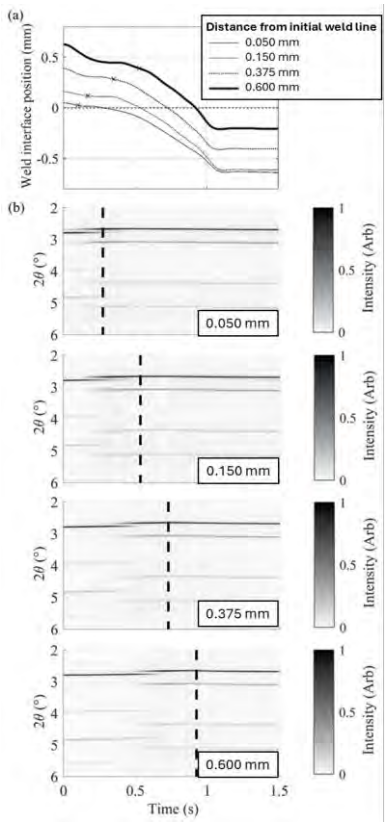


Figure 8.5: In situ high speed synchrotron X-ray diffraction analysis of phase evolution during inertia friction welding of high-carbon steel

Reproduced from M. Rowson et al. J. Synchrotron Rad. ***28****, 790-803 (2021) under the terms of a Creative Commons Attribution International License. DOI: 10.1107/S1600577521001569*

that do not consider the rapid and transient nature of the thermal and thermomechanical fields during friction welding. Such a limitation hinders the development of models to predict the microstructure-property development in friction welds. Some of the proposed work can include in-situ X-ray diffraction measurements and wide-field X-ray dynamic imaging during high strain rate testing (Hopkinson bar) at high temperature, to deliver both flow-stress/strain behaviour as well as microstructural (phase transformation) information to understand the microstructural phenomena (e.g. dynamic recrystallisation, precipitation, etc.) and micromechanical development (e.g. crystallographic texture). Furthermore, the influence of rapid heating on the phase transformations kinetics and other microstructural phenomena (e.g. liquation) can be explored to model the microstructural development within the heat-affected zone (HAZ).

Additive manufacturing: Laser-material Interaction

Recently, there has been a growing interest in the development and utilisation of in situ X-ray techniques[69] and high-speed imaging[19, 70] to study the physical phenomena of additive manufacturing (**Figure 8.6**), especially the laser-material interaction, to understand the defect formation mechanisms.

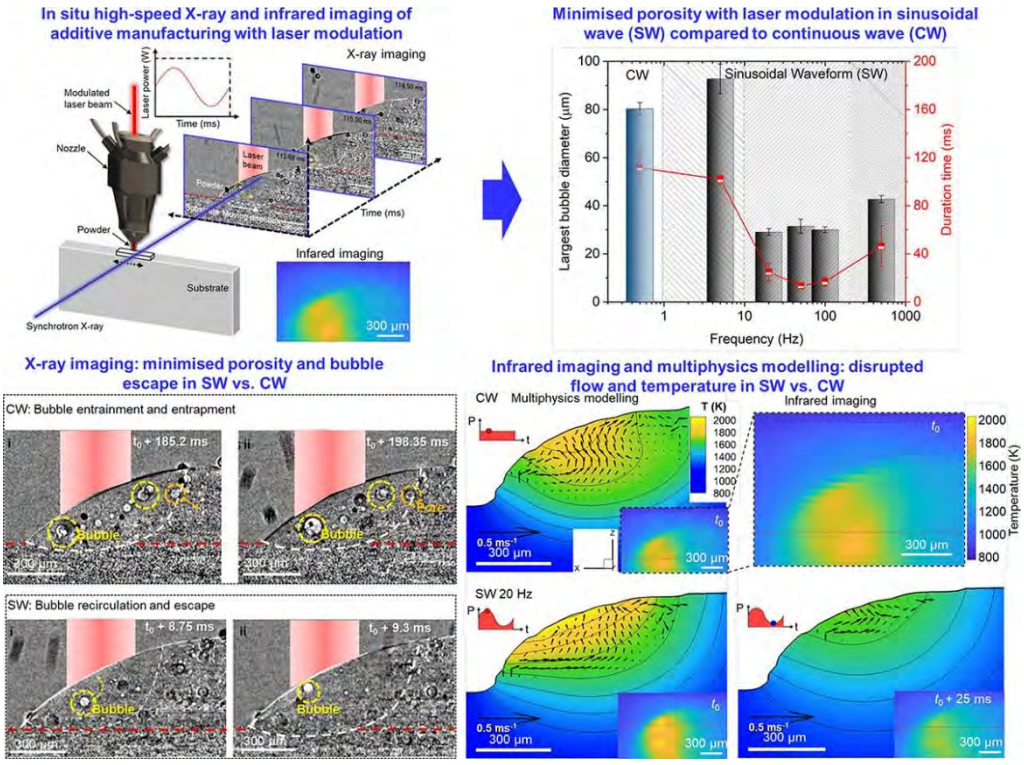


Figure 8.6: In situ high speed synchrotron X-ray and infrared imaging analysis of a laser additive manufacturing process with a nickel-based superalloy

*Reproduced from K. Zhang et al. Acta Materialia **301**, 121515 (2025) under the terms of a Creative Commons Attribution International License. DOI: 10.1016/j.actamat.2025.121515*

Further studies are needed to improve our understanding of the rapid phenomena during additive manufacturing, specifically by exploring the following areas:

- Residual stress development: it is important to understand the influence of the repeated thermal cycling during additive manufacturing on the development of residual stresses, due to their detrimental impact on the mechanical properties, part tolerances and process.
- Phase transformations: additive manufacturing is estimated to have a cooling rate of 10^6 K/s, and a very high heating rate. Understanding the impact of the rapid phenomena on the solid-to-solid and liquid-to-solid phase transformation will achieve the holy grail of additive manufacturing, which is enabling localised microstructural control and customisation of the local properties to improve the product performance.



Figure 8.7: Example additive manufacturing platform that can fit within the experimental facilities, the 'shoe box' laser additive manufacturing system which was used by Bidare et al. in monitoring the process using high-speed imaging

To implement this research, ultrafast hard X-ray pulses are needed along with 2D detectors required to record crystallographic information, and EDX detectors to record residual stress development. Sample environments that allow us to mimic the real-world processes (see **Figure 8.7**) need to be further developed. Acquisition rates should be faster than > 1 kHz.

*Figure reproduced from P. Bidare et al. Additive Manufacturing **16** 177-185 (2017) under the terms of a Creative Commons Attribution International License 4.0 DOI: 10.1016/j.addma.2017.06.007*

8.3.2 Laser Machining

Laser machining is a widely used technology in UK industrial production and there are domestic companies providing automated tooling for this process. In engineering literature, there is ongoing discussion on the choice between short-pulse (fs), long-pulse (ns) or continuous-wave (CW) lasers. Often different solutions are used for different applications, but there are fundamental questions why these choices produce such different results.

The high-power laser research world is similarly divided between the "petawatt (PW)" communities exploring very fast electron processes in molecules or materials, and the "kilojoule" communities interested in compression, ramping, pressure generation and heating processes in materials. These represent the same differences between the fs and ns laser worlds. Comparisons of the results of femtosecond and nanosecond laser hole drilling, carried out side-by-side on samples of thin sheets of aluminium[71] and steel,[72] are shown in **Figure 8.8**. The authors both note striking improvements in the sharpness of the laser cut obtained with the fs pulses, and also the presence of a "heat affected zone" in the case of the ns cutting. This is only qualitatively understood at the present time.

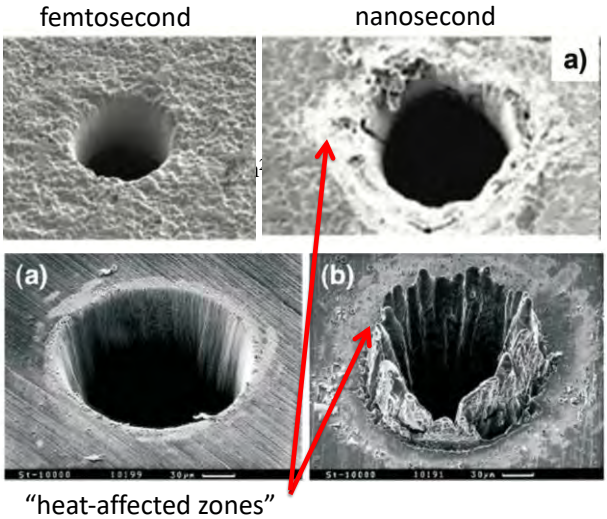


Figure 8.8: Comparisons of the results of fs and ns laser machining, in thin sheets of aluminium[71] and steel[72]

Top left and right figures reproduced from T. Aizawa and T. Inohara, "Pico- and Femtosecond Laser Micromachining for Surface Texturing", Micromachining (2019). Published by IntechOpen. DOI: 10.5772/intechopen.83741
*Bottom left and right figures reprinted by permission from Springer Nature: B.N. Chichkov et al. Appl. Phys. A **63**, 109–115 (1996). DOI: 10.1007/BF01567637 Copyright (1996)*

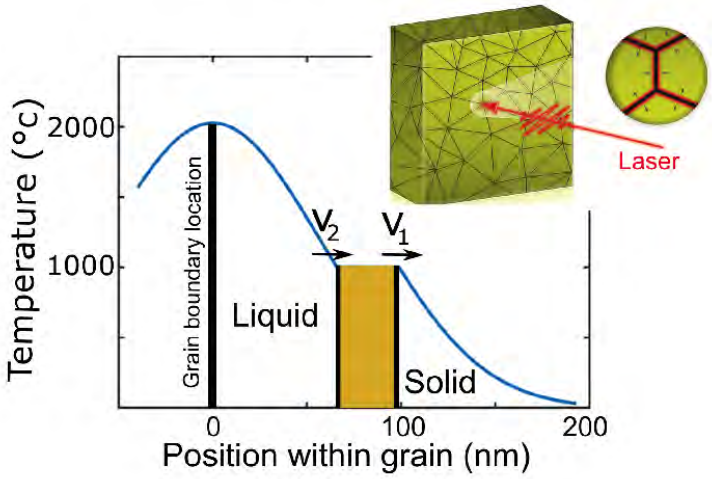


Figure 8.9: Model of the behaviour seen in laser pump, XFEL X-ray probe measurements of the spatial of melting of a 300 nm gold thin film near a grain boundary[73]

*Figure reproduced from T.A. Assefa et al. Science Advances **6**, 3, eaax2445 (2020) under the terms of a Creative Commons 4.0 Attribution International License.*
DOI: 10.1126/sciadv.aax2445

An example of a recent result[73] representing a possible future direction of study that could be undertaken at a next generation XFEL is illustrated in **Figure 8.9**. A 300 nm thin film of gold was melted with a single laser pulse tuned to just provide enough heat to melt the film over a 100 µm focused area. A single X-ray pulse from the PAL XFEL facility in South Korea was brought in to measure the X-ray diffraction pattern of a 50 µm region in the centre of the focus, as a function of time delay. From the shape of the diffraction showing a split peak, it was clear that the melting of the polycrystalline film takes place inhomogeneously. The model in the figure assumes that all the energy is deposited at the grain boundaries, where the heated electrons couple to the crystal lattice. This heat conducts on a picosecond time scale into the surrounding grains, which are micron-sized. The result is a pair of melt fronts, separating in time, which bracket a block of gold undergoing melting by absorption of the latent heat of melting. This block gives the distinct second peak in the transient diffraction pattern seen.

8.3.3 Extreme ultraviolet lithography

Standard lithography of semiconductor chips with ArF laser-produced 193 nm radiation is gradually being augmented/replaced by the finer patterning enabled by 13.5 nm illumination, referred to in the industry as EUV. This is the main contemporary technique allowing the industry to keep up with Moore's Law. Currently, EUV is produced through the excitation of a tin or xenon plasma with an excimer laser. Commercial scanners can now produce EUV at the few 100 W level. An alternative method would be the deployment at chip fabrication plants of an EUV FEL capable of operating at multi-kW average power. Such a possibility has been investigated in detail by a leading company in lithography apparatus, but previously the low level of technical maturity of FELs had prohibited commercial commitment. In recent years a number of start-up companies have been established to exploit this route. There is hence a great opportunity for X-ray FEL experimental studies of short wavelength lithography (EUV and SXR) that can be performed using the high repetition rate of a next generation XFEL.

An upgrade of a next-generation XFEL might include a soft X-ray FEL with a ~1 GeV Energy Recovery Linac (ERL) that would enable multi-kW production of EUV (see **Appendix 2**). Such a possibility is also currently under consideration in Japan[74]. This would benefit the global semiconductor industry by allowing study of FEL capabilities at an industrial output level, and developing and proving kW-capable EUV optical elements/beamlines for photon transport to chip scanners. Such a flexible, industrial research-led tool would also facilitate investigations beyond the current industry state-of-the-art. The superior flexibility and controllability of FEL photons as compared to "brute-force" laser-plasma produced photons would have far-reaching implications for many diverse aspects of lithography. Examples of this could include shorter wavelengths, or indeed variation of wavelength (two-colour exposures), variation of polarisation or transverse coherence in differentiating patterning layers, or generation of orbital angular momentum photons to manipulate helicity within a wafer. There is clear potential for novel semiconductor devices to be developed utilising such source capability.

8.4 Applied and Industrial Catalysis

Catalysis is one of the most economically relevant technologies underpinning the roadmap to sustainable chemicals manufacturing and energy generation. The next generation XFEL will provide crucial insights into the dynamics of the transition states associated with active catalytic sites, paving the way for a rational design of catalytic processes with optimal resource efficiency. The development of sample environments for multi-technique XFEL studies of catalytic systems in situ and operando will be essential to achieve this aim.

Catalytic processes, especially those involving heterogeneous catalysts, are seen as key technologies for addressing the most pressing contemporary sustainability challenges in the chemicals and energy technology sectors.[75] By their very nature, catalytic processes proceed at the molecular level through transient species in active sites that typically exist only under conditions far from equilibrium, i.e., under elevated temperatures and, often, pressures in catalytic reactors. The research fields of fundamental (see **Section 6.4**) and applied catalysis have consequently, for decades, been at the forefront of developing sample environments for *in situ* and *operando* studies with advanced X-ray analytical technology at synchrotron radiation sources. Traditionally, X-ray diffraction (XRD) and hard X-ray absorption spectroscopy (XAS) methodologies (including extended X-ray absorption fine-structure, EXAFS, and X-ray near edge structure, XANES), often in combination with X-ray fluorescence (XRF), have been the most widely used *in situ* and *operando* X-ray techniques for studies of catalysts. X-ray photoelectron spectroscopy (XPS) and near-edge X-ray absorption fine structure (NEXAFS) have long been used to perform complementary surface science studies of model catalysts. With the advent of 3rd generation synchrotron sources, the use of even more advanced hard X-ray techniques, such as high-energy resolution fluorescence-detected (HERFD) XAS, X-ray emission spectroscopies (XES), resonant inelastic X-ray scattering (RIXS), X-ray Raman scattering (XRS), X-ray pair distribution function (XPDF) measurements by total X-ray scattering, and various modalities (phase contrast, XRD, XPDF, small angle X-ray scattering, SAXS) of X-ray computed tomography (XCT) have emerged as techniques providing even deeper insight into the electronic and geometric structure of catalysts at the molecular level. At the same time, the development of near-ambient pressure (NAP) and ambient pressure (AP) instrumentation has facilitated the transition of XPS and NEXAFS from ultra-high vacuum surface science techniques to *in situ* and *operando* analysis methods that can also be applied to practical catalysis. The interested reader is referred to **Chapter 6**, where prospects for taking these techniques into the ultrafast domain at a next-generation XFEL have already been presented. The challenge for catalysis remains to interrogate the active site to establish structure-function relationships in realtime under realistic conditions. Elucidating the ultrafast dynamics taking place at active sites using experimental XFEL science is already an accepted part of the Roadmap for Science and Technology of Catalysis (see reference [75]).

8.4.1 Methodology Developments: Experiment & Theory

To drive this understanding forward in the context of applied research, methodological developments have been made in the design of sample environments for higher throughput, e.g. multi-capillary setups for loading different gas compositions/pressures for heterogeneous catalysis. Access to higher temperatures and pressures is pursued as well as correlative imaging/spectroscopy experiments or surface diffraction. To better distinguish the active site against the strong background signal of spectator species time-resolved methods such as modulated excitation with time and phase-retrieved EXAFS data have been developed.[76] Addressing dynamics on millisecond timescales is possible using pump-probe XAFS techniques.[77] With the higher flux upgrades such as EBS at the ESRF and Diamond-II high-throughput multi-dimensional catalytic studies will be possible as well as fast imaging (CDI with fast ptychography) and of systems with low concentration (e.g. of metalloenzyme systems), with time resolution down to the ns to microsecond range.

However, probing the crucial ultrafast structural and electronic dynamics in catalysts, which are required to elucidate the transition states in the active sites for catalytic transformations will only be

possible with X-ray free electron lasers. For example, at Swiss FEL and European XFEL studies of photocatalysis and energy conversion with 100 fs to ps time resolution are now possible with single-shot dispersive resonant and non-resonant probing, including XES, XDS, XAS, RIXS, WAXS and single crystal diffraction possible.[78-83] Large solid samples can be studied by raster scanning, while liquid jets permit studies of liquid homogeneous systems.[78-80]

The development of pump-probe techniques relevant for homogeneous catalysis are already under way. Giving just one example of research, a study at SwissFEL in the context of C-H and C-C bond functionalisation, relevant for green chemistry, examined C-H activation at a transition metal (Rh) carbonyl complex using photoexcitation with a 266 nm laser. The photoexcitation causes loss of a CO ligand, enabling the Rh d orbital to activate the C-H bond. Detecting the fluorescence from Rh provides a local probe for the metal electronic orbitals, complementing vibrational spectroscopy.[84]

An example of catalysts inspired by nature are high-valence iron (IV) oxo molecular catalysts.[85] The Fe centre mimics those in heme and non-heme enzymatic systems and is highly amenable to 2D X-ray spectroscopy, e.g., 2p3d RIXS, XAS and XES.[86,87] At XFELs there is potential for enzymatic reactions with microfluidics and mixing/freeze quench cycle studies to examine the dynamics at the centres further, especially when XES and XAS are applied as multicolour absorption edge combinations, e.g. Se/Fe or P/Mo ligand-metal centre pairs.

The interpretation of advanced X-ray spectroscopic data relies on structure and dynamics modelling. Modelling that takes into account the complex effects of environmental interactions remains a challenge, and even more so when X-ray spectra need to be calculated. Additional information from complementary analytical techniques is crucial to identify the right molecular structures for the computational studies. Theory research has made strides forward in the last decade, as exemplified by studies of photomagnets[88] and electron/hole dynamics in ZnO.[78,79] Opportunities for further progress also arise from applying machine learning to improve calculation speed.[89,90]

8.4.2 An Integrated Vision of Complementary Capabilities

The abovementioned complementary use of other analytical techniques, including synchrotron, electron microscopy, neutron techniques as well as non-XFEL pump-probe techniques, will be crucial to realise the full potential of applied next-generation XFEL science. An example for state of the art pump-probe infrastructure in the UK are the capabilities of the ULTRA facility (IR/Vis spectroscopy, Raman, 2D-IR, 2D-ES, Kerr gated Raman) and especially the HILUX upgrade.[91,92]

A dream XFEL imaging experiment would be “chemical imaging” XRD-CT scans[93] probing atomic structure on mesoscopic scale. High average XFEL brightness will enable this on timescales (< 1 hour) realistic for operando or in situ studies. Likewise, XFEL-based XAS/XES would likely be fast enough to catch reaction intermediates e.g. in catalytic NO_x reductions. There is strong complementarity in this area with sample handling capabilities developed in XFEL life science, e.g., tape sample delivery system for optical excitation and fast droplet delivery methods. An example of how such XAS studies could look like are fsXAS studies at SACLA on hot electron injection in plasmonic materials (TiO_2) probing Au to Ti electron transfer.[94] The next generation XFEL would for example provide an opportunity for developing sample environments for triggering fast dynamics by controllable heating e.g. microwave heating, magnetic induction or plasma induction.

Next-generation XFEL science in applied catalysis can build on the established track record of close collaboration between industry (Johnson Matthey, JM) and central facilities in the UK. Access to the latest analytical methods and a pipeline of trained scientists through close collaboration creates not only a pathway to economic impact but also for wider benefit through the development of new national user facilities. JM have for example established an aberration corrected STEM in the EPSIC facility at Diamond for both proprietary R&D and open user access. The full integration with high resolution X-ray imaging (see **Figure 8.10**), XAS, XPS/NEXAFS & XRD in JM’s R&D also provides new training opportunities, e.g. through part-funded PhDs and Fellowships. This model integrating advanced techniques and training is expected to continue at the next-generation XFEL. Science areas

where next-generation XFEL would impact could be Cu dynamics and dimer formation for NO_x control in lean burn applications.[95,96] A static picture of the catalyst has been established using modelling and XAS established but direct evidence of the formation of transient Cu dimers under reaction conditions[97] will be crucial to understanding and designing better processes. Other areas are fuel cells and electrolysers, where investigations using *operando* XRD at the ESRF[98] have revealed degradation of catalysts under fuel cell conditions with operando XRD.

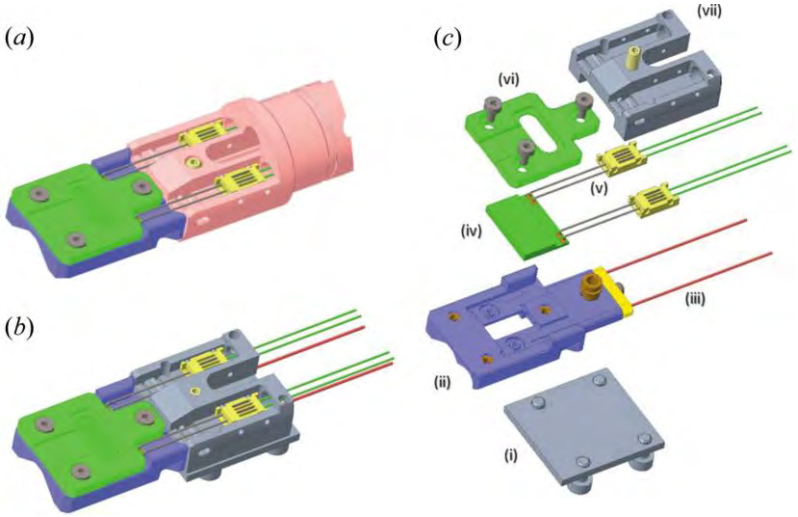


Figure 8.10: Example of a correlative hard X-ray nanoprobe and electron microscopy studies of catalysts under in situ conditions [99]

Figure reproduced from J.E. Parker et al. J. Synchrotron Rad. 29, 431–438 (2022) under the terms of a Creative Commons Attribution License DOI: 10.1107/S1600577521013576

8.4.3 Conclusions

For catalysis research "photochemistry" approaches for activation (laser pulses to excite target electronic states in a tight temporal window) can be useful, but alternative trigger processes are emerging for catalysis: fast electrical activation (with picosecond switch speeds) via nano-electrodes or THz fields, laser pulses for hot electron injection, laser pulses to induce fast T-jumps in the matrix, laser pulses in MIR for fast heating of critical bonds. Nevertheless, access to the full UV-Vis-IR tuneable laser ranges for pumping excited electronic states will be important and there are applications requiring electron beam and ion/proton beam pumping of radiolytic processes.

The time looks ripe to go beyond the basic model systems so far studied to more complex systems where the sample – rather than the X-ray technique – is the centre of attention. High throughput allowing many samples, variation of conditions (temperature and pressure) and positions within a sample will permit significantly more impact.

Complementary techniques will be key and multiple measurement modalities on a single sample are highly desirable to fully interrogate the behaviour of the system, including several different X-ray methods (e.g. spectroscopy and scattering). The case to perform these measurements simultaneously is impacted by the need to optimise S/N for each and instead an approach that gives access to sequential measurements on the same sample is generally favoured and likely to be well supported by a high productivity next-generation XFEL.

8.5 Industrial inspirations from deeper insights into biology: Pharma to clean energy

Industrial XFEL users in life science want faster, better structures from smaller samples. They demand reliability and automation, especially for proprietary R&D efforts. Industry is already using Diamond and eBIC extensively, and starting to explore options at XFELs. They are watching for developments in cryo-EM, serial crystallography and time-resolved studies that couple structure and function from the same sample. New opportunities for drug discovery impacting human health are profound and progress has recently been demonstrated with serial femtosecond crystallography (SFX) results on several membrane proteins involved cell signalling. Time-resolved SFX results targeting photosystem II, hydrogenases, and nitrogenases promise molecular level insights that will inspire the next generation of solar and fuel cells, and green catalysts to convert N_2 into fertiliser.

An outstanding grand challenge in the life sciences is to understand the molecular basis of symbiosis *versus* pathogenicity. *Why are some interactions beneficial, and how can these be protected or enhanced while simultaneously degrading those that cause disease?* The need to distinguish between "friend or foe" impacts the entire biosphere and is one of the critical factors that drives evolution on Earth; often a life or death process. This ongoing struggle is a fundamental underlying basis of the $1.2 trillion pharmaceutical industry focused upon human health, and similar global efforts targeting agriculture. Despite the extinction of more than 99% of all organisms that have ever lived on Earth (see **Chapter 7**), the current diversity of life is immense and always evolving.[100]

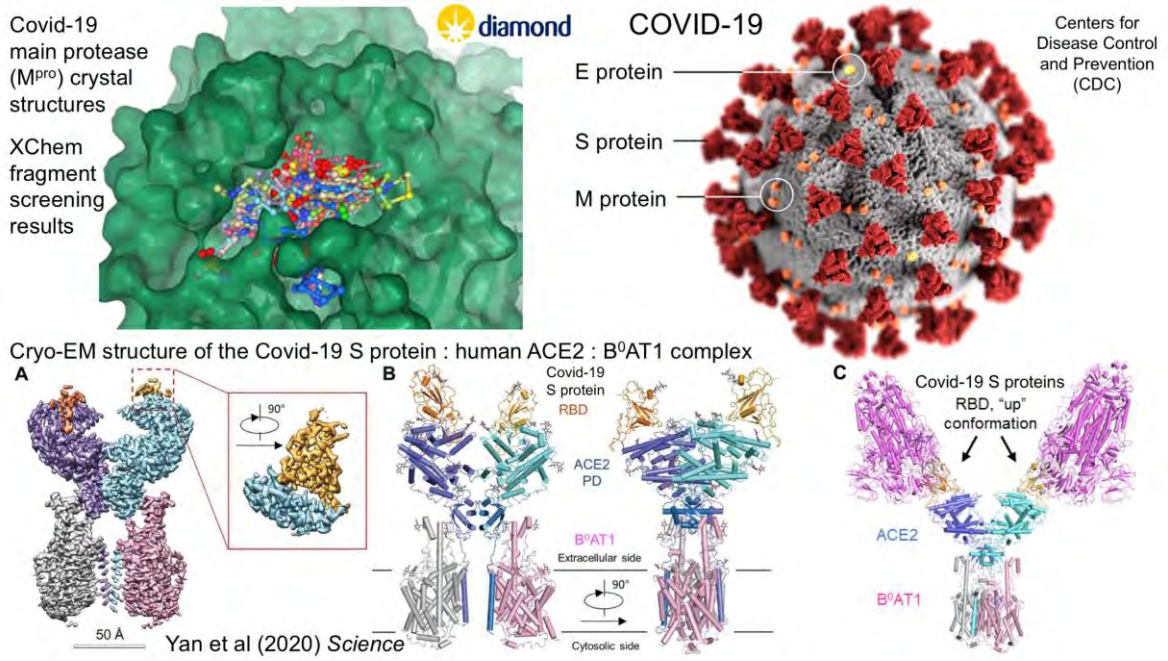


Figure 8.11: Morphology of the COVID-19 virus (top right) and structure-based drug discovery. (top left) Fragment screening by crystallography of the M^{pro} protease at Diamond identified > 50 ligand hits in and around the active site. (bottom) 2.9 Å resolution cryo-EM map (A) and overall structure (B) of the RBD-ACE2-B^0AT1 ternary complex. (C) The ternary complex superimposed with the S protein of COVID-19 (PDB code: 6VSB)

*Top figure (left): Joint initiative announced to accelerate the search for COVID-19 drugs - - Diamond Light Source, © Diamond Light Source, with permission; Top figure (right): Source: CDC; Bottom figure: Reproduced from R. Yan et al. Science **367**, 6485, 1444-1448 (2020) under the terms of a Creative Commons 4.0 Attribution International License. DOI: 10.1126/science.abb2762*

It is in this context instructive to remind ourselves how structural biologists in academic and industrial labs around the world quickly and vigorously responded to the COVID-19 pandemic, including analyses of key proteins from the COVID-19 virus genome using cryo-EM, X-ray crystallography and homology

modelling approaches.[101–107] Among the first results were cryo-EM single particle analysis of the whole virus and the complex that likely mediates entry into human cells.

Although very successful, these approaches largely ignore dynamic components because they derive from samples held at cryogenic temperature. In contrast, many of the XFEL-based approaches described in **Chapter 7** are performed at physiological temperature and thereby enable scientists to simultaneously probe dynamics and structure. This capability was germane to COVID-19 R&D efforts. Fragment screening results do not address any of the dynamic steps within the protease reaction kinetics or catalytic mechanism.

Structure-based drug discovery and/or design remains a hallmark strategy across the pharmaceutical industry. Its success is illustrated by the fact that more than 90% of new molecular entities (NEM) to receive US FDA approval since 2010 leveraged structural biology.[108 – 110] Almost all of the atomic models for the new drug targets were released into the public domain, and many about 10 years before a drug compound came to market. Thus, the linkages between the public and private sectors are historic and extensive.[111] At Diamond, up to 10% of the available experiment time is set aside for proprietary access used by many industrial partners.

XFEL-based structural biology methods efficiently use slurries of micron-size crystals to generate high resolution atomic models. An example of the impact is illustrated with G protein-coupled receptors (GPCRs, **Figure 8.12**).[112 – 117] These integral membrane proteins tend to exhibit a seven transmembrane protein fold that is often difficult to crystallise and study by traditional methods. Nevertheless, many have produced microcrystals with lipidic cubic phase conditions, that have generated important results from XFELs using SFX approaches.[118 – 129] There are more than 800 human GPCRs that respond to thousands of chemicals or photons, and elicit responses that touch nearly every physiological aspect of cells. Ligand binding or photoisomerisation elicit dynamic conformational changes that propagate across the membrane and initiate intracellular signalling cascades. More than 40% of all prescribed drugs target GPCRs with impact to the central nervous, cardiovascular, immune, metabolic, and reproductive systems, as well as to many human cancers. The importance of GPCRs was recognised by the 2012 Nobel Prize in Chemistry to Lefkowitz and Kobilka “for studies of G-protein-coupled receptors.” Membrane proteins, and especially GPCRs, will be a strong use case for Industrial users for XFELs in the coming decades.

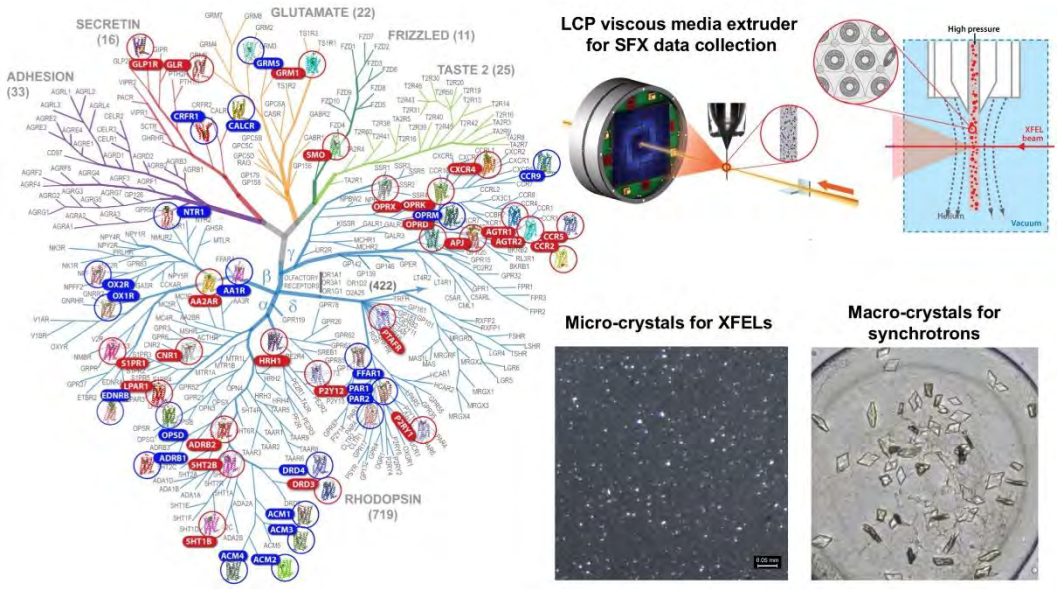


Figure 8.12: (Left) High-resolution crystal structures of GPCRs in 2019 superimposed upon the phylogenomic family tree. (Top right) SFX data collection strategy using an LCP injector at XFELs and microcrystal. (Bottom right) Comparison of micro- and macro-crystals.

Figure (left): Courtesy of Vadim Cherezov and adapted from V. Katritch et al. Trends Pharmacol Sci 33, 17-27 (2012). DOI: 10.1016/j.tips.2011.09.003; Figure right (top): Adapted with permission from W. Liu et al. Science 342 1521-1524. DOI: 10.1126/science.1244142. Copyright The American Association for the Advancement of Science (2013); Figure right (bottom): Courtesy of Vadim Cherezov

Metalloenzymes catalyse the most difficult reactions in biology.[130 – 134] They evolve to produce high energy intermediates when and where they are needed to transform a wide range of compounds. For instance, **Section 7.2** highlights photosystem II and how XFELs provide experimental approaches to watch visible light photons elicit charge separation, that sequentially oxidises the Mn atoms within the oxygen evolving complex, that ultimately converts two H_2O molecules into O_2.[135 – 145] These mechanistic insights serve as inspiration for advanced generation photovoltaic cells for industrial applications. Fuel cells will also take inspiration from hydrogenases, metalloenzyme that use complex iron-sulfur and nickel clusters to catalyse the reversible reaction of two H^+ plus two electrons to produce H_2.[146 – 156] Methane monooxygenase uses dinuclear iron centre to catalyse the conversion of methane into methanol by creating a bis-Fe(IV)=O reactive intermediate.[157 – 169] Indeed, Fe(IV)=O intermediates are critically important across all aerobic life and are extraordinarily difficult to study by traditional synchrotron methods, because they are easily perturbed by photoelectrons generated during the X-ray exposure.[161,164,170, 171] Metalloproteins will be a strong use case at XFELs and will inspire small molecule catalysis for many industrial applications.

For most of the Earth's history, natural sources have provided enough bio-available nitrogen to support all life in the biosphere. The most important reason is nitrogenase, a class of complex metalloenzymes that evolved in microbes to fix N_2 at atmospheric pressure and ambient temperature, converting it to NH_3.[172, 173] The enzyme needs eight electrons and uses the energy released by ATP hydrolysis to drive protein conformational changes (**Figure 8.13**). Microbial species that carry genes for nitrogenase are widely distributed across terrestrial and oceanic environments. Some symbiotic bacteria inhabit the root nodules of legumes and express nitrogenases, which supply all of the reduced nitrogen needed by the plant. In exchange, the plants supply reduced carbon from photosynthesis to the microbes, which is used for carbon and energy needed to fix N_2. The photosynthetic cyanobacteria *Crocosphaera watsonii* in the ocean expresses photosystem II during the day to generate electrons and fix CO_2, then during the night, it expresses nitrogenase to fix N_2.[174 – 176] An outstanding frontier challenge is to understand the molecular basis of nitrogenase catalysis, especially how protein and metal cluster dynamics impact reactivity. Indeed, structural and spectroscopic results demonstrate that the ground-state crystal structures of nitrogenase determined at cryogenic temperatures are inactive.[177 – 189] This supports the hypothesis that dynamic motion of the active site cluster is essential to catalysis.

The Haber-Bosch process is the industrial equivalent of nitrogenase and N_2 fixation.[172,173] It was invented just over 110 years ago and now produces as much NH_3 globally as all natural sources. It has not changed significantly over the past century. Unfortunately, the Haber-Bosch process requires high pressure and temperature, as well as annually consuming about 5% of the global natural gas; thus, it is not sustainable. Moreover, feeding the current world population of ~7.7 billion critically depends upon industrial fertilisers; but natural N_2 fixation processes alone can support only about 50% of the current population.[173,190,191] Consequently, there is an urgent need to develop alternatives to the Haber-Bosch process. Clearly a better understanding of the structure, dynamics and function of nitrogenase is an inspirational guidepost and XFELs will play a major role in the R&D effort in the years to come. The industrial scale application of green chemistry strategies to produce new N_2 fixing catalysts inspired by structural biology is essential to human survival.

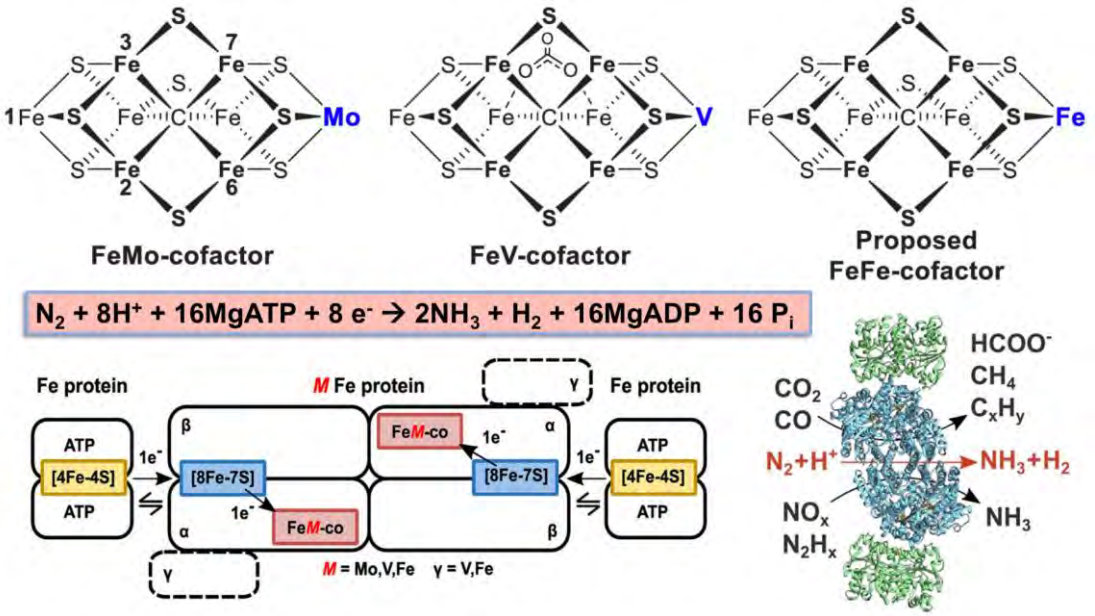


Figure 8.13: (Bottom, left) Schematic of nitrogenase structures showing the electron delivery Fe protein component and the catalytic MFe protein component (M = Mo, V, Fe).
(Bottom, right) Overall structure of Fe protein - MoFe protein complex and reactions catalysed.
(Centre) The nitrogenase reaction is catalysed by the metal FeM-co centres (top) that incorporate similar but distinct clusters from various microbes.

Adapted with permission from American Chemical Society: L.C. Seefeldt et al. Chem. Rev. 120, 12, 5082–5106 Copyright (2020)
DOI: 10.1021/acs.chemrev.9b00556

8.6 Energy materials and devices: Solar cells and batteries

Our energy systems are rapidly evolving, driven by the challenges associated with decarbonisation, an ageing infrastructure, and shifts in societal expectations. Achieving a radical shift in how we supply, manage and consume energy calls for new materials and a detailed understanding of how they function. Yet in many energy technologies there remain fundamental processes related to function that we simply do not understand, and this is severely impeding progress. Ultrafast X-ray probing will provide unprecedented insight into the function of materials on the atomic scale of time (femtosecond) and length (ångströms), leading to a greatly improved understanding of structure-property relationships in materials for energy applications.

8.6.1 Introduction

Energy demands are increasing throughout the world (increased by 65% since 1990) and provision is currently being met by a mix of sources, including fossil fuels, nuclear power, hydroelectricity and renewables, such as wind and solar energy. However, many challenges remain and need to be overcome to realise the global energy revolution required to limit the detrimental effects on the planet. Solutions must be found that allow an increase in energy consumption whilst reducing the environmental impact, in order to meet the UK's obligations under the Paris Agreement on Climate Change[192] and the ambition of a net zero emissions energy policy by 2050.[193] This will only be possible by improving all aspects of energy conversion, storage, transmission and low-power device efficiency.

For energy conversion, technologies focus upon the transition from polluting fossil fuels to low-carbon sources, such as wind, tidal and solar power. These technologies are, however, inherently intermittent and consequently must be developed alongside new directions for highly efficient grid and off-grid storage solutions, such as batteries or chemical storage. Crucially, solutions will not be found without new classes of zero-carbon materials that can be produced sustainably and that allow higher efficiency energy conversion with better operational stability than current materials.

The challenge is that materials underpinning many energy conversion/storage processes are complex and poorly understood, especially on the atomic scale. Indeed, they often exhibit functional structural disorder and contain dynamical properties that are needed for their operation, but which are also responsible for energy losses and device instabilities and degradation during decade-long operation under harsh, non-equilibrium conditions. This lack of understanding means that the design of new materials is often focused upon large-scale synthetic programs as epitomised by the extensive literature reporting new potential candidates. Ultimately, few candidate materials make the transition to application in practically useful devices. This *status-quo* leads to incremental progress, stagnation of research fields and makes designing materials costly and time-consuming.

The development and utilisation of ultrafast X-ray methods will play an important role in providing crucial understanding of material properties down to the atomic scale of time (femtosecond) and length (ångströms). One of the key advantages of X-ray methods in the context of materials and devices is that they offer the potential to probe these dynamics under operando conditions, for example, inside an operating battery or at the solid-liquid interfaces of heterogeneous catalysts. Such experiments have the potential to yield unique understanding, that can subsequently be used to control the physics and chemistry of emerging materials for energy conversion/storage, and to guide the design of devices.

By exploiting a broad range of excitation (pump) pulses in the UV, visible, IR or THz region, it will be possible to address a wide range of challenges in energy materials using optical, vibrational and thermal excitations. Probe techniques, such as Resonant X-ray Emission Spectroscopy (RXES), will provide powerful insights into the properties of the materials required to address the above challenges. At present, the repetition rate of XFELs currently available severely limits their ability to acquire RXES spectra, while third generation light sources cannot achieve the temporal resolution for

the required understanding. These techniques will also be combined with complementary techniques, such as X-ray Photoelectron Spectroscopy (XPS), X-ray Scattering, X-ray Magnetic Circular Dichroism and X-ray Raman, to facilitate the study of dynamic process interfaces. Indeed, by exploiting the unique atomic sensitivity, these X-ray techniques can disentangle the coupled motion of the spins, electrons and nuclear dynamics, making them uniquely powerful for studying energy materials. Combined with the X-ray capabilities of a next generation XFEL (ultrafast time resolution, transform-limited bandwidth and high repetition rate), these measurements will deliver potentially transformative new approaches to address fundamental and use-inspired questions in energy materials.

8.6.2 Photovoltaics

Approximately 360 W m^{-2} of radiant energy in the form of natural light arrives on earth from the sun, providing around 100 PW of solar energy. The ability to convert this solar radiation into energy is core to attempts to reduce our reliance on unsustainable fuel sources. Crystalline and amorphous silicon photovoltaics (PV) are used owing to their stability and high-power conversion efficiency, but they have distinct drawbacks including, for example, indirect band gap and processing costs. The global PV market is forecast to grow significantly in the coming years, with emerging technologies, including dye-sensitised nanoparticles, organic bulk heterojunctions, thin film semiconductors, such as lead-halide perovskites, predicted to account for 25% of this market.

These emerging technologies are appealing, as they are based around low-cost solution processing or vacuum deposition, and are highly scalable. They are, however, currently limited by a number of factors, including efficiency and stability. They rely on sunlight to generate charge carriers (electrons and holes) and, consequently, improvements in performance relies on supporting the desirable processes, such as the creation, separation, transport of photogenerated holes and electrons, while suppressing the undesirable processes, such as trapping and recombination over a wide distribution of time and length scales. These dynamics begin on the ultrafast timescale and therefore require ultrashort pulses to track all of the competing processes. The ultrashort timescales, and the complex interplay of structural and electronic effects, means that many of these processes and various relaxation pathways remain poorly understood.

Recently, time-resolved X-ray spectroscopy has increasingly been used to investigate the fate of charge carriers in these photovoltaic materials.[79,194] The element-specificity of X-ray spectroscopy can be exploited to directly probe the valence and conduction, to establish a detailed understanding of the interplay between the electronic and nuclear degrees of freedom. This can reduce the complexity of these materials, to provide important insights into the charge carrier dynamics and the effect of morphology, defects and band level alignment.

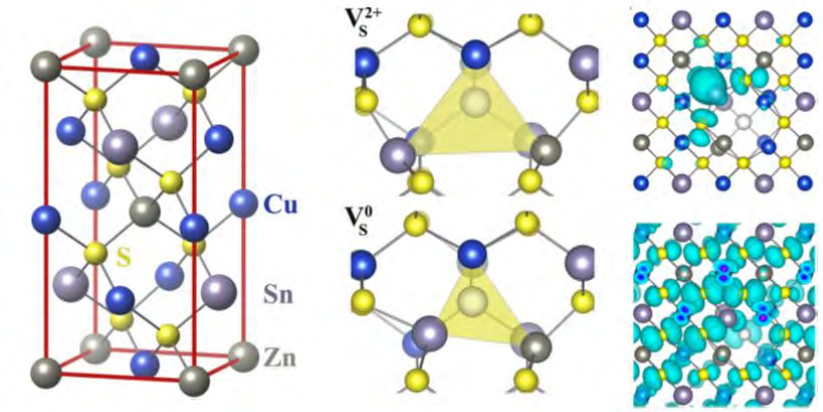


Figure 8.14: (Left) The atomic structure of the Kesterite like Cu_2ZnSnS_4 (CZTS) system; (Right) Key defects proposed to be responsible for nonradiative electron-hole recombination and charge density associated with them.[195]

*Figure reproduced from S. Kim et al. ACS Energy Lett. **3**, 496-500 (2018) under the terms of a Creative Commons Attribution 4.0 International License. DOI: 10.1021/acsenergylett.7b01313*

In this area, there has been a significant research effort in the development of ternary and quaternary semiconductors such as CIGS ($CuIn_xGa_{1-x}Se_2$), kesterite structures (**Figure 8.14**) such as CZTS (Cu_2ZnSnS_4), or halide perovskite structured semiconductors such as methylammonium lead iodide ($CH_3NH_3PbI_3$).[196] Specifically, for the case of the earth abundant solar absorber, CZTS, band gap excitation would excite an electron from the Cu-3d/S-3p state (valence band) to the Sn-5s/S-3p state (conduction band).[197] Time-resolved X-ray absorption and emission spectroscopy can be used to monitor the photocarrier generation, localisation and recombination occurring on the femto- and picosecond timescale from the perspective of multiple atomic sites. Through chemical modifications, the effect of the interstitial atoms, vacancies and grain boundary on the excited carrier dynamics can be investigated,[198] while dopants can be introduced to improve photon absorption and shift the energy levels to refine the performance of promising materials. The capability of femtosecond X-ray spectroscopy, and the insights obtained from these measurements, will enable detailed structural understanding of ultrafast charge carrier dynamics and enable us to propose avenues for improving the performance of these materials (see for example **Box 8.1**).

Organic semiconductors offer clean, flexible and low-cost opto-electronic devices such as solar cells[199], thin film transistors and more recently energy storage devices[200]. Designing organic materials as alternatives to existing technology is vital as these can be sustainably sourced and solution processed from earth-abundant materials. Recently there has been significant development in the efficiency of organic photovoltaic devices due to the introduction of new non-fullerene acceptors. Organic solar cells utilizing the flagship non-fullerene-acceptor (NFA) molecule have achieved power conversion efficiencies exceeding 20% when blended with a polymer donor[201] [202] [203] .

Efficient free charge generation has also been observed in neat Y6 thin films[204] which has led to interest in functionalizing Y6 in single component devices such as organic photodetectors and solar cells. The mechanism and excited state nature behind this efficient generation is a subject of intense study (hundreds of groups globally) and as yet no clear consensus has arisen as to the nature of these processes. Quantum localisation and delocalisation of charge carriers and excitons in organic semiconductors is seen as a critical issue in determining exciton diffusion rates and conversion efficiency. This view is supported by recent theoretical modelling advances[205] and recent experimental investigations in a variety of systems all pointing to the importance of delocalised polarons in boosting the charge extraction.[206,207] Direct measurements of the character and dynamics of the intra- and inter-molecular electronically excited states of these materials are currently largely lacking.

Time resolved X-ray spectroscopy can deliver precisely the incisive insights into the charge dynamics and the nature of the excited states yielding few-fs temporal resolution and atomic localisation needed to advance our understanding and aid intelligent design of organic semiconductors. Charge transfer between atomic sites can be tracked through the shifts in the core level binding energy upon changes of the local electron density (i.e. oxidation/reduction). This enables tracking of the charge distribution of a complex system either by addressing different elemental absorption edges or by exploiting chemical shifts to address atoms in distinct chemical environments.

In recent work, performed at the FLASH XFEL, it was shown how the chemical sensitivity of XPS (X-ray photoelectron spectroscopy) at the carbon K edge can be used to track charge transfer across a bilayer heterojunction on femtosecond timescales[208]. Of direct relevance to future XFEL based time resolved spectroscopies was the observation in a polythiophene polymer (P3HT) of the initial exciton delocalisation. This was inferred to occur across several chains in the first few tens of femtoseconds after excitation, followed by the electron cooling and localisation, by comparing calculations to measurements using High Harmonic Generation (HHG) based time-resolved carbon K-edge X-ray spectroscopy that directly measuring the delay dependent absorption[209] (see **Figure 8.15**).

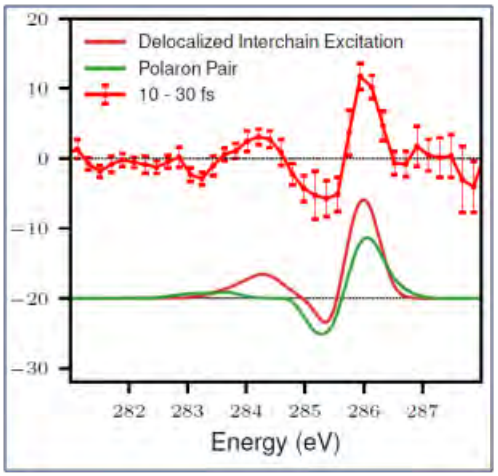


Figure 8.15: Experimental time-resolved XAS of P3HT ΔA (mOD) at the carbon K edge. [209]

Photoexcitation leads to a blue shift in the C1s to π transition due to a transfer of electron density away from the carbon atoms. The energy and amplitude of the pre-edge feature (284.5 eV) is sensitive to delocalisation between polymer chains and polaron pair formation, allowing the rapid localisation of the P3HT exciton to be tracked on a few tens of femtoseconds timescale.*

Figure reproduced from D. Garratt et al. "Direct observation of ultrafast exciton localization in an organic semiconductor with soft X-ray transient absorption spectroscopy." Nat Commun 13, 3414 (2022) under the terms of a Creative Commons Attribution 4.0 International License. DOI: 10.1038/s41467-022-31008-w

8.6.3 Electrochemical Energy Storage

Many forms of renewable energy, like solar and wind, are intermittent. Consequently, to meet the current worldwide energy demand and control the load exerted on the national grid, a wide variety of energy storage solutions need to be integrated. The development of the Li-ion battery[210] has revolutionised the technology; however, the ever-increasing need for energy storage beyond portable electronics places an increasingly heavy demand on battery capacity and on developing other approaches to electrochemical storage, e.g. redox flow batteries.[211] This calls for further improvements in energy density and a continuous reduction of cost. The need for affordable, large-scale grid storage is urgent and can only be achieved through a detailed understanding of the competing processes occurring in operational batteries.

The operation of all electrochemical storage solutions relies on the movement and/or changes in the chemical state of ions, which is accompanied by solvation and desolvation processes of these ions. The rate of electron transfer involved in the redox process strongly determines the electrochemical activity, and therefore achieving a detailed understanding is essential. The energy and temporal resolution provided by a next generation XFEL combined with the high repetition rate will enable X-ray spectroscopy, X-ray Raman, X-ray scattering and photoelectron spectroscopy measurements capable of deeper understanding of the fundamental processes involved in battery performance and degradation. The high time resolution which can be achieved by a next generation XFEL will be exploited to probe fundamental charge transfer and solvation dynamics around the ions that occur on the femto- to picosecond timescale.[212] The accessibility to this time domain offers the enticing prospect of directly capturing the phenomena that drive diffusion of electroactive ions in complex electrode materials, to improve the functionality, synthesis and stability of electrochemical energy storage materials.[213]

Pulse radiolysis pump combined with X-ray probe experiments can be used to enable the study, on the picosecond timescale, of the reaction of the electrons with the ions and the electrolytes,[214] and to reveal the structural dynamics leading to degradation mechanisms. IR-pump / X-ray probe studies will provide structural insights into the solvation dynamics so important to the systems.[215]The increased brightness will concurrently allow the collection of high-quality data of weak signal from in situ studies of systems under operational conditions, such as materials/liquid interfaces in batteries.

An example of where a next generation XFEL could contribute a step-change includes providing new insights into the mechanism for intercalation observed in Li-ion batteries (LIB) and Na-ion batteries (NIBs). Synchrotron-based high resolution X-ray imaging (**Figure 8.16**) already provides spatially highly resolved insight into the relationships between the charge state of a battery and internal composition, material stresses and mass transport. Research in NIBs is of interest owing to the elemental abundance of sodium in the earth's crust, which is about three orders of magnitude larger than that of lithium.[216] However, NIBs exhibit inferior power density and reversibility compared to LIBs.

Overcoming these performance limitations requires a fundamental understanding of electrode materials and of the effect of the larger ionic radius of the Na-ion. For example, it has been shown that Na-ion intercalation in graphite electrodes includes its solvation shell and, consequently, usually an ether-based electrolyte such as di-glyme is used. In this case, the graphite interlayer spacing expands almost three-fold, from 3.35 to 10.9 Å.[217] Given this large expansion, it is astonishing that these systems can be cycled several thousand times without a significant loss in capacity. A next-generation XFEL, with its ability to probe the absorption edges of all of the constituent atoms, would provide ultrafast insight into the solvation and exchange dynamics of the Na and Li ions, and into how these change upon intercalation.

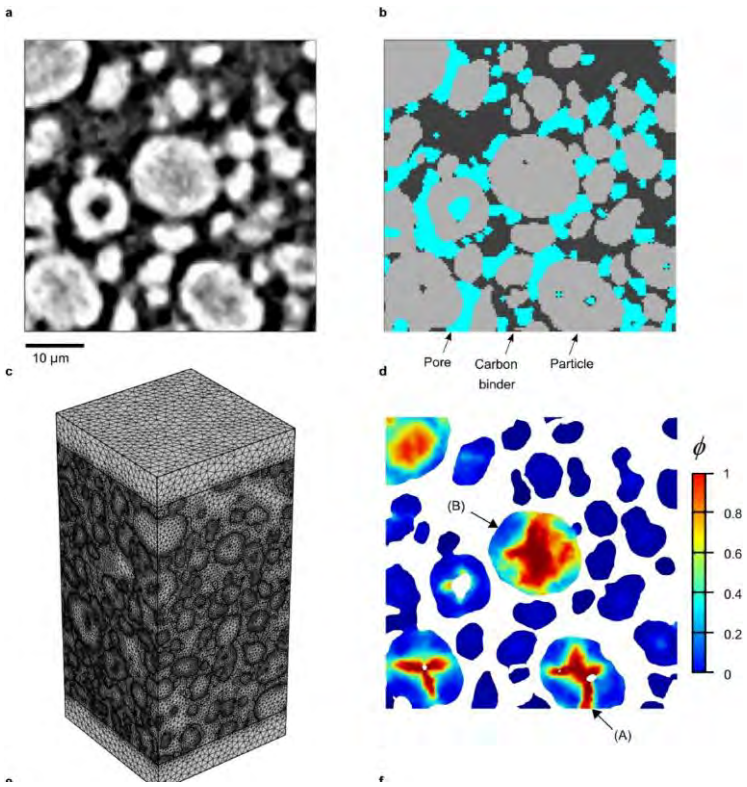


Figure 8.16: X-ray tomography, segmentation, meshing and simulation of an electrode. a) Tomogram of cropped three-phase image, b) segmentation of CT image, c) computational mesh of segmented 3D volume, d) example of model output showing fracture at a slice equivalent to a) and b).

*Figure reproduced from A.M. Boyce et al. J. Power Sources. **526**, 231119 (2022) under the terms of a Creative Commons Attribution 4.0 International License.*
DOI: 0.1016/j.jpowsour.2022.231119

A combination of X-ray Raman and resonant X-ray emission can be used to investigate the dynamic properties of electrodes during fast charge/discharge process from the perspective of the electrode material, the ions and the solvent. The visualisation of ion dynamics with pico- to femtosecond time resolution will shed new insight into the mechanism responsible for the migration of ions and what drives their diffusion. It will also enable investigations into the reduction of an electrolyte on an anode surface, the initial step towards the formation of an solid-electrolyte interface film: it is challenging to capture the reactions at the electrode/electrolyte interface experimentally, as some of the reactions could occur at the picosecond (ps) timescale.[218] Another example includes atomic scale insight into the crucial electron transfer mechanism between redox couples in redox flow batteries.[196] Besides the timescale for these processes, the high brightness of a next generation XFEL will facilitate the collection of high-quality data of photon-in/photon-out spectroscopies in operando, which have previously been shown to provide significant insight into the dynamical mechanism in batteries. Note that in **Section 9.4, Flagship Programmes IV and V** are both concerned with batteries research.

8.6.4 New generation data storage

Magnetism in novel nanoscale materials is a key ingredient in modern information technology. Manipulating magnetic materials is the cornerstone of hard drive technology, where binary digital information is recorded by aligning the direction of the magnetic poles in the hard drive. New technologies are urgently needed because it is estimated that soon over 20% of the world's energy will be consumed by information technologies, where data centres consume a large fraction of this energy. Data storage servers are already emitting as much carbon dioxide as the whole aviation industry. With the ever-increasing use of big data for driverless cars, robots, video surveillance, artificial intelligence etc, there is an urgent need to develop new generation data storage devices.

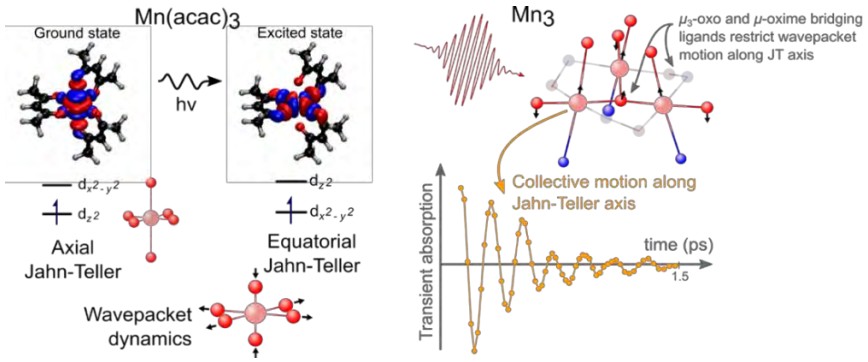


Figure 8.17: Photophysics of Mn^{3+} complexes. The antibonding nature of the e_g orbitals lead to a rapid switch of the JT distortion in the excited state of $Mn(acac)_3$ (left). In Mn_3, the strong bonds in the triangle prevent equatorial expansion and the Mn ion (right).[88]

*Figure reproduced with permission from F. Liedy et al. "Vibrational coherences in manganese single-molecule magnets after ultrafast photoexcitation" Nat. Chem. **12**, 452-458 (2020) Springer Nature. DOI: 10.1038/s41557-020-0431-6*

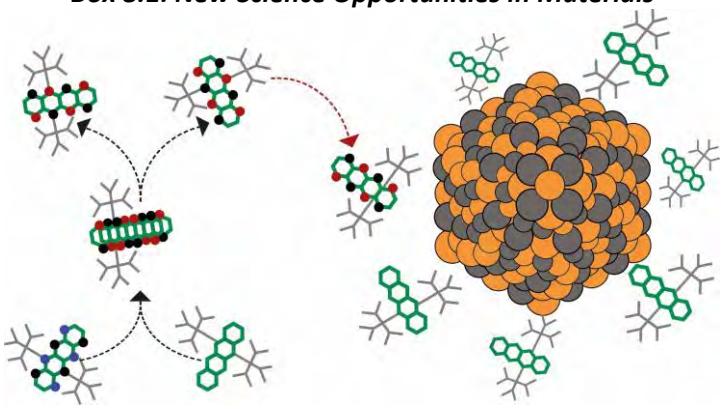
Recent developments in ultrafast magnetism have resulted in photo-magnetic recording in materials which has the distinct advantage of faster sequential switching rates due to the non-thermal mechanism.[219] These experiments make use of specific optical transitions, exciting the electrons from one atomic orbital to another, which in turn changes the magneto-crystalline anisotropy.[219] However, the microscopic mechanisms responsible are difficult to understand because they involve a high density of electronically excited states, vibrational motion, and different spin states, which are all highly coupled (see **Section 6.1**). At present, this lack of detailed understanding is hindering the development of new materials to achieve fast, energy-efficient operation and also miniaturising the magnetic grains towards the nanoscale.

The capability of fs X-ray spectroscopy will facilitate unprecedented new insights into the mechanism of emerging photo-magnetic materials, such as the trinuclear SMM $[Mn^{III}_3O(Et\text{-}sao)_3(\beta\text{-}pic)_3(ClO_4)]$,[220] as performed for light-induced excited spin-state trapping (LIESST) systems.[221, 222] In this case, the excitation of a vibrational wavepacket, closely linked to the Jahn-Teller distortion (**Figure 8.17**) was found to be closely linked the magnitude and orientation of the magnetic anisotropy. These results highlight the strong coupling between electronic and nuclear degrees of freedom, and the strong electron correlation between electrons on Mn sites in the polynuclear molecule, important for the photo-magnetic properties. The ability to probe the electronic (XAS, XES), structural (XAS) and spin (XES) dynamics of these complex materials and related analogues on the timescale upon which they operate, i.e. femtoseconds, will enable fine control of the magnetic properties and coherence times of these materials, and provide crucial new insights urgently required to develop to new storage materials.

8.6.5 Conclusion and future vision

In summary, the importance of new tools to disentangle the complex dynamics, and subsequently feed these into design rules for new energy materials, cannot be underestimated. Brute force trial and error approaches to develop new materials do not work, because we cannot test the high number of candidate molecules. The requirement of achieving increased understanding is also crucial to the ongoing digital revolution that is enabling the design process to be increasingly automated, with the potential to rapidly speed-up molecule and materials discovery.

Box 8.1: New Science Opportunities in Materials



Adapted from J. Allerdice et al. J. Am. Chem. Soc. ***141****, 32, 12907-12915 (2019) DOI: 10.1021/jacs.9b06584*

Singlet exciton fission *occurs on sub-100 fs timescales and has the potential to deliver photovoltaic devices which achieve external quantum efficiencies above 100%. However, a grand challenge is to harness singlet fission and to break the Shockley–Queisser limit on the efficiency of single-junction photovoltaics. It has been shown that the triplet states generated by singlet fission can be harvested by inorganic quantum dots, but further work is needed to fully explore triplet energy transfer to inorganic semiconductors and harness it into a device. A next-generation XFEL will make it possible to following the singlet fission and energy transfer processes responsible, providing the new understanding required to achieve high efficiency in photovoltaics.*

Indeed, to take full advantage of these developments, it is essential to achieve an understanding of the important underlying principles and competing processes. This understanding will lead to the definition of descriptors in automated methods and therefore, without careful definition, approaches based upon artificial intelligence are likely to have built in bias and are extremely unlikely to identify step-changing materials.

The next-generation XFEL will deliver the ability to investigate these fundamental dynamical processes using a range of techniques. In addition, over the next 10 years, the developments in methods such as Coherent Diffractive Imaging (CDI) and X-ray photon correlation spectroscopy (XPCS) will enable the dynamical imaging of structural domains within what are likely to be heterogenous materials into the picosecond and even femtosecond domain. This will complement the local information obtained from techniques such as XAS and XES. Developments required to support this venture include data analysis for heterogenous systems and also the challenges of performing extended studies, while ensuring uniformity of conditions and sample integrity.

8.7 References for Chapter 8

1 Project 2035 - The chemical industry transition: Pathways for a resilient and sustainable future; S&P Global (2024). Abridged version available at https://www.cia.org.uk/cia-news/the-chemical-industry-transition-pathways-for-a-resilient-and-sustainable-future/1015.article

2 M.A. Meyers, "Dynamic Behavior of Materials" (Wiley & Sons, New York, 1994), DOI: 10.1002/9780470172278

3 A.C. Fletcher *et al.* "Particle-in-cell simulations of an RF emission mechanism associated with hypervelocity impact plasmas." *Physics of Plasmas* **24**, 053102 (2017); DOI: 10.1063/1.4980833

4 R. Sundar, P. Ganesh, R.K. Gupta *et al.* "Laser Shock Peening and its Applications: A Review." *Lasers in Manufacturing and Materials Processing* **6**, 424–463 (2019); DOI: 10.1007/s40516-019-00098-8

5 S.J. Lainé *et al.* "Microstructural characterisation of metallic shot peened and laser shock peened Ti-6Al-4V." *Acta Materialia* **123**, 350 (2017); DOI: 10.1016/j.actamat.2016.10.044

6 E. Bringa, K. Rosolankova, R. Rudd *et al.* "Shock deformation of face-centred-cubic metals on subnanosecond timescales." *Nature Mater* **5**, 805-809 (2006) DOI: 10.1038/nmat1735

7 D. Milathianaki *et al.* "Femtosecond visualization of lattice dynamics in shock-compressed matter." *Science* **342** 220-223 (2013) DOI: 10.1126/science.1239566

8 R. Briggs *et al.* "Ultrafast X-ray Diffraction Studies of the Phase Transitions and Equation of State of Scandium Shock Compressed to 82 GPa." *Phys. Rev. Lett.* **118**, 025501 (2017) DOI: 10.1103/PhysRevLett.118.025501

9 A.L. Coleman *et al.* "Identification of Phase Transitions and Metastability in Dynamically Compressed Antimony Using Ultrafast X-ray Diffraction." *Phys. Rev. Lett*. **122**, 255704 (2019) DOI: 10.1103/PhysRevLett.122.255704

10 C.E. Wehrenberg, D. McGonegle, C. Bolme *et al.* "In situ X-ray diffraction measurement of shock-wave-driven twinning and lattice dynamics." *Nature* **550**, 496–499 (2017) DOI: 10.1038/nature24061

11 M. Sliwa *et al.* "Femtosecond X-ray Diffraction Studies of the Reversal of the Microstructural Effects of Plastic Deformation during Shock Release of Tantalum." *Phys. Rev. Lett*. **120** 265502 (2018) DOI: 10.1103/PhysRevLett.120.265502

12 J. Coakley *et al*., "Femtosecond quantification of void evolution during rapid material failure." *Sci. Adv*. **6**: eabb4434 (2020) DOI: 10.1126/sciadv.abb4434

13 https://www.lanl.gov/science-innovation/science-facilities/dmmsc/index.php

14 P.D. Heighway *et al.* "Molecular dynamics simulations of grain interactions in shock-compressed highly textured columnar nanocrystals." *Phys. Rev. Materials* **3**,083602 (2019) DOI: 10.1103/PhysRevMaterials.3.083602

15 B. Lambourn and C. Handley, "A two-temperature model for shocked porous explosive." *AIP Conf. Proc*. **1793**, 120025 (2017) DOI: 10.1063/1.4971707

16 C. Handley *et al.* "Understanding the shock and detonation response of high explosives at the continuum and meso scales." *Appl. Phys. Rev*. **5**, 011303 (2018) DOI: 10.1063/1.5005997

17 R.L. Sandberg *et al.* "Studying Shocked Material Dynamics with Ultrafast X-rays." *Microsc. Microanal*. **21** (Suppl 3), 1851 (2015) DOI: 10.1017/S143192761501003X

18 P.G. Frankel *et al.* "Residual stress fields after FOD impact on flat and aerofoil-shaped leading edges." *Mechanics of Materials* **55**, 130 (2012).DOI: 10.1016/j.mechmat.2012.08.007

19 C.L.A. Leung, S. Marussi, R.C. Atwood *et al.* "In situ X-ray imaging of defect and molten pool dynamics in laser additive manufacturing." *Nat Commun* **9** 1355 (2018) DOI: 10.1038/s41467-018-03734-7

20 N.J. Sanchez *et al.* "Dynamic exploding foil initiator imaging at the advanced photon source." *AIP Conference Proceedings* **1979**, 160023 (2018) DOI: 10.1063/1.5045022

21 B.R. Maddox *et al.* "Single-pulse X-ray diffraction using polycapillary optics for in situ dynamic diffraction." *Rev. Sci. Inst*. **87**, 083901 (2016) DOI: 10.1063/1.4960812

22 P. Mason *et al.* "Development of a 100J, 10Hz laser for compression experiments at the High Energy Density instrument at the European XFEL." *High Power Laser Science and Engineering* **6**, E65 (2018) DOI: 10.1017/hpl.2018.56

23 S.N. Luo *et al.* "Gas gun shock experiments with single-pulse X-ray phase contrast imaging and diffraction at the Advanced Photon Source." *Rev. Sci. Inst*. **83**, 073903 (2012); DOI: 10.1063/1.4733704

24 T.A. Kathyola *et al.* "X-ray Absorption Spectroscopy as a Process Analytical Technology: Reaction Studies for the Manufacture of Sulfonate-Stabilized Calcium Carbonate Particles." *Ind. Eng. Chem. Res.* **62**, 40, 16198–16206 (2023) DOI: 10.1021/acs.iecr.3c02540

25 T.A. Kathyola *et al.* "Reactive $CaCO_3$ Formation from CO_2 and Methanolic $Ca(OH)_2$ Dispersions: Transient Methoxide Salts, Carbonate Esters and Sol-Gels." *ACS physical chemistry Au* **4**,5 555-567 (2024) DOI: 10.1021/acsphyschemau.4c00041

26 T.A. Kathyola *et al.* "How non-aqueous media direct the reaction of $Ca(OH)_2$ with CO_2 to different forms of $CaCO_3$: *operando* mid-infrared and X-ray absorption spectroscopy studies." *Phys. Chem. Chem. Phys.* **27**, 9668-9675 (2025) DOI: 10.1039/D4CP04774E

27 I. Kicior, L. Matthews, A.J. Britton *et al.* "Friction and wear reduction by glycerol oleates: The molecular basis for performance variations in the presence of water and acetic acid." *Tribology International*, **214** (Part A). 111140 (2026) DOI: 10.1016/j.triboint.2025.111140

[28] G. Tsagkaropoulou, C.P. Warrens and P.J. Camp, "Interactions between Friction Modifiers and Dispersants in Lubricants: The Case of Glycerol Monooleate and Polyisobutylsuccinimide-Polyamine." *ACS Appl. Mater. Interfaces* **11**, 28359-28369 (2019) DOI: 10.1021/acsami.9b05718

[29] M.P. Grubb, P. Coulter, H. Marroux *et al.* "Translational, rotational and vibrational relaxation dynamics of a solute molecule in a non-interacting solvent." *Nat. Chem.* **8**, 1042-1046 (2016) DOI: 10.1038/nchem.2570

[30] R.J. Davey, S.L.M. Schroeder and J.H. ter Horst, "Nucleation of organic crystals - A molecular perspective." *Angew. Chem. Int. Ed*. **52**, 2166–2179 (2013) DOI: 10.1002/anie.201204824

[31] G.C. Sosso at al. "Crystal Nucleation in Liquids: Open Questions and Future Challenges in Molecular Dynamics Simulations." *Chem. Rev*. **116**, 7078–7116 (2016) DOI: 10.1021/acs.chemrev.5b00744

[32] D. Gebauer *et al.* "Pre-nucleation clusters as solute precursors in crystallisation." *Chem. Soc. Rev*. **43**(7), 2348–2371 (2014) DOI: 10.1039/c3cs60451a

[33] D. Kashchiev and G.M. van Rosmalen, "Review: Nucleation in solutions revisited." *Cryst. Res. Technol.* **38**, 555–574 (2003) DOI: 10.1002/crat.200310070

[34] D. Kashchiev, "Nucleation: Basic Theory with Applications." Butterworth-Heinemann, Oxford (2000) DOI: 10.1016/B978-0-7506-4682-6.X5000-8

[35] D. Erdemir, A.Y. Lee and A.S. Myerson, "Nucleation of Crystals from Solution: Classical and Two-Step Models." *Acc. Chem. Res*. **42**, 5, 621–629 (2009) DOI: 10.1021/ar800217x

[36] S.Y. Chang, S.L.M. Schroeder *et al.* "Detection and characterisation of sub-critical nuclei during reactive Pd metal nucleation by X-ray absorption spectroscopy." *CrystEngComm* **18**, 674–682 (2016) DOI: 10.1039/C5CE01883H

[37] M.H. Nielsen, S. Aloni and J.J. De Yoreo, "In situ TEM imaging of $CaCO_3$ nucleation reveals coexistence of direct and indirect pathways." *Science* **345**, 1158–1162 (2014) DOI: 10.1126/science.1254051

[38] H.N. Chapman, "X-ray Free-Electron Lasers for the Structure and Dynamics of Macromolecules." *Annu Rev Biochem* **88**, 35-58 (2019) DOI: 10.1146/annurev-biochem-013118-110744

[39] P. Fromme, "XFELs open a new era in structural chemical biology." *Nat Chem Biol* **11**, 895-899 (2015) DOI: 10.1038/nchembio.1968

[40] I. Schlichting, "Serial femtosecond crystallography: the first five years*." IUCrJ* **2**, 246-255 (2015) DOI: 10.1107/S205225251402702X

[41] J.C.H. Spence, "XFELs for structure and dynamics in biology." *IUCrJ* **4**, 322-339 (2017) DOI: 10.1107/S2052252517005760

[42] M. Schmidt, "Time-Resolved Macromolecular Crystallography at Pulsed X-ray Sources*." Int. J. Mol. Sci.* **20**(6) 1401 (2019) DOI: 10.3390/ijms20061401

[43] M. Schmidt, "Time-Resolved Macromolecular Crystallography at Modern X-ray Sources." *Methods Mol Biol* **1607**, 273-294 (2017) DOI: 10.1007/978-1-4939-7000-1_11

[44] M. Schmidt and D.K. Saldin, "Enzyme transient state kinetics in crystal and solution from the perspective of a time-resolved crystallographer." *Struct Dyn* **1**, 024701 (2014) DOI: 10.1063/1.4869472

[45] M. Schmidt, "Mix and Inject: Reaction Initiation by Diffusion for Time-Resolved Macromolecular Crystallography." *Advances in Condensed Matter Physics* 2013, (5-6):1-10 (2013) DOI: 10.1155/2013/167276

[46] C.X. Weichenberger and B. Rupp, "Ten years of probabilistic estimates of biocrystal solvent content: new insights via nonparametric kernel density estimate." *Acta Crystallogr D Biol Crystallogr* **70**, 1579-1588 (2014) DOI: 10.1107/S1399004714005550

[47] M. Chruszcz *et al.* "Analysis of solvent content and oligomeric states in protein crystals--does symmetry matter?." *Protein Sci* **17**, 623-632 (2008) DOI: 10.1110/ps.073360508

[48] K.A. Kantardjieff and B. Rupp, "Matthews coefficient probabilities: Improved estimates for unit cell contents of proteins, DNA, and protein-nucleic acid complex crystals." *Protein Sci* **12**, 1865-1871 (2003) DOI: 10.1110/ps.0350503

[49] B.W. Matthews, "Solvent content of protein crystals." *J Mol Biol* **33**, 491-497 (1968) DOI: 10.1016/0022-2836(68)90205-2

[50] L. Pravda, K. Berka, R. Svobodová Vařeková *et al.* "Anatomy of enzyme channels." *BMC Bioinformatics* **15**, 379 (2014) DOI: 10.1186/s12859-014-0379-x

[51] D.H. Juers and J. Ruffin, "MAP_CHANNELS: a computation tool to aid in the visualization and characterization of solvent channels in macromolecular crystals." *J Appl Crystallogr* **47**, 2105-2108 (2014) DOI: 10.1107/S160057671402281X

[52] R.G. Coleman and K.A. Sharp, "Finding and characterizing tunnels in macromolecules with application to ion channels and pores." *Biophys J* **96**, 632-645 (2009) DOI: 10.1529/biophysj.108.135970

[53] J.L. Olmos, S. Pandey, J.M. Martin-Garcia, M. Schmidt *et al. "*Enzyme intermediates captured "on the fly" by mix-and-inject serial crystallography." *BMC Biol* **16**, 59 (2018) DOI: 10.1186/s12915-018-0524-5

[54] D. Oberthuer, J. Knoška, M. Wiedorn *et al.* "Double-flow focused liquid injector for efficient serial femtosecond crystallography." *Sci Rep* **7**, 44628 (2017) DOI: 10.1038/srep44628

[55] C. Kupitz, J.L. Olmos Jr, M. Holl *et al.* "Structural enzymology using X-ray free electron lasers." *Struct Dyn* **4**(4):044003 (2017) DOI: 10.1063/1.4972069

[56] J. Knoška, L. Adriano, S. Awel *et al.* "Ultracompact 3D microfluidics for time-resolved structural biology." *Nat Commun* **11**, 657 (2020) DOI: 10.1038/s41467-020-14434-6

[57] S. Bohne, M. Heymann, H.N. Chapman, H.K. Trieu, S. Baht, "3D printed nozzles on a silicon fluidic chip." *Rev Sci Instrum* **90**, 035108 (2019) DOI: 10.1063/1.5080428

[58] M.O. Wiedorn, S. Awel, A.J. Morgan *et al.* "Rapid sample delivery for megahertz serial crystallography at X-ray FELs." *IUCrJ* **5**, 574-584 (2018) DOI: 10.1107/S2052252518008369

[59] J.R. Stagno, Y. Liu, Y.R. Bhandari *et al.* "Structures of riboswitch RNA reaction states by mix-and-inject XFEL serial crystallography." *Nature* **541**, 242-246 (2017) DOI: 10.1038/nature20599

[60] B.G. Abdallah, N.A. Zatsepin, S. Roy-Chowdhury *et al.* "Microfluidic sorting of protein nanocrystals by size for X-ray free-electron laser diffraction." *Struct Dyn* **2**, 041719 (2015) DOI: 10.1063/1.4928688

[61] J. Luo, K.A. Muratore, E.A. Arriaga, A. Ros, "Deterministic Absolute Negative Mobility for Micro- and Submicrometer Particles Induced in a Microfluidic Device." *Anal Chem* **88**, 5920-5927 (2016) DOI: 10.1021/acs.analchem.6b00837

[62] B.G. Abdallah, S. Roy-Chowdhury, J. Coe, P. Fromme, A. Ros, "High throughput protein nanocrystal fractionation in a microfluidic sorter." *Anal Chem* **87**, 4159-4167 (2015) DOI: 10.1021/acs.analchem.5b00589

[63] M. Heymann, A. Opthalage, J.L. Wierman *et al.* "Room-temperature serial crystallography using a kinetically optimized microfluidic device for protein crystallization and on-chip X-ray diffraction." *IUCrJ* **1**(Pt 5), 349-360 (2014) DOI: 10.1107/S2052252514016960

[64] G. Brändén, G. Hammarin, R. Harimoothy et al. "Coherent diffractive imaging of microtubules using an X-ray laser." Nat Commun 10, 2589 (2019) DOI: 10.1038/s41467-019-10448-x

[65] D.H. Wojtas, K. Ayyer, M. Liang *et al*. "Analysis of XFEL serial diffraction data from individual crystalline fibrils." *IUCrJ* **4**, 795–811 (2017) DOI: 10.1107/S2052252517014324

[66] C. Seuring, K. Ayyer, E. Filippaki *et al*. "Femtosecond X-ray coherent diffraction of aligned amyloid fibrils on low background grapheme." *Nat Commun* **9**, 1836 (2018) DOI: 10.1038/s41467-018-04116-9

[67] S.-Y. Ow and D.E. Dunstan, "A brief overview of amyloids and Alzheimer's disease." *Protein Sci*. **23**, 1315–1331 (2014) DOI: 10.1002/pro.2524

[68] K. Araki, N. Yagi, K. Aoyama *et al*. "Parkinson's disease is a type of amyloidosis featuring accumulation of amyloid fibrils of α-synuclein". *Proc Natl Acad Sci U S A.* **116**, 17963–17969 (2019) DOI: 10.1073/pnas.1906124116

[69] C.L.A. Leung *et al*, "Laser-matter interactions in additive manufacturing of stainless steel SS316L and 13-93 bioactive glass revealed by *in* situ X-ray imaging." *Additive Manu*. **24**, 647-657 (2018) DOI: 10.1016/j.addma.2018.08.025

[70] P. Bidare, I. Bitharas, R.M. Ward, M.M. Attallah, A.J. Moore, "Fluid and particle dynamics in laser powder bed fusion." *Acta Materialia* **142**, 107-120 (2018) DOI: 10.1016/j.actamat.2017.09.051

[71] T. Aizawa and T. Inohara, "Pico- and Femtosecond Laser Micromachining for Surface Texturing." *InTech Open Book* (2018) DOI: 10.5772/intechopen.83741

[72] K. Sugioka and Y. Cheng, "Femtosecond laser three-dimensional micro- and nanofabrication." Appl. Phys. Rev. **1**, 041303 (2014) DOI: 10.1063/1.4904320

[73] T.A. Assefa, Y. Cao, S. Banerjee *et al.* "Ultrafast X-ray diffraction study of melt-front dynamics in polycrystalline thin films." *Sci Adv*. **6**(3):eaax2445 (2020), DOI: 10.1126/sciadv.aax2445

[74] N. Nakamura et al. "Research and development of the EUV-FEL light source for lithography." Proc. SPIE 13177, Photomask Japan 2024: XXX Symposium on Photomask and Next-Generation Lithography Mask Technology, 131770L (2024) DOI: 10.1117/12.3033966

[75] S. Perathoner (Ed.) "Science and Technology Roadmap on Catalysis for Europe a Path To Create a Sustainable Future." European Research Institute for Catalysis (ERIC aisbl) (2016) http://www.euchems.eu/roadmap-on-catalysis-for-europe/

[76] G.L. Chiarello and D. Ferri, "Modulated excitation extended X-ray absorption fine structure spectroscopy." *Phys. Chem. Chem. Phys.* **17**(16), 10579–10591 (2015) DOI: 10.1039/C5CP00609K

[77] T. Yokoyama, Y. Uemura, "Pump Probe XAFS." In: Y. Iwasawa, K. Asakura, M. Tada (eds) *XAFS Techniques for Catalysts, Nanomaterials, and Surfaces*. Springer, Cham. DOI: 10.1007/978-3-319-43866-5_9

[78] C.J. Milne *et al*. "Disentangling the evolution of electrons and holes in photoexcited ZnO nanoparticles." *Struct. Dyn*. **10**, 064501 (2023) DOI: 10.1063/4.0000204

[79] T.J. Penfold, J. Szlachetko, F.G. Santomauro *et al.* "Revealing hole trapping in zinc oxide nanoparticles by time-resolved X-ray spectroscopy." *Nat Commun* **9**, 478 (2018) DOI: 10.1038/s41467-018-02870-4

[80] M.H. Rittmann-Frank *et al*. "Mapping of the photoinduced electron traps in TiO_2 by picosecond X-ray absorption spectroscopy." *Angewandte Chemie (International ed. in English)* vol. **53**, 23:5858-62 (2014) DOI: 10.1002/anie.201310522

[81] G. Smolentsev, C.J. Milne, A. Guda *et al.* "Taking a snapshot of the triplet excited state of an OLED organometallic luminophore using X-rays." *Nat Commun* **11**, 2131 (2020) DOI: 10.1038/s41467-020-15998-z

[82] R. Boll, J.M. Schäfer, B. Richard *et al.* "X-ray multiphoton-induced Coulomb explosion images complex single molecules." *Nat. Phys.* **18**, 423–428 (2022) DOI: 10.1038/s41567-022-01507-0

[83] M. Aleksich *et al*. "XFEL Microcrystallography of Self-Assembling Silver *n*-Alkanethiolates." *J. Am. Chem. Soc.* **145**, 31, 17042–17055 (2023) DOI: 10.1021/jacs.3c02183

[84] R.M. Jay *et al.* "Tracking C-H activation with orbital resolution." *Science* **380**, 955-960 (2023) DOI: 10.1126/science.adf8042

[85] J-U. Rohde *et al*. "Crystallographic and spectroscopic characterization of a nonheme Fe(IV)-O complex." *Science* **299**,5609: 1037-9 (2003) DOI: 10.1126/science.299.5609.1037

[86] A.W. Hahn *et al.* "Measurement of the Ligand Field Spectra of Ferrous and Ferric Iron Chlorides Using

2p3d RIXS." *Inorg. Chem*. **56**, 14, 8203–8211 (2017) DOI: 10.1021/acs.inorgchem.7b00940

87 R.G. Castillo *et al.* "Probing Physical Oxidation State by Resonant X-ray Emission Spectroscopy: Applications to Iron Model Complexes and Nitrogenase." *Angew. Chem. Int. Ed.* **60**, 10112 (2021) DOI: 10.1002/anie.202015669

88 F. Liedy, J. Eng, R. McNab *et al*. "Vibrational coherences in manganese single-molecule magnets after ultrafast photoexcitation." *Nat. Chem*. **12**, 452–458 (2020) DOI: 10.1038/s41557-020-0431-6

89 C. Middleton, C.D. Rankine and T.J. Penfold, "An on-the-fly deep neural network for simulating time-resolved spectroscopy: predicting the ultrafast ring opening dynamics of 1,2-dithiane." *Phys. Chem. Chem. Phys.* **25**, 13325-13334 (2023) DOI: 10.1039/D3CP00510K

90 L. Watson *et al.* "A Δ-learning strategy for interpretation of spectroscopic observables." *Struct. Dyn.* **1** 10 (6): 064101 (2023) DOI: 10.1063/4.0000215

91 P.M. Donaldson *et al*. "Breaking Barriers in Ultrafast Spectroscopy and Imaging Using 100 kHz Amplified Yb-Laser Systems**."** *Acc. Chem. Res*. **56**, 15, 2062–2071 (2023) DOI: 10.1021/acs.accounts.3c00152

92 P.M. Donaldson, "Photon echoes and two dimensional spectra of the amide I band of proteins measured by femtosecond IR – Raman spectroscopy." *Chem. Sci.* **11**, 8862-8874 (2020) DOI: 10.1039/D0SC02978E

93 F. Meirer, B.M. Weckhuysen, "Spatial and temporal exploration of heterogeneous catalysts with synchrotron radiation." *Nat Rev Mater* **3**, 324–340 (2018) DOI: 10.1038/s41578-018-0044-5

94 Y. Obara *et al.* "Femtosecond time-resolved X-ray absorption spectroscopy of anatase TiO_2 nanoparticles using XFEL." *Struct. Dyn*. **4**, 044033 (2017) DOI: 10.1063/1.4989862

95 C. Paolucci *et al*. "Dynamic multinuclear sites formed by mobilized copper ions in NO_x selective catalytic reduction**.**" *Science* **357**, 898 (2017) DOI10.1126/science.aan5630

96 L. Chen *et al.* "A Complete Multisite Reaction Mechanism for Low-Temperature NH_3-SCR over Cu-CHA." *ACS Catal*. **10**, 10, 5646–5656 (2020) DOI: 10.1021/acscatal.0c00440

97 C. Paolucci *et al*. "Catalysis in a Cage: Condition-Dependent Speciation and Dynamics of Exchanged Cu Cations in SSZ-13 Zeolites." J. Am. Chem. Soc. 2016, 138, 18, 6028–6048 (2016) DOI: 10.1021/jacs.6b02651

98 M. Ronovsky *et al*. "Assessing Utilization Boundaries for Pt-Based Catalysts in an Operating Proton-Exchange Membrane Fuel Cell." *ACS Appl. Energy. Mater.* **6**, 17, 8660 (2023) DOI: 10.1021/acsaem.3c01243

99 J.E. Parker *et al*. "A cell design for correlative hard X-ray nanoprobe and electron microscopy studies of catalysts under in situ conditions." *J. Synch. Rad.* **29**(2), 431–438 (2022) DOI: 10.1107/S1600577521013576

100 A. Barnosky, N. Matzke, S. Tomiya *et al.* "Has the Earth's sixth mass extinction already arrived?." *Nature* **471**, 51-57 (2011) DOI: 10.1038/nature09678

101 L. Zhang, D. Lin, X. Sun, U. Curth, C. Drosten, L. Sauerhering, R. Hilgenfeld *et al.* "Crystal structure of SARS-CoV-2 main protease provides a basis for design of improved alpha-ketoamide inhibitors." *Science* **368**, 409-412 (2020) DOI: 10.1126/science.abb3405

102 R. Yan, Y. Zhang, Y. Li, L. Xia, Y. Guo and Q. Zhou, "Structural basis for the recognition of the SARS-CoV-2 by full-length human ACE2." *Science* **367**, 1444-1448 (2020) DOI: 10.1126/science.abb2762

103 D. Wrapp, N. Wang, K.S. Corbett *et al.* "Cryo-EM structure of the 2019-nCoV spike in the prefusion conformation." *Science* **367**, 1260-1263 (2020) DOI: 10.1126/science.abb2507

104 S. Dong, J. Sun, Z. Mao, L. Wang, Y.L. Lu, Y. L. and J. Li, "A guideline for homology modeling of the proteins from newly discovered betacoronavirus, 2019 novel coronavirus (2019-nCoV)." *J Med Virol.* (2020) DOI: 10.1002/jmv.25768

105 J. Lan, J. Ge, J. Yu *et al.* "Structure of the SARS-CoV-2 spike receptor-binding domain bound to the ACE2 receptor". *Nature* **581,** 215–220 (2020). DOI: 10.1038/s41586-020-2180-5

106 Z. Jin, X. Du, Y. Xu *et al.* "Structure of M^{pro} from COVID-19 virus and discovery of its inhibitors." *Nature* **582**, 289-293 (2020) DOI: 10.1038/s41586-020-2223-y

107 A.C. Walls, Y.J. Park, M.A. Tortorici, A. Wall, A.T. McGuire and D. Veesler, "Structure, Function, and Antigenicity of the SARS-CoV-2 Spike Glycoprotein." *Cell* (2020) DOI: 10.1016/j.cell.2020.02.058

108 J.D. Westbrook, R. Soskind, B.P. Hudson and S.K. Burley, "Impact of the Protein Data Bank on antineoplastic approvals." *Drug Discov Today* S1359-6446(20)30070-2 (2020) DOI: 10.1016/j.drudis.2020.02.002

109 D.S. Goodsell, C. Zardecki, L. Di Costanzo *et al.* "RCSB Protein Data Bank: Enabling biomedical research and drug discovery." *Protein Science* **29**(1): 52-65 (2020) DOI: 10.1002/pro.3730

110 J.D. Westbrook and S.K. Burley, "How Structural Biologists and the Protein Data Bank Contributed to Recent FDA New Drug Approvals." *Structure* **27**, 211-217 (2019) DOI: 10.1016/j.str.2018.11.007

111 T.L. Blundell, "Protein crystallography and drug discovery: recollections of knowledge exchange between academia and industry." *IUCrJ* **4**, 308-321 (2017) DOI: 10.1107/S2052252517009241

112 I. Shimada, T. Ueda, Y. Kofuku *et al*. "GPCR drug discovery: integrating solution NMR data with crystal and cryo-EM structures." *Nat Rev Drug Discov* **18**, 59-82 (2019) DOI: 10.1038/nrd.2018.180

113 C. Munk, E. Mutt, V. Isberg *et al.* "An online resource for GPCR structure determination and analysis." *Nat Methods* **16**, 151-162 (2019) DOI: 10.1038/s41592-018-0302-x

114 W.I. Weis and B.K. Kobilka, "The Molecular Basis of G Protein-Coupled Receptor Activation*." Annu Rev Biochem* **87**, 897-919 (2018) DOI: 10.1146/annurev-biochem-060614-033910

[115] D. Hilger, M. Masureel and B.K. Kobilka, "Structure and dynamics of GPCR signaling complexes." *Nat Struct Mol Biol* **25**, 4-12 (2018) DOI: 10.1038/s41594-017-0011-7

[116] N.R. Latorraca, A.J. Venkatakrishnan and R.O. Dror, "GPCR Dynamics: Structures in Motion." *Chem Rev* **117**(1): 139-155 (2017) DOI: 10.1021/acs.chemrev.6b00177

[117] V. Katritch, V. Cherezov and R.C. Stevens, "Diversity and modularity of G protein-coupled receptor structures." *Trends Pharmacol Sci* **33**(1), 17-27 (2012) DOI: 10.1016/j.tips.2011.09.003

[118] D. Li and M. Caffrey, "Structure and Functional Characterization of Membrane Integral Proteins in the Lipid Cubic Phase." *Journal of Molecular Biology* Feb (2020) DOI: 10.1016/j.jmb.2020.02.024

[119] R.M. Stein, H.J. Kang, J.D McCorvy *et al.* "Virtual discovery of melatonin receptor ligands to modulate circadian rhythms." *Nature* **579**, 609-614 (2020) DOI: 10.1038/s41586-020-2027-0

[120] B. Stauch, L.C. Johansson, J.D. McCorvy *et al.* "Structural basis of ligand recognition at the human MT_1 melatonin receptor." *Nature* **569**, 284-288 (2019) DOI: 10.1038/s41586-019-1141-3

[121] L.C. Johansson, B. Stauch, J.D. McCorvy *et al.* "XFEL structures of the human MT_2 melatonin receptor reveal the basis of subtype selectivity." *Nature* **569**, 289-292 (2019) DOI: 10.1038/s41586-019-1144-0

[122] A. Gusach, A. Luginina, E. Marin *et al.* "Structural basis of ligand selectivity and disease mutations in cysteinyl leukotriene receptors." *Nat Commun* **10**, 5573 (2019) DOI: 10.1038/s41467-019-13348-2

[123] B. Stauch and V. Cherezov, "Serial Femtosecond Crystallography of G Protein-Coupled Receptors." *Annu Rev Biophys* **47**, 377-397 (2018) DOI: 10.1146/annurev-biophys-070317-033239

[124] T. Che, S. Majumdar, S.A. Zaidi *et al.* "Structure of the Nanobody-Stabilized Active State of the Kappa Opioid Receptor." *Cell* **172**, 55-67 e15 (2018) DOI: 10.1016/j.cell.2017.12.011

[125] H. Zhang, H. Unal, C. Gati *et al.* "Structure of the Angiotensin receptor revealed by serial femtosecond crystallography." *Cell* **161**(4): 833-844 (2015) DOI: 10.1016/j.cell.2015.04.011

[126] Y. Kang, X.E. Zhou, X. Gao *et al.* "Crystal structure of rhodopsin bound to arrestin by femtosecond X-ray laser." *Nature* **523**, 561-567 (2015) DOI: 10.1038/nature14656

[127] U. Weierstall, D. James, C. Wang *et al.* "Lipidic cubic phase injector facilitates membrane protein serial femtosecond crystallography." *Nat Commun* **5**, 3309 (2014) DOI: 10.1038/ncomms4309

[128] W. Liu, D. Wacker, C. Gati *et al.* "Serial femtosecond crystallography of G protein-coupled receptors." *Science* **342**, 1521-1524 (2013) DOI: 10.1126/science.1244142

[129] A. Ishchenko, B. Stauch, G.W. Han *et al.* "Toward G protein-coupled receptor structure-based drug design using X-ray lasers." *IUCrJ* **6**, 1106-1119 (2019) DOI: doi:10.1107/S2052252519013137

[130] K.K. Meier, S.M. Jones, T. Kaper *et al.* "Oxygen Activation by Cu LPMOs in Recalcitrant Carbohydrate Polysaccharide Conversion to Monomer Sugars." *Chem Rev* **118**(5): 2593-2635 (2018) DOI: 10.1021/acs.chemrev.7b00421

[131] A.J. Jasniewski and L. Que Jr. "Dioxygen Activation by Nonheme Diiron Enzymes: Diverse Dioxygen Adducts, High-Valent Intermediates, and Related Model Complexes." *Chem Rev* **118**, 5,2554-2592 (2018) DOI: 10.1021/acs.chemrev.7b00457

[132] X. Huang and J.T. Groves, "Oxygen Activation and Radical Transformations in Heme Proteins and Metalloporphyrins." *Chem Rev* **118**, 5, 2491-2553 (2018) DOI: 10.1021/acs.chemrev.7b00373

[133] R.H. Holm, P. Kennepohl and E.I. Solomon, "Structural and Functional Aspects of Metal Sites in Biology." *Chem Rev* **96**, 7, 2239-2314 (1996) DOI: 10.1021/cr9500390

[134] E.I. Solomon, S. Goudarzi and K.D. Sutherlin, "O_2 Activation by Non-Heme Iron Enzymes." *Biochemistry* **55**(46), 6363-6374 (2016) DOI: 10.1021/acs.biochem.6b00635

[135] F. Muh and A. Zouni, "Structural basis of light-harvesting in the photosystem II core complex." *Protein Sci* **29**(5): 1090-1119 (2020) DOI: 10.1002/pro.3841

[136] N. Cox, D.A. Pantazis and W. Lubitz, "Current Understanding of the Mechanism of Water Oxidation in Photosystem II and Its Relation to XFEL Data." *Annu Rev Biochem* (2020) DOI: 10.1146/annurev-biochem-011520-104801

[137] J. Kern, R. Chatterjee, I.D. Young *et al.* "Structures of the intermediates of Kok's photosynthetic water oxidation clock." *Nature* **563**, 421-425 (2018) DOI: 10.1038/s41586-018-0681-2

[138] I. Young, M. Ibrahim, R. Chatterjee *et al.* "Structure of photosystem II and substrate binding at room temperature." *Nature* **540**, 453-457 (2016) DOI: 10.1038/nature20161

[139] J. Kern, R. Tran, R. Alonso-Mori *et al.* "Taking snapshots of photosynthetic water oxidation using femtosecond X-ray diffraction and spectroscopy." *Nat Commun* **5**, 4371 (2014) DOI: 10.1038/ncomms5371

[140] J. Kern, R. Alonso-Mori, R. Tran *et al.* "Simultaneous femtosecond X-ray spectroscopy and diffraction of photosystem II at room temperature." *Science* **340**(6131), 491-495 (2013) DOI: 10.1126/science.1234273

[141] M. Suga, F. Akita, K. Yamashita *et al.* "An oxyl/oxo mechanism for oxygen-oxygen coupling in PSII revealed by an x-ray free-electron laser." *Science* **366**(6463):334-338 (2019) DOI: 10.1126/science.aax6998

[142] M. Suga, F. Akita, M. Sugahara *et al.* "Light-induced structural changes and the site of O=O bond formation in PSII caught by XFEL." *Nature* **543**, 131-135 (2017) DOI: 10.1038/nature21400

[143] M. Suga, X. Qin, T. Kuang and J.R. Shen, "Structure and energy transfer pathways of the plant photosystem I-LHCI supercomplex." *Curr Opin Struct Biol* **39**, 46-53 (2016) DOI: 10.1016/j.sbi.2016.04.004

[144] K. Ayyer, O.M. Yefanov, D. Oberthür *et al.* "Macromolecular diffractive imaging using

imperfect crystals." *Nature* **530**, 202-206 (2016) DOI: 10.1038/nature16949

145 C. Kupitz, S. Basu, I. Grotjohann *et al.* "Serial time-resolved crystallography of photosystem II using a femtosecond X-ray laser." *Nature* **513**, 261-265 (2014) DOI: 10.1038/nature13453

146 Y. Lu and J. Koo, "O_2 sensitivity and H_2 production activity of hydrogenases-A review." *Biotechnol Bioeng* **116**(11):3124-3135 (2019) DOI: 10.1002/bit.27136

147 Y. Ilina, C. Lorent, S. Katz *et al.* "X-ray Crystallography and Vibrational Spectroscopy Reveal the Key Determinants of Biocatalytic Dihydrogen Cycling by [NiFe] Hydrogenases." *Angew Chem Int Ed Engl* **58**(51):18710-18714 (2019) DOI: 10.1002/anie.201908258

148 A. Volbeda, J.M. Mouesca, C. Darnault *et al*. "X-ray structural, functional and computational studies of the O_2-sensitive E. coli hydrogenase-1 C19G variant reveal an unusual [4Fe-4S] cluster." *Chemical Communications (Cambridge, England)* **54**(52): 7175-7178 (2018) DOI: 10.1039/c8cc02896f

149 K. Schuchmann, N.P. Chowdhury and V. Muller, "Complex Multimeric [FeFe] Hydrogenases: Biochemistry, Physiology and New Opportunities for the Hydrogen Economy." *Front Microbiol* **9**, 2911 (2018) DOI: 10.3389/fmicb.2018.02911

150 S.E. Beaton, R.M. Evans, A.J. Finney *et al*. "The structure of hydrogenase-2 from Escherichia coli: implications for H2-driven proton pumping." *The Biochemical Journal* **475**(7):1353-1370 (2018) DOI: 10.1042/BCJ20180053

151 Y. Shomura, M. Taketa, H. Nakashima *et al.* "Structural basis of the redox switches in the NAD^+-reducing soluble [NiFe]-hydrogenase." *Science* **357**(6354):928-932 (2017) DOI: 10.1126/science.aan4497

152 J. Kalms, A. Schmidt, S. Frielingsdorf, P. van der Linden, D. von Stetten, O. Lenz, P. Carpentier, P. Scheerer, "Krypton Derivatization of an O_2-Tolerant Membrane-Bound [NiFe] Hydrogenase Reveals a Hydrophobic Tunnel Network for Gas Transport." *Angew Chem Int Ed Engl* **55**, 5586 (2016) DOI: 10.1002/anie.201508976

153 R. Evans, E. Brooke, S. Wehlin *et al.* "Mechanism of hydrogen activation by [NiFe] hydrogenases." *Nat Chem Biol* **12**, 46-50 (2016) DOI: 10.1038/nchembio.1976

154 H. Ogata, K. Nishikawa and W. Lubitz, "Hydrogens detected by subatomic resolution protein crystallography in a [NiFe] hydrogenase." *Nature* **520**, 571-574 (2015) DOI: 10.1038/nature14110

155 J. Fritsch, O. Lenz and B. Friedrich, "Structure, function and biosynthesis of O_2-tolerant hydrogenases." *Nat Rev Microbiol* **11**, 106-114 (2013) DOI: 10.1038/nrmicro2940

156 A. Volbeda, P. Amara, C. Darnault *et al.* "X-ray crystallographic and computational studies of the O_2-tolerant [NiFe]-hydrogenase 1 from Escherichia coli." *Proc Natl Acad Sci USA* **109**, 5305-5310 (2012) DOI: 10.1073/pnas.1119806109

157 R. Banerjee, J.C. Jones and J.D. Lipscomb, "Soluble Methane Monooxygenase." *Annu Rev Biochem* **88**:1, 409-431 (2019) DOI: 10.1146/annurev-biochem-013118-111529

158 N. Elango, R. Radhakrishnan, W.A. Froland *et al*. "Crystal structure of the hydroxylase component of methane monooxygenase from Methylosinus trichosporium OB3b." *Protein Sci* **6**(3): 556-568 (1997) DOI: 10.1002/pro.5560060305

159 R. Banerjee, Y. Proshlyakov, J. Lipscomb and D.A. Proshlyakov, "Structure of the key species in the enzymatic oxidation of methane to methanol." *Nature* **518**, 431-434 (2015) DOI: 10.1038/nature14160

160 L. Shu, J.C. Nesheim, K. Kauffmann, E. Münck, J.D. Lipscomb and L. Que Jr. "An Fe_2IVO_2 diamond core structure for the key intermediate Q of methane monooxygenase." *Science* **275**(5299): 515-518 (1997) DOI: 10.1126/science.275.5299.515

161 J.C. Nesheim and J.D. Lipscomb, "Large kinetic isotope effects in methane oxidation catalyzed by methane monooxygenase: evidence for C-H bond cleavage in a reaction cycle intermediate." *Biochemistry* **35**, 31, 10240-10247 (1996) DOI: 10.1021/bi960596w

162 S.K. Lee, J.C. Nesheim and J.D. Lipscomb, "Transient intermediates of the methane monooxygenase catalytic cycle." *J Biol Chem* **268**(29): 21569-21577 (1993)

163 S.J. Lee, M.S. McCormick, S.J. Lippard and U.S. Cho, "Control of substrate access to the active site in methane monooxygenase." *Nature* **494**, 380-384 (2013) DOI: 10.1038/nature11880

164 M.H. Sazinsky and S.J. Lippard, "Product bound structures of the soluble methane monooxygenase hydroxylase from Methylococcus capsulatus (Bath): protein motion in the alpha-subunit*." J Am Chem Soc* **127**, 5814-5825 (2005) DOI: 10.1021/ja044099b

165 D.A. Whittington, A.C. Rosenzweig, C.A. Frederick and S.J. Lippard, "Xenon and halogenated alkanes track putative substrate binding cavities in the soluble methane monooxygenase hydroxylase." *Biochemistry* **40**, 3476-3482 (2001) DOI: 10.1021/bi0022487

166 D.A. Whittington and S.J. Lippard, "Crystal structures of the soluble methane monooxygenase hydroxylase from *Methylococcus capsulatus* (Bath) demonstrating geometrical variability at the dinuclear iron active site." *J Am Chem Soc* **123**, 827-838 (2001) DOI: 10.1021/ja003240n

167 A.C. Rosenzweig, H. Brandstetter, D.A. Whittington, P. Nordlund, S.J. Lippard and C.A. Frederick, "Crystal structures of the methane monooxygenase hydroxylase from *Methylococcus capsulatus* (Bath): implications for substrate gating and component interactions." *Proteins* **29**, 141-152 (1997) PMID: 9329079

168 A.C. Rosenzweig, C.A. Frederick, S.J. Lippard and P. Nordlund, "Crystal structure of a bacterial non-haem iron hydroxylase that catalyses the biological oxidation of methane." *Nature* **366**, 537-543 (1993) DOI: 10.1038/366537a0

169 G.E. Cutsail III, R. Banerjee, A. Zhou, L. Que Jr., J.D. Lipscomb and S. DeBeer, "High-Resolution Extended X-ray Absorption Fine Structure Analysis Provides

Evidence for a Longer Fe...Fe Distance in the Q Intermediate of Methane Monooxygenase.*" J Am Chem Soc* **140**, 48, 16807-16820 (2018) DOI: 10.1021/jacs.8b10313

170 S. Kal, S. Xu and L. Que Jr. "Bio-inspired Nonheme Iron Oxidation Catalysis: Involvement of Oxoiron(V) Oxidants in Cleaving Strong C-H Bonds." *Angew Chem Int Ed Engl* 59(19):7332-7349 (2019) DOI: 10.1002/anie.201906551

171 M.Y. Pau, J.D. Lipscomb and E.I. Solomon, "Substrate activation for O_2 reactions by oxidized metal centers in biology." *Proc Natl Acad Sci USA* **104**, 18355-18362 (2007) DOI: 10.1073/pnas.0704191104

172 L.C. Seefeldt, Z.Y. Yang, D.A. Lukoyanov *et al*. "Reduction of Substrates by Nitrogenases." *Chem Rev* 2020;10.1021/acs.chemrev.9b00556 (2020) DOI: 10.1021/acs.chemrev.9b00556

173 J.G. Chen, R.M. Crooks, L.C. Seefeldt *et al.* "Beyond fossil fuel-driven nitrogen transformations." *Science* **360** eaar6611 (2018) DOI: 10.1126/science.aar6611

174 M.A. Saito, E.M. Bertrand, S. Dutkiewicz *et al.* "Iron conservation by reduction of metalloenzyme inventories in the marine diazotroph Crocosphaera watsonii." *Proc Natl Acad Sci USA* **108**, 2184-2189 (2011) DOI: 10.1073/pnas.1006943108

175 M.A. Saito, M.R. McIlvin, D.M. Moran *et al*. "Multiple nutrient stresses at intersecting Pacific Ocean biomes detected by protein biomarkers." *Science* **345**, 1173-1177 (2014) DOI: 10.1126/science.1256450

176 A. Tagliabue, A. Bowie, P. Boyd *et al.* "The integral role of iron in ocean biogeochemistry." *Nature* **543**, 51-59 (2017) DOI: 10.1038/nature21058

177 S.M. Keable, J. Vertemara, O.A. Zadvornyy *et al.* "Structural characterization of the nitrogenase molybdenum-iron protein with the substrate acetylene trapped near the active site." *J Inorg Biochem* **180**, 129-134 (2018) DOI: 10.1016/j.jinorgbio.2017.12.008

178 D. Sippel and O. Einsle, "The structure of vanadium nitrogenase reveals an unusual bridging ligand." *Nat Chem Biol* **13**, 956-960 (2017) DOI: 10.1038/nchembio.2428

179 C.N. Morrison, T. Spatzal and D.C. Rees, "Reversible Protonated Resting State of the Nitrogenase Active Site." *J Am Chem Soc* **139**(31): 10856-10862 (2017) DOI: 10.1021/jacs.7b05695

180 J. McGale, G.E. Cutsail III, C. Joseph, M.J. Rose and S. DeBeer, "Spectroscopic X-ray and Mossbauer Characterization of M_6 and M_5 Iron(Molybdenum)-Carbonyl Carbide Clusters: High Carbide-Iron Covalency Enhances Local Iron Site Electron Density Despite Cluster Oxidation." *Inorg Chem* **58**(19): 12918-12932 (2019) DOI: 10.1021/acs.inorgchem.9b01870

181 S.M. Keable, O.A. Zadvornyy, L.E. Johnson *et al.* "Structural characterization of the P^{1+} intermediate state of the P-cluster of nitrogenase." *J Biol Chem* **293**(25): 9629-9635 (2018) DOI: 10.1074/jbc.RA118.002435

182 F.A. Tezcan, J.T. Kaiser, J. B. Howard and D.C. Rees, "Structural evidence for asymmetrical nucleotide interactions in nitrogenase." *J Am Chem Soc* **137**(1): 146-149 (2015) DOI: 10.1021/ja511945e

183 J.T. Henthorn, R.J. Arias, S. Koroidov *et al.* Localized Electronic Structure of Nitrogenase FeMoco Revealed by Selenium K-Edge High Resolution X-ray Absorption Spectroscopy, *J Am Chem Soc* **141**(34): 13676-13688 (2019) DOI: 10.1021/jacs.9b06988

184 D. Sippel, M. Rohde, J. Netzer, *et al.* "A bound reaction intermediate sheds light on the mechanism of nitrogenase." *Science* **359**, 1484-1489 (2018) DOI: 10.1126/science.aar2765

185 T. Spatzal, K.A. Perez, O. Einsle, J.B. Howard and D.C. Rees, "Ligand binding to the FeMo-cofactor: structures of CO-bound and reactivated nitrogenase." *Science* **345**, 1620-1623 (2014) DOI: 10.1126/science.1256679

186 T. Spatzal, M. Aksoyoglu, L. Zhang *et al.* "Evidence for interstitial carbon in nitrogenase FeMo cofactor." *Science* **334**, 940 (2011) DOI: 10.1126/science.1214025

187 B. Schmid, M.W. Ribbe, O. Einsle *et al.* "Structure of a cofactor-deficient nitrogenase MoFe protein." *Science* **296**, 352-356 (2002) DOI: 10.1126/science.1070010

188 O. Einsle, F.A. Tezcan, S.L. Andrade *et al*. "Nitrogenase MoFe-protein at 1.16 A resolution: a central ligand in the FeMo-cofactor." *Science* **297**, 1696-1700 (2002) DOI: 10.1126/science.1073877

189 H. Schindelin, C. Kisker, J. Schlessman *et al*. "Structure of ADP•AlF_4^--stabilized nitrogenase complex and its implications for signal transduction." *Nature* **387**, 370-376 (1997) DOI: 10.1038/387370a0

190 V. Smil, "Detonator of the population explosion." *Nature* **400**, 415-415 (1999) DOI: 10.1038/22672

191 J. Erisman, M. Sutton, J. Galloway *et al*. "How a century of ammonia synthesis changed the world." *Nature Geosci* **1**, 636-639 (2008) DOI: 10.1038/ngeo325

192 Adoption of the Paris Agreement FCCC/CP/2015/L.9/Rev.1 (UNFCCC, 2015)

193 Committee on Climate Change Report to Parliament – Meeting Carbon Budgets: Closing the Policy Gap (2017) https://www.theccc.org.uk/publication/2017-report-to-parliament-meeting-carbon-budgets-closing-the-policy-gap/

194 Y. Uemura, D. Kido, Y. Wakisaka *et al.* "Dynamics of Photoelectrons and Structural Changes of Tungsten Trioxide Observed by Femtosecond Transient XAFS." *Angew. Chem. Int. Ed.* **55**, 1364 (2016) DOI: 10.1002/anie.201509252

195 S. Kim, J-S. Park, A. Walsh, "Identification of Killer Defects in Kesterite Thin-Film Solar Cells." *ACS Energy Lett*. **3**, 2 409-500 (2018) DOI: 10.1021/acsenergylett.7b01313

196 H.J. Snaith, "Present status and future prospects of perovskite photovoltaics." *Nature Mater* **17**, 372-376 (2018) DOI : 10.1038/s41563-018-0071-z

197 J. Paier, R. Asahi, A. Nagoya, G. Kresse, "Cu_2ZnSnS_4 as a potential photovoltaic material: A hybrid Hartree-Fock density functional theory study." *Phys.*

Rev. B **79**, 115126 (2009) DOI: 10.1103/PhysRevB.79.115126

198 J.S. Park, S. Kim, Z. Xie *et al.* "Point defect engineering in thin-film solar cells." *Nat Rev Mater* **3**, 194-210 (2018) DOI: 10.1038/s41578-018-0026-7

199 G. Li, R. Zhu & Y. Yang, "Polymer solar cells." *Nature Photon* **6**, 153–161 (2012) DOI: 10.1038/nphoton.2012.11

200 J. Lopez, D.G. Mackanic, Y. Cui *et al*. "Designing polymers for advanced battery chemistries." *Nat Rev Mater* **4**, 312–330 (2019) DOI: 10.1038/s41578-019-0103-6

201 G. Zhang *et al.* "Renewed Prospects for Organic Photovoltaics." *Chemical Reviews* **122**,18,14180-14274 (2022) DOI: 10.1021/acs.chemrev.1c00955

202 C. Li, J. Song, H. Lai *et al.* "Non-fullerene acceptors with high crystallinity and photoluminescence quantum yield enable >20% efficiency organic solar cells. " *Nat. Mater.* **24**, 433–443 (2025) DOI: 10.1038/s41563-024-02087-5

203 H. Chen, Y. Huang, R. Zhang *et al*. "Organic solar cells with 20.82% efficiency and high tolerance of active layer thickness through crystallization sequence manipulation." *Nat. Mater*. **24**, 444–453 (2025) DOI: 10.1038/s41563-024-02062-0

204 M.B. Price, P.A. Hume, A. Ilina *et al*. "Free charge photogeneration in a single component high photovoltaic efficiency organic semiconductor." *Nat Commun* **13**, 2827 (2022) DOI: 10.1038/s41467-022-30127-8

205 S. Giannini, A. Carof, M. Ellis *et al.* "Quantum localization and delocalization of charge carriers in organic semiconducting crystals." *Nat Commun* **10**, 3843 (2019) DOI: 10.1038/s41467-019-11775-9

206 S. Prodhan *et al.* "Long range interactions boost singlet exciton diffusion in nanofibers of pi-extended polymer chains." *J Phys. Chem. Lett* **12**, 8188 (2021) DOI: 10.1021/acs.jpclett.2c00127 Exciton transport in molecular organic semiconductors boosted by transient quantum delocalisation, S.Giannini et al, Nat.Comm. 13, 2755 (2022)

207 S. Giannini, W.T. Peng, L. Cupellini *et al.* "Exciton transport in molecular organic semiconductors boosted by transient quantum delocalization." *Nat Commun* **13**, 2755 (2022) DOI: 10.1038/s41467-022-30308-5

208 F. Roth, M. Borgwardt, L. Wenthaus *et al.* "Direct observation of charge separation in an organic light harvesting system by femtosecond time-resolved XPS." *Nat Commun* **12**, 1, 1196 (2021) DOI: 10.1038/s41467-021-21454-3

209 D. Garratt, L. Mikiekis, D. Wood *et al* "Direct observation of ultrafast exciton localization in an organic semiconductor with soft X-ray transient absorption spectroscopy." *Nat Commun* **13**, 3414 (2022) DOI: 10.1038/s41467-022-31008-w

210 F. Wu, J. Maier, Y. Yu, "Guidelines and trends for next-generation rechargeable lithum and lithium-ion batteries." *Chem. Soc. Rev.* **49**, 1569-1614 (2020) DOI: 10.1039/C7CS00863E

211 P. Leung, A.A. Shah, L. Sanz *et al. "*Recent developments in organic redox flow batteries: A critical review." *J. Power Sources* **360**, 243-283 (2017) DOI: 10.1016/j.jpowsour.2017.05.057

212 V.T. Pham. T.J. Penfold, R.M. van der Veen *et al. "*Probing the Transition from Hydrophilic to Hydrophobic Solvation with Atomic Scale Resolution." J. Am. Chem. Soc. **133**, 12740-12748 (2011) DOI: 10.1021/ja203882y

213 M. Dunne, "X-ray free-electron lasers light up materials science." *Nat Rev Mater* **3**, 290-292 (2018) DOI: 10.1038/s41578-018-0048-1

214 D. Ortiz, I. Gordon Jiménez, J.P. Baltaze *et al.* "Electrolytes Ageing in Lithium-ion Batteries: A Mechanistic Study from Picosecond to Long Timescales." *ChemSusChem* **8**, 3605-3616 (2015) DOI: 10.1002/cssc.201500641

215 K. Lee, K. Park, H. Lee *et al. "*Ultrafast fluxional exchange dynamics in electrolyte solvation sheath of lithium ion battery." *Nat Commun* **8** 14658 (2017) DOI: 10.1038/ncomms14658

216 V. Palomares, P. Serras, I. Villaluenga *et al.* "Na-ion batteries, recent advances and present challenges to become low cost energy storage systems." *Energy Environ. Sci.* **5**, 5884-5901 (2012) DOI: 10.1039/c2ee02781j

217 L. Seidl, N. Bucher, E. Chu *et al.* "Intercalation of solvated Na-ions into graphite." *Energy Environ. Sci*. **10**, 1631-1642 (2017). DOI: 10.1039/C7EE00546F

218 A. Wang, S. Kadam, H. Li *et al.* "Review on modeling of the anode solid electrolyte interphase (SEI) for lithium-ion batteries." *npj Comput Mater* **4**,15 (2018) DOI: 10.1038/s41524-018-0064-0

219 A. Stupakiewicz, K. Szerenos, D. Afanasiev *et al.* "Ultrafast nonthermal photo-magnetic recording in a transparent medium." *Nature* **542**, 71-74 (2017) DOI: 10.1038/nature20807

220 K. Barlow, R. Phelps, J. Eng *et al*. "Tracking nuclear motion in single-molecule magnets using femtosecond X-ray absorption spectroscopy." Nat Commun 15, 4043 (2024) DOI: 10.1038/s41467-024-48411-0

221 W. Zhang, R. Alonsi-Mori, U. Bergmann *et al.* "Tracking excited-state charge and spin dynamics in iron coordination complexes.." *Nature* **509**, 345 (2014) DOI: 10.1038/nature13252

222 G. Auböck, M. Chergui, "Sub-50-fs photoinduced spin crossover in $[Fe(bpy)_3]^{2+}$." *Nat Chem*. **7**(8):629-633 (2015) DOI: 10.1038/nchem.2305

9. Next-generation XFEL Capabilities and Unique High Impact Opportunities

Any XFEL that is in the planning stage today would take on the order of a decade to become operational. It is therefore imperative that plans consider the science and technology that is likely to be served by XFELs in the future, to identify the key capabilities required for a machine that will still be cutting edge when it comes online and remain so for decades after. This chapter explores the key next-generation capabilities, explains the additional requirements for delivering the highest quality research outcomes, and maps out the future opportunities that a next-generation XFEL may deliver across a broad range of science and technology.

The 2020 UK XFEL Science Case[1] was predicated on the notion that XFEL science was in a state of rapid advance, and that any future facility would need to anticipate critical technical capability improvements if it were to fully serve science and technology when it came online. The 2020 Science Case therefore considered the feasible advances and identified opportunities that would be made possible by a machine with capabilities beyond those available anywhere at that time. Significant advances, that are still accelerating, have occurred since 2020 fully vindicating this approach.

Advances in science and technology have been matched by developments in XFEL machine capabilities, which were already anticipated as being close to realisation in 2020. Amongst the new capabilities are: externally seeded XFELs achieving stable narrow bandwidth soft X-ray fields (FERMI at Elettra in Trieste and now the FLASH I upgrade), attosecond near transform limited operation with single and two pulse/two colour capability (LCLS, LCLS II, European XFEL and Swiss FEL), high repetition rate XFELs driven by superconducting CW linacs (LCLS II operational, and now LCLS II HE and Shine, Shanghai under construction) and narrow band operation with high brightness SASE (recently demonstrated at Swiss FEL) and a first demonstration of the XFELO oscillator concept at European XFEL.

In late September 2020, after the Case had been published, the UK XFEL project team began preparing for a Project Review (led by Professor Mike Dunne, Director of LCLS). This preparation work prompted us to formalise and simplify the ***critical next-generation capabilities*** of a future XFEL machine, and to identify what would be required from an XFEL to address the full spectrum of science and technology opportunities highlighted in the 2020 Case. In addition to these next-generation capabilities the essential X-ray characteristics already available at existing XFELs must be retained, including intense X-ray pulses of femtosecond duration, wide tunablity across the entire X-ray range, full polarisation control and excellent transverse coherence. The science and technology opportunities that were identified in the 2020 Science Case – and even more so those identified in this 2026 Science and Technology Case – remain critically dependent on the availability of next-generation capabilities alongside an array of more standard features, all of which are incorporated in the Conceptual Design.

This chapter explores the advanced capabilities and other features that a next-generation XFEL facility should offer and provides some examples of **Flagship Science and Technology Programmes** that would specifically be enabled by such a machine.

9.1 Next-generation XFEL capabilities

*A diverse and ambitious range of scientific and technology opportunities has been described in **Chapters 3 to 8**. This section summarises the new XFEL capabilities that would be needed to fully address these science and technology opportunities.*

Both the 2020 UK XFEL Project Review and our International Advisory Board (IAB) have strongly endorsed our approach to defining **next-generation XFEL capabilities**. It is worth noting that the LCLS X future upgrade project has adopted a very similar approach to defining the essential new capabilities. The need to deliver these capabilities was the starting point for the current **Conceptual Design and Options Analysis (CDOA) project**.

9.1.1 Defining next-generation capabilities

The approach taken in defining the essential next-generation XFEL capabilities was to identify the impediments that are currently preventing XFELs from delivering the very best science and technology, and what can be done to remove them so that research outputs can thrive in the future.

The list that follows shows the current limitation (in blue) before the critical next-generation capability (in black) that would address the issue.

1: The X-ray output is currently very noisy as a consequence of the stochastic nature of the SASE process; in contrast many advanced measurements require smooth, reproducible pulses like a laser

- **Near transform-limited operation across the X-ray range by using modes that go beyond conventional SASE**

2: Current facilities only permit a few dozen experiments per year; to significantly widen access and extend the science and technology impact, this needs to go to many hundreds of experiments per year

- **A high-efficiency facility, with a step-change in the simultaneous operation of multiple end stations**

3: Current facilities provide 100 - 4,000 pulses per second due to the limits of normal conducting linacs and pulse-loaded superconducting linacs; many scientific applications/measurements need 100,000 pulses per second

- **Evenly spaced, high repetition rate pulses to match samples, lasers, and detectors**
- **New AI approaches for data acquisition, analysis and interpretation of the vast volumes of data generated**

4: Current facilities synchronisation/timing to ~ 50 fs due to intrinsic jitter between the X-rays and optical lasers and restrictions of current time-tools; many applications need < 1 fs to fully unlock access to the dynamics in myriad processes

- **Improved synchronisation/timing data with external lasers to < 1 fs**

5: Current facilities deliver two similar X-ray colours; key applications also require the combination of two very different X-ray colours to open up new measurement capability

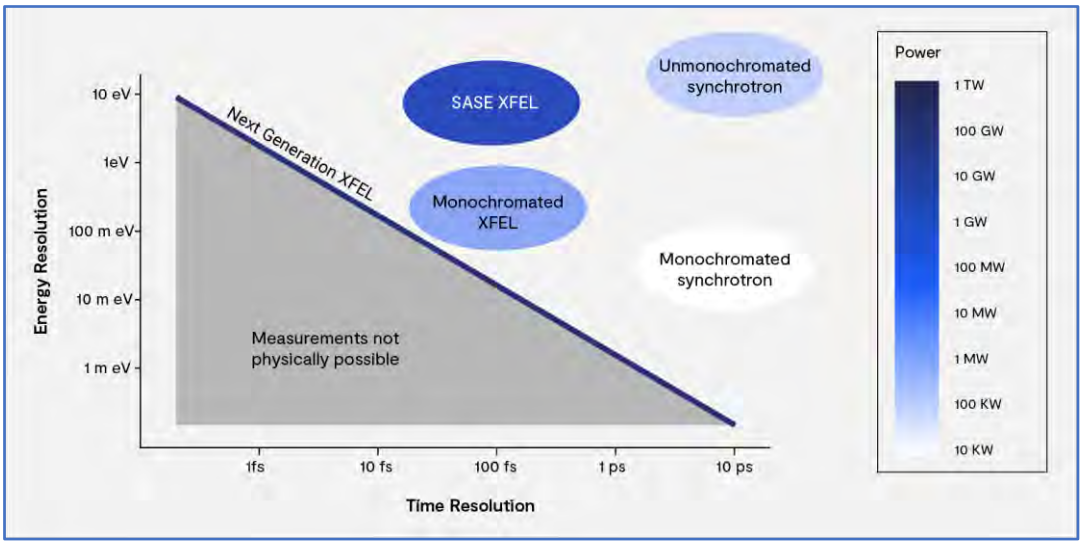
- **Widely separated, multiple colour X-rays to at least one end station by combining the outputs from two FELs**

6: Current facilities have a limited range of pump options due to the limits of laser and non-linear optical technology operating at existing facilities; pumps from XUV – THz + particle beams are required to address the full range of potential measurements

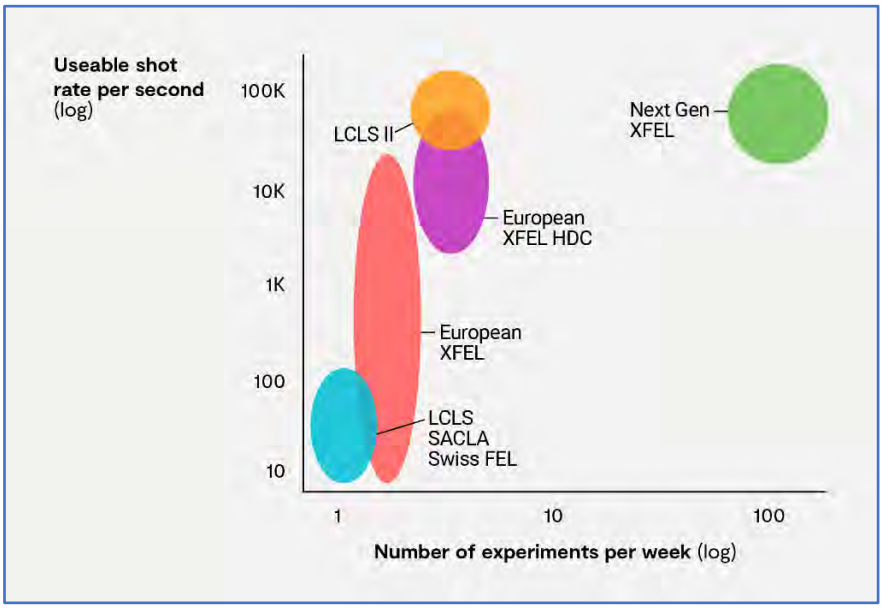
- **A full array of synchronised sources including optical lasers and non-linear optical conversion across the electromagnetic spectrum from XUV – THz, charge particle beams, high energy and high power lasers**
- **A sustainable facility meeting Net Zero targets**

How transformative each of these new capabilities will be is briefly discussed below.

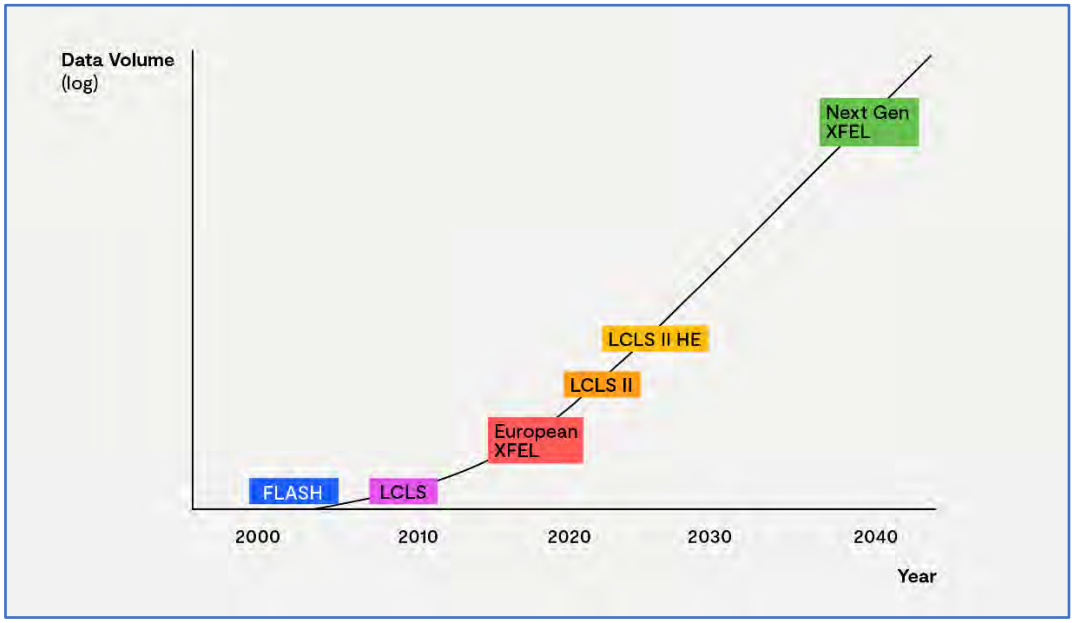
Near transform-limited operation across the X-ray range will permit measurements at the physical limit of combined temporal and energy resolution. In addition, a whole array of as yet untapped non-linear X-ray methods (e.g. second-harmonic generation with surface sensitivity, hard X-ray Raman methods to measure chemical dynamics in dense environments, impulsive stimulated X-ray Raman to enable attosecond measurements of electronic dynamics within complex systems) will only be made possible with high quality and reproducible transform-limited X-ray fields. Moreover, the improved X-ray properties, compared to the current stochastic properties, will vastly increase the useful data rate and so, combined with high repetition rate, enable measurements that previously took weeks and days to be completed in hours and minutes.



A high efficiency facility, with a step-change in the simultaneous operation of multiple end stations in parallel, will open XFEL measurements to many new branches of science and technology and to the needs of industry, by dramatically lowering the barriers to access. Multiplexing along with the high useful data rate will enable more than an order of magnitude increase in the number of measurements that can be completed every week. Moreover, some scientific programmes of high potential impact (see Flagship Programmes in **Section 9.4**) will only be feasible with extended and repeated beamtime access (as is the case at Synchrotron facilities).



Evenly spaced, high repetition rate pulses are an essential prerequisite for many measurements that need to reach high signal-to-noise, or for which the signals are inherently weak (e.g. measurements of chemical dynamics in low concentration, as might occur in nature). This capability would also unlock enormously high average spectral flux, which will enable entirely new dynamic and chemically-sensitive imaging capabilities that are impossible with current light sources. The huge data volumes generated will require the most ***advanced AI tools*** for efficient optimisation, acquisition, analysis and interpretation to deliver the best possible research outcomes from the large datasets. This will also act as a driver for innovations in the use of AI in science and technology.



Improved synchronisation/timing data to ~ 1 fs between optical lasers and the X-ray pulses will enable the fully resolved study of dynamics of electronically excited states that underpin ALL solar energy, solar fuel generation, photodetectors, optoelectronics devices and photosynthesis, and will offer a major advance over the current status (see **Figure 9.1**).

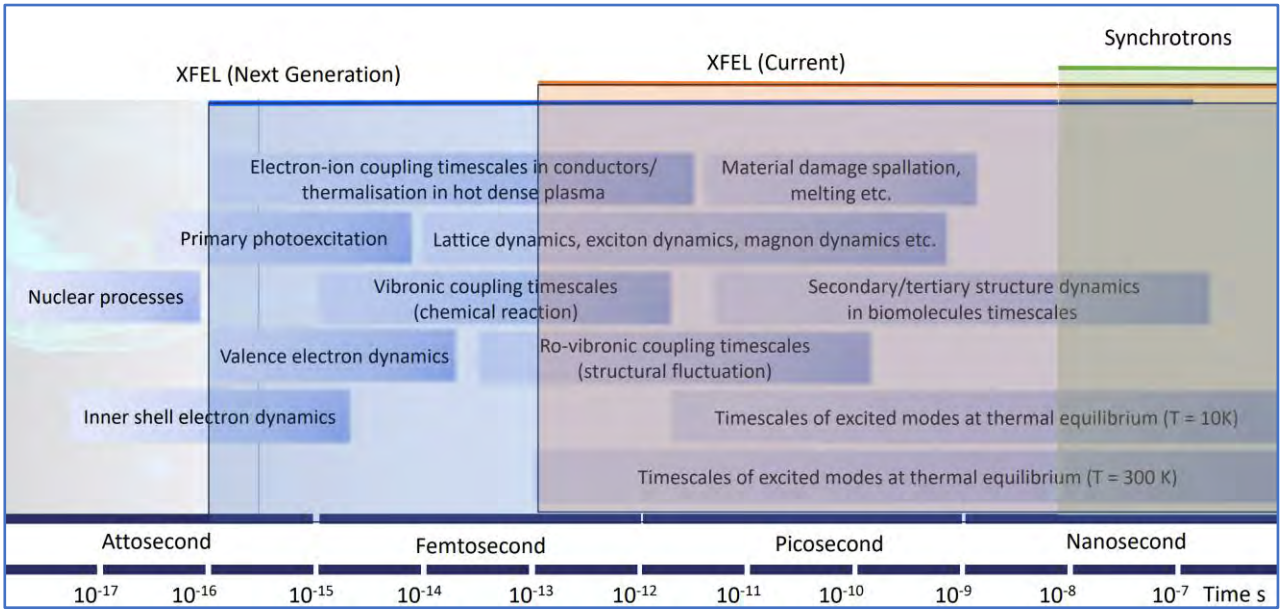
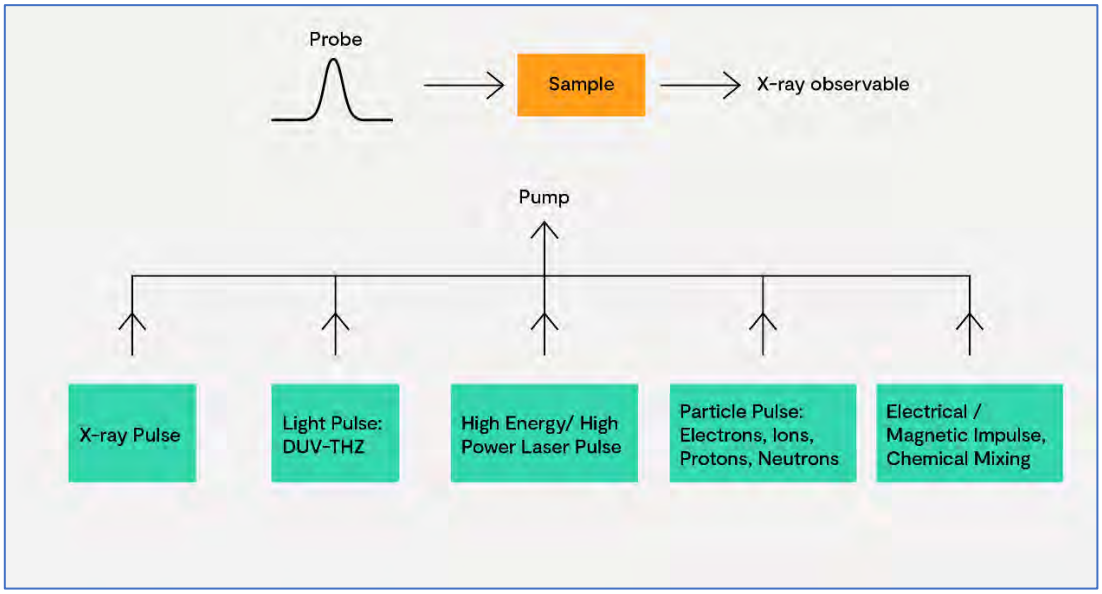


Figure 9.1: Access to the fastest dynamics – important in nanoscopic processes in science and technology – will be enabled at a next-generation XFEL by having pump-probe pulse timing tools with 1 fs fidelity (optical - X-ray) and 0.1 fs fidelity (X-ray - X-ray)

Widely separated, multiple colour X-rays to at least one end station will provide a unique set of measurement possibilities, where the sample is first pumped by soft X-rays and then probed by hard X-rays (or vice versa) to time resolve the effects. An example is **Flagship Programme III** in **Section 9.4** that uses this capability to measure dynamics in systems far from equilibrium. Having a ***full array of synchronised sources*** will unlock the measurement of photodynamics initiated across the electromagnetic spectrum from deep UV to mid IR. In addition, the use of THz directly to drive lattice motions is vital in the study of quantum materials, and for providing precise temperature jumps to trigger dynamics in many other systems. Particle beams including electrons, protons, neutrons and ions will open the way to measuring the dynamics in a vast array of radiolysis and radiation damage situations.



A summary of the next-generation capabilities and what they will enable, over and above what is currently readily available, is summarised in **Box 9.1** below.

Box 9.1: Mapping of next generation capabilities to scientific opportunities and productivity

Future Opportunities Unlocked With:

Transform limited operation across entire X-ray range

Fully resolving dynamics at the combined limits of temporal and energy resolution from uncovering the fastest electron dynamics to subtle excitations in quantum materials

High efficiency facility with a step-change in the simultaneous operation of multiple end stations

Expanding access to researchers by providing scope for many hundreds of unique experiments every year to ensure science and technology reaps the full benefits of XFELs

Evenly spaced, high-rep rate pulses to match lasers, samples & detectors

Enabling the most advanced measurement methodologies whilst supporting high throughput measurements with standard capabilities using the most suitable combinations of lasers, sample delivery and detectors for time resolved studies and nano-scale imaging

Improved synchronisation/timing data with external lasers to < 1 fs

Realising the full temporal resolution of x-rays and lasers to see dynamics unfold across multiple timescales down to ~ 1 fs or better

Multiple colour X-rays at one end-station and full array of synchronised sources:

To interrogate multiple electronic, vibronic, excitonic etc. modes to completely uncover the complex dynamical pathways and couplings in matter and to access extreme states of matter

Data and computing matched to the high repetition rate:

To enable AI approaches to unlock the maximum scientific benefit from the data

9.1.2 Specific requirements identified through the 2023-25 community engagements

Defining the next-generation capabilities was a vital step in the conceptual design process, to identify the required specifications that must be targeted.

The validity of these capabilities has been explored and confirmed through the recent round of Science and Technology Community Engagements during 2023 and 2025, with no gaps or omissions coming to light. The recent engagements did, however, add useful nuance and suggested prioritisation for the capabilities, especially as we have increased our emphasis on Technology and Applications at these events, as is reflected in the updated Science and Technology Case.

Some of the main findings from the 2023-25 Community Engagements were:

- Electronic processes (e.g. in photo-chemical dynamics, photovoltaics, photobiology, radiolysis, quantum materials) demand access to few femtosecond, and even attosecond, timescales for both soft and hard X-rays
- Probing light-induced states (e.g. superconducting and other hidden phases) demands sub-cycle locking with MIR/THz lasers (< 1 fs synchronisation)
- Chiral dynamics and ultrafast magnetism demand full polarisation control of X-rays at all colours, with pulse durations down to attoseconds
- Time-resolving the development of material disorder in the condensed phase, and accessing *in operando* battery and catalytic dynamics, requires ultrafast hard X-rays at high repetition rate
- Matter under extreme conditions (MEC) requires high energy pulses in the 5 – 10 keV range and 20 - 40 keV pulses at moderate repetition rates (compatible with high energy optical lasers), with a short burst mode option available
- Life sciences, both dynamic structural biology and biochemistry, require ultrafast scattering and spectroscopy capabilities at repetition rates ultimately limited by detectors and samples.

These particular requirements have been fed into the ongoing technical design work within the CDOA project.

9.2 Facility general requirements to match scientific needs

Although the X-ray properties are at the core of the new science made possible by XFELs, a successful XFEL facility with exceptional scientific and technological reach must have provision for many other features. These features, if properly configured, can add greatly to the capability of a world-leading next-generation XFEL.

A great deal of the added value of a next-generation XFEL facility can come from auxiliary features that will enable much new science and technology not possible elsewhere. These general requirements for the facility have been informed by **Chapters 3 to 8** of this Case, and by the many years of collective experience of XFEL users and operators of existing facilities.

Since the time-resolved capabilities of XFELs arise largely from pump-probe measurements, it is inevitable that ultrafast lasers are a key requirement. By looking to the latest optical technologies, we can ensure the availability of ultrafast pulses spanning the wavelength range from 10 µm to less than 10 nm (photon energies 0.12 - 120 eV). The synchronisation and time tool strategies explained in the Conceptual Design can then be used to deliver pump-probe timing resolution approaching 1 fs (and potentially better than this in the future). For still longer wavelengths of importance to, for example, chemistry and condensed phase systems, there are non-linear optical and accelerator-based THz options (based on bends or short undulators) that will continue to be developed over the coming years. For some of the most adventurous physical science in this case (**Sections 3.5** and **3.6**, and **Chapter 4**), high power lasers capable of reaching focused intensities > 10^{22} W cm^{-2} are required to operate at a repetition rate matching to the hard X-ray (HXR) beamlines. For shock compression and high energy density systems, a rep-rated (> 10 Hz) high energy laser (kilojoule-class) would permit world-leading science. Electron beams and high magnetic fields are other capabilities that, when offered at the interaction points with the X-rays, will greatly extend the science range. Beyond this, advanced sample preparation and sample delivery are required to enable a truly world-leading range of experiments. The most advanced detectors for X-rays and emitted charged particles – of exceptional sensitivity, dynamic range and ability to accept the full repetition rate of the X-rays pulses – are also essential. All the detectors and diagnostic systems will generate vast quantities of data at the increased repetition rates planned, and the hardware, software, AI tools and administrative strategies to handle these must be designed into the facility at the outset.

9.2.1 Femtosecond optical pump sources of wavelength 10 µm to 10 nm

Provision of synchronised sources of high temporal resolution spanning the electromagnetic spectrum is a key capability for a next-generation XFEL, and goes well beyond the routine provision at existing facilities. The dynamics of matter can be studied by selectively probing excitations, e.g. electronic, vibrational and rotational. These naturally lie across a range of photon energies (wavelengths) ranging from the deep UV through the optical to the far IR part of the electromagnetic spectrum, as reflected by the commensurate timescales illustrated in **Figure 9.1**. Electronic excitations of the valence states of neutrals and ions lie in energy ranges typically from 20 eV to 0.4 eV (50 nm to 2 µm). Vibrational excitations/phonons lie in the range from 0.4 eV to 0.02 eV (2 to 20 µm), whilst rotations are at still lower energies/longer wavelengths. Raman excitation, as opposed to direct single photon excitation, offers ways to access these excitations using shorter wavelength sources (including X-rays), but often direct excitation is required. This sets a wide range of target photon energies/wavelengths that must be provided from a femtosecond laser. This is generally done using a variety of non-linear optical techniques: optical parametric amplification (OPA), difference frequency generation (DFG), harmonic generation (second to fifth), and high harmonic generation. OPAs are especially attractive, as they offer continuous tunability over significantly wide wavelength ranges and can produce a wide range of other wavelengths through coupling to the other non-linear techniques.

Most early experiments at XFELs used titanium-sapphire (Ti:S) chirped pulse amplified (CPA) architecture femtosecond lasers but, as the repetition rates of XFELs have increased, this technology

is limiting. New technologies include: industrial grade Yb platforms, disc laser pumped OPCPA lasers offering 100 – 200 kHz repetition rate and intrinsically short pulses; and fibre lasers using coherent combination of multiple fibre outputs that can approach the 1 MHz repetition rate, be pulse compressed to short duration, and be used in conjunction with OPAs and other non-linear methods to cover the required spectral ranges. It is likely that a next-generation XFEL will embrace all of these technologies, plus others currently under development, to provide the full range of required wavelengths at the required repetition rate.

Although in most current XFEL facilities, pump laser pulse durations of 30 fs have been deemed adequate, as the X-ray pulses become shorter and the synchronisation is improved, the laser pump pulses must be matched with comparably short pulses. Some XFEL end-stations are starting to use hollow core fibre pulse compression, and new fibre and structured fibre technologies are likely to see widespread use across diverse wavelength ranges. Recent work has shown the utility of structured (Kagome) fibres for deep UV pulses of ~ 3 fs duration,[2] and exceptional performance of stretched hollow core fibres in non-linear pulse generation across a broad spectral range[3].

The need to go to longer wavelengths will require a combination of laser-based THz generation methods to reach 10 THz, and potentially electron beam-based THz methods to cover the 10 to 30 THz range (see below). These pulses are necessarily far longer in duration than the optical domain pulses (picoseconds rather than femtoseconds), but their key role in exciting the modes of importance to thermally-excited samples (**Chapter 6**), and of driving condensed phase systems beyond normal equilibrium including non-linear driving of phononic modes (**Chapter 5**), mandate that they be available.

For wavelengths shorter than 220 nm a number of options exist[4]. There are some promising structured and hollow fibre-based approaches that offer relatively high power to around 120 nm [5] [6]. To reach into the VUV – XUV range (10 – 100 eV/ 120 – 12 nm), the conventional choice is high order harmonic generation that has been shown to be driven by high repetition rate lasers[7]. In the energy range to 25 eV, relatively high conversion efficiencies (10^{-5} – 10^{-6}) have been demonstrated, so pulses of 1 – 10 nJ are possible, even for high repetition rates, which are of sufficient energy to pump the small sample volumes probed in typical XFEL experiments.

9.2.2 High energy and high power lasers

The requirement for LWFA and other MEC-related high energy density pumping (**Chapter 4**) necessitates the availability of a high power multi-petawatt class laser with < 30 fs pulse duration, which can be focused to intensities from 10^{19} W cm^{-2} to those exceeding 10^{22} W cm^{-2}. Multiple focusing geometries (and hence focused laser intensities), coupled with high repetition-rate target delivery, would permit access to a broad range of extreme conditions and laser-driven secondary sources. In order to access extreme fields, and many of the regimes needed for the fundamental physics experiments described in **Section 3.5**, laser powers on the order of 100 PW (and focused intensities exceeding 10^{24} W cm^{-2}) could be required. While this would require long-term technological development, it would be viable for a next-generation XFEL facility.

To provide a really unique capability, we should aspire to a 100 Hz repetition rate laser system. These higher repetition rates will greatly benefit the observation of rare events, including the study of non-linear QED systems driven by ultra-intense electromagnetic fields, where statistical analysis of multiple events will be required. Many applications of secondary sources generated by high intensity lasers will also require higher repetition rates. A new high repetition-rate, high intensity laser would provide an attractive platform to optimise existing applications, and draw users from a broad range of research fields when coupled with a powerful X-ray probe. Conversely a high-power laser could also be used to probe XFEL-driven non-linear dynamics; hence a high-repetition rate source should be a priority, to exploit the capability of an ultra-intense hard X-ray source.

The rapid advancement of diode-pumped laser technology has made possible the construction of lasers such as D100-X (DiPOLE laser technology developed by the Central Laser Facility in the UK and

installed at the HIBEF (Helmholtz International Beamline for Extreme Fields) end-station of the European XFEL). D100-X uses innovative diode-pumped, cryogenically gas cooled amplification media to produce high energy (> 100 J) laser pulses at high repetition rates (10 Hz). The same diode pumped laser system will also power the 10 Hz petawatt-class laser source for the new Extreme Photonics Applications Centre (EPAC), coming into operation at the CLF in 2026. This innovative technology could be scaled to produce higher energies and/or repetition rates, depending on the evolution of the science drivers.

To ensure unique new science is possible in the dynamic compression area and studies of warm dense matter (WDM), a high-energy frequency-tripled kJ class nanosecond laser is required in order to reach the highest energy densities and pressures. A 10 Hz repetition rate is highly desirable – going to higher rep rates as the technology evolves. Multiple high-energy beams could be combined in order to provide novel geometries for compressed matter experiments, as well as to provide a more scalable path to the highest laser energies (and hence experimental pressures). The laser temporal profile should be highly controllable (as per D100-X), in order to provide access to the largest possible range of energy states. The scalable and flexible nature of the DiPOLE laser technology would underpin the operation of both a high power and high energy laser system, thus delivering a wide range of experimental capability at a considerably lower cost compared to that required to build two independent laser systems. A high-repetition rate, multi-petawatt class laser would require hundreds of joules of pump energy (possibly over a kilojoule for the highest powers); hence when not in use (or running at lower power), the high energy DiPOLE system could be fully customised and optimised for dynamic compression experiments. Should both ultra-high power (multi-petawatt) and high energy lasers be required simultaneously in the future, then the total pumping capacity could easily be expanded to meet the requirements of the user community. Upgrade paths to still higher energy, for e.g. a spherical compression capability, should be retained as a future option.

9.2.3 THz, high magnetic fields and relativistic e-beams at interaction points

It is possible to obtain intense pulses of THz light, synchronised to the FEL pulse, from electron beams using a number of different mechanisms. The FEL electron beam is used at the TeraFERMI beamline[8] after it has passed through the FEL and just before it is dumped. In this example, the electrons pass through a thin metal foil and emit coherent transition radiation. An alternative is to pass the spent beam through a long period undulator to generate the THz, as is the case at FLASH[9]. Recent technological breakthroughs in this method[10] make it feasible to use the GeV-scale electron bunches at hard X-ray FELs to generate synchronised, narrowband THz with the required 100 MV cm^{-1} peak electric fields and > 10 T peak magnetic fields specified in this Science and Technology Case (**Section 6.2**). Another option to consider would be the generation of a low energy, short bunch, electron beam (of order 10 MeV) close to the FEL beamline for efficient undulator light production. This electron beam would be well synchronised to the FEL pulse using established techniques, and could also be used as a source for electron radiolysis and diffraction at the end-stations.

The interaction of materials with magnetic fields is a rich source of information on their magnetic and spin quantum properties. Work at LCLS investigating X-ray scattering from materials using their 30 T pulsed magnetic field apparatus has revealed new insights into quantum materials[11]. It would seem an excellent aspiration to equip at least one hard X-ray end-station with a pulsed high B field facility to progress research in this direction. The possibility for a high field DC magnet might also be considered, given that the pulse repetition rate in both hard- and soft-X-ray would deliver unprecedented measurement sensitivity that could transform our understanding. The options for doing this would need to be further reviewed under the activities associated with preparing a Technical Design Report.

The demands for pulsed radiolysis (**Chapter 6**) and the prospects for Ultrafast Electron Diffraction (UED) (**Appendix 1.3**) potentially combined with correlated X-ray spectroscopy and X-ray scattering on the same sample, demand that a synchronised relativistic (1 – 5 MeV) electron gun be located at least at one of the end-stations. This will open up new science not available at any existing XFEL facility, as well as enabling an independent programme of research driven by UED alone. The technology of these

guns is now mature enough that we can be confident that this is achievable[12] [13]. A future Technical Design process will need to analyse the strategies for synchronisation with the X-rays, the extent to which a common suite of scattering detectors can be used, as well as addressing any radiological protection issues. Other laser accelerated electron and ion beam capabilities will be developed to extend possibilities to higher energy electrons to the GeV range (see **Section 4.3**), accelerated protons, pulsed neutrons and various ions. This will lead to a world-leading capability.

9.2.4 Sample delivery, sample environments and fabrication

Across all XFEL application areas, delivering the samples to be probed in suitable sample environments is an essential aspect of the research. A flexible combination of approaches to match in-vacuum, atmospheric or more exotic environments must be provided, to enable *near-operando* probing of catalysis, batteries and industrial processes through to the probing of sensitive thin film materials or solution phase molecules. Fast rastering of targets and arrays, fast low-volume liquid sheet jets, nanofabricated arrays, and injection on demand are among the solutions currently being developed, with ongoing effort being led by researchers across different facilities (including XFELs, synchrotrons and UED facilities).

The particular characteristics of X-ray scattering experiments at XFELs – i.e. the powerful concept of "diffract-before-destroy" that has driven progress in serial femtosecond nano-crystallography and coherent diffraction imaging – have demanded the development of new concepts in sample delivery. There is an essential need to reduce the consumption rate of high value samples and ensure the maximum number of nanocrystals yield X-ray scattering signal. Great progress has produced an array of sample delivery methods, starting with liquid injector and gas dynamic virtual nozzle (GVDN) injectors[14], and expanding into several alternatives as described in **Chapter 7**.

Table 9.1 shows the typical data collection rates across XFEL facilities in operation now and under construction. These rates are driven by a combination of the X-ray pulse repetition-rate and the detector capabilities. For example, the LCLS-II-HE facility anticipates fielding a 35 kHz ePixUHR detector with 4M – 16M pixels for SFX[15] which will collect scattered photons from only a fraction of their 1 MHz pulses. The impact will be profound, as shown by the expectation that a 25,000 image dataset will require only 14 seconds even with a very modest 5% hit ratio. For comparison, at LCLS it would take over an hour to collect this same dataset at 120 Hz. Moreover, if a 70% hit ratio is realised, then slower XFELs still yield datasets relatively fast – e.g. a 70% index ratio requires approximately 20 or 5 minutes to collect SFX data at 30 Hz or 120 Hz, respectfully[16] [17]. If a high sample hit ratio is ultimately coupled with high X-ray pulse repetition rate, then each dataset may only require a few seconds. This also highlights the need for automatic instrument alignments and fast-feedback strategies that maximize overlap between the sample delivery and X-ray pulse. Some of the current on-demand sample delivery methods can operate at up to about 50 kHz, but further developments are needed to achieve 0.5 MHz or faster delivery strategies. For instance, in November 2024 the XFEL Hub at Diamond executed some drop-on-demand SFX experiments at the SPB/SFX downstream instrument (in air) at the European XFEL that delivered ~ 50 pL droplets at between 20k – 56.4 kHz to intersect between 7 – 16 X-ray pulses within a 310 µs pulse train. The team collected from about a dozen samples and some produced 30,000 lattices and refined atomic models to 1.2 Å resolution using only a few µL of precious sample. This sample efficiency was only possible because no sample was wasted during the 99.4 ms gap between pulse trains. Similar experiments were also demonstrated at the FXE instrument at the European XFEL [18]. Thus, the XFEL Hub at Diamond and others have already demonstrated that drop-on-demand strategies can yield high resolution SFX data to meet LCLS-II-HE conditions that exploit 35 kHz ePixUHR detector.

The remaining challenges include increasing the throughput and developing sample on-demand technology that will ensure every X-ray pulse yields useful data (rather than the high fraction of "misses" that is the current norm for some sample delivery methods). Technology is moving quickly, with sample array technologies as well as sample on-demand injectors being developed. The aspiration is to ensure the most efficient data collection and the highest throughput. A further aspiration is that users will not even need to accompany their samples to the XFEL, which will greatly increase the

number of scientists and Pharma companies using XFELs as a routine part of their research efforts. Finally, the XFEL Single Particle Imaging Initiative strives to collect scattering data from macromolecules under near physiological conditions, to support sub-nanometre resolution atomic models and time-resolved studies. Recent theoretical analysis suggests that 3 Å resolution models might be reconstructed from about 66,000 good quality images [19] [20]. With appropriate noise mitigation strategies, improved algorithms, and more images, then the resolution will improve even further [21] [22].

For X-ray spectroscopy, a similarly wide array of liquid jet technologies is available that can optimise the measurement using XAS and XES [23] [24]. An important motivation for high repetition rate is that very dilute samples, for example those consistent with the concentrations in naturally occurring biochemistry, can be studied; optimised sample environments that minimise noise in the detection channel must be further developed.

Table 9.1: Minimum time required for one SFX dataset with 25,000 indexed images

Facility	Detector	Image Rate Hz	Time to Collect Dataset with			
			5% hit ratio		70% hit ratio	
			seconds	minutes	seconds	minutes
LCLS	CSPAD / ePIX / Jungfrau 16M	120	4167	69.4	298	5.0
LCLS	Rayonix [a]	10	50000	933.3	3571	59.5
LCLS	Rayonix [a]	30	16667	277.9	1190	19.8
SACLA / PAL-XFEL	MPCCD	60	8333	138.9	595	9.9
SwissFEL	Jungfrau	100	5000	83.3	357	6.0
European XFEL	Jungfrau [b]	160	3125	52.1	195	3.3
Diamond VMXi	Eiger2 [c]	500	1000	16.7	71	1.2
European XFEL	AGPID [d]	3,520	142	2.4	10	--
LCLS-II-HE	ePixUHR [e]	35,000	14	--	1.02	--
SHINE	tbd [f]	17,000	29	--	2.1	--

[a] Rayonix MX340-XFEL detector with different on-chip pixel binning modes impact pixel size and image readout rate; e.g. 2x2 = 10 Hz, 4x4 = 30 Hz

[b] A JUNGFRAU detector with 16 "on-board" memory cells that can collect 16 images across a pulse train (300 – 600 µs long) arriving at 10 Hz (99.4 ms between trains, equivalent to up to ~ 50 kHz intra-train frequency) at the Eu.XFEL.

[c] The Dectris Eiger2 is a counting detector and is shown for comparison at the VMXi beamline at Diamond Light Source. The detector does permit electronic gating to collect factions of the 2 ms image rate.

[d] The European XFEL can deliver up to 27,000 pulses in 600 µs duration trains at 10 Hz, to achieve an intra-train frequency of 4.5 MHz. The Adaptive Gain Integrating Pixel Detector has "on-board" memory sufficient to save 352 images per train at 10 Hz.

[e] Under development and likely to collect at 35 kHz evenly spaced across the 1 MHz pulses with 4M – 16M pixels

[f] Under development and likely to collect at ~17 kHz evenly spaced across the 1 MHz pulses

Solid state samples of importance in materials science face a limitation due to sample damage (both pump beam and X-ray induced). This effect has hitherto limited data acquisition to relatively low repetition rates. To fully exploit the capabilities of the XFEL it is important to develop sample growth facilities to provide a ready supply of high-quality samples, moving sample holders that allow a fresh region to be probed even at a high repetition rate, and *in situ* sample cooling to ameliorate damage. Solid samples for high energy density (HED) science, and diamond anvil cells transparent to X-ray probing, will also need to be developed. HED science has traditionally been performed at low-repetition rate, high energy laser facilities (with shot repetition rates below one per minute) and, as the sample must be replaced for each shot, this has become the low throughput working mode. It is reasonable to move towards faster sample refreshment that could see a step change in data quality,

enabled by far higher repetition rate X-ray pulses (for directly creating WDM) and the rep-rated high energy laser. To achieve the higher-rep rate objective, developments in target fabrication and presentation to the beams will be required. These are synergistic with the needs of the inertial fusion energy research community.

For solid crystalline samples, the ultrafast excitations of interest are often at low temperatures, requiring cryostats. This is challenging for pump-probe applications because two vacuum windows are needed, one for the pump and one for the X-ray probe, and few materials are transparent to both. The availability of cryostats at existing XFEL facilities is patchy, and the choice of samples or facilities is often constrained by this. “Cryostream” gas jets are often used with nitrogen or helium cooling gas to avoid the window problem, but these lead to icing and sample stability issues. Sample vibration is a second, related issue in the implementation of a cryostat. A next-generation XFEL new build option will benefit from expertise at existing neutron and X-ray facilities, as well as the national presence of the Oxford Instruments company to strive to deliver innovative solutions. For example, fixed window, feedthrough-based solutions have been proposed and are under development at Diamond’s I-16 beamline.

9.2.5 Advanced X-ray detectors

X-ray imaging detectors of high sensitivity and dynamic range, and operable at high repetition rate, are essential for all X-ray scattering measurement, and also for momentum-spectrum resolved RIXS and spectroscopy measurements. This has been an area of dedicated progress across several organisations over a long period of time (including RAL UK, PSI Switzerland, DESY Germany and SLAC USA) and excellent detectors for the current range of repetition rates are available. New detectors are already being developed for the higher repetition rates anticipated (> 50 kHz) but the near future 1 MHz rates are still seen as a major challenge.

The development of hybrid technology detectors, with charge integrating front-end electronics instead of photon counting, has been critical for XFEL sources, where many photons arrive at the detector in a very short period of time due to the pulsed nature of the source. These detectors need to have single photon sensitivity (i.e. the detector equivalent noise charge must be smaller than the charge released in the sensor by a single photon event) and they also need to be able to detect a large number of photons at one time (up to 10^6 photons/pulse) without going into saturation. Hybrid integrating detectors are in use at existing XFEL sources, such as LPD, AGIPD, and DSSC developed for the European XFEL, ePix detector developed for LCLS at Stanford, and the JUNGFRAU detector developed for the SwissFEL. The JUNGFRAU detector can run at a frame rate up to 2.4 kHz, and the development team is planning further improvements of the chip that aim to bring the maximum frame rate to around 4 kHz. At SACLA, CITIUS, an integrating detector with a frame rate of 17.4 kHz, is under development.

Further initiatives are currently underway to meet the challenges that are posed by the next generation of XFELs, such as LCLS-II or the upgrade of the European XFEL. These new sources will require detectors running at a frame rate of 100 kHz and above, expected to be in routine operation within the next 10 years. For instance, at LCLS the plans are based around the ePIX detector family with ePIXHR (5 kHz) now being rolled out for LCLS II, and future models ePIXHR2.5D (25 kHz) and ePIXUHR (100 kHz – 1 MHz) in the development pipeline. Nevertheless, at SLAC it has been recognised that no single detector solution will satisfy all future applications. There remains an urgent need for innovation and continuing R&D in this arena, but on the timescale of 10 years, it is likely that off-the-shelf solutions up to the 100 kHz rate will be ready for a next-generation XFEL.

9.2.6 Electron and charge particle detection

Many measurement modes utilise emitted electrons and ions that carry the signatures of dynamical changes, e.g. in X-ray photoelectron spectroscopy (XPS), angle resolved electron spectroscopy (ARPES), and coincidence-based momentum imaging. Favoured techniques, such as velocity map imaging (VMI) and electron/ion time-of-flight (TOF) measurements, can still be used at higher rep-rates, but there will be limits placed at high repetition rates (on readout speeds in the case of VMI and flight times in

the case of TOFs). Technical developments to provide efficient high throughput analogues to TOF and VMI will be required to optimise instruments at a number of end-stations. ARPES using standard hemispherical analysers is, in principle, compatible with high repetition rates, but, unless integration over many shots is required, upgraded fast readout detectors will need to be used to access single-shot data. Momentum imaging techniques, such as COLTRIMs, are intrinsically designed for high data rate acquisition, and the REMI instrument at the European XFEL and the recently commissioned DREAM instrument at LCLS are already able to handle the higher repetition rates.

9.2.7 Data infrastructure and AI

Along with the massive scientific advantages associated with the high data rate from a high repetition rate XFEL comes a heavy demand in terms of data transfer, storage and management. At the existing high repetition rate facilities, it has been realised that the cost of proceeding without significant data compression and intelligent data retention policies is too high to be viable (estimated at around $0.25 billion in the case of LCLS-II and would grow further). Analysis of LCLS-II suggests that each working end-station operating at 1 MHz will generate in the range of 100 Gb/s – 1 TB/s. In their planning, they account for a factor of 10 reduction through data compression to 10 GB/s – 100 Gb/s. Part of this compression will be in the form of on-chip data reduction using field programmable gate arrays (FPGAs) integrated to the front-end detectors. Compression via feature extraction, vetos, and multi-event reduction must all form part of the strategy. At the same time, it is vital to provide the possibility of fast feedback to the users in real-time during the experiment, to ensure efficient use of beamtime. Very large off-line data storage and analysis capability will be essential, requiring multiple 100 PB storage capacity. To manage this will require the implementation of a forward-looking set of policies on data retention. It is important to start planning hardware, software and administrative policies from the outset, to avoid serious problems later.

New opportunities enabled by AI in online data analysis are likely to revolutionise how we conduct complex experiments, including those at next-generation XFELs. It is clear, for instance, that future SFX experiments will tax computational resources by generating very large datasets, which may require varying degrees of image triage, and will need merging as fast as possible so that scientists can make the most effective use of XFEL beamtime. Thus, very quickly one will ask these fundamental questions that get to the heart of the data processing and sample delivery aspects of SFX research at XFEL facilities: *When will I know the overall quality of the SFX data we just collected? How long will it take to collect the second, third, fourth, … datasets, especially in a time-resolved series?* Fast AI aided online analysis will effectively address these questions.

The advantage of greater coherence and stability of X-rays by going beyond SASE modes (seeding, eSASE, superradiance schemes) is that the required experimental signal may be measured in a greatly reduced number of shots compared to conventional SASE operation. Experience with two-pulse SASE X-ray modes, where spectral/temporal/intensity fluctuations affecting both pulses in the pair requires aggressive data sorting, has shown that a down-selection by several orders of magnitude is often required, which would be greatly improved were seeded and stable operation to be available. In addition, the pulse-to-pulse X-ray diagnostics are very expensive in terms of data volume, especially if they involve detector arrays (e.g. spectral or temporal measurements like XTCAV) – it has been shown that machine learning approaches to X-ray diagnostics can be hugely beneficial in this regard[25].

A fully integrated controls environment must be developed for the entire facility, including all end-stations and experimental installations. The experience required to do this is available from Diamond, LCLS, European XFEL, etc. We anticipate an AI-optimised facility/experiment optimisation using all the available tools such as digital twinning of end-station instruments, full remote access and use of robotics. The advantages of AI in machine tune-up and optimisation and in rapidly optimising the end-station set-up for an experiment are now being explored at XFEL facilities, and this approach is likely to lead to a massive improvement in operational efficiency in the next decades.

9.2.8 Auxiliary support facilities

To allow the efficient delivery of the science mission, a next-generation XFEL will require an extensive array of state-of-the-art support facilities, as well as excellently equipped end-stations. These facilities need to be accessible easily and, in some cases, on-site location is desirable.

Capability for sample preparation and fabrication will be central to supporting the best science. Nanofabrication capability on-site, including nanoscribe, fast-ion beam (FIB), sample growth and nano-lithography, will be required, along with laboratories for the safe preparation of high-quality chemical and biological samples. If the industry demand arises, there may need to be facilities for handling nuclear materials. Additionally, a first-class machine shop, optical testing and coating, and electronics workshop facilities will be needed to support both in-house facility development and R&D programmes, as well as the user science programme. This will include local testing and measurement laboratories equipped with sample characterisation capability, such as LEED, TEM, and SEM, as well as standard optical and two-photon microscopy.

Further measurement modalities, other than X-ray based, can be very valuable in establishing integrative approaches to the science and thereby stretching the scientific capability; an example of this is co-location of UED capabilities (**Appendix 1.3**). Laser laboratories for optical only time-resolved measurements, cryo-electron microscopy (Cryo-EM) capability for single molecule imaging, and NMR capability might also be integrated into the scientific offer of a next-generation XFEL, either at the same site or distributed across the STFC facility network.

9.2.9 Lowering barriers to access

Users are at the core of the scientific and technological success of any facility. Lowering the barriers to access is a critical goal for a next-generation XFEL, and a systematic approach to managing needs to be developed by applying best practice from existing facilities, as well as identifying and implementing innovative approaches.

One of the main ways in which a next-generation XFEL will be able to radically lower the barrier to access is by providing more than an order of magnitude increase in research throughput compared to existing machines, e.g. through the parallel operation of end-stations, AI driven efficiencies in set-up and high intrinsic data rates. This will directly translate to being able to serve more users as many measurements will be conducted much faster, in hours rather than in days, compared to the situation now.

As for any other large-scale user facility, such as the CLF, Diamond or ISIS, a next-generation XFEL must offer appropriate user support. Any new facility will need to adopt best practice in user support infrastructure in terms of accommodation, transport, catering, safety initiation and training, technical training, offsite user support, and data policies, which are continuing to develop within existing facilities. Attention must be given to ensure that the user experience is as efficient and productive as possible, and that innovations and measures to lower barriers to access are applied at all points of operation with engagement of new user communities and dedicated fast access routes for industry.

The use of XFELs is perceived to be much more challenging than for more established methods and this has presented a significant barrier to the adoption of their use for routine science. A next-generation XFEL must do all that is possible to support new users and substantially reduce this barrier, both that perceived and the actual one caused by the complexity of end-stations and the rapid development that the technology is still undergoing. Measures to accomplish this are being pioneered at existing facilities in terms of offering end-station scientist support and transparent to operate end-station controls, and a new facility would need to adopt all best practice. Some classes of measurement, e.g. diffract-before-destroy CDI, serial nano-crystallography, time-resolved X-ray spectroscopy and RIXS, should be made far more routine and fully supported, so that in the future users need only submit samples and collaborate with the staff scientists on the data analysis. Where this is not practical, standard end-station configurations should be developed that minimise facility

staff and user time in swapping between experiments, thus making high quality data taking more certain and efficient.

Most end-stations should be configured with a dedicated set of high calibre instrumentation, to ensure high quality data and high scientific productivity. Automation of end-station setups using AI tools is already being developed at existing facilities and it is likely that this will be at a very advanced level 10 years from now, hugely accelerating experiment set-up times and massively reducing facility staff load. Nevertheless, some provision for “roll-up” user supplied end-stations should be retained, to ensure operational flexibility and future-proofing through the development of new experimental concepts.

Finally, an extensive training support programme will need to be offered by the facility to provide new users with the necessary skills: this ought to be strongly mirrored and enhanced by university-based academic training actions.

9.3 Facility end-stations and their capabilities

At an XFEL facility, the experiments and measurements are performed at experimental end-stations using the instruments with which these are equipped. It is at the end-stations that the X-rays, secondary sources, samples and detection systems are brought together to interact, and so they are central to the scientific capability. When planning a next-generation XFEL, it is essential that the provision of end-stations be carefully planned and matched to the scientific requirements. A planning process has been undertaken as part of the CDOA project to identify the end-stations that would need to be provided to meet the science needs identified in the earlier chapters of this Case. This process is explained in more detail in the Conceptual Design, which also defines the end-stations required for the first phase of the operation of a proposed next-generation XFEL in appropriate technical detail.

The process of identifying and specifying the end-stations has involved many interactions between the Conceptual Design Team, the Science Team, and a significant number of potential end users. Two in-person Away Days were held at the CLF in February 2024 and January 2025, and a significant number of additional online discussions have taken place around specific end-stations.

Figure 9.2 shows the array of end stations that are currently envisioned and their associated FELs, followed by a brief description of the capabilities and the science that would be served by each end-station. Other end-stations and/or capabilities may need to be included in future upgrade phases. Note: Seven independent FEL undulators have been identified and the end-stations group around these, as the X-ray optics and instrument details are X-ray photon energy dependent.

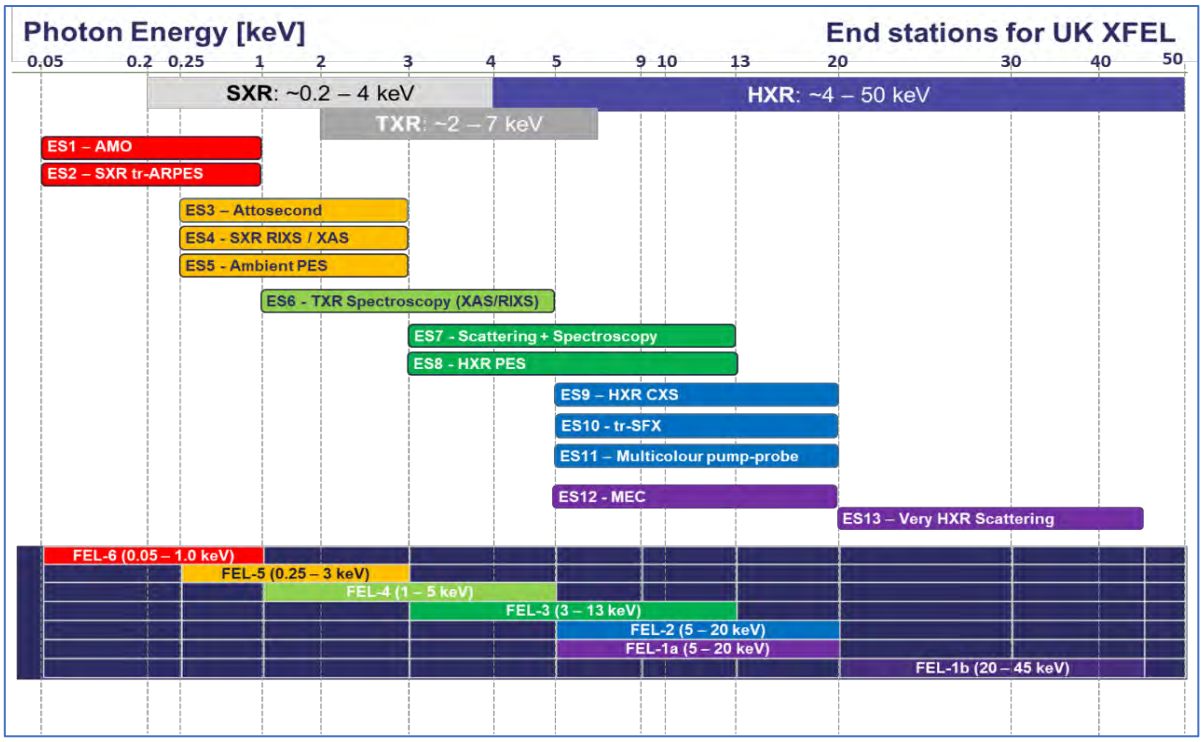


Figure 9.2: Overview of end-stations from the Conceptual Design process, with mapping to science and technology areas

ES1 – AMO – Research in atomic, molecular, and optical (AMO) physics and chemistry aimed at resolving complex single- and multi-photon processes on ultrafast timescales, utilising the combination of high intensity, coherence, and repetition rate of a next-generation XFEL.

ES2 – SXR tr-ARPES – Angle-resolved photoemission spectroscopy techniques over a broad XUV-SXR range (0.05 – 1 keV) for high throughput studies of ultrafast processes at surfaces and quantum materials.

ES3 – Attosecond – Very highest X-ray time resolution for studying attosecond electron dynamics for AMO and photo-induced processes in chemistry, condensed matter and biology (note multiple end-stations will also be able to field Attosecond experiments).

ES4 – SXR RIXS / XAS – High-resolution, time-resolved RIXS, XAS, and XES methods across 0.25 - 3 keV for studying ultrafast dynamics in quantum materials and complex chemical systems.

ES5 – Ambient PES – Application of PES techniques over SXR-TXR range (0.25-3 keV) with complex sample configurations relevant to catalysis, batteries and biomaterials.

ES6 – TXR Spectroscopy – Flexible platform for time-resolved X-ray spectroscopy (and scattering) in the tender X-ray range (2 – 7 keV), enabling ultrafast studies of catalytic, biological, and magnetic dynamics with high spectral and spatial resolution.

ES7 – Scattering and Spectroscopy – Ultrafast time-resolved spectroscopy and scattering in the hard X-ray regime (3 – 13 keV), with flexible sample environments and pump-probe capabilities for studying structural and electronic dynamics.

ES8 – HXR PES – Hard X-ray photoelectron spectroscopy (HAXPES) for bulk-sensitive chemical analysis of buried interfaces and materials in-operando.

ES9 – HXR CXS – Application of coherent X-ray scattering (CXR) techniques to investigate nanoscale materials and dynamic processes in complex systems, enabled by flexible detector and sample setups for a wide-range of experimental configurations.

ES10 – tr-SFX – Time-resolved X-ray serial femtosecond crystallography (tr-SFX) at high repetition rates to study macromolecules and small chemical systems with the very highest spatial and temporal resolutions.

ES11 – Multi-colour pump-probe – Flexible experimental platform for advanced dual-colour X-ray experiments with widely separated, independent soft and hard X-rays for pump-probe or sequential probing of transient states.

ES12 – MEC – Cutting-edge platform for studying materials under extreme conditions (MEC), driven primarily by high-power lasers for the application of hard X-ray spectroscopy and scattering techniques, supporting research in laboratory astrophysics, inertial confined fusion (ICF)and materials under dynamic compression.

ES13 – Very HXR Scattering – Dedicated platform for imaging and time-resolved scattering at very hard X-ray energies (20 – 45 keV), enabling studies of high-density materials under dynamic compression or *in operando* conditions, as well as high-resolution, time-resolved pair distribution function (PDF) measurements.

The design of these end-stations has been driven by the science requirements outlined in the earlier chapters of this Case and the current plan would satisfy most of the research needs. The instrumentation used would be state-of-the-art that, as a minimum, matches anything currently available. It is anticipated that there will be improvements to instrumentation, especially in the critical areas of high frame rate/high bit depth detectors, during the facility planning stages and the eventual instrumentation map will reflect that progress.

9.4 High impact Flagship Science and Technology Programmes

Based on the science opportunities outlined in Chapters 3 to 8 of this Science and Technology Case, we have defined the capabilities (including the end-stations) that are required of the Conceptual Design to deliver a next-generation XFEL that will meet future research needs. Starting from the specifications that would be delivered by the Conceptual Design, we have then 'closed the loop,' by identifying some high impact Flagship Programmes that would specifically be enabled by such a machine.

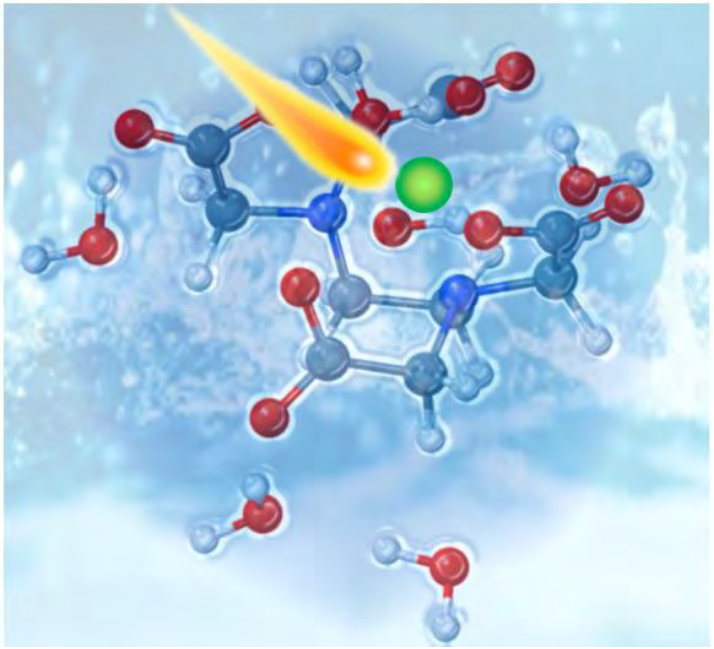
The combination of XFEL capabilities and end-stations defined through the Conceptual Design process has been extensively discussed with the Science Team and an extended set of users. It has been used as a starting point to define a series of Flagship Science and Technology Programmes that could be undertaken in the first few years of operation and that would have high Impact. The criteria used to identify these Flagship Programmes were that they:

- **should aim to answer a key question in a field or be opening a new sub-field**
- **should be near future (i.e. imagining that a next-generation XFEL would be available within a decade)**
- **must use the key capabilities of the Conceptual Design and end-stations**
- **could use multiple end-stations and measurement techniques (e.g. SXR spectroscopy, XRD, PDF & IXRS), and even include some non-XFEL components**
- **should be multi-beamtime, to leverage the high throughput and easier access ambitions**
- **could be jointly proposed by several of the Science Team groups**
- **would ideally be supported by various funding agencies as a collaborative programme; in such cases, we asked for the names of agencies that were likely to support the programme.**

The 11 example programmes developed in this exercise are given in the following pages. It is important to note that ***all*** these cases require a ***high efficiency facility, with a step-change in the simultaneous operation of multiple end stations in parallel***. Provision of significant XFEL beamtime is essential to drive forwards strategically important science and technology programmes. The restricted availability of beamtime at present is a huge inhibitor to realising the full scientific potential of XFELs, and it is only likely to be fully overcome by the combination of a next generation XFEL, as envisioned by the UK XFEL project, alongside collaborating with other higher throughput facilities being developed in SLAC, European XFEL and Shanghai.

I. Enabling Routes to Greener Chemical Synthesis

The chemical manufacturing industry is one of the world's most energy-intensive and polluting industries, in terms of both CO_2 production and hazardous waste. In 2012, 16.5 % of all industrial energy usage was dedicated for chemical manufacturing. All key advances in critical research areas, such as renewable energy generation and storage, and pharmaceuticals, are underpinned by the creation and manufacture of new chemicals. Finding routes to 'greenify' chemistry is therefore essential.



The programme will tackle three key challenges in greener chemical synthesis: how to redesign synthesis to use greener, alternative chemical feedstocks; how to use alternative solvents or reduce solvent use; and how to do industrial-scale reactions under milder conditions.

A next-generation XFEL will enable a suite of advanced experimental techniques (time-resolved-XAS/XRS/XES etc.) at high data rates to access chemically relevant concentrations (< mM) to probe fundamental questions about the role of reactants and solvents, including site-specific information in solvolytic reactions.[1] How to more efficiently catalyse solvolysis reactions for bond breaking is a key issue in polymer recycling, for example.[2]

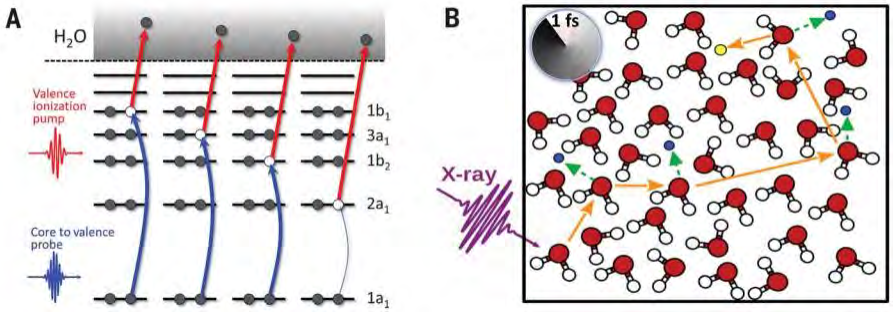
The proposed work will make use of both hard and soft X-rays at a variety of end-stations, in particular HRIXs/XAS, TXR Spectroscopy and Scattering and Spectroscopy. Potential funders including EPSRC, BBSRC, the Royal Society and industrial partners at AstraZeneca and Bayer.

[1] E.J. Mascarenhas, M. Fondell, R. Büchner, S. Eckert, V. Vaz da Cruz, and A. Föhlisch, "*The Role of the Lowest Excited Triplet State in Defining the Rate of Photoaquation of Hexacyanometalates*,", *JCP Lett.*, **15(1)**, 241–247 (2024). https://doi.org/10.1021/acs.jpclett.3c02775

[2] F. G. Cirujano et al., "*On the metal- and bio-catalyzed solvolysis of polyesters and polyurethanes wastes*," *RSC Sustainability*, 2(10), 2781–2804 (2024). https://doi.org/10.1039/d4su00233d

II. Tracking the fastest dynamics of radiation damage in materials for nuclear and space technology

To further space exploration and nuclear technology, including future fusion reactors, we need our technology to operate in a hostile environment with fast ionising radiation (gamma rays, beta particles, neutrons, protons, alpha particles) bombarding electronics, confinement materials and water coolant. It is therefore essential to characterise the mechanisms of interaction and damage to build understanding of the multi-timescale damage processes, and to fully work out mitigation strategies. Using X-ray ionisation (core and valence level) by attosecond X-ray pulses[1] is a realistic proxy for other fast ionising radiations and then leverages the implementation of pump-probe studies at temporal resolution ranging from attoseconds to nanoseconds via methods such as time-resolved X-ray absorption, resonant inelastic scattering and total scattering (to establish the evolving pair-distribution function).



This ambitious extended programme will employ soft and hard X-ray attosecond pulses and operate in X-ray/X-ray pump-probe configurations at high repetition rate, the former to establish the electronic pathways following damage, and the latter to track subsequent structural reorganisation and disorder. Consequently, both the Attosecond end-station and the HXR scattering capabilities operating with sub-femtosecond modes would be employed.

Liquid water[2], bulk metals, semiconductors, glasses and ceramics would all be within the scope of this investigation, which would unleash advanced XFEL measurement methods on this important range of real world problems. Extension to unravelling radiation damage mechanisms of biomolecules in hydrated environments would be expected in a future programme. Agencies who might fund such a programme include EPSRC, BBSRC, MRC, ESA/NASA, UKAEA, MOD.

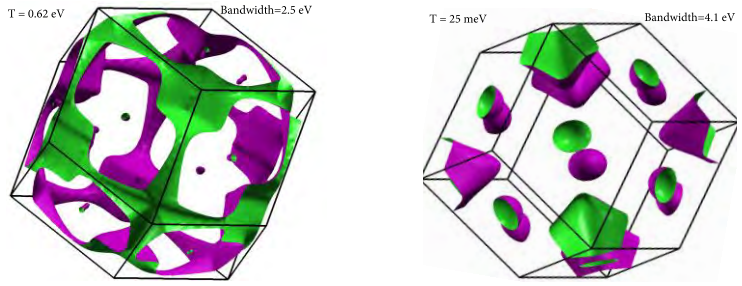
[1] Z. Guo, T. Driver, S. Beauvarlet *et al*. "*Experimental demonstration of attosecond pump–probe spectroscopy with an X-ray free-electron laser*," *Nat. Photon.* **18**, 691-697 (2024). https://doi.org/10.1038/s41566-024-01419-w

[2] S. Li *et al. "Attosecond-pump attosecond-probe x-ray spectroscopy of liquid water," Science*, **383** (6687), 1118 (2024). https://doi.org/10.1126/science.adn6059

*Illustration reproduced with permission from [2] S. Li et al. Science, **383** (6687), 1118 (2024). DOI: 10.1126/science.adn6059*

III. Measuring the dynamics of materials far from equilibrium

Materials exhibit exotic behaviour when driven to highly nonthermal, far-from-equilibrium states. Examples include nonthermal melting in semiconductors, bond hardening in metals, laser-induced phase transitions in covalently bonded materials, and, more recently, spin and phase transitions, including magnetic disordering in ferromagnets, antiferromagnets, and metals [1-5]. While theory and simulations have advanced our understanding of such processes, progress remains limited by the lack of experimental techniques capable of both generating and probing these states on their intrinsic spatial and temporal scales. Given their relevance across fields, from fusion energy to laser machining, experimental tools that can produce bulk samples under extreme conditions and probe their electronic and lattice dynamics on femtosecond timescales are of critical importance.



Fermi surface of two spin-down bands at electronic temperatures of 0.025 and 0.62 eV plotted inside the first BZ of the BCC structure. Increasing the electronic temperature reduces the bandwidth and localises the band near the Fermi surface. Figure reproduced from ref. [4].

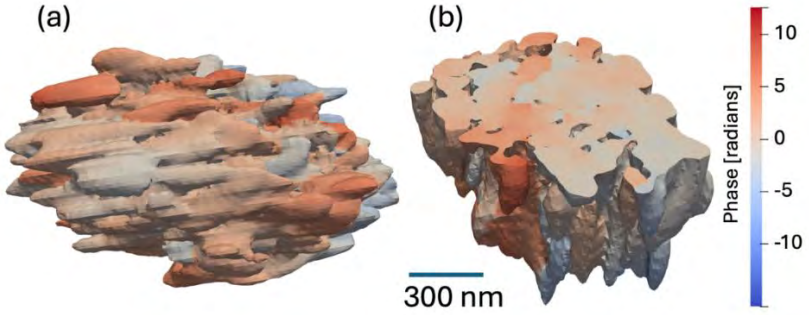
This programme will harness the two-colour soft X-ray pump/hard X-ray probe capabilities of a next-generation XFEL to advance our understanding of non-equilibrium systems on atomic length scales and electron dynamics timescales. Using a soft X-ray pump (0.5 – 2 keV), bulk samples spanning tens of cubic microns can be rapidly heated to temperatures exceeding 10,000 K within femtoseconds, while preserving the atomic lattice structure. A subsequent hard X-ray probe will track the lattice evolution via X-ray diffraction, complemented by SAXS and X-ray photon correlation spectroscopy, and will also interrogate electronic structural dynamics through X-ray scattering techniques, RIXS, EXAFS, XANES. By tuning the pump-probe delay, the full equilibration pathway, from the initial nonthermal electron distribution to electron relaxation, coupling with lattice, spin system, and beyond, will be resolved.

The programme will accommodate a broad class of materials, including semiconductors, insulators, metals, alloys, and strongly correlated systems, across sample types from thin films to bulk structures with varied morphologies. It is poised to deliver insights into ultrafast electron, spin, and ion dynamics, while also addressing challenges in materials science with industrial relevance. Potential funding agencies include EPSRC, STFC, ESA/NASA, UKAEA, and MOD.

[1] C.W. Siders *et al*., *"Detection of nonthermal melting by ultrafast X-ray diffraction," Science* **286**, 1340 (1999). https://doi.org/10.1126/science.286.5443.1340
[2] S. Wall *et al*., *"Ultrafast disordering of vanadium dimers in photoexcited VO_2," Science* **362**, 572 (2018). https://doi.org/10.1126/science.aau3873
[3] M.Z. Mo *et al. "Heterogeneous to homogeneous melting transition visualized with ultrafast electron diffraction," Science* **360**, 6396 (2018). https://doi.org/10.1126/science.aar2058
[4] S. Azadi *et al*., *"Nonthermal solid-solid phase transition in ferromagnetic iron," Phys. Rev. B* **110**, 214434 (2024). https://doi.org/10.1103/PhysRevB.110.214434
[5] A. Amouretti *et al*., *"Isostructural Phase Transition of Fe_2O_3 under Laser Shock Compression," Phys. Rev Lett*. **134**, 176102 (2025). https://doi.org/10.1103/PhysRevLett.134.176102

IV. Ion-conductor solid state electrolytes

Batteries made with solid state electrolytes (SSEs) are promising to revolutionise the electric vehicles (EV) industry with long range, fast charging and higher safety. "High-entropy" versions of NASICON ion conductor SSEs have a very fine grain structure of crystallographically aligned "phase domains," as shown in the figure below. Their order-of-magnitude larger ion conductivity (with respect to low entropy versions) may be due to ion conduction along the many grain boundaries revealed by X-ray Bragg Coherent Diffraction Imaging (BCDI). One proposed mechanism of ion conduction is Li-ion hopping between adjacent vacancy sites in the partially filled spinel lattice[1]. The strains associated with the lattice distortions around these sites can be imaged with BCDI as a function of time to map out the energy barriers associated with ion hopping.



(a) External surface of a 1600 nm sized $Li_3Ti_2(PO_4)_3$ crystal measured by BCDI on a 110 Bragg peak. The cigar shaped domains are oriented along the hexagonal crystal's c-axis, horizontally on the page. (b) Cross section perpendicular to the c-axis showing a network of phase domains. Ion diffusion is expected to take place along the domain boundaries.

This idea will be tested with SSE particles coated with a proto anode and cathode material. Laser pumping will then drive the ion current which will be time resolved by BCDI. This could be done by jet-based methods at high rep-rate (above) or on particles attached to substrates. **A next-generation XFEL, running with high rep-rate in CW operation, is expected to be considerably more stable, so will preserve the transverse coherence from one shot to the next**. High rep-rate pump-probe experiments with such beams are expected to be less destructive to the samples, so high quality BCDI data can be accumulated as a function of picosecond time delay.

The impact to society of developing advanced SSE materials is enormous. Armed with the understanding of the ion-conduction mechanism, scientist could design batteries for EVs that would be safe from fire and explosions, would hold considerably higher energy density, and would charge considerably faster than current technologies. An EV with 400 km range could be charged in around five minutes, similar to traditional fuelling times[2]. This work may attract investment from the Faraday Institution, and such as UKBic, Ilkia and Johnson Matthey.

[1] Y. Chen, Z. Lun, X. Zhao *et al. "Unlocking Li superionic conductivity in face-centred cubic oxides via face-sharing configurations," Nat. Mater*. **23**, 535-542 (2024). https://doi.org/10.1038/s41563-024-01800-8

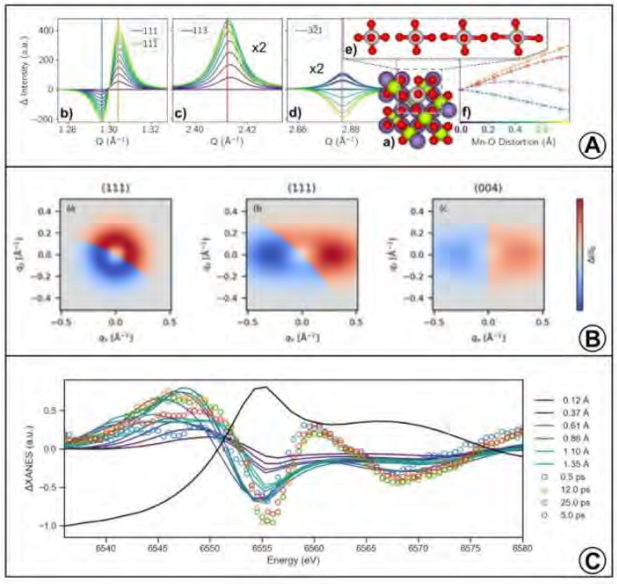
[2] Jeremy Hsu, *"Will we soon be able to charge electric cars in minutes?" New Scientist*, 18 March 2025 https://www.newscientist.com/article/2472602

Illustration reproduced with permission from I.K. Robinson et al. "Phase Domains Introduced in NASICON Ion Conductors after Ball Milling," in preparation for ACS Nano (2026)

V. Probing and controlling elementary steps in batteries

Li-ion batteries are a critical technology for meeting the world's clean energy transition[1]. At their core, batteries are governed by a range of elementary charge transfer steps such as ion hopping, electron tunnelling and solvent reorganisation, that together build up to give the macroscopic operational battery response. For example, it is the path electrons take after injection into the electrode (and before equilibrating) that will set the ultimate achievable battery cell capacity. Similarly, ion (de)solvation and solid-state hopping will determine electrode charging rates and interfacial/bulk stability. While we can probe the *effect* of these elementary processes, on long-timescales (seconds to hours), probing the individual building steps of battery charge/discharge remains challenging. This is due to the ultrafast femtosecond/picosecond timescales and nanoscopic lengths scales on which they occur[2]. Nonetheless, without understanding battery chemistry in this ultrafast regime, our ability to engineer energy storage systems from the bottom-up will remain limited.

With their widely tuneable energy range, femtosecond time resolution and nanoscopic spatial resolution XFELs can meet this gap. **A range of different next-generation XFEL end-stations would be used over an extended series of beamtimes to reveal the elementary inner working steps of batteries.** For instance, a THz pump, hard X-ray probe station would be ideal for capturing the structural dynamics that impede ion motion during battery charging, key for creating faster charging cells. Similarly, femtosecond X-ray liquid scattering with IR pumping would be ideal for probing which electrolyte structures are responsible for inhibiting solvation at battery interfaces. And picosecond X-ray photon correlation measurements[3] and soft X-ray imaging could finally reveal how Li-heterogeneities develop in battery materials an outstanding question for pushing their durability.



Left: Simulations and experiments of polaron (electronic charge carrier) formation in $Li_xMn_2O_4$ a key electrode material. From UltraBat Consortium[4].

An XFEL programme on batteries would hence explore a range of electrode and solid or liquid electrolyte materials from those in commercial use, such as Li_xCoO_2 (interfacing with the large battery industry on optimisation), to those being developed for the next generation of high-rate capacity durable batteries, such as anionic redox compounds. The measurements would open a new paradigm for the bottom-up, rational design of battery (and related energy storage materials) based on the understanding of building block ultrafast processes.

We anticipate support from UKRI, ERC, national and international hubs in battery materials (e.g. Faraday Institution) and those working on related problems in other similar ionic/electronic conductors (e.g. catalysis; UK Catalysis Hub).

[1] J.M. Tarascon, M. Armand, *"Issues and challenges facing rechargeable lithium batteries," Nature* **414**, 359–367 (2001). https://doi.org/10.1038/35104644

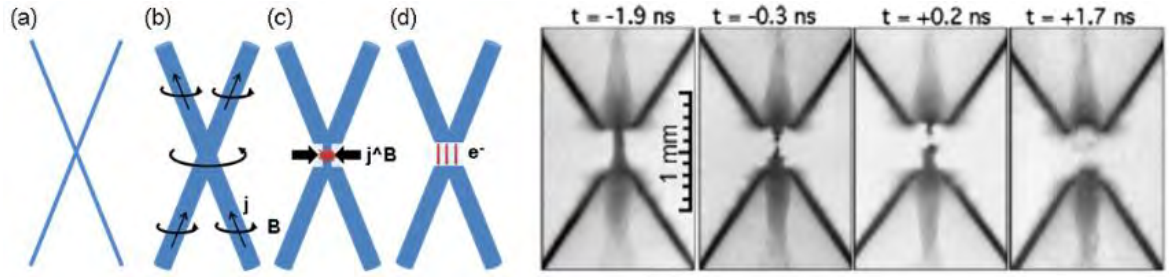
[2] A. Sood, A.D. Poletayev, D.A. Cogswell *et al. "Electrochemical ion insertion from the atomic to the device scale," Nat Rev Mater* **6**, 847–867 (2021). https://doi.org/10.1038/s41578-021-00314-y

[3] Y. Shinohara, T. Osaka, I. Inoue *et al. "Split-pulse X-ray photon correlation spectroscopy with seeded X-rays from X-ray laser to study atomic-level dynamics," Nat Commun* **11**, 6213 (2020). https://doi.org/10.1038/s41467-020-20036-z

[4] https://battery2030.eu/battery2030/projects/ultrabat/

VI. Exploring extreme material conditions in current driven X-pinch implosions

Current driven magneto-hydrodynamic instabilities influence the behaviour of many systems – from lightning conductors to Tokamaks. To localise an m=0 'sausage' instability in high density plasmas, and enable it to be studied in more detail, 'X-pinches' were developed in the 1980s. The magnetic hot spot at the crossing point in the pinch emits high power, sub-ns bursts of X-ray radiation from a few micron wide volume. Whilst there is significant understanding of the dynamics of material in an X-pinch [1], there is a lack of sufficiently time-resolved, quantitative measurements of these processes. Simulations[2] suggest that the implosion and instability development result in solid density, highly magnetised plasmas with pressures >100 Mbar and temperatures ~KeV, conditions typically found only in inertial fusion experiments and planetary/stellar physics.



Left: Implosion of an X-pinch showing initial expansion of the wires into dense plasmas (b), m=0 development at the crossing point and emission of X-ray burst (c), break up of column and micro-diode formation (d). Right: Radiographs of different X-pinch experiments show the evolution of the X-pinch at the neck region driven by the m=0 instability occurs on the ns – sub ns timescale.

Figures reproduced with permission from (left) Zucchini et al. Rev. Sci. Instrum. 86, 033507 (2015) DOI: 10.1063/1.4915496; (right) Pikuz et al. Phys Rev Lett. 89(3):035003 (2002) DOI: 10.1103/PhysRevLett.89.035003

A next-generation XFEL would provide unprecedented capabilities in analysing these extreme conditions using a rapid train of X-ray pulses alongside the latest in X-ray cameras, e.g. the Daedalus Ultrafast Imager[3], enabling quantitative X-ray radiography to explore X-pinch dynamics on the nanosecond scale in a single experiment. Novel techniques, such as the split and delay system pioneered at the European XFEL[4] , would enable multiple radiographs to be taken with << nanosecond interframe times ('GHz imaging'), vital for examining instability driven processes in such rapidly evolving plasmas. The open geometry of a two wire X-pinch could also enable direct temperature measurements through XANES / XRTS. Together these measurements would allow the first accurate code and theory validation in these extreme conditions complimenting measurements made with high energy lasers.

The research could initially accommodate a broad class of metals, enabling atomic physics effects (e.g. radiatively cooling rates) to be related to properties at these extreme conditions. Recent improvements to X-pinch drivers and loads extend this to gases and mixtures of insulating materials[5] with improved reproducibility and turn round time. The same XFEL based radiography systems would also be ideal for studying instabilities driven in convergent inertial fusion targets. Potential funding agencies include EPSRC, NNSA, and MoD.

[1] S.A. Pikuz, T.A. Shelkovenko, D.A. Hammer, *"X-pinch. Part I," Plasma Phys. Rep*. **41**, 291–342 (2015). https://doi.org/10.1134/S1063780X15040054

[2] J.P. Chittenden, A. Ciardi, C.A. Jennings *et al*. *"Structural Evolution and Formation of High-Pressure Plasmas in X Pinches,"* *Phys. Rev. Lett*. **98**, 025003 (2007). https://doi.org/10.1103/PhysRevLett.98.025003

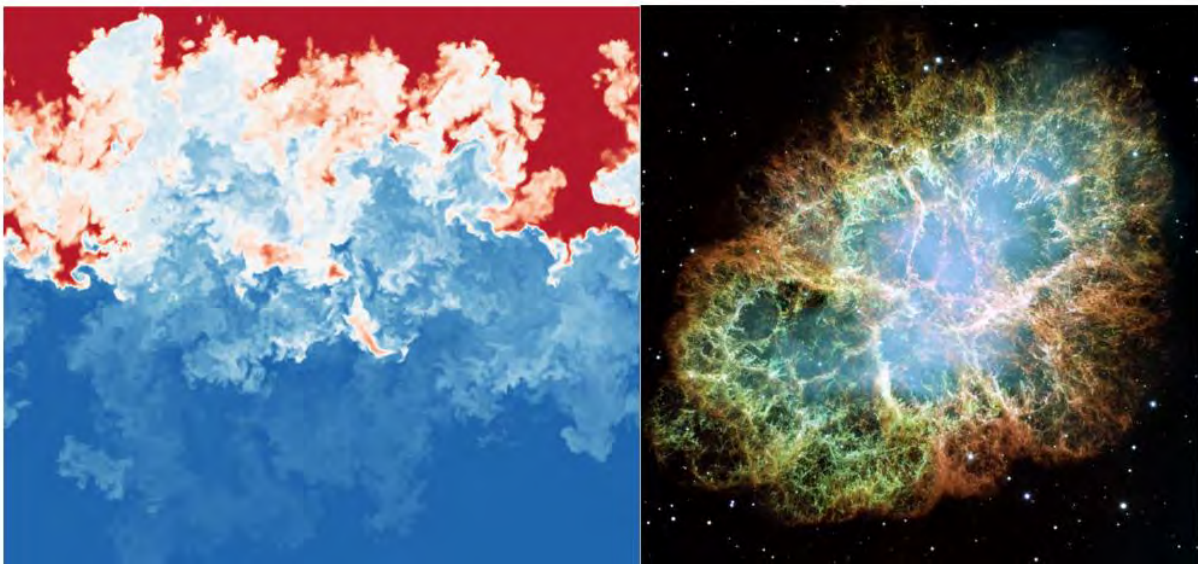
[3] Q. Looker, M. Kimmel, C. Yang, J.L. Porter, *"Optical and x-ray characterization of the Daedalus ultrafast x-ray imager," Rev. Sci. Inst.* **94**, 113505 (2023) https://doi.org/10.1063/5.0171222

[4] Under development at the SPB/SFX beamline European XFEL, by P. Vagovic *et al.*

[5] T.A. Shelkovenko, S.A. Pikuz, S.A. Mishin *et al. "Hybrid X-pinches," Plasma Phys. Rep*. **38**, 359–381 (2012). https://doi.org/10.1134/S1063780X1204006X

VII. Understanding magneto-hydrodynamic stability and fluid mixing

Fluid mixing dominates the dynamics of many natural systems[1] – from development of complex structures in nebulae, to planetary impacts, inertial confinement fusion energy or combustion engines. Modelling the nonlinear dynamics that drive the cascade from large-scale flows to molecular mixing (or vice versa) is one of the few remaining scientific challenges in classical physics. Understanding magneto-hydrodynamic mixing is important in situations ranging from industrial uses – such as stabilisation of fuel compression in fusion energy, which is commonly unstable to swiftly developing Richtmyer-Meshkov or Rayleigh-Taylor instabilities[2] – to purely scientific ones. These include the development of magnetic fields in astrophysical turbulence or explaining the similarity of elemental composition between the Moon and the Earth, suggested to result from fluid-like mixing during an impact between the proto-Earth and the approximately Mars-sized 'Theia'.



Left: Simulation of a turbulent fluid mixing during shock-compression of an imperfect interface from [1].
Right: A composite Hubble Space Telescope image of the Crab Nebula. © NASA

This programme will leverage the **coupling of a next-generation XFEL over multiple beamtimes to a suite of dynamic drivers** to enable measurement of material mixing dynamics, from well-defined initial stages (e.g. jetting from well-known interfaces) through to deeply nonlinear stages of turbulent development. The envisaged measurements will utilise various imaging techniques, such as near-field holography or Talbot imaging, to understand early-time effects of geometry, viscosity and material strength, as well as the measurement of mixing fractions in the nonlinear regime. X-ray speckle techniques, such as XPCS, will be used to understand how the structure factor evolves over time.

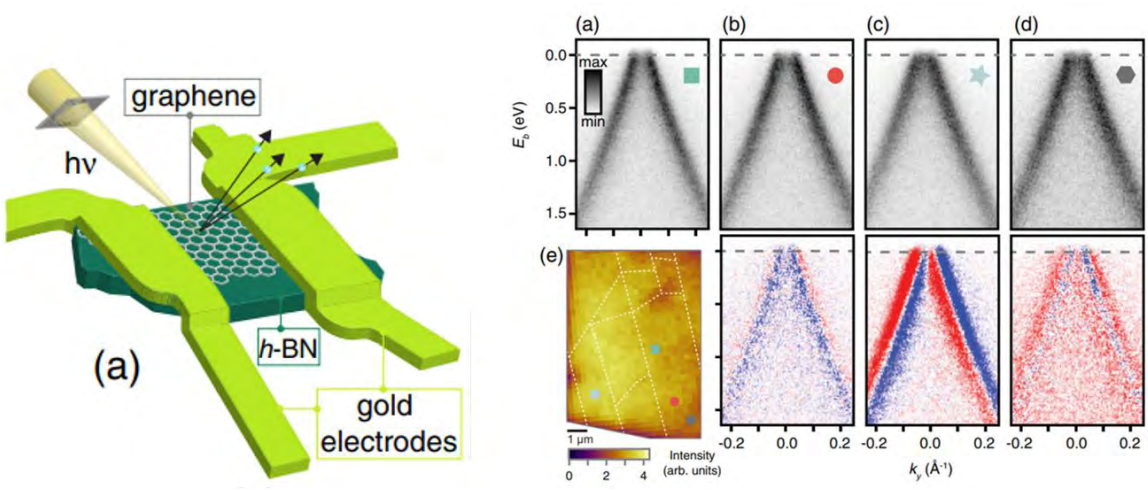
Additionally, utilisation of pulsed-power high-current discharges will enable the systematic study of astrophysical scenarios and dense plasma mixing in the presence of strong magnetic fields – spearheading the development of novel measurement techniques for magnetised dynamics, such as X-ray Faraday rotation imaging. Potential funding partners include EPSRC, ESA/NASA, DOE/DOD, and private fusion companies.

[1] Y. Zhou, R.J.R. Williams, P. Ramaprabhu *et al*. "Rayleigh–Taylor and Richtmyer–Meshkov instabilities: A journey through scales," *Physica D: Nonlinear Phenomena*, **423**, 132838 (2021). https://doi.org/10.1016/j.physd.2020.132838

[2] A.B. Zylstra, O.A. Hurricane *et al. "Burning plasma achieved in inertial fusion," Nature **601**, 542–548 (2022).* https://doi.org/10.1038/s41586-021-04281-w

VIII. Probing THz electron transport in graphene

When a conduction electron in graphene is exposed to a DC electric field, it will rapidly accelerate from the drain electrode towards the source electrode reaching the Fermi velocity in an attosecond[1,2]. In contrast, in an AC electric field the electron will oscillate, at the Fermi velocity, at the frequency of the applied field[2]. For electric fields below THz frequency, the electron will experience numerous scattering events due to electron-electron, electron-phonon, impurity interactions etc. The emergence of graphene and other 2D materials (G2DMs) has opened a plethora of novel potential applications in quantum computing, communications and sensing, as well as petahertz electronics, energy storage and medical technologies. Minimising dissipative processes in G2DMs will be crucial to the realisation of these technologies in the future.



Left: Graphene on h-BN with gold source-drain electrodes to inject 'transport current' at THz frequencies. Right: Intensity of the Dirac cone spectra taken in different locations of the device, as given by the corresponding markers in (e) [reproduced with permission from 3].

This requires an accurate understanding of the electron transport scattering mechanisms[3,4] in G2DM, to enable development of novel materials that consume exceptionally low amounts of energy whilst providing robust performance. Experimental observation of these interactions using a THz pump and soft X-ray probe in a nano/time-resolved ARPES set-up (using the soft X-ray tr-ARPES on FEL 6: 0.05-1 keV) would allow unique insights into electron 'transport dynamics' in G2DMs. By **harnessing the inherent high (~ 10^5 Hz) pulse rate and pump-probe capability of a next-generation XFEL** we can study the electronic dynamics over the delay from 0.1 – 1000 fs to fully capture the electron transport scattering processes and interactions in G2DMs for optimising material properties and enabling real world applications.

This programme would be targeted for support from EPSRC, BBSRC, MRC, STFC, Innovate UK, Horizon Europe and industry.

[1] K.S. Novoselov *et al. "Electric field effect in atomically thin carbon films," Science*, **306**, 666-669 (2004). https://doi.org/10.1126/science.1102896

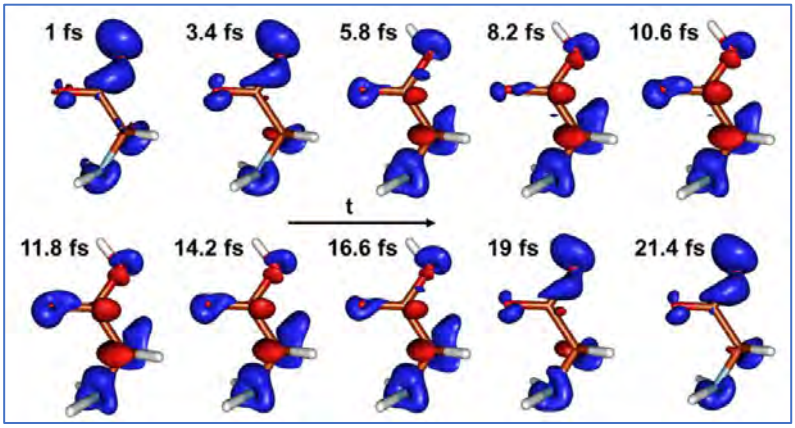
[2] S.A. Awan *et al, "Transport conductivity of graphene at RF and microwave frequencies," 2D Mater.* **3,** 015010 (2016). https://doi.org/10.1088/2053-1583/3/1/015010

[3] D. Curcio *et al. "Accessing the spectral function in a current-carrying device," Phys. Rev. Lett.* **125**, 236403 (2020). https://doi.org/10.1103/PhysRevLett.125.236403

[4] S. Ulstrup *et al.* "Ultrafast electron dynamics in epitaxial graphene investigated with time- and angle-resolved photoemission spectroscopy," *J. Phys.: Condens. Matter* **27**, 164206 (2015). https://doi.org/10.1088/0953-8984/27/16/164206

IX. New chemical dynamics induced by sudden ionisation

When a valence electron is suddenly removed from a molecule, by an attosecond soft X-ray pulse[1] or a collision with a fast charged particle (such as a cosmic ray), the resulting wavepacket of the electronic states of the cation can manifest new oscillatory electron density dynamics (charge migration) and induce unique new modes of fragmentation[2]. The oscillatory charge migration leads to new time dependent forces absent under normal "slow" initiation. This is a channel of "attochemical" activity previously unobserved, due to the absence of fast enough pumps for impulsive initiation and subsequent probing of the unfolding electronic and nuclear dynamics.



Ultrafast charge motion in suddenly ionised glycine calculated via ADC(2) theory and measured with few femtosecond resolution

Figure reproduced from D. Schwickert et al. Sci. Adv. 8, eabn6848 (2022) DOI: 10.1126/sciadv.abn6848

By harnessing the high data rate attosecond pump-probe capability of a next-generation XFEL we can study the electronic dynamics and electron-nuclear coupling over the delay from 0.1 – 1000 fs to fully capture the unfolding dynamics of the molecular ion undergoing these new chemical modes. This would use time-resolved multi-edge X-ray absorption and X-ray photoelectron spectroscopy combined, in covariance or coincidence, with ion mass and ion momentum measurement at the SXR Attosecond End-Station. High quality data and the ability to study dynamics at high temporal resolution (~300 as) over long delay times will be enabled by the inherent high (~ 10^5 Hz) pulse rate.

This programme would explore an appropriate range of small molecules from methane to amino acids (including potentially anionic and cationic systems) to build a conceptual picture of the physics and chemistry within this new paradigm of charge migration initiated chemistry. There would be a particular emphasis on those molecules identified in environments, like space and the outer layers of planetary atmospheres, where sudden ionisation from ionising radiation will be naturally present. This programme could be targeted for support from EPSRC, NERC and ESA/NASA.

[1] J. Duris, S. Li, T. Driver *et al. "Tunable isolated attosecond X-ray pulses with gigawatt peak power from a free-electron laser," Nat. Photonics* **14**, 30–36 (2020). https://doi.org/10.1038/s41566-019-0549-5

[2] D. Schwickert *et al. "Electronic quantum coherence in glycine molecules probed with ultrashort x-ray pulses in real time," Science Advances* **8**, 22 (2022). https://doi.org/10.1126/sciadv.abn6848
D. Schwickert *et al. "Charge-induced chemical dynamics in glycine probed with time-resolved Auger electron spectroscopy," Struct. Dyn*. **9**(6):064301 (2022). https://doi.org/10.1063/4.0000165

X. Probing exciton and spin dynamics in optoelectronic materials

Optoelectronic materials, such as metal porphyrins (e.g. Zinc(II)-tetraphenyl porphyrin (ZnTPP)), are prototypical 'closed system' molecules used as thin films and in a crystalline state in device integration of organic and inorganic semiconductors. Understanding the exciton and spin dynamics in these materials is critical to fully optimise such devices. Time-resolved X-ray spectroscopy and diffraction are ideal for this purpose but, to fully reveal the key coherences in mixed electronic-valence pathways critical in these functional materials, new techniques that combine multi-dimensional optical and X-ray spectroscopy must be implemented.

Two-dimensional Electronic-X-ray spectroscopy (2DEX) will be developed[1] that combines the power of electronic multi-dimensional spectroscopy with incisive (electronic and spin state resolved) X-ray spectroscopy and **leverages the very high repetition rate of a next-generation XFEL**.

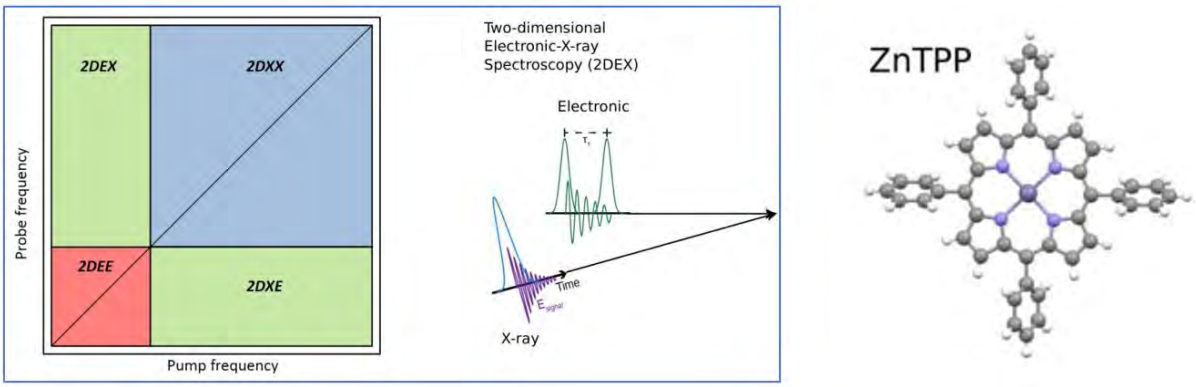


Figure adapted from Ref [1]

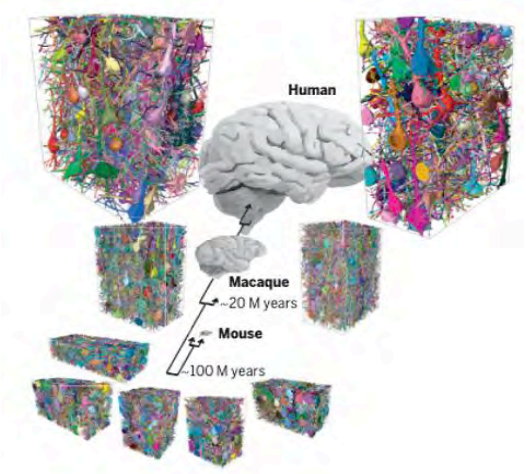
By replacing a single laser pulse in a pump-probe X-ray experiment with a phase locked pulse pair, the frequency correlation of the valence electron dynamics can be retrieved by incrementing the inter-pulse delay in a phase stable manner. The key requirement for this work is that such datasets can only be collected at very high repetition rate, since many hundreds or thousands of repeat measurements of kinetic series are required to create the Fourier domain of frequency correlation. The frequency correlation of the electronic dimension provides high energy resolution and will separate the low frequency, fingerprint region and high frequency vibrations.

An important further application will be the measurement of spin changes in metal complexes including enzymes, which is expected to resolve the spin-vibration coupling. Extensions of the frequency correlation technique are proposed for any time resolved X-ray experiment, including XRD, XES, RIXS, EXAFS, and so can be rolled out across multiple end-stations of a next-generation XFEL. Agencies likely to support such work include EPSRC, BBSRC, ERC and Innovate UK.

[1] J. van Thor "*Coherent two-dimensional electronic-x-ray spectroscopy*" J. Chem. Phys. 164, 044117 (2026) https://doi.org/10.1063/5.0304001

XI. Nanobioimaging in tissues and organs – wiring diagrams for whole brains

Life science is rapidly moving from a cellular to a tissue age, where ultrastructure and functional detail must be resolved in the context of intact tissues and organs. Nowhere is this more critical than in neuroscience: information processing in the brain depends on the connectome—the precise map of how millions of neurons interconnect[1-3]. To reveal this wiring, one must image axons, dendrites, and synapses at <20 nm resolution while tracing fibres over millimetre scales. At present, connectomics relies on volume electron microscopy[4]. Because electrons penetrate only nanometres into tissue, physical sectioning or ablation is required. This destructive, slow, and error-prone process limits accessible volumes to ~0.01 mm³ and demands specialised laboratories, restricting the field to a handful of groups worldwide. Scaling to statistically meaningful brain volumes (≥1 mm³) is currently beyond reach.



Wiring diagrams from mouse, macaque and human tissues
Figure reproduced with permission from ref [3]

Next-generation X-ray free electron lasers (XFELs) offer a revolutionary alternative. They will deliver 3 orders of magnitude higher flux than even state-of-the-art 4th-generation synchrotrons, with the stability required for nanoscale tomography imaging, pioneered at synchrotron light sources[5]. This leap will enable non-destructive imaging of soft tissue volumes at tens-of-nanometre resolution across millimetre to centimetre-sized samples, possibly opening up whole-brain imaging for mammals including primates. Crucially, XFELs will allow this whole-organ imaging without sectioning, bypassing the throughput bottlenecks of electron microscopy.

Like genome sequencing in molecular biology, routine acquisition of connectomes would transform neuroscience, providing structural basis for psychiatric diseases, as well as new network architectures for neural network models. We anticipate support from MRC, EPSRC, BBSRC, as well as charities such as Wellcome[4].

[1] D.A. Pospisil, M.J. Aragon, S. Dorkenwald *et al*. "*The fly connectome reveals a path to the effectome*," *Nature* **634**, 201-209 (2024). https://doi.org/10.1038/s41586-024-07982-0
[2] The MICrONS Consortium. *"Functional connectomics spanning multiple areas of mouse visual cortex," Nature* **640**, 435–447 (2025). https://doi.org/10.1038/s41586-025-08790-w
[3] S. Loomba, J. Straehle, V. Gangadharan *et al*. *"Connectomic comparison of mouse and human cortex," Science* **377**, 6602 (2022). https://doi.org/10.1126/science.abo0924
[4] G.S. Jefferis, L. Collinson, C. Bosch *et al*. "*Scaling up connectomics - The road to a whole mouse brain connectome*" (2023). Wellcome Trust Report. https://cms.wellcome.org/sites/default/files/2023-06/Connectomics-scaling-up-connectomics.pdf
[5] T. Aidukas, N.W. Phillips, A. Diaz *et al*. "*High-performance 4-nm-resolution X-ray tomography using burst ptychography,*" *Nature* **632**, 81–88 (2024). https://doi.org/10.1038/s41586-024-07615-6

9.5 References for Chapter 9

1 A.Burnett, M. Borghesi, A. Comley, M. Dean, S. Diaz-Moreno, D. Dye, J. Greenwood *et al*. "UK XFEL Science Case" (2020) DOI: 10.5286/stfctr.2026008

2 C. Brahms, D. Austin, F. Tani, A. Johnson, D. Garratt, J. Travers, J. Tisch, P. Russell and J. Marangos, "Direct characterization of tuneable few-femtosecond dispersive wave pulses in the deep UV," *Opt. Letts*. **44**, 2990 (2019) DOI: 10.1364/OL.44.000731

3 J.C. Travers, T.F. Grigorova, C. Brahms *et al.* "High energy pulse self-compression and ultraviolet generation through soliton dynamics in hollow capillary fibres," *Nat. Photonics* **13**, 547-554 (2019) DOI: 10.1039/s41566-019-0416-4

4 J. Lee *et al*. "Few-femtosecond soft X-ray transient absorption spectroscopy with tuneable DUV-Vis pump pulses," *Optica*, 11, 1320 (2024) DOI: 10.1364/OPTICA.530964

5 A. Ermolov, K.F. Mak, M.H. Frosz, J.C. Travers and P.St.J. Russell, "Supercontinuum generation in the vacuum ultraviolet through dispersive-wave and soliton-plasma interaction in a noble-gas filled hollow core photonic crystal fibre," *Phys. Rev. A* **92**, 033921 (2015) DOI: 10.1103/PhysRevA.92.033921

6 H. Bromberger *et al.*"Angle-resolved photoemission spectroscopy with 9 eV photon-energy pulses generated in a gas filled hollow core photonic crystal fibre" *Appl. Phys. Lett*. 107, 091101 (2015) DOI: 10.1063/1.4929542

7 M. Krebs, S. Hädrich, S. Demmler *et al.*"Towards isolated attosecond pulses at megahertz repetition rates" *Nature Photon* **7**, 555 (2013) DOI: 10.1039/nphoton.2013.131

8 A. Perucchi *et al.* "The TeraFERMI terahertz source at the seeded FERMI free-electron-laser facility," *Rev. Sci. Instrum.* **94**(2), 022702 (2013) DOI: 10.1063/1.4790429

9 M. Först, M. Gensch, R. Riedel, F. Tavella, E.A. Schneidmiller, N. Stojanovic, M.V. Yurkov, "Optical Afterburner for a SASE FEL: First Results from FLASH," THPC94, IPAC2011, San Sebastián, Spain (2011)

10 J. Tanikawa et al. "Volt-per-Ångstrom terahertz fields from X-ray free-electron lasers," *J Synchrotron Radiat*. 27, 796-799 (2020) DOI: 10.1107/S1600577520004245

11 S. Gerber, H. Jang, D. Zhu, J.-S. Lee, W.-S. Lee *et al.* "Three-dimensional charge density wave order in $YBa_2Cu_3O_{6.67}$ at high magnetic fields" *Science* **350**, 949-952 (2015) DOI: 10.1126/science.aac6257

12 J. Yang. M. Guehr, T. Vecchione *et al.* "Diffractive imaging of a rotational wavepacket in nitrogen molecules with femtosecond megaelectronvolt electron pulses," *Nat Commun* **7**, 11232 (2016) DOI: 10.1039/ncomms11232

13 S.P. Weathersby, R.K. Li *et al.* "Mega-electron-volt ultrafast electron diffraction at SLAC National Accelerator Laboratory," *Rev. Sci. Instrum*. **96**, 073702 (2015) DOI: 10.1063/1.4926994

14 U. Weierstall, J.C.H. Spence and R.B. Doak, "Injector for scattering measurements on fully solvated biospecies," *Rev. Sci. Instrum*. **93**, 035109 (2012) DOI: 10.1063/1.3693040

15 Mous, S., Hunter, M. S., Poitevin, F., Boutet, S. & Gee, L. B. Macromolecular crystallography and biology at the Linac Coherent Light Source. *Journal of Synchrotron Radiation* **32**, 548-566 (2025) DOI: 10.1107/S1600577525002735

16 F.D. Fuller, S. Gul, R. Chatterjee *et al.* "Drop-on-demand sample delivery for studying biocatalysts in action at X-ray free-electron lasers," *Nat Methods* **14**, 443-449 (2017) DOI: 10.1038/nmeth.4195

17 S. Oghbaey, A. Sarracini, H.M. Ginn *et al.* "Fixed target combined with spectral mapping: approaching 100% hit rates for serial crystallography," *Acta Crystallographica D Struct Biol* **72**, 944-955 (2016) DOI: 10.1107/S2059798316010834

18 Perrett, S. *et al.* Kilohertz droplet-on-demand serial femtosecond crystallography at the European XFEL station FXE. *Struct Dyn* **11**, 024310 (2024) DOI:10.1063/4.0000248

19 Poudyal, M. Schmidt, and P. Schwander, "Single-particle imaging by X-ray free-electron lasers-How many snapshots are needed?" *Struct Dyn* ***7***, 024102 (2020) DOI: 10.1063/1.514451

20 H.N. Chapman, "X-Ray Free-Electron Lasers for the Structure and Dynamics of Macromolecules," *Annu Rev* Biochem **88**, 35-58 (2019) DOI: 10.1146/annurev-biochem-013118-110744

21 Z.B. Sun, J.D. Fan, H.Y. Li, H.D. Jiang, "Current Status of Single Particle Imaging with X-ray Lasers," *Appl Sci-Basel* **8** (2018) DOI: 10.3390/app8010132

22 A. Aquila, A. Barty, C. Bostedt *et al.* "The linac coherent light source single particle imaging road map," *Struct Dyn* **2**:4, 041701 (2015) DOI: 10.1063/1.4918726

23 G. Galinis, J. Strucka, J.C.T. Barnard, A. Braun, R.A. Smith, J.P. Marangos, "Micrometer-thickness liquid sheet jets flowing in vacuum," *Rev. Sci. Instrum*. **88**, 083117 (2017) DOI: 10.1063/1.4990130

24 J.D. Koralek, J.B. Kim, P. Brůža *et al.*"Generation and characterisation of ultrathin free-flowing liquid sheets," *Nat Commun* **9**, 1353 (2018) DOI: 10.1038/s41467-018-03696-w

25 A. Sanchez-Gonzalez, P. Micaelli, C. Olivier *et al.* "Accurate prediction of X-ray pulse properties from a free-electron laser using machine learning," *Nat Commun* **8**, 15461 (2017) DOI: 10.1038/ncomms15461

10. Alignment to National Priorities and International Engagement for a Next-generation XFEL

A next-generation XFEL will be orders of magnitude greater in both peak and average power than the most advanced synchrotron. It is thus the future for light sources that will deliver the essential structural and dynamical insights to propel science, industry, defence and medicine forwards into the second half of this century. This potential has been fully grasped internationally and plans are advancing in China and the USA for next-generation XFELs. If the UK and Europe are not to be left behind, they need to act strategically now or significantly lose competitiveness over the long-term in industry and defence.

As presented in the **Executive Summary** and **Overview**, the next generation of XFELs will be the most advanced light sources the world has ever seen. They will have an average X-ray brightness more than a thousand times higher than fourth generation storage rings like Diamond-II, and a peak brightness a billion times higher. This will provide revolutionary X-ray structure and imaging capabilities that will impact industry, defence, biotechnology, batteries, solar energy and catalysis (see **Chapters 8** and **9**). Still more importantly this will give access to the intrinsic timescales for physical, chemical and biological changes of matter that are governed by the motion of the constituent electrons (moving on typical timescales of a femtosecond or less) and atoms (moving on typical timescales of 100 femtoseconds). This is largely out of reach of even fourth generation storage rings that cannot resolve processes significantly faster than nanoseconds. This capability will transform science and technology, providing access to unprecedented information.

XFELs provide unique real-time access to electronic and structural dynamics in matter at the quantum scale. Understanding these dynamics will unlock new science, new technology and new biotech opportunities. Emerging XFEL technologies that provide boosted access, and the fullest range of advanced capabilities, are being developed in China and the USA. The UK XFEL project is in part a response to this and the CDOA has been exploring ways to deliver a next-generation XFEL that will serve wide areas of science and technology and increase core competitiveness in the UK and partner nations.

In this chapter, we overview how a next-generation XFEL would:

- impact national strategic priorities in technology
- serve the interests of defence technology and industry
- integrate into the broader facilities infrastructure available to the UK
- engage and interact with international partners.

10.1 Addressing national strategic priorities in technology

The impact of a next-generation XFEL aligns with government ambition in all key sectors of the economy by building the UK skills and technology base. In five of the IS-8 sectors it would directly address key challenges. Access to a next-generation XFEL is of critical importance to the UK, providing industry, defence and academia with vital tools to advance their research and deliver advanced, competitive solutions.

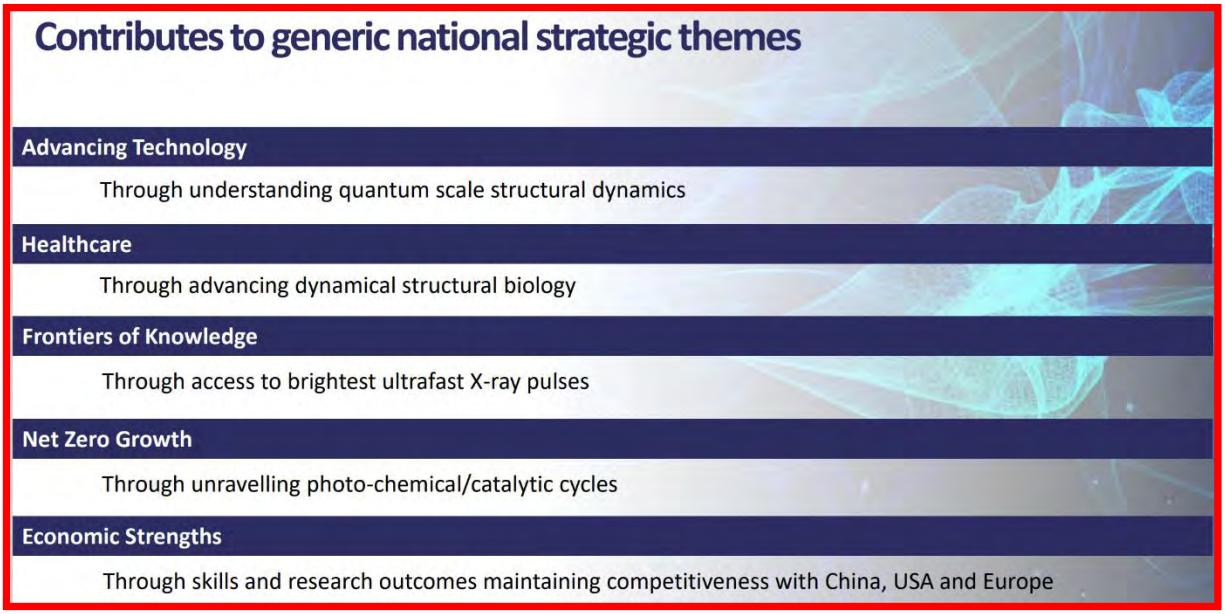
The UK government's recent reports, **Invest 2035: the UK's modern industrial strategy**[1] and **The UK's Modern Industrial Strategy**[2], set out the ambition for the country and identify priority growth sectors for the UK economy. The industrial strategy is focussed on the sectors which offer the highest growth opportunity for the economy and business. The eight growth-driving sectors, the **IS-8**, are:

- Advanced manufacturing *
- Clean energy industries *
- Creative industries
- Defence *
- Digital and technologies *
- Financial services
- Life sciences *
- Professional and business services.

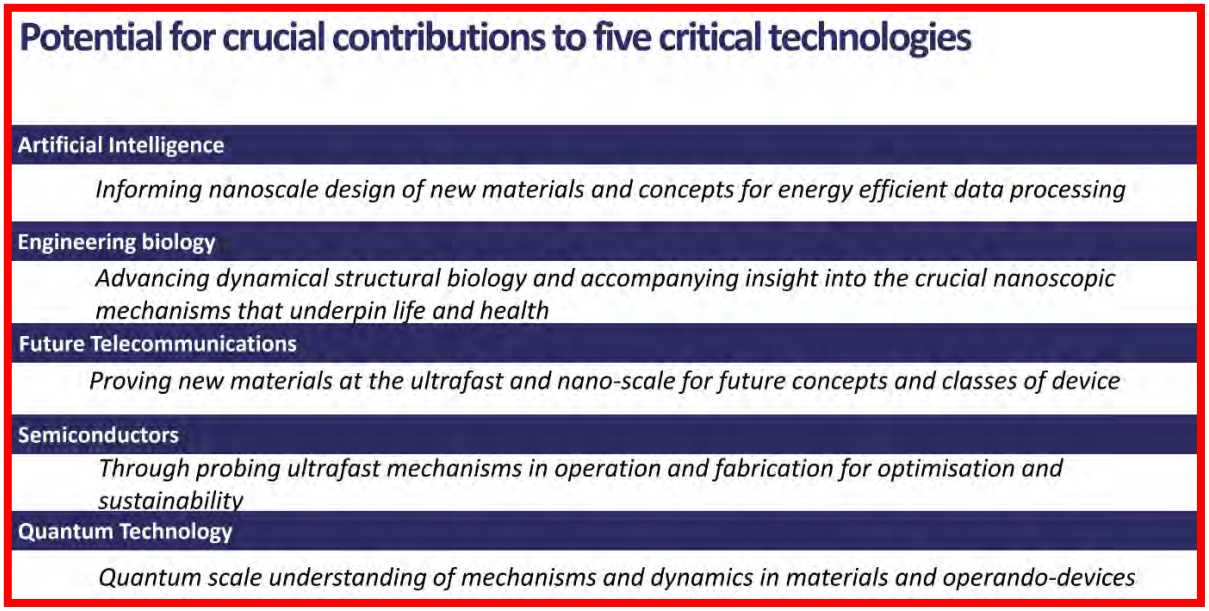
The impact of a next-generation XFEL aligns with government ambitions in all of these sectors by building the UK skills and technology base. It is directly aligned to the advanced science and technology needed by sectors marked with * above, and indeed all of these sectors are heavily featured in this Science and Technology Case. Advanced XFEL capabilities would be able to address key technology challenges for **Advanced Manufacturing**, **Clean Energy Industries**, **Digital and Technologies**, **Life Sciences** and **Defence**. Moreover, next-generation XFELs will be some of the biggest sources of high-value data in the world; they will have a highly synergistic relationship with AI and we would seek to capitalise on the value of this data for the UK. The vast amounts of data generated by an advanced facility will require the development of cutting-edge concepts to facilitate efficient processing, providing a pioneering environment and incubator for new ideas in **Data, AI and Machine Learning** that can quickly propagate into the wider economy. Large numbers of highly trained scientists and engineers, whose skills will be honed working with the facility, will ultimately join the workforce, thereby boosting all sectors including the **Creative Industries**, **Financial Services** and **Professional and Business Services**.

Access to an advanced XFEL is of critical importance to the UK to boost the science and technology base, provide companies with vital tools for their missions, and maintain competitiveness in industry and defence. Within the context of the 2025 UKRI strategy[3], an advanced XFEL provides the tools needed for addressing the science and technology at the core of: **Building a green future, Building a secure and resilient world, Tackling infections, Securing better health, ageing and wellbeing** and **Creating opportunities, creating outcomes.** The text box below highlights in which respects a next generation XFEL would be crucial to generic national strategic themes – those set out by the UK government in 2023, which informed our 2023-25 engagement process, and those reflected in the 2025 strategy.

1 Invest 2035 - GOV.UK
2 https://www.gov.uk/government/collections/the-uks-modern-industrial-strategy-2025
3 https://www.ukri.org/who-we-are/our-vision-and-strategy/ukri-strategic-themes/



We can map key areas where an XFEL will boost the IS-8 priorities and other critical sectors of technology. The **Five Critical Technologies** (2023 and 2025)[4] **Artificial Intelligence**, **Engineering Biology, Advance Connectivity Technologies, Semiconductors** and **Quantum Technology**, are all directly supported by a next-generation XFEL. The text box below explicitly maps the strong contributions from a next-generation XFEL to each (note the April 2025 policy renames *Future Telecoms* as *Advanced Connectivity Technologies*).



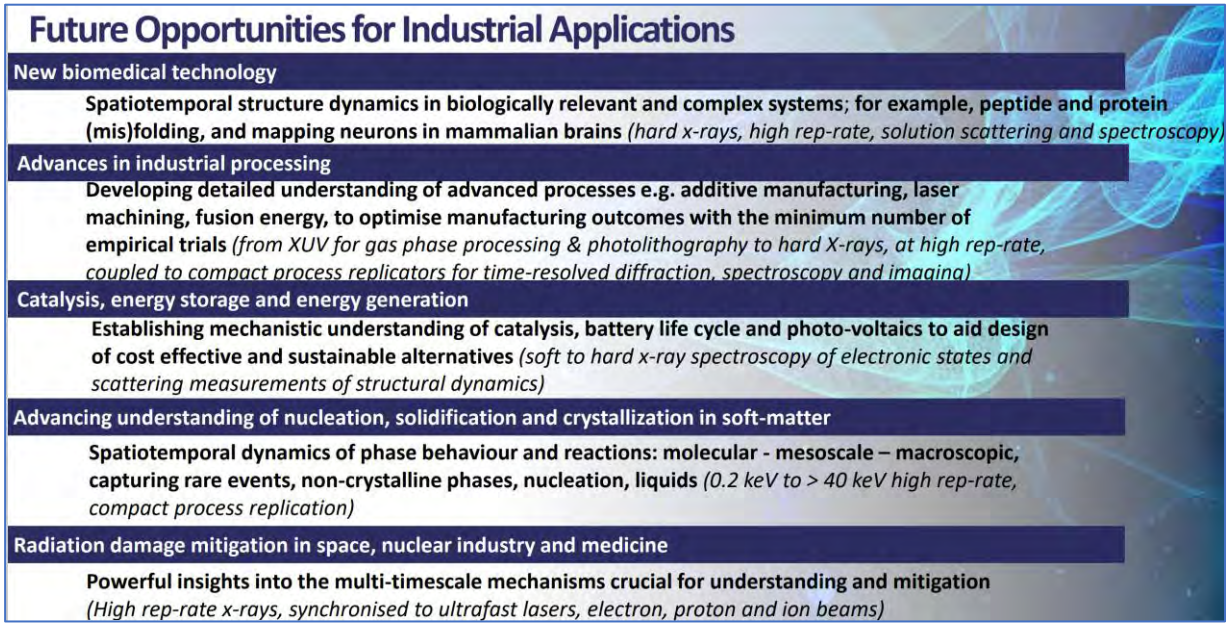
This mapping to key technological sectors was reflected in the themes of the seven Townhall meetings held around the UK in 2023-2025 as part of the UK XFEL CDOA Project. The theme and the meeting locations were:

- **Frontiers of measurement technology – Queen's University Belfast**
- **Materials, chemistry and biology at extreme conditions – University of Strathclyde, Glasgow**
- **AI, quantum computing and fundamental physics – University of Plymouth**
- **Engineering biology and healthcare – Royal Society London**

[4] https://www.gov.uk/government/publications/science-and-technology-framework/science-and-technology-framework

- **Energy, environmental and climate technologies – University of Sheffield**
- **Electronics, photonics and quantum technologies – Henry Royce Institute, Manchester**
- **Advanced materials and manufacturing – University of Cardiff.**

An extended list of XFEL applications is emerging that will impact multiple industrial sectors, and we have examined leading examples of these (full details in **Chapter 8** and summarised in **Section 10.3**). Many other applications are likely to emerge in the coming years. Mindful of this, we have consciously increased our engagement with industry and other end-users of technology through our Townhall meetings and Workshops. Examples of some emerging technological impacts and the key parameters of a next-generation XFEL that they will require are highlighted below:



10.2 Defence technology

In our engagement process, national security and defence were featured in recognition that defence technologies will require use of the best and most advanced measurement methodologies to stay ahead of potential adversaries. This included direct discussions with a number of key agencies and a dedicated Defence Technology Workshop.

A number of Townhall meetings dealt with topics directly relevant to defence technology (**Frontiers of measurement technology, Belfast; Materials, chemistry and biology at extreme conditions, Glasgow; and Advanced materials and manufacturing, Cardiff**). Direct engagements were also made via presentations by Professor Jon Marangos at **Dstl, Porton Down** (2023) and at **AWE** (January 2024).

This engagement culminated in the **Defence Technology Workshop**, held in the CLF Visitors Centre in October 2024. This Workshop was attended by 38 participants from various agencies, including MOD, AWE, Dstl, Qinetiq, Rolls-Royce, SLAC/DOE and the UK XFEL team. The programme (see below) allowed ample time for an open discussion of the needs and issues specific to this community.

Defence Technology Workshop – Programme

	Talk Title	Speaker
09:45	Arrive and Coffee	
10:00	Welcome Opening and Introduction	John Collier
10:05	UK XFEL Overview	UK XFEL Team
10:40	DSTL Related Work and Requirements	Stephen Boyes / Matt Lunt
11:00	AWE High Level Requirements	Andy Comley
11:20	Defence Materials Science Sector (DMSS) at the APS	Matt Cotton
11:40	DST Summary	Stephen Robinson
12:00	Lunch	
13:00	Discussions – Preceded by a talk by Mikael Martinez on LCLS MEC-U	
15:00	Close	

This workshop was held in part to highlight the UK XFEL project and to signal the potential science and technology impacts to the defence technology community; and in part to enable the project to gain a better understanding of the needs and future requirements of that community, to ensure that all the required features were incorporated in the Conceptual Design.

The potential for advances enabled by a next-generation XFEL that were highlighted included:

- **Matter at extreme conditions**
- **Shocked materials**
- **Additive manufacturing**
- **Understanding material damage (both by mechanical and radiation processes)**
- **Supporting the development of new materials**
- **Providing incisive benchmarking of measurement methodologies for application in the field.**

Topics that were discussed regarding future needs included: the need for hard X-ray (> 10 keV) and very hard X-rays (> 40 keV); provision to locate special end-station equipment like gas guns; and special X-ray delivery modes. There is a strong appetite for dynamic wide-field volumetric imaging to be available, which was also found with our industrial engagements. The requirement for high energy and high-power lasers was also emphasised, as these are seen as essential to access high temperature and pressure conditions: again, this requirement is similar to that of the academic MEC community. In the

long term, access to a very high energy laser system (e.g. an Orion successor) was seen as an important aspiration.

Careful consideration will need to be given to security to enable a successful international research facility to sit alongside the requirements of developing sovereign defence capability. In the main it was felt the defence community could work alongside the user community at the facility, but some secure, isolated, infrastructure may ultimately be required for sensitive projects. In terms of operation, it is envisioned that provision will be made for a secure data pipeline (as in the case at EPAC) and dedicated access channels. Nevertheless, it was seen as desirable to have some selected UK academic access to dedicated facilities, as happens at Orion, as the advantages of this to the long-term mission have been demonstrated. In considering non-UK location options, security was seen as significantly more problematic, and probably not viable.

10.3 Industrial engagement

*A next-generation XFEL will be a highly valued tool for multiple industrial sectors. Although industrial users make up a small proportion of overall XFEL usage today, it must be appreciated that XFELs have only been available for a relatively short time, and an industrial applications culture has yet to fully develop. Nevertheless, in **Chapter 8** we present a rich array of industry applications for XFELs spanning diverse sectors and that have the potential to offer major advantages to companies.*

As part of our engagement process, we consulted with a sizeable number of industry-facing academics and industry representatives. These engagements were managed through the Townhall meetings, all of which contained significant applications components, as well as auxiliary online meetings and specialist workshops, most notably the Ion beam interaction (UK nuclear industry via Dalton Nuclear Institute), Catalysis (UK chemical sector via the UK Catalysis Hub), and Defence technology (highlighted above) workshops. We engaged with a significant number of industry sectors, including Engineering and Chemicals (Rolls-Royce, Johnson Matthey, Infineum), Pharma (Nxera, leadXpro, GSK), and Fusion Energy (First Light Fusion), as well as multiple industry-facing organisations, for example, the Institute of Compound Semiconductors, Cardiff and the Henry Royce Institute, Manchester.

From our side, a striking discovery from these engagements was the knowledge that industrial scientists were already thinking about future measurement opportunities with XFELs, which they see as making strategic impacts upon their businesses. It must be anticipated that, as with synchrotrons, the industrial uptake will start to build strongly over the next decade. These opportunities are more fully explored in **Chapter 8**, but here we highlight a few case studies to illustrate the wide interest from industry for significantly more XFEL access.

10.3.1 Catalysis

Around 80% of manufactured products, including fuels, fertilisers, food and drink, cars, mobile phones and medicines, rely upon catalysts for their production. Catalysis research is already a big user of Diamond Light Source, using X-ray spectroscopy to focus in on the atomic sites at which catalytic activity is occurring within a larger molecular complex, and diffraction to observe the accompanying structural changes. The high average brightness and temporal resolution of a next-generation XFEL will enable access to the full temporal range of catalytic mechanisms, from femtoseconds to microseconds, and at realistic concentrations. A dream experiment to resolve mechanisms across the spatial scales relevant to catalytic materials, suggested by Andrew Beale (UCL), would be chemical imaging XRD-CT scans probing atomic structure over mesoscopic scales. A high brightness XFEL would enable this to be measured on timescales of minutes. Other mid-term measurements of great impact, highlighted by Dave Thompsett (Johnson-Matthey), were measurement of the mechanisms at copper centres in metal-doped zeolites to control NOx emissions in lean burn combustion, and understanding oxidation of octahedra (oh) PtNiX/C catalysts in fuel cells under *in operando* conditions with less than millisecond resolution. With accompanying capabilities for *in operando* studies, a wide range of measurements will become possible, with the goal of making catalysis greener and more sustainable by systematically replacing some of the rarer materials currently used with Earth-abundant elements (see **Flagship Programme I** in **Chapter 9)**.

10.3.2 Batteries

Batteries are a critical technology in the green transition, and gains from increased efficiency and options to reduce reliance on a supply of a single element, lithium, are seen as strategically important. Several opportunities that would be transformative with FELs were identified by Rob House (Oxford), including resolving the ultrafast structural dynamics accompanying structural rearrangement under battery operation, identifying intermediate species in the battery operating cycle, determining ion dynamics, and diffusion mechanisms. Louis Piper and Raj Pandya (Warwick) pointed out that the timescales of interest in batteries range from femtoseconds/picoseconds (electron transport), nanoseconds/milliseconds (polaronic transport), redox (milliseconds to minutes), degradation (weeks

to years). To get a picture of the full operation of a battery, over its whole cycle, requires access to all these timescales as well as probing of large-scale analogues of a real battery (see **Flagship Programmes IV** and **V** in **Chapter 9**). With XFELs, all measurements will become much faster (due to brightness) with the unique possibility of focusing on the fastest timescale critical processes.

10.3.3 Fuel additives and lubricants

Fuel additives and lubricants are vital to the mechanical efficiency, energy consumption and lifetime of combustion engines. Even with the green transition, such engines will remain essential to society for decades to come. Peter Dowding (Infineum) pointed out some important potential applications of XFELs in this sector, which included: studies of the dynamics of barrier-crossing in the complex network of reactive nucleation processes (e.g. sulphonate stabilised calcium carbonate nanoparticles used as detergents in engine lubricants) that are vital for the control of product properties; X-ray reflectivity studies of self-assembly dynamics at the interfaces of the polymers used to reduce friction between components; ultrafast dynamical studies of the mechanistic basis of friction modifiers; and understanding the molecular basis of the kinetics of component interactions (e.g. of detergents and dispersants) via time-resolved ultrafast spectroscopy and imaging.

10.3.4 Semiconductors

The smooth supply of semiconductor wafers for chip manufacture is strategically essential for the economy. In the fabrication of semiconductors, full control over the integrity of the process is essential. Peter Smowton (Institute for Compound Semiconductors, Cardiff) and Ian Robinson (UCL/Brookhaven National Laboratory) highlighted that defects are a critical impediment and, for certain classes of defects that may be light or current induced, there is a need to track their formation and transport *in operando* on picosecond/femtosecond timescales. XFELs could play a crucial role here and in resolving the connection between carrier lifetimes and crystal defects in semiconductors. Again, it would be important to have the appropriate end-station instrumentation to do this under *in operando* conditions (see **Flagship Programmes VIII** and **X** in **Chapter 9**). There is also a growing industrial interest in pushing photolithography to shorter (XUV and X-ray) wavelengths and understanding this option through studies with XFELs could be critical for next generation chip manufacture along with consideration of using a high-repetition rate XFEL in fabrication at scale (see **Appendix 2 A2.4.1**).

10.3.5 Engineering materials

The response of engineering materials to shocks and stresses is vital to the engineering industry, as well as to our safety (e.g. the integrity of aeroengines). Advances in understanding this are closely connected to the scientific efforts in MEC with, for instance, the pioneering SAXS/WAXS studies of laser shocked metals resolving void formation and failure at high strain rates by members of our Science Team (e.g. Andrew Higginbotham (York) and David Dye (Imperial)). Residual stress from the manufacturing process is an important factor leading to failure of materials, as was raised by Mike Fitzpatrick (Coventry). Some processes are too fast to be captured by other methods (e.g. neutron scattering) and require access to sub-millisecond timescales only available at an XFEL. Mitigation methods to relieve residual stress include laser shock peening, widely used in aeroengine components, but to understand this requires fast temporal resolution as recently applied at the SACLA XFEL. See **Flagship Programme III** in **Chapter 9**.

10.3.6 Additive manufacturing

Laser additive manufacturing via laser bed fusion is an industrially important method but involves complex processes on multiple spatial and temporal scales. Peter Lee (UCL) pointed out that residual strain and the complexity of the process are large challenges to our understanding of how to improve the product quality. Given that important components of the process take place on sub-microsecond to picosecond timescales, XFELs are a critical technology. Understanding how the laser penetrates the material is a key example of how XFEL-based dynamic imaging can be incisive. Cracking can also arise due to the high thermal gradients and large residual strain can build up in the material. Time-resolved X-ray imaging and diffraction of the cracking mechanism are an excellent opportunity to progress the

issues. Likewise, imaging melting dynamics in laser machining for drilling and cutting is a critical issue that only an XFEL can resolve.

10.3.7 Fusion technology

Both magnetic and inertial confined routes to fusion energy can benefit from the availability of XFEL measurements, as time-resolved X-ray probing of electronic and structural dynamics is a key capability for both understanding and mitigating radiation damage within the first wall materials of the fusion reactor. Further they can, for example, advance understanding of radiation induced quenching of High Temperature Superconducting (HTS) magnets, efficient lithium isotope enrichment strategies, radiation damage in structural materials and coolants, and diffusion of hydrogen isotopes through interfaces, which are all of importance in magnetic confinement technology. This aligns with the **LIBRTI**[5] project within the **Fusion Futures**[6] programme and would support **STEP**[7] by providing probing opportunities of irradiated first wall materials following initial operation. For inertial confinement, the same methodologies used in MEC science, such as XRD and EXAFs, can be used to study dense plasmas. Moreover, dynamic tomographic imaging will provide unique insights into instabilities, vital to understand for ensuring efficient compression. Already there is excellent contrast in images obtained at the European XFEL compared to those obtained at ESRF when looking at shocks, and only XFELs can reach the multiple frames per few nanoseconds that are required to completely characterise a compression. A dedicated beamline is being planned at the European XFEL for fusion technology, signposting that XFELs are becoming an essential component in ongoing developments. See **Flagship Programmes II, VI** and **VII** in **Chapter 9**.

10.3.8 Biotechnology and Engineering Biology

The Townhall meeting at the Royal Society in London (29 – 30 July 2024) explored the multiple impacts of structural dynamics mechanisms to understanding the essential processes of life, with implications for biotechnology. The meeting had 143 registered in-person participants and 29 on-line. It had partial financial support from UKRI STFC, UKRI BBSRC, the International Science Partnerships Fund (ISPF) and the INEOS Oxford Institute for antimicrobial research (IOI). The presentations included three keynote talks by Ilme Schlichting, Richard Neutze and Sir David Stuart, with some concluding remarks by James Naismith. Other presentations included one by Vadim Cherezov (University of Southern California), who stressed the importance of G protein-coupled receptors (GPCRs) in cell membranes in the development of many drugs and he demonstrated the structural solutions of melatonin receptors, MT1 and MT2, that were solved via the power of the XFEL-based serial nano-crystallography approach. Michael Henning (leadXpro) and Tian Geng (Nxera Pharma) explained the importance – in their view – of XFELs to the pharma industry for structure-based drug discovery, with the potential importance of structural dynamics studies also highlighted. They both advocated for more access to XFELs for the Pharma industry. See **Flagship Programme XI** in **Chapter 9.**

5 LIBRTI | UKAEA Fusion Energy

6 Fusion Futures | UKAEA Fusion Energy

7 STEP | UKAEA Fusion Energy

10.4 Synergies with other national facilities and capability: Synergistic technology transfer among XFELs, neutrons, synchrotrons, and electron microscopy/diffraction

No single method can solve all scientific problems, so it is essential that a next-generation XFEL is fully integrated into the wider UK science infrastructure. In the physical sciences, methods to probe the chemistry and physics of matter will impact new technologies, advanced manufacturing, industrial processes and energy technology. In the life sciences, several complementary methods exploiting X-rays and electrons will yield atomic level structural and functional insights with increasing temporal resolution, which can be applied to individual macromolecules through to whole cells and tissues. By enhancing critical interactions and cooperation between a next-generation XFEL and, for example, Diamond-II, ISIS, the Central Laser Facility, and the electron imaging centres for physical (ePSIC) and life sciences (eBIC), there will be a large multiplying impact upon the science and upon each facility, as synergistic technologies are developed and shared between them.

10.4.1 Fostering relationships with other institutes and facilities

A next-generation XFEL will not 'operate in a vacuum' but rather will leverage the significant opportunities for in-depth cooperation with many national facilities and research organisations. For example, cooperation is envisaged with the Diamond Light Source upgrade (Diamond-II), ISIS Neutron and Muon Source, the Electron Physical Science Imaging Centre (ePSIC), the Electron Bio-Imaging Centre (eBIC), the Central Laser Facility (CLF), the Rosalind Franklin Institute (RFI), the Francis Crick Institute, the Henry Royce Institute and the wider university sector. The diverse set of capabilities and expertise available at these facilities and organisations together enable a large cross-section of the science community to carry out advanced research, thereby creating a powerful research and development ecosystem. Moreover, the opportunities they offer guarantee that even the most ambitious science that people may wish to undertake in the future can be tackled by the UK.

The **STFC's CLF** carries out research using lasers to investigate a broad range of science areas, spanning physics, chemistry and biology. It provides a broad spectrum of laser facilities, from high intensity laser systems to ultrafast sources and laser microscopy techniques. The CLF instruments are enabling capabilities that underpin time-resolved spectroscopy and structural biology with pump-probe strategies, computational plasma physics to target micro-fabrication, and laser tweezers. Some of these efforts already include close cooperation with Diamond Light Source to enable time-resolved dynamic structural biology and spectroscopic studies. Artemis, one of the CLF's facilities, is a leading ultrafast XUV research facility, based upon high harmonic generation with a strong programme on time-resolved ARPES and CDI, and will be strongly connected to part of the science mission of a next-generation XFEL. Indeed, pump-probe optical laser-based capabilities are also common and critical at all XFEL facilities around the world. The world-leading expertise in ultrafast lasers available at the CLF will be an essential asset for a next-generation XFEL facility, as will the synergistic R&D being carried out for the CLF's EPAC project[8].

In early 2020, and within the framework of the Helmholtz International Beamline for Extreme Fields (HiBEF) user consortium, STFC and the CLF delivered a 10 Hz repetition rate, high-energy laser, D100-X, to the High-Energy Density (HED) instrument at the European XFEL. The experimental set-up at the HED instrument enables scientists to generate and study extreme temperatures and pressures in materials that are similar to the interior of exoplanets, with temperatures of up to 10,000°C, and pressures of up to 10,000 tons per square centimetre. Without question, the UK XFEL project will include very close interactions with the CLF, as reflected in the plans here to incorporate the DiPOLE technology into the proposed end-stations.

[8] https://www.clf.stfc.ac.uk/Pages/EPAC-introduction-page.aspx

The **RFI (Rosalind Franklin Institute)** is a national institute, funded by the UK government through UK Research and Innovation (UKRI), dedicated to bringing about transformative changes in life science through interdisciplinary research and technology development. It brings together academia and industry to solve the most pressing problems in the life sciences (Industrial Biotechnology, Pharmaceutical, Agrichemical). The RFI has a Hub at Harwell and currently ten university partners (Spokes). The RFI has five interlinked scientific themes: structural biology, next generation chemistry, imaging with sound and light, mass spectrometry and next-generation electron microscopy. The new building for the RFI is on the Harwell Campus and is already interacting with Diamond Light Source, the CLF, and the Research Complex at Harwell (RCaH). There is every expectation that it will also interact with the next-generation XFEL project, especially within the structural biology and next-generation chemistry thrusts.

Diamond-II is a coordinated programme, funded by the UK government and the Wellcome Trust, for a major machine upgrade [1,2]. In April 2020, the project cleared CD1 status, the technical designs were completed in August 2022, and in July 2023 approval was received for the project and the start of funding (£519.4M total cost). In August 2025 the Diamond Extension Building was completed: here, much of the girder assembly for the new, six bend achromat lattice will take place. The 'dark period' will run from December 2027 through to June 2029 for Diamond-II installation, with commissioning starting in December 2028. The first phase of beamlines operations will begin in September 2029, with the first users at the flagship beamlines in January 2030. Diamond-II will be a diffraction limited, fourth-generation synchrotron source based upon a novel multibend-achromat (MBA) storage ring lattice and electron beam accelerator operating at 3.5 GeV to provide dramatic gains in photon brightness (especially at high energy) and coherence. The project includes complementary improvements to optics, detectors, sample delivery, and computing, as well as integrated and correlative methods. As a result, Diamond-II will be transformative in speed and resolution, and will offer scientists streamlined access to enhanced instruments for life and physical sciences. Diamond-II will enable a wide range of science at its > 34 beamlines as well as a suite of complementary facilities – eBIC[3], ePSIC, HeXI (a MeV electron diffraction instrument), the MPL (Membrane Protein Lab)[4], the XChem Fragment Screening service [5–10] and the XFEL Hub at Diamond [11,12], which develops technology for sample delivery and data analysis for XFELs for life sciences. In addition, the world-recognised strengths of the collaborative computing projects (CCP4[13], CCPN[14] and CCPEM [15,16]) in structural biology based at the RCaH and the Diamond structural biology software groups, provide an excellent environment for future software developments. More information about these opportunities is detailed in **Appendix 1**.

HeXI at Diamond was funded through the Wellcome Trust's "Electrifying Life Science" grant. This grant aimed to support the development of electron imaging physical sciences technologies with the capacity to revolutionise how we see life, and included an electron diffraction instrument to investigate the use of mega-electron volt (MeV) electrons in macromolecular structure determination. Higher acceleration energies will enable the benefits of electrons for interrogating charged states to be exploited for XFEL-scale crystals, hence offering excellent complementarity to state-of-the-art light source beamlines and XFELs. Instrument construction and commissioning will be completed in 2027 and will be available to users during the Diamond 'dark period'.

ISIS Neutron and Muon Source at the STFC Rutherford Appleton Laboratory on the Harwell Campus produces beams of neutrons and muons that allow scientists to study materials at the atomic level using neutron diffraction, neutron imaging, and neutron and muon spectroscopy. With multiple instruments each individually optimised for the study of different types of matter, this provides the UK with a leading capability to understand the structure of matter. Neutron and muon experiments are non-destructive and provide results that cannot be achieved by other techniques. There is a large national and international community of more than 2000 scientists who use neutrons and muons for research in physics, chemistry, materials science, geology, engineering, and biology. The complementarity with the structural dynamics capabilities of a next-generation XFEL is clear. Combining the capabilities of ISIS, Diamond-II, the CLF and a next-generation XFEL will enable scientists to study all aspects of the structure, structural dynamics and electronic dynamics of matter.

ePSIC and **eBIC** are national user facilities operated by Diamond Light Source to provide access to state-of-the-art transmission electron microscopes for the physical and life sciences. ePSIC is equipped with two aberration corrected microscopes for studying materials at the atomic scale. eBIC already offers high-end Titan Krios instruments equipped with direct electron detectors and automated data collection software for single particle cryo-electron microscopy. eBIC also supports molecular cryo-electron tomography, cellular cryo-electron tomography, focused ion beam milling and imaging, and will soon offer electron crystallography. More information with respect to the synergistic relationships between XFEL, cryo-EM, and eBIC is detailed in **Appendix 1**.

As of April 2026, the ultrafast electron diffraction (UED) component of the **RUEDI** – Relativistic Ultrafast Electron Diffraction and Imaging – proposal is still under development at the STFC Daresbury Laboratory in collaboration with the University of Liverpool and a network of national partners. It is hoped to deliver the ultrafast electron diffraction platform (UED) via a compact relativistic electron beam technology, and to offer access to users via EPSRC funding. An ultrafast electron microscope (UEM) is also being contemplated that will enable electron imaging of assemblies (e.g. tissue, complex materials, devices) undergoing dynamics to a temporal resolution of picoseconds, whereas the UED will permit ultrafast electron diffraction of matter with the ability to resolve structural dynamics to ~<100 fs temporal resolution. Thus, this instrumentation will serve a growing need in UK science and technology for dynamical studies of matter. It will be available in early 2030 and will help to boost the structural dynamics community in readiness for a next-generation XFEL. More detail is given in **Appendix 1**, where the synergies between an XFEL and UED are further explored.

10.4.2 Examples of synergistic efforts in structural biology

Structural biology is experiencing parallel step-changes in X-ray crystallography, AI approaches and cryo-EM methods [17–23]. The former is related to XFELs and emerging opportunities in SFX, time-resolved SFX, and time-resolved single particle imaging.

The 2024 Nobel Prize in Chemistry was awarded to Hassibis and Jumper (Google Deep Mind, London) “for protein structure prediction” and Baker (University of Washington) “for computational protein design,” underlining how AI and computational approaches are revolutionising structural biology. The AlphaFold AI protein structure prediction system is built upon data from around 200,000 experimental protein structures already deposited in the protein database. An interesting question is how much dynamical structure from XFELs, and other measurement methods, will be needed before AI predictions of new drug complexes and/or protein structural dynamics become feasible.[24–27]

The impact of CryoEM was highlighted by the 2017 Nobel Prize in Chemistry, which was awarded to Dubochet, Frank and Henderson for “developing cryo-electron microscopy (cryo-EM) for the high-resolution structure determination of biomolecules in solution” [28,29]. Because methods and microscopes are improving rapidly [30–32], and national centres supporting the high-end instruments are more common, more high-resolution structures of smaller macromolecules are being released annually such that the method is approaching similar productivity numbers as X-ray crystallography (**Figure 10-1**). Facilities like eBIC at Diamond provide scientists with state-of-the-art experimental equipment and expertise, for both single particle analysis and cryo-tomography[33–36]. This is part of the UK infrastructure that overall fields more than 20 high-end microscopes. Similarly, three US NIH-funded national electron microscopy centres are operational in New York, Oregon and California. There are also analogous initiatives in many European countries and Asia.

There is, however, still room to improve cryo-EM technologies especially with respect to the quantum efficiency of detectors, recovering all of the high-resolution signal in the presence of various types of noise, selection of the appropriate electron energy, sample preparations methods and data analysis algorithms. Improvements in all these areas will bring the method closer to its theoretical limits. Together, MX, cryo-EM and X-ray and electron tomography have the potential over the coming decade(s) to provide the necessary tools to establish the structural basis of nearly every functional aspect from any type of cell.

Indeed, with such large global effort and many important biological targets (see also **Table 7.1**), progress across all of biology has been profound and will continue with increasing pace[37]. This is reflected in the recent trend in PDB statistics (**Figure 10.1**) indicating that the ratio of newly released atomic models determined X-ray crystallography to cryo-EM is likely to reach parity very soon. Between 01 June 2024 and 01 June 2025, the wwPDB released 9,490 atomic models based upon X-ray diffraction data (58.5% of new experimental models), which were linked to many publications, including *Science* (19 publications linking to 48 atomic models), *Nature* (9 publications linking to 105 atomic models), and *Cell* (24 publications linking to 40 atomic models). For comparison, across the same time period the wwPDB released 6,410 atomic models based upon cryo-EM data (39.5% of new experimental models), which were linked to publications in *Science* (45 publications linking to 181 atomic models), *Nature* (100 publications linking to 471 atomic models), and *Cell* (52 publications linking to 235 atomic models), as well as other high-profile journals. These new X-ray crystallography atomic models had an average resolution of 2.04 Å and 20% of these datasets extended to atomic resolution or better as defined by the typical C-C bond distance of 1.54 Å. The resolution of the cryo-EM atomic models is steadily improving, and the newly released atomic models had an average resolution of 3.33 Å. Moreover, average size proteins (46 kilo dalton (kDa))[38] and smaller have been a problem for single particle cryo-EM structure determination. However, conjugating small proteins with Llama nanobodies increases the molecular weight and introduces symmetry such that structural analysis of average and smaller proteins becomes tenable. This was recently demonstrated for maltose binding protein (42 kDa, 2.45 Å resolution) and lysozyme (15 kDa, 3.1 Å resolution).[39,40]

Although cryo-EM does not require a crystal lattice, the data is collected under cryo-conditions that are far from physiological and do not allow for dynamic conformational changes. However, freeze-quench methods are being developed to enable time-resolved cryo-EM with about millisecond time resolution.[25,41–49] In addition, temperature jump methods that use a “laser melting and revitrification process” enable time-resolved cryo-EM results with microsecond temporal resolution.[50,51] This complements the sub-microsecond to femtosecond temporal resolution potential of XFELs under near physiological conditions.

Sample preparation and delivery are unmet challenges in both serial MX and cryo-EM methods. This offers significant opportunities for technology transfer between the fields.[44] They each must manipulate on-demand nano- to picolitre volumes of either macromolecules in solutions or as a slurry of micro-crystals.[52–56] Freeze-quench methods in cryo-EM will likely be limited to about 100s µs to the millisecond time range because of constraints linked to sample grid preparation; however, this is an active area of R&D. High-quality SFX and time-resolved SFX data collected at XFEL facilities already approach fs time resolution for light-triggered reactions. For mixing strategies, it is likely that enzyme reactions will be studied from 100s of µs through seconds. With more XFEL facilities, some running with MHz repetition rates, scientists will be able to significantly improve the correlations between the electronic and atomic structures, even potentially on a crystal-by-crystal basis.

Scientists working at the forefront of biology will use many of the tools available to them in an increasingly integrative approach (**Figure 7.2**). For structural biology, some frontier challenges for synchrotrons, XFELs and cryo-EM / electron diffraction (ED) are summarised in **Table 10.1.** Several areas of common synergistic overlap are identified in **Chapter 7** and **Appendix 1**. Consequently, R&D effort in one area is very likely to be transferred rapidly to other areas.

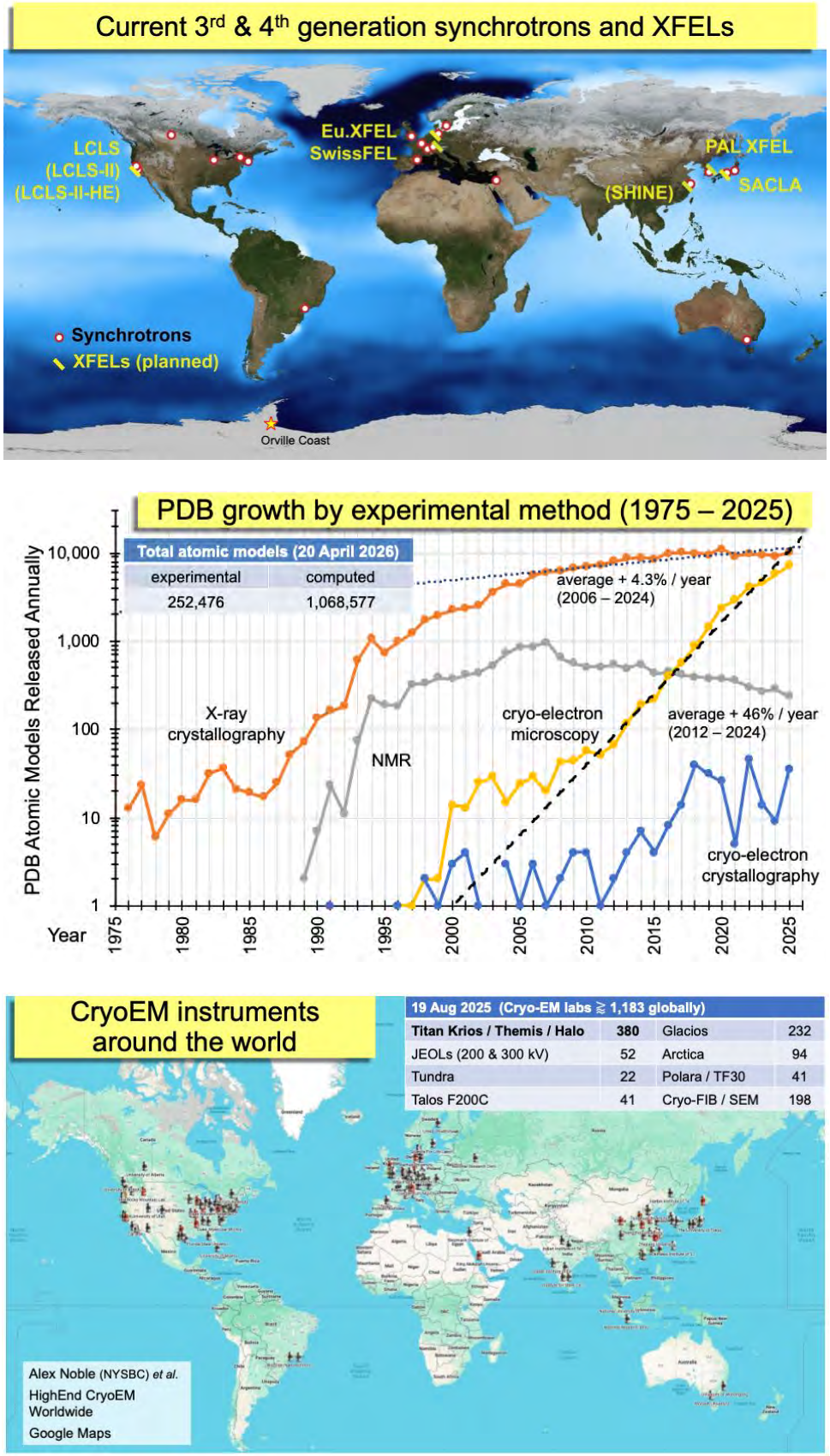


Figure 10.1: ***Growth of the PDB archive from X-ray and cryo-EM methods*** *(compiled April 2026)*

(Top) In 2025 there are currently 22 modern synchrotrons and 5 + 1 hard X-ray XFELs distributed around the world. (Middle) The growth of the Protein Data Bank as a function of experimental method reveals that X-ray crystallography and cryo-EM are the major contributors of new data. (Bottom) More than 390 high-end cryo-EM instruments serve more than 1200 labs around the world.

Table 10.1: Frontier challenges in structural biology and some approaches for progress

Goal	Synchrotrons	XFELs	cryo-EM & ED
To determine time-resolved structures directly from systems engaged in catalysis at physiological temperature and pressure	• RT serial µ-crystal methods • focused µ-beams • µs – ms datasets to dose limits • kinetics within µ-crystals correlated w/ spectroscopy	• on-demand sample delivery methods • mixing injectors • kinetics within n – µ-crystals correlated w/ spectroscopy • SFX processing pipelines	• automated, time-resolved sample grid preparation • high resolution from smaller targets • RT serial & time-resolved ED
To determine structures from single molecules in native-like conditions (in solution or membranes, in pure complexes)	• continuous diffractive imaging from n – µ-crystals with coherent sources	• single particle imaging & sample delivery methods • continuous diffractive imaging	• imaging processing & better detectors • low-energy electron holography
To understand structure / function / dynamics in native context	• X-ray microscopy with correlated imaging of metals and/or labels • X-ray tomography of relatively thick specimens	• *In situ* SFX of n – µ-crystals • Imaging processing • Coherent X-ray imaging	• liquid / whole cells • high resolution microscopy • *in situ* cryo-electron tomography of FIB milled samples

Exciting future challenges lie in the ability to observe dynamic enzymes and macromolecular complexes at high spatial and temporal resolution, both in purified/reconstituted forms and *in situ/in vivo*, and the ability to correlate these dynamics with physiological changes from the cell to the tissue and organism. There are clear opportunities to exploit the synergies between all of the current structural biology techniques including, but not limited to:

- synchrotron- and XFEL-based MX including serial methods
- XFEL based SFX for structural dynamics
- cryo-EM single particle techniques
- cryo-electron tomography
- X-ray tomography with synchrotrons and XFELs
- serial and time-resolved electron diffraction from sub-micron macromolecular crystals
- NMR
- other spectroscopic methods.

10.5 International engagement and partnerships

XFEL research benefits from international collaborations and partnerships, as they offer access to diverse expertise, resources, and perspectives that can significantly enhance research quality and impact. The UK XFEL CDOA project has actively engaged with the international community to gain input to this Science and Technology Case and to the Conceptual Design itself. It is also likely that new international partnerships will be formed in developing a path to a next-generation XFEL.

XFEL research is intrinsically built around international collaborations. In part, this is due to there currently being only a handful of facilities around the world and so, for instance, UK users must always travel overseas. In addition, the complexity of XFEL research requires multiple types of expertise, for example in sample preparation, detection systems, lasers, simulation, data analysis and so on, which has, up until now, demanded large, multi-institutional teams, often spanning several countries as well as the XFEL host country. As XFEL research matures, and the relative proportion of 'standard' measurements grows, it is anticipated that smaller teams will become the norm. Although this may reduce the need for international collaboration, it is likely to remain at the level seen at other major international facilities (synchrotron, neutron source, high-power laser). XFEL research will continue to be an activity that benefits from international collaborations and partnerships, and that will naturally serve as a catalyst for growing and exploring new collaborations.

The international aspect of XFEL use is strongly reflected in the national usage charts for LCLS (USA) and the European XFEL (Germany) (**Figure 10.2**), which show the percentages of users from non-host countries.

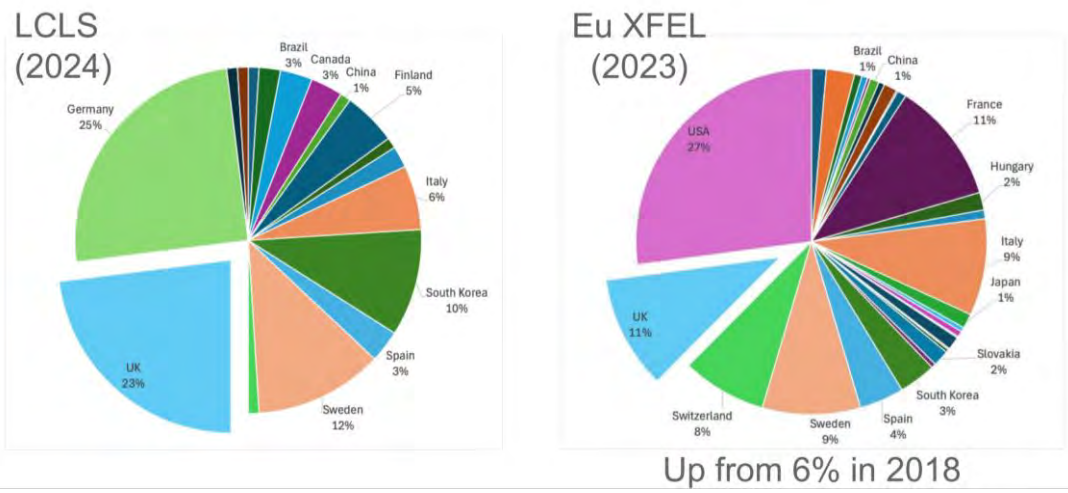


Figure 10.2: Users of LCLS and the European XFEL

Notably it can be seen that, other than the two respective host nations, the UK accounts for the highest number of users at both facilities (i.e. aside from the USA and Germany who each host one of the facilities). The two host nations have a strong track record of using each other's facilities, underscoring how the presence of an XFEL facility in their countries has energised their national scientific communities. That the UK has such a high usage illustrates the increasing appetite for using XFELs in research. The proportion of UK users for the European XFEL has almost doubled since 2018 and appears to be continuing to grow. UK users are also very active at FERMI (Italy), SACLA (Japan), PAL (Korea) and SwissFEL (Switzerland).

UK users have been especially active in advancing some key areas of XFEL research: matter at extreme conditions, chemical dynamics, phase changes in correlated materials, SFX and structural dynamics of proteins, attosecond science, gas phase molecular scattering, applications of scattering and imaging to materials dynamics, and chemical physics. This is evidenced by UK groups playing leading roles in

strategic developments, for example at European XFEL, in the HIBEF early science programme, UK users led work on hard X-ray total scattering and pair distribution function measurements, and in the axion search experiment. The Life Sciences XFEL hub has played a lead role in developing sample delivery and mixing strategies for dynamic structural biology being applied at multiple XFELs. Moreover, UK scientists are now involved in multiple scientific and leadership roles at many XFEL facilities (e.g. Mike Dunne, former Director of LCLS).

The UK XFEL CDOA project has actively engaged with the international community and many contributions to the updated Science and Technology Case have been informed by discussions with international partners. When we conducted the Community Engagements during 2023 and 2025, we were mindful of the need to engage international, as well as national, expertise. Indeed, of the 95 speakers at our seven Townhall meetings, 43 came from overseas institutions. This strong international involvement is indicative of the fact that UK users of XFELs have been building strong partnerships across many scientific disciplines with existing international facilities and their networks of users.

In addition, the UK XFEL CDOA project has engaged directly with international XFEL facilities. The depth and breadth of engagement with the European XFEL and LCLS has been especially notable, and includes facility visits, technical collaborations and ongoing strategic discussions with the senior leaderships of these facilities. This level of engagement reflects the fact that an investment at one or both of these facilities is seen as a core option for providing UK access to a next-generation XFEL. The project team also paid an onsite visit to Swiss FEL, and conducted in depth online discussions with key staff from SACLA and PAL. Informal facility visits were made to other facilities including FERMI (Trieste, Italy), FLASH (Hamburg, Germany), SHINE (Shanghai, China), and the new Sirius fourth generation synchrotron (Campinas, Brazil), helping to extend the reach of our engagement and build potential partnerships. Additional contacts were made through workshops and visits with India, Denmark and Slovakia, regarding joint activities.

The UK is, of course, a shareholder in the European XFEL, along with Germany, France, Denmark, Sweden, Switzerland, Spain, Slovakia, Poland, Hungary, Italy and Russia (Russia is not currently permitted research access) and so the UK has direct influence over future strategy developments, as well as operations. For the other XFELs, whilst the UK community is very active as users, and punches above its weight in terms of memberships of Proposal Prioritisation Panels and Science and Technical Advisory Committees, it has no formal role in shaping their future directions. As things currently stand, only SHINE (China) and LCLS (USA) (through LCLS II and the putative LCLS X) have ambitions for a high repetition rate multiplexed superconducting machine serving multiple users simultaneously, although the high duty cycle modes currently being analysed for the European XFEL may partially allow this.

Looking ahead to a next-generation XFEL located in the UK (or with a strong UK contribution but constructed elsewhere), a significant number of potential partners might be willing to provide technical, in-kind and financial contributions to construction and operation.

In addition to the current European XFEL shareholders, and the host countries of superconducting machines (USA, Germany and China), with whom future additional partnerships are likely, further partnerships may come from a range of countries with economies of significant size and a commitment to science and technology. Based on World Bank data on GDP, it is possible to rank the first 20 such countries in order of GDP (highest to lowest): Japan, India, Brazil, Canada, Mexico, Australia, South Korea, Indonesia, Netherlands, Turkey, Saudi Arabia, Argentina, Belgium, Ireland, Thailand, UAE, Israel, Austria, Singapore, and Norway.

The UK already has a strong history of scientific collaborations and deep partnerships with many of these nations. Developing a next-generation XFEL would deepen existing relationships and build new ones for the UK with the international science and technology community.

10.6 References for Chapter 10

1 L.C. Chapon, I. Boscaro-Clarke, A.J. Dent, A. Harrison, M. Launchbury, D.I. Stuart, R.P. Walker, (2019) "Diamond-II — Conceptual Design Report," https://www.diamond.ac.uk/dam/jcr:ec67b7e1-fb91-4a65-b1ce-f646490b564d/Diamond-II%20Conceptual%20Design%20Report.pdf

2 I. Boscaro-Clarke, L.C. Chapon, A.J. Dent, S. Dhesi, S. Diaz-Moreno, G. Evans, H. Wilhelm, *et al*. (2019) "Diamond-II — Advancing Science," https://www.diamond.ac.uk/dam/jcr:2ddff8c5-80fe-43aa-8a00-321be9c02cc6/Diamond%20II%20Science%20Interactive%20_%20Dec%202019%20Update.pdf

3 D.K. Clare, C.A. Siebert, C. Hecksel, C. Hagen, V. Mordhorst, M. Grange, P. Zhang *et al.* "Electron Bio-Imaging Centre (eBIC): the UK national research facility for biological electron microscopy," *Acta Crystallogr D Struct Biol* **73**, 488-495 (2017) DOI: 10.1107/S2059798317007756

4 Moraes, G. Evans, J. Sanchez-Weatherby, S. Newstead, P.D. Stewart (2014) "Membrane protein structure determination - the next generation," *Biochim Biophys Acta* **1838**, 78-87 DOI: 10.1016/j.bbamem.2013.07.010

5 S.E. Thomas, P. Collins, R.H. James, V. Mendes, S. Charoensutthivarakul, C. Radoux, T.L. Blundell *et al*. "Structure-guided fragment-based drug discovery at the synchrotron: screening binding sites and correlations with hotspot mapping," *Philos Trans A Math Phys Eng Sci* **377**, 20180422 (2019) DOI: 10.1098/rsta.2018.0422

6 P.M. Collins, A. Douangamath, R. Talon, A. Dias, J. Brandao-Neto, T. Krojer, F. von Delft, "Achieving a Good Crystal System for Crystallographic X-Ray Fragment Screening," *Methods Enzymol* **610**, 251-264 (2018) DOI: 10.1016/bs.mie.2018.09.027

7 D. Bowkett, R. Talon, C. Tallant, C. Schofield, F. von Delft, S. Knapp, P.E. Brennan, *et al*. "Identifying Small-Molecule Binding Sites for Epigenetic Proteins at Domain-Domain Interfaces," *ChemMedChem* **13**, 1051-1057 (2018) DOI: 10.1002/cmdc.201800030

8 N.M. Pearce, T. Krojer, A.R. Bradley, P. Collins, R.P. Nowak, R. Talon, F. von Delft *et al*. "A multi-crystal method for extracting obscured crystallographic states from conventionally uninterpretable electron density," *Nat Commun* **8**, 15123 (2017) DOI: 10.1038/ncomms15123

9 N.M. Pearce, A.R. Bradley, T. Krojer, B.D. Marsden, C. M. Deane, F. von Delft, "Partial-occupancy binders identified by the Pan-Dataset Density Analysis method offer new chemical opportunities and reveal cryptic binding sites," *Struct Dyn* **4**, 032104 (2017) DOI: 10.1063/1.4974176

10 T. Krojer, R. Talon, N. Pearce, P. Collins, A. Douangamath, J. Brandao-Neto, F. von Delft *et al*. "The XChemExplorer graphical workflow tool for routine or large-scale protein-ligand structure determination," *Acta Crystallogr D Struct Biol* **73**, 267-278 (2017) DOI: 10.1107/S2059798316020234

11 J.M. Grimes, D.R. Hall, A.W. Ashton, G. Evans, R.L. Owen, A. Wagner, *et al*. "Where is crystallography going?," *Acta Crystallogr D Struct Biol* **74**, 152-166 (2018) DOI: 10.1107/S2059798317016709

12 A.M. Orville, "The XFEL Hub at Diamond: A Bridge between Structural Biologists and Facilities," *Synchrotron Radiation News* **30**, 37-39 (2017) DOI: 10.1080/08940886.2017.1387000

13 M.D. Winn, C.C. Ballard, K.D. Cowtan *et al*. "Overview of the CCP4 suite and current developments," *Acta Crystallogr D Biol Crystallogr* **67**, 235-242 (2011) DOI: 10.1107/S0907444910045749

14 S.P. Skinner, R.H. Fogh, W. Boucher *et al.* "CcpNmr AnalysisAssign: a flexible platform for integrated NMR analysis," *J Biomol NMR* **66**, 111-124 (2016) DOI: 10.1007/s10858-016-0060-y

15 T. Burnley, C.M. Palmer, M. Winn, "Recent developments in the CCP-EM software suite," *Acta Crystallogr D Struct Biol* **73**, 469-477 (2017) DOI: 10.1107/S2059798317007859

16 C. Wood, T. Burnley, A. Patwardhan, S. Scheres, M. Topf, A. Roseman, M. Winn, "Collaborative computational project for electron cryo-microscopy," *Acta Crystallogr D Biol Crystallogr* **71**, 123-126 (2015)DOI: 10.1107/S1399004714018070

17 I. Schlichting, "Serial femtosecond crystallography: the first five years," *IUCrJ* **2**, 246-255 (2015) DOI: 10.1107/S205225251402702X

18 P. Fromme, "XFELs open a new era in structural chemical biology," *Nat Chem Biol* **11**, 895-899 (2015) DOI: 10.1038/nchembio.1968

19 J.C.H. Spence, "XFELs for structure and dynamics in biology," *IUCrJ* **4**, 322-339 (2017) DOI: 10.1107/S2052252517005760

20 R. Fernandez-Leiro, S.H. Scheres, "Unravelling biological macromolecules with cryo-electron microscopy," *Nature* **537**, 339-346 (2016) DOI: 10.1038/nature19948

21 D. Elmlund, H. Elmlund, "Cryogenic electron microscopy and single-particle analysis," *Annu Rev Biochem* **84**, 499-517 (2015) DOI: 10.1146/annurev-biochem-060614-034226

22 Y. Cheng, N. Grigorieff, P.A. Penczek, T. Walz, "A primer to single-particle cryo-electron microscopy," *Cell* **161**, 438-449 (2015) DOI: 10.1016/j.cell.2015.03.050

23 R.M. Glaeser, "How Good Can Single-Particle Cryo-EM Become? What Remains Before It Approaches Its Physical Limits?," *Annu Rev Biophys* **48**, 45-61 (2019) DOI: 10.1146/annurev-biophys-070317-032828

24 S.K. Burley, "Protein data bank: From two epidemics to the global pandemic to mRNA vaccines and Paxlovid." *Curr Opin Struct Biol* **90**, 102954 (2025) DOI: 10.1016/j.sbi.2024.102954

25 Y. Mao, "Dynamics-based drug discovery by time-resolved cryo-EM." *Curr Opin Struct Biol* **91**, 103001 (2025) DOI: 10.1016/j.sbi.2025.103001

[26] A. King, "Four ways to power-up AI for drug discovery." *Nature* (2025) DOI: 10.1038/d41586-025-00602-5

[27] K. Zhang *et al.* "Artificial intelligence in drug development." *Nat Med* **31**, 45-59 (2025) DOI: 10.1038/s41591-024-03434-4

[28] P.S. Shen, "The 2017 Nobel Prize in Chemistry: cryo-EM comes of age," *Anal Bioanal Chem* **410**, 2053-2057 (2018) DOI: 10.1007/s00216-018-0899-8

[29] Nobelprize.org. The 2017 Nobel Prize in Chemistry - Press Release, Nobel Media AB 2014, (2017) https://www.nobelprize.org/nobel_prizes/chemistry/laureates/2017/

[30] S. Subramaniam, "The cryo-EM revolution: fueling the next phase," *IUCrJ* **6**, 1-2 (2019) DOI: 10.1107/S2052252519000277

[31] S.P. Muench, S.V. Antonyuk, S.S. Hasnain, "The expanding toolkit for structural biology: synchrotrons, X-ray lasers and cryoEM," *IUCrJ* **6**, 167-177 (2019) DOI: 10.1107/S2052252519002422

[32] A. Ourmazd, "Cryo-EM, XFELs and the structure conundrum in structural biology," *Nat Methods* **16**, 941-944 (2019) DOI: 10.1038/s41592-019-0587-4

[33] A. Horstmann, A. *et al.* A service-based approach to cryoEM facility processing pipelines at eBIC. *Acta Crystallogr D Struct Biol* **80**, 174-180, doi:10.1107/S2059798324000986 (2024).

[34] D.K. Clare *et al.* "Electron Bio-Imaging Centre (eBIC): the UK national research facility for biological electron microscopy." *Acta Cryst. D Struct Biol* **73**, 488-495 (2017) DOI: 10.1107/S2059798317007756

[35] P. Majumder and P. Zhang, "In situ cryo-electron microscopy and tomography of cellular and organismal samples." *Curr Opin Struct Biol* **93**, 103076 (2025) DOI: 10.1016/j.sbi.2025.103076

[36] P.N.M. Shah, R. Sanchez-Garcia and D.I. Stuart, "TomoCPT: a generalizable model for 3D particle detection and localization in cryo-electron tomograms." *Acta Cryst. D Struct Biol* **81**, 63-76 (2025) DOI: 10.1107/S2059798325000865

[37] E. Callaway, "Revolutionary cryo-EM is taking over structural biology," *Nature* **578**, 201 (2020) DOI: 10.1038/d41586-020-00341-9

[38] R. Milo, P. Jorgensen, U. Moran, G. Weber and M. Springer, "BioNumbers--the database of key numbers in molecular and cell biology." *Nucleic Acids Res* **38**, D750-753 (2010) DOI: 10.1093/nar/gkp889

[39] G. Yi, D. Mamalis, M. Ye *et al.* "Covalently constrained 'Di-Gembodies' enable parallel structure solutions by cryo-EM." *Nat Chem Biol (2025)* DOI: 10.1038/s41589-025-01972-7

[40] M.S.A. Gilman and M.A. Skiba, "Hidden gems bring proteins into view." *Nat Chem Biol (2025)* DOI: 10.1038/s41589-025-01959-4

[41] S. Kaledhonkar, Z. Fu, H. White, J. Frank, "Time-Resolved Cryo-electron Microscopy Using a Microfluidic Chip," *Methods Mol Biol* **1764**, 59-71 (2018) DOI: 10.1007/978-1-4939-7759-8_1

[42] J. Frank, "Time-resolved cryo-electron microscopy: Recent progress," *J Struct Biol* **200**, 303-306 (2017) DOI: 10.1016/j.jsb.2017.06.005

[43] D. Kontziampasis, D.P. Klebl, M.G. Iadanza, S.P. Muench *et al*. "A cryo-EM grid preparation device for time-resolved structural studies," *IUCrJ* **6**(Pt 6):1024-1031 (2019) DOI: 10.1107/S2052252519011345

[44] A. Banari, A.K. Samanta, A. Munke *et al.* "Advancing time-resolved structural biology: latest strategies in cryo-EM and X-ray crystallography." *Nat Methods* **22**, 1420–1435 (2025) DOI: 10.1038/s41592-025-02659-6

[45] M.M. Papasergi-Scott, G. Pérez-Hernández, H. Batebi *et al.* "Time-resolved cryo-EM of G-protein activation by a GPCR." *Nature* **629**, 1182–1191 (2024) DOI: 10.1038/s41586-024-07153-1

[46] S. Bhattacharjee *et al.* "Time resolution in cryo-EM using a PDMS-based microfluidic chip assembly and its application to the study of HflX-mediated ribosome recycling." *Cell* **187**, 782-796 e723 (2024) DOI: 10.1016/j.cell.2023.12.027

[47] S. Torino, M. Dhurandhar, A. Stroobants *et al.* "Time-resolved cryo-EM using a combination of droplet microfluidics with on-demand jetting." *Nat Methods* **20**, 1400–1408 (2023) DOI: 10.1038/s41592-023-01967-z

[48] S.J. Amann *et al*. "Frozen in time: analyzing molecular dynamics with time-resolved cryo-EM." *Structure* **31**,1:4-19 (2023) DOI: 10.1016/j.str.2022.11.014

[49] M.E. Maeots and R.I. Enchev, "Structural dynamics: review of time-resolved cryo-EM." *Acta Cryst. D Struct Biol* **78**, 927-935 (2022) DOI: 10.1107/S2059798322006155

[50] U.J. Lorenz, "Microsecond time-resolved cryo-electron microscopy." *Curr Opin Struct Biol* **87**, 102840 (2024) DOI: 10.1016/j.sbi.2024.102840

[51] O.F. Harder, S.V. Barrass, M. Drabbels *et al.* "Fast viral dynamics revealed by microsecond time-resolved cryo-EM." *Nat Commun* **14**, 5649 (2023) DOI: 10.1038/s41467-023-41444-x

[52] T. Jain, P. Sheehan, J. Crum, B. Carragher, C.S. Potter, "Spotiton: a prototype for an integrated inkjet dispense and vitrification system for cryo-TEM," *J Struct Biol* **179**, 68-75 (2012) DOI: 10.1016/j.jsb.2012.04.020

[53] V.P. Dandey, H. Wei, Z. Zhang *et al*. (2018) "Spotiton: New features and applications," *J Struct Biol* **202**, 161-169 DOI: 10.1016/j.jsb.2018.01.002

[54] S. Kaledhonkar, Z. Fu, K. Caban *et al*. "Late steps in bacterial translation initiation visualized using time-resolved cryo-EM," *Nature* **570**, 400-404 (2019) DOI: 10.1038/s41586-019-1249-5

[55] C.G. Roessler, A.M. Orville, R. Agarwal, M. Allaire *et al*. "Acoustic Injectors for Drop-On-Demand Serial Femtosecond Crystallography," *Structure* **24**, 631-640 (2016) DOI: 10.1016/j.str.2016.02.007

[56] B. Davy, R.L. Owen, P. Aller *et al*. "Reducing sample consumption for serial crystallography using acoustic drop ejection," *Journal of Synchrotron Radiation* **26**, 1820-1825 (2019) DOI: 10.1107/s1600577519009329

Appendix 1: Complementarity of Techniques

A1.1 Cryo-electron microscopy (cryo-EM), tomography (cryo-ET) and diffraction (cryo-ED)

Cryo-EM, following the resolution revolution, has become a major method for macromolecular structural studies. An active R&D area includes time-resolved studies with samples trapped by freeze-quench methods at the millisecond and longer timeframe. Current challenges in cryo-EM include the development of new approaches towards sample preparation, reaction triggering and delivery to improve efficiency and reduce the time required from pure proteins to structures, and the ability to assign structures to functional states during a dynamic process. Cryo-ET provides structural detail within context, such as whole cells, albeit without as high a resolution. Cryo-ED yields atomic resolution models from sub-micron size crystals and time-resolved methods are a very active R&D area. These all complement macromolecular crystallography (MX), which remains a major technique in structural biology. Time-resolved serial MX data collected at physiological temperatures at XFELs probe femtoseconds and longer, whereas studies at microfocus synchrotron sources probe reactions from ~nanoseconds to microseconds and longer. Together, these complementary approaches share R&D efforts in sample delivery, reaction triggering strategies and data analysis algorithms.

For decades, macromolecular crystallography (MX) has been the main technique in structural biology.[1–5] As of 1 October 2025, the worldwide Protein Data Bank (wwPDB) curates 242,847 atomic models based upon experimental data (e.g. MX and cryo-EM), and 1,068,577 atomic models based upon computational predictions (e.g. AlphaFold); they are all released to the public for the benefit of the entire research community.[6–9] Between 1 June 2024 and 1 June 2025, the wwPDB released 9,490 new atomic models based upon X-ray diffraction data (58.5% of new experimental models), which were linked to many publications, including *Science* (19 publications linked to 48 atomic models), *Nature* (9 publications linked to 105 atomic models), and Cell (24 publications linked to 40 atomic models). An unavoidable issue of MX is the need to obtain well-ordered crystals, which remains a trial-and-error process. Although often automated and using nanolitre volumes per condition, crystallisation trials can consume large amounts of samples and take significant time to optimise. In addition, the crystallisation process requires a homogenous macromolecular conformation, which poses challenges for large, dynamic and transient complexes that play key roles in mediating many biological processes.

The 2017 Nobel Prize in Chemistry was awarded to Dubochet, Frank, and Henderson *"for developing cryo-electron microscopy for the high-resolution structure determination of biomolecules in solution."* This reinforces the recent revolutionary advances in cryo-EM.[10–23] These include microscope instrumentation, detector developments and image processing algorithms. An advantage of cryo-EM is that it only needs a relatively small amount of sample at a significantly lower (100 – 1000 times) concentration compared to MX. Consequently, structural determination by cryo-EM is an attainable goal for many large proteins and complexes that are difficult to produce, purify or crystallise. The method allows fast structural determination for many proteins, as demonstrated by the recent structures of COVID-19 spike protein, which were resolved within weeks of genes being sequenced (see also **Section 8.5**).[24] Furthermore, since each particle is imaged individually, and can be sorted out *in silico* according to their conformation, even dynamic proteins and complexes can now be imaged and their structures determined, provided that their different structural classes are sufficiently differentiated. Between 1 June 2024 and 1 June 2025, the wwPDB released 6,410 new atomic models based upon cryo-EM data (39.5% of new experimental models). Stunning cryo-EM results are frequently published in *Science* (45 publications linked to 181 atomic models released between 1 June 2024 and 1 June 2025), *Nature* (100 publications linked to 471 atomic models released between the same dates), and *Cell* (52 publications linked to 235 atomic models released between the same dates), as well as other high profile journals; a selected subset are listed here.[24–45]

The principal structural methods that use frozen-hydrated samples and a transmission electron microscope apply to macromolecular samples in pure states in solution (cryo-EM) or submicron crystals (cryo-ED) to heterogenous samples in complex environments such as whole cells (cryo-ET) (**Figure A1.1**).[46–53] Current cryo-EM single particle analysis methods focus on biomolecules ranging from ~50 kilodaltons (kDa) to several megadaltons (MDa), covering the majority of macromolecules complexes as well as viruses.[50,54–58] Indeed, recent examples demonstrate that even haemoglobin (64 kDa) can be studied by cryo-EM and 10 of the 4,641 atomic models released by the PDB (29 March 2020) are to better than 2 Å resolution.[49,50,54–61] However, conjugating small proteins with Llama nanobodies increases the molecular weight and introduces symmetry such that structural analysis of average and smaller proteins becomes even more tractable. This was recently demonstrated for maltose binding protein (42 kDa, 2.45 Å resolution) and lysozyme (15 kDa, 3.1 Å resolution).[62,63]

Cryo-ET provides structural information *in situ* and with the extraordinarily valuable context of whole cells.[10,12,64–71] The technique is very likely to unravel new biology as we start to observe links between different macromolecular complexes inside the cell and organelles, track how different macromolecular complexes change in response to environment stimuli, and complexes associate and dissociate (**Figure A1.2**).[45,72] Despite the ability to resolve large macromolecular complexes within cellular context, average size proteins and enzymes are beyond the reach of cryo-ET methods. Moreover, samples for cryo-ET must be less than 500 nanometres thick and often require cryo-focused ion beam (FIB) milling, a laborious and time-consuming process. Similarly, cryo-ED requires sub-micron size crystals to reduce or eliminate multiple diffraction events from the sample, but it can provide truly atomic resolution results.[46,47,52,73–78] To date, all cryo-ED structures have been solved by molecular replacement, with the exception of the very high resolution dataset of a prion peptide that enabled direct methods to calculate phases and further advancements are always emerging.[51,79–84] Analogous to cryogenic X-ray crystallography, most cryo-ED data are collected with continuous-rotation methods. In comparison to X-rays, however, electrons interact much more strongly with matter and thereby yield high resolution diffraction from much smaller samples.

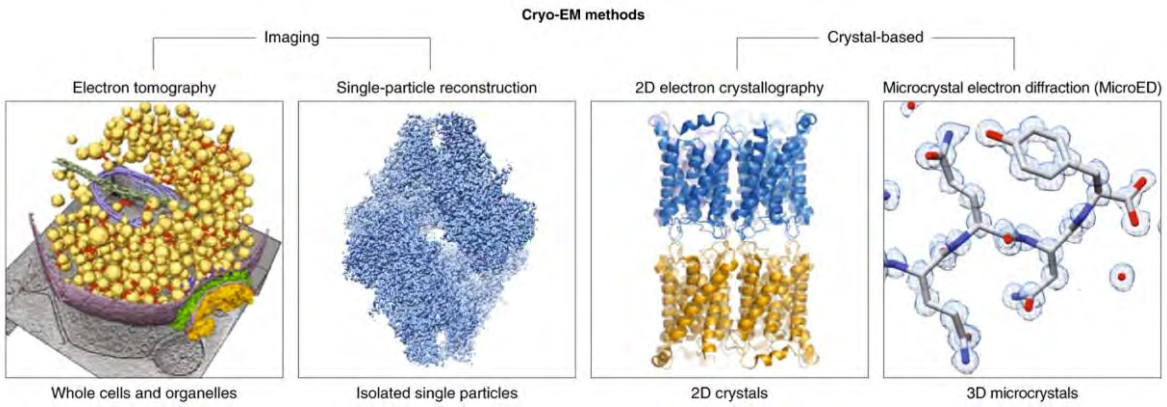


Figure A1.1: The diverse imaging-based and diffraction-based techniques used in cryo-EM can provide structural information from a wide range of samples

Images acquired with the different techniques are shown here, depicting the synaptosome (electron tomography), a 2.2 Å reconstruction of β-galactosidase (single-particle reconstruction), a 1.9 Å structure of aquaporin-0 (2D electron crystallography) and a 1.0 Å structure of the NNQQNY Sup35 prion fragment (MicroED).

*Reproduced by permission from Springer Nature: B.L. Nannenga and T. Gonen, Nat. Methods **16**: 369–379 (2019)*
DOI: 10.1038/s41592-019-0395-x Copyright (2019)

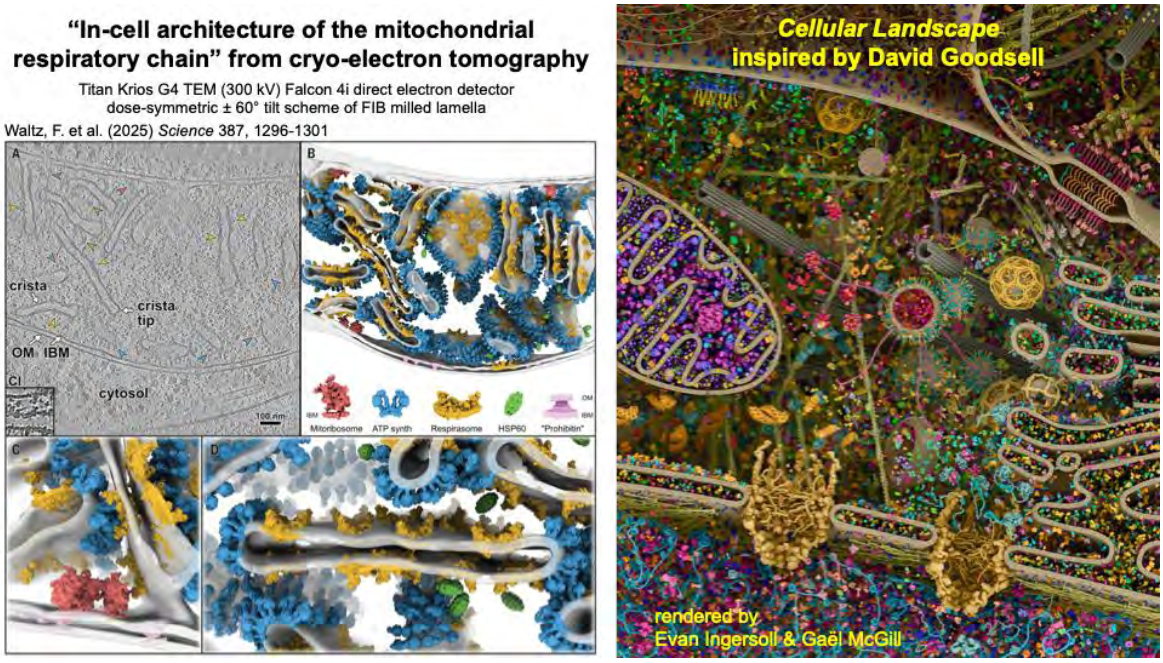


Figure A1.2: Imaging based upon cryo-ET data compared to a simulated model of a whole eucaryotic cell with mitochondria in context using several types of biophysical data

(Left) Molecular landscape of Chlamydomonas mitochondria. (A) Slice of a tomogram depicting a mitochondrion within a native C. reinhardtii cell. (Inset) Zoomed-in view showing complex I. Arrowheads point to complexes coloured in (B). (B) Corresponding segmentation of the tomogram with STA structures of the molecular complexes mapped back into their respective particle positions. Gray, mitochondrial membranes; red, mitoribosomes; blue, ATP synthase dimers; orange, respirasomes; green, HSP60; pink, putative prohibitins. Enlarged views of the STA maps are displayed below the segmentation. (C and D) Close-up views of the mapped-in complexes, showing the organisation of mitoribosomes and putative prohibitins at the IBM (C) and the organisation of ATP synthases and respirasomes in cristae (D). See also movie S1 available with the full paper.[45]

*Reproduced with permission from: F. Waltz et al. In-cell architecture of the mitochondrial respiratory chain. Science **387**, 1296-1301 (2025) DOI: 10.1126/science.ads8738*

(Right) Cellular landscape cross-section through a eukaryotic cell, by Evan Ingersoll and Gaël McGill. Created for Cell Signalling Technology, Inc., and inspired by the stunning art of David Goodsell, this 3D rendering of a eukaryotic cell is modelled using X-ray, nuclear magnetic resonance (NMR), and cryo-electron microscopy datasets for all its molecular actors. It is an attempt to recapitulate the myriad pathways involved in signal transduction, protein synthesis, endocytosis, vesicular transport, cell-cell adhesion, apoptosis and other processes. Although dilute in its concentration relative to a real cell, this rendering is also an attempt to visualise the great complexity and beauty of the cell's molecular choreography.

Reproduced with permission from: https://gaelmcgill.artstation.com/projects/Pm0JL1

The requirement to use sub-micron size samples also makes cryo-ED synergistic with SFX and serial MX methods at XFELs and synchrotrons. The parallels continue with serial cryo-ED strategies wherein nanocrystals are randomly dispersed on a TEM grid, located with a low-dose exposure, then a still cryo-ED pattern is collected from each sample, and the whole dataset is merged together from tens of thousands of still images.[73,85] The use of nanocrystals also makes serial electron diffraction an attractive and complementary method for time-resolved studies. This still needs significant R&D effort and is likely to exploit freeze quench methods on TEM grids with a minimum time resolution on the order of hundreds of microseconds to tens of milliseconds. An alternative is to use a mega-electron-volt (MeV) ultrafast electron diffraction instrument and exploiting pump-probe or mix-inject jets to deliver thin streams or sheets of nanocrystal slurries at room temperature to achieve a temporal resolution of approximately 200 fs.[86,87,88]

To achieve the highest resolution in single particle imaging by cryo-EM requires optimum samples and sufficient microscope time. Rapidly improving technologies and high end instruments are becoming

more widespread, which in aggregate are producing many new results on a daily basis.[11] All of the 4,629 cryo-EM models released by the PDB as of 29 March 2020, give an average 5.92 Å resolution; however, for those 485 models released in 2020 (as of 29 March) the average was 3.9 Å resolution. The obvious trend is more structures and to higher resolution, such that between 1 June 2024 and 1 June 2025, the 6,410 atomic models determined by cryo-EM have an average resolution of 3.33 Å. Over the same period, the 9,490 atomic models determined by X-ray crystallography have an average resolution of 2.04 Å and 1,870 datasets (~ 20%) went to "atomic resolution" or beyond as defined by the typical C-C bond distance of 1.54 Å. Thus, cryo-EM is clearly a very important method for many structural biology projects, including structural studies to characterise ligand and/or inhibitor binding.

Cryo-EM methods complement MX, wherein the latter often provides atomic resolution to well beyond 2 Å resolution and sometimes even with direct correlations with spectroscopic data from the same samples. Although time-resolved MX studies at physiological conditions with XFELs is a major use case, time-resolved cryo-EM is also being actively pursued by several research groups.[89–92] For instance, the Frank group has recently published freeze-quench cryo-EM studies of the ribosome initiation of translation with time points at 20, 80, 200 and 600 ms, wherein the rapid formation of the 70S initiation complex transitions into 70S elongation-competent complex.[93] The collaboration between Muench, Scharff, White *et al.* produced time-resolved cryo-EM structures at 10 ms and 120 ms timepoints to almost 4 Å resolution of the force generation triggered by ATP hydrolysis of the actin-myosin motor complex.[94,95] Skiniotis *et al.* used 'freeze trapping' at distinct time points and cryo-EM to examine the evolution of a G-protein-coupled receptor (GPCR) activated by a heterotrimeric G protein (GPCR–G-protein complex) through 20 pre-steady-state intermediates across the reaction coordinate.[96]

In addition to resolving multiple conformations and composition heterogeneity within a single sample, cryo-EM is well suited to the study of dynamic systems at the milliseconds to seconds time frame dictated by freeze-quench methods, within which many macromolecular assembling, co-factor binding, conformational changes, and signalling events take place. However, in order to track a dynamic process, precise and well controlled sample preparation, triggering and delivery systems are required to capture different functional states, or distributions of functional states, during a dynamic biological process.

Despite these clear advantages and capabilities, there are a number of challenges and limitations that hinder cryo-EM to reach its full potential:

1) *Instrumentation capacity*
   A significant problem for cryo-EM is the limited access and long waits to use extraordinarily expensive microscopes. In the last few years, the UKRI and Wellcome Trust, as well as individual universities/institutes, have invested significantly in high end instrumentation. This includes establishing the national electron bio-imaging centre (eBIC) at Diamond Light Source, a successful model that is now widely adopted in many other countries. However, these instruments are expensive to purchase, maintain and require expertise to operate; they are thus best placed in centres or institutions with sufficient user groups. To best utilise these high-end instruments and to allow more scientists to have access to cryo-EM, samples need to be screened first, which should be assessed locally. There is currently limited access to screening instruments across the whole UK structural biology community. Fortunately, there are a number of current efforts and approaches to address this; for instance, the development of a 100 keV instrument that aims to democratise cryo-EM.[97,98]

2) *Sample preparation and delivery*
   Current methods in cryo-EM sample and grids preparation date back to the 1980s. Although blotting works for many samples, it is increasingly becoming a major bottleneck as the numbers of samples and their complexity increases.[99] The difficulty is that many macromolecular complexes dissociate, aggregate, denature or simply do not go into the holes of the cryo-EM grids. A further complication is the lack of rapid and easy quality assessment early in the process, which now happens after the samples have been imaged using a cryo-

EM instrument and analysed computationally. The lack of robust and reliable specimen preparations, and the inability to assess sample quality prior to cryo-EM imaging, hinder the overall efficiency of structural determinations by cryo-EM. Fortunately, these areas are experiencing rapid development and have even spawned new product lines (e.g. VitroJet™ by Cryosol, Maastricht, The Netherlands and chameleon™ by SPT Labtech Ltd, UK.[100–105] Given that sample delivery is a major area of development required for successful XFEL experiments, as detailed in **Chapter 7**, there is significant synergy with the sample delivery systems developed for serial methods at XFELs.

3) *Cryo-ET development*

One of the most exciting but least developed areas is the ability to image and recognise macromolecules to high resolution *in situ*. Electron cryo-tomography reconstructs a three-dimensional image from a series of tilted images, which limits resolution to about 15 – 20 Å. Furthermore, the limited penetration power of electrons in the available microscopes (100 – 300 keV, limiting to ~ 200 nm) requires many of the biological samples to be thinned first, currently through focused-ion beam milling.[69] The resolution limitation can be overcome and 3 – 4 Å resolution has been achieved through sub-tomographic averaging in some cases;[106,107] this is not always possible, however, due to the small numbers and small sizes of the objects within the biological specimen. There remain significant technical challenges to develop methodologies to improve the resolution, to increase penetration power and develop new ways to obtain thinner specimens, and to enable particles to be identified in tomograms.

A1.2 Next-generation synchrotron light sources

The emerging generation of high-brightness synchrotron sources provides scientific capability that is highly complementary to that of XFELs, particularly in respect to the time domain and the peak X-ray intensity that XFELs deliver. Current XFELs do not compete on average spectral brightness with diffraction limited synchrotrons, but next-generation XFELs will exceed the average spectral brightness of these machines by as much as three orders of magnitude.

A1.2.1 Time domain

Synchrotrons, such as Diamond Light Source and its upgrade to Diamond-II (**Figure A1-3**), are designed for the study of a wide range of processes under functional conditions, on timescales down to microseconds, and with high spatial resolution. This time resolution can be further enhanced by taking advantage of the electron bunch structure of the synchrotron, and this can facilitate dynamic studies using system snapshots taken in hundreds of picoseconds. One way to achieve this is by operating the synchrotron with distinct separation between the electron bunches to facilitate stroboscopic measurements with fast pulses of X-rays, as is the case of the hybrid or single bunch mode available at Diamond. Higher time resolutions have been achieved at synchrotrons using novel time schemes such as laser-electron slicing[108,109] or by producing shorter, more intense X-ray pulses with crab cavities[110] or low alpha optics.[111] In all these cases, the higher time resolutions are attained at a large cost in flux. Of these options, the low alpha mode is currently the high time resolution mode offered at Diamond, achieving time resolutions of the order of 10 ps.[112]

The development of Diffraction Limited Storage Rings (DLSR) or fourth generation synchrotrons, with reduced horizontal emittance values by between one to two orders of magnitude, offers the scientific community the opportunity to exploit much brighter photon beams and an increased coherence. These beam characteristics are being exploited for the study of materials with nanometric spatial resolution. From the perspective of time-resolved studies, the ultralow emittance sources are in conflict with the optimum requirements for the timing schemes usually used for pump-probe experiments, as these require highly charged electron bunches. In general, these new low emittance machines will make use of longer electron bunches, that in turn reduce the time resolution achievable. Some of the upgrades being planned are consequently considering implementing two different operation modes: a brightness mode and a timing mode. In the case of the APS upgrade, APS-U,[113] the timing mode maximises the brightness of a single bunch, at the expense of the attainable vertical emittance. Forty-eight bunches of approximately 4 mA will be used in that mode with a bunch length larger than 200 ps. Petra IV,[114,115] on the other hand, is planning to operate the timing mode with eighty bunches, approximately 150 ps long, separated by 96 ns, each with a current of 1 mA. In the case of Diamond-II,[116,117] it is expected that the bunch length will be of the order of 100 ps, and advanced timing modes such as the low alpha will not be available.

The hundreds of picoseconds time resolution offered in synchrotrons and diffraction limited machines are suitable for increasing our understanding of chemical and biological process mechanisms, by solving the electronic and geometrical structures of the transient states on the time scales of ns to hours. XFELs, on the other hand, with photon pulse lengths more than 10,000 times shorter than those on fourth generation synchrotron sources, enable the study of complex systems on femtosecond timescales with high flux, opening the door to the study of electron and nuclear dynamics under system conditions that are far from thermal equilibrium. These very high time resolutions can also provide access to transient states of matter that can be induced, for example, by the application of extreme pressures by shockwave methods, or high transient electric or magnetic fields.

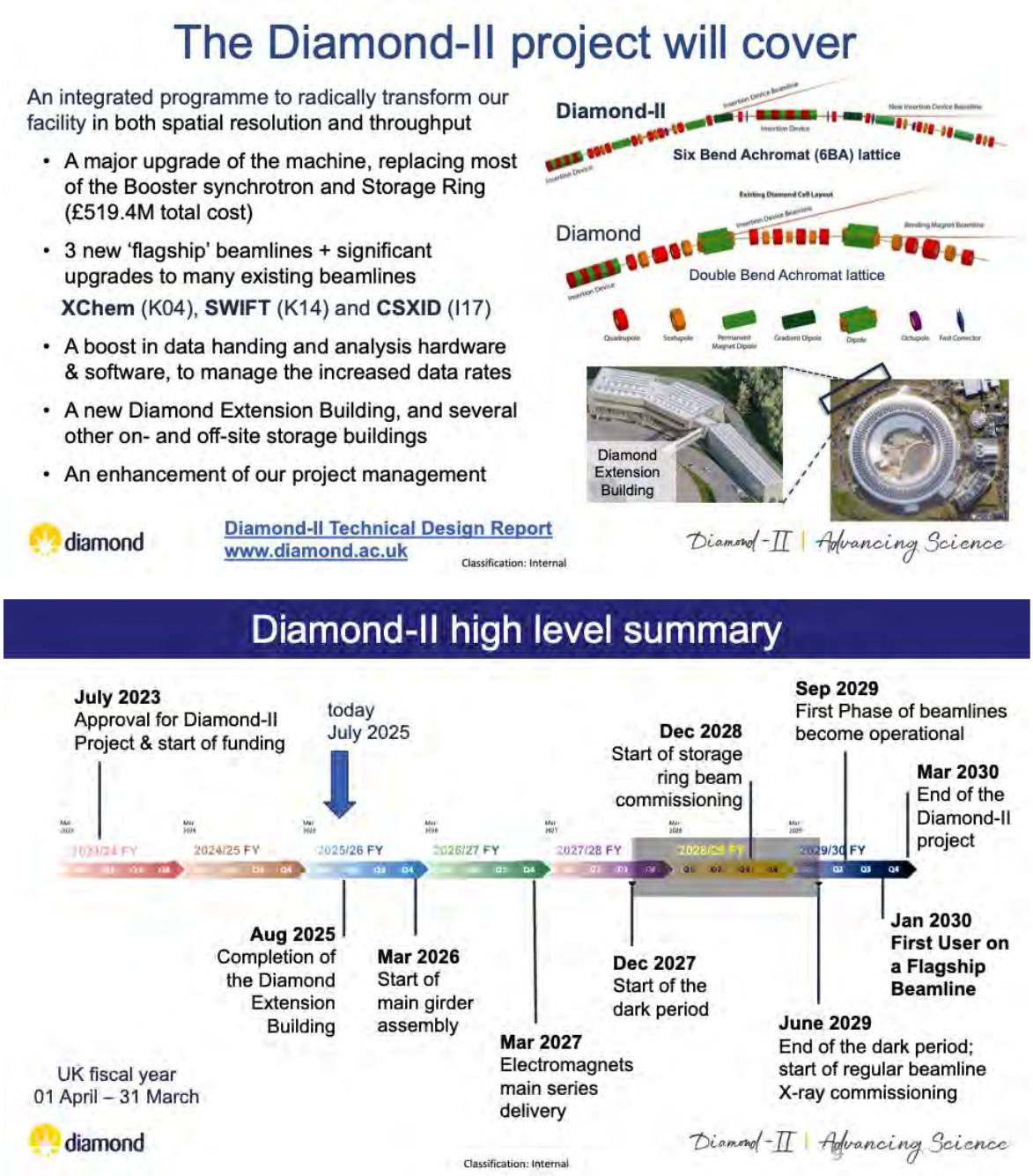


Figure A1.3: An overview of the Diamond-II upgrade project and delivery schedule

A1.2.2 Peak intensity

Synchrotron sources and XFELs are also complementary in the peak intensity they deliver. These intensities can be different by up to 10 orders of magnitude. The high peak intensity delivered by XFEL sources is enabling novel experiments that cannot be performed at synchrotron sources. For example, XFELs are used to study the atomic structures of delicate biological systems from micron to submicron size samples and before radiation-induced effects damage the samples, and their high peak power is also well suited to the study of high energy density systems. Furthermore, high peak intensities are opening the way to non-linear X-ray methods that give rise to powerful new probing capabilities. For example, second harmonic emission is a surface sensitive method that is a promising route to revolutionise the investigation of processes at interfaces, whilst various Raman methodologies offer to allow chemical sensitive probes of dense environments (e.g. in detonations and projectile propellants) and of ultrafast electronic dynamics in the condensed phase.

Many examples of applications of the use of the high time resolutions and high peak intensities achieved at XFEL sources can be found in this Science and Technology Case. These applications span many different areas, from chemistry and energy materials to life sciences, quantum chemistry and matter under extreme conditions.

The complementarity of synchrotrons, including diffraction limited sources, and XFELs is increasingly being recognised by the scientific community, and there many examples of co-location of these sources, such as Petra III and the European XFEL, the SLS and the SwissFEL, Elettra and FERMI, and SPring-8 and SACLA. By combining the capabilities of both sources, studies of the dynamics of complex materials can be investigated over the full range of timescales, from below femtoseconds to minutes and even hours, and also across a large energy range.

Ultimately, next-generation XFELs may supersede synchrotrons as the light sources of choice not only for time-resolved measurements but also for imaging and other applications that require the highest average, as well as peak, brightness.

A1.3 Ultrafast electron diffraction

Ultrafast electron diffraction (UED) with a relativistic electron gun is an emerging method in structural dynamics. We discuss the synergy with an XFEL facility and point to unique scientific possibilities if UED apparatus were synchronised with the XFEL. We also review the synergies between the UED project and XFELs, and in particular a next-generation XFEL.

The use of monoenergetic electron beams for atomic scale structure determination by diffraction has a long history, stretching back to the Nobel Prize winning work of Thompson, Davisson and Germer in 1926. Electron diffraction is a natural complement to X-ray diffraction, as it has different sensitivities and characteristics. Electrons have $10^4 - 10^6$ higher scattering cross-sections than X-rays, making them more suitable for thin or diffuse samples. In 1930, Mark and Wierl realised that diffraction patterns for the molecule CCl_4 in the gas phase could be acquired in a fraction of the time required for X-rays.[118] A few short years later, the structure of 146 molecules in the gas phase had been determined[119] and structural determination of gas phase molecules using electron diffraction became an important technique that remains in use.[118] Electrons scatter from both the electrons and the nuclei in the target, in contrast to X-rays that scatter only from the electrons, making electron diffraction more sensitive to low Z atoms. In principle, it can be used to detect H atoms, which are effectively invisible to X-ray diffraction. The possibility of using diffraction of ultrafast electron pulses to image structural dynamics has therefore caused substantial interest in the chemical dynamics and materials communities in recent decades. Not unexpectedly, the impact has been greatest for probing dynamics in gas phase molecules and thin films of crystalline material. Early work by Zeweil[120] and Miller[121] and others on ultrafast electron diffraction (UED) demonstrated what is possible. There is a strong consensus that, along with time-resolved X-ray diffraction, UED is a powerful route to access structural dynamics in molecules undergoing chemical reactions[122] and in crystalline materials undergoing phase changes.[123]

Despite this promise, there are severe limits to temporal resolution set by space-charge repulsion between electrons in an electron bunch. Unless the number of electrons in the bunch is kept unrealistically low, the time-resolution becomes badly degraded (although single electron "attosecond" experiments are possible when sampling periodic dynamics[124]). This has limited the temporal resolution in most UED experiments to picoseconds, despite efforts to design optimal electron optics. A big improvement is gained by using relativistic electron guns that rapidly accelerate the electron bunch to > 1 MeV. In this case, relativistic Lorentz contraction reduces the effective space-charge by an enormous factor so allowing simultaneously very short pulses (< 100 fs) and high bunch charges that enable good signal to noise measurements. A UED facility based upon a relativistic electron gun operating at 2 – 4 MeV with ~100 fs pulses has been established at SLAC,[125,126] and this has been running as a user facility alongside LCLS for the last seven years. The SLAC facility has achieved significant scientific impact in this short time with measurements in photochemistry[127,128] and condensed matter physics[129] among prominent recent results. The high scattering cross-section and small de Broglie wavelength of the electrons is likely to enable time-resolved pair-distribution function retrieval in liquids in the future.

A relativistic UED instrument of the type operating at SLAC, or the REGAE system being developed at DESY, is arguably two orders of magnitude cheaper than a hard X-ray FEL and far more compact. It can be synchronised with external pump lasers to enable a wide range of pump-probe studies. It can deliver a range of structural dynamics information in gas phase, thin films and in liquid samples (**Figure A1.4**) with

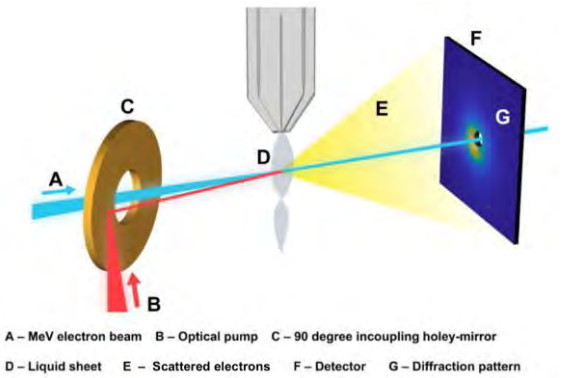


Figure A1.4: Schematic representation of the liquid-phase MeV UED experimental setup

*Figure reproduced from J.P.F. Nunes et al. Struct. Dyn. **7**, 024301 (2020) DOI: 10.1063/1.5144518 licensed under a Creative Commons Attribution 3.0 Unported license*

temporal resolution < 100 fs. In particular, liquid samples are constrained to thickness < 20% of the electron mean free path (approximately 1 µm in water for electrons at 3.7 MeV). To this end, Nunes *et al.*[86] exploited a water sheet using a microfluidic chip to produce a 20 µm cylindrical liquid jet that was flatted with gas flow into a sheet with a profile that decreases from 700 nm near the top to < 100 nm at the bottom. As discussed in **Section A1.1** above, the requirement to use nanocrystals also makes time-resolved studies well-suited to serial electron diffraction with biological macromolecules. Although the present SLAC gun is operating at 540 Hz, higher repetition rate reaching 1080 kHz has been established. The pulse duration at SLAC has recently been reduced, e.g. using THz driven electron beam compression, to around 35 fs in development experiments and so higher temporal resolution is expected to be achievable.

Overcoming space-charge broadening in relativistic electron pulses has seen significant success, but is not without side-effects that need careful consideration. MeV electron pulses can transport much higher fluxes as compared to non-relativistic pulses over the range 40 – 100 keV. The study of thin, high-Z or, particularly, biological samples can undergo knock-on or polarisation damage when high bunch charge and energy are combined. In some cases, with a carefully controlled electron beam, longer exposure can be possible with lower energies, as advocated by the SALVE Consortium for conventional electron microscopy. Longer exposure and less damage can result in higher contrast and resolution. Furthermore, non-relativistic pulsed electron instruments can be operated without RF acceleration, rather making use of highly stable DC acceleration, reducing the uncertainty in bunch charge and energy distribution, hence duration. A consequence is that THz/IR compression has higher shot-to-shot stability at non-relativistic energies, hence a temporal resolution down to around ten fs is possible. Considering linear electron-EM field interactions, transient fields as driven by a laser E-field or intensity envelope scatter lower energy electrons more effectively, therefore non-relativistic electron pulses are well-suited to observing diffraction from, for example magnetic devices. Practically, implementing a non-relativistic UED is cheaper as RF infrastructure is not required, and is far more compact. With careful design, such an instrument could also be operated as a conventional transmission electron microscope, albeit with limited performance as compared to the current state-of-the-art, however routine sample monitoring and characterisation would be invaluable.

As of April 2026 a UED ultrafast electron diffraction instrument of RUEDI is under development at the STFC Daresbury Laboratory in collaboration with the University of Liverpool and a network of national partners. It is contemplated also to deliver ultrafast electron microscopy (UEM) alongside the ultrafast electron diffraction platform (UED), both leveraging a compact relativistic electron beam technology. UEM would enable electron imaging of assemblies (e.g. tissue, complex materials, devices) undergoing dynamics to a temporal resolution of picoseconds, and the UED will permit ultrafast electron diffraction of matter with the ability to resolve structural dynamics to ~ 20 fs temporal resolution. Thus, this instrumentation would serve a growing need in UK science and technology for dynamical studies of matter. It will be available in early 2030 and will help to boost the structural dynamics community in readiness for a next-generation XFEL. It will also complement the existing landscape of XFELs currently accessed by UK users, most especially the European XFEL.

Table A1.1 summarises the capabilities of state-of-the-art UED and UEM instrumentation and a next-generation XFEL. This shows that UEM would offer time-resolved (TR) electron microscopy to ~ 10 ps temporal resolution and time-resolved electron diffraction to ~ 50 fs temporal resolution. In contrast, the next-generation XFEL will offer femtosecond resolution X-ray microscopy (at a lower resolution but able to penetrate bulk matter) and temporal resolution in diffraction and spectroscopy to ~ 0.2 fs. The next-generation XFEL will also deliver a much higher measurement capacity.

Table A1.1: Summary of state-of-the art UED/UEM and next-generation XFEL capabilities

Capability	UED/UEM	Next-generation XFEL
Time resolution	~ 50 fs UED / ~10 ps UEM	~ 0.25 fs
Rep-rate	~100 Hz – 1 kHz	100 kHz (x 10 end-stations in parallel)
Methodologies	TR electron scattering / TR microscopy	TR X-ray scattering / TR and static X-ray imaging in bulk samples TR X-ray spectroscopy

The complementarity with XFELs is best understood by considering the limitations, as well as the strengths, of UED. First and foremost, the penetration length, due to the inherent high scattering cross-section, is much less than hard X-rays and so precludes the study of bulk material properties, buried structures and 3D biological samples such as multicellular tissue . The temporal resolution is currently two orders of magnitude worse than that achieved with eSASE modes of an XFEL and is only likely to see modest improvements in the foreseeable future. Moreover, whilst electron diffraction can retrieve crystalline structures, there is no method equivalent to X-ray CDI that permits the time-resolved retrieval of irregular structures, limiting the application mainly to macroscopically crystalline samples and gas phase molecules. Volumetric X-ray dynamic imaging of bulk industrially relevant processes as is just emerging at LCLS and European XFEL cannot be matched via electron techniques. Likewise, there is no equivalent to inelastic scattering currently stimulating powerful new notions in X-ray scattering measurement (see discussion of coherent mixed scattering and quantum imaging in **Section 3.2**). The strong interaction of electrons with electric, magnetic and electromagnetic field is also a significant limit when investigating interactions with field dressed materials, whereas X-rays are immune to any perturbation. Finally, the argument has been advanced that new high-flux X-ray photon sources can achieve higher spatial resolution than UED during realistic exposure times, due to significantly lower noise in the large momentum-transfer data where UED suffers from much stronger quenching than X-ray scattering.[130] Ultimately, the greatest strength of electron scattering is as a structural technique and we will still need the power of X-ray spectroscopy, XES, RIXS and XPS, plus the emerging non-linear techniques, to address the electronic quantum state dynamics that accompany, and drive, structural changes. A state-of-the-art relativistic UED facility would be far less versatile and scientifically pervasive than an XFEL but would still likely find an enthusiastic user base. **Table A1.2** details the exciting synergies that access to next-generation XFEL and UED/UEM capabilities would deliver to UK science.

To understand the synergies of techniques we can look at a recent case study from Dr Alice Green of the University of Edinburgh, who led a collaboration using multiple ultrafast techniques to image the gas-phase photochemistry of small cyclic carbonyl molecules. Dr Green reports: "*The photochemistry of carbonyls is of particular interest as these species form major components of secondary organic aerosols, prominent atmospheric pollutants with potential major impacts for global climate and public health. The experimental techniques used were enabled by modern XFELs and MeV-UED sources: ultrafast X-ray scattering, time-resolved X-ray Coulomb explosion imaging and ultrafast electron diffraction. Each of these techniques are sensitive to the ultrafast nuclear dynamics that underpin molecular photochemistry but, in our studies, we found that each technique is differentially sensitive to particular aspects of the complicated, multi-dimensional photoinduced dynamics. As such, combining the insights from these XFEL and MeV-UED based techniques leads to a more complete and comprehensive view of the underlying photochemistry. For instance, ultrafast X-ray scattering at the LCLS excels in terms of signal-to-noise and time resolution, whilst ultrafast electron diffraction at the SLAC MeV-UED facility offers improved spatial resolution and higher sensitivity to electronic dynamics. Time-resolved X-ray Coulomb explosion imaging promises to offer a wealth of complementary information, as it can probe higher-dimensional structural information (e.g. directly pertaining to bond angles and three-dimensional conformation) than these diffractive imaging approaches, but requires acquiring data over many XFEL shots, as will be better enabled by high repetition rate XFELs*."

In view of this, it is reasonable to consider the development of additional UED facilities alongside a next-generation XFEL, to complement the capabilities and increase capacity for users who are addressing questions of structural dynamics that the more limited temporal resolution of UED can deliver. This model of co-location has been effective at SLAC and has led to significant extra scientific productivity and reach for that laboratory. We do not, however, advocate merely co-location of UED and XFEL capability. Instead, we would consider developing a more synergistic model, where an end-station for time-resolved X-ray diffraction and X-ray spectroscopy can also be equipped with a UED gun that delivers electrons close to collinearly with the X-ray beam. In this way, some common installations and equipment can be shared, and the end-station can maintain productivity even when X-rays are not available. Sharing of the pump beam capabilities, including a wide spectral range of advanced femtosecond laser and THz sources that will be established at a next-generation XFEL, can thus be used with significant scientific benefit for UED studies.

Further there is then the possibility of interrogating the dynamics of the same systems via multiple channels, e.g. XES, UED and time-resolved X-ray diffraction, thus exploiting the strengths of each method in an integrative methodology. Additionally, this configuration would open-up new scientific possibilities where an electron or an X-ray pulse is used as a pump and the other synchronised, but controllably delayed, X-ray or electron pulse is used as a probe. One possible scientific application is touched on in Chemical Dynamics, **Section 6.3**, where research into fast radiolysis processes could be enabled by such a configuration. The chemical and physical effects of an electron ionisation can thus be probed by X-ray spectroscopy and allied X-ray methods. A wide range of other scientific possibilities is also foreseen with this dual XFEL/UED capability.

Table A1.2: The scientific synergy between UED/UEM and a next-generation XFEL
Note: This table is intended as indicative rather than exhaustive

Capability	UED/UEM	Next-generation XFEL
Time Resolution	~ 50 fs UED / ~10 ps UEM	~ 0.25 fs
Rep-rate	~100 Hz – 1 kHz	100 kHz (x 10 end-stations in parallel)
Sub-nm imaging of biological and nanotechnology	Dedicated imaging end-station (10 ps res/sub nm)	CDI partial image retrieval (20 fs res/nm) in SXR and HXR, and Tomographic imaging (nm)
MEC	Imaging of shocked materials (~10 ps)	< 100 fs structural and electronics dynamics
Gas phase diffraction	Sensitive to protons/high Q	Excellent signal to noise
Thin film (2D and photovoltaics)	Structural dynamics	Electronic and ultrafast structural dynamics
Liquid phase scattering	High Q < 25 fs	Bulk trPDF at high resolution < 1 fs
Processes in bulk materials	Micron-scale nm dynamics	Millimetre-scale *in operando* nm dynamics
Field dressed states	Imaging fields (< 10 ps)	Imaging matter (< 10 fs)
Crystallographic structure solution	Limited	Excellent
Quantum materials	Structural and spin dynamics	Spin, electronic and structural dynamics
Chemical dynamics/Energy storage	Structural dynamics	Resolution to < 1 fs/site resolved/electronic state dynamics
Electronic dynamics in solids	Inter-domain transport	Valence state evolution/nm transport
Photobiology	Dynamic imaging of complexes	Structural and electronic dynamics
Sub-cellular function	Imaging organelles	Resolution sub-cellular chemical dynamics

A1.4 Life Sciences Hub and roadmap

The options available to the life sciences community are broad and range from the currently active (e.g. the XFEL Hub at Diamond) to long-term developments (e.g. a next-generation XFEL project) with additional opportunities in between (e.g. partnerships with existing XFEL facilities).

Table A1.3: Some options for life sciences in XFEL research and development

Time frame	Main objectives and/or goals	Relative cost
Short term (0 – 2 years)	• Full support &/or expansion of the XFEL Hub at Diamond and XFEL Hub for physical sciences • CDT / DTP PhD studentships in life and physical sciences dedicated to XFEL research • Sample delivery collaboration between Diamond and SwissFEL for time-resolved SFX ± XES (currently ongoing)	0.005 – 0.02
Medium term (3 – 5 years)	• Partnership with SwissFEL &/or European XFEL to construct hard X-ray beamline(s) within existing accelerator tunnel for dynamic structural biology & imaging • Institute for XFEL Science	0.02 – 0.125
Long term (> 10 years)	• Build a next-generation XFEL with hard X-ray capability for dynamic structural biology and imaging • Develop time resolved and single molecule imaging capability	1.0

For instance, the XFEL Hub at Diamond is a first in the world and was formed with grant support from the Wellcome Trust, MRC and BBSRC awarded to Jim Naismith *et al.* in 2014. Three full-time Hub scientists reside at Diamond, develop technologies for XFELs, and look to take advantage of synergies between XFELs and synchrotrons to better enable users to solve biomedical questions, especially by accessing the time domain with high resolution structural biology. The Hub helps users compete for beamtime on the global XFEL market. XFEL beamtime is massively oversubscribed, so we take it as a measure of success that the Hub has participated in more than 95 XFEL experiments at all five hard X-ray XFEL facilities worldwide since October 2015. The Hub has also provided travel assistance to more than 400 UK-based scientists for their participation in XFEL experiments. The overwhelming majority of these were given to students and postdocs to participate directly in XFEL experiments. Staff at the XFEL Hub at Diamond also pursue science driven projects in close collaboration with users and other synchrotron and XFEL scientists. To these ends, the Hub has active R&D projects with Diamond beamline staff at I04, I24, VMXi, VMXm and HeXI, as well as with eBIC. These activities and the historical collaborative ties between the XFEL Hub at Diamond and the SFX Consortium at the SPB/SFX Instrument at the European XFEL were recently recognised, with the European XFEL granting the first of its kind "Block Allocation Group (BAG)" for XFEL beamtime in autumn 2024. The SFX Consortium BAG is currently being led by the XFEL Hub at Diamond and anticipates receiving beamtime each run at the European XFEL to be used for R&D projects championed by Consortium members and collaborators, ongoing methods development, and training new groups including PhD students and Postdoctoral fellows.

The XFEL Hub at Diamond has also established a "*Dynamic Structural Biology at Diamond and XFELs*" BAG at Diamond. This introduces and brings serial MX capabilities to users, advances dynamic structural biology, and helps reduce the barrier to access to XFELs for SFX and time-resolved studies of reactive intermediates generated *in situ*. Moreover, it provides valuable training to new users, enables scientists to collect important preliminary data for XFEL beamtime applications, and also generates results that stand on their own. Judging from the increasing access of UK to XFEL sources, the XFEL Hub has already had a useful catalytic role, despite its modest scale. There is strong consensus

in the UK that the XFEL Hub at Diamond should be fully supported by UKRI STFC, and expanded to increase its impact across a larger cross-section of structural biology R&D.

Although the XFEL Hub at Diamond is much smaller in scale, there are parallels between it and BioXFEL (https://www.bioxfel.org/), a Science and Technology Center funded by the US National Science Foundation. BioXFEL is a multi-institutional and international centre established with a $25M grant in 2013, which was awarded a five-year renewal in 2018 with a $22.5M grant. BioXFEL does not have a specific user support role; rather it is mandated to address education, outreach, research and development with aims to develop biological applications for XFELs. As a result, BioXFEL has extensive collaborations throughout the global SFX community.

Mid-term options to life sciences include partnerships with existing facilities to build out their infrastructure. For instance, two unoccupied tunnels are already drilled at the European XFEL. One of these is in early discussions to be developed for Fusion Energy Research. The other tunnel could be developed to support dynamic structural biology. The current intra-train pulse rate of up to 4 MHz is delivered across a short burst train that is currently limited to 600 µs and with new trains arriving at 10 Hz. The European XFEL may strive to achieve CW-like operations and to that end are actively developing scenarios to deliver significantly longer duration pulse trains. SwissFEL also has room for another hard X-ray beamline that will deliver X-ray pulses at 100 Hz and at lower flux density. Finally, an Institute for XFEL Science would bring research groups into a coordinated space similar to the Center for Free-Electron Laser Science (CFEL) (https://www.cfel.de/) on the DESY campus in Hamburg, Germany. These options all have significant merits and should be considered further by UKRI and UK universities.

Long-term options include building a next-generation XFEL or contributing to a related development elsewhere. For life sciences, the desired machine will deliver 5 - 25 keV X-ray pulses at about 100 kHz or faster, of 0.1 - 25 fs duration, in a well-focused beam (~0.02 - 2 μm^2) with at least 10^{12} photons per pulse. Further details of a potential machine are detailed in the accompanying **Conceptual Design Report** following the demands of the analysis in **Chapter 9**. There are also strong incentives to tightly integrate the science programmes of a next-generation XFEL with Diamond-II, RUEDI, cryo-EM and serial electron diffraction, and the Rosalind Franklin Institute.

A1.5 References for Appendix 1

1 L. Maveyraud, L. Mourey, "Protein X-ray Crystallography and Drug Discovery." *Molecules* **25**(5):1030 (2020) DOI: 10.3390/molecules25051030

2 D.J. Haas, "The early history of cryo-cooling for macromolecular crystallography." *IUCrJ* **7**, 148-157 (2020) DOI: 10.1107/S2052252519016993

3 H.N. Chapman, "X-Ray Free-Electron Lasers for the Structure and Dynamics of Macromolecules." *Annu Rev Biochem* **88**, 35-58 (2019**)** DOI: 10.1146/annurev-biochem-013118-110744

4 J.M. Grimes, D.R. Hall, A.W. Ashton *et al.* "Where is crystallography going?" *Acta Crystallogr D Struct Biol* **74**, 152-166 (2018) DOI: 10.1107/S2059798317016709

5 R.L. Owen, J. Juanhuix, M. Fuchs, "Current advances in synchrotron radiation instrumentation for MX experiments." *Arch Biochem Biophys* **602**, 21-31 (2016) DOI: 10.1016/j.abb.2016.03.021

6 S.K. Burley, "Protein data bank: From two epidemics to the global pandemic to mRNA vaccines and Paxlovid." *Curr Opin Struct Biol* **90**, 102954 (2025) DOI: 10.1016/j.sbi.2024.102954

7 PDB consortium, "Protein Data Bank: the single global archive for 3D macromolecular structure data." *Nucleic Acids Res* **47**, D520-D528 (2019) DOI: 10.1093/nar/gky949 (2019)

8 H.M. Berman *et al.* "The Protein Data Bank." *Nucleic Acids Res* **28**, 235-242 (2000) DOI: 10.1093/nar/28.1.235

9 "Crystallography: Protein Data Bank." *Nature New Biology* **233**, 223 (1971) DOI: 10.1038/newbio233223b0

10 X. Benjin, L. Ling, "Developments, applications, and prospects of cryo-electron microscopy." *Protein Sci* **29**, 872-882 (2020) DOI: 10.1002/pro.3805

11 E. Callaway, "Revolutionary cryo-EM is taking over structural biology." *Nature* **578**(7794): 201 (2020) DOI: 10.1038/d41586-020-00341-9

12 Y. Cheng, "Single-particle cryo-EM-How did it get here and where will it go." *Science* **361**(6405): 876-880 (2018) DOI: 10.1126/science.aat4346

13 S. Subramaniam, "The cryo-EM revolution: fueling the next phase." *IUCrJ* **6**, 1-2 (2019) DOI: 10.1107/S2052252519000277

14 D. Lyumkis, "Challenges and opportunities in cryo-EM single-particle analysis." *J Biol Chem* **294**(13): 5181-5197 (2019) DOI: 10.1074/jbc.REV118.005602

15 "Method of the Year 2015." *Nat Methods* **13**, 1 (2016) DOI: 10.1038/nmeth.3730

16 D. Elmlund, H. Elmlund, "Cryogenic electron microscopy and single-particle analysis." *Annu Rev Biochem* **84**, 499-517 (2015) DOI: 10.1146/annurev-biochem-060614-034226

17 Y. Cheng, "Single-Particle Cryo-EM at Crystallographic Resolution." *Cell* **161**, 450-457 (2015) DOI: 10.1016/j.cell.2015.03.049

18 A. Ourmazd, "Cryo-EM, XFELs and the structure conundrum in structural biology." *Nat Methods* **16**, 941-944 (2019) DOI: 10.1038/s41592-019-0587-4

19 A. Patwardhan, R. Henderson and C.J. Russo, "Extending the reach of single-particle cryoEM." *Current Opinion in Structural Biology* **92**, 103005 (2025) DOI: 10.1016/j.sbi.2025.103005

20 S.J. Amann, D. Keihsler, T. Bodrug, N.G. Brown and D. Haselbach, "Frozen in time: analyzing molecular dynamics with time-resolved cryo-EM." *Structure* **31**, 4-19 (2023) DOI: 10.1016/j.str.2022.11.014

21 P. Majumder and P. Zhang, "In situ cryo-electron microscopy and tomography of cellular and organismal samples." *Curr Opin Struct Biol* **93**, 103076 (2025) DOI: 10.1016/j.sbi.2025.103076

22 A. Banari, A.K. Samanta, A. Munke*et al.* "Advancing time-resolved structural biology: latest strategies in cryo-EM and X-ray crystallography." *Nat Methods* **22**, 1420-1435 (2025) DOI: 10.1038/s41592-025-02659-6

23 E.Y.D. Chua *et al.* "Better, Faster, Cheaper: Recent Advances in Cryo-Electron Microscopy." *Annu Rev Biochem* **91**, 1-32 (2022) DOI: 10.1146/annurev-biochem-032620-110705

24 A.C. Walls, Y.J. Park, M.A. Tortorici, A. Wall, A.T. McGuire, D. Veesler, "Structure, Function, and Antigenicity of the SARS-CoV-2 Spike Glycoprotein." *Cell* **181**(2): 281-292.e6 (2020) DOI: 10.1016/j.cell.2020.02.058

25 F. Coscia, A. Taler-Verčič, V.T. Chang *et al.* "The structure of human thyroglobulin." *Nature* **578**, 627-630 (2020) DOI: 10.1038/s41586-020-1995-4

26 W. Huang, M. Masureel, Q. Qu *et al.* "Structure of the neurotensin receptor 1 in complex with β-arrestin 1." *Nature* **579**, 303-308 (2020) DOI: 10.1038/s41586-020-1953-1

27 J. Ma, X. You, S. Sun *et al*. "Structural basis of energy transfer in *Porphyridium purpureum* phycobilisome." *Nature* **579**, 146-151 (2020) DOI: 10.1038/s41586-020-2020-7

28 D.P. Staus, H. Hu, M.J. Robertson *et al*. "Structure of the M2 muscarinic receptor-β-arrestin complex in a lipid nanodisc." *Nature* **579**, 297-302 (2020) DOI: 10.1038/s41586-020-1954-0

29 F.R. Wagner, C. Dienemann, H. Wang *et al*. "Structure of SWI/SNF chromatin remodeller RSC bound to a nucleosome." *Nature* **579**, 448-451 (2020) DOI: 10.1038/s41586-020-2088-0

30 W. Zhang, A. Tarutani, K.L. Newell *et al*. "Novel tau filament fold in corticobasal degeneration." *Nature* **580**, 283-287 (2020) DOI: 10.1038/s41586-020-2043-0

31 Y.M. Abbas, D. Wu, S.A. Bueler, C.V. Robinson, J.L. Rubinstein, "Structure of V-ATPase from the mammalian brain." *Science* **367**, 1240-1246 (2020) DOI: 10.1126/science.aaz2924

32 N.J. Cook, W. Li. D. Berta *et al*. "Structural basis of second-generation HIV integrase inhibitor action and viral resistance." *Science* **367**, 806-810 (2020) DOI: 10.1126/science.aay4919

[33] S. He, Z. Wu, Y. Tian *et al*. "Structure of nucleosome-bound human BAF complex." *Science* **367**, 875-881 (2020) DOI: 10.1126/science.aaz9761

[34] D.P. Hoffman, G. Shtengel, C.S. Xu *et al*. "Correlative three-dimensional super-resolution and block-face electron microscopy of whole vitreously frozen cells." *Science* **367**(6745): eaaz5357 (2020) DOI: 10.1126/science.aaz5357

[35] G. Kang, A.T. Taguchi, J. Stubbe, C.L. Drennan, "Structure of a trapped radical transfer pathway within a ribonucleotide reductase holocomplex." *Science* **368**, 424-427 (2020) DOI: 10.1126/science.aba6794

[36] A. Qiao, S. Han, X. Li *et al*. "Structural basis of G_s and G_i recognition by the human glucagon receptor." *Science* **367**, 1346-1352 (2020) DOI: 10.1126/science.aaz5346

[37] D. Wrapp, N. Wang, K.S. Corbett *et al*. "Cryo-EM structure of the 2019-nCoV spike in the prefusion conformation." *Science* **367**, 1260-1263 (2020) DOI: 10.1126/science.abb2507

[38] R. Yan, Y. Zhang, Y. Li, L. Xia, Y. Guo, Q. Zhou, "Structural basis for the recognition of SARS-CoV-2 by full-length human ACE2." *Science* **367**, 1444-1448 (2020) DOI: 10.1126/science.abb2762

[39] P. Schommers, H. Gruell, M.E. Abernathy *et al*. "Restriction of HIV-1 Escape by a Highly Broad and Potent Neutralizing Antibody." *Cell* **180**, 471-489.e22 (2020) DOI: 10.1016/j.cell.2020.01.010

[40] M.M. Papasergi-Scott, G. Pérez-Hernández, H. Batebi *et al.* "Time-resolved cryo-EM of G-protein activation by a GPCR." *Nature* **629**, 1182-1191 (2024) DOI:10.1038/s41586-024-07153-1

[41] D.P. Klebl, S.N. McMillan, C. Risi *et al.* "Swinging lever mechanism of myosin directly shown by time-resolved cryo-EM." *Nature* **642**, 519-526 (2025) DOI: 10.1038/s41586-025-08876-5

[42] S. Bhattacharjee, X. Feng, S. Maji *et al.* "Time resolution in cryo-EM using a PDMS-based microfluidic chip assembly and its application to the study of HflX-mediated ribosome recycling." *Cell* **187**, 782-796 e723 (2024) DOI: 10.1016/j.cell.2023.12.027

[43] L. Shen *et al.* "Structure and function of a huge photosystem I–fucoxanthin chlorophyll supercomplex from a coccolithophore." *Science* **389**, eadv2132 (2025) DOI: 10.1126/science.adv2132

[44] R. Hussein *et al.* "Cryo-electron microscopy reveals hydrogen positions and water networks in photosystem II." *Science* **384**, 1349-1355 (2024) DOI: 10.1126/science.adn6541

[45] F. Waltz *et al.* "In-cell architecture of the mitochondrial respiratory chain." *Science* **387**, 1296-1301 (2025) DOI: 10.1126/science.ads8738

[46] B.L. Nannenga, T. Gonen, "The cryo-EM method microcrystal electron diffraction (MicroED)." *Nat Methods* **16**, 369-379 (2019) DOI: 10.1038/s41592-019-0395-x

[47] B.L. Nannenga, T. Gonen, "MicroED opens a new era for biological structure determination." *Curr Opin Struct Biol* **40**, 128-135 (2016) DOI: 10.1016/j.sbi.2016.09.007

[48] R. Fernandez-Busnadiego, N. Schrod, Z. Kochovski *et al*. "Insights into the molecular organization of the neuron by cryo-electron tomography." *J Electron Microsc (Tokyo)* **60** Suppl 1: S137-S148 (2011) DOI: 10.1093/jmicro/dfr018

[49] A. Bartesaghi, C. Aguerrebere, V. Falconieri *et al*. "Atomic Resolution Cryo-EM Structure of β-Galactosidase." *Structure* **26**, 848-856 e3 (2018) DOI: 10.1016/j.str.2018.04.004

[50] A. Bartesaghi, A. Merk, S. Banerjee *et al*. "2.2 Å resolution cryo-EM structure of beta-galactosidase in complex with a cell-permeant inhibitor." *Science* **348**, 1147-1151 (2015) DOI: 10.1126/science.aab1576

[51] T. Gonen, Y. Cheng, P. Sliz *et al*. "Lipid-protein interactions in double-layered two-dimensional AQP0 crystals." *Nature* **438**, 633-638 (2005) DOI: 10.1038/nature04321

[52] M.R. Sawaya, J. Rodriguez, D. Cascio *et al*. "Ab initio structure determination from prion nanocrystals at atomic resolution by MicroED." *Proc Natl Acad Sci U S A* **113**, 11232-11236 (2016) DOI: 10.1073/pnas.1606287113

[53] W.J. Nicolas, C. Gilman, S.J. Weaver *et al.* "Comprehensive microcrystal electron diffraction sample preparation for cryo-EM." *Nat Protoc* **20**(5):1275-1309 (2025) DOI: 10.1038/s41596-024-01088-7

[54] J. Zivanov, T. Nakane, B.O. Forsberg *et al*. "New tools for automated high-resolution cryo-EM structure determination in RELION-3." *Elife* **7***:e42166* (2018) DOI: 10.7554/eLife.42166

[55] A. Peña, A. Sweeney, A.D. Cook, J. Locke, M. Topf, C.A. Moores, "Structure of Microtubule-Trapped Human Kinesin-5 and Its Mechanism of Inhibition Revealed Using Cryoelectron Microscopy." *Structure* **28**(4): 450-457.e5 (2020) DOI: 10.1016/j.str.2020.01.013

[56] S. Yuan, J. Wang, D. Zhu *et al*. "Cryo-EM structure of a herpesvirus capsid at 3.1 Å." *Science* **360**(6384): eaao7283 (2018) DOI: 10.1126/science.aao7283

[57] M.A. Herzik Jr, M. Wu, G.C. Lander, "High-resolution structure determination of sub-100 kDa complexes using conventional cryo-EM." *Nat Commun* **10**, 1032 (2019) DOI: 10.1038/s41467-019-08991-8

[58] L. Shen, Z. Huang, S. Chang *et al*. "Structure of a $C_2S_2M_2N_2$-type PSII-LHCII supercomplex from the green alga *Chlamydomonas reinhardtii*." *Proc Natl Acad Sci U S A* **116**, 21246-21255 (2019) DOI: 10.1073/pnas.1912462116

[59] A. Merk, A. Bartesaghi, S. Banerjee *et al*. "Breaking Cryo-EM Resolution Barriers to Facilitate Drug Discovery." *Cell* **165**, 1698-1707 (2016) DOI: 10.1016/j.cell.2016.05.040

[60] Y.Z. Tan, S. Aiyer, M. Mietzsch *et al*. "Sub-2 Å Ewald curvature corrected structure of an AAV2 capsid variant." *Nat Commun* **9**, 3628 (2018) DOI: 10.1038/s41467-018-06076-6

[61] F. Weis, M. Beckers, I. von der Hocht,C. Sachse, "Elucidation of the viral disassembly switch of

tobacco mosaic virus." *EMBO Rep* **20**, e48451 (2019) DOI: 10.15252/embr.201948451

62 G. Yi, D. Mamalis, M. Ye *et al.* "Covalently constrained 'Di-Gembodies' enable parallel structure solutions by cryo-EM." *Nat Cheml Biol* (2025) DOI: 10.1038/s41589-025-01972-7

63 M.S.A. Gilman, M.A. Skiba, "Hidden gems bring proteins into view." *Nat Chem Biol* (2025) DOI: 10.1038/s41589-025-01959-4

64 M. Do, S.A. Isaacson, G. McDermott, M.A. Le gros, C.A. Larabell, "Imaging and characterizing cells using tomography." *Arch Biochem Biophys* **581**, 111-121 (2015) DOI: 10.1016/j.abb.2015.01.011

65 F.K. Schur, "Toward high-resolution in situ structural biology with cryo-electron tomography and subtomogram averaging." *Curr Opin Struct Biol* **58**, 1-9 (2019) DOI: 10.1016/j.sbi.2019.03.018

66 V. Lučič, A. Rigort, W. Baumeister, "Cryo-electron tomography: the challenge of doing structural biology in situ." *J Cell Biol* **202**, 407-419 (2013) DOI: 10.1083/jcb.201304193

67 A. Burt, C.K. Cassidy, P. Ames *et al*. "Complete structure of the chemosensory array core signalling unit in an E. coli minicell strain." *Nat Commun* **11**, 743 (2020) DOI: 10.1038/s41467-020-14350-9

68 B. Turoňová, W.J.H. Hagen, M. Obr *et al.* "Benchmarking tomographic acquisition schemes for high-resolution structural biology." *Nat Commun* **11**, 876 (2020) DOI: 10.1038/s41467-020-14535-2

69 M. Schaffer, S. Pfeffer, J. Mahamid *et al*. "A cryo-FIB lift-out technique enables molecular-resolution cryo-ET within native Caenorhabditis elegans tissue." *Nat Methods* **16**, 757-762 (2019) DOI: 10.1038/s41592-019-0497-5

70 M. Beck, W. Baumeister, "Cryo-Electron Tomography: Can it Reveal the Molecular Sociology of Cells in Atomic Detail?." *Trends Cell Biol* **26**, 825-837 (2016) DOI: 10.1016/j.tcb.2016.08.006

71 R. Strack, "Structures in situ." *Nat Methods* **17**, 21 (2020) DOI: 10.1038/s41592-019-0704-4

72 Y. Zhu, C.W. Koo, C.K. Cassidy *et al.* "Structure and activity of particulate methane monooxygenase arrays in methanotrophs." *Nat Commun* **13**, 5221 (2022) DOI: 10.1038/s41467-022-32752-9

73 R. Bücker, P. Hogan-Lamarre, P. Mehrabi *et al*. "Serial protein crystallography in an electron microscope." *Nat Commun* **11**, 996 (2020) DOI: 10.1038/s41467-020-14793-0

74 A.M. Wolff, I.D. Young, R.G. Sierra *et al*. "Comparing serial X-ray crystallography and microcrystal electron diffraction (MicroED) as methods for routine structure determination from small macromolecular crystals." *IUCrJ* **7**, 306-323 (2020) DOI: 10.1107/S205225252000072X

75 M.W. Martynowycz, W. Zhao, J. Hattne, G.J. Jensen, T. Gonen, "Qualitative Analyses of Polishing and Precoating FIB Milled Crystals for MicroED." *Structure* **27**, 1594-1600.e2 (2019) DOI: 10.1016/j.str.2019.07.004

76 D. Shi, B.L. Nannega, M.J. de la Cruz *et al*. "The collection of MicroED data for macromolecular crystallography." *Nat Protoc* **11**, 895-904 (2016) DOI: 10.1038/nprot.2016.046

77 D. Shi, B.L. Nannega, M.G. Iadanza, T. Gonen, "Three-dimensional electron crystallography of protein microcrystals." *Elife* **2**:e01345 (2013) DOI: 10.7554/eLife.01345

78 M.W. Martynowycz, W. Zhao, J. Hattne, G.J. Jensen, T. Gonen, "Collection of Continuous Rotation MicroED Data from Ion Beam-Milled Crystals of Any Size." *Structure* **27**, 545-548.e2 (2019) DOI: 10.1016/j.str.2018.12.003

79 N.W. Vlahakis *et al.* "Combining MicroED and native mass spectrometry for structural discovery of enzyme-small molecule complexes." *Proc Natl Acad Sci U S A* **122**, e2503780122 (2025) DOI: 10.1073/pnas.2503780122

80 S. Mahmoudi, T. Gruene, C. Schröder *et al.* "Experimental determination of partial charges with electron diffraction." *Nature* **645**, 88–94 (2025) DOI: 10.1038/s41586-025-09405-0

81 P. Hogan-Lamarre, Y. Luo, R. Bucker, R.J.D. Miller and X. Zou, "STEM SerialED: achieving high-resolution data for ab initio structure determination of beam-sensitive nanocrystalline materials." *IUCrJ* **11**, 62-72 (2024) DOI: 10.1107/S2052252523009661

82 K. Yonekura, S. Maki-Yonekura and K. Takaba, "Applications and limitations of electron 3D crystallography." *Structure* **31**, 1328-1334 (2023) DOI: 10.1016/j.str.2023.09.007

83 M.T.B. Clabbers, A. Shiriaeva and T. Gonen, "MicroED: conception, practice and future opportunities." *IUCrJ* **9**, 169-179 (2022) DOI: 10.1107/S2052252521013063

84 X. Mu, C. Gillman, C. Nguyen and T. Gonen, "An Overview of Microcrystal Electron Diffraction (MicroED)." *Annu Rev Biochem* **90**, 431-450 (2021) DOI: 10.1146/annurev-biochem-081720-020121

85 Y. Gevorkov, A. Barty, W. Brehm *et al*. "pinkIndexer - a universal indexer for pink-beam X-ray and electron diffraction snapshots." *Acta Crystallogr A Found Adv* **76**, 121-131 (2020) DOI: 10.1107/S2053273319015559

86 J.P.F. Nunes, K. Ledbetter, M. Lin *et al*. "Liquid-phase mega-electron-volt ultrafast electron diffraction." *Struct Dyn* **7**, 024301 (2020) DOI: 10.1063/1.5144518

87 J. Knoška, L. Adriano, S. Awel *et al*. "Ultracompact 3D microfluidics for time-resolved structural biology." *Nat Commun* **11**, 657 (2020) DOI: 10.1038/s41467-020-14434-6

88 D.P. Deponte, J.T. McKeown, U. Weierstall, R.B. Doak, J.C. Spence, "Towards ETEM serial crystallography: Electron diffraction from liquid jets." *Ultramicroscopy* **111**, 824-827 (2011) DOI: 10.1016/j.ultramic.2010.11.036

89 C. Schmidli, S. Albiez, L. Rima *et al*. "Microfluidic protein isolation and sample preparation for high-resolution cryo-EM." *Proc Natl Acad Sci U S A* **116**, 15007-15012 (2019) DOI: 10.1073/pnas.1907214116

90 D. Kontziampasis D.P. Klebl, M.G. Iadanza *et al*. "A cryo-EM grid preparation device for time-resolved

structural studies." *IUCrJ* **6** 1024-1031 (2019) DOI: 10.1107/S2052252519011345

91 S. Kaledhonkar, Z. Fu, H. White, J. Frank, "Time-Resolved Cryo-electron Microscopy Using a Microfluidic Chip." *Methods Mol Biol 1764*, 59-71 (2018) DOI: 10.1007/978-1-4939-7759-8_4

92 J. Frank, "Time-resolved cryo-electron microscopy: Recent progress." *J Struct Biol* **200**, 303-306 (2017) DOI: 10.1016/j.jsb.2017.06.005

93 S. Kaledhonkar, Z. Fu, K. Caban *et al*. "Late steps in bacterial translation initiation visualized using time-resolved cryo-EM." *Nature* **570**, 400-404 (2019) DOI: 10.1038/s41586-019-1249-5

94 D.P. Klebl, S.N. McMillan, C. Risi *et al.* "Swinging lever mechanism of myosin directly shown by time-resolved cryo-EM." *Nature* **642**, 519–526 (2025) DOI: 10.1038/s41586-025-08876-5

95 J. Robert-Paganin, O. Pylypenko, C. Kikuti, H.L. Sweeney and A. Houdusse, "Force Generation by Myosin Motors: A Structural Perspective." *Chem. Rev.* **120**, 1, 5-35 (2020) DOI: 10.1021/acs.chemrev.9b00264

96 M.M. Papasergi-Scott, G. Pérez-Hernández, H. Batebi *et al.* "Time-resolved cryo-EM of G-protein activation by a GPCR." *Nature* **629**, 1182–1191 (2024) DOI: 10.1038/s41586-024-07153-1

97 E. Hand, "'We need a people's cryo-EM.' Scientists hope to bring revolutionary microscope to the masses." *American Association for the Advancement of Science, Sciencemag.org* (2020) https://www.sciencemag.org/news/2020/01/we-need-people-s-cryo-em-scientists-hope-bring-revolutionary-microscope-masses#, access date (30 March 2020)

98 K. Naydenova, G. McMullan, M.J. Peet *et al*. "CryoEM at 100 keV: a demonstration and prospects." *IUCrJ* **6**, 1086-1098 (2019) DOI: 10.1107/S2052252519012612

99 B. Carragher, Y. Cheng, A. Frost *et al*. "Current outcomes when optimising 'standard' sample preparation for single-particle cryo-EM." *J Microsc* **276**, 39-45 (2019) DOI: 10.1111/jmi.12834

100 D.P. Klebl, D.C.F. Monteiro, D. Kontziampasis *et al*. "Sample deposition onto cryo-EM grids: from sprays to jets and back." *Acta Crystallogr D Struct Biol* **76**, 340-349 (2020) DOI: 10.1107/S2059798320002958

101 N. Liu, J. Zhang, Y. Chen *et al*. "Bioactive Functionalized Monolayer Graphene for High-Resolution Cryo-Electron Microscopy." *J Am Chem Soc* **141**, 4016-4025 (2019) DOI: 10.1021/jacs.8b13038

102 H. Wei, V.P. Dandey, Z. Zhang *et al.* "Optimising "self-wicking" nanowire grids." *J Struct Biol* **202**, 170-174 (2018) DOI: 10.1016/j.jsb.2018.01.001

103 A.J. Noble, H. Wei, V.P. Dandey *et al*. "Reducing effects of particle adsorption to the air-water interface in cryo-EM." *Nat Methods* **15**, 793-795 (2018) DOI: 10.1038/s41592-018-0139-3

104 V.P. Dandey, H. Wei, Z. Zhang *et al*. "Spotiton: New features and applications." *J Struct Biol* **202**, 161-169 (2018) DOI: 10.1016/j.jsb.2018.01.002

105 I. Razinkov, V.P. Dandey, H. Wei *et al*. "A new method for vitrifying samples for cryoEM." *J Struct Biol* **195**, 190-198 (2016) DOI: 10.1016/j.jsb.2016.06.001

106 F.K. Schur, M. Obr, W.J. Hagen *et al*. "An atomic model of HIV-1 capsid-SP1 reveals structures regulating assembly and maturation." *Science* **353**, 506-508 (2016) DOI: 10.1126/science.aaf9620

107 B.A. Himes, P. Zhang, "emClarity: software for high-resolution cryo-electron tomography and subtomogram averaging." *Nat Methods* **15**, 955-961 (2018) DOI: 10.1038/s41592-018-0167-z

108 R.W. Schoenlein, S. Chattopadhyay, H.H. Chong *et al.* "Generation of femtosecond pulses of synchrotron radiation." *Science* **287**, 2237–2240 (2000) DOI: 10.1126/science.287.5461.2237

109 P. Beaud, S.L. Johnson, A. Streun *et al.* "Spatiotemporal stability of a femtosecond hard-X-ray undulator source studied by control of coherent optical phonons." *Phys. Rev. Lett.* **99**, 1–4 (2007) DOI: 10.1103/PhysRevLett.99.174801

110 K. Harkay *et al.* "Generation of short X-ray pulses using crab cavities at the advanced photon source." *Proceedings of the 2005 Particle Accelerator Conference*, Knoxville, TN, USA, 2005, pp. 668-670, DOI: 10.1109/PAC.2005.1590522

111 I.P.S. Martin, G. Rehm, C. Thomas, R. Bartolini, "Experience with low-alpha lattices at the Diamond Light Source." *Phys. Rev. ST Accel. Beams* **14**, 040705 (2011) DOI: 10.1103/PhysRevSTAB.14.040705

112 H. Ehrke, R.I. Tobey, S. Wall *et al.* "Photoinduced melting of antiferromagnetic order in $La_{0.5}Sr_{1.5}MnO_4$ measured using ultrafast resonant soft X-ray diffraction." *Phys. Rev. Lett.* **106**, 25–28 (2011) DOI: 10.1103/PhysRevLett.106.217401

113 "Advanced Photon Source Upgrade Project, Final Design Report, May 2019." Argonne National Laboratory, Document Number : APSU-2.01-RPT-003 ICMS Content ID : APSU_2032071 (2019). DOI: 10.2172/1543138

114 C.G. Schroer *et al.* "PETRA IV: the ultralow-emittance source project at DESY." *J. Synchrotron Radiat.* **25**, 1277–1290 (2018) DOI: 10.1107/S1600577518008858

115 K. Wittenburg, "PETRA IV. Upgrade of Petra III to the Ultimate 3D X-ray Microscope. Conceptual Design Report." (2019) DOI: 10.3204/PUBDB-2019-03613

116 L.C. Chapon, I. Boscaro-Clarke, A.J. Dent, A. Harrison, M. Launchbury, D.I. Stuart and R.P. Walker (Eds), "Diamond-II — Conceptual Design Report." (2019) https://www.diamond.ac.uk/dam/jcr:ec67b7e1-fb91-4a65-b1ce-f646490b564d/Diamond-II%20Conceptual%20Design%20Report.pdf, access date 12 May 2020

117 I. Boscaro-Clarke, L.C. Chapon, A.J. Dent *et al*. "Diamond-II — Advancing Science." (2019) https://www.diamond.ac.uk/dam/jcr:2ddff8c5-80fe-43aa-8a00-321be9c02cc6/Diamond%20II%20Science%20Intera

ctive%20_%20Dec%202019%20Update.pdf, access date 12 May 2020

118 I. Hargittai and M. Hargittai, "Stereochemical Applications of Gas-Phase Electron Diffraction : Part A The Electron Diffraction Technique." VCH Publishers, 1988, ISBN 0-89573-337-4

119 L.O. Browckway, "Electron Diffraction by Gas Molecules." *Rev. Mod. Phys*. **8**, 231 (1936) DOI: 10.1103/RevModPhys.8.231

120 J.C. Williamson and A.H. Zewail, "Ultrafast Electron Diffraction. 4. Molecular Structures and Coherent Dynamics." *J. Phys. Chem*. **98**, 11, 2766-2781 (1994) DOI: 10.1021/j100062a010

121 B.J. Siwick, J.R. Dwyer, R.E. Jordan, R.J. Miller, "An atomic level view of melting using femtosecond electron diffraction." *Science* **302**, 1382-1385 (2003) DOI: 10.1126/science.1090052

122 A.A. Ischenko, P.M. Weber, R.J.D. Miller, "Capturing chemistry in action with electrons: Realization of atomically resolved reaction dynamics." Chem. Rev. **117**, 11, 11066 (2017) DOI: 10.1021/acs.chemrev.6b00770

123 T. Ishikawa, S.A. Hayes, S. Keskin *et al*. "Direct observation of collective modes coupled to molecular orbital-driven charge transfer." *Science* **350**(6267): 1501-1505 (2015) DOI: 10.1126/science.aab3480

124 Y. Morimoto and P. Baum, "Diffraction and microscopy with attosecond electron pulse trains." *Nature Phys* **14**, 252-256 (2018) DOI: 10.1038/s41567-017-0007-6

125 J. Yang, M. Guehr, T. Vecchione *et al*. "Diffractive imaging of a rotational wavepacket in nitrogen molecules with femtosecond megaeletronvolt pulses." *Nat Commun* **7**, 11232 (2016) DOI: 10.1038/ncomms11232

126 S.P. Weathersby, G. Brown, M. Centurion *et al*, "Mega-electron-volt ultrafast electron diffraction at SLAC National Accelerator Laboratory." *Rev. Sci. Inst* **86**, 073702 (2015) DOI: 10.1063/1.4926994

127 J. Yang, X. Zhu, T.J.A. Wolf *et al*. "Imaging CF_3I conical intersection and photodissociation dynamics with ultrafast electron diffraction." *Science* **361**, 64 (2018) DOI: 10.1126/science.aat0049

128 T.J.A. Wolf, D.M. Sanchez, J. Yang *et al*. "The photochemical ring-opening of 1,3 cyclohexadiene imaged by ultrafast electron diffraction." *Nat. Chem*. **11**, 504-509 (2019) DOI: 10.1036/s41557-019-0252-7

129 E.J. Sie, C.M. Nyby, C.D. Pemmaraju *et al*. "An ultrafast symmetry switch in a Weyl semimetal." *Nature* **565**, 61-66 (2019) DOI: 10.1038/s41586-018-0809-4

130 L. Ma *et al.* "Ultrafast x-ray and electron scattering of free molecules: A comparative evaluation." *Struct. Dyn*. **7**(3):034102 (2020) DOI: 10.1063/4.0000010

Appendix 2: Complementary Technologies and Future Upgrade Opportunities

A2.1 Complementary pulsed X-ray technologies

Two nascent compact pulse X-ray source technologies based upon electron pre-bunching and radiation either in an undulator or via inverse Compton scattering are discussed. These technologies hold promise of short X-ray pulses, albeit at much lower peak powers and repetition rates than a full scale XFEL. These ideas are being developed at UCLA and Arizona State University, where demonstration systems are being built. If these demonstrations are successful, we recognise synergies with a next-generation XFEL in providing additional X-ray pulse pumping/probing capability, and the possibility of their use as sources for hard X-ray seeding in a future enhancement of the XFEL.

Only a multi-GeV superconducting facility can cover the full range of next-generation XFEL user requirements, in particular the requirement for high photon flux and millijoule pulse energies and multiple simultaneous experiments. This is because the XFEL is a device for converting electron beam kinetic energy into photon beam energy and, while it may be possible to produce HXR photons with significantly lower beam energies, there are two fundamental factors which compound one another to limit the flux. First, to obtain the required wavelength with a low energy beam, the undulator period must be very short. Technologies are available, or under development, to achieve this, but the efficiency of the FEL, i.e. the fraction of electron beam power converted to photon beam power, scales with undulator period so will be low with a short undulator period. Second, the electron beam power is itself proportional to the beam energy. Taken together, these two factors prohibit the production of high photon flux and mJ pulse energies from a low energy facility. To obtain FEL pulses appropriate for high energy density science, multi-GeV electron beams are essential.

Proposals are, however, under development for compact, university scale, accelerator-based HXR sources. Such sources can be seen as complementary, offering pulse energies only a few percent of that available from a full-scale facility, but which may be appropriate for some science applications, as discussed below. By co-locating such sources at a large facility, they could provide additional pump-probe capability and potentially be used as HXR seed sources. It is therefore a potential future upgrade path to incorporate such a compact X-ray source at a next-generation XFEL. **Table A2.1** shows the main parameters of two well developed proposals.

The first concept is from UCLA[1] (UC-XFEL). It features high gradient cryogenically-cooled accelerating sections and a short period cryogenically-cooled undulator. The electron bunch would be modulated with a laser and converted into a train of microbunches – by doing so, the beam quality in each low charge microbunch can be conserved, and the peak current in each microbunch is high enough that FEL saturation is reached in a few metres. The micro-modulated beam is less susceptible to wakefield degradation in the undulator than a conventional bunch, allowing a very small gap of 2 mm, so that the undulator period can be made very short whilst maintaining sufficient on-axis field. For this reason, 8 keV photons might be produced with a beam energy of only 1.6 GeV the pulse energy is predicted to be around 12 μJ.

The second proposal is by Arizona State University[2] (CXFEL), with funding secured for construction and experimental verification, and development is ongoing. The hard x-ray CXLS (Inverse Compton Scattering) source is currently being commissioned, whilst the CXFEL (soft x-ray coherent laser) is being constructed. The method for the CXFEL is to generate a pre-bunched electron beam by translating the transverse diffraction pattern of the electron beam incident on a nano-patterned silicon crystal into a longitudinal modulation. The photons are then emitted through coherent Inverse Compton Scattering off an incident laser, demonstrating good temporal coherence with a pulse energy of 0.13 μJ. This source could potentially be used as a direct HXR seed for an FEL amplifier driven by a multi-GeV beam, because the peak power is sufficient to dominate the noise from the SASE process.

Table A2.1: Performance parameters (simulated) of the UCLA and Arizona State University compact light source projects

Performance parameter	UC-XFEL [1]	CXFEL [2]
Beam Energy	1.6 GeV	35 MeV
Photon Energy	7.8 keV	8 keV
Peak Power	8 GW	2 MW
Pulse Energy	12 µJ	0.13 µJ
Bandwidth	0.1%	0.01%
Repetition Rate	100 Hz	1 kHz
Facility Length	40 m	10 m

A2.2 Plasma and laser wakefield acceleration

Plasma and laser wakefields are promising concepts for electron acceleration that are likely to have technology impact in the future. While this technology is advancing rapidly, it remains insufficiently mature to replace a MHz-repetition-rate conventional linear accelerator in a next-generation XFEL in the foreseeable future. However, we identify strong synergies and opportunities to enhance the capabilities of a next-generation XFEL facility, by incorporating laser wakefield capability at some end-stations, and integrating plasma wakefield accelerator test beamlines into the facility design as potential upgrade paths to energy and brightness booster stages.

Plasma wakefield accelerators utilise the huge electric fields generated within plasma waves driven by intense laser pulses or particle beams. These fields are of order 100 GV m^{-1}, or around one thousand times greater than those possible with conventional radio-frequency (RF) technology. In addition to being extremely compact, plasma accelerators generate electron bunches with several highly desirable properties. These include:

- few-femtosecond bunch duration
- multi-kA peak current
- sub-micron normalised transverse emittance, with prospects for reaching emittances in the nanometre range
- for laser-driven or hybrid plasma accelerators, tight synchronisation with an ultrafast laser system.

To date, plasma accelerators have accelerated electrons to tens of GeV energies in accelerator stages only a few tens of centimetres long [3,4,5,6,7,8] . The electron bunches they produce have been used to generate radiation from 100 eV to GeV in magnetic undulators[9,10], via betatron oscillations in the plasma accelerator[11,12], and by Compton scattering[13,14,15,16,17]. They have also been used to generate positron beams[18] , positron-electron plasmas[19], pions[20], and muons[21] and have been employed in fundamental physics tests[22,23].

Compared to superconducting RF linac technology laser driven electron accelerators have a major weakness, low repetition rate, set by the limits of the available high power laser technology. Although progress has been made with laser technology over several decades current limits of a few to a few tens of Hz make laser driven accelerators unsuitable for a high throughput multiplexed facility as required by the next generation criteria. Plasma wakefield accelerators, that accelerate a following electron bunch in the wakefield of a first bunch, are promising as an add-on to a superconducting RF linac based facility as their repetition rate is set by the linac and not by the repetition rate of a high power laser.

The UK is a world leader in the development of both laser-driven and electron-driven plasma wakefield acceleration (laser wakefield accelerators (LWFA) and plasma wakefield accelerators (PWFA), respectively). This work is coordinated by the Plasma Wakefield Accelerator Steering Committee (PWASC, http://pwasc.org.uk/), which represents UK universities, ASTeC, the CLF, and the two Accelerator Institutes. In 2019, the PWASC summarised the rapid developments in plasma wakefield accelerators, and published a roadmap[24] for research and development to 2040. The potential of laser wakefield accelerators, and the applications they enable, has proved a major driver for significant investments, such as the Extreme Photonics Application Centre (EPAC) at RAL, the Compact Linear Accelerator for Research and Applications (CLARA) at Daresbury Laboratory, and university-centred initiatives including the Scottish Centre for the Application of Plasma-based Accelerators (SCAPA) and upgrades to several university-based systems across the UK. The importance of novel accelerator science has also been recognised by STFC, which selected the UK Novel Accelerator project as a 'priority project'.

The repetition rate, energy gain and bunch properties of plasma accelerators continue to improve[25,26] and the number of applications they enable continues to grow. Recently the group at DESY

demonstrated active compression of a laser accelerated electron beam with energy spread and stability suitable for electron beam injection into a compact storage ring[27]. Current laser technology is limiting the repetition rate of laser-driven, GeV-scale plasma accelerators to around 10 Hz, but a variety of approaches for increasing the repetition rate of LWFAs is being pursued. One approach is the development of more efficient, higher-repetition rate lasers, such as the CLF's DiPOLE technology. A complementary approach is the use of different methods for driving the plasma wave; for example, in the multi-pulse approach[28,29], the drive energy is delivered over many plasma periods, which allows the use of novel lasers, such as thin-disk lasers, that can deliver picosecond-duration, joule-class laser pulses with high wall-plug efficiency and at multi-kHz repetition rates. Also, recently, laboratory-scale PWFA stages powered by LWFA-generated electron beams (known as 'Hybrid PWFA2LWFA') have made significant experimental progress[30,31,32] . This growing maturity is supported by increasing international collaboration, further accelerating its path toward real-world application.

To improve the quality of the electron bunches, potentially transformative prospects are being pursued through projects such as the STFC PWFA-FEL, H2020 EuPRAXIA and NeXource. One prospect, the use of plasma photocathodes ('Trojan Horse'), offers the potential to improve the stability, energy spread[33], emittance and brightness[34] by orders of magnitude, and reached LCLS-level emittances in the first proof-of-concept. If optimised, these electron beams could become orders of magnitude brighter than even those used in state-of-the-art hard X-ray facilities today. It is worth noting that laser-plasma accelerators and hybrid plasma wakefield accelerators[35] offer intrinsic time-synchronisation, for example, for pump-probe experiments.

Although very promising, this new accelerator technology is not yet at a point that would allow a coherent X-ray light source MHz-repetition-rate facility to be planned around it. However, high profile CDR-level studies explore pathways of employing plasma accelerators for applications in light sources and high-energy physics in the future[36,37]. In recent years plasma accelerators have made significant advances in the levels of energy spread, emittance, and shot-to-shot stability which, in the best cases, can approach those delivered by conventional linacs. The high-repetition-rate bunches delivered by the next-generation XFEL linac could be used to drive a high average power PWFA stage due to the nanosecond-scale plasma recovery time[38]. However, for laser wakefield accelerators, the high pulse energy required limits the repetition rates to around 10 Hz with today's laser technology. In contrast the "first generation XFELs" operate at ~100 Hz and the "second generation" at 1 - 1000 kHz. As reflected in this Science and Technology Case, there is a widespread demand for these higher repetition rates across the proposed applications. While the quality and repetition rate of beams from plasma accelerators obtained experimentally are currently far below those from conventional linac technology, prospects for improving both could add unique opportunities for a next-generation XFEL in future upgrades.

Synergies between plasma wakefield acceleration and XFEL output and performance are strong. Consequently, it appears opportune to integrate laser- and electron-beam driven plasma wakefield acceleration capabilities and capacities into the design of a future, cutting-edge XFEL machine, although significant R&D would be required. Auxiliary compact betatron[10,11] or inverse Compton scattering-based secondary light sources[13,14] (e.g. for poly-X-ray beam illumination), with tight synchronisation to ultrafast visible lasers, could complement these features, as discussed in **Chapters 3** and **4**. Plasma wakefield accelerators and laser-driven plasmas and auxiliary radiation sources are already employed in XFELs, such as the Matter at Extreme Conditions station at LCLS and the HIBEF beamline at the European XFEL. Driving FELs directly with plasma accelerators is a goal that is being pursued by several groups worldwide, with FEL gain being reported recently[39,40,41] . Furthermore, in view of the superior emittance and brightness offered, programmes have been initiated at Daresbury Laboratory, within the UK XFEL CD-OA project and SLAC (for example, via the STFC PWFA-FEL project), and at DESY, to integrate plasma accelerators into existing and future (X)FELs such as UK XFEL design, as discussed in **Section 3.6**. Using PWFA at the next-generation XFEL facility would enable additional capabilities, including the use of plasma stages to boost the bunch energy (by a factor of two to five), and the use of plasma photocathodes as compact electron brightness afterburners (which could

increase brightness by up to 100,000 times). Such an energy and brightness plasma booster stage for XFELs[42] would open pathways to higher photon energies at reduced electron energies and/or sub-femtosecond, higher brilliance photon pulses, and intrinsically synchronised pump-probe multi-colour experiments. Unlike LWFA schemes these PWFA can run at the repetition rate of the driving SC Linac and so the upgrade path can be achieved with no loss of capacity. Recently, a conceptual simulation study highlighted a pathway toward a plasma-driven, attosecond–Ångstrom-class XFEL module with prospects for enabling very hard photon energies[43], which can be integrated as energy and brightness plasma booster stage at existing and future (X)FELs such as a next-generation XFEL (see **Figure A2.1**).

Plasma wakefield accelerators are compact and highly flexible and could be implemented after the FEL undulator stages or in dedicated test beamlines, to provide energy and brightness afterburners for unique water-window mJ-class soft XFELs pulses[44] and exploitation of novel XFEL modalities in compact undulators instead of wasting the electrons in beam dumps. A dedicated research stations could also be used for related applications, such as high-field science[22,23] and exploration of PWFA staging physics towards high-energy physics. For example, realisation of Hybrid PWFA2LWFA in collider geometry at a dedicated end-station would allow colliding ultra-high-brightness electron beams at multi-GeV energies and, in combination with fs-duration TW–PW-class laser pulses, could open novel research modalities[45]. These extreme electron beams (X-Beams) with extreme number densities, high field strengths and ultrashort durations achievable in plasma-based accelerators in turn could reveal novel beam-matter interactions via field and impact ionisation physics and strong-field QED signature for unparalleled opportunities to probe the frontiers of fundamental physics[45,45]. Bringing together researchers with expertise in conventional accelerators, plasma accelerators and XFELs is likely to promote advances at the interface of these disciplines and beyond, such as the development of novel lasers, fusion reactor and XFEL diagnostics.

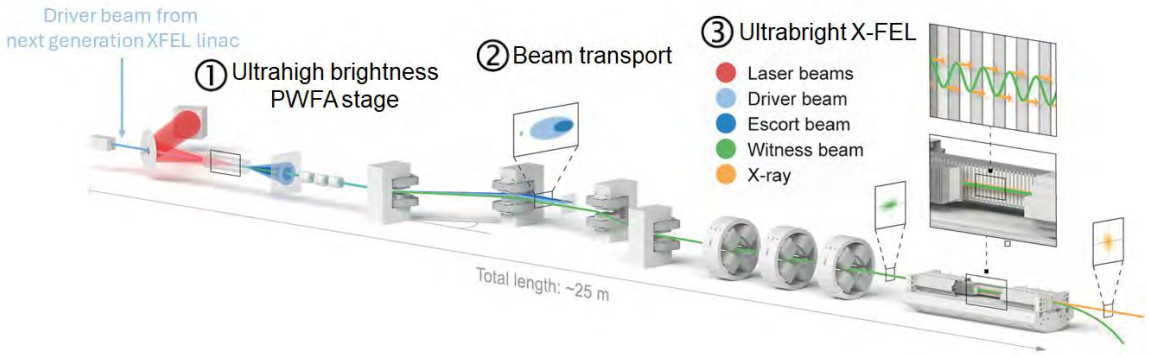


Figure A2.1: PWFA energy and brightness booster stage for a next-generation XFEL

Figure reproduced from A. F. Habib et al. Nat Commun 14, 1054 (2023) under the terms of a Creative Commons Attribution License 2.0.
DOI: 10.1038/s41467-023-36592-z

We see incorporation of a plasma wakefield capability as a potential future upgrade path to provide a higher energy, high rep-rate, ultrahigh brightness electron beams for a harder X-ray high rep-rate XFEL. These unique capabilities will ensure that the next-generation XFEL machine remains at the forefront of accelerator R&D for years to come.

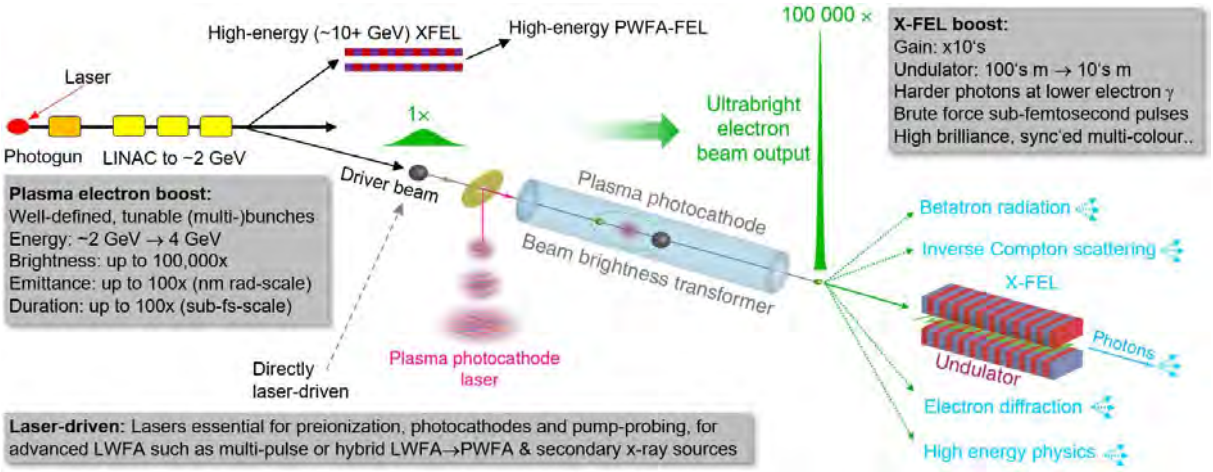


Figure A2.2: Schematic diagram of the capabilities enabled by combining XFEL beamlines and plasma accelerators

A2.3 High harmonic sources

High order harmonic generation (HHG) driven by high power ultrashort pulse optical lasers is a standard technique for generating short wavelength coherent radiation in the 10 – 500 eV photon energy range. Until the recent eSASE demonstration, it was the only way to generate attosecond pulses and remains the workhorse for attosecond science. Although pulse energies are low, it is a compact and versatile method that naturally offers itself for incorporation into XFEL pump-probe experiments.

Both HHG-based attosecond sources and XFELs are now established methods for generating light of unique characteristics. HHG driven by infrared lasers was first studied by the Saclay team of L'Huillier, for which she was awarded the 2023 Nobel Prize in Physics, along with Agostini and Krausz, for the discovery and development of attosecond physics and technology.[1] HHG and XFELs are both sources of short wavelength (VUV to X-ray), ultrashort light pulses with durations in the range 100 fs to < 0.25 fs (250 attoseconds). This is having an impact through the rich scientific applications so far achieved. In the scientific sphere, both have proved extraordinary in enabling things not possible before. Both are unique tools that are finding growing applications in science and technology. For HHG sources, the brightness in the spectral range from 10 – 100 eV has proved sufficient to enable a wide range of applications, for example in time-resolved photoelectron spectroscopy, coherent diffraction imaging and time-resolved absorption spectroscopy in a variety of settings including surface science, photochemical reaction dynamics, time-resolved band structure imaging, nanostructure and biological structure imaging.

A significant number of facility scale beamlines have been developed at institutions around the world with some made available to a wider user base (e.g. Artemis (CLF) in the UK, various LaserLab Europe facilities, and the ELI facilities) and a number of commercialisations are now being made available. The importance is reflected in a significant level of public investment in these facilities, amounting to hundreds of millions of Euros globally. There has been a steady stream of applications, and it is clear that this capability is firmly established in the repertoire of ultrafast probing methods available to science and technology. HHG has been widely applied as a short pulse (femtosecond domain) source of coherent X-rays for imaging and time-resolved spectroscopy applications[46,47,48].

A unique selling point of HHG sources has been the potential to do something hitherto no other source could – to provide sub-femtosecond time domain pulses for directly measuring and controlling electronic dynamics in matter. This latter possibility termed *attosecond science* has generated a great deal of excitement and effort over the past two decades. This is not surprising as HHG is an enabling tool to probe the most fundamental events of electronic dynamics in matter. There have been remarkable developments and insights obtained over the years from laboratories all around the world. The first unambiguous confirmation of the production of attosecond pulses (a pulse train) in HHG was carried out using a side-band modulation (RABBIT) method by Agostini's group at Saclay[49]. The sideband method has now been widely used with considerable success in characterising ionisation (phase) delays at the attosecond level in atoms and molecules, with work progressing in a number of groups around the world. The first demonstration of isolated attosecond pulses was, however, made by the MPQ Garching group of Krausz using the streaking idea. Isolated pulses are an essential measurement tool for the most general implementation of attosecond science[50,51,52,53,54,55] . More recently attention has also turned to attosecond electron control concepts in condensed phase systems[56,57], new concepts in ultrafast field metrology[58] and applications towards photochemistry[59,60,61]. The field continues to flourish and expand backed by accompanying technical work pushing HHG attosecond sources deeper into the soft X-ray range.

A large-scale European facility the ELI-ALPS (Extreme Light Infrastructure – Attosecond Light Pulse Source) in Szeged, Hungary, illustrates the maturity of the technology and the confidence for impact. This facility concentrates on delivering XUV attosecond capability (up to 100 eV) with (for HHG sources)

[1] https://www.nobelprize.org/prizes/physics/2023/summary/

unprecedented brightness. Pulse energies of 100s nJ are likely in the lower photon energy range of operation, below 30 eV, with pulse energies approaching the microjoule range have been demonstrated using high power drive lasers. Potentially this is an excellent complement to the soft-X-ray ESASE capabilities being developed at XFELs such as Fermi, Flash and LCLS, and which we anticipate also being an integral part of any next-generation XFEL. HHG is now reaching into the soft X-ray range[62], but above 100 eV the demonstrated efficiency of HHG falls rather rapidly[63] (see **Figure 3.8**). This is due to scaling limits placed on efficiency when the required longer wavelength lasers are used[64], so that pJ pulses are likely to remain the norm in the soft X-ray range. In contrast, eSASE has so far shown exceptional brightness between 500 – 1000 eV (> 20 μJ pulses across this range with no fall off with photon energy)[65]. SXR HHG research will still continue to be an important area for the time being and even in the long term, especially where perfect synchronisation to optical fields is required and for exploratory and complementary studies in collaboration with XFELs. Future eSASE developments are likely to extend this range down towards 100 eV and have already been established into the hard X-ray range. Although currently eSASE pulses are somewhat longer than the best HHG-based sources (by around a factor of five), we should anticipate continued improvement in pulse duration especially as harder X-rays are developed. Current HHG sources, nor none currently predicted, can compete with the eSASE FEL attosecond pulse brightness in the X-ray range.

Nevertheless, high repetition rate drive lasers based on OPCPA and fibre laser technology are now making an impact, even on attosecond generation[66]. These are pushing towards the MHz repetition rate with moderate pulse energies sufficient for reaching the XUV via HHG. We can therefore expect significant improvements in average flux performance in the XUV. Therefore, we anticipate XFEL-based sources to be dominant in attosecond applications above 100 eV photon energy, whilst HHG-based systems will continue to be competitive and probably the source of choice up to around 100 eV. For non-linear X-ray interactions, diffract-and-destroy and other single shot measurement schemes and probing hot plasmas XFELs will dominate across the XUV – X-ray range.

An alternative route to HHG, based upon the relativistic acceleration of particles at surfaces, has excited substantial interest over the last decades[67]. Development at various laser facilities has proceeded to improve the performance and to establish attosecond capability[68,69] .These sources promise to be high brightness with significant energy conversion efficiency from the laser pulse to the HHG. Currently proven performance is limited to the soft X-ray range. Moreover, a relativistic laser intensity (> 10^{18} W cm^{-2}) is required, which limits the repetition rate to around 10 Hz at current laser technology. Efforts to develop these sources continue at facilities such as ELI-ALP and through laser development programmes and so, in the longer term, they may prove more competitive, although they cannot form the basis of a facility plan at the current time.

Importantly the availability of XUV pump sources based on HHG alongside higher photon energy XFEL based eSASE sources at a facility end-station is an exciting and so far untapped opportunity that should add considerable additional attosecond and ultrafast measurement capability. It is thus likely that there will be substantial synergy with HHG sources at future XFEL facilities, especially as techniques for synchronisation and time stamping improve to the sub-femtosecond range. We would plan to make such capability an integral part of the facility at some end-stations, as the incremental cost of setting this up beyond the already installed high-repetition rate femtosecond lasers is on the order of just £100k.

A2.4 Energy Recovery Linac upgrade

An Energy Recovery Linac (ERL) is a potential future upgrade to a next generation XFEL. It would enable two unique research and development platforms: a prototype production platform for XUV semiconductor chip manufacture, and a high brightness gamma ray source. Both of these platforms would offer an enormous boost to industrial applications of the facility.

A next-generation XFEL machine already offers enormous potential for science and technology advances and for supporting critical industries. An Energy Recovery Linac (ERL) is a potential future upgrade that we envision could build upon the infrastructure already in place for a next-generation XFEL. Such an upgrade would not substantively impact the operation of the rest of the facility, but would provide a high current, high repetition rate, energy tuneable electron beam that could drive two platforms that will enable technology and industrial applications – an XUV beamline for advance lithography and chip manufacture, and the brightest gamma-ray source in the world to serve the needs of the nuclear industry. This upgrade would provide unique additional capability and could be delivered after the main facility is fully operational if the baseline design makes an allowance for the space and electron beam configurations to enable such a future step.

A2.4.1 Extreme ultraviolet lithography

Standard lithography of semiconductor chips with ArF laser-produced 193 nm radiation is gradually being augmented/replaced by the finer patterning enabled by 13.5 nm illumination, referred to in the industry as EUV lithography. This is the main contemporary technique allowing the industry to keep up with Moore's Law. Currently, EUV is produced through the excitation of a tin or xenon plasma with an excimer laser (Laser Produced Plasma, LPP), and commercial scanners can now produce EUV at 600 W[70]. It is recognised that substantially more power will be required in the future, and that this will require a technology change, as will any industry move to beyond-EUV. A promising alternative to LPP at chip fabrication plants would be the deployment of an EUV-FEL capable of operating at multi-kW average power. Such a possibility has been investigated in detail by ASML, the leading established company in lithography apparatus, and additionally by xLight, a venture-backed start-up. However, to date the low level of technical maturity of FELs has prohibited commercial commitment.

The global semiconductor industry recognises FELs as a promising future EUV production technology, as evidenced by engagement with the yearly EUV-FEL workshop[71]. The KEK laboratory in Japan is currently most advanced in addressing the R&D needs for a high-power EUV-FEL. It is adapting its 20 MeV ERL to drive a FEL, albeit at infrared wavelengths[72] . There is a clear need for a high-power EUV-FEL test facility to conduct R&D, but it does not exist anywhere in the world at this time.

Driving a soft X-ray FEL with a ~1 GeV ERL would enable multi-kW production of EUV. This would benefit the global semiconductor industry by allowing the study of FEL capabilities at an industrial output level, and developing and proving kW-capable EUV optical elements/beamlines for photon transport to chip scanners. Such a flexible, industrial research-led tool would also facilitate investigations beyond the current industry state-of-the-art. The superior flexibility and controllability of FEL photons as compared to 'brute-force' LPP photons would have far-reaching implications for many diverse aspects of lithography. Examples of this could include shorter wavelengths, or indeed variation of wavelength (two-colour exposures), variation of polarisation or transverse coherence in differentiating patterning layers, or generation of orbital angular momentum photons to manipulate helicity within a wafer. There is clear potential for novel semiconductor devices to be developed utilising such source capability.

A2.4.2 Inverse Compton Scattering gamma source

The use of Inverse Compton Scattering (ICS) with the primary 8 GeV beam is a possibility with the Conceptual Design. A still more versatile and internationally unique ICS gamma source could be developed with a future ERL upgrade. The injector and first ~1 GeV of the superconducting electron accelerator at MHz repetition rate could be readily adapted to include Energy Recovery (SC-ERL). The

resulting capability to produce high average electron currents (10 –100 mA) would enable a high-flux, narrowband gamma source based on ICS.[73,74]

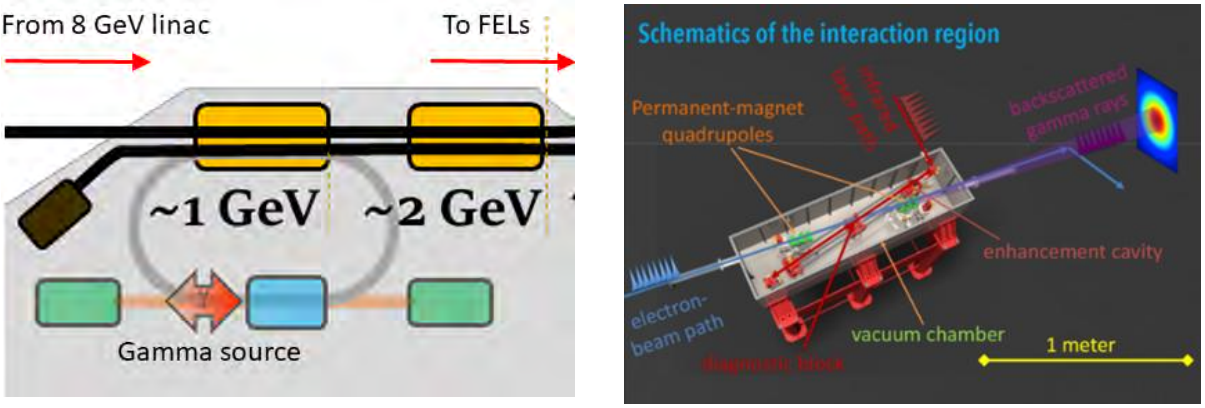


Figure A2.3: (Left) Illustration of ERL-driven ICS gamma source located within a full next-generation XFEL facility and (right) details of example laser-electron interaction point, comprising high finesse four-mirror bowtie laser cavity and permanent magnet quadrupole focused electron spot

Figure courtesy of Philippe Piot

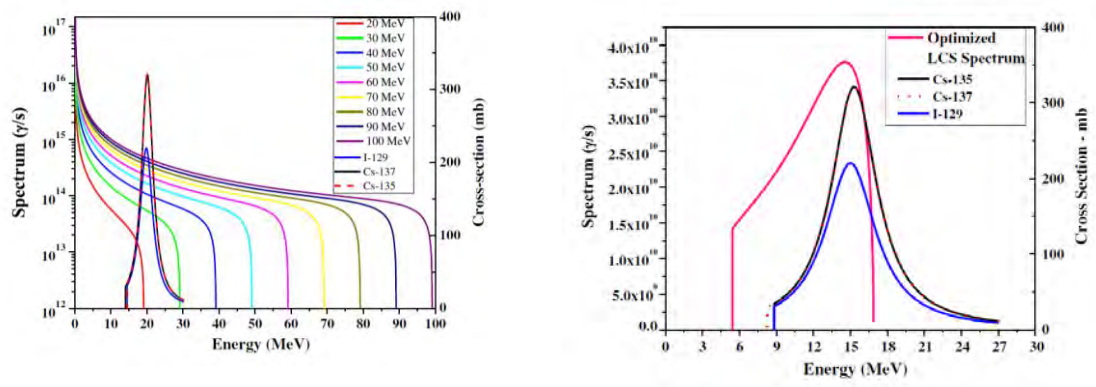


Figure A2.4: (Left) Bremsstrahlung and (right) collimated ICS gamma spectra compared to photonuclear dipole resonances of Cs-135, Cs-135 and I-129 (right only).[75]

Reprinted by permission from John Wiley & Sons, Ltd: H.U. Rehman et al. International Journal of Energy Research 42, 236-244. DOI: 10.1002/er.3904 Copyright (2017)

The production of 1 – 100 MeV gamma-rays via ICS of relativistic electrons in an external laser field results in gamma properties fundamentally improved with respect to standard bremsstrahlung generation. Bremsstrahlung is broadband emission peaked at low energy with a cut-off at the electron energy. ICS has a correlation between the angle of emission and energy; therefore, in combination with angular collimation, narrowband (or 'monoenergetic') gamma beams can be produced.[76,77] In addition, ICS preserves the polarisation of the incident laser. Presently the world's brightest narrowband gamma source is the High Intensity Gamma Source (HIGS) at Duke University.[76] The EU-funded Extreme Light Infrastructure – Nuclear Physics (ELI-NP) Variable Energy Gamma (VEGA) System is in the construction phase in Magurele, Romania.[77]

To quantify the potential of an ICS source driven by an SC-ERL enabled XFEL front end, initial calculations of the source properties have been produced and are shown in **Table A2.2** and **Figure A2.5**. This ICS source has a spectral energy density at least two orders of magnitude greater than HIGS, and is likely to similarly exceed the performance of ELI-NP-GBS. It should be noted that this calculation assumes conservative, previously demonstrated, parameters and should therefore be viewed as a lower bound. Narrowing the energy bandwidth below 0.5% whilst retaining significant flux, as shown in **Table A2.3**, will enable the resolution of individual nuclear excitations according to the nuclear shell model.

Table A2.2: Conservative input parameters used for ICS source calculation for electron beam and laser system

This covers the nominal gamma energy from 1 - 100 MeV using the electron beam extracted at three locations. The laser-electron interaction point assumes a Fabry-Perot bowtie like resonator cavity, as demonstrated at KEK.[78]

Beam Parameters	Value		
Beam Energy (MeV)	340	680	1020
RF Frequency (MHz)	802		
Repetition Rate (MHz)	100		
Bunch Charge (pC)	100		
Average Beam Current (mA)	10		
Normalised Transverse Emittance (mm-mrad)	0.5		
Recoil Parameter	0.006	0.012	0.018

Nd:YAG Laser System Parameters	Value
Wavelength (nm)	1064
Repetition Rate (MHz)	100
Pulse Energy (µJ)	100
Average Stored Cavity Power (kW)	10
Spot Size at IP (circular spot) (µm)	25
Stored Pulse Width (ps)	5.7
Field Strength of the Normalised Laser Vector Potential a_0	6.05×10^{-4}

Table A2.3: Resulting ICS source brilliances and spectral energy densities for the three extracted electron beam energies detailed in Table A2.2

Parameter Beam Energy	γ-ray Peak Energy (MeV)	Flux per Shot (ph)	Band-width	Flux	Average Brilliance (ph/s mm^2-mrad^2)	Peak Brilliance (ph/s mm^2-mrad^2)	Spectral Density (ph/s eV)
340 MeV	2.05	4076	Raw	4.08×10^{11}	–	–	–
			0.50%	6.24×10^{9}	2.79×10^{14}	3.77×10^{16}	2.41×10^{5}
			0.10%	4.05×10^{9}	1.81×10^{13}	2.45×10^{15}	7.81×10^{4}
680 MeV	8.17	4750	Raw	4.75×10^{11}	–	–	–
			0.50%	6.24×10^{9}	1.12×10^{15}	1.51×10^{17}	6.01×10^{4}
			0.10%	4.08×10^{8}	7.32×10^{13}	9.88×10^{15}	1.96×10^{4}
1020 MeV	18.27	5027	Raw	5.03×10^{11}	–	–	–
			0.50%	6.24×10^{9}	2.52×10^{15}	3.40×10^{17}	2.67×10^{4}
			0.10%	4.11×10^{8}	1.66×10^{14}	2.24×10^{16}	8.79×10^{3}

Simulated improvement in the knowledge of an example photonuclear cross-section is shown in **Figure A2.5**. The ICS source would be a step change in high-flux, tunable, narrowband gamma production. As such, it would lead to the establishment/consolidation of a new field of science, Nuclear Photonics, named by analogy to the field of atomic photonics opened up by lasers from the 1960s.

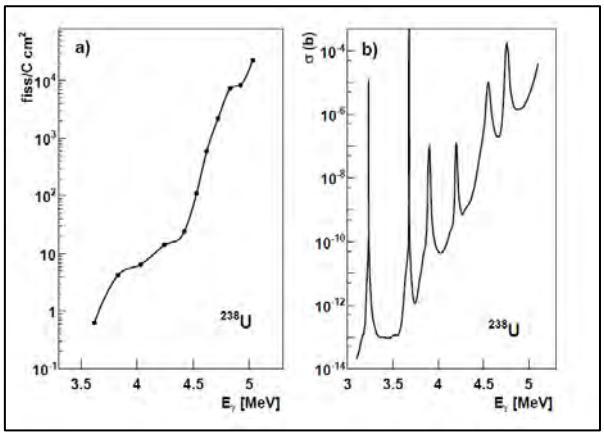


Figure A2.5: (Left) Observed, bremsstrahlung induced photo-fission Giant Dipole Resonance (GDR) of ^{238}U, and (right) predicted "hidden" resonances within GDR revealed by an ICS narrowband gamma source.[79]

Figure reproduced from P.G. Thirolf et al. EPJ Web of Conferences 38, 08001 (2012) under the terms of a Creative Commons Attribution License 2.0. DOI: 10.1051/epjconf/20123808001

In particular, the use of fully linearly-polarised gamma beams in photon induced reaction results in distinct angular distributions for the two transition multipolarities (electric E or magnetic M), and the associated excitation modes can then easily be disentangled. Hence, ICS gamma beams are a sensitive probe of the nuclear electric (E1)[80] and magnetic (M1)[81] dipole response. Since the photon is not charged, for an interaction it physically needs to hit the object nucleus, resulting in a low scattering cross-section. In order to compensate for this, existing facilities use large amounts of target material (order of grams is required), which limits the application to stable or quasi-stable nuclei with a half-life in the order of 100 years. The 100-fold increase in flux enabled by an SC-ERL driven source will eliminate this restriction.

The E1 response is dominated by the well-known Giant Dipole Resonance (GDR).[82,83] In the last two decades, however, an additional E1 contribution has been established on the low-energy tail of the GDR. This so-called Pygmy Dipole Resonance (PDR)[84,85] is located near the particle thresholds and has been shown to have an enormous influence on neutron capture rates as encountered in the astrophysical rapid and slow neutron capture processes,[86] which synthesise all chemical elements heavier than iron. The PDR is often visualised as an oscillation of a neutron skin versus a core with nearly equal proton and neutron numbers, although this interpretation is controversial. Nevertheless, this geometric interpretation suggests a connection to the asymmetry term of the nuclear equation of state, required to describe properties of the heaviest known objects: neutron stars. Recently, the PDR has even been linked to the reactor antineutrino anomaly,[87] which causes a previously unexplained heat generation in operational nuclear reactors.

For the M1 response, the Gamow-Teller (spin-isospin) resonances are of particular importance, dominating inelastic neutrino-nucleus interactions. These provide an additional heating to supernova type-II events, which otherwise would not explode.[88] Furthermore, they are mandatory in order to reliably estimate the cross-sections for neutrino detectors (e.g. see [89]).

Various interesting physics cases are not feasible with the gamma fluxes presently available (HIGS) or at facilities under construction (ELI-NP-VEGA), but would become so with an SC-ERL driven ICS source. One example is the investigation of the E1 response of the octupole-correlated nucleus ^{226}Ra ($T_{1/2}$ = 1600 years), which very likely has a strong quadrupole-octupole coupling enhanced CP-violating Schiff moment in the ground state.[90] Recently, admixtures of the low-lying E1 strength have been proposed as a second enhancement mechanism.[91] Another example is the measurement of parity violating physics exploiting $J^{\pi} = 1^{\pm}$ parity doublets (close lying 1- and 1+ levels) as, for example, found in ^{20}Ne.[92]

In the context of particle physics, the ICS gamma source would enable unprecedented measurements of Delbrück scattering (QED vacuum) and light-by-light scattering. A SC-ERL driven ICS source would

not only be of great interest in academic physics and astrophysics, but would also have direct societal and economic benefits in the nuclear security, civil nuclear power and medical radio-nuclide sectors.

With the exception of the repetition rate, the electron beam properties required within the ERL to drive the ICS gamma source will be the same as those required to drive the soft X-ray FELs. This allows sharing of the injector and indeed for one of the FELs to be located within the ERL itself, opening seeding and industrial opportunities (e.g. short-wavelength photolithography) from the high average power thereby enabled. The 1 MHz bunches required to drive the soft X-ray FELs can be separated from the remaining 99 MHz energy recovery bunches using resonant RF kickers, as demonstrated for the Electron-Ion collider project.[93,94] The hard X-ray bunches can be injected into, and separated from, the ERL accelerating section utilising standard magnetic separation. Simultaneous and mutually transparent operation of all three source types would therefore be possible.

A2.4.3 High luminosity internal gas target interaction point

A 1 GeV, high current (10 – 100 mA), high brightness (< 1 mm mrad), low energy spread (< 10^{-5}) electron beam, such as that capable of being produced by a next-generation XFEL SC front end with energy recovery, is recognised as having high potential for fundamental physics studies requiring highly intense electron beams.

High luminosity (> 10^{36} cm^{-2} s^{-1}) e-A scattering can be used as precision tests of Standard Model and Beyond the Standard Model physics; for example, measurements of the weak mixing angle and direct searches for dark matter particles. The DarkLight experiment at Jefferson Lab[95] and MAGIX at MESA, U. Mainz[96] are examples of present and future experiments of this type. The paradigm is to bring the electron beam into collision with a supersonic gas jet surrounded by a 4-pi tracking detector, then recover the energy of the electron beam after disruption to enable large currents (and correspondingly high luminosities). This setup has potential to greatly exceed limits established by beam dump and storage ring alternatives, such as those at CEBAF. Of utmost importance in these types of experiment is the precision with which one knows the electron energy, and therefore the ERL transport should be optimised to minimise the energy spread. It should be possible to maintain the gun-projected energy spread to the IP (300 – 1000 MeV), leading to energy spreads potentially at the 10^{-5} level.

A2.4.4 Gamma source application in nuclear security and materials in nuclear industry

The availability of a gamma source as described would be a unique capability globally. As such, it would comprise an advantage for both UK defence and the civil nuclear industry, with significant potential for high-value spin off activity. Locating it as part of a larger XFEL facility would be advantageous in two respects: firstly, the electron beam infrastructure required is common to both FEL and ICS sources; secondly, the analytic capability of FELs is complementary. The wider infrastructural considerations of enabling handling of nuclear materials within an XFEL facility presents challenges, but also significant opportunities, and could be evaluated in the ERL conceptual design phase.

Presently, the most intense dedicated ICS source at MeV energies is the High Intensity Gamma Source (HIGS) at Duke University, USA. Important measurements have been made, such as photonuclear resonances in ^{235}U, where 13 new resonances were identified. This data was important in the development of nuclear resonance fluorescence as an assay methodology. HIGS is, however, limited in flux and bandwidth, as it is a storage ring-based source. The key technology improvement proposed for the next generation XFEL ICS source is the replacement of the electron storage ring with an Energy Recovery Linac (ERL), which allows for orders of magnitude increase in flux (and narrowing of bandwidth). Higher flux means shorter integration times in the applications described below; narrower bandwidth means better energy resolution and the ability to tune into narrow nuclear resonances with less background signal and less absorbed dose into the object under inspection.

A2.4.5 Non-destructive assay via radiography, nuclear resonance fluorescence and photofission

Radiographic imaging (< 10 MeV) of assemblies (e.g. shipping container contents) can be conducted with broadband (bremsstrahlung) systems, but a near-monoenergetic ICS source would significantly

simplify the deconvolution of detector and filter responses during the post-processing of radiographic data whilst reducing dose to the object. Tunability of the source (including below 1 MeV) may permit some degree of discrimination between materials.

1 – 5 MeV photons with around few percent bandwidth are expected to enable development of verification techniques for non-proliferation security through nuclear resonance fluorescence (NRF) computed tomography. AWE would be interested in being partners, as this would be a source of high-quality underpinning data for future, smaller systems deployable in the field (e.g. at ports of entry into the UK, or at other locations where there is a requirement to rapidly detect and diagnose materials of concern, including possible contraband). Specifically, nuclear cross-sections and the resonance characteristics of materials could be acquired across the photon energy range of operational interest. The narrow bandwidth and tunability of the source are also key, in that specific resonances can be targeted with the aim of demonstrating materials identification from the resulting fluorescence signature. Furthermore, the narrowband nature of the ICS source would ensure that the input dose to the target could be significantly reduced compared to existing broadband sources. NNL would be interested in being partners in the context of the non-destructive assay of components through the whole nuclear fuel cycle, for example spent fuels and unknown legacy wastes. The gamma rays from the ICS system would allow fast, high-resolution, isotopically sensitive probing of waste packages, allowing nuclear assay even through shielded flask walls.

From a national security perspective, the ICS source could be used to demonstrate the feasibility of using induced photofission signatures (5 MeV < E < 10 MeV) for low-dose identification of specific isotopes. As for NRF, underpinning materials data (in this case, nuclear photofission cross-sections) acquired using the ICS source would be central for developing this new detection methodology

A2.4.6 Nuclear waste management via photonuclear transmutation

Combining NRF with irradiation at higher photon energy (5 – 40 MeV) and narrower bandwidth (0.1 – 0.01 %) is expected to enable development of techniques to selectively transmute specific isotopes. This would allow investigation of improved nuclear waste management techniques via induced photofission of actinides and long-lived fission products. Crucially, a high value source or product oxide could be purified without the need for wet chemical partitioning, thus allowing purification of a mixture of isotopes or, alternatively, selective destruction of a contaminant that has grown into a material. For example, ingrowth of ^{241}Am in a can of PuO_2 greatly increases operator dose when this is recycled as MOX fuel. This could be mitigated if the ^{241}Am could be eliminated in situ.

For future reprocessing plant, new reprocessing strategies are being investigated to segregate actinides in differing combinations, to improve long term waste handling options. It may be practical to selectively destroy a specific high hazard actinide or alternatively a fission product waste such as ^{129}I or ^{99}Tc. To be economically viable, the waste quantity would need to be small and specific long-term waste storage and waste stabilisation costs be high. Major economic benefit may therefore arise in, for example, reconfiguring the long-term management of the UK's current and future stockpiles of problematic legacy wastes on the Sellafield site

A2.4.7 Medical radionuclide production

The high spectral flux available may make the production of novel medical radioisotopes economically viable, including by harvesting them from legacy material currently considered as waste. The pencil nature of the gamma beam implies potential for very high specific activity in the material produced. Applications would include new medical diagnostic techniques, such as gamma-PET (photonuclear generation of ^{44}Ti, ^{195m}Pt, ^{117m}Sn, ^{44}Sc).

A2.4.8 Detector calibration

For example, calibrated gas Cherenkov detectors (GCD) are routinely used to monitor burn characteristics in Inertial Confinement Fusion (ICF) schemes[97]. The monochromatic but tuneable characteristics of the ICS source are ideal for determining detector response as a function of gamma photon energy.

A2.5 References for Appendix 2

[1] J.B. Rosenzweig *et al. "An Ultra-Compact X-Ray Free-Electron Laser"*, arXiv:2003.06083 [physics.acc-ph], 13 March 2020

[2] W.S. Graves *et al.* "ASU Compact XFEL", *Proceedings of FEL2017*, Santa Fe, NM, USA, p225, **TUB03**, DOI: 10.18429/JACoW-FEL2017-TUB0

[3] M.J. Hogan, C.D. Barnes, C.E. Clayton *et al.* "Multi-GeV energy gain in a plasma-wakefield accelerator", *Phys. Rev. Lett.* **95**, 054802, (2005) DOI: 10.1103/PhysRevLett.95.054802

[4] W.P. Leemans, B. Nagler, A. Gonsalves *et al.* "GeV electron beams from a centimetre-scale accelerator", *Nature Phys* **2**, 696-699 (2006) DOI: 10.1038/nphys418

[5] I. Blumenfeld, C. Clayton, F. Decker *et al.* "Energy doubling of 42 GeV electrons in a metre-scale plasma wakefield accelerator", *Nature* **445**, 741-744 (2007) DOI: 10.1038/nature05538

[6] S. Kneip *et al.* "Near-GeV acceleration of electrons by a nonlinear plasma wave driven by a self-guided laser pulse", *Phys. Rev. Lett.* **103**, 035002 (2009) DOI: 10.1103/PhysRevLett.103.035002

[7] A.J. Gonsalves, K. Nakamura, J. Daniels *et al.*, "Petawatt laser guiding and electron beam acceleration to 8 GeV in a laser-heated capillary discharge waveguide", *Phys. Rev. Lett.* **122**, 084801 (2019) DOI: 10.1103/PhysRevLett.122.084801

[8] A. Picksley et al., Matched Guiding and Controlled Injection in Dark-Current-Free, 10-GeV-Class, Channel-Guided Laser-Plasma Accelerators, Phys. Rev. Lett. 133, 255001 (2024).

[9] H.-P. Schlenvoigt, K, Haupt, A. Debus *et al.* "A compact synchrotron radiation source driven by a laser-plasma wakefield accelerator", *Nature Phys* **4**, 130-133 (2008) DOI: 10.1038/nphys811

[10] M. Fuchs, R. Weingartner, A. Popp *et al.* "Laser-driven soft-X-ray undulator source", *Nature Phys* **5**, 826-829 (2009) DOI: 10.1038/nphys1404

[11] S. Kneip, C. McGuffey, J. Martins *et al.* "Bright spatially coherent synchrotron X-rays from a table-top source", *Nature Phys* **6**, 980-983 (2010) DOI: 10.1038/nphys1789

[12] S. Cipiccia, M. Islam, B. Ersfeld *et al.* "Gamma-rays from harmonically resonant betatron oscillations in a plasma wake", *Nature Phys* **7**, 867-871 (2011) DOI: 10.1038/nphys2090

[13] N.D. Powers, I. Ghebregziabher, G. Golovin *et al.* "Quasi-monoenergetic and tunable X-rays from a laser-driven Compton light source", *Nature Photon* **8**, 28-31 (2014) DOI: 10.1038/nphoton.2013.314

[14] K. Khrennikov, J. Wenz, A. Buck *et al.* "Tunable all-optical quasimonochromatic Thomson X-ray source in the nonlinear regime", *Phys. Rev. Lett.* **114**, 195003 (2015) DOI: 10.1103/PhysRevLett.114.195003

[15] H.-E. Tsai, X. Wang, J.M. Shaw *et al.* "Compact tunable Compton X-ray source from laser-plasma accelerator and plasma mirror", *Phys. Plasmas* **22**, 023106 (2015) DOI: 10.1063/1.4907655

[16] M. Mirzaie et al., All-optical nonlinear Compton scattering performed with a multi-petawatt laser, Nat. Photonics 18, 1212 (2024).

[17] A. Matheron et al., Compton photons at the GeV scale from self-aligned collisions with a plasma mirror, arXiv:2412.19337

[18] G. Sarri, W. Schumaker, A. Di Piazza *et al.*, "Table-top laser-based source of femtosecond, collimated, ultrarelativistic positron beams", *Phys. Rev. Lett.* **110**, 255002 (2013) DOI: 10.1103/PhysRevLett.110.255002

[19] G. Sarri, K. Poder, J. Cole *et al.*, "Generation of neutral and high-density electron-positron pair plasmas in the laboratory", *Nat Commun* **6**, 6747 (2015) DOI: 10.1038/ncomms7747

[20] W. Schumaker *et al.*, "Making pions with laser light", *New J Phys* **20**, 073008 (2018) DOI: 10.1088/1367-2630/aace0c

[21] F. Zhang et al., Proof-of-principle demonstration of muon production with an ultrashort high-intensity laser, Nat. Phys. : https://www.nature.com/articles/s41567-025-02872-2

[22] K. Poder, M. Tamburini, G. Sarri *et al.* "Experimental signatures of the quantum nature of radiation reaction in the field of an ultraintense laser", *Phys Rev X* **8**, 031004 (2018) DOI: 10.1103/PhysRevX.8.031004

[23] J.M. Cole, K.T. Behm, E. Gerstmayr *et al.* "Experimental evidence of radiation reaction in the collision of a high-intensity laser pulse with a laser-wakefield accelerated electron beam", *Phys Rev X* **8**, 011020 (2018) DOI: 10.1103/PhysRevX.8.011020

[24] B. Hidding, S. Hooker, S. Jamison *et al.*, "Plasma Wakefield Accelerator Research 2019 - 2040: A community-driven UK roadmap compiled by the Plasma Wakefield Accelerator Steering Committee (PWASC)," arXiv:1904.09205 [physics.acc-ph], 19 April 2019

[25] S.M. Hooker, "Developments in laser-driven plasma accelerators", *Nature Photon* **7**, 775-782 (2013) DOI: 10.1038/nphoton.2013.234

[26] Lindstrøm, C. A. et al. Beam-driven plasma-wakefield acceleration, *arXiv:2504.05558* [physics.acc-ph], 7 April 2025

[27] Winkler, P.et al, Active energy compression of a laser-plasma electron beam Nature 907, 060 (2025) DOI: 10.1038/s41586-025-08772-y

[28] O. Jakobsson, S. M. Hooker, and R. Walczak, Gev-Scale Accelerators Driven by Plasma-Modulated Pulses from Kilohertz Lasers, Phys Rev Lett 127, 184801 (2021).

[29] A. J. Ross et al., Resonant excitation of plasma waves in a plasma channel, Phys. Rev. Res. 6, L022001 (2024).

[30] B. Hidding et al. Progress in Hybrid Plasma Wakefield Acceleration. Photonics 10.2, p. 99 (2023) DOI: 10.3390/photonics10020099

[31] T. Kurz et al., Demonstration of a Compact Plasma Accelerator Powered by Laser-Accelerated Electron Beams, *Nat. Commun.* **12**, 2895 (2021)

[32] F M Foerster et al. Stable and High-Quality Electron Beams from Staged Laser and Plasma Wakefield Accelerators. *Phys. Rev. X* **12**, 41016 (2022) DOI: 10.1103/PhysRevX.12.041016

[33] G.G. Manahan, A. Habib, P. Scherkl *et al.* "Single-stage plasma-based correlated energy spread compensation for ultrahigh 6D brightness electron beams", *Nat Commun* **8**, 15705 (2017) DOI: 10.1038/ncomms15705

[34] A. Deng, O.S. Karger, T. Heinemann *et al.* "Generation and acceleration of electron bunches from a plasma photocathode", *Nat Phys* **15**, 1156-1160 (2019) DOI: 10.1038/s41567-019-0610-9

[35] S. Chou, J. Xu, K. Khrennikov *et al.*, "Collective deceleration of laser-driven electron bunches", *Phys. Rev. Lett.* **117**, 144801 (2016) DOI: 10.1103/PhysRevLett.117.144801

[36] R. W. Assmann et al. EuPRAXIA Conceptual Design Report. *The European Physical Journal Special Topics* **229.24**, 3675-4284 (2020) DOI: 10.1140/epjst/e2020-000127-8

[37] B Foster, R D'Arcy, and C A Lindstrom. A hybrid, asymmetric, linear Higgs factory based on plasma-wakefield and radio-frequency acceleration. *New Journal of Physics* **25.9**, 93037 (2023) DOI: 10.1088/1367-2630/acf395

[38] D'Arcy, R., Chappell, J., Beinortaite, J. et al. Recovery time of a plasma-wakefield accelerator, Nature **603**, 58–62 (2022). DOI: https://doi.org/10.1038/s41586-021-04348-8

[39] W. Wang et al., Free-electron lasing at 27 nanometres based on a laser wakefield accelerator, Nature 595, 516 (2021).

[40] R. Pompili et al., Free-electron lasing with compact beam-driven plasma wakefield accelerator, Nature 605, 659 (2022).

[41] M. Labat et al., Seeded free-electron laser driven by a compact laser plasma accelerator, Nat Photonics 17, 150 (2022).

[42] A.F. Habib et al. Plasma accelerator-based ultrabright X-ray beams from ultrabright electron beams, *Advances in Laboratory-based X-Ray Sources, Optics, and Applications VII.* ***Vol. 11110.*** *SPIE, (2019)* DOI: 10.1117/12.2530976.

[43] A.F. Habib et al. Attosecond-Angstrom free-electron laser towards the cold beam limit, *Nat. Comm.* **14.1**, 1054 (2023) DOI:10.1038/s41467-023-36592-z.

[44] Berman, L. H. et al. Ultra-high-gain water-window X-ray laser driven by plasma photocathode wakefield acceleration, arXiv:2507.06403 [physics.acc-ph], 8 July 2025.

[45] A.F. Habib et al. Plasma Photocathodes. *Annalen der Physik* **535.10**, 2200655 (2023), DOI: 10.1002/andp.202200655

[46] M.Kovacev, S.V. Fomichev, E. Priori *et al.* "Extreme ultraviolet Fourier-transform spectroscopy with high order harmonics", *Phys. Rev. Lett.* **95**, 223903 (2005) DOI: 10.1103/PhysRevLett.95.223903

[47] E. Gagnon, P. Ranitovic, X.M. Tong *et al.* "Soft X-ray driven femtosecond molecular dynamics", *Science* **317,** 1374-1378 (2007) DOI: 10.1126/science.1144920

[48] P. Wernet, M. Odelius, K. Godeshusen, J. GGaudin, O. Schwartzkopf, W. Eberhardt,"Real-time evolution of the valence electronic structure in a dissociating molecule", *Phys. Rev. Lett.* **103**, 013001 (2009) DOI: 10.1103/PhysRevLett.103.013001

[49] P.M. Paul, E.S. Toma, P. Breger *et al.* "Observation of a train of attosecond pulses from high harmonic generation", *Science* **292**, 1689-1692 (2001) DOI: 10.1126/science.1059413

[50] M. Hentschel, R. Kienberger, C. Spielmann *et al.* "Attosecond metrology", *Nature* **414**, 509-513 (2001) DOI: 10.1038/35107000

[51] R. Kienberger, M. Hentschel, M. Uiberacker *et al.* "Steering attosecond electron wave packets with light", *Science* **297**, 1144-1148 (2002) DOI: 10.1126/science.1073866

[52] A. Baltuška, T. Udem, M. Uiberacker *et al.* "Attosecond control of electronic processes by intense light fields", *Nature* **421**, 611-615 (2003) DOI: 10.1038/nature01414

[53] R. Kienberger, E. Goulielmakis, M. Uiberacker *et al.* "Atomic transient recorder", *Nature* **427**, 817-821 (2004) DOI: 10.1038/nature02277

[54] E. Goulielmakis, M. Uiberacker, R. Kienberger *et al.* "Direct measurement of light waves", *Science* **305**, 1267-1269 (2004) DOI: 10.1126/science.1100866

[55] E. Goulielmakis. M. Schultze, M. Hofstetter *et al.* "Single cycle nonlinear optics", *Science* **320**, 1614-1617 (2008) DOI: 10.1126/science.1157846

[56] S. Ghimire, A. DiChiara, E. Sistrunk *et al.* "Observation of high-order harmonic generation in a bulk crystal", *Nature Phys* **7** , 138-141 (2011) DOI: 10.1038/nphys1847

[57] M. Schultze, K. Ramasesha, C.D. Pemmaraju *et al.* "Attosecond band-gap dynamics in silicon", *Science* **346**, 1348-1352 (2014) DOI: 10.1126/science.1260311

[58] S. Keiber, S. Sederberg, A. Schwarz *et al.* "Electro-optic sampling of near infrared waveforms", *Nature Photon* **10**, 159-162 (2016) DOI: 10.1038/nphoton.2015.269

[59] F. Calegari, D. Ayuso, A. Trabattoni *et al.* "Ultrafast electron dynamics in phenylalanine initiated by attosecond pulses", *Science* **346**, 336 (2014) DOI: 10.1126/science.1254061

[60] Y. Pertot, C. Schmidt, M. Matthews et al. "Time-resolved X-ray absorption spectroscopy with a water window high-harmonic source". *Science* **355**(6322):264-267 (2017). DOI: 10.1126/science.aah6114

[61] A.R. Attar, A. Bhattacherjee, C.D. Pemmaraju *et al.* "Femtosecond X-ray spectroscopy of an

electrocyclic ring opening reaction", *Science* **356**, 54-59 (2017) DOI: 10.1126/science.aaj2198

62 T. Popmintchev, M.C. Chen, D. Popmintchev *et al.* "Bright coherent ultrahigh harmonics in the keV X-ray regime from IR femtosecond lasers" *Science* **336**, 1287-1291 (2012) DOI: 10.1126/science.1218497

63 S.M. Teichmann, F. Silva, S. Cousin *et al.* "0.5-keV soft X-ray attosecond continua", *Nat Commun* **7**, 11493 (2016) DOI: 10.1038/ncomms11493

64 A.S. Johnson, D.R. Austin, D.A. Wood *et al.* "High flux soft X-ray harmonic generation from ionization-shaped few-cycle pulses", *Sci Adv*. **4**, eaar3761 (2018) DOI: 10.1126/sciadv.aar3761

65 J. Duris, S. Li, T. Driver *et al.* "Tunable isolated attosecond X-ray pulses with gigawatt peak power from a free-electron laser", *Nat Photonics* **14**, 30-36 (2020) DOI: 10.1038/s41566-019-0549-5

66 M. Krebs, S. Hädrich, S. Demmler *et al.* "Towards isolated attosecond pulses at megahertz repetition rates", *Nature Photon* **7**, 555-559 (2013), DOI: 10.1038/nphoton.2013.131

67 Y. Nomura, R. Hörlein, P. Tzallas *et al.* "Attosecond phase locking of harmonics emitted from laser produced plasmas", *Nature Phys* **5**, 124-128 (2009) DOI: 10.1038/nphys1155

68 A. Borot, A. Malvache, X. Chen *et al.* "Attosecond control of collective electron motions in plasmas", *Nature Phys* **8**, 416-421 (2012) DOI: 10.1038/nphys2269

69 J. Wheeler, A. Borot, S. Monchocé *et al.* "Attosecond lighthouses from plasma mirrors", *Nature Photon* **6**, 829-833 (2012) DOI: 10.1038/nphoton.2012.284

70 J. van Schoot et al. "Next step in Moore's law: high NA EUV system overview and first imaging and overlay performance," J. Micro/Nanopattern. Mats. Metro. 24(1) 011009 (2024) DOI: 10.1117/1.JMM.24.1.011009

71 9th workshop on EUV-FELs, 4th February 2025, Institute of Science, Tokyo, https://conference-indico.kek.jp/event/303/

72 N. Nakamura et al. "Research and development of the EUV-FEL light source for lithography", Proc. SPIE 13177, Photomask Japan 2024: XXX Symposium on Photomask and Next-Generation Lithography Mask Technology, 131770L (2024) DOI: 10.1117/12.3033966

73 D. Mihalcea, A. Murokh, P. Piot, J. Ruan, "Development of a Watt-level gamma-ray source based on high-repetition-rate inverse Compton scattering", *Nucl. Inst. Meth. Phys. Res. B* **402**, 212-215 (2017) DOI: 10.1016/j.nimb.2017.03.140

74 T. Akagi, A. Kosuge, S. Araki *et al.* "Narrow-band photon beam via laser Compton scattering in an energy recovery linac", *Phys. Rev. Accel. Beams* **19**, 114701 (2016) DOI: 10.1103/PhysRevAccelBeams.19.114701

75 H.U. Rehman, J. Lee, Y. Kim, "Comparison of the laser-Compton scattering and the conventional Bremsstrahlung X-rays for photonuclear transmutation", *Int J Energy Res*. **42**:236-244 (2018) DOI: 10.1002/er.3904

76 H. Weller *et al.* "Research opportunities at the upgraded HIγS facility", *Prog. Part. Nucl. Phys*. **62**, 257-303 (2009) DOI: 10.1016/j.ppnp.2008.07.001

77 G. Mourou, G. Korn, W. Sandner, and J.L. Collier, *ELI-Whitebook*, https://eli-lasers.eu/media/1019/eli-whitebook.pdf, page 134 and following

78 T. Akagi *et al.* "Development of optical resonant cavities for laser-Compton scattering", *Nucl. Inst. Meth. Phys. Res. B* **402**, 370–372 (2017) DOI: 10.1016/j.nimb.2017.03.081

79 P. G. Thirolf *et al.* "Perspectives for photofission studies with highly brilliant, monochromatic γ–ray beams", *EPJ Web of Conferences* **38**, 08001 (2012) DOI: 10.1051/epjconf/20123808001

80 U. Kneissl, N. Pietralla, and A. Zilges, "Low-lying dipole modes in vibrational nuclei studied by photon scattering", *J. Phys. G* **32**, R217-R252 (2006) DOI: 10.1088/0954-3899/32/8/R01

81 K. Heyde, A. Richter, and P. von Neumann-Cosel, "Magnetic dipole excitations in nuclei: Elementary modes of nucleonic motion", *Rev. Mod. Phys.* **82**, 2365 (2010) DOI: 10.1103/RevModPhys.82.2365

82 M.N. Harakeh and A. van der Woude, "Giant Resonances: Fundamental high-frequency modes of nuclear excitation", *Oxford University Press*, *Oxford* (2001)

83 F. Bortignon, A. Bracco, and R.A.Broglia, "Giant Resonances – Nuclear Structure at Finite Temperatures", *CRC Press* (1998)

84 D. Savran, T. Aumann, and A. Zilges, "Experimental studies of the Pygmy Dipole Resonance", *Prog. Part. Nucl. Phys*. **70**, 210-245 (2013) DOI: 10.1016/j.ppnp.2013.02.003

85 A. Bracco, E.G. Lanza, and A. Tamii, "Isoscalar and isovector dipole excitations: Nuclear properties…", *Prog. Part. Nucl. Phys.* **106**, 360-433 (2019) DOI: 10.1016/j.ppnp.2019.02.001

86 S. Goriely, "Radiative neutron captures by neutron-rich nuclei and the r-process nucleosynthesis", *Phys. Lett. B* **436**, 10-18 (1998) DOI: 10.1016/S0370-2693(98)00907-1

87 K.R. Mashtakov, V. Yu. Ponomarev, M. Sheck, S.W. Finch, J. Isaak *et al.* "Structure of high-lying levels populated in the ^{96}Y → ^{96}Zr β decay" (2020) **arXiv:2003.11572 [nucl-ex]**

88 K.-H. Langanke, G. Martinez-Pinedo, P. Von Neumann Cosel and A. Richter, "Supernova Inelastic Neutrino-Nucleus Cross Sections from High-Resolution Electron Scattering Experiments and Shell-Model Calculations", *Phys. Rev. Lett*. **93**, 202501 (2004) DOI: 10.1103/PhysRevLett.93.202501

89 J. Wilhelmy, U. Gayer *et al.* "Investigation of J=1 states and their γ-decay behavior in ^{52}Cr", *Phys. Rev. C* **98**, 034315 (2018) DOI: 10.1103/PhysRevC.98.034315

[90] J. Engel, M.J. Ramsey-Musolf, and U. van Kolck, "Electric dipole moments of nucleons, nuclei, and atoms: The Standard Model and beyond", *Prog. Part. Nucl. Phys*. **71**, 21-74 (2013) DOI: 10.1016/j.ppnp.2013.03.003

[91] N. Auerbach, Ch. Stoyanov, M.R. Anders and S. Shlomo, "Isoscalar and isovector dipole strength distributions in nuclei and the Schiff moment", *Phys. Rev. C* **89**, 014335 (2014) DOI: 10.1103/PhysRevC.89.014335

[92] J. Beller, N. Pietralla *et al.* "Separation of the $1^+/1^-$ parity doublet in ^{20}Ne", *Phys. Lett. B* **741**, 128-133 (2015) DOI: 10.1016/j.physletb.2014.12.018

[93] Y. Huang, H. Wang *et al.* "Ultrafast harmonic rf kicker design and beam dynamics analysis for an energy recovery linac based electron circulator cooler ring", *Phys. Rev. Accel. Bea*ms **19** 084201 (2016) DOI: 10.1103/PhysRevAccelBeams.19.084201

[94] Y. Huang, H. Wang *et al.* "Multiple harmonic frequencies resonant cavity design and half-scale prototype measurements for a fast kicker", Phys. Rev. Accel. Beams 19 122001 (2016) DOI: 10.1103/PhysRevAccelBeams.19.122001

[95] R. Alarcon *et al.* "Transmission of Megawatt Relativistic Electron Beams through Millimeter Apertures", *Phys. Rev. Lett.* **111**, 164801 (2013) DOI: 10.1103/PhysRevLett.111.164801

[96] S. Grieser *et al.* "A Cryogenic Supersonic Jet Target for Electron Scattering Experiments at MAGIX@MESA and MAMI", *Nucl. Instrum. Meth. A* **906**, 120-126 (2018) DOI: 10.1016/j.nima.2018.07.076

[97] M.S.Rubery et Al, "Monte Carlo validation for the gas Cherenkov detectors at the National Ignition Facility and Omega", Rev.Sci.Inst., 84, 073504,(2014) DOI: 10.1063/1.4812572

Appendix 3: Community Engagement

This Appendix summarises the various community engagements that have been carried out to gather the information for this Science and Technology Case Update. A full list of contributors is included. We also include a summary of the engagements carried out for the 2020 edition and details of a survey of UK users of XFELs that was carried out at that time.

A3.1 Townhall Events and Workshops

A3.1.1 Townhall Events 2023-24

Townhall Events were held to engage with the UK research and innovation community at locations around the nation. To extend the Case from the 2020 edition, which had focused mainly on basic science research opportunities, additional efforts were made to capture technological research by reaching out to an extended community, including researchers working in catalysis, batteries, pharma, AI, quantum tech, energy, biomedicine, defence and engineering. The objective was two-fold:

- To inform local communities of the UK XFEL project and the research opportunities already underway at XFELs around the world
- To learn of the main research questions in the broad fields covered by the Townhall events, to ensure these were accurately reflected in the Science and Technology Case and to optimise the Conceptual Design so that it could address a significant number of these questions.

Launch Event – The Royal Society, London, 30th January 2023

Speakers:
Massimo Altarelli *(MPSD, Hamburg) – Project context*
Jim Clarke and David Dunning *(Daresbury) – UK XFEL conceptual design process*
Adrian Mancuso *(Diamond Light Source) and* ***James Green*** *(Central Laser Facility) – End-stations and instruments*
Robert Feidenhansl *(European XFEL) – Future developments at European XFEL*
Mike Dunne *(LCLS) – Future developments at LCLS*
Ago Marinelli *(SLAC) – Attosecond XFEL sources*
Claudio Masciovecchio *(Elettra ST) – Seeding of FELs*
Patrick Rauer *(DESY) – XFELO*
Brian McNeil *(University of Strathclyde) – New polarisation and angular momentum modes*

There were 150 in-person attendees plus a further 150 attendees online.

Frontiers of Measurement Technology – Queen's University Belfast, 20th and 21st June 2023

Speakers:
Cristian Svetina *(IMDEA, Madrid) – Hard X-ray transient grating measurements*
Andrew Brown *(QUB, Belfast) – Multiphoton theory of multielectron systems*
Henry Chapman *(CFEL DESY) – Nanoscale imaging with X-rays*
Carlo Callegari *(Fermi, Trieste) – Coherent control with X-ray radiation*
Adam Kirrander *(University of Oxford) – Ultrafast X-ray scattering*
Mark Dean *(Brookhaven University) – RIXS measurements in condensed phase*
David Keen *(Diamond Light Source) – Time resolved pair distribution functions*
Rebecca Boll *(European XFEL) – Coulomb explosion imaging at XFELs*
David Ayuso *(Imperial College London) – Chiral dynamics of matter and fields*
John Costello *(Dublin City University) – Attosecond chronoscopy at SASE XFELs*
Nina Rohringer *(DESY, Hamburg) – X-ray non-linear optics*

There were 30 in-person attendees plus a further 25 attendees online.

Matter, chemistry and biology at extreme conditions – University of Strathclyde, Glasgow, October 2nd and 3rd 2023

Speakers:

David McGonegle *(AWE) – AWE's extreme environment experiments at European XFEL and LCLS*

Malcolm McMahon *(University of Edinburgh) – Results from Static and Dynamic Compression Experiments at European XFEL*

Colin Pulham *(University of Edinburgh) – Putting the squeeze on molecular materials – high pressure studies of fuels, lubricants, pharmaceuticals and explosives*

Tom Cowan *(Dresden) – XFEL probing of extreme conditions in ultra-relativistic laser-produced plasmas – Status of HED/HIBEF at European XFEL*

Robbie Scott *(Central Laser Facility) – Combining a UK XFEL with spherical compression: Laser fusion science possibilities*

Claudio Stan *(Rutgers) – Discovering and investigating soft matter phenomena with XFELs*

Simon Gerber *(PSI) – Exploring quantum matter at extreme conditions – low temperature and high magnetic fields*

Archie Bott *(University of Oxford) – The role of magnetic fields in turbulent high-energy density plasmas*

Sam Vinko *(University of Oxford) – Unravelling material properties with intense X-rays*

Emma McBride *(Queen's University Belfast) – Towards making high resolution inelastic X-ray scattering measurements at extreme conditions*

There were 40 in-person attendees and a further 30 attendees online.

Fundamental Physics, Quantum Computing and AI – New Babbage Building, University of Plymouth, 18th -19th January 2024

Speakers:

Abbas Ourmazd *(University of Wisconsin at Milwaukee) – Few-fs atomic resolution movies of a photoactive protein traversing a conical intersection*

Gianluca Gregori *(University of Oxford) – Measuring Unruh radiation from accelerated electrons*

James Cryan *(SLAC) – On Spectral domain ghost imaging and attosecond campaign*

Stewart Boogert *(Cockroft Institute) – Towards a FEL based "fundamental physics" facility*

Alvaro Sanchez Gonzalez *(Google Deep Mind) – Applying AI to complex problems in the physical sciences*

Luigi Genovese *(CEA, Grenoble) – Challenges and Opportunities from Electronic Structure Calculations of Systems at the Nanoscale*

Giulio Cerullo *(Politecnico Milan) – Real-time visualization of conical intersections in biomolecules using XFELs*

Sir Peter Knight FRS *(Imperial College London) – Developing a National Strategy for Quantum Technology*

Alice Bowen *(University of Manchester) – EPR overview from National Research Facility for EPR*

Graham Smith *(University of St Andrews) – EPR experiments and XFELs*

Tom Blackburn *(University of Gothenburg) – Simulation of strong-field QED in XFEL beams*

Ralf Schuetzhold *(HZDR) – Fundamental Physics with XFELs*

Leszek Frasinski *(Imperial College London) – On covariance mapping and multi-dimensional extensions*

Stuart Mangles *(Imperial College London) – Physics using XFELs and high intensity lasers*

Bernhard Hidding *(Heinrich-Heine-University Düsseldorf) – Novel capabilities from plasma wakefield-based high-brightness X-FELs*

There were 40 in-person attendees and a further 20 attendees online.

Energy, environmental and climate technologies – University of Sheffield, 4th and 5th June 2024

Speakers: ***Jenny Clark*** *(University of Sheffield) – Excitonic up- and down-conversion for solar energy harvesting applications*
Rob House *(University of Oxford) – Probing charge storage chemistry in battery materials*
Majed Chergui *(Trieste) – Non-linear Extreme Ultraviolet (EUV) to hard X-ray spectroscopy*
Adrien Chauvet *(University of Sheffield) – Non-precious metal catalysts investigation for hydrogen fuel cells*
Camila Bacellar *(SwissFEL) – Femtosecond Chemical and Biological Dynamics at the Alvra End-station*
Thomas Wolf *(LCLS, SLAC) – Opportunities for ultrafast gas phase photochemistry at an advanced XFEL*
Thomas Feurer *(European XFEL) – European XFEL: Recent highlights and upcoming opportunities*
Basile Curchod *(University of Bristol) – Atmospheric chemistry from a computational and theoretical perspective*
Louis Piper *(University of Warwick) – Li-ion batteries: picoseconds to years*
Kiyoshi Ueda *(Tohoku University) – Catching and steering electrons and atoms in action with light*
Soonam Kwon *(PAL) – Carrier capture at the active sites in metal-oxide photo-catalysts*
Nils Huse *(University of Hamburg) – Investigating chemical reactions in solution with ultrafast X-ray spectroscopy methods*

There were 50 in-person attendees and a further 23 attendees online.

Lifesciences and Bio-Medicine – The Royal Society, London, 29th and 30th July 2024

Speakers: ***Ilme Schlichting*** *(MPI Medical Research) – Keynote: The sample is the science*
Patrick Rabe *(University of Oxford) – Monitoring penicillin ring formation through a crystallographic and spectroscopic lens*
Briony Yorke *(University of Leeds) – Time-resolved studies of the role of UV in cataract formation*
Alastair Siebert *(Diamond Light Source) – HeXI and eBIC using electrons for structural biology*
Radoslav Enchev *(Francis Crick Institute) – Enabling time-resolved cryoEM*
Keith Moffat *(University of Chicago) – Dynamics and kinetics in XFEL-based structural biology*
Randy J.Read *(University of Cambridge) – Prospects for the post-Alpha Fold era of structural biology*
Eriko Nango *(Tohuko University) – Status of time-resolved serial femtosecond crystallography at SACLA*
Richard Neutze *(University of Gothenburg) – Keynote: Time-resolved studies using XFEL radiation: Approaches and opportunities*
Philip Johnson *(PSI/Swiss FEL) – Time-resolved biology at Swiss FEL*
Richard Bean *(European XFEL) – Biology at the European XFEL*
Katerina Dörner *(European XFEL) – Sample preparation and delivery at the European XFEL*
Daniela Rupp *(ETH, Zurich) – Imaging free nanoparticles and their ultrafast dynamics with time-resolved coherent diffraction imaging*
Alan Orville *(Diamond Light Source) – The XFEL Life Sciences Hub at Diamond*
Elizabeth Shotton *(Diamond Industrial Liaison) – Industrial science at large research infrastructures*

Vadim Cherezov *(UCSC) – GPCRs, revealing their secrets*
Michael Hennig *(leadXpro) – Structure based drug discovery using XFELs*
Tian Geng *(Nxera Pharma) – Industrial perspectives on XFELs*
Thomas (TJ) Lane *(DESY/Cambridge) – Time-resolved crystallography captures light driven DNA repair*
David Leys *(University of Manchester) – Time-resolved MX of light-dependent systems*
Sir Dave Stuart FRS *(University of Oxford) – Keynote: Synergies between X-rays and electrons in life science research*

Closing remarks were given by ***Jim Naismith FRS (University of Oxford)*** and a mid-morning discussion was convened on the second day by ***John Helliwell FRS (University of Manchester)*** that helped raise issues regarding the range of attitudes within this community as to the appetite for a next-generation XFEL facility.

There were 110 in-person attendees and 20 attendees online.

Electronic, Photonic and Quantum Technologies and THz Workshop – Royce Institute, Manchester, 8th and 9th August 2024

Speakers:
Simon Wall *(Aarhus University) – Tracking ultrafast heterogeneity and disorder in quantum materials*
Richard Curry *(University of Manchester) – Scaling silicon-based qubit technologies*
Phil King *(University of St Andrews) – Time and angle resolved photoemission of interlayer charge transfer and charge density wave dynamics in monolayer TiSe2*
Charlotte Sanders *(Central Laser Facility – Artemis) – Time-resolved Photoelectron Diffraction*
Jens Biegert *(ICFO) – Attosecond quantum dynamics in materials and molecules*
Oleana Fedchenko *(Mainz University) – Implementation of momentum microscopy for the study of quantum materials*
Artem Bakulin *(Imperial College London) – Ultrafast action spectroscopy of processible electronic materials and devices*

THz Workshop introduced by Andrew Burnett (Leeds)

Speakers:
Steve Johnson *(PSI/ETH) – Coherent dynamics at multiple length scales via tr XRD and XRS*
Ben Murdin *(University of Surrey) – THz FEL studies of silicon impurities, and X-ray studies for impurity diagnosis*
Matthias Hoffman *(SLAC) – THz pump/X-ray probe at LCLS*
Dave Walsh *(Daresbury) – THz options for UK XFEL*
Darren Graham *(University of Manchester/Cockcroft) – Laser based THz sources*

There were 42 in-person attendees and 15 attendees online.

Advanced Manufacturing and Materials –SPARC, Cardiff University, 17th and 18th September 2024

Speakers:
David Dye *(Imperial College London) – XFEL diffraction and SAXS measurements of stress and void evolution at high rates – and thoughts on industrial applications*
Mike Fitzpatrick *(Coventry University) – Residual stress and damage in engineering materials*
Lauren Hatcher *(Cardiff University) Advanced micro-crystallization solutions for serial crystallography*
Peter Smowton *(Cardiff University – Institute for Compound Semiconductors) – Institute for Compound Semiconductors and Issues in Compound Semiconductor Manufacture*

Peter Lee *(University College London) – Is XFEL needed to image additive manufacturing processes in real and reciprocal space?*
Leora Dresselhas-Marais *(Stanford University) – Ultrafast XFEL imaging for metals manufacturing*
Ian Robinson *(University College London) – Role of ultrafast heterogeneous melting in laser machining dynamics*
Colin Berry *(Cardiff University) – XFEL analysis of naturally crystalline protein inclusions from Bacillus thuringiensis*
Sneha Banerjee *(Central Laser Facility) – Johnson Matthey and potential XFEL collaborations*
Peter Dowding *(Infineum) – Unlocking the properties and dynamics of commercial oil additives using X-rays*
Andrea Folli *(Cardiff University) – Opportunities for X-ray free-electron laser in photocatalysis and electrocatalysis*

There were 20 in-person attendees and 20 attendees online (note there was serious travel disruption on 17th September).

A3.1.2 Workshops and engagement summary 2023-25

As well as the Townhalls meetings, a series of more specialised Workshops was held to explore some important specific emerging areas of XFEL research opportunity and to ensure the Conceptual Design incorporated the required features to further these fields. These Workshops were on the topics of **Ion and particle beams**, **Catalysis**, **THz**, and **Defence Technology**. In addition, an **XFEL Theory** Workshop was held in July 2025, in part convened by the UK XFEL Project.

Ion and particle beams – University of Manchester, 18th May 2023

Speakers:
Fred Currell *(University of Manchester) – The Dalton Cumbrian Facility, radiation science at the heart of the UK's nuclear industry*
Peter Williams *(STFC) – A tuneable, mono-energetic, 1-100 MeV gamma source as part of UK-XFEL: potential and applications*
Kenneth Long *(Imperial College London) – LhARA, the Laser-hybrid Accelerator for Radiobiological Applications*
James Green *(Central Laser Facility) – Current and future status of laser-driven ion sources at the Central Laser Facility*
Ross Gray *(University of Strathclyde) – Progress in the development of laser-driven ion sources*
Mike Yueng *(replacing Brendan Dromey who could not attend) (Queen's University Belfast) – Exploiting ultrafast capabilities and future applications*
Jason Parsons *(University of Birmingham) – Analysing the radiobiological response to photons and particle ions in tumour cell models: The potential for FLASH*
Matthew Bird, ***Dave Grills*** *and* ***Andrew Cook*** *(Brookhaven National Laboratory, USA) – Pulse radiolysis: current applications and possibilities at UK XFEL (via Zoom)*
Linda Young *(Argonne National Laboratory, USA) – Ultrafast processes in the radiolysis of water studied with XFELs (via Zoom)*
Alex Baidak *(University of Manchester) – New frontiers in radiation chemistry reachable by ultrafast time resolution*

There were 15 in-person attendees and 5 attendees online.

Catalysis – RAL/Harwell, 27th November 2023, with a specialised discussion on End-Stations at Imperial College London on 28th November 2023

Speakers:
Sofia Diaz-Moreno *(Diamond Light Source) – Catalysis science at Diamond Light Source and future directions*

Chris Milne *(European XFEL) – Probing ultrafast structural and electronic dynamics in functional materials using X-ray free electron lasers*
Phillipe Wernet *(Uppsala University) – Orbital-level control of catalysis enabled by X-ray spectroscopy*
Kelly Gaffney *(SLAC, Stanford) – Capturing light-driven chemistry with atomic specificity and resolution*
Tom Penfold *(Newcastle University) – Achievements, Opportunities and Challenges for Theory at X-FELs*
Serena DeBeer *(Max Planck) – X-ray Spectroscopic Studies of Biological and Chemical Catalysis – New Opportunities at XFELs*
Andrew Beale *(University College London/FINDEN Ltd) – XFELs and operando catalysis: challenges and opportunities*
Paul Donaldson *(Central laser Facility – Ultra) – Impacts of ultrafast time resolved optical spectroscopy on catalysis. A helping hand for the UK XFEL case?*
David Thomsett *(Johnson Matthey) – JM and potential XFEL collaboration: Industrial analysis requirements*
Jason Lynam *(University of York) – Unveiling the hidden steps in catalysis with time-resolved spectroscopy*
Gabriel Karras *(Diamond Light Source) – Addressing questions in photocatalysis with optical-pump X-ray probe pulses*

There were 50 in-person attendees.

THz – Royce Institute, Manchester, 8th and 9th August 2024

The **THz workshop** took place as part of the Electronic, Photonic and Quantum Technologies Townhall event in Manchester in August 2024 (see **Section A3.1.1**).

There were 42 in-person attendees and 15 attendees online.

Defence Technology – CLF Visitors Centre, October 2024

This Workshop was attended by 38 participants from various agencies, including MOD, AWE, Dstl, Qinetiq, Rolls-Royce, SLAC/DOE and the UK XFEL team. The programme allowed ample time for an open discussion of the needs and issues specific to this community. Further details are provided in **Section 10.2**.

XFEL Theory Workshop – Imperial College London, 1st and 2nd July 2025 (in part convened by the UK XFEL Project)

This Workshop focused on strengthening the theory pipeline for chemical dynamics and condensed matter investigations at XFELs. Speakers included **Majed Chergui, Nana List, Nils Huse, William Glover, Rebecca Ingle, Nadja Doslic, Lina Fransen, Gilberto Teobaldi, Daria Popovla-Gorelova, Sonia Coriani, Andrei Benediktovitch** and **Matthew Foulkes**.

A3.2 Community engagement summary

Altogether, **more than 950 people participated** in our engagements (Townhalls and Workshops). We regard this as an excellent measure of the interest in a next-generation XFEL from the UK research and innovation community, many of whom may not be using XFELs in their research yet, but who recognise the significant potential of these facilities in future research in their fields.

A3.3 Other external engagements of UK XFEL team

A separate set of engagements (both in-person and online) was convened by James Green (Central Laser Facility) to help in defining the required End-Station Instrumentation. Two in-person End-Station Away Days were held at the RAL Visitors Centre on 28th February 2024 and 28th January 2025. This process is discussed further in the **Conceptual Design report.**

In addition, monthly online meetings were held with the **Science Team,** and a range of single topic online engagements with the UK community. For example:

- **Astrochemistry at a next generation XFEL** – held 26th March 2025, with participants including Wendy Brown (University of Sussex), Jimena Gorfinkiel (Open University), Cate Anstorter (University of Edinburgh), Martin Mc Coustra (Heriot Watt University), Nigel Mason (University of Kent), Jonathan Tennyson (University College London) and Claire Vallance (University of Oxford).
- **Time-resolved X-ray volumetric imaging at a UK XFEL** – **held** 3rd April 2025 (online), with participants including Manolis Gavaises (City University/Magdeburg), Colin Nave (Diamond Light Source), Jiawei Mi (University of Hull), Hugo Doyle (First Light Fusion), Simon Bland (Imperial College London), Patrik Vagovic (European XFEL/DESY), Matthew Cotton (AWE), Andrew Comley (AWE) and David Dunning (Daresbury). This meeting was followed by online discussions also with Colin Nave and Andreas Schaefer (Crick) on static volumetric imaging, e.g. of whole mammalian brains.
- **XFELs and Fusion Technology** – held on 8th September 2025, with participants including Graham Appleby (UKAEA), Mark Gilbert (UKAEA Materials) and Peter Williams (Daresbury),

Project team participation in externally organised workshops and conferences has also fed into both the Science and Technology Case and the Conceptual Design. Examples of such activity are:

- David Dunning and Jon Marangos, Online Seminar to the European XFEL User Community in European XFEL Series on 7th October 2024
- Paul Aden, David Dunning and Jon Marangos, UKXFEL Project Lecture, Pickavance Lecture Theatre, Harwell on 28th January 2025
- Jon Marangos and Paul Aden presented at the Dynamic Imaging workshop, Slovak Embassy, London on 19th March 2025
- Talks given by UK XFEL team members at various facilities, discussing both Conceptual Design and Science and Technology case, including:
    - Swiss FEL/PSI, Villigen, Switzerland
    - European XFEL, Hamburg, Germany
    - LCLS, SLAC, USA
    - Fermi@Elettra, Trieste, Italy
    - Sirius Light Source, Campinas, Brazil
    - SHINE, Shanghai, China
    - Online with SACLA, Harima, Japan
    - Online with PAL, Pohang, South Korea

A3.4 Science Team

The Science Team played a vital role throughout the project (starting in 2019) in developing the Science and Technology Case, feeding expert views into the Conceptual Design, organising the various engagements (including identifying speakers and making local arrangements), and in authoring the main sections of the Case. All of the Science Team members are listed below.

Physics and X-ray photonics

Jason Greenwood (Queen's University Belfast)
Adam Kirrander (University of Oxford)
Jon Marangos – Science Team Lead (Imperial College London)
Elaine Seddon (Cockroft Institute/University of Manchester)
Amelle Zair – Chapter Editor (King's College London)

Matter at extreme conditions

Marco Borghesi (Queen's University Belfast)
Andrew Comley (AWE)
Andrew Higginbotham (University of York)
Emma McBride (Queen's University Belfast)
Malcolm McMahon (University of Edinburgh)
Sam Vinko – Chapter Editor (University of Oxford)
Justin Wark (University of Oxford)

Quantum materials, nanotechnology, condensed matter

Shakil Awan (University of Plymouth)
Mark Dean (Brookhaven National Laboratory)
Sarnjeet Dhesi (Diamond Light Source)
Marcus Newton – Chapter Editor (University of Southampton)
Paolo Radaelli (University of Oxford)
Anna Regoutz (University of Oxford)
Ian Robinson (UCL)
Simon Wall (Aarhus University)

Chemical Sciences

Alex Baidak (University of Manchester)
Mark Brouard (University of Oxford)
Andrew Burnett (University of Leeds)
Sofia Diaz Moreno (Diamond Light Source)
Rebecca Ingle (UCL)
Russell Minns (University of Southampton)
Tom Penfold (University of Newcastle)
Claire Vallance (University of Oxford)
Julia Weinstein – Chapter Editor (University of Sheffield)

Life Sciences

Tian Geng (Nxera Pharma)
Adrian Mancuso (Diamond Light Source)
Allen Orville – Chapter Editor (Diamond Light Source)
Jasper van Thor (Imperial College London)
Xiaodong Zhang FRS (Imperial College London)

Industrial Applications

David Dye (Imperial College London)
Dan Eakins (University of Oxford)
Mike Fitzpatrick (University of Coventry)
David Rugg (formerly of Rolls Royce)
Sven Schroeder – Chapter Editor (University of Leeds)
Shakil Awan*
Andrew Comley*
Sofia Diaz Moreno*
Allen Orville*

** provided additional assistance*

A3.5 Contributors to the 2026 Science and Technology Case update

We list below all those who have directly contributed to the updated Science and Technology Case through direct authorship of material, critical consultations, speaking at Townhall meetings/ workshops, and editing and reviewing text. Those who were willing are included in the list of contributing authors at the front of this document, along with those who contributed to the original 2020 Science Case that formed the basis for this update. Other contributors are acknowledged accordingly.

Title	First Name	Family Name	Role	Affiliation
Dr	Paul	Aden	UK XFEL Team	Daresbury
Prof.	Massimo	Altarelli	Speaker/IAB	MPISD
Dr	Deepa	Angal-Kalinin	UK XFEL Team	Daresbury
Dr	Graham	Appleby	Consultant	UKAEA
Dr	Shakil	Awan	Science Team	University of Plymouth
Dr	David	Ayuso	Speaker	Imperial College London
Dr	Camila	Bacellar	Speaker	Paul Scherrer Institute, Switzerland
Dr	Aliaksandr	Baidak	Science Team	University of Manchester
Dr	Artem	Bakulin	Speaker	Imperial College London
Dr	Sneha	Banerjee	Speaker	Johnson Matthey PLC/CLF
Prof.	Andrew	Beale	Speaker	University College London
Dr	Richard	Bean	Speaker	European XFEL
Prof.	Colin	Berry	Speaker	University of Cardiff
Prof.	Jens	Biegert	Speaker	ICFO, Barcelona
Dr	Matthew	Bird	Speaker	Brookhaven National Laboratory, USA
Dr	Thomas	Blackburn	Speaker/Consultant	University of Gothenburg
Prof.	Simon	Bland	Consultant	Imperial College London
Dr	Rebecca	Boll	Speaker	European XFEL
Prof	Stewart	Boogert	Speaker	Cockroft Institute/ University of Manchester
Prof.	Marco	Borghesi	Science Team	Queen's University Belfast
Dr	Archie	Bott	Speaker	University of Oxford
Dr	Alice	Bowen	Speaker	University of Manchester
Dr	Steven	Boyes	Speaker	DSTL
Prof.	Mark	Brouard	Science Team	University of Oxford
Dr	Andrew	Brown	Speaker	Queen's University Belfast
Mrs	Tracey	Burge	Technical Author	Central Laser Facility
Dr	Andrew	Burnett	Science Team	University of Leeds
Dr	Carlo	Callegari	Speaker	FERMI, Elettra Sincrotrone, Trieste
Prof. Sir	Richard	Catlow FRS	Consultant	University College London
Prof.	Giulio	Cerullo	Speaker	Politecnico di Milano
Prof.	Henry	Chapman FRS	Speaker	DESY, Hamburg
Dr	Adrien	Chauvet	Speaker	University of Sheffield
Prof.	Vadim	Cherezov	Speaker	University of Southern California
Prof	Majed	Chergui	Speaker	EPFL/Trieste

Title	First Name	Family Name	Role	Affiliation
Prof.	Jenny	Clark	Speaker	University of Sheffield
Prof.	Jim	Clarke	UK XFEL Team	Daresbury
Prof.	John	Collier	UK XFEL Team	Central Laser Facility
Dr	Andrew	Comley	Science Team	AWE
Dr	Andrew	Cook	Speaker	Brookhaven National Lab., USA
Prof.	John	Costello	Speaker	Dublin City University
Dr	Matthew	Cotton	Speaker	AWE
Prof.	Tom	Cowan	Speaker	Helmholtz Zentrum Dresden Rosendorf
Dr	James	Cryan	Speaker	Stanford Linear Accelerator Centre, USA
Prof.	Basile	Curchod	Speaker	University of Bristol
Prof.	Frederick	Currell	Speaker	Dalton Cumbria Facility
Prof.	Richard	Curry	Speaker/Organiser	University of Manchester
Prof.	Serena	de Beer	Speaker	Max Planck Inst for Chemical Energy Conversion
Dr	Mark	Dean	Speaker/Science Team	Brookhaven National Laboratory, USA
Dr	Sarnjeet	Dhesi	Science Team	Diamond Light Source
Dr	Sofia	Diaz Moreno	Speaker/Science Team	Diamond Light Source
Dr	Katerina	Dörner	Speaker	European XFEL
Prof.	Paul	Donaldson	Speaker	Central Laser Facility
Prof.	Peter	Dowding	Speaker	Infineum Ltd
Dr	Leora	Dresselhaus-Marais	Speaker	Stanford Linear Accelerator Centre, USA
Prof.	Brendan	Dromey	Consultant	Queen's University Belfast
Prof.	Mike	Dunne	Speaker	Stanford Linear Accelerator Centre, USA
Dr	David	Dunning	UK XFEL Team	Daresbury
Prof.	David	Dye	Speaker/Science Team	Imperial College London
Prof.	Daniel	Eakins	Speaker	University of Oxford
Dr	Radoslav	Enchev	Speaker	Crick Institute
Prof.	Olena	Fedchenko	Speaker	Goethe University Frankfurt
Prof.	Robert	Feidenhansl	Speaker	European XFEL
Prof.	Thomas	Feurer	Speaker	European XFEL
Prof.	Mike	Fitzpatrick	Speaker/Science Team	University of Coventry
Dr	Andrea	Folli	Speaker	University of Cardiff
Prof	Leszek	Frasinski	Speaker	Imperial College London
Prof.	Kelly	Gaffney	Speaker	Stanford Linear Accelerator Centre, USA
Dr	Tian	Geng	Speaker/Science Team	Nxera Pharma
Dr	Luigi	Genovese	Speaker	CEA/University of Grenoble
Dr	Simon	Gerber	Speaker	Paul Scherrer Institute, Switzerland
Prof.	Gianluca	Gregori	Fund. Physics	University of Oxford

Title	First Name	Family Name	Role	Affiliation
Dr	Mark	Gilbert	Consultant	UKAEA
Dr	Darren	Graham	Speaker	University of Manchester/Cockroft
Dr	Ross	Gray	Speaker	University of Strathclyde
Dr	James	Green	Design Team	Central Laser Facility
Dr	Alice	Green	Consultant	University of Edinburgh
Dr	Jason	Greenwood	Science Team	Queen's University Belfast
Dr	Dave	Grills	Speaker	Brookhaven National Lab., USA
Dr	Ahmad Fahim	Habib	Speaker	Cockroft Institute
Dr	Lauren	Hatcher	Speaker	University of Cardiff
Dr	Thomas	Heinzl	Consultant	University of Plymouth
Dr	Michael	Hennig	Speaker	LeadXPro AG
Prof	Bernhard	Hidding	Speaker	University of Dusseldorf
Dr	Andrew	Higginbotham	Science Team	University of York
Dr	Matthias	Hoffmann	Speaker	Stanford Linear Accelerator Centre, USA
Prof.	Simon	Hooker	Wakefield case	University of Oxford
Dr	Robert	House	Speaker	University of Oxford
Prof.	Nils	Huse	Speaker	University of Hamburg
Dr	Rebecca	Ingle	Science Team	University College London
Dr	Philip	Johnson	Speaker	Paul Scherrer Institute, Switzerland
Prof.	Steve	Johnson	Speaker	ETH Switzerland/Paul Scherrer Institute
Dr	Gabriel	Karras	Speaker	Diamond Light Source
Prof.	David	Keen	Speaker	ISIS Neutron and Muon Source
Prof.	Philip	King	Speaker	St Andrews University
Dr	Ben	King	Consultant	University of Plymouth
Prof.	Adam	Kirrander	Science Team	University of Oxford
Prof. Sir	Peter	Knight FRS	Speaker	Imperial College London
Dr	Soonam	Kwon	Speaker	PAL FEL
Dr	Thomas	Lane	Speaker	DESY
Prof.	Cristina	Lazzeroni FRS	Kaon case	University of Birmingham
Prof.	Peter	Lee	Speaker	University College London
Prof.	David	Leys	Speaker	University of Manchester
Prof.	Ken	Long	Speaker	Imperial College London
Dr	Matt	Lunt	Speaker	DSTL
Prof.	Jason	Lynam	Speaker	University of York
Dr	Adrian	Mancuso	Speaker	Diamond Light Source
Prof	Stuart	Mangles	Speaker/Consultant	Imperial College London
Prof.	Jon	Marangos	Science Team Lead	Imperial College London
Prof.	Agostino	Marinelli	Speaker	Stanford Linear Accelerator Centre, USA
Dr	Mikael	Martinez	Speaker	Stanford Linear Accelerator Centre, USA

Title	First Name	Family Name	Role	Affiliation
Prof.	Claudio	Masciovecchio	Speaker	FERMI@Elettra
Dr	Karim	Massri	Kaon case	University of Lancaster
Dr	Emma	McBride	Science Team	Queen's University Belfast
Dr	David	McGonegle	Speaker	AWE
Prof.	Paul	McKenna	Speaker	University of Strathclyde
Prof.	Malcolm	McMahon	Speaker/Science Team	University of Edinburgh
Prof.	Brian	McNeil	Speaker	University of Strathclyde
Dr	Christopher	Milne	Speaker	European XFEL
Prof.	Russell	Minns	Science Team	University of Southampton
Prof.	Keith	Moffat	Speaker	University of Chicago
Prof.	Ben	Murdin	Speaker	University of Surrey
Prof.	James	Naismith FRS	Advisor/Speaker	University of Oxford
Prof.	Eriko	Nango	Speaker	Tohoku University
Dr	Colin	Nave	Consultant	Diamond Light Source
Prof.	Richard	Neutze	Speaker	University of Gothenburg
Dr	Marcus	Newton	Science Team	University of Southampton
Prof.	Allen	Orville	Science Team	Diamond Light Source
Prof	Abbas	Ourmazd	Speaker	University of Wisconsin Milwaukee
Dr	Raj	Pandya	Consultant	University of Warwick
Prof.	Jason	Parsons	Speaker	University of Birmingham
Prof.	Mitesh	Patel	Kaon case	Imperial College London
Prof.	Thomas	Penfold	Science Team	University of Newcastle
Prof.	Louis	Piper	Speaker	University of Warwick
Prof.	Colin	Pulham	Speaker	University of Edinburgh
Dr	Patrick	Rabe	Speaker	University of Oxford
Prof.	Paolo	Radaelli	Science Team	University of Oxford
Dr	Patrick	Rauer	Speaker	DESY, Hamburg
Prof.	Randy	Read FRS	Speaker	University of Cambridge
Prof.	Anna	Regoutz	Science Team	University of Oxford
Prof.	Ian	Robinson	Science Team	University College London
Dr	Steven	Robinson	Speaker	MOD
Prof.	Nina	Rohringer	Speaker	DESY, Hamburg
Prof.	Daniela	Rupp	Speaker	ETH Switzerland
Dr	Danny	Sahtoe	Speaker	Hubrecht Institute
Dr	Alvaro	Sanchez-Gonzalez	Speaker	Google Deep Mind
Dr	Charlotte	Sanders	Speaker	Central Laser Facility
Prof.	Subir	Sarkar	Speaker	University of Oxford
Dr	Andreas	Schaefer	Consultant	Crick Institute
Prof.	Ilme	Schlichting	Speaker	Max Planck Institute for Medical Research
Prof.	Sven	Schroeder	Science Team	University of Leeds
Prof.	Ralf	Schützhold	Speaker	Helmholtz Zentrum Dresden Rosendorf
Dr	Robbie	Scott	Speaker	Central Laser Facility

Title	First Name	Family Name	Role	Affiliation
Prof.	Elaine	Seddon	Science Team	Cockroft Institute/ University of Manchester
Dr	Elizabeth	Shotton	Speaker	Diamond Light Source
Dr	Alistair	Siebert	Speaker	Diamond Light Source
Prof	Graham	Smith	Speaker	St Andrews University
Prof.	Peter	Smowton	Speaker	University of Cardiff
Dr	Edward	Snedden	UK XFEL Team	Daresbury
Dr	Claudiu	Stan	Speaker	Rutgers University, USA
Dr	Jergus	Strucka	Consultant	Imperial College London
Prof. Sir	David	Stuart FRS	Speaker	Diamond Light Source
Prof.	Cristian	Svetina	Speaker	IMDEA Nanoscience, Madrid
Dr	David	Thompsett	Speaker	Johnson Matthey PLC
Prof	Kiyoshi	Ueda	Speaker	Shanghai Tech/University of Tohoku
Dr	Patrick	Vagovic	Consultant	DESY
Prof.	Claire	Vallance	Science Team	University of Oxford
Prof.	Jasper	van Thor	Science Team	Imperial College London
Prof.	Sam	Vinko	Speaker/Science Team	University of Oxford
Prof.	Simon	Wall	Science Team	University of Aarhus, Denmark
Dr	Dave	Walsh	Speaker	Daresbury
Prof.	Ryan	Wang	Consultant	University College London
Prof.	Justin	Wark	Science Team	University of Oxford
Prof.	Dan	Watts	Speaker	University of York
Prof.	Julia	Weinstein	Science Team	University of Sheffield
Prof.	Philippe	Wernet	Speaker	Uppsala University, Sweden
Dr	Peter	Williams	Speaker	Daresbury
Dr	Thomas	Wolf	Speaker	Stanford Linear Accelerator Centre, USA
Dr	Mark	Yeung	Speaker	Queen's University Belfast
Dr	Briony	Yorke	Speaker	University of Leeds
Prof.	Linda	Young	Speaker/IAB	Argonne National Laboratory, USA
Dr	Amelle	Zair	Science Team	King's College London
Prof.	Xiaodong	Zhang FRS	Science Team	Imperial College London

A3.6 Engagements and surveys from the 2020 edition of the Science Case

A3.6.1 Workshops and community engagement events 2019

Table A3.1: Workshops and numbers attending event in 2019

Event	No. of attendees
Launch Meeting (Royal Society, London, July 16th 2019)	72
Matter at Extreme Conditions (University of Edinburgh, Oct 2nd 2019)	27
Life Sciences (Crick Institute, London, Nov 5th 2019)	160
Frontiers in Physical Sciences (Imperial College, London, Nov 13th 2019)	102
Quantum and Nanomaterials (University of Southampton, Nov 27th 2019)	40
Applications to Industry (University of Warwick, Dec 4th 2019)	29
Chemical Dynamics and Energy (University of Newcastle, Dec 11th 2019)	50

A website was established dedicated to community engagement with presentations from workshops and opportunity to input:

https://www.clf.stfc.ac.uk/Pages/UK-XFEL-Scientific-Case-Consultations.aspx

A number of discussion meetings were organised for the science and technical teams; these were arranged to facilitate the development of machine specification and construction of the science case:

- Meeting of Science and Technical teams 27th September 2019, King's College London
- Meeting of full Science team 15th and 16th January 2020, Cosener's House, Abingdon

A3.6.2 Development of UK XFEL user community up to 2020

Up to 2020, the UK had a strong and growing community of scientists who use existing operational XFEL facilities, such as the European XFEL, LCLS or SACLA, to conduct research in a broad range of areas from protein structural dynamics to matter at extreme conditions and ultrafast electron dynamics. UK users had been benefiting from beam time since first operations on most facilities, either through FAP awarded beamtime or collaborative commissioning campaigns. For the most established facilities, LCLS and SACLA, there was already a clear record of increasing engagement from the UK community. A survey of research groups in the UK (across the Life and Physical Sciences) indicated that over 500 UK scientists had had active involvement in XFEL science in the last decade. This was a conservative estimate, as our survey was partial and many university groups working with XFELs were likely missed. In STFC alone, there were over 150 people across multiple departments working both to upgrade the capabilities of existing XFELs and to explore new and ambitious technologies that could pave the way for a UK XFEL.

The UK research community at that time comprised a diverse range of academics consisting of university staff, post-doctoral researchers and post-graduates, who had either attended beamtime or undertaken theoretical and computational analysis. In a 10-year period, the UK's research groups had established a strong reputation in many areas of activity including, for example, structural biology, protein structural dynamics, matter at extreme conditions, materials, chemical sciences and nanoscience and ultrafast X-ray-matter interactions.

The 2016 STFC FEL Review identified that the existing potential XFEL user community should be helped to grow, especially following construction of, and UK investment in, the European XFEL. The Life and Physical Sciences Hubs (based at Diamond and the Central Laser Facility, respectively) were

established to support and grow the UK community through various initiatives, including funding travel for experimenters, development of hardware and sample technologies, joint funding of PhD studentships and support for networking activities. Whilst they operate on different models, both Hubs share the common strategic aim to assist users, some of whom will never have visited an XFEL, in gaining the experience and capability to make the most of these cutting-edge facilities. Since XFEL beamtime is in great demand, it is critical that these programmes continue in order to lower the barriers to access that many UK groups face and enable them to deliver greater scientific impact and foster new international collaborations.

SACLA publication data (see **Figure A3.1**) highlighted the growth in UK users at this hard X-ray FEL. This was also reflected in the fraction of UK scientists that make up the total number of domestic and international users at the facility. This relatively small, but emergent UK base at SACLA had already delivering scientific impact by 2019, with UK authors featuring on 10% of all XFEL user publications at the facility in the preceding five years. As the first hard X-ray FEL, LCLS-I has been a draw for the UK academic community since the first year of operations in 2009, with an average of 50 unique UK users using the facility annually between 2014 and 2019. Accounting for shutdown periods for the development of LCLS-II, the facility had seen a steady increase in UK engagement over that period, with an approximate growth of 10% per annum.

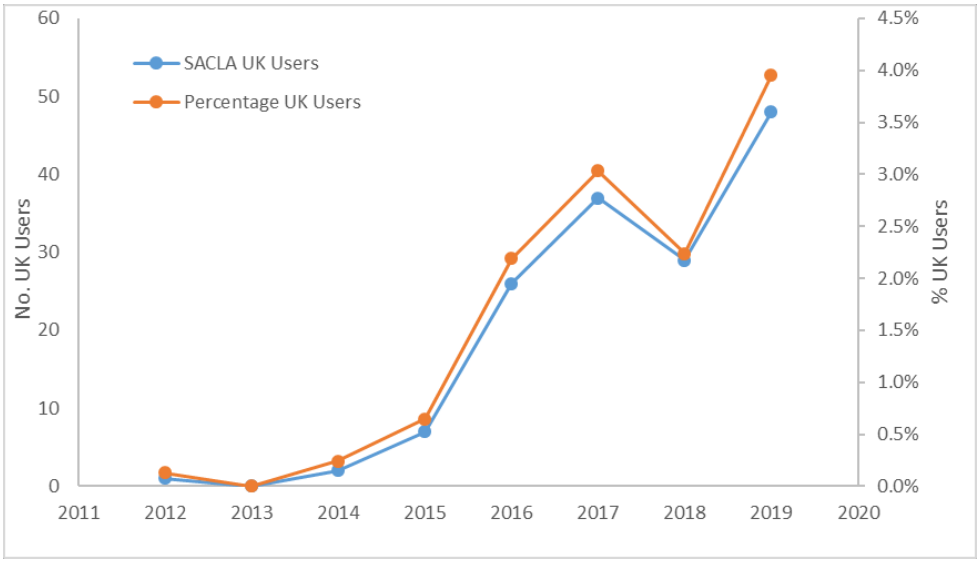


Figure A3.1: Number of UK team members on experiments at the SACLA XFEL to 2019. The relative percentage that UK users made up of the total number of users from all countries is also shown.

By 2020, the UK community was currently moderate in number (in 2018 there were 98 users at LCLS and SACLA), and it is still smaller compared to the communities in Germany, Japan and the USA. Whilst increasing international capacity was welcomed by UK scientists to meet immediate needs (especially with the European XFEL recently coming online), output from existing host countries shows how domestic user communities rapidly grow to build and exploit new capabilities. As the geographically closest XFEL facility to the UK currently, as well as offering state-of-the-art capability, the European XFEL remains an attractive destination to address a range of scientific challenges for UK scientists. Although it had only been operational for a couple of years in 2019, there were 891 unique users at the facility overall that year, 31 of which whom from the UK. Although UK participation in the European XFEL was anticipated to grow significantly over the coming years, the number of users was dwarfed by the number of domestic users at the facility who totalled 303 (34%) unique users. The presence of large domestic user communities was also reflected at established FELs like LCLS and SACLA, the latter of which had 1214 user visits in 2019, with 58% of these consisting of Japanese academic and industrial sectors. It was recognised in 2020 that a UK XFEL would undoubtedly be extremely valuable in guaranteeing UK access to an ultra-fast X-ray facility and importantly, lowering the barriers to access. In addition, as international demand increases, competition for beamtime on existing facilities is only likely to grow over the next 5 – 10 years.

The cutting-edge nature of the research performed at XFELs is reflected in the quality of the publications produced from the facilities. As the most established hard X-ray facility, and the one most in demand by UK users in over the last five years, LCLS provides useful statistics in this regard. **Figure A3.2** shows how publication numbers from X-ray beam time increased since first user operations began in 2009, as scientists discovered how the new capability could be used to answer significant scientific questions and developed new experimental techniques to make the most of their limited beamtime. In the five years from 2014 to 2019, LCLS averaged almost 100 publications per year. LCLS, like many other XFELs, produced significant numbers of high impact publications across a range of fields. Almost one-third of all LCLS X-ray science publications have been in published in high impact journals (Impact Factor > 10). The facility as a whole averaged 186 publications in the same period, owing to additional FEL and accelerator science, as well as publication of scientific work performed by LCLS scientists at other facilities. A UK XFEL would also be expected to produce significant output from these additional activities as the facility developed new techniques, including novel acceleration techniques, X-ray beam characterisation, detector development, sample delivery, and data analysis. As a world-leading facility, we would expect to attract a high calibre of facility scientists, who would also pursue their own scientific programmes at the UK FEL and facilities worldwide.

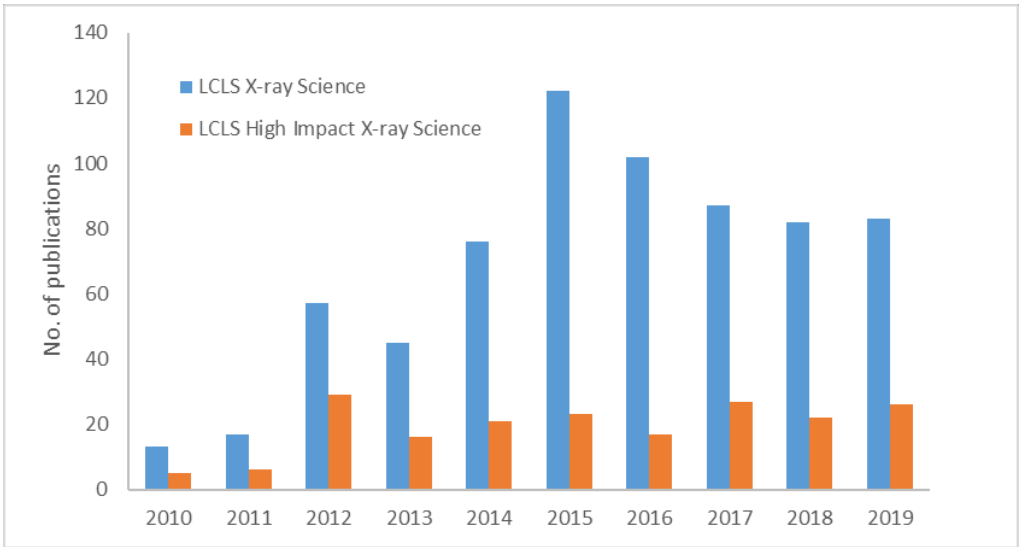


Figure A3.2: Number of LCLS publications based on X-ray science performed at the facility between 2009 and 2019. The number of high impact publications (impact factor of 10+) is also shown. Note – FY17 and FY19 had limited beam time (6 months and 3 months respectively) due to LCLS-II development work, hence we would expect this to have negatively impacted publication rates from 2017 onwards.

It should be noted that whilst the average number of publications per year from an XFEL such as LCLS was lower than many established X-ray synchrotron facilities, there are a number of key differences. Most synchrotrons are able to operate with multiple end-stations in parallel (typically 20 – 30), significantly boosting the quantity of scientific output. For most operational XFELs in 2019, only a single end-station could operate at any one time, which was a limiting factor. However, next-generation XFELs (including LCLS-II, the European XFEL and the UK XFEL proposed in 2020) would be capable of multiplexing in order to utilise multiple end-stations simultaneously. In addition, as a mature technology, synchrotrons use established techniques to produce their scientific results, so most beamtime results in a publication of some sort. As a new technology, not only are experimental techniques on XFELs in their relative infancy, but the nature of experiments is often testing the capability of the machine rather than utilising known methods to measure certain material parameters. Whilst these early experiments can yield high impact publications from the first application of cutting-edge techniques (as demonstrated on machines like LCLS), the overall publication rate that results will be lower initially, especially when additional facility development is often continually ongoing in parallel.

As use of XFELs becomes more established across a range of physical and life sciences, and additional capacity is unlocked through the use of multiplexing and higher repetition rates, it is anticipated that the degree of scientific productivity from these facilities will increase significantly.

Whilst we cannot precisely predict how long the current XFEL capacity will sufficiently meet scientific demand, we highlight two important trends. Firstly, everywhere the number of users is steadily growing. Secondly, already at all XFELs beamtime is heavily oversubscribed by typically high-quality proposals, so that of proposals deemed competitive only about one in four receive beamtime. Extra capacity will alleviate this, but demand will also grow as more scientists recognise the benefits of XFEL measurements to their research. Moreover, new capabilities, such as those that will be offered by UK XFEL, will create new areas of demand. It is therefore our anticipation that within the next decade the demand will drive the need for additional XFELs and new capabilities. A UK XFEL would be well placed to satisfy this demand from both national and overseas scientists.

Glossary

ARPES	Angle-resolved Photoemission Spectroscopy
CDI	Coherent Diffractive Imaging
CLF	Central Laser Facility
Cryo-EM	Cryogenic Electron Microscopy
ESCA	Electron Spectroscopy for Chemical Analysis
EUV /XUV	Extreme Ultraviolet (20 - 200 eV)
EXAFS	Extended X-ray Absorption Fine Structure
HAXPES	Hard X-ray Photoelectron Spectroscopy
HED	High Energy Density
HHG	High Harmonic Generation
HXR	Hard X-ray (4 keV - 100 keV)
ICS	Inverse Compton Scattering
IR	Infrared
Linac	Linear Accelerator
LWFA	Laser Wakefield Acceleration
MX	Macromolecular Crystallography
NC	Normal Conducting
ODL	Orbital Degeneracy Lifting
PDF	Pair Distribution Function
PWFA	Plasma Wakefield Acceleration
QED	Quantum Electro-Dynamics
RAL	Rutherford Appleton Laboratory
RIXS	Resonant Inelastic X-ray Scattering
SASE	Self-amplified Spontaneous Emission
SC	Super Conducting
SCO	Spin-crossover
SFX	Serial Femtosecond Crystallography
STFC	Science and Technology Facilities Council
SXR	Soft X-ray (200 - 4 keV)
THz	Terahertz (10^{12} Hz)
UED	Ultrafast Electron Diffraction
UKRI	UK Research and Innovation
UV	Ultraviolet
VUV	Vacuum Ultraviolet (10 - 20 eV)
WAXS	Wide Angle X-ray Scattering
WDM	Warm Dense Matter
XANES	X-ray Absorption Near Edge Structure
XAS	X-ray Absorption Spectroscopy
XES	X-ray Emission Spectroscopy
XFEL	X-ray Free Electron Laser
XFELO	XFEL Oscillator
XPCS	X-ray Photon Correlation Spectroscopy
XPS	X-ray Photoelectron Spectroscopy

Units

Time

Attosecond	1 as = 10^{-18} s
	Attosecond range 1 - 1000 as
Femtosecond	1 fs = 10^{-15} s
	Femtosecond range 1 - 1000 fs
Picosecond	1 ps = 10^{-12} s
	Picosecond range 1 - 1000 ps
Nanosecond	1 ns = 10^{-9} s
	Nanosecond range 1 - 1000 ns

Length

Ångstrom	1 Å = 10^{-10} m
Nanometre	1 nm = 10^{-9} m

Metric prefixes

exa	E	10^{18}
peta	P	10^{15}
tera	T	10^{12}
giga	G	10^{9}
mega	M	10^{6}
kilo	k	10^{3}
hecto	h	10^{2}
deca	da	10^{1}
		10^{0}
deci	d	10^{-1}
centi	c	10^{-2}
milli	m	10^{-3}
micro	μ	10^{-6}
nano	n	10^{-9}
pico	p	10^{-12}
femto	f	10^{-15}
atto	a	10^{-18}

Science and Technology Facilities Council



Copyright 2026 UK Research and Innovation

To read the full reports go to
xfel.ac.uk